Photochemistry and Photophysics of Coordination Compounds

Edited by
H. Yersin and A. Vogler

With 145 Figures and 38 Tables

Springer-Verlag
Berlin Heidelberg New York
London Paris Tokyo

Proceedings of the Seventh International Symposium
on the Photochemistry and Photophysics of Coordination Compounds
Elmau/FRG, March 29–April 2, 1987

Priv.-Doz. Dr. Hartmut Yersin
Institut für Physikalische und Theoretische Chemie
Universität Regensburg
Universitätsstr. 31, 8400 Regensburg, FRG

Prof. Dr. Arnd Vogler
Institut für Anorganische Chemie, Universität Regensburg
8400 Regensburg, FRG

ISBN 3-540-17808-2 Springer-Verlag Berlin Heidelberg New York
ISBN 0-387-17808-2 Springer-Verlag New York Berlin Heidelberg

Printing and Binding: Druckhaus Beltz, Hemsbach/Bergstr.
2152/3140-543210

PREFACE

The "Seventh International Symposium on the Photochemistry and Photophysics of Coordination Compounds" was held in the charming Schloß Elmau lying in a hidden valley of the Bavarian Alps above Garmisch-Partenkirchen, Federal Republic of Germany, from March 29 to April 2, 1987.

About ninety participants from seventeen countries including about thirty non-European scientists as far away as Japan and Australia came together for this symposium. Forty-five oral and twenty-five poster contributions were presented. These presentations and the opportunity for many formal and informal discussions stimulated an intense scientific interaction between the participants.

This meeting followed previous symposia held in Mühlheim 1974 (Koerner von Gustorf), Ferrara 1976 (Carassiti, Scandola), Köln 1978 (Wasgestian), Montreal 1980 (Serpone), Paris 1982 (Gianotti) and London 1984 (Harriman). The main fields covered by this 7^{th} Symposium were photo-redox processes, organometallic photochemistry, and properties of metal centered excited states. Furthermore, special complexes such as $[Ru(bpy)_3]^{2+}$ and related compounds as well as Cr(III)-complexes were discussed extensively. Moreover, a series of potential applications such as solar energy conversion and storage (e.g. water splitting) and photoresist technology were important subjects of this meeting. Thus, it was shown again that the rapidly expanding field of excited-state chemistry and physics of coordination compounds has become an important part of inorganic chemistry.

The organization of this symposium was made possible financially through the generosity of Deutsche Forschungsgemeinschaft, Fonds der Chemischen Industrie, BASF AG, Bayer AG, BMW AG, CIBA-GEIGY AG, CYANAMID GMBH , Degussa AG , HOECHST AG , DR. SEITNER-Meßtechnik, Siemens AG, and Wacker-Chemie GmbH.

Regensburg, July 1987

Arnd Vogler and Hartmut Yersin

TABLE OF CONTENTS

---

* Contributions marked with an asterix (*) are dedicated to Prof. A.W. Adamson by his former graduate students and post doctoral associates.

TOPIC 1

Metal-Centered Excited States

POLARIZED LUMINESCENCE OF ($Pt(CN)_2bipy$) SINGLE CRYSTALS-MAGNETIC FIELD AND TEMPERATURE EFFECTS

J.Biedermann, M.Wallfahrer, and G.Gliemann

Institut für Physikalische und Theoretische Chemie, Universität Regensburg, 8400 Regensburg, FRG

ABSTRACT

The polarized luminescence of single crystal [$Pt(CN)_2bipy$] is reported. On raising the temperature from 1.9 K to 7 K or increasing the magnetic field from 0 to 1 T the **E**$\perp$**a**-polarized emission band (**E**: electric field vector, **a**: crystallographic **a** axis) is blue shifted by ~175 cm^{-1}. A temperature increase to 295 K or a magnetic field increase to 6 T reduces the emission lifetime by a factor of ~10^3 and ~10^2, respectively.

EXPERIMENTAL

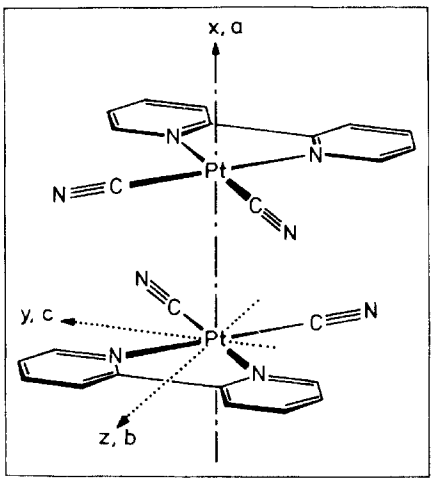

Fig. 1. Part of the proposed columnar structure of the red modification of [$Pt(CN)_2bipy$], schematic.[1,2]

The anhydrous red modification of [$Pt(CN)_2bipy$] was synthesized by a procedure described by Bielli [3]. [$Pt(CN)_2bipy$] belongs to the group

Photochemistry and Photophysics
of Coordination Compounds, Ed. by H. Yersin/A. Vogler

of planar d^8-transition metal complexes which form quasi-one dimensional columns in the solid state with short Pt-Pt distances, see Fig. 1. The apparatus and methods for the polarized emission measurements and for the magnetic field studies are described in Ref. [4].

RESULTS

Temperature Behavior of the Polarized Emission

Figure 2 presents the polarized emission spectra of single crystal [$Pt(CN)_2$bipy] at T = 1.9 K. The energies of the **E⊥a** and **E∥a** emission

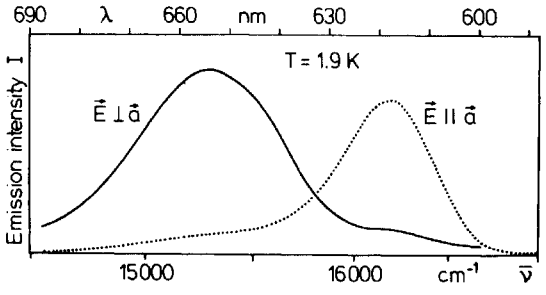

Fig. 2. **E∥a** and **E⊥a** polarized emission spectra of [$Pt(CN)_2$bipy] single crystal at T=1.9 K (λ_{ex}=364 nm).

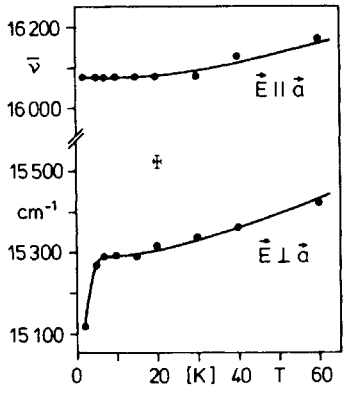

Fig. 3. Temperature dependence of the wave numbers $\bar{\nu}_{\parallel}$ and $\bar{\nu}_{\perp}$ of the emission maxima of a [$Pt(CN)_2$bipy] single crystal (λ_{ex}=364 nm).

maxima vs. temperature are plotted in Fig. 3. Below 20 K the **E∥a** emission maximum does not depend on temperature. Above 20 K it is blue shifted monotonically and the intensity $I_{\parallel}$ decreases with increasing temperature. Within the temperature range 1.9 K ≤ T ≤ 295 K, the lifetime $\tau_{\parallel}$ is shorter than 3 ns. Between 1.9 K and 7 K the **E⊥a** emission maximum is blue shifted by ~175 cm^{-1} and the corresponding intensity $I_{\perp}$ increases by a factor of ~20. Above T > 7 K the energy of the **E⊥a** emission increases monotonically and the intensity $I_{\perp}$ becomes weaker with increasing temperature. The lifetime $\tau_{\perp}$ at T = 1.9 K is ~ 2 ms. It becomes shorter by a factor of ~10^3 when the temperature increases up to 295 K.

Polarized Emission in the Presence of Magnetic Fields

The energy and the intensity of the **E⊥a** emission maximum at 1.9 K as functions of the strength of a magnetic field **H⊥a** is presented in Fig. 4 and 5, respectively. Between 0 and 1 T a blue shift of

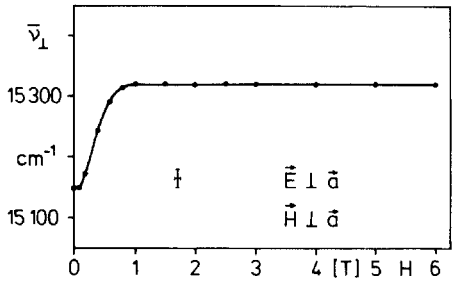

Fig. 4. Magnetic field dependence of the wavenumber $\bar{\nu}_\perp$ of the **E⊥a** emission maximum of a $[Pt(CN)_2(bipy)]$ single crystal at T=1.9 K (λ_{ex}=364 nm). **H⊥a**.

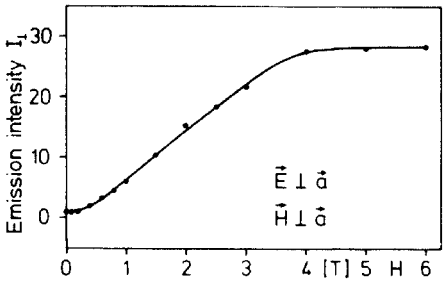

Fig. 5. Intensity $I_\perp$ of the **E⊥a** emission of a $[Pt(CN)_2(bipy)]$ single crystal in dependence of magnetic field strength at T=1.9 K (λ_{ex}=364 nm). **H⊥a**.

~175 cm^{-1} is observed. Above H = 1 T the spectral position of the **E⊥a** emission remains constant, indicating a saturation effect (Fig. 4). The relative intensity $I_\perp(H)/I_\perp(H=0)$ increases between 0 and 4 T by a factor of ~28 reaching a constant value at 4 T (Fig. 5). Application of a magnetic field of strength H = 6 T yields a reduction of the lifetime $\tau_\perp$ by a factor of ~10^2. The **E∥a** emission is found to be not influenced by magnetic fields.

DISCUSSION

The observed properties can be described by a system of interacting complexes of C'_{2v} symmetry. The energies of the electronic states are described by a valence band and a conduction band generated by an interchain coupling of the molecular states Pt5d and $Pt6p_x/CN^-\pi^*$, respectively.[5] Taking electron coupling and spin-orbit coupling into account, the resulting ground state has symmetry $A'_1(^1A_1)$ and the lowest excited states can be classified according to $A'_2, A'_1, B'_2(^3B_1)$ and $B'_1(^1B_1)$.

The **E⊥a** emission originates from (self-trapped) states A_2',A_1',B_2' of $^3B_1$ parentage, which are positioned below the lower edge of the conduction band. These states are shown at the left hand side (I and II) of Fig. 6. At 1.9 K the emission belongs to the transition $A_2' \rightarrow A_1'$ which

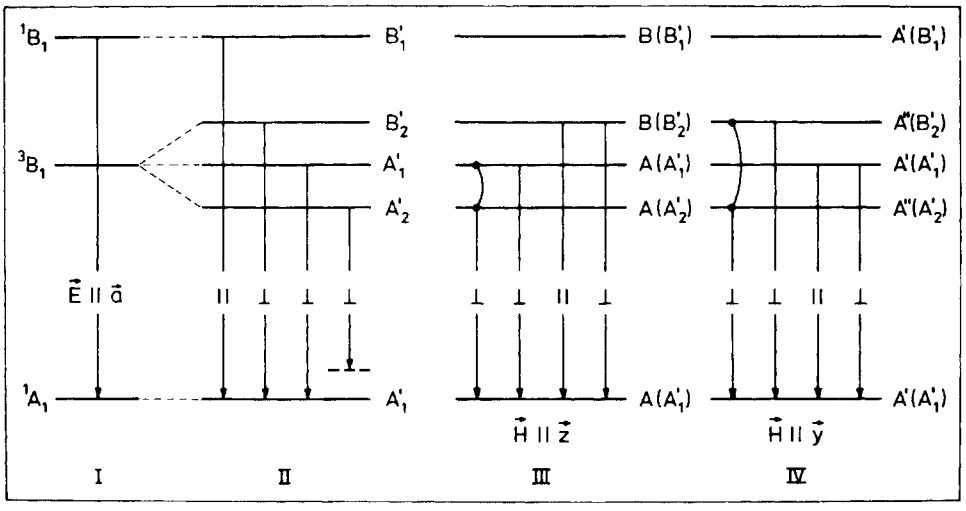

Fig. 6. Proposed energy-level diagram of $[Pt(CN)_2(bipy)]$ and radiative transitons (schematic). I: spin-orbit coupling neglected (symmetry C_{2v}), II: spin-orbit coupling included (symmetry C_{2v}'), III: magnetic field **H∥z** (symmetry C_2), IV: magnetic field **H∥y** (symmetry C_s).

is only vibronically allowed. At temperatures > 1.9 K the higher spin-orbit components A_1' and B_2' become thermally repopulated and emit directly (non-vibronically) into the ground state, resulting in a blue shift of ~175 cm^{-1}, an increase of the emission intensity and a reduction of the lifetime. The blue shift is on the order of one vibrational quantum. The **E∥a** emission corresponds to the singlet-singlet transition $B_1' \rightarrow A_1'$ (short lifetime $\tau_{\parallel} < 3$ ns).

The right hand side of Fig. 6 presents the energy levels of $[Pt(CN)_2bipy]$ in a homogeneous magnetic field **H⊥a**. For **H∥z** and **H∥y** the magnetic field lowers the symmetry C_{2v}' to the subgroup C_2 (case III) and C_s (case IV), respectively. A consequence of the symmetry lowering is a magnetic field induced interaction of the excited states A_2' and A_1'/B_2'.[6] As a result of the corresponding mixing of these states, a new additional radiative channel from the lowest excited state $A/A''(A_2')$ into the vibrationally non-excited ground state $A/A'(A_1')$ is opened. This explains the magnetic field induced blue shift and the lifetime decrease of the **E⊥a** emission at 1.9 K.

ACKNOWLEDGEMENT

We would like to thank the Fonds der Chemischen Industrie and the Deutsche Forschungsgemeinschaft for support of our work.

References:

[1] Textor, M., Oswald, H. R., Röntgenographische und spektroskopische Untersuchungen an zwei Modifikationen von Dichloro-2,2'-dipyridyl-platin(II). Z. anorg. allg. Chem. 407, 244 (1974).

[2] Biedermann, J., Wallfahrer, M., Gliemann, G., Magnetic-field and temperature effects on the optical properties of dicyano-2,2'-bipyridyl-platinum(II) single crystals. J. of Luminescence (1987) in press.

[3] Bielli, E., Gidney, P.M., Gillard, R.D., Heaton, B.T., Spectroscopic studies on some compounds (including dimorphic solids) of platinum(II) with 2,2'-bipyridyl and its analogeous. J. C. S. Dalton 4, 2133 (1974).

[4] Hidvegi, I., Ammon, W. v., Gliemann, G., Magnetic field effects on the luminescence of quasi-one-dimensional crystals $M_x[Pt(CN)_4]\cdot yH_2O$. J. Chem. Phys. 76, 4361 (1982); Ammon, W. v., Hidvegi, I., Gliemann, G., Magnetic field effects on the luminescence of $Ln_2[Pt(CN)_4]_3\cdot yH_2O$ single crystals. J. Chem. Phys. 80, 2837 (1984).

[5] Gliemann, G., Yersin, H ., Spectroscopic properties of the quasi one-dimensional tetracyanoplatinate(II) compounds. Structure and Bonding 62, 87 (1985).

[6] Gliemann, G., Magnetic field effects on the luminescence of transition metal complexes. Comments Inorg. Chem. 5, 263 (1986).

LIGHT-INDUCED EXCITED SPIN STATE TRAPPING IN IRON(II) COMPLEXES

S.Decurtins, P.Gütlich, A.Hauser, and H.Spiering

Institut für Anorganische Chemie und Analytische Chemie,
Johannes Gutenberg-Universität, 6500 Mainz, FRG

In the course of our studies on the thermally induced high spin (HS) ↔ low spin (LS) transition in iron(II) complexes /1/, $^5T_{2g} \leftrightarrow {}^1A_{1g}$ in the approximation of O_h symmetry, we have observed in 1984 a new photophysical effect /2/: If, at sufficiently low temperature, the solid spin crossover complex is irradiated with green light into the $^1A_1 \rightarrow {}^1T_1$ ligand field absorption band, the thermodynamically stable LS state can be converted to the metastable HS state and trapped with practically infinite lifetime. We have called this unusual phenomenon "Light-Induced Excited Spin State Trapping (LIESST)".

The first example, where we have seen the LIESST effect, is $[Fe(ptz)_6](BF_4)_2$ (ptz = 1-propyltetrazole) /2/. This coordination compound is known to exhibit thermally-induced spin transition with hysteresis of ca. 7 K width around 130 K /3,4/. The transition from the HS($^5T_2$) state to the LS($^1A_1$) state is accompanied by a dramatic color change from white to purple. Accordingly, the single-crystal absorption spectra of this complex are quite different in the two spin states as can be seen from Fig. 1 /5/. At 273 K, there is only one absorption band around 12250 cm^{-1} arising from the quintet-quintet transition $^5T_2 \rightarrow {}^5E$ in the HS molecules. At 8 K this absorption band has completely disappeared in favour of two singlet-singlet transitions, centered at 18400 and 26650 cm^{-1}, corresponding to $^1A_1 \rightarrow {}^1T_1$ and $^1A_1 \rightarrow {}^1T_2$ in the LS molecules. After bleaching the crystal with white light for ca. 2 min one sees again the typical HS absorption spectrum. Around 10 K, the trapped

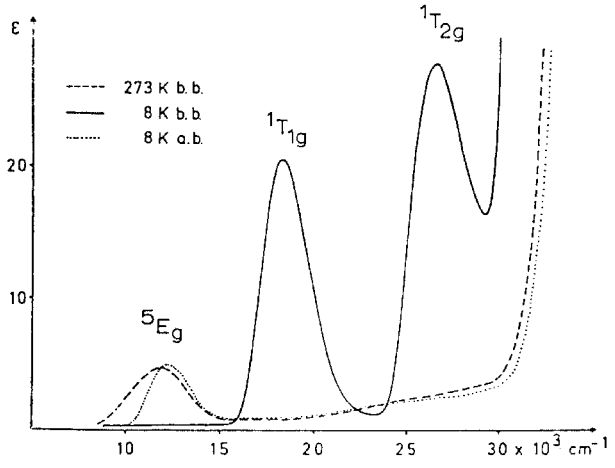

Fig. 1: Single-crystal absorption spectra (unpolarized) of $[Fe(ptz)_6](BF_4)_2$ before bleaching (b.b.) at 273 K and 8 K, and after bleaching (a.b.) for 2min with white light (tungsten lamp) at 8 K (from /5/).

Photochemistry and Photophysics
of Coordination Compounds, Ed. by H. Yersin/A. Vogler

metastable HS state does not decay to any noticeable extent within several days, excluding any tunnelling processes. Back relaxation to the thermodynamically stable LS($^1A_1$) state occurs only if the temperature is raised to 50–55 K. If the sample is heated further, one finally observes the well established thermally-induced LS → HS transition around 130 K.

We have followed the LIESST effect in $[Fe(ptz)_6](BF_4)_2$ also by magnetic susceptibility measurements /5/ and ^{57}Fe Mössbauer spectroscopy /2/. Figure 2 shows a sequence of Mössbauer spectra of $[Fe(ptz)_6](BF_4)_2$ for the light-induced LS → HS conversion at 15 K (a → b), the thermally induced back relaxation HS → LS around 50–55 K (c,d), and the thermally induced LS → HS conversion around 130 K (e → f). The HS state produced by LIESST has the same Mössbauer parameters as the thermodynamically stable HS state above 130 K (compare spectra b and f in Fig. 2).

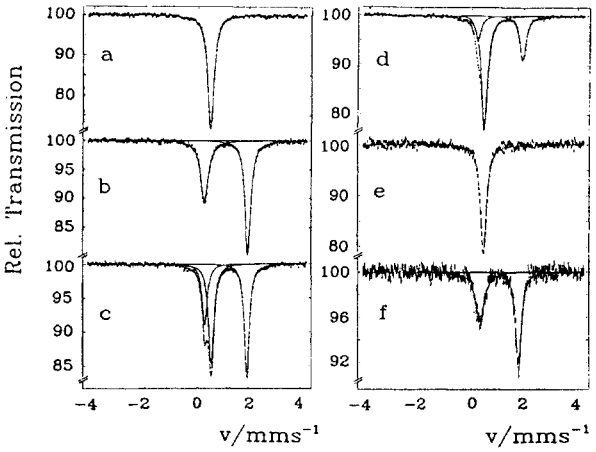

Fig. 2: Mössbauer spectra of $[Fe(ptz)_6](BF_4)_2$. (a) Before bleaching (measuring temperature T_M = 15 K); (b) after bleaching for 1 h at 15 K (T_M = 15 K); (c) after bleaching to 50–55 K and cooling to T_M = 15 K; (d) after second heating to 50–55 K and cooling to T_M = 15 K; (e) after subsequent heating to 97 K (T_M = 97 K); (f) after heating to 148 K (T_M = 148 K) (from /2/).

The mechanism of LIESST can be explained on the basis of Fig. 3: Irradiating the cold sample induces spin-allowed transitions $^1A_{1g} \rightarrow {}^1T_{1g}$ and $^1A_{1g} \rightarrow {}^1T_{2g}$ (s. Fig. 1). The excited spin-singlet states are short-lived and can decay back to the $^1A_{1g}$ ground state within nanoseconds. There is, however, an alternative decay path, favoured by spin-orbit coupling, which leads to a population of the spin triplet states $^3T_{1g}$ and $^3T_{2g}$ (intersystem crossing). These again decay via intersystem crossing, either to the $^1A_{1g}$ ground state or to the metastable $^5T_{2g}$ state. There is no radiative decay path from the $^5T_{2g}$ to the $^1A_{1g}$ state, and the $^5T_{2g}$(HS) state remains trapped with practically infinite lifetime as long as the temperature is sufficiently low so that the energy barrier between the $^5T_{2g}$ and the $^1A_{1g}$ potential surfaces, which are well separated by the large difference in the metal-ligand bond length of ca. 0.2 Å between the two spin states /6/, is not thermally overcome. But the trapped HS state can be pumped back to the LS state by irradiating with red light (of ca. 850 nm) into the $^5T_{2g} \rightarrow {}^5E_g$ absorption band /7/.

The $^5T_2 \rightarrow {}^1A_1$ relaxation kinetics was examined to pure $[Fe(ptz)_6](BF_4)_2$ crystals as well as for mixed crystals $[Fe_xZn_{1-x}(ptz)_6](BF_4)_2$ using optical spectroscopy /8/. It was shown that (a) for $x \approx 0.1$ a single-ion treatment of both the spin equili-

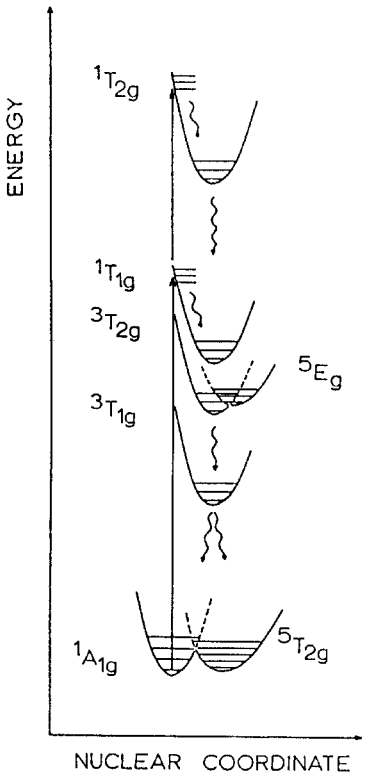

Fig. 3: Potential surface diagram according to experimental and calculated energies of the ligand field states of $[Fe(ptz)_6](BF_4)_2$ (from ref. /5/).

brium (with $\Delta H_{HL} = H_{HS}-H_{LS} = 510(12)$ cm^{-1}, $\Delta S_{HL} = S_{HS}-S_{LS} = 5.1(2)$ cm^{-1}/K at T = 100K and the $^5T_2 \rightarrow {}^1A_1$ relaxation of the light-induced trapped HS state (with Arrhenius activation energy $E_a^o = 810(30)$ cm^{-1} and frequency factor $A \approx 10^5$/s) is appropriate and (b) with increasing x cooperative effects become more and more important for both the HS $\rightleftharpoons$ LS equilibrium and the relaxation of the trapped HS state. These statements become apparent from Figs. 4-7.

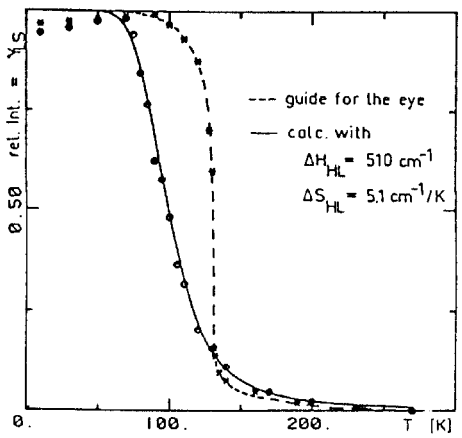

Fig. 4: Relative intensity of the $^1A_1 \rightarrow {}^1T_1$ transition vs. temperature for (*) $[Fe(ptz)_6](BF_4)_2$ and (o) $[Fe_xZn_{1-x}(ptz)_6](BF_4)_2$ ($x \approx 0.1$) (from /8/). The abrupt transition for the pure iron complex is typical for a first-order phase transition due to cooperative effects and agrees with the results from Mössbauer and magnetic susceptibility measurements /4/. For the dilute material cooperative effects are less important, and the spin conversion curve can be interpreted as a continuous LS $\leftrightarrow$ HS equi-

librium with $\Delta G = G_{HS}-G_{LS} = H_{HS}-H_{LS}-T(S_{HS}-S_{LS}) = \Delta H_{HL}-T\Delta S_{HL} = -k_B T \ln K_{HL} = -k_B T \ln[(1-\gamma_{LS})/\gamma_{LS}]$ (γ_{LS} = mole fraction of LS molecules).

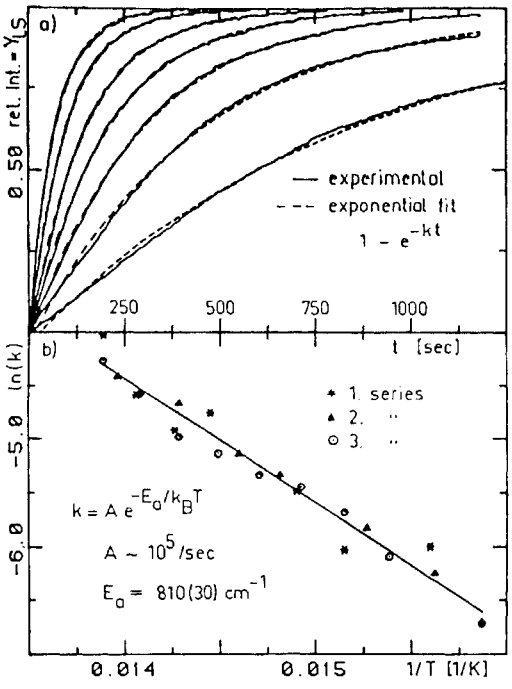

Fig. 5: (a) Normalized $^5T_2 \rightarrow {}^1A_1$ relaxation curves for $[Fe_xZn_{1-x}(ptz)_6](BF_4)_2$ ($x \approx 0.1$) at various temperatures.
(b) Arrhenius plot ln k vs. 1/T. As shown, an exponential fit $\gamma_{LS}(t) = 1-\exp(-kt)$ describes well the relaxation curves in the dilute material ($x \lesssim 0.1$) with constant activation energy E_a^o = 810(30) cm^{-1} and frequency factor $A \approx 10^5 s^{-1}$ (from /8/).

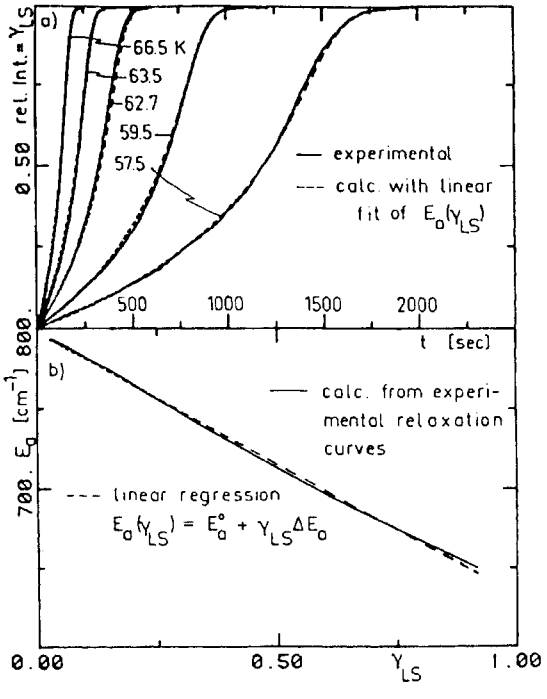

Fig. 6: (a) Normalized $^5T_2 \rightarrow {}^1A_1$ relaxation curves for pure $[Fe(ptz)_6](BF_4)_2$ at various temperatures. The sigmoidal (rather than exponential) form of the decay curves is due to cooperative effects. The activation energy E_a is now a linear function of γ_{LS} as shown in (b). The solid line in (b) was obtained from a simultaneous fit of the five measured decay curves of Fig. 6a. The broken line results from a linear regression (slope ΔE_a = -164 cm^{-1}; intercept E_a^o = 797 cm^{-1}) (from /8/).

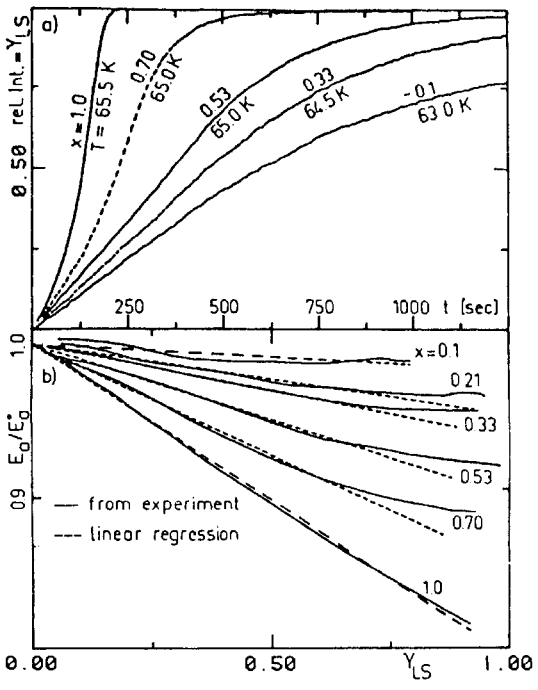

Fig. 7: (a) Normalized $^5T_2 \rightarrow {}^1A_1$ relaxation curves at approximately the same temperature for various concentrations of Fe(II) in the mixed crystals $[Fe_xZn_{1-x}(ptz)_6](BF_4)_2$. The decay curves follow a simple first-order law only in the dilute systems, but show more and more sigmoidal characteristics with increasing iron concentration due to cooperative effects. The activation energy turns out to be a function of γ_{LS} and x according to $E_a(\gamma_{LS},x) = E^o + \gamma_{LS}\ (\Delta E_a(x))$ as shown in Fig. 7b (from /8/).

$\Delta E_a(x)$ has been found to depend linearly on x; this supports our suggestion that the cooperative effects are of elastic and thus long-range rather than of electronic origin. The so-called "lattice expansion model" /9/ based on long-range elastic interactions arising from the drastic volume change $(V_{HS}-V_{LS})$ /6/ is well suited to explain these observations.

The LIESST effect has also been seen in other iron(II) spin crossover compounds, such as $[Fe(2\text{-pic})_3]Cl_2 \cdot EtOH$ (2-pic = 2-aminomethylpyridine) /10/ (see Fig. 8), $[Fe(phen)_2(NCS)_2]$ /10,11/ (see Fig. 9), and $[Fe(2\text{-Y-phen})_3]X_2$ (Y = CH_3, X_2 = ClO_4; Y = CH_3, X = BPh_4; Y = CH_3O, X_2 = $(ClO_4)_2 \cdot H_2O$) /12/.

Extensive studies on the LIESST effect are currently going on in our laboratory, particularly towards possible application in optical storage.

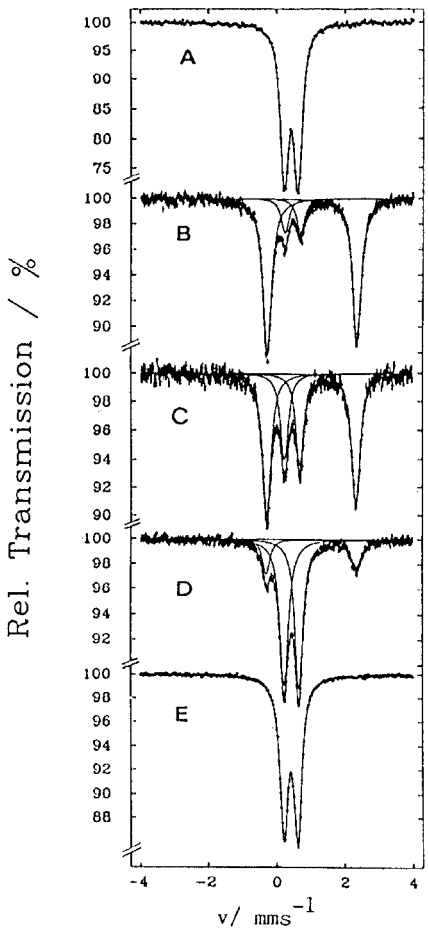

Fig. 8: Mössbauer spectra of $[Fe(2\text{-pic})_3]Cl_2$ EtOH recorded at T_M = 4.2 K (A) before bleaching, (B) after bleaching with white light for 1h, and (C,D,E) warming up to 30–32 K for a short time and cooling back to 4.2 K in three cycles. The outer two lines refer to the quadrupole doublet of the HS state, the inner two lines to that of the LS state (from /10/).

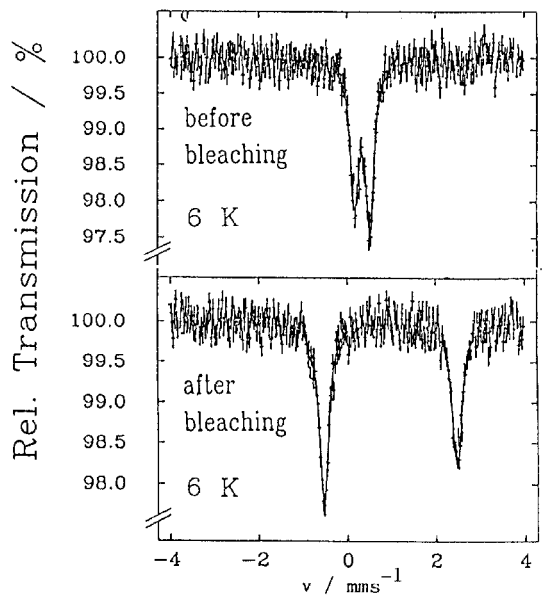

Fig. 9: Mössbauer spectra of $[Fe(phen)_2(NCS)_2]$ recorded at T_M = 6 K before and after bleaching with white light for 1 h (from /10/).

Acknowledgement

Financial support from the Bundesministerium für Forschung und Technologie (Grant No. NT 2723 7), the Deutsche Forschungsgemeinschaft, the Stiftung Volkswagenwerk, and the Fonds der Chemischen Industrie is gratefully acknowledged.
We wish to thank Professor H.U. Güdel (Bern) for fruitful cooperation.

References

/1/ Gütlich, P. In Structure and Bonding; Springer-Verlag: Berlin, 1981; Vol. 44, p. 83

/2/ Decurtins, S.; Gütlich, P.; Köhler, C.P.; Spiering, H.; Hauser, A. Chem. Phys. Lett. **1984**, 105, 1

/3/ Franke, P.L.; Haasnoot, J.G.; Zuur, A.P. Inorg. Chim. Acta **1982**, 59, 5

/4/ Müller, E.W.; Ensling, J.; Spiering, H.; Gütlich, P. Inorg. Chem. **1983**, 22, 1074

/5/ Decurtins, S.; Gütlich, P.; Hasselbach, K.M.; Hauser, A.; Spiering, H. Inorg. Chem. **1985**, 24, 2174

/6/ Mikami, M.; Konno, M.; Saito, Y. Chem. Phys. Lett. **1979**, 63, 566

/7/ Hauser, A. Chem. Phys. Lett. **1986**, 124, 543

/8/ Hauser, A.; Gütlich, P.; Spiering, H. Inorg. Chem. **1986**, 25, 4245

/9/ Spiering, H.; Meissner, E.; Köppen, H.; Müller, E.W.; Gütlich, P. Chem. Phys. **1982**, 68, 65

/10/ Decurtins, S.; Gütlich, P.; Köhler, C.P.; Spiering, H. J. Chem. Soc. Chem. Commun. **1985**, 430

/11/ Herber, R.; Casson, L.M. Inorg. Chem. **1986**, 25, 847

/12/ Poganiuch, P.; Gütlich, P. Inorg. Chem. **1987**, 26, 455

INFRARED LUMINESCENCE SPECTROSCOPY OF V^{3+} DOPED Cs_2NaYX_6 (X=Cl,Br)

C.Reber and H.U.Güdel

Institut für anorganische Chemie, Universität Bern, 3000 Bern 9, SWITZERLAND

1. Introduction

The luminescence properties of V^{3+} have received very little interest. The present work represents the first study of exactly octahedral VX_6^{3-} (X=Cl,Br) units which were obtained by doping the elpasolite lattices Cs_2NaYCl_6 with V^{3+} and growing single crystals by the Bridgman technique. Synthesis, crystal growth and the structure of the host lattices are described in the literature (Morss et al 1970; Mermant et al 1979). V^{3+} has a $3d^2$ electron configuration and therefore $^3T_{1g}$ as ground state in O_h symmetry. The lowest energy excited state is either $^1T_{2g}$ or $^3T_{2g}$, depending on the ligand field strength. In both situations luminescence in the near infrared region is expected, either as sharp lines ($^1T_{2g} \rightarrow {}^3T_{1g}$) or as a broad emission band ($^3T_{2g} \rightarrow {}^3T_{1g}$). Such transition metal systems are investigated as possible solid state laser materials (Imbusch et al 1985).

In the title crystals we are in the crossover region between sharp-line singlet and broad-band triplet emission. This situation in the excited state makes the luminescence spectroscopy particularly interesting and informative. From studies of the temperature dependence of the luminescence and decay properties a rather detailed picture of the relevant excited states is obtained. In addition, the spin-orbit splitting of the ground state can be determined. In non-cubic crystals luminescence spectroscopy of d^2 ions such as Ti^{2+} or V^{3+} is an excellent probe of the geometric distortions, because the low-symmetry splittings of $^3T_{1g}$ can be resolved. Ti^{2+} in $MgCl_2$ provides a nice example of this (Jacobsen et al 1986).

2. Experimental results

The luminescence spectrum of $Cs_2NaYCl_6:V^{3+}$ is presented in Fig. 1 at three temperatures. At 2K rich fine structure is observed. There is a pronounced change of the spectrum with temperature, above 100K a broad band becomes dominant. In contrast, $Cs_2NaYBr_6:V^{3+}$ shows broadband luminescence already at the lowest temperatures (peak energy 7500cm^{-1} at 4.2K).

In Fig. 2 the temperature dependence of the luminescence decay times is shown. All the decay curves are single exponentials. In the chloride host the decay time is 17.2msec at 21K, and it drops by nearly two orders of magnitude on increasing T to 270K. In contrast, the decay time in the bromide lattice is only 228µsec at 16K, similar to the chloride values at high temperatures, and it drops by only a factor of 3 on warming to 250K.

3. Discussion

a) Low-temperature luminescence spectrum of Cs_2NaYCl_6

The rich fine structure in the luminescence spectrum of $Cs_2NaYCl_6:V^{3+}$ at 2K (Fig. 1) together with the narrow overall width of the spectrum clearly indicate a $^1T_{2g} \rightarrow {}^3T_{1g}$ transition. The observed peaks can be assigned as electronic origins to the spin-orbit split components of the $^3T_{1g}$ ground state and as vibronic t_{1u} and t_{2u} origins built on these.

Photochemistry and Photophysics
of Coordination Compounds, Ed. by H. Yersin/A. Vogler

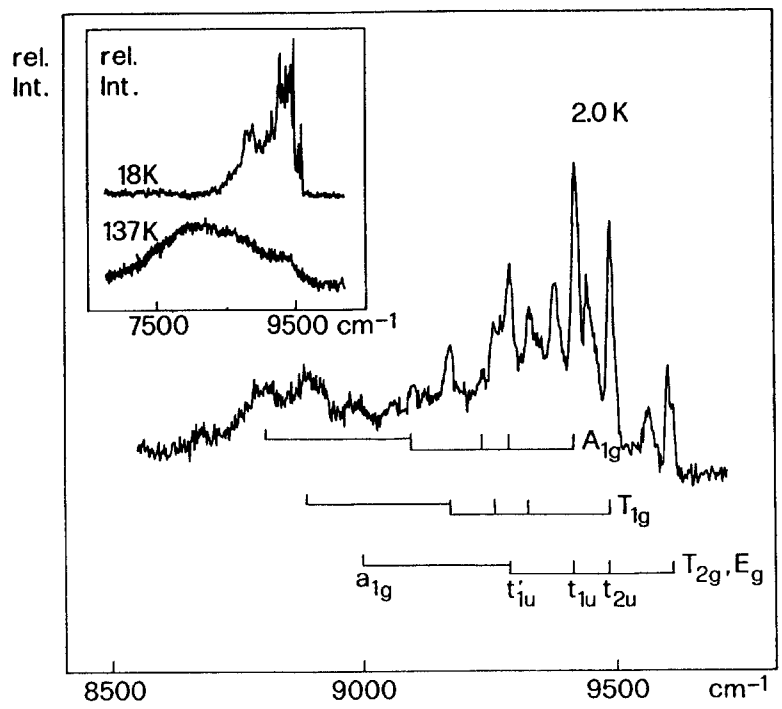

Figure 1 Low-temperature single crystal luminescence spectra of $Cs_2NaYCl_6:V^{3+}$ (0.05 mole%). The fine structure is assigned in terms of electronic transitions to the spin-orbit split ground state components and vibronic origins involving ungerade modes of the VCl_6^{3-} unit as indicated in the 2K spectrum. Built on the vibronic origins weak a_{1g} sidebands are indicated.

Although there is an overlap of electronic origins and vibronic sidebands an unambigous assignment of the bands is possible by using all the observed transitions. The lowest-energy components of the $^3T_{1g}$ ground state are the T_{2g} and E_g spinor states, which are degenerate in first order. Our spectra show that they are separated by $9.3cm^{-1}$, with E_g lower in energy, as could be shown with MCD (Neuenschwander 1981) and magnetic susceptibility measurements. The T_{1g} and A_{1g} origins lie at energies of $132.6cm^{-1}$ and $201.0cm^{-1}$, respectively. From these splittings we determine a spin-orbit coupling parameter ζ of $130cm^{-1}$. This is 62% of the free ion value, and we conclude that there is no Jahn-Teller effect in the ground state.
Three vibronic sidebands with energy displacements of $318cm^{-1}$, $186cm^{-1}$ and $128cm^{-1}$ are observed on all the electronic origins. The ground state vibrational energies of t_{1u}, t_{1u} and t_{2u} modes in the same host lattice doped with Cr^{3+} are $322cm^{-1}$, $187cm^{-1}$ and $120cm^{-1}$, respectively (Knochenmuss et al 1986). The vibronic sidebands in our spectrum can thus be assigned as t_{1u}, t_{1u} and t_{2u} vibronic origins. These modes are internal VCl_6^{3-} modes (Lentz 1974). A group of relatively broad and weak bands, which is displaced by approximately $300cm^{-1}$ from the intense group of vibronic origins, consists of a_{1g} sidebands.

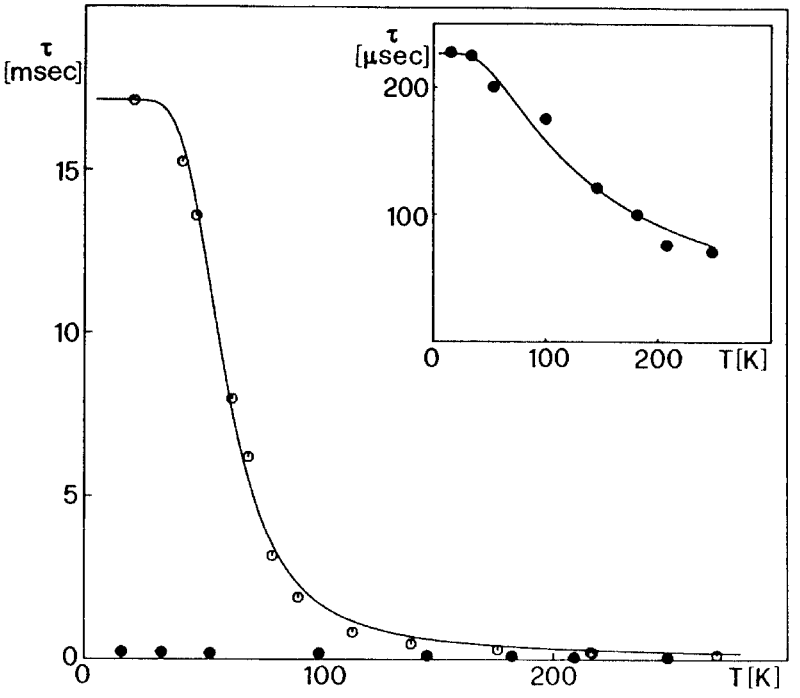

Figure 2 Temperature dependence of the luminescence decay times for $Cs_2NaYCl_6:V^{3+}$ (0.1 mole%, open circles) and $Cs_2NaYBr_6:V^{3+}$ (0.5 mole%, filled circles). The insert shows the bromide decay times on an expanded ordinate scale. The solid lines are fits to eq 1 and eq 2 for the chloride and bromide, respectively, as explained in the text.

b) Radiative relaxation in $Cs_2NaYCl_6:V^{3+}$

It is clear from the luminescence spectra in Fig. 1 that with increasing temperature the $^3T_{2g}$ excited state becomes thermally populated and broadband luminescence is observed. This is confirmed by the luminescence decay times in Fig. 2 which can be considered as radiative below 200K. The decay time of 17.2msec at 21K is typical for a spinforbidden transition. The high temperature values of 100-200μsec are in the typical range for spin-allowed vibronic transitions. In order to obtain a more quantitative picture a simple model was fitted to the decay times. We assume thermal equilibration within the $^1T_{2g}$ and $^3T_{2g}$ excited states to occur much faster than the luminescence transitions to the ground state. Neglecting the ^1E_g excited state, whose energy is unknown, as well as spin-orbit coupling within and between $^1T_{2g}$ and $^3T_{2g}$, we obtain equation 1 for the total radiative decay rate τ^{-1}:

$$\tau^{-1} = \tau_s^{-1} \cdot P_s + \tau_t^{-1} \cdot \coth(\hbar\omega/2kT) \cdot P_t \qquad (1)$$

with $P_s = 3/Z$

$P_t = 9 \cdot \exp(-\Delta E/kT)/Z$

$Z = 3 + 9 \cdot \exp(-\Delta E/kT)$

where τ_s and τ_t are the intrinsic decay times of the $^1T_{2g}$ and $^3T_{2g}$ states, respectively and ΔE is their energy difference. The coth term describes the temperature dependence of the $^3T_{2g} \rightarrow {}^3T_{1g}$ radiative rate with an enabling mode frequency of $179cm^{-1}$ which was determined from the temperature dependence of the $^3T_{1g} \rightarrow {}^3T_{2g}$ absorption intensity. τ_s was set to 17.2 msec, the observed low-temperature value, and τ_t as

well as ΔE were varied in the least squares fitting process. The parameter values are τ_t = 213 µsec and ΔE = 231cm^{-1}. The model is clearly oversimplified, but the fit is very good and the parameters are in quantitative agreement with the observed ratios of sharp-line to broadband emission.

c) Luminescence properties of $Cs_2NaYBr_6:V^{3+}$

The observation of broadband luminescence from $Cs_2NaYBr_6:V^{3+}$ as well as the different temperature dependence of the decay times show that the order of the lowest energy excited states is not the same as in the chloride host. Due to the weaker ligand field of Br^- compared to Cl^- $^3T_{2g}$ is the emitting state in the bromide at all temperatures. This is confirmed by the luminescence decay times. In analogy to eq 1, eq 2 gives the temperature dependence of the radiative decay rate:

$$\tau^{-1} = \tau_t^{-1} \coth(\hbar\omega/2kT) \qquad (2)$$

τ_t and $\hbar\omega$, the energy of the effective enabling mode, were treated as parameters. The resulting fit with values of 225 µsec and 122cm^{-1} for τ_t and $\hbar\omega$,respectively, is shown in Fig. 2. In contrast to the chloride lattice it is not possible to obtain any information on the energy separation of $^3T_{2g}$ and $^1T_{2g}$ in the bromide lattice from our decay time measurements. This is due to the fact that the faster radiative decay channel from $^3T_{2g}$ is dominant at all temperatures. The possibility of strong spin-orbit mixing between $^3T_{2g}$ and a close lying $^1T_{2g}$ cannot be excluded.

4. References

Imbusch GF, Donegan JF, Bergin FJ (1985) Transition Metal Ion-doped Materials of Laser Interest. In: Di Bartolo B (ed) Spectroscopy of Solid-state Laser Materials. Plenum Press, New York, in press

Jacobsen SM, Smith WE, Reber C, Güdel HU (1986) Near-infrared luminescence from Ti^{2+} in $MgCl_2$. J Chem Phys 84: 5205-5206

Knochenmuss R, Reber C, Rajasekharan MV, Güdel HU (1986) Broadband near-infrared luminescence of Cr^{3+} in the elpasolite lattices $Cs_2NaInCl_6$, Cs_2NaYCl_6, and Cs_2NaYBr_6. J Chem Phys 85: 4280-4289

Lentz A (1974) Lattice Vibration Analysis of Cryolite $A_3B'X_6$ and Elpasolite $A_2BB'X_6$ Compounds. A Force Constant Calculation of Sr_2ZnTeO_6. J Phys Chem Solids 35: 827-832

Mermant G, Primot J (1979) Préparation, crystallogenese et caracterization des bromures mixtes de lanthanide, de sodium et de césium $Cs_2NaLn(III)Br_6$. Mat Res Bull 14: 45-50

Morss LR, Siegal M, Stenger L, Edelstein N (1970) Preparation of Cubic Chloro Complex Compounds of Trivalent Metals: Cs_2NaMCl_6. Inorg Chem 9: 1771-1775

Neuenschwander K (1981) Hexachlorokomplexe von dreiwertigem Titan, Vanadium, Chrom und Eisen. Kristallzucht und magnetooptische Untersuchung der Elektronentransferbanden. Inauguraldissertation, Universität Bern, p 109-136

RECENT PROGRESS IN URANYL PHOTO-PHYSICS

R.Reisfeld and C.K.Jørgensen

Section de Chimie, Université de Genève, 1211 Geneva 4, SWITZERLAND

The fluorescence of triatomic linear OUO^{+2} was first studied by Brewster in 1833,and formed the basis of the law of Stokes,in modern wording: The photons emitted from a photoluminescent material have lower energy than corresponding to the absorption band,except perhaps for a coinciding threshold,indicating an electronic origin without vibrational co-excitation.Uranyl salts were the first inorganic materials not needing a trace activator,and the familiarity of Henri Becquerel with uranyl luminescence triggered the discovery of radioactivity in 1896.A rich experimental set of data about crystalline and vitreous materials (Rabinowitch and Belford 1964;Burrows and Kemp 1974) is less extended, as far goes solutions.In many cases,the non-radiative de-excitation, decreasing the quantum yield η below 0.1,if not 0.001,is due not only to multi-phonon relaxation well-known from internal transitions in the 4f shell of trivalent lanthanides (Reisfeld and Jørgensen 1977,1987) but also to photochemical abstraction of hydrogen atoms from organic molecules and to removal of an electron from moderately reducing anions and cations present in solution (Rabinowitch and Belford 1964;Burrows and Kemp 1974).Marcantonatos (1980) argues that η is below 0.01 for aqua ions,at pH below 2,due to ephemeric hydrogen atom abstraction from an adjacent water molecule,recombining without luminescence. This water molecule must be close to one of the two oxo ligands,since a single perchlorate or phosphate (Lieblich-Sofer et al.1978) ligand present in the equatorial plane increases η to above 0.1.The striking similarity of the emission spectra of $UO_2F_5^{-3}$ with the aqua ion suggests the latter (Görrler-Walrand and Colen 1982,1984)is $UO_2(OH_2)_5^{+2}$. One anion in the equatorial plane only replaces one or two water molecules,but it may modify the oxidizing character and reactivity of the oxo ligands in the excited state.

In close analogy to yellow and orange colours of chromate and cerium (IV),there is no doubt that the uranyl absorption bands are electron transfer bands (Jørgensen 1970) due to one,or several,reducing ligands transferring one electron in the excited state to an oxidizing central atom.The first absorption band providing the long-lived fluorescent state has a position hardly dependent on the reducing character of the anion X.The same is true for orange $XCrO_3^-$ (X = Br,Cl,F,OH).In both cases,the transferred electron comes essentially from the oxo ligands. There have been two arguments for hesitation to accept this classification of uranyl electron transfer bands.One is the much lower wavenumbers compared with tungstates and other tungsten(VI) compounds,in spite of U(VI) being,chemically speaking,only slightly more oxidizing than W(VI).It is now established (McDiarmid 1976,1980) that gaseous UF_6 has a weak electron transfer band at 25700 cm^{-1} whereas WF_6 has the first band at 58000 cm^{-1} and MoF_6 at 47600 cm^{-1}.The other,quite unexpected,fact is that the uranyl bands below 30000 cm^{-1} are 100 to 2000 times weaker than electron transfer to the empty 4f shell of cerium(IV) and to the partly filled 5d shell (Jørgensen 1963,1970) of osmium(IV),iridium(IV) and platinum(IV) complexes.

Photochemistry and Photophysics
of Coordination Compounds, Ed. by H. Yersin/A. Vogler

Until 1975,it was the general opinion (Burrows and Kemp 1974) that the first excited M.O.(molecular orbital) configuration of the uranyl ion consists of one or more triplet (S = 1) states followed by singlet (S = 0)at higher energy,as usual for luminescent organic molecules.This opinion is even true (Jørgensen 1963) for d^6 transitions of octahedral rhodium(III) and iridium(III) complexes,though the spin-forbidden bands here have acquired intensities 3,and 15,percent of those of subsequent singlet-singlet transitions.However,because of the almost coinciding energies of at least four (two fφ and two fδ) among the seven empty 5f orbitals,combined with strong effects of spin-orbit coupling ($^2F_{7/2}$ is 7609 cm^{-1} above $^2F_{5/2}$ in gaseous U^{+5} indicating ζ_{5f}=2174 cm^{-1}) the transfer of an electron from one M.O. to the 5f shell provides 16 energy levels (Jørgensen and Reisfeld 1975,1982) characterized by the quantum number Ω in linear symmetry,having the same relation to $|M_J|$ in spherical symmetry as Λ has to $|M_L|$.Deviations from linear symmetry induced by the equatorial ligands (normally 4,5 or 6 atoms) can,at the most,produce two separate states from each Ω level.Nearly all these Ω values represent mixtures of comparable amounts of triplet and singlet character,and it has no meaning to speak about spin-forbidden transitions.A major step in identifying Ω was Denning et al.(1976) substituting ^{18}O in $Cs_2UO_2Cl_4$ allowing a distinction between vibrational components and electronic origins.The first excited level at 20096 cm^{-1} has Ω=1; the two next levels at 20406 and 21310 cm^{-1} are ascribed to a splitting of Ω=2;and 8 further origins up to 27758 cm^{-1} assigned Ω=3,2,3 (or 5), and 4.Comparable results were obtained (Denning et al.1979) for $CsUO_2(O_2NO)_3$ and $NaUO_2(O_2CCH_3)_3$ starting with Ω=1 at 21089 and 21104 cm^{-1},respectively.Both these crystals have 6 equatorial ligating atoms. Contrary to halide complexes (Jørgensen 1963,1970) the minor shift of the first excited state is not related to ligand electronegativity. Mixed oxides with octahedral $U(VI)O_6$ have the first origin (Bleijenberg 1980) between 19100 and 20300 cm^{-1},and salts of $UO_2F_4^{-2}$ at 19240,but of $UO_2F_5^{-3}$ at 19985 cm^{-1} (Flint and Tanner 1984).On the whole,the origin shifts toward lower energy with decreasing number of equatorial atoms, and apparently also with shorter U-X distances,since $UO_2Cl_4^{-2}$ syncrystallized in cubic Cs_2SnCl_6 has the fluorescent origin already at 19692 cm^{-1} (Flint and Tanner 1979).The aqua ion in solution has the origin close to 20600 cm^{-1}.The values in glasses are less precise (because of multiple sites) such as 19063 to 20400 cm^{-1} in borosilicate glass (Flint et al. 1983) and 19800 cm^{-1} in indium lead barium fluoride glass (Reisfeld et al. 1986) but seems as high as 20500 cm^{-1} in $NaPO_3$ glass (Lieblich-Sofer et al. 1978).

The extraordinary low intensity of the uranyl electron transfer bands leave no doubt that the M.O. losing an electron to the empty 5f shell has odd parity,in spite of 4 among 6 recent approximate M.O.calculations (Jørgensen and Reisfeld 1982,1983) suggesting the loosest bound M.O. to have even parity,or being at most 0.4 eV above an even M.O.Extrapolation from halide complexes (Jørgensen 1970) would suggest that the two π_u formed in the L.C.A.O. model from oxygen 2p orbitals are easier to excite or ionize than σ_u.The problem is (Jørgensen and Reisfeld 1982) that $\pi_u \rightarrow [5f(\varphi,\delta)\Omega=5/2^u]$ provides Ω=1,4,2 and 3 (among which Ω=4 has not been detected) but $\sigma_u \rightarrow 5f(\varphi,\delta)$ should give Ω=2 and 3 followed at 2000 cm^{-1} higher energy by Ω=1 and 2.Denning et al.1976,1979) argue that the ligands in the equatorial plane destabilize 5fφ by about this amount relative to 5fδ.One might have hoped that the neptunyl(VI) salts would show informative $5f^1$ transitions,but the evidence (Denning et al. 1982) does not seem conclusive.Though this dilemma has not been resolved

the conceivable easier excitation of σ_u can be due to anti-bonding on the closed shell U6p (Jørgensen,1982; DeKock et al.1984) in analogy to the loosest bound M.O. of N_2 being "pushed from below" by the σ_g combination of the two N2s orbitals.In any case,in a sufficiently large wave-number interval,the parity-forbidden uranyl electron transfer bands comprise all 16 Ω levels due to σ_u and 32 Ω levels due to π_u.

Until recently,only fluorescence of the first excited level had been detected,though higher excited states might easily show η around 10^{-4} with τ of order 10^{-8} s (Jørgensen and Reisfeld 1983).However,crystalline $CsUO_2(NO_3)_3$;$UO_2(NO_3)_2$,6 H_2O;hydrated uranyl sulfate;and uranyl-containing borosilicate glass were shown (Marcantonatos et al.1986) each to emit about 30 narrow bands in the interval 20800 to 30000 cm^{-1} with low intensity (η of order 10^{-3}) at 77 K.Already the vibrational structure connected with emission from the "classical" first excited state is more complicated than in a diatomic molecule.Though the major peaks of the emission spectrum are roughly equidistant,much lower frequencies are superposed,and it is expected from group-theory that nearly all transitions involve one (or three) odd normal modes of vibration.The absorption bands above 20000 cm^{-1} were thought of as a roughly equidistant set generated by a frequency known to be 0.85 times that of the electronic groundstate.Today,this seems to be a coincidence after 22000 cm^{-1},where the strong peaks involve several higher electronic levels,which happen to be separated by a multiple of the vibration.Continued work by Marcantonatos shows a quite short-lived electronic state close to 22700 cm^{-1} and at least one somewhat longer-lived state around 29000 cm^{-1} (related to the $^2F_{7/2}$ components expected some 8000 cm^{-1} above the first excited state).The difficulty for interpreting some 30 vibrational components is that the equidistant manifold of groundstate vibrations seems strongly modified.A plausible rationalization is that the "classical" first excited state remains linear,with two equally elongated U-O internuclear distances,whereas several of the (15 or 47) higher Ω levels tend to be thermalized,with equilibrium distances corresponding to a bending angle well below 180° and perhaps two different U-O ,not to speak about rearrangement of the ligands in the equatorial plane.

Anyhow,a major conclusion is that uranyl absorption is not followed by exclusively non-radiative relaxation to the first excited state,but cascades down with perceptible short-lived steps of luminescence toward the groundstate.Such cascading is known for eight J-levels of $4f^{10}$ holmium(III) in fluoride glasses (Reisfeld and Jørgensen,1987).Since the oscillator strength of the second and following excited Ω levels is very difficult to separate clearly from the first excited state,the observed τ above 1 ms in anhydrous salts is not an invariant radiative life-time since $Cs_2(SnCl_6)_{1-x}(UO_2Cl_4)_x$ has τ = 3.2 ms (Flint and Tanner 1979).τ of hydrated salts increase moderately by substitution with deuterium oxide, but the mere presence of protons is not (like in lanthanides,Reisfeld & Jørgensen 1977,1987) a sufficient condition for pronounced non-radiative de-excitation.The distant equatorial methyl groups in $NaUO_2(O_2CCH_3)_3$ interfere much less than most organic compounds in solution.
The highest known τ for a glass is 0.63 ms in a fluoride glass (Reisfeld et al.1986) in spite of simultaneously present uranium(IV).The average oscillator strength of distorted sites in most glasses is higher than in comparable crystals,decreasing the radiative life-time.Direct comparison with τ/η might be quite informative.This would also be highly significant for the luminescence from higher electronic states (Marcantonatos et al. 1986).There may be an initial rise of intensity,due to feeding from higher states,but the maximum should be proportional to the concentration of the short-lived,emitting state.

Acknowledgement

We are grateful to Professor Minas Marcantonatos for valuable discussions,and to Professor Charles Jacoboni for fluoride glasses for the spectroscopic studies.The collaboration was furthered by 2.820-0.85 and previous grants from the Swiss National Science Foundation.

Bleijenberg K C (1980) Structure and Bonding 42: 97-128
Burrows H D,Kemp T J (1974) Chem.Soc.Rev.(London) 3: 139-165
DeKock R L,Baerends E J,Boerrigter M,Snijders J G (1984) Chem.Phys.Lett. 105: 308-316
Denning R G,Snellgrove T R,Woodwark D R (1976) Mol.Phys. 32: 419-442
Denning R G,Foster D N P,Snellgrove T R,Woodwark D R (1979) Mol.Phys. 37: 1089-1107 & 1109-1143
Denning R G,Norris J O W,Brown D (1982) Mol.Phys. 46: 287-323 & 325-364
Flint C D,Tanner P A (1979) J.Lumin. 18: 69-72
Flint C D,Tanner P A,Reisfeld R,Tzehoval H (1983) Chem.Phys.Lett. 102: 249-253
Flint C D,Tanner P A (1984) J.C.S.Faraday Trans.II 80: 219-226
Görrler-Walrand C,Colen W (1982) Chem.Phys.Lett. 93: 82-85
Görrler-Walrand C,Colen W (1984) Inorg.Chim.Acta 94: 183-188
Jørgensen C K (1963) Adv.Chem.Phys. 5: 33-146
Jørgensen C K (1970) Progress Inorg.Chem. 12: 101-158
Jørgensen C K,Reisfeld R (1975) Chem.Phys.Lett. 35: 441-443
Jørgensen C K (1982) Chem.Phys.Lett. 89: 455-458
Jørgensen C K,Reisfeld R (1982) Structure and Bonding 50: 121-171
Jørgensen C K,Reisfeld R (1983) J.Electrochem.Soc. 130: 681-684
Lieblich-Sofer N,Reisfeld R,Jørgensen C K (1978) Inorg.Chim.Acta 30: 259-265
Marcantonatos M D (1980) J.C.S.Faraday Trans.I 76: 1093-1115
Marcantonatos M D,Altheer C,Reisfeld R,Jørgensen C K (1986) Chem.Phys.Lett. 132: 247-251
McDiarmid R (1976) J.Chem.Phys. 65: 168-173
McDiarmid R (1980) Chem.Phys.Lett. 76: 300-303
Rabinowitch E,Belford R L (1964) Spectroscopy and photochemistry of uranyl compounds.Pergamon,Oxford
Reisfeld R,Jørgensen C K (1977) Lasers and excited states of rare earths. Springer,Berlin Heidelberg New York
Reisfeld R,Eyal M,Jørgensen C K (1986) Chem.Phys.Lett. 132: 252-255
Reisfeld R,Jørgensen C K (1987) Excited state phenomena in vitreous materials.In: Gschneidner K A,Eyring L (eds) Handbook on the physics and chemistry of rare earths,vol. 9,chapter 58.North-Holland Publ.Co. Amsterdam

EFFECTS OF MACROCYCLIC AND CRYPTAND LIGANDS ON PHOTOPHYSICS OF Eu^{3+} IONS

N.Sabbatini, S.Perathoner, and L.De Cola

Dipartimento di Chimica "G.Ciamician" dell 'Universita', Bologna, ITALY

INTRODUCTION

The effects of second-sphere perturbations on the photochemical and photophysical properties of transition metal complexes have been discussed in a recent review paper (Balzani 1986). In the frame of that study lanthanide complexes were also considered, assuming that an analogy could be seen between the effects produced by the second coordination sphere on the d-block metal complexes and the first coordination sphere on the f-block metal ions.

In the current development of coordination chemistry an important role is played by complexes with macrocyclic and cage-type ligands (Voegtle 1981; Lehn 1982; Izatt 1985). For lanthanide ions, which usually give rise to weak complexes having ill-defined composition and structure in solution, those ligands are particularly valuable because they provide a means to obtain stable complexes.

In this paper we report preliminary results on the effects produced on the photophysics of Eu^{3+} in water solution on complexation of Eu^{3+} with the $C_{22}H_{26}N_6$ hexa-aza-macrocyclic ligand in the presence of acetate anions and ion-pair association of the $[Eu{\subset}2.2.1]^{3+}$ cryptate with F^- anions.

A detailed analysis of the properties of the luminescent excited state of Eu^{3+} is known to be a powerful means to elucidate molecular structures in solution (Horrocks 1984; Balzani 1986).

The excited state properties of complexes of some lanthanide ions with the macrobicyclic 2.2.1 cryptand ligand have been recently studied in our laboratory (Sabbatini 1984; 1986).

RESULTS AND DISCUSSION

The $[Eu(C_{22}H_{26}N_6)(CH_3COO)]^{2+}$ Complex

The complex was synthesized as previously described (De Cola 1986). The

Photochemistry and Photophysics
of Coordination Compounds, Ed. by H. Yersin/A. Vogler

experiments were performed in solutions containing 1.0×10^{-1}M CH_3COONa to minimize dissociation of the coordinated acetate anion.

Besides the weak f-f transitions of Eu^{3+}, the absorption spectrum shows three intense (ξ of the order of 10^4) bands in the near U.V. region (λ_{max}=214, 245, and 300 nm). These bands are attributed to transitions within the ligand because of their high intensity and because they are also observed in the analogous Gd^{3+} and Tb^{3+} compounds.

The excitation spectrum shows the same pattern as the absorption spectrum. This means that intramolecular energy transfer from the excited ligand to the emitting $^5D_0$ level of Eu^{3+} takes place.

The emission spectrum under high-resolution conditions shows only one peak ($\tilde{\nu}$ =17250 cm^{-1}) in correspondence with the $^5D_0 \rightarrow {}^7F_0$ transition of Eu^{3+}. This indicates that only one Eu^{3+} containing species is present in solution (Horrocks 1984; Balzani 1986).

The lifetimes for the emission from the $^5D_0$ excited state of Eu^{3+} are 0.70 ms (at 300 K) and 1.4 ms (at 77 K) in H_2O solution and 2.0 ms (at 300 K) and 2.1 ms (at 77 K) in D_2O solution. These values indicate that (i) the luminescent excited state of Eu^{3+} is partly quenched by vibronic coupling with the high-frequency O-H vibrations (longer lifetimes in D_2O than in H_2O solution) (Horrocks 1984), (ii) no low-lying, thermally occupied excited state is present (temperature independent lifetimes in D_2O solution) (Blasse 1986). The temperature dependence of the lifetime in H_2O may be attributed to a slight modification in coordination of H_2O molecules in the glassy state.

From the Horrocks' equation (Horrocks 1984) which makes use of lifetime measurements carried out in H_2O or D_2O solution, we obtain that 1 H_2O molecule is coordinated to Eu^{3+} in the macrocyclic complex at room temperature.

The $[Eu\subset 2.2.1]^{3+}$-F^- and $[Eu\subset 2.2.1]^{3+}$-$2F^-$ Ion Pairs

The $[Eu\subset 2.2.1]^{3+}$ cryptate was prepared as previously described (Sabbatini 1984). The two ion pairs with 1:1 and 1:2 $[Eu\subset 2.2.1]^{3+}$:F^- stoichiometries were obtained in the following conditions: $[Eu\subset 2.2.1]^{3+}=5.0 \times 10^{-3}$M, $[F^-]=5.0 \times 10^{-3}$M or

5.0×10^{-1}M, respectively, and ionic strength 5.0×10^{-1}M obtained by addition of KCl, on the basis of the reported association constants (Yee 1980).

The absorption spectra show that the N—>Eu^{3+} and O—>Eu^{3+} charge transfer bands (Sabbatini 1984) are blue shifted by $\sim$2000 cm^{-1} in going from $[Eu\subset 2.2.1]^{3+}$ to $[Eu\subset 2.2.1]^{3+}$-F^- and by $\sim$3000 cm^{-1} in going from $[Eu\subset 2.2.1]^{3+}$-F^- to $[Eu\subset 2.2.1]^{3+}$-$2F^-$. This fact can be explained by considering that association with F^- anions reduces the effective positive charge of Eu^{3+}, with a consequent increase in the energy of the LMCT transitions involving the nitrogen and oxygen donor atoms of the cryptand.

In Table I the luminescence lifetimes of the two ion pairs are reported and

Table I. Lifetimes (in ms) of the luminescent $^5D_0$ excited state

Solvent	T(K)	$[Eu\subset 2.2.1]^{3+}$	$[Eu\subset 2.2.1]^{3+}$-F^-	$Eu\subset 2.2.1]^{3+}$-$2F^-$
H_2O	300	0.22	0.50	1.0
	77	0.34	0.62	1.2
D_2O	300	0.64	1.5	1.7
	77	1.2	1.5	1.8

compared with those of the "free" $[Eu\subset 2.2.1]^{3+}$ cryptate. The increase in the lifetimes observed in H_2O solution with increasing F^- concentration shows that F^- ions replace water molecules which were found to be present in the coordination sphere of Eu^{3+} in the 2.2.1 cryptate (Sabbatini 1984), i.e. $[Eu\subset 2.2.1]^{3+}$-F^- and $[Eu\subset 2.2.1]^{3+}$-$2F^-$ are not solvent-separated ion pairs. The lifetimes of the two ion pairs are practically temperature independent. This is explained considering that radiationless decay via low-lying charge-transfer levels (Blasse 1986) is prevented because the LMCT excited states of the cryptate move to higher energies (see above) and become inaccessible when F^- replaces water in the holes of the cryptate structure.

The pattern of the luminescence spectrum of $[Eu\subset 2.2.1]^{3+}$ cryptate (Sabbatini 1984) is markedly affected by association with F^-. It shows (i) changes in the

crystal field splitting, related to changes in the site symmetry of Eu^{3+} and (ii) shift of all transitions to higher energies, ascribed to a reduction of the nephelauxetic effect upon replacing H_2O by F^-.

CONCLUSION

This study presents new examples of perturbations of the absorption and luminescence properties of the Eu^{3+} ion by suitable complexation and ion-pair association and confirms the utility of the photophysical characteristics of Eu^{3+} in enlarging the knowledge on the properties of macrocyclic and cryptand ligands. It is well-known that these molecules have recently revealed a particularly important class of ligands because they offer new possibilities in the field of coordination chemistry (Lehn 1982; Balzani 1986).

Acknowledgments. The authors wish to thank Prof. V. Balzani for helpful discussions.

References

Balzani V, Sabbatini N, Scandola F (1986) Chem. Rev. 86:319

Blasse G, Buys M, Sabbatini N (1986) Chem. Phys. Lett. 124:538

De Cola L, Smailes DL, Vallarino LM (1986) Inorg. Chem. 25:1729

Horrocks W, Albin M (1984) Progr. Inorg. Chem. 31:1

Izatt RM, Bradshaw JS, Nielsen SA, Lam JD, Christensen JJ, Sen D (1985) Chem. Rev. 85:271

Lehn JM (1982) In: Laidler KJ (ed) Frontiers of Chemistry (IUPAC) Pergamon, New York

Sabbatini N, Dellonte S, Ciano M, Bonazzi A, Balzani V (1984) Chem. Phys. Lett. 107:212

Sabbatini N, Dellonte S, Blasse G (1986) Chem. Phys. Lett. 129:541

Voegtle F (ed) (1981) Host Guest Complex Chemistry I, Top. Curr. Chem., 98

Yee EL, Gansow OA, Weaver MJ (1980) J. Am. Chem. Soc. 102:2278

TOPIC 2

Photophysics and Photochemistry of Cr (III) Complexes

LIGAND FIELD ANALYSIS OF THE DOUBLET EXCITED STATES IN CHROMIUM(III) TRISCHELATED COMPLEXES

A.Ceulemans, N.Bongaerts, and L.G.Vanquickenborne

Department of Chemistry, University of Leuven, 3030 Leuven, BELGIUM

THE ORGEL EFFECT IN TRISCHELATES

Trischelated complexes with bidentate ligands containing a π-conjugated bridge may show a pronounced trigonal splitting of the t_{2g} orbitals. As has been pointed out by Orgel (1961) this splitting is due to the electronic interaction between the pπ-orbitals of the ligator atoms via the conjugated bridge. An extended angular overlap model, which takes this interaction into account, has recently been developed (Ceulemans et al. 1985). If in the frontier molecular orbital (MO) on the bidentate ligand the ligator pπ-functions are *in phase*, a ψ-type Orgel effect results, described by a $\pi_{\perp}(\psi)$ parameter. Conversely if in the frontier MO of the ligand the pπ-functions are *out of phase*, a χ-type coupling occurs, described by a parameter $\pi_{\perp}(\chi)$. In principle more than one MO interaction can be important so that both ψ- and χ-effects may be operative simultaneously. Defining the trigonal splitting of the t_{2g} shell, $\Delta\tau_2$, as the energy difference between the e and a_1 orbitals of t_{2g} signature

$$\Delta\tau_2 = \varepsilon(e) - \varepsilon(a_1)$$

the Orgel effect in trischelated complexes is given by :

$$\Delta\tau_2 = 3\pi_{\perp}(\psi) - 3\pi_{\perp}(\chi)$$

Quite often ligand donor and acceptor levels display opposite phase coupling so that $\pi_{\perp}(\psi)$ and $\pi_{\perp}(\chi)$ will adopt opposite signs. In this way quite pronounced trigonal splittings may be obtained.

LIGAND FIELD CALCULATIONS

Within the framework of ligand field theory complete state calculations have been performed on hexacoordinated d^3 complexes, showing a variable trigonal splitting of the t_{2g} orbitals. In Fig. 1 we present the variation of the $(t_{2g})^3$ doublet energies as a function of the trigonal splitting. The input parameters of the calculation are specified in the figure legend. From the figure several observations may be made :

Photochemistry and Photophysics
of Coordination Compounds, Ed. by H. Yersin/A. Vogler

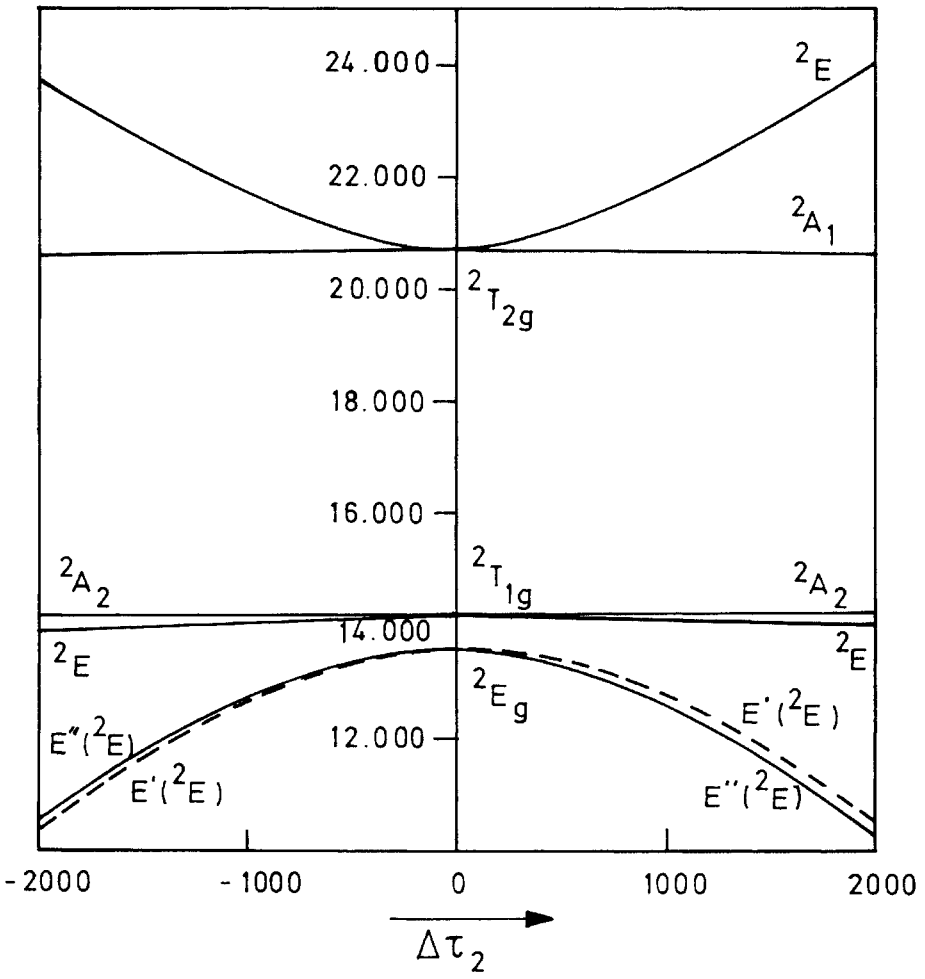

Figure 1 : Energies of the $(t_{2g})^3$ doublet states as a function of the trigonal orbital splitting $\Delta\tau_2$. These energies were obtained from complete d^3 ligand field calculations, using B = 700 cm^{-1}, C = 4B, ζ = 200 cm^{-1} and 10 Dq = 18500 cm^{-1}. In the centre of the figure one recognizes the three parent O_h states : ^2E_g, $^2T_{1g}$ and $^2T_{2g}$. Other symmetry labels refer to D_3 representations. The spin orbit components of the lowest ^2E emitting level are also represented. A full line is used for the E" component and a dashed line for the E' component.

a) There is no first order splitting of the octahedral doublet levels ^2E_g, $^2T_{1g}$ and $^2T_{2g}$. This is a result of their half-filled shell character (Ceulemans et al. 1982).
b) Spin orbit splitting of the ^2E levels is similarly small. The E' and E" components of the lowest ^2E level have been indicated on the figure. Their relative ordering depends on the sign of the trigonal splitting. Remark that for positive values of $\Delta\tau_2$ the spin orbit splitting of the lowest ^2E is more pronounced than for negative values of $\Delta\tau_2$.
c) In a recent study (Ceulemans et al. 1987) we have also calculated orbital density distributions for the lowest ^2E level of Fig. 1. From these calculations it was concluded that the trigonal field induces an anisotropic charge distribution. In all cases this anisotropy corresponds to a charge flow into the lower lying t_{2g} component, and a concomitant depletion of the higher lying component.

APPLICATIONS

Two typical trischelated Cr(III) complexes of great interest in photochemistry and photophysics, which are likely to exhibit a pronounced Orgel effect, are $Cr(acac)_3$ and $Cr(bipy)_3^{3+}$.

The *acac*$^-$ ligand (acetylacetonate) is iso-electronic with the pentadienyl anion. Consequently its π-donor HOMO will be of the ψ-type ($\pi_\perp(\psi) > 0$) while its π^*-acceptor LUMO will be of the χ-type ($\pi_\perp(\chi) < 0$). The sign of $\Delta\tau_2$ for $Cr(acac)_3$ is thus unambiguously determined to be positive. Accordingly the spin orbit components of the emitting ^2E level will be ordered as in the righthand side of Fig. 1 with E' above E". The spectral origin at 12900 cm^{-1} is therefore associated with the E"(^2E) component while the next transition near 13200 cm^1 is assigned as E'(^2E). (Armendarez and Forster 1964; Schönherr et al. 1983). This assignment is consistent with the ligand field analysis of the spin allowed quartet bands (Piper and Carlin 1960; Atanasov et al. 1987). Additional confirmation can be obtained from low temperature Zeeman luminescence spectra, published by Field and coworkers (1984). Some features of these spectra remain puzzling though.

The *bipy* ligand ($\alpha\alpha'$-bipyridyl) is iso-electronic with the butadiene system and therefore should show opposite phase coupling characteristics. With $\pi_\perp(\psi) < 0$ and $\pi_\perp(\chi) > 0$ the $\Delta\tau_2$ splitting in $Cr(bipy)_3^{3+}$ is clearly predicted to be negative. The spin orbit

components E" and E' are therefore expected to be ordered as in the lefthand side of Fig. 1 with E' below E". These predictions have recently been confirmed by detailed Zeeman spectra of $Cr(bipy)_3^{3+}$ in crystalline hosts (Hauser et al. 1987). The E'(^{2}E) component corresponds to the spectral origin around 13775 cm^{-1} while the E"(^{2}E) component is associated with a transition near 13800 cm^{-1}. Remark that the spin orbit splitting of the ^{2}E level in $Cr(bipy)_3^{3+}$ is substantially lower than in $Cr(acac)_3$. The effect is more pronounced than could be expected on the basis of the ligand field calculations in Fig. 1 and is probably due to a trigonal twist of the $Cr(bipy)_3^{3+}$ coordination sphere which counteracts the Orgel splitting.

Acknowledgement : We thank Prof. H.-H. Schmidtke and Dr. A. Hauser for communicating their results prior to publication. AC is indebted to the Belgian National Science Foundation (NFWO) for a research grant.

References :

Armendarez PX, Forster LS (1964) J. Chem. Phys. 40: 273

Atanasov MA, Schönherr T, Schmidtke H-H (1987) Theoret. Chim. Acta (Berlin)(to be published)

Ceulemans A, Beyens D, Vanquickenborne LG (1982) J. Am. Chem. Soc. 104: 2988

Ceulemans A, Dendooven M, Vanquickenborne LG (1985) Inorg. Chem. 24: 1153

Ceulemans A, Bongaerts N, Vanquickenborne LG (1987) Inorg. Chem. (to be published)

Field RA, Haidl E, Winscom CJ, Kahn ZH, Plato M, Möbius K (1984) J. Chem. Phys. 80: 3082

Hauser A, Mäder M, Robinson WT, Murugesan R, Ferguson J (1987) Inorg. Chem. (submitted for publication)

Orgel LE (1961) J. Chem. Soc. 1961: 3683

Piper TS, Carlin RL (1960) J. Chem. Phys. 33: 1208

Schönherr T, Eyring G., Linder R. (1983) Z. Naturforsch. 38A: 736

QUENCHING OF THREE PHOTOAQUATION MODES OF A CHROMIUM(III) ACIDOAMMINE

A.Damiani, P.Riccieri, and E.Zinato

Dipartimento di Chimica, Università di Perugia, 06100 Perugia, ITALY

INTRODUCTION. *Trans*-$Cr(NH_3)_4(CN)X^{z+}$ complexes with X = H_2O, Cl^-, F^-, NCS^-, etc. are photochemically unusual, since the spectrochemical strengths of the two ligands on the tetragonal axis are respectively higher and lower than that of the equatorial NH_3 groups. The situation is intermediate between those of *trans*-$Cr(NH_3)_4X_2^{z+}$ [1] and *trans*-$Cr(NH_3)_4(CN)_2^+$ ions,[2] which are characterized by different energy orderings of the ligand-field states, hence, by different antibonding properties of the lowest excited quartet: mainly axial (^4E_g state) for the former, and equatorial ($^4B_{2g}$) for the latter. The opposing effects of CN^- and X on the splittings of the octahedral energy levels make these species electronically quasi O_h, although their actual geometries are C_{4v}. Therefore, the ligand-field excitation energy can be distributed almost evenly among the different types of metal-ligand bonds. A recent investigation[3] of some members of this family has provided a test for the degree of detail the current photolabilization models[4] are able to handle when three concurrent photosubstitutions are involved.

The above ions phosphoresce from the lowest doublet excited state(s) in room-temperature solution, and for the X = NCS^- complex such emission is fairly intense and long lived. A study of its quenching was thus possible, in parallel with that of three different and reasonably efficient photoaquation modes. The aim was to seek further information as to the long debated[5] origin of the quenchable part of chromium(III) photochemistry.

RESULTS. The ligand-field absorption bands of *trans*-$Cr(NH_3)_4(CN)(NCS)^+$ are octahedral-like, with maxima at 466 and 355 nm for the $^4A_{2g} \rightarrow {}^4T_{2g}$ and $^4A_{2g} \rightarrow {}^4T_{1g}$ transitions. Irradiation of these features in acidic aqueous solution (10^{-3} M $HClO_4$) results in

Photochemistry and Photophysics
of Coordination Compounds, Ed. by H. Yersin/A. Vogler

the simultaneous aquation of NH_3, CN^-, and NCS^-, with virtually wavelength independent quantum yields of 0.25±0.01, 0.07±0.01, and 0.019±0.001, respectively. Such independence extends to the low-energy side of the first absorption band.[3]

The phosphorescence spectrum under photochemical conditions (Fig. 1) shows a peak at 709 nm. The emission lifetime is 30.0±0.5 μs at 20°C, and its temperature dependence in the 5-30°C range gives an apparent activation energy of 9.1±0.3 kcal mol^{-1}.

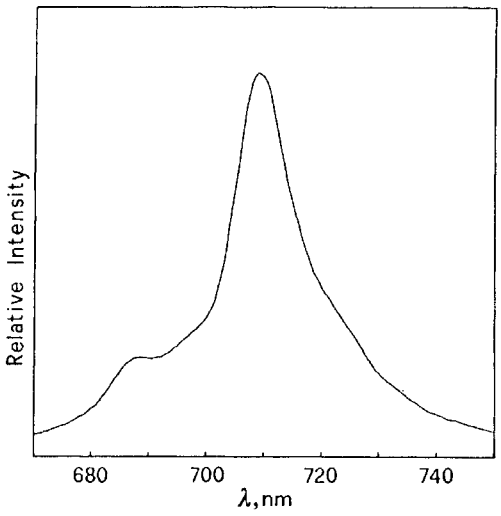

Figure 1. Emission spectrum of *trans*-$Cr(NH_3)_4(CN)(NCS)^+$ in $1x10^{-3}$ M $HClO_4$ solution at room temperature.

The trisoxalatochromate(III) ion, $Cr(C_2O_4)_3^{3-}$, quenches the emission (k_q = $5.6x10^8$ $M^{-1}s^{-1}$ at 20°C) and the three photoreactions. The findings of a systematic study are the following. (a) Photochemistry and emission are quenched in parallel, as indicated by the linearity of a plot of photoreaction vs. doublet lifetime quenching (Fig. 2). (b) Upon complete quenching of the lowest doublet state(s), 25±2% of the photoreactivity remains unquenched. (c) The quantum yield ratios of the three photoaquation modes are the same for both the unquenchable and the quenchable components.

DISCUSSION. The energy separation between the two sublevels of the octahedral $^4T_{2g}$ state of *trans*-$Cr(NH_3)_4(CN)(NCS)^+$, evaluated by means of the parameters of the two-dimensional spectrochemical series,[4] is relatively small, ca. 300 cm^{-1}, in agreement with the absence of any band splitting. Establishment of thermal equilibrium between the photochemically relevant $^4B_2$ and ^4E states can thus explain: (i) the comparable extents of the equatorial (NH_3) and axial (CN^- + NCS^-) photoreactivities, and (ii) the wavelength independence of quantum yields and, more significantly, of their ratios.

The quenching results are interpreted with reference to the d^3 excited-state scheme of Fig. 3. The unquenchable part of each photoaquation mode pertains to molecules which never pass through the doublet state(s). Partial unquenchability is well known for Cr(III),[5] and these contributions are unanimously assigned to the short-lived quartet excited state(s), formed in competition with intersystem crossing to the doublet(s) during vibrational relaxation of the Franck-Condon (FC) state(s) (route 1 of Fig. 3).

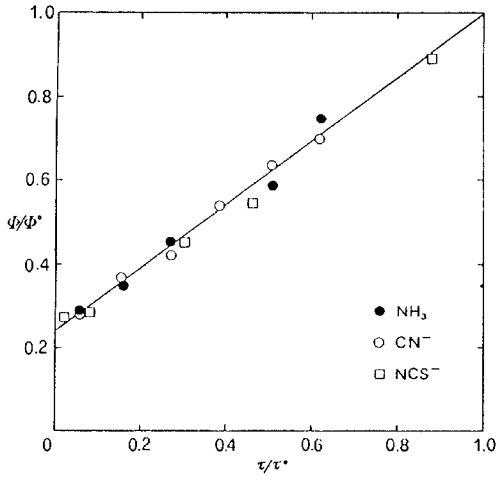

Figure 2. Photoreaction vs. emission quenching by $Cr(C_2O_4)_3^{3-}$.

The quenchable parts are then attributed to excited molecules traversing the longer-lived, emitting doublet(s). However, at least three possibilities are currently at issue about the actual precursor(s) of these contributions: (a) direct doublet reaction,[6] (b) delayed quartet reaction following back intersystem crossing,[7-9] and (c) crossing from the doublet to a reactive ground-state intermediate.[10] All three pathways are expected to be activated, hence, compatible with the observed temperature dependence of the doublet decay. The quenching behavior instead strongly supports pathway (b) (route 2 of Fig. 3). The same proportion in ligand labilization for both the unquenchable and the quenchable photoreactivity points to a single source for all photochemistry which, in the above context, must be $^4B_2/^4E$. It is highly improbable that the $^4B_2/^4E$ and $^2A_1/^2B_1$ states, of different electronic configurations (t_{2g}^2 e_g and t_{2g}^3), and conceivably different equilibrium structures, be characterized by identical preferences in the cleavage of *three* distinct metal-ligand bonds. Similar considerations apply to comparison between $^4B_2/^4E$ and a possible ground-state intermediate, originated from $^2A_1/^2B_1$ and branching into various substitutional channels plus vibrational relaxation.[10] This test appears more severe than previous studies, where analogous results for either two photoreactions,[11,12] or two-isomer product

mixtures,[9,13] were taken as evidence for back intersystem crossing. In such cases a fortuitous constancy of the mode ratio for the fast and slow photochemistry could not be completely ruled out. The present conclusions are also in line with the fact that the photoreactivity is entirely explainable by the models based on the antibonding charge distribution of the excited quartet(s).[4] If the postulated unique reactive entity is not an excited quartet, but some intermediate generated by excited-state deactivation, its bond labilization properties should at least resemble those of the $^4B_2/^4E$ states.

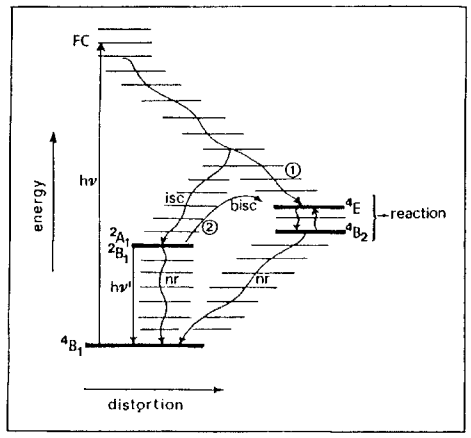

Figure 3. Energy-level diagram for a C_{4v} chromium(III) complex.

(1) Zinato E (1975) in Concepts of Inorganic Photochemistry; Adamson AW, Fleischauer PD eds. Wiley, New York, p 143

(2) Zinato E, Riccieri P, Prelati M (1981) Inorg Chem 20: 1432

(3) Riccieri P, Zinato E, Damiani A (1987) Inorg Chem 26 (in press)

(4) Vanquickenborne LG, Ceulemans A (1983) Coord Chem Rev 48: 157

(5) Kirk AD (1981) Coord Chem Rev 39: 225

(6) Walters RT, Adamson AW (1979) Acta Chem Scand Ser A 33: 53

(7) Kirk AD, Rampi-Scandola MA (1982) J Phys Chem 86: 4141

(8) Linck NJ, Berens SJ, Magde D, Linck RG (1983) J Phys Chem 87: 1733

(9) Cimolino MC, Linck RG (1981) Inorg Chem 20: 3499

(10) Endicott JF (1983) J Chem Educ 60: 824

(11) Sandrini D, Gandolfi MT, Moggi L, Balzani V (1978) J Am Chem Soc 100: 1463

(12) Krause HH, Wasgestian F (1981) Inorg Chim Acta 49: 231

(13) Zinato E, Adamson AW, Reed JL, Puaux JP, Riccieri P (1984) Inorg Chem 23: 1138

STEREOCHEMICAL CONSTRAINTS ON THE EXCITED STATE BEHAVIOR OF CHROMIUM(III)

J.F.Endicott*, Chong Kul Ryu*, R.B.Lessard*, and P.E.Hoggard**

* Department of Chemistry, Wayne State University, Detroit, MI 48202, USA
** Department of Chemistry, North Dakota State University, Fargo, ND 58102, USA

INTRODUCTION

The lifetimes of the lowest energy doublet excited states of Cr(III) complexes in solutions at ambient temperatures have long been known to span a wide range (Kirk 1981), with some complexes having subnanosecond lifetimes, while others persist for a few ms (Endicott, *et. al.* 1986, 1987). The non-radiative decay of the shorter lived excited state species is thermally activated and medium dependent. The origin of the thermally activated decay pathway(s) has been the focus of some discussion for several years (see reviews by Kirk 1981 and Endicott *et. al.* 1987 for discussion and references) and alternative single channel decay mechanisms have been proposed; for example: (a) back intersystem crossing to a very unstable quartet excited state; (b) direct chemical reaction of the doublet state; (c) a partially forbidden crossing to the potential energy surface of a ground state reaction intermediate.

In this report we describe the photophysical behavior of three series of Cr(III) complexes. These, and many of the earlier observations suggest that several channels can contribute to (^{2}E)Cr(III) decay and that the excited state lifetimes and reaction behavior can be dramatically altered by the stereochemical constraints imposed by the ligands.

EXPERIMENTAL SECTION

Compounds Studied

Most of the compounds studied fall into three classes: (a) *cis-* and *trans-* $Cr^{III}(MCL)X_2$ (where MCL = a tetraazamacrocyclic ligand and X = CN^- or NH_3); (b) $Cr^{III}([9]aneN_3)X_3$ (where X_3 = $[9]aneN_3$, $[NH_3]_3$, $[H_2O]_3$, $[CN]_3^{3-}$, $[NCS]_3^{3-}$) and the N-derivatized complexes Cr^{III}(DTNE) (DTNE = 1,2-bis(1,4,7-triazacyclononyl)ethane) and Cr^{III}(TCTA) (TCTA = 1,4,7-tris(acetato)-1,4,7-triazacyclononane); and
(c) $Cr^{III}(PP)_nX_{6-2n}$ (PP = phen or bpy; X = NCS^-, CN^-, en/2, NH_3). Literature techniques, or variations on them, have been employed in all syntheses and the compounds have been characterized using standard uv-vis and IR spectrophotometry, cyclic voltammetry and elemental analyses. X-ray crystal structures have been determined for a few of these compounds.

Instrumental techniques

Emission spectra and lifetimes have been determined using a Molectron UV 1000 pumped tunable dye laser for excitation, P.A.R.-O.M.A.- I (SIT - Vidicon) or an RCA 980 PM tube mounted in a Products for Research thermo-regulated housing (± 1.0) coupled to a Gould 4500 digital oscilloscope for luminescence detection. The operation of these instruments and the signal averaging, curve fitting, *etc.* routines are controlled by means of a Zenith 158 computer using software developed by On Line Instrument Systems Inc.

Excitation spectra were obtained at North Dakota State using instrumental techniques described by Hoggard (1986).

Photochemistry and Photophysics
of Coordination Compounds, Ed. by H. Yersin/A. Vogler

RESULTS AND DISCUSSION

These compounds exhibit three kinds of photophysical behavior (Table I): (a) long lived *trans*-$Cr^{III}(MCL)X_2$ complexes (X = CN^- or NH_3) for which the 298 and 77K lifetimes are nearly the same; (b) very short lived molecules at 298K ($\tau << 0.1$ μs) which have sterically strained ground states (Cr(TCTA) and $Cr(DTNE)^{3+}$); and (c) intermediate behavior of most of the complexes in which the excited state decay is thermally activated and the ambient lifetimes are typically 0.1 to 10μs. There are some qualitatively striking features of these observations: (i) if ligand motion is sterically restricted, as with the *trans*-MCL ligands, the thermally activated quenching pathway is repressed; (ii) if the ligand system is strained in the ground state in such a way that there is some driving force for ligand rearrangement, as with the DTNE and TCTA ligands, the thermally activated quenching pathway is enhanced; (iii) the mixed ligand polypyridine complexes are surprisingly short lived at 298K in fluid solution; and (iv) variation of the ligands, X = NCS^-, NH_3 and CN^-, has only a minor influence on the thermally activated decay patterns. The major factors influencing the thermally activated decay behavior appear to be the solvent medium and ligand stereochemistry.

The emission spectra of most Cr(III) complexes are not markedly solvent dependent with the O-O' and vibronic bands being only a little broadened in glassy or solution matrices compared to the solid state. Several of the triazacyclononane derivatives are exceptions. The most striking such complex is $Cr(DTNE)^{3+}$ for which the emission maximum occurs at about 300 cm^{-1} higher energy in DMSO-H_2O glass at 77K than in the solid state (ClO_4^- salt) and the band width is about 360 cm^{-1}. Matrix dependent broadening of the emission bands, without appreciable shifts in the emission maxima, is observed for several $Cr^{III}([9]aneN_3)X_3$ complexes. The phenomenon has been examined most closely for $Cr([9]aneN_3)_2^{3+}$ for which the emission band width increases with temperature in the range 200-270K in DMSO-H_2O (apparent activation energy 300-400 cm^{-1}). It may be pertinent that the $^2T_{1g}(O_h)$ component electronic origins are found about 360, 400 and 650 cm^{-1} above the energy of the ^2E state in this complex. Thus some part of the line broadening in the emission from electronically excited $Cr([9]aneN_3)_2^{3+}$ may arise from superposition of the intense vibronic satellites of the upper doublet state emissions onto the ^2E emission.

The small energy differences between the different doublet components of $Cr([9]aneN_3)_2^{3+}$ raises the possibility that thermally activated relaxation through the different doublet electronic states may be a feature of the photophysics of many Cr(III) complexes. It seems clear that a large number of factors can contribute to thermally activated (^2E)Cr(III) relaxation. Some of these are electronic (such as the proximity of states with different electronic configurations), some stereochemical (as in the constraints imposed by various cyclic ligands) and some environmental. Work described here and in the literature cited is helping to establish the limiting cases.

ACKNOWLEDGEMENTS

The work presented here has been partly supported by the National Science Foundationand by Wayne State University.

Table I. Excited State Decay Parametes for Cr(III) Complexes[a]

Complex	$E(^2E)$ $cm^{-1}/10^4$	$E(^4T_2)_{max}$[b] $cm^{-1}/10^4$	τ_{lim} μs	τ_{298} μs	E_A kJ mol^{-1}
t-$CrL_1(CN)_2^+$	1.426	2.35[c]	379	380	---
c-$CrL_2(CN)_2^+$	1.379	2.16[c]	208	2.1	50
t-$Cr(d_4\text{-}L_1)(CN)_2^+$	1.43	2.35[c]	5600	1752	---
c-$Cr(d_4\text{-}L_2)(CN)_2^+$	1.38	2.16[c]	1854	2	46
t-$Cr(L_3)(CN)_2^+$	1.404	2.42[d]	355[d]	361[d]	---
t-$Cr(d_4\text{-}L_3)(CN)_2^+$	1.4	2.42[d]	3060	1499	---
t-$Cr(L_3)(NH_3)_2^{3+}$	1.47[e]	2.2[e]	180	136 [e]	6 [c]
c-$Cr(L_3)(NH_3)_2^{3+}$	1.47[e]	2.14[e]	116[e]	1.0[e]	43[e]
$Cr(L_4)_2^{3+}$	1.472	2.28[c]	400	30	41
$Cr(L_4)(NH_3)_3^{3+}$	1.498	2.17	104	6.7	35
$Cr(L_4)(CN)_3$	1.35	2.41	402	6.1	32
$Cr(L_4)(NCS)_3$	1.332	1.98	112	18	10
$Cr(L_4)(OH_2)_3^{3+}$	1.483	1.98	65	---	---
$Cr(DTNE)^{3+}$	1.37	2.08[c]	50	(6×10^{-5})[f]	32
Cr(TCTA)	1.398	1.95[c]	395	(2×10^{-5})[f]	38
$Cr(phen)_2(NH_3)_2^{3+}$	1.422	2.31[c]	190	3.6	35
$Cr(phen)(en)_2^{3+}$	1.436	2.20[c]	155	0.5	30
$Cr(bpy)(en)_2^{3+}$	1.437	2.15[c]	164	0.5	30
$Cr(phen)(CN)_4^-$	1.275	2.40[c]	4320	0.4	33
$Cr(bpy)_2(CN)_2^+$	1.322	2.22[c]	3600	0.11	34
$Cr(phen)_2(NCS)_2^+$	1.263	1.96	660	2.2	35
$Cr(bpy)_2(NCS)_2^+$	1.265	1.98	610	2.8	35

Notes for Table I

[a]In DMSO:H_2O (1:1v/v) except at noted
[b]Lowest energy quartet absorption maximum
[c]As cited in Endicott, *et. al.* (1986,1987)
[d]Kane-Maguire, et. al. (1983)
[e]Kane-Maguire, et. al. (1985)
[f]Extrapolated value

Ligand abbreviations: L_1 = 5,12-*meso*-5,7,7,12,14,14-hexamethyl-1,4,8,11-tetraazacyclotetradecane (teta); d_4 - L_1 = 1,4,8,1-deutero-teta; L_2 = 5,12-*rac*-5,7,7,12,14,14-hexamethyl-1,4,8,11-tetraazacyclotetradecane (tet*b*); d_4 - L_2 = 1,4,8,11-deutero-tet*b*; L_3 = 1,4,8,11-tetraazacyclotetradecane (cyclam); L_4 = 1,4,7-triazacyclononane ([9]aneN_3).

REFERENCES

Ditze A, Wasgestion F. (1985) Photophysics of bis(1,4,7-triazacyclononane)chromiumIII. J. Phys. Chem. 89:426

Endicott JF, Lessard RB, Lei Y, Ryu CK, Tamilarasan R (1986) Manipulation of doublet excited state lifetimes in chromium(III) complexes. In: Lever APB (ed) Excited states and reactive intermediates. ACS Symposium Series No. 307. Amer Chem Soc, Washington DC, p. 85.

Endicott JF, Ramasami T, Tamilarasan R, Lessard RB, Ryu CK (1987) Structure and reactivity of metal-centered transition metal excited states. Coord Chem Rev, in press.

Hoggard PE (1986) Sharp line electronic spectra and metal-ligand angular geometry. Coord Chem Rev 70:85.

Kane-Maguire NAP, Crippen WS, Miller PK (1983) Unusual photobehavior of *trans*-dicyano(1,4,8,11-tetraazacyclotetradecane)-chromium(III) perchlorate. Inorg Chem 22: 696.

Kane-Maguire NAP, Wallace KC, Miller DB (1985) Synthesis, characterization, and photobehavior of *cis*- and *trans*-diammine(1,4,8,11-tetraazacyclotetradecane)chromium(III) and some related compounds. Inorg Chem 24:597.

Kirk AD (1981) Chromium(III) photochemistry and photophysics. Coord Chem Rev 39:225-263.

EXCITED STATE BEHAVIOR AS A PROBE OF GROUND-STATE ION-PAIR INTERACTIONS IN CHROMIUM(III)-POLYPYRIDYL COMPLEXES

M.Z.Hoffman* and N.Serpone**

* Department of Chemistry, Boston University, Boston, MA, USA
** Department of Chemistry, Concordia University, Montreal, CANADA

INTRODUCTION

The tris-polypyridyl complexes of Cr(III) ($Cr(NN)_3^{3+}$) are remarkable in that the observed lifetimes (τ_{obs}) of their thermally-equilibrated lowest doublet metal-centered excited states ($^2T_1/^2E$) are amongst the longest known for transition metal coordination complexes in fluid solution at room temperature, ranging from 0.070 ms for $Cr(bpy)_3^{3+}$ (bpy = 2,2'-bipyridine) to 0.64 ms for $Cr(3,4,7,8\text{-}Me_4phen)_3^{3+}$ (phen = 1,10-phenanthroline) (Brunschwig 1978; Serpone 1979, 1981). These long lifetimes, the high ionic charges of the complexes, and the hydrophobic nature of the ligand environment make τ_{obs} extremely sensitive to solution medium parameters such as solvent (Van Houten 1978; Jamieson 1983a), presence of anions (Henry 1977; Sriram 1980; Jamieson 1983b), and [substrate] at high anion concentrations (Sriram 1980; Jamieson 1983b). In addition, because the $^2T_1/^2E$ excited states and the $^4A_2$ ground states of the complexes have the same geometry, there being no Stokes shift in the absorption and emission between those states (Balzani 1970), the nature of the solution medium environment in the immediate vicinity of the cation will be the same for $^2T_1/^2E$ as it was prior to the absorption of light. Thus, the behavior of $^2T_1/^2E$ can be interpreted in terms of ground-state interactions. For OH^-, which quenches $^2T_1/^2E$ directly in highly alkaline solution (Bolletta 1983), and Cl^-, the ion-pair formation constants can be estimated as ~1 M^{-1} by analogy to the $Ru(bpy)_3^{3+}/OH^-$ (Ghosh 1984) and Cr^{III}/Cl^- (Wrona 1984) systems. It is easy to see that when the complex concentration is initially ~10 μM, the anion concentration must be ~0.1-1 M in order for the ion-pairing to be appreciable.

In the study (Neshvad) from which this paper was derived, τ_{obs} was measured for $Cr(NN)_3^{3+}$ (NN = phen, 5-Clphen, 5-Mephen, 5-Phphen, 4,7-Me_2phen, 3,4,7,8-Me_4phen, and 4,4'-Me_2bpy) as a function of pH and $[Cl^-]$ at 5°, a temperature chosen to optimize the experimental conditions.

EFFECT OF Cl^-

Figure 1 shows the dependence of τ_{obs} on $[Cl^-]$ in acidic solution for $Cr(phen)_3^{3+}$ and four substituted-phen complexes. The inflections are consistent with the occurrence of reaction 1 with $\underline{K}_1 \sim 1\ M^{-1}$.

$$Cr(NN)_3^{3+} + Cl^- \rightleftharpoons Cr(NN)_3^{3+},Cl^- \qquad [1]$$

EFFECT OF pH

Figure 2 shows the dependence of τ_{obs} on pH for $Cr(phen)_3^{3+}$; τ_{obs} was not a function of the nature of the buffer used to control pH. The reversibility of τ_{obs} was demonstrated with a solution at pH 9.2 made acidic to pH 3.1 and returned to the original pH. The intensity of

Photochemistry and Photophysics
of Coordination Compounds, Ed. by H. Yersin/A. Vogler

the emission from the complex as a function of pH paralleled τ_{obs} in Fig. 2. This dependence of τ_{obs} on pH was a general phenomenon for those $Cr(NN)_3^{3+}$ examined (Table 1). The measurement of τ_{obs} at pH 3-4 and 9-10 as a function of temperature (5-35°) yielded activation energies for the decays of $*Cr(phen)_3^{3+}$ (37 and 31 kJ mol^{-1}) and $*Cr(5\text{-}Mephen)_3^{3+}$ (41 and 30 kJ mol^{-1}).

Table 1. Values of τ_{obs} for $Cr(NN)_3^{3+}$ at 5° in Ar-purged solutions.

NN	pH	τ_{obs},[a] ms	τ_{obs},[b] ms
phen	3.32	1.03	0.62
	9.50	0.65	0.61
5-Clphen	3.32	0.46	0.31
	9.50	0.40	0.32
5-Mephen	3.18	0.95	
	3.32		0.46
	9.19	0.67	
	9.50		0.52
5-Phphen	3.32	0.77	0.33
	9.50	0.52	
4,7-Me_2phen	3.32	1.28	0.75[c]
	9.50	0.55	0.65[c]
3,4,7,8-Me_4phen	3.38	1.68	0.75
	8.96	0.64	0.64
4,4'-Me_2bpy[d]	3.32	0.46	0.46
	8.89		0.41
	9.05	0.34	
	9.63		0.43

[a] absence of added NaCl
[b] presence of 1.0 M NaCl
[c] presence of 0.93 M NaCl
[d] in 4% v/v CH_3CN/H_2O

It should be noted that our previous measurements of τ_{obs} for $Cr(bpy)_3^{3+}$ and $Cr(phen)_3^{3+}$, performed in aerated solution containing 1 M NaCl at 15°, did not reveal any dependence on pH (Maestri 1978; Bolletta 1983). Similar measurements by Lilie and Waltz (1983) on $Cr(bpy)_3^{3+}$ in deaerated solutions in the absence of added solutes also showed no variation of τ_{obs} with pH; for $Cr(phen)_3^{3+}$ under the same conditions (Lilie 1986), τ_{obs} was shorter in alkaline than in acidic solution. Kane-Maquire and Langford (1976) reported that the intensity of luminescence from aerated solutions of $Cr(phen)_3^{3+}$ was higher in acidic than in alkaline solution. As Table 1 shows, the presence of 1 M NaCl, in general, reduces τ_{obs} in acidic solution at 5° by a significant factor while not affecting the value in alkaline medium to any great extent (if at all), resulting in a great diminution of the pH-effect.

INTERACTIONS OF $Cr(NN)_3^{3+}$

Inasmuch as the complexes do not possess moieties that have acid-base properties, the effect of pH on τ_{obs} must be attributed to an interaction that exhibits an inflection point at pH ~ 6-7, is reversible, and does not result in a change in the energy levels of the states involved in absorption and emission. At the same time, the kinetics of the nonradiative decay of $^2T_1/^2E$, which involves transfer of metal-centered electronic energy to the vibrational modes of the ligands (Henry 1978), are changed so that τ_{obs} exhibits slightly different E_a values in acidic and alkaline solution; the pH effect is emphasized at low temperatures, with the values of τ_{obs} approaching each other at ambient conditions. Interactions for which the equilibrium constant is small, such as deprotonation of an acidic ring-carbon (Serpone 1983a), direct attack of OH^- on the metal center (Maestri 1976; Jamieson 1978; Bolletta 1983), and the formation of a pseudo-base (Ghosh 1984), can be ruled out. For the same reason, ion-pairing reaction 2 cannot be important as the sole source of the pH effect.

$$Cr(NN)_3^{3+} + OH^- \rightleftharpoons Cr(NN)_3^{3+},OH^- \qquad [2]$$

In order to explain the pH-dependence of the photoaquation quantum yields of $Cr(NN)_3^{3+}$, we proposed several years ago (Maestri 1978) that $^2T_1/^2E$ can react with H_2O in competition with its nonradiative decay to form a "seven-coordinate" intermediate; deprotonation of this intermediate in the pH ~ 6-7 range is viewed to lead to the final products. The similarity of the pH-profiles of τ_{obs} and Φ strongly suggests that the photochemical and nonradiative decay modes of $^2T_1/^2E$ are coupled and involve the same intermediates. We propose here that the "seven-coordinate" aqua intermediate (Jamieson 1981; Serpone 1983b) exists in the ground-state (reaction 3) and undergoes acid-base equilibrium (reaction 4) in the neutral pH range. Excitation of these species results in $^2T_1/^2E$ with the same configuration. The nonradiative behavior of $^2T_1/^2E$ as a function of pH reflects the subtle change of the vibrational modes of the complex as H_2O is deprotonated; the photochemical pathway can be viewed as a relatively minor branch off the same potential energy surface.

$$Cr(NN)_3^{3+} + H_2O \rightleftharpoons H_2O\cdots Cr(NN)_3^{3+} \qquad [3]$$

$$H_2O\cdots Cr(NN)_3^{3+} \rightleftharpoons {}^-HO\cdots Cr(NN)_3^{3+} + H^+ \qquad [4]$$

At high $[Cl^-]$, reaction 5 could compete with reaction 3 in acidic solution, bringing Cl^- into the inner-sphere and resulting in a diminution in τ_{obs}. In alkaline solution, the driving force of reaction 4, and the interaction of OH^- with the metal center and, perhaps, the nitrogen-heterocyclic ligands, would minimize the presence of Cl^- in the inner-sphere.

$$Cr(NN)_3^{3+},Cl^- \rightleftharpoons {}^-Cl\cdots Cr(NN)_3^{3+} \qquad [5]$$

ACKNOWLEDGEMENTS

This research was supported in part by the Office of Basic Energy Sciences, Division of Chemical Sciences, U.S. Department of Energy, and in part by the Natural Sciences and Engineering Research Council of Canada. The authors acknowledge the work of their associates, Drs. G. Neshvad, M. Bolte, and R. Sriram

REFERENCES

Balzani V, Carassiti V (1970) Photochemistry of coordination compounds. Academic Press, New York

Bolletta F, Maestri M, Moggi L, Jamieson MA, Serpone N, Henry MS, Hoffman MZ (1983) Photochemical, photophysical, and thermal behavior of tris(1,10-phenanthroline)chromium(III) ion in aqueous solution. Inorg Chem 22: 2502-2509

Brunschwig B, Sutin N (1978) Reactions of the excited states of substituted polypyridinechromium(III) complexes with oxygen, iron(II) ions, ruthenium(II) and -(III), and osmium(II) and -(III) complexes. J Am Chem Soc 100: 7568-7577

Ghosh, PK, Brunschwig BS, Chou M, Creutz C, Sutin N (1984) Thermal and light-induced reduction of $Ru(bpy)_3^{3+}$ in aqueous solution. J Am Chem Soc 106: 4772-4783

Henry MS (1977) Prolongation of the lifetime of the ^2E state of tris-(2,2'-bipyridine)chromium(III) ion by anions in aqueous solution. J Am Chem Soc 99: 6138-6139

Henry MS, Hoffman MZ (1978) Solution medium effects on the photophysics and photochemistry of polypyridyl complexes of chromium-(III). Adv Chem Ser 168: 91-114

Jamieson MA, Serpone N, Maestri M (1978) Hydroxide ion assisted aquation of tris(2,2'-bipyridine)chromium(III) ion. Inorg Chem 17: 2432-2436

Jamieson MA, Serpone N, Hoffman MZ (1981) Recent advances in the photochemistry and photophysics of chromium(III) polypyridyl complexes in fluid media. Coord Chem Rev 39: 121-179

Jamieson MA, Langford CH, Serpone N, Hersey MW (1983a) Medium effects in chromium(III) photochemistry. Dynamic vs. static processes in tris(bipyridine)chromium(III) and trans-diammine(tetrathiocyanato)-chromium(III) ions in acetonitrile-water mixtures. J Phys Chem 87: 1004-1008

Jamieson MA, Serpone N, Hoffman MZ, Bolletta F (1983b) Ground-state quenching of $(^2T_1/^2E)Cr(NN)_3^{3+}$. Anion and temperature dependence. Inorg Chim Acta 72: 247-252

Kane-Maguire NAP, Langford CH (1976) Effects of quenchers on the emission and photoracemization of tris(1,10-phenanthroline)-chromium(III). Inorg Chem 15: 464-466

Lilie J, Waltz WL (1983) Pulsed-laser photochemical study of tris-(2,2'-bipyridine)chromium(III) ion in acidic and alkaline aqueous media. Inorg Chem 22: 1473-1478

Lilie J, Waltz WL, Lee SH, Gregor LL (1986) Pulsed-laser photochemical study of tris(1,10-phenanthroline)chromium(III) ion in acidic and alkaline aqueous media. Inorg Chem 25: 4487-4492

Maestri M, Bolletta F, Serpone N, Moggi L, Balzani V (1976) Kinetics of ligand substitution of tris(2,2'-bipyridine)chromium(III) in aqueous solution. Inorg Chem 15: 2048-2051

Maestri M, Bolletta F, Moggi L, Balzani V, Henry MS, Hoffman MZ (1978) Mechanism of the photochemistry and photophysics of the tris(2,2'-bipyridine)chromium(III) ion in aqueous solution. J Am Chem Soc 100: 2694-2701

Neshvad G, Hoffman MZ, Bolte M, Sriram R, Serpone N (to be published) Photophysics of chromium(III)-polypyridyl complexes. Behavior of the $^2T_1/^2E$ excited states a a probe of ground-state ion-pair interactions. Inorg Chem

Serpone N, Jamieson MA, Henry MS, Hoffman MZ, Bolletta F, Maestri M (1979) Excited state behavior of polypyridyl complexes of chromium-(III). J Am Chem Soc 101: 2907-2916

Serpone N, Jamieson MA, Sriram R, Hoffman MZ (1981) Photophysics and photochemistry of polypyridyl complexes of chromium(III). Inorg Chem 20: 3983-3988

Serpone N, Ponterini G, Jamieson MA, Bolletta F, Maestri M (1983a) Covalent hydration and pseudobase formation in transition metal polypyridyl complexes: Reality or myth? Coord Chem Rev 50: 209-302
Serpone N, Hoffman MZ (1983b) Photochemistry and photophysics of chromium(III)-polypyridyls. A case study. J Chem Educ 60: 853-860
Sriram R, Hoffman MZ, Jamieson MA, Serpone N (1980) Ground state quenching of ^2E excited states of $Cr(bpy)_3^{3+}$ and $Cr(phen)_3^{3+}$. J Am Chem Soc 102: 1754-1756
Van Houten J, Porter GB (1978) Autocatalytic chain reaction in the photochemical decomposition of tris(2,2'-bipyridyl)chromium(III) in dimethylformamide. Inorg Chem 18: 2053-2054
Wrona PK (1984) Equilibrium constants of chromium(III) and chromium-(II) inner- and outer-sphere complexes with chloride, bromide, and iodide ions. Inorg Chem 23: 1558-1562

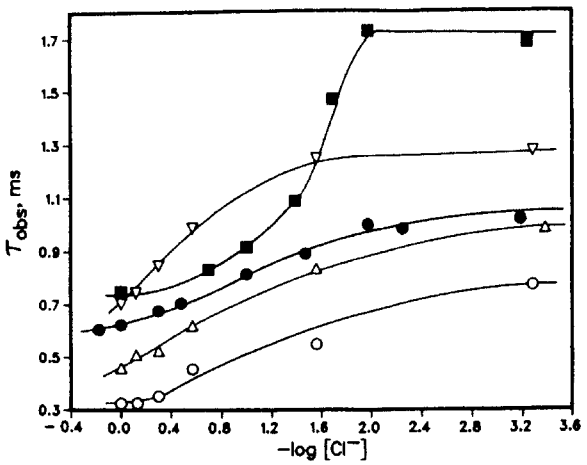

Fig. 1. τ_{obs} as a function of the total concentration of Cl^- (addition of NaCl) for Ar-purged solutions at 5° and pH 3.3 (controlled with HCl). ●, 15 μM $Cr(phen)_3^{3+}$; △, 10 μM $Cr(5\text{-}Mephen)_3^{3+}$; ○, 10 μM $Cr(5\text{-}Phphen)_3^{3+}$; ▽, 10 μM $Cr(4,7\text{-}Me_2phen)_3^{3+}$; ■, 10 μM $Cr(3,4,7,8\text{-}Me_4phen)_3^{3+}$.

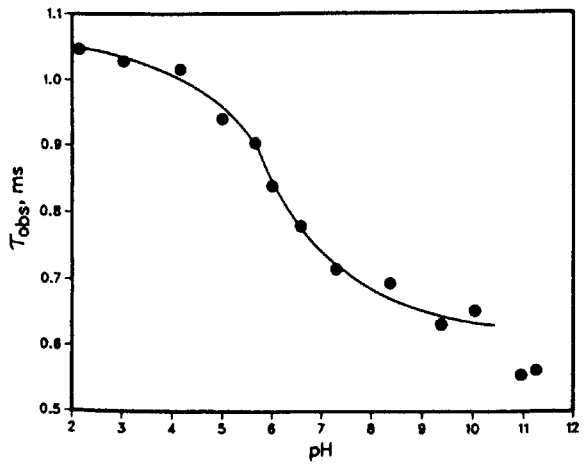

Fig. 2. τ_{obs} as a function of pH for Ar-purged solutions at 5° containing 10-15 μM $Cr(phen)_3^{3+}$.

COUNTERION EFFECTS ON DOUBLET SPLITTINGS OF CHROMIUM(III) COMPLEXES

P.E.Hoggard and Kyu-Wang Lee

Department of Chemistry, North Dakota State University, Fargo, ND 58102, USA

Splittings within the intraconfigurational doublet bands in d^3 ions are sensitive to the exact metal-ligand angular geometry, but not very strongly affected by differences in the values of the ligand field splitting parameter, 10Dq, of the coordinating groups (Hoggard 1981, 1986). Since the transitions are, to the first approximation, within the t_{2g} subshell, ligand e_π effects can be expected to dominate in determining the splittings, although we have found that $e_\sigma + e_\pi$ is a better predictor of splittings calculated from a ligand field model including spin-orbit coupling (Hoggard 1981). Ligand pi anisotropy is another factor that can make large contributions to the doublet splittings, but can in principle be accounted for if the exact geometry is known (Hoggard 1986)

It appears, however, that for some very simple compounds, with relatively high symmetry, no pi anisotropy, and little deviation from orthoaxiality, substantial splittings are seen, beyond the ability of ligand field theory to explain (given reasonable bounds on the parameters), and causing the widespread conclusion that ligand field theory is simply incapable of effectively predicting splittings with magnitudes of tens of reciprocal centimeters (Flint 1977). Table 1 presents some of these data. The theory should not, however, be thrown out as long as there are still effects that can reasonably be incorporated into calculations.

All of the data in Table 1 are problematic. In an octahedral environment, a ^2E state is unsplit by spin-orbit coupling, so that splittings much smaller than 50 cm^{-1} would be expected for any octahedral complex. In the pentaammine series, the differences in 10Dq between NH_3 and the other ligand are often large enough to produce easily visible splitting of the first quartet band. But it is not 10Dq differences that matter for the doublet splittings, and in fact the $e_\sigma + e_\pi$ values of NH_3, Cl^-, Br^-, I^-, and H_2O are not markedly

Photochemistry and Photophysics
of Coordination Compounds, Ed. by H. Yersin/A. Vogler

Table 1
^2E_g Splittings in Nearly Orthoaxial Chromium(III) Complexes

Complex	Splitting, cm^{-1}	Reference
$K_3[Cr(CN)_6]$	49	Flint 1974
$[Cr(NH_3)_5Cl]Cl_2$	175	Flint 1973
$[Cr(NH_3)_5Br]Br_2$	225	"
$[Cr(NH_3)_5I]I_2$	305	"
$[Cr(NH_3)_5H_2O](ClO_4)_3$	205	"

different. Thus calculations show splittings of at most 50 cm^{-1}, and more typically very close to zero.

The luminescence spectra of a number of hexacyanochromium(III) complexes with different cations reveal a considerable variation in ^2E_g splittings (Schlafer 1971), from 78 cm^{-1} for the Li^+ salt to 41 cm^{-1} for the Ph_4As^+ salt. Similar variations are seen for $[Cr(CN)_6]^{3-}$ substituted into hexacyanocobaltate(III) lattices (Flint 1977). This suggests a strong influence of the counterions. We have thus used the known crystal structure of $K_3[Cr(CN)_6]$ (Jagner 1974; Figgis 1981), and have determined the crystal structure of $[Cr(NH_3)_5Cl]Cl_2$, in order to test the hypothesis that the splittings in Table 1 might be explained by energetic effects on the metal d orbitals derived from the counterions.

The Angular Overlap Model provides a simple method to incorporate contributions from any number of counterions. It is also reasonable to assume that pi-bonding effects will be very minimal, and consequently the counterions need only be characterized by a single parameter to represent sigma bonding (e_σ in the AOM). However, since the counterions in general do not reside at equal distances from the metal ion, a radial dependence for e_σ of the counterions must be established. At typical counterion distances they may be well represented as point charges, so that the crystal field treatment is appropriate. This is based on the expression for the potential of an electron at (r, θ, ϕ) in the field generated by a single point charge q at (R, θ_o, ϕ_o) in terms of an infinite sum of spherical harmonics.

$$V(r,\theta,\phi) = q\sum_{n=0}^{\infty}\frac{r^n}{R^{n+1}} \cdot \frac{4\pi}{2\ell+1}\sum_{m=-\ell}^{+\ell} Y_{\ell m}(\theta,\phi)\cdot\bar{Y}_{\ell m}(\theta_o,\phi_o)$$

When an integral of $V(r,\theta,\phi)$ is taken between two d wavefunctions, terms with odd n and all terms with n greater than 4 drop out. The potential may thus effectively be represented as

$$V = \frac{C_0}{R} + \frac{C_2}{R^3}\left[Y_{2,-2}(\theta_0,\phi_0)\bar{Y}_{2,-2}(\theta,\phi) + Y_{2,-1}(\theta_0,\phi_0)\bar{Y}_{2,-1}(\theta,\phi) + \ldots\right]$$

$$+ \frac{C_4}{R^5}\left[Y_{4,-4}(\theta_0,\phi_0)\bar{Y}_{4,-4}(\theta,\phi) + Y_{4,-3}(\theta_0,\phi_0)\bar{Y}_{4,-3}(\theta,\phi) + \ldots\right]$$

The R^{-1} term has a spherical angular dependence and is incorporated into the central field potential. The radial dependence can thus in general be described as a complicated function of R^{-3} and R^{-5}. For the often-cited octahedral case the R^{-3} coefficients drop out. For most actual counterion arrangements both R^{-3} and R^{-5} dependences will exist. We assume the R^{-5} terms will be negligible at typical counterion distances of 4 Å or more, and in the calculations to follow the counterion field is always considered to decline as R^{-3}. Typical e_σ values for counterions at 4 to 4.5 Å will be seen to be around 300 cm^{-1}, which may appear to represent a more rapid falloff with R, compared to typical values for ligands at about 2 Å of around 6000 cm^{-1}. In fact, the R^{-5} terms would be expected to be more important at shorter distances, and an even stronger dependence on R should be reached at metal-ligand distances, approximating that of Born repulsion.

The experimental data for all of the sharp-line doublets of $K_3[Cr(CN)_6]$ are listed in Table 2. The ^2E_g splitting of 53 cm^{-1} is accompanied by $^2T_{1g}$ and $^2T_{2g}$ splittings of around 60 and 100 cm^{-1} between the highest and lowest components. Before looking at the cations, the effects of the chromophore geometry must be examined. Even though the deviations from orthoaxiality are small, generally less than 0.5°, they are still capable of causing significant splitting, primarily within the $^2T_{2g}$ state, as shown in the second column of Table 2. In fact the calculated $^2T_{2g}$ splittings are larger

than the experimental with no contribution from the cations, while the ^2E_g state is split hardly at all.

The cation geometry around the chromium center in $K_3[Cr(CN)_6]$ is not a simple one. There are 14 K^+ ions at distances spread irregularly from 4.2 to 6.0 Å, which we have treated as the "second coordination sphere". It is possible that still more remote K^+, and $[Cr(CN)_6]^{3-}$ ions as well, could make significant contributions. Figure 1 shows the calculated effects on the doublet transition energies of introducing a field from the 14 cations up to an e_σ value of 450 cm^{-1}. It is seen that the $^2T_{2g}$ splitting is decreased markedly from $e_{\sigma(K^+)} = 0$ to about -300 cm^{-1}, while the splittings of the ^2E_g and $^2T_{1g}$ states increase. Near -300 cm^{-1} the experimental splittings are close to being well reproduced. An optimization yielded the values in column 3 of Table 2.

Table 2

Experimental and Calculated Doublet Transition Energies for $K_3[Cr(CN)_6]$. All data in cm^{-1}.

	Exptl, 13K	Calculated[a] Chromophore geometry only	Calculated[b] Cations Included
^2E_g	12447	12518	12480
	12500	12521	12511
$^2T_{1g}$	13101	13090	13067
	13121	13104	13118
	13164	13117	13154
$^2T_{2g}$	18388	18301	18359
	18435	18383	18440
	18487	18500	18504

[a] Parameters used: $e_{\sigma CN} = 8760$, $e_{\pi CN} = 0$, B = 715, C = 1900, (Trees correction) = 215, = 150.

[b] $e_{\sigma CN} = 9508$, $e_{\pi CN} = 607$, B= 737, C = 1848, = 217, = 222, $e_{\sigma K^+} = -334$.

Although the fit is not perfect, it is close enough to conclude that the doublet splittings can in the main be accounted for through geometric effects arising both from the chromophore and from the counterion sphere.

It is a different story with $[Cr(NH_3)_5Cl]Cl_2$. There are eight nearest-neighbor chloride ions, with Cr-N distances from 4.25 to 4.41 Å. These form a distorted cube that is nevertheless close enough to a perfect cube with the ligands oriented towards the centers of the faces that only a slight amount of additional splitting of the ^2E_g or the other states is predicted, even at $e_{\sigma(Cl^-)} = 500\ cm^{-1}$. Thus the anions are not responsible for splittings on the order of 200 cm^{-1} in this complex, and probably not for the other pentaammines as well.

Is the large ^2E_g splitting in the pentaammine series real? One way to obtain such splittings is for a component of the $^2T_{1g}$ state

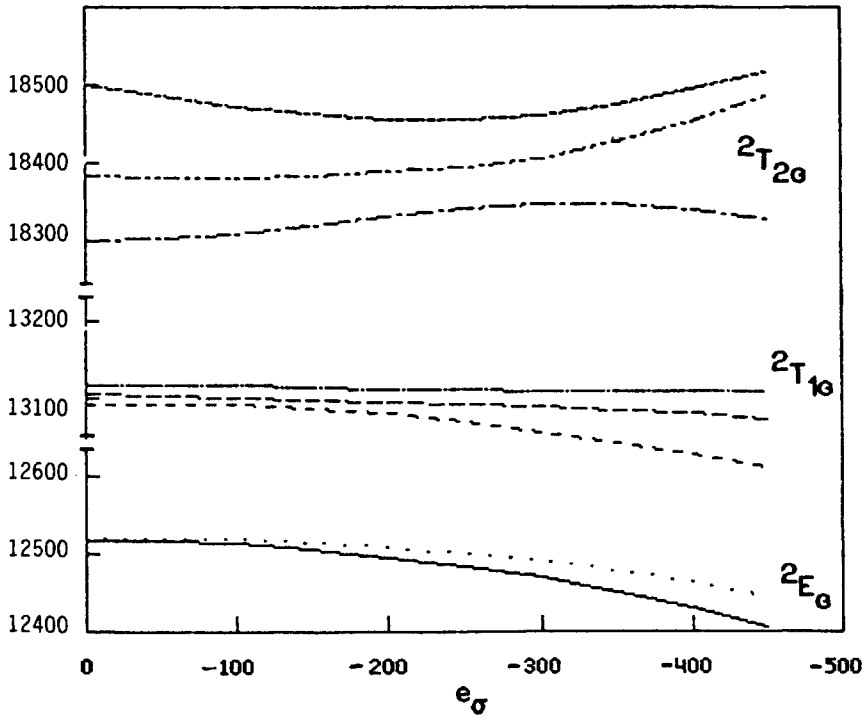

Figure 1. Calculated doublet transition energies for $K_3[Cr(CN)_6]$ as a function of e_σ of the nearest K^+ ion. The potential from the 14 nearest cations was taken into account. The other parameters are those from the second column of Table 2.

to become the lowest doublet. This would, however, require that e_π for Cl^- be at least 1500 cm^{-1}, which is unlikely. We have recently measured small splittings, between 10 and 15 cm^{-1}, of the 0-0 lines in several pentaammine complexes in both luminescence and excitation spectra. It remains to be seen whether these can be assigned to the ^2E_g state, but from the standpoint of ligand field theory, the assignment of the electronic transitions listed in Table 1 to a component of the $^2T_{1g}$ state is quite reasonable.

References

Figgis, BN, Reynolds PA, Williams GA (1981) Acta Cryst B37:504-508

Flint CD, Matthews AP (1973) J Chem Soc Faraday Trans II 69: 419-425

Flint CD, Greenough P (1974) J Chem Soc Faraday Trans II 70: 815-825

Flint CD, Matthews AP, O'Grady, PJ (1977) J Chem Soc Faraday Trans II 73: 655-663

Hoggard PE (1981) Z Naturforsch A 36:1276-1288

Hoggard PE (1986) Coord Chem Rev 70:85-120

Jagner S, Ljungstrom E, Vannerberg NG (1974) Acta Chem Scand A28:623-630

Schlafer HL, Wagener H, Wasgestian F, Herzog G (1971) Ber Bunsenges Phys Chem 75:878-883

SPECTRUM-STRUCTURE CORRELATIONS IN HEXACOORDINATED TRANSITION METAL COMPLEXES

T.Schönherr

Institut für Theoretische Chemie, Universität Düsseldorf, 4000 Düsseldorf 1, FRG

To understand the photophysical and photochemical processes a comprehensive knowledge of the molecular energy level scheme is required. It has been found in recent years that even slight changes of the geometric structure can significantly alter the electronic properties of transition metal complexes. This has led to a growing interest in the study of spectrum-structure correlations, in particular for chromium(III) compounds which are of current interest as possible candidates for luminescent solar concentrators (1). In the first section of this paper the potential of common ligand field theory (LFT) will be illustrated to describe trigonal distortions for complexes near to high symmetry. For the properties considered the hexaamminechromate(III) ion represents an ideal system for the global parametrization within the LFT which is reflected by the high molecular symmetry and the absence of metal-ligand π-bonding. The angular overlap model (AOM), on the other hand, is based on an additive description of metal-ligand interactions using local bonding parameters of σ- and π-type which are more adequate to the chemical way of thinking. One of its advantages over the LFT is that it is easier to include the molecular geometry into energy level calculations, since the AOM parameters are independent of angular distortions within the coordination sphere (2). In the case of osmium(IV) complexes a great deal of information about electronic and geometric structure can be derived from detailed studies of intraconfigurational transitions, and model parameters are given here for the first time. In order to explain spectroscopic properties of transition group metal acetylacetonates an extended AOM is required. Directional π-bonding effects resulting from the phase coupling of chelate molecular orbitals lead to non-additive contributions to the d-orbital energies. We will give an illustration of this type of study below.

Molecular Structure Determination of $[Cr(NH_3)_6]^{3+}$-Salts

The lowest states $^4A_{2g}$, ^2E_g, and $^2T_{1g}$ (in O_h-notation) all derive from the (t_{2g}^3) electron configuration leading to sharp line spectra in the low energy spin-forbidden region. Information about the transition into

Photochemistry and Photophysics
of Coordination Compounds, Ed. by H. Yersin/A. Vogler

the higher $^2T_{1g}$ is very rare because the vibronic structure of the $^4A_{2g} \longrightarrow {}^2E_g$ transition usually covers the less intense $^2T_{1g}$ lines in absorption spectra. Recently, a new optical device, which provides for low temperature spectroscopy of solid materials, was applied for measuring an extremely rich vibronic band pattern in the 4.2K absorption spectra of the pentachlorocadmium and -copper salts of the hexaammine complex. As elaborated in detail in Ref. 3 all five spin-orbit components (Kramers' doublets) of ^2E_g and $^2T_{1g}$ were identified including assingments for about sixty vibronic sidebands in both cases (cf. Fig. 1). The electronic level schemes have been rationalized by complete ligand field calculations considering certain limitations for the trigonal LF parameters K and K' due to reasonable radial parts of the d-electron wavefunctions. Trigonal distortions of the CrN_6 chromophore can be calculated from the parameter relation

$$(K+K') \;/\; Dq \;=\; 10/\sqrt{2} \cdot (\theta_{cub} - \theta) \cdot \pi/180^{\circ} \;, \qquad (1)$$

where θ denotes the angle between the octahedral trigonal axis and one

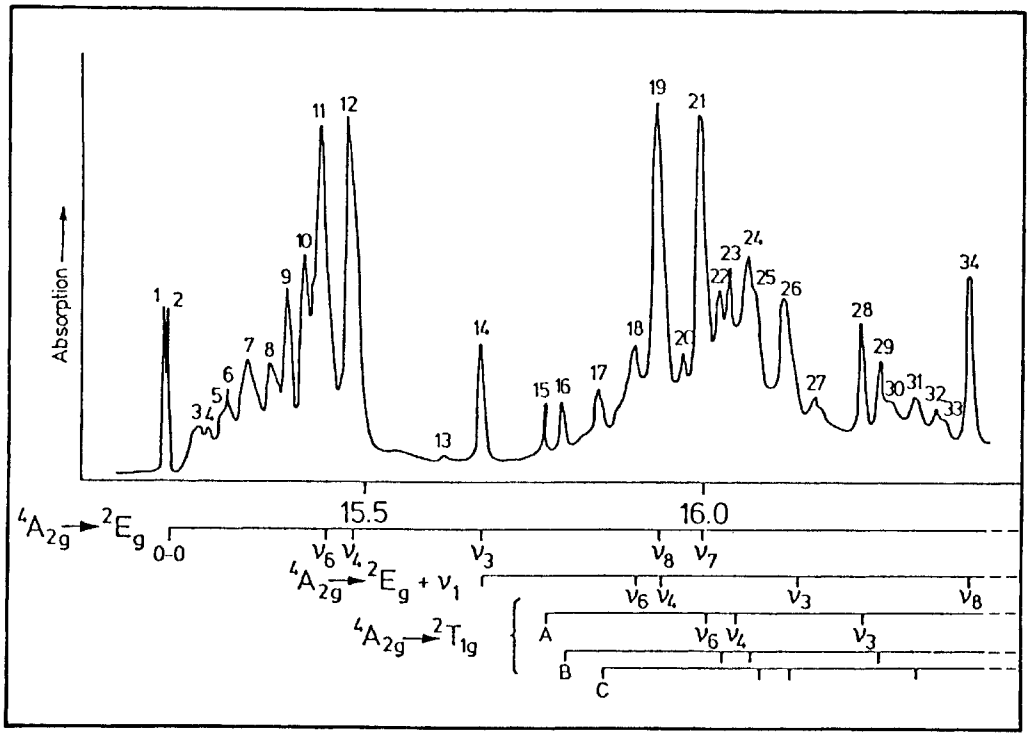

Figure 1 Low energy part of the absorption spectrum of crystalline $[Cr(NH_3)_6](CdCl_5)$ at 4.2K.

of the metal-ligand vectors (4). The calculated doublet energies as well as ground state splittings are in excellent agreement with the experimental findings, and θ is determined to be 0.19^{o} in the Cd-salt and 0.23^{o} in the Cu-salt, respectively, indicating a slight compression along the trigonal axis. This reflects the expected distortions of the chromium complex in the two lattices, the value for the copper salt also coincides with X-ray results (0.22^{o}). Therefore, it is concluded that conventional LFT can rationalize experimental energies up to high accuracy when complexes possess a high symmetry and π-bonding can be neglected. Otherwise more sophisticated treatments of electron repulsion (usually spheric parameters are used) or extensions referring to molecular orbital theory are required (vide infra).

Angular Overlap Calculations for Os^{4+} Complexes

In comparision with the ions from the first transition period, much less is known about d-electronic states of heavier metal ions in complex compounds. Though in recent years several papers have been published dealing with absorption and luminescence spectroscopy of hexacoordinated Os^{4+} compounds (e.g. Refs. 5-8), assingments even of the best investigated intraconfigurational transitions are still open for discussion. The first calculation of energy levels for octahedrally surrounded osmium(IV), including spin-orbit coupling, was performed in 1968 (Dorain et al.) using conventional LFT. Low symmetry d^4 complexes have not been theoretically treated up to now. To assign spectra, band splittings of low symmetry compounds as well as selection rules for zero-phonon and vibronic transitions have been used (6). Nevertheless, the given assignments are still speculative and partially even in contradiction to the predictions of group theory (8). Therefore, in order to elucidate the electronic structures and determine hitherto unknown AOM parameters of osmium complexes, we have fitted calculated energy levels to the experimental ones by adaptation of the geometrical properties of the molecules. By this procedure was found for $OsCl_6^{2-}$, when doped into low symmetry K_2SnCl_6 host lattice, that the experimental splitting pattern of the spin-orbit states resulting from $^3T_{1g}$ (6,7) is reproduced by use of antibonding parameters e_σ = 9500 cm^{-1} and e_π = 1800 cm^{-1}. Investigations on the energy level schemes of mixed hexahalide compounds support this result (9). In the following, the obtained findings are applied to the well resolved $\Gamma_1 \longrightarrow \Gamma_3, \Gamma_5$ (all from $^3T_{1g}$) transitions in $[OsCl_4ox]^{2-}$, ox = oxalate, (8). In this molecule a strong deviation from octahedral surrounding appears due to the rigidity of the oxalate ion. From geometrical considerations a bite angle of about 74^{o} is expected. In our AOM calcula-

tions the chloride antibonding parameters are used as given above while for the oxalate parameters the guide lines of the spectrochemical series should hold. Fig. 2 shows that an almost perfect fit of the experimental findings has been achieved by varying the bite angle α. The obtained result ($\alpha = 78 \pm 1^{\circ}$) reflects the influence of covalency ($\alpha > 74^{\circ}$) as well as the rigidity of the chelate ligand ($\alpha << 90^{\circ}$). This example demonstrates that spectrum-structure correlations can be quite significant though easy to handle when appropriate models are used providing a good field for future theoretical and experimental investigations.

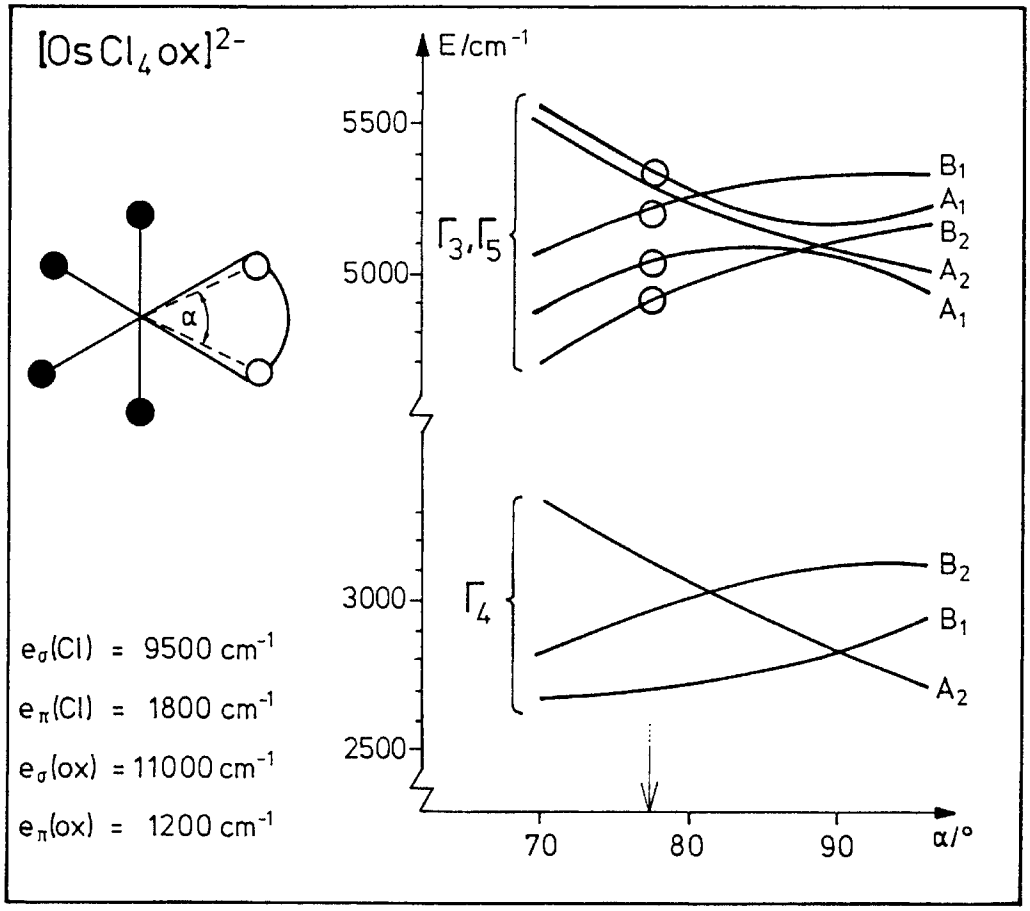

Figure 2 Calculated (——) and experimental (O) spin-orbit energy levels of $^3T_{1g}(O_h)$. B = 370, C = 5 B, ζ = 2650 (in cm^{-1}).

Orbital Phase Coupling Effects in Metal Acetylacetonates

The molecular geometry of trisbidentate complexes has been the subject of many investigations in the past twenty years. However, various approaches have failed to describe the structural properties of transition metal acetylacetonates. Furthermore, assingments of some d-d transitions are not clear up to now. Most recently, it has been shown that usual LFT (although this model is able to fit the experimental energy level scheme (10)) and the AOM cannot account for the trigonal level splittings in $Cr(acac)_3$, for which the coordination sphere of oxygen atoms is nearly octahedrally arranged (11). Consideration of anisotropic π-bonding using different AOM parameters for in plane and out of plane interactions, $e_{\pi c}$ and $e_{\pi s}$, is not able to change the situation, since for reasons of symmetry a "pseudoisotropic" electron density results for this compound. However, a more profound extension of the AOM, which becomes important for chelate complexes (12), can reproduce the experimental findings. The phase relations of ligand orbitals influence the d-orbital splitting in a different way as the point symmetry of the chromophore would predict, leading to a non-additive model for the metal-ligand interactions. For trisacetylacetonates in phase coupling is present in accordance with the fact that the HOMO's of the acac ligands are of Ψ-type (Fig.3).
Finally, this is applied to the geometry of such compounds. From analytical expressions of the matrx elements $\langle d_i | V_{trig} | d_j \rangle$, which depend on the chelate bite angle α and on antibonding parameters, the trigonal

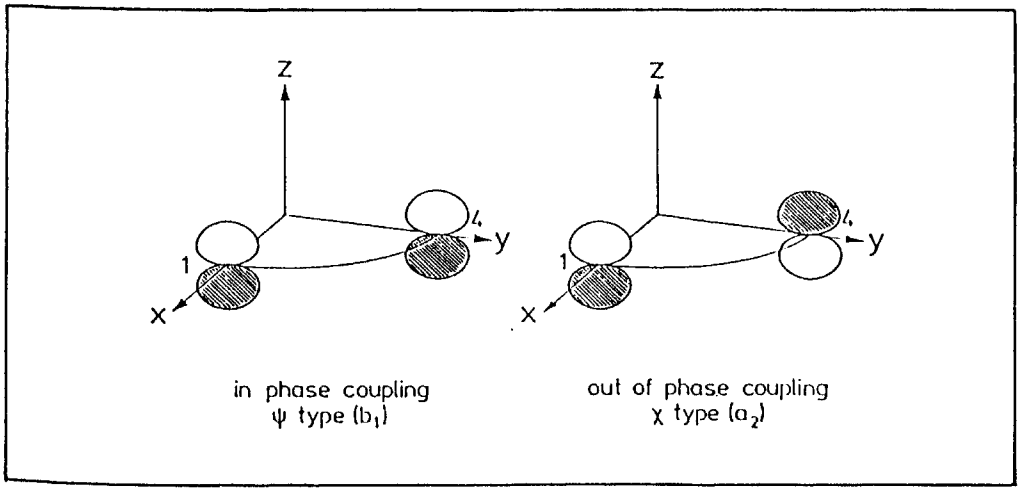

Figure 3 p-orbital phase coupling scheme for bidentate ligands (C_{2v})

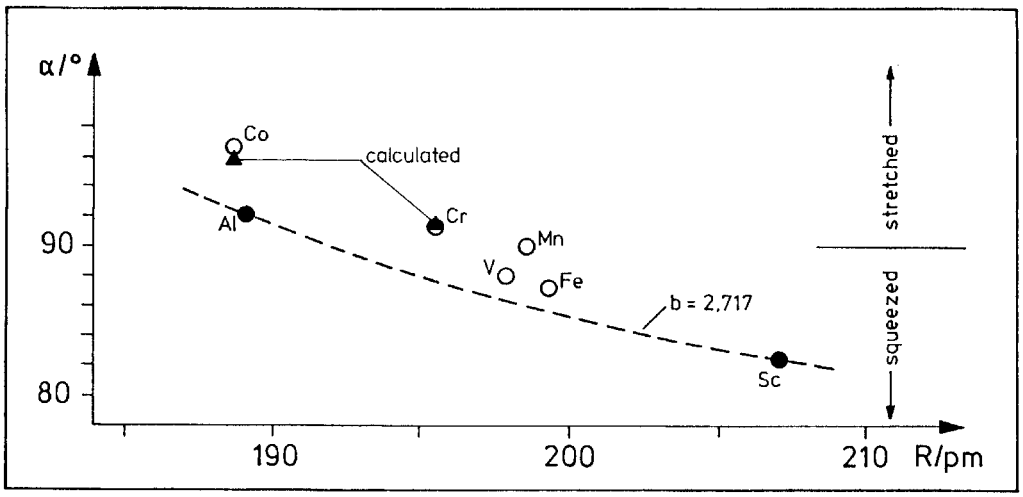

Figure 4 Bite angle to metal-ligand distance plot from X-ray data. The dependence for constant O-O bite is given by the dashed line.

distortion of the MO_6 skeleton from octahedral symmetry can be calculated. For example, the total energy of a d^3 or d^6 system is minimal with respect to variation of α for

$$\cos \alpha = - e_{\pi s} / (3e_{\sigma} - 4e_{\pi c}) . \qquad (2)$$

Since the denominator must be positive (σ-bonding is larger than corresponding π-bonding) as is the case for $e_{\pi s}$ (donor ligands), the increase of O-O bites in transition group acetylacetonates compared to closed shell compounds is well explained (Fig. 4). Quantitative results are derived for the Cr^{3+} and Co^{3+} complexes (13), where AOM parameters can be obtained from trigonal band splittings in polarized absorption spectra.

References

(1) Reisfeld, R. Mater. Sci. Eng. 1985, 71, 375
(2) Hoggard, P.E. Coord. Chem. Rev. 1986, 70, 85
(3) Urushiyama, A.; Schönherr, T.; Schmidtke, H.-H. Ber. Bunsenges. Phys. Chem. 1986, 90, 1195
(4) Schoenen, N.; Schmidtke, H.-H. Mol. Phys. 1986, 57, 983
(5) Dorain, P.B.; Patterson, H.H.; Jordan, P.C. J.Chem.Phys.1968,3845
(6) Schönherr, T.; Wernicke, R.; Schmidtke, H.-H. Spectrochim. Acta 1982, 28A, 679
(7) Kozikowski, B.A.; Keiderling, T.A. J. Chem. Phys. 1983, 87, 4630
(8) Homborg, H.; Preetz, W.; Schätzel, G. Z.Naturforsch. 1980,35b,554
(9) Strand, D. unpublished results
(10) Schönherr, T., Linder, R.; Eyring, G. Z. Naturforsch.1983,38a,736
(11) Atanasov,M.;Schönherr,T.;Schmidtke,H.-H. Theor.Chim.Acta, in press
(12) Ceuleman, A.; Dendooven, M.; Vanquickenborne, L.G. Inorg. Chem. 1985, 24, 1153
(13) Schönherr,T.;Atanasov,M.;Schmidtke,H.-H. Inorg.Chim.Acta, submitted

MULTIPHOTON-INDUCED PICOSECOND PHOTOPHYSICS OF CHROMIUM(III)- POLYPYRIDYL COMPLEXES

N.Serpone* and M.Z.Hoffman **

* Department of Chemistry, Concordia University, Montreal, CANADA
**Department of Chemistry, Boston University, Boston, MA, USA

INTRODUCTION

The photophysics of Cr(III)-polypyridyl complexes, $Cr(NN)_3^{3+}$, have been the object of many studies in attempts at understanding the behaviour of these systems on absorption of light (Jamieson 1981; Serpone 1983). The usual photochemically relevant states of $Cr(NN)_3^{3+}$ (Fig. 1) are: the ground state, $^4A_2$; the lowest energy spin-allowed quartet state, $^4T_2$; and the lowest energy spin-forbidden doublet states, $^2T_1/^2E$. Also, shown are the other higher energy quartet and doublet states, and the ligand-centred states (Ohno 1983 1986) depicted as dashed curves; not shown are some 12 additional doublet states. Several studies have been

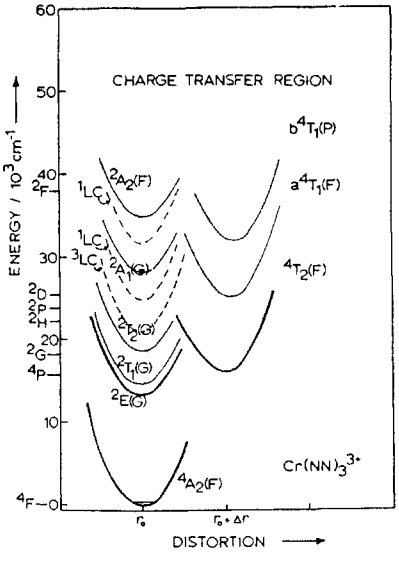

Fig. 1: Qualitative energy level diagram as a function of a distortion coordinate. Solid lines denote metal-centred state surfaces; dashed lines show ligand-centred surfaces. From (Serpone 1987).

directed toward the long-lived ($\tau \sim 0.1$ - 1 ms) luminescent $^2T_1/^2E$ states; prompt fluorescence from $^4T_2$ has not been observed in fluid media at ambient temperatures, implying either that the lifetime of $^4T_2$ is too short or that this state is not populated. Recent pulsed laser transient absorption spectroscopy experiments have indicated that τ of $^4T_2$ of $Cr(acac)_3$, $Cr(NCS)_6^{3-}$, t-$Cr(NH_3)_2(NCS)_4^-$, t-$Cr(en)_2(NCS)_2^+$, $Cr(en)_3^{3+}$, and $Cr(bpy)_3^{3+}$ are a few ps or less (Kirk 1976; Rojas 1986 1987; Pyke 1978; LeSage 1983; Nicollin 1980).

Recently, we reported (Serpone 1984) that 355-nm excitation of $Cr(bpy)_3^{3+}$ and $Cr(4,7\text{-}Me_2phen)_3^{3+}$ in 1M HCl aqueous media results in a grow-in of the luminescence from their $^2T_1/^2E$ states with τ(rise) $\sim$ 10-20 ns, attributed to intersystem crossing from the quartet to the doublet mani-

Photochemistry and Photophysics
of Coordination Compounds, Ed. by H. Yersin/A. Vogler

folds. We also observed a rapid increase in transient absorption in the 400-600 nm region within the integrated laser pulse (∿ 30 ps, fwhm) followed by a slower absorption rise to 12 ns, just outside of experimental error ($\pm\sigma$). Kirk (1986) has questioned our results from the standpoint of a (a) lack of observable fluorescence from $^4T_2$, (b) possible artifact (Raman effects, filter emission,...) in our data, (c) the emission concaves upward, and (d) $\pm 2\sigma$ should be used rather than our $\pm\sigma$. In our reply (Serpone 1986) we emphasized that the slow rise in emission did not originate from artifactual sources; also, the computer fitting of the grow-in did not show unreasonable errors (see below). *Curiously,* Kirk (1986) carried out *neither* transient emission experiments, *nor* transient absorption experiments beyond 400 ps. Rojas (1987) was surprised at our results on the basis of their own work in which they employed low-power laser pulses (photon fluxes $\lesssim 10^{11}$ photons/cm^2); they did concede (1986) that perhaps Cr(III)-polypyridyl may have photophysical properties different from those of other Cr(III) complexes.

We report here our extensive examination of the ps transient emission properties of several $Cr(NN)_3^{3+}$ complexes, and in detail the transient absorption properties for $Cr(5,6\text{-}Me_2phen)_3^{3+}$; transient emission was determined *under identical experimental conditions* as those of t-$Cr(NH_3)_2(NCS)_4^-$, t-$Cr(en)_2(NCS)_2^+$, $Cr(en)_2F_2^+$, $Cr(en)_3^{3+}$, $Cr(terpy)_2^{3+}$, and $Cr(cyclam)(NH_3)_2^{3+}$. To further test for potential artifactual sources, we also examined $Ru(bpy)_3^{2+}$, $Fe(bpy)_3^{2+}$, eosine-Y, and biacetyl.

MATERIALS AND PROCEDURES

These have been reported elsewhere in some detail (Serpone 1987).

RESULTS AND DISCUSSION

In the present work (Serpone 1987) and in our earlier communication (Serpone 1984) we employed a solid-state Nd:Yag laser system (∿30 ps pulses; 2-3 mj/pulse); photon flux per pulse ∿ 10^{16}-10^{17} photons/cm^2, some 5-6 orders of magnitude greater than that used by Rojas (1986 1987).

Transient Emission: A survey of $Cr(NN)_3^{3+}$ complexes (where NN is bpy, 4,4'-Me_2bpy, 4,4'-Ph_2bpy, phen, 5-Brphen, 5-Clphen, 5-Mephen, 5-Phphen, 5,6-Me_2phen, 4,7-Me_2phen, 4,7-Ph_2phen, 3,4,7,8-Me_4phen) revealed that excitation (355 nm) of all these complexes results in a fast emission component below 650 nm that decays in ∿ 50 ps (Fig. 2a), and, with the exception of NN = 5-Phphen, 4,4'-Ph_2bpy, and $Cr(terpy)_2^{3+}$, a slow emission rise at ∿ 700 nm. The slow rise has also been observed with $Cr(cyclam)(NH_3)_2^{3+}$ (Kane-Maguire 1984). The following emitting systems showed *neither* a slow rise in luminescence *nor* a fast emission component, but only showed their normal decays as seen by others: $Ru(bpy)_3^{2+}/H_2O$, t-$Cr(NH_3)_3(NCS)_4^-/H_2O$, $Cr(en)_2F_2^+/H_2O$, $Cr(en)_3^{3+}/H_2O$, eosine-Y/H_2O, biacetyl/methanol, and biacetyl/heptane. With 266-nm excitation (Fig. 2b), $Cr(5,6\text{-}Me_2phen)_3^{3+}$ shows a prompt emission rise (at $\lambda \gtrsim 305$ nm; plot A) levelling off to a plateau in the 0-7 ns time window of the streak camera.However, plot A is a composite of the emission features in plot B (decay time ∿ 13 ns) and plot C; the latter is similar to plot B of Fig. 2a.

In our previous paper (Serpone 1984), we treated the kinetics of the slow emission rise by the model of Castelli (1977) {$I_t = K(1 + e^{-kt})$, where K is a constant and k was taken as the rate of intersystem crossing between $^4T_2$ and $^2T_1/^2E$} which assumes that *thexi* $^4T_2{}^o$ and $^2T_1/^2E$

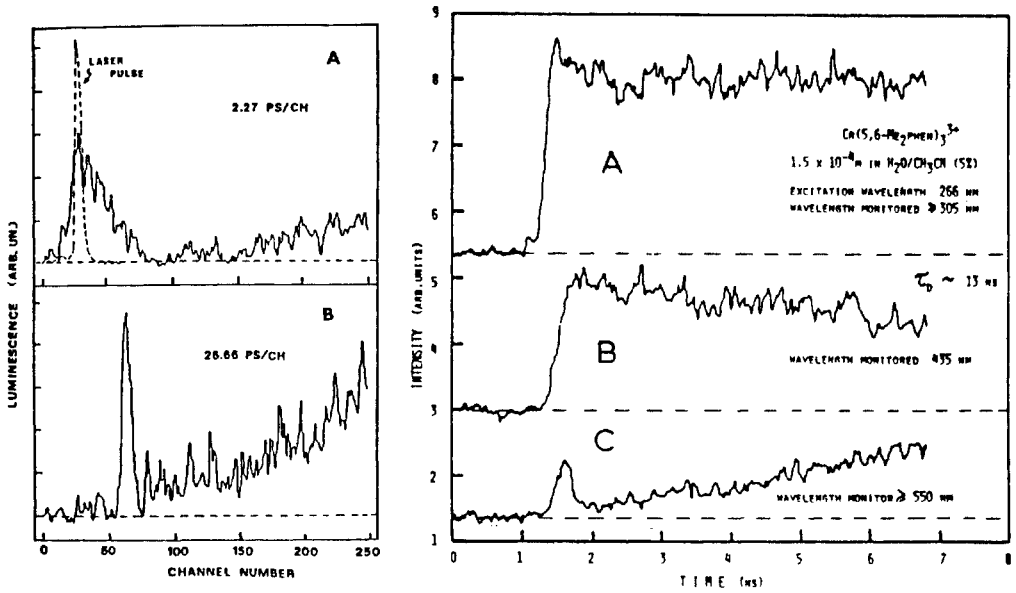

(a) (b)

Fig. 2: (a) Time-resolved emission from the 355-nm excitation of Cr(5,6-Me_2phen)$_3^3$; A, time window 568 ps; B time window 6.7 ns. Dashed line in A is the laser pulse. (b) Time-resolved emission from the 266-nm laser excitation of Cr(5,6-Me_2phen)$_3^3$. From (Serpone 1987).

states are involved and that back intersystem crossing is negligible. Application of this model leads to the unreasonable requirement that $^4T_2{}^o$ be sufficiently long-lived for steady-state fluorescence to be observed (Kirk 1986). The model of Castelli (1977) is in retrospect not appropriate since $^4T_2{}^o$ is not populated (Serpone 1981). Rather, the slow emission grow-in (B of Fig. 2b) can be fitted (Fig. 3) to a model for two consecutive first-order reactions (eqn 1; Frost 1961); where τ_1

$$A \xrightarrow{k_1} B \xrightarrow{k_2} C \qquad (1)$$

$= 1/k_1 \sim 500$ ps and $\tau_2 = 1/k_2 \sim 10$ ns (Serpone 1987). It is interesting to note that I^-, a well known quencher of $^2T_1/^2E$ states, totally quenches the slow emission growth and slightly quenches the fast emission component. It is not inconceivable then that the slow rise identifies with formation of the $^2T_1/^2E$ manifolds (species *C*). Wavelength-resolved emission spectra (Fig. 4) reveal two emissions: one centred at $\sim$ 570 nm ($\tau \sim$50 ps) and the other centred at $\sim$ 460 nm (biphasic decay with $\tau_1 \sim$ 0.65 ns and $\tau_2 \sim$ 11 ns). The former is identified (Serpone 1987) with *unrelaxed fluorescence from the $^4T_2$ manifold*; the emission band at $\sim$ 460 nm is identified with emission originating with the coordinated NN ligands, by analogy with the steady-state luminescence. Note the congruence between the NN emission decay times with the risetimes of the slow emission grow-in.

Figure 5a shows the transient absorption spectra at four delay times; the absorption at 460 nm decreases dramatically between 0 and 50 ps delay times. Figure 5b shows the inverse formation {ΔA(x ps)-ΔA(0 ps}

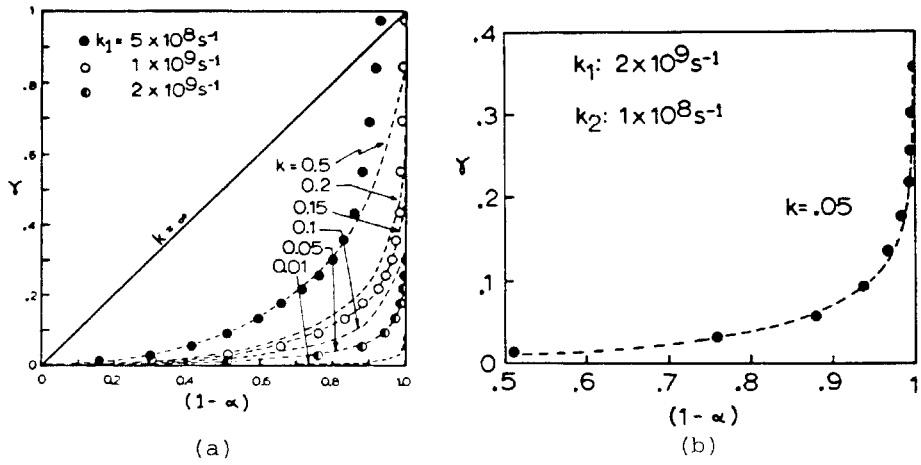

Fig. 3: Theoretical curve fit of the slow emission rise of $^2T_1/^2E$ from 355-nm laser excitation of $Cr(5,6\text{-}Me_2phen)_3^{3+}$. (a) Various curve fits for different values of k; the circles denote experimental data. (b) Best curve fit for $k \sim 0.05$ and for $k_1 \sim 2 \times 10^9 s^{-1}$.

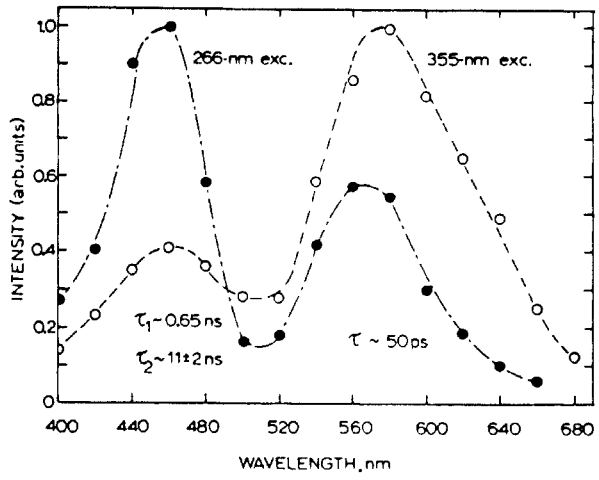

Fig. 4: Wavelength-resolved transient emission spectra taken at 0 ps from the 266-nm and 355-nm laser excitation of $Cr(5,6\text{-}Me_2phen)_3^{3+}$. Both spectra were taken under identical conditions except for the excitation wavelength.

(decay) of the 460-nm band; $\tau \sim 50$ ps. Figure 6 summarizes the transient absorption results as ΔA vs. time. Clearly, there are two decaying transients at $\sim$ 460 nm and there is one at 541 nm (see insert in Fig. 6). More important, there is an absorption rise from $\sim$ 1 ns to 10 ns, which is outside of $\pm 2\sigma$ at both wavelengths. Excitation of $Cr(5,6\text{-}Me_2phen)_3^{3+}$ at 266 nm shows a spectrum (Fig. 7a) reminiscent of solvated electrons (thus a CTTS state is populated; eqn 2); the transient spectrum of the free ligand in 1M HCl (Fig. 7b) also shows features

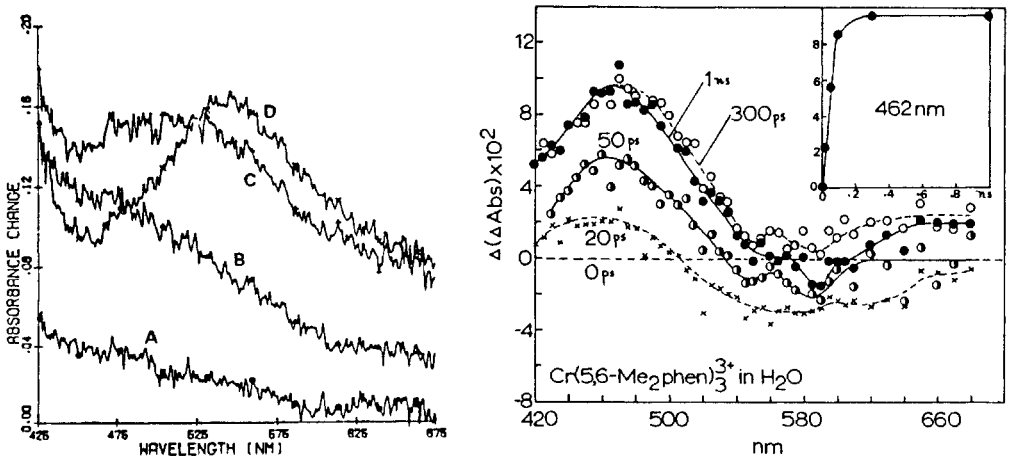

(a) (b)

Fig. 5: (a) Transient absorption spectra at -50 ps (A), -20 ps (B), 0 ps (C), and +50 ps (D) delay times from the 355-nm excitation of $Cr(5,6\text{-}Me_2phen)_3^{3+}$. From (Serpone 1987). (b) Difference spectra at various times against that at 0 ps; insert shows the inverse decay of the 460-nm band.

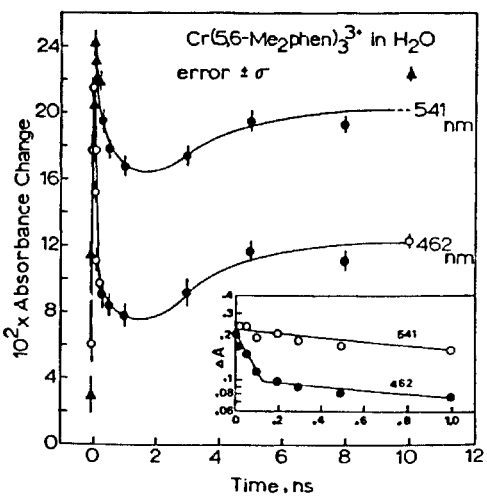

Fig. 6: Absorbance change vs. time at 462 nm and 541 nm from the 355-nm excitation of $Cr(5,6\text{-}Me_2phen)_3^{3+}$. Inset shows a semilogarithmic plot of ΔA vs. time. From (Serpone 1987).

$$\{Cr(5,6\text{-}Me_2phen)_3\}^{3+} \xrightarrow[266\ nm]{h\nu} \{Cr(5,6\text{-}Me_2phen)_3\}^{4+} + e^-(aq) \qquad (2)$$

consistent with solvated electrons (additional absorptions are seen at lower wavelengths).

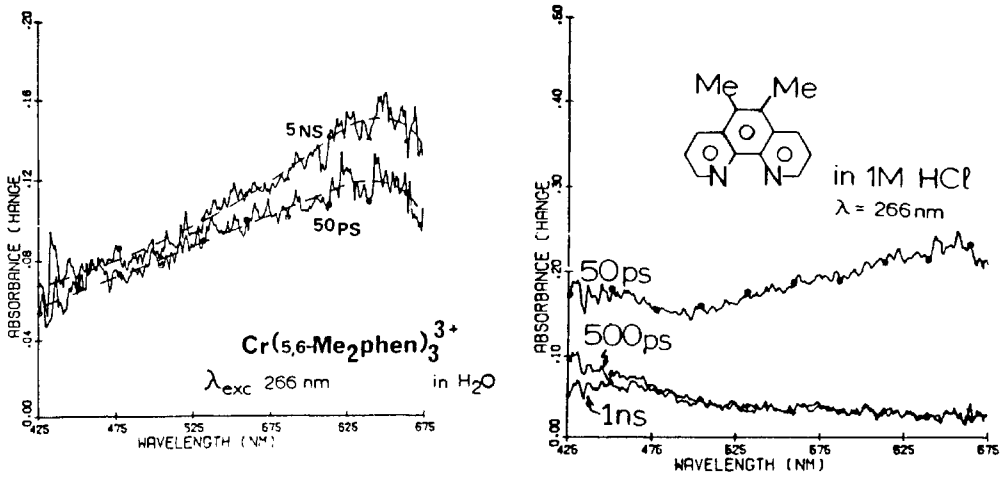

Fig. 7: Transient absorption spectra at 50 ps and 5 ns from the 266-nm excitation of an aqueous solution of $Cr(5,6\text{-}Me_2phen)_3^{3+}$; from (Serpone 1987). (b) Transient absorption spectra at 50 ps, 500 ps and 1 ns from the 266-nm excitation of the 5,6-Me_2phen ligand in 1M HCl/CH_3CN aqueous media.

CONCLUSIONS

In summary, we have identified (Serpone 1987) four transient species: (i) transients *A* and *B* with lifetimes ∿ 0.5-0.65 ns and 11-13 ns, respectively, are the ^{1}LC and ^{3}LC coordinated ligand states which are the direct and principal precursors to transient *C* ($^2T_1/^2E$ states), and (ii) transient *D* with τ ∿ 50 ps is identified with the *unrelaxed* $^4T_2$ *state*. The model proposed is shown in Fig. 8 and is based on data known to date. That is, excitation of the Cr(III) complex by a laser pulse

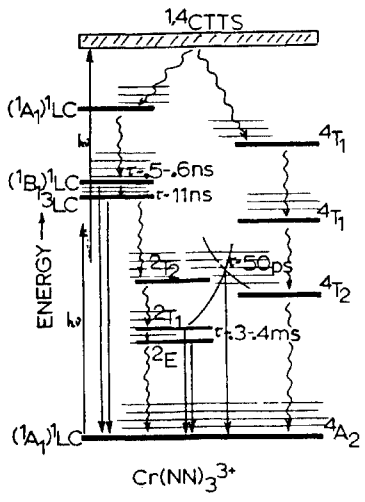

Fig. 8: Jablonsky-type diagram showing the tentative relaxation pathways for the photophysical events arising from multiphoton excitation of $Cr(NN)_3^{3+}$. From (Serpone 1987).

with such a high photon flux, as used in our work, leads to multiphotonic events, whereby it is evident at 266-nm excitation that a CTTS state is formed, unlike excitation at 355 nm. Following formation of the CTTS manifold, energy partitioning ensues that populates the LC states preferentially (see eg. Fig. 4). It is these two ligand-centred states that are the primary precursors to the $^2T_1/^2E$ states, *under our experimental conditions*, with both 266- and 355-nm excitation.

Clearly, the multiphoton induced events presented here contrast, but are not inconsistent with those reported by Rojas (1987) from single-photon excitation. High-power laser excitation can therefore discover and probe new photophysics, not available with low-power laser excitation. It is also evident that the polypyridine complexes of chromium examined here (Serpone 1987) afford the 'right' pathology of ground and excited states with which to view these multiphotonic events.

ACKNOWLEDGEMENTS

Our work is supported by the Natural Sciences and Engineering Research Council of Canada, and by the Office of Basic Energy Sciences, Division of Chemical Sciences, US Department of Energy. We are grateful to Dr. D.K. Sharma of Concordia University for expert technical assistance in running the laser experiments.

REFERENCES

Castelli F, Forster LS (1977) J Phys Chem 81: 403

Frost AA, Pearson RG (1961) Kinetics and Mechanisms, Wiley, New York

Jamieson MA, Serpone N, Hoffman MZ (1981) Coord Chem Rev 39: 121

Kane-Maguire NAP, Sharma DK (1984) unpublished results

Kirk AD, Hoggard PE, Porter GB, Rockley MG, Windsor MW (1976) Chem Phys Lett 37: 199

Kirk AD, Porter GB, Sharma DK (1986) Chem Phys Lett 123: 548

LeSage R, Sala KL, Yip RW, Langford CH (1983) Can J Chem 61: 2761

Nicollin D, Bertels P, Koningstein JA (1980) Can J Chem 58: 1334

Ohno T, Kato S, Kaizaki S, Hanazaki I (1983) Chem Phys Lett 102: 471

Ohno T, Kato S, Kaizaki S, Hanazaki I (1986) Inorg Chem 25: 3853

Pyke SC, Windsor MW (1978) J Am Chem Soc 100: 6518

Rojas GE, Dupuy C, Sexton DA, Magde D (1986) J Phys Chem 90: 87

Rojas GE, Magde D (1987) J Phys Chem 91: 689

Serpone N, Hoffman MZ (1983) J Chem Educ 60: 853

Serpone N, Jamieson MA, Sharma DK, Danesh R, Bolletta F, Hoffman MZ (1984) Chem Phys Lett 104: 87

Serpone N, Hoffman MZ (1986) Chem Phys Lett 123: 551

Serpone N, Jamieson MA, Maestri M (1981) unpublished results

Serpone N, Hoffman MZ (1987) J Phys Chem 91: 0000

TOPIC 3

Excited State Properties of Tris-2,2'-Bipyridine Ruthenium (II) and Related Complexes

ON THE ORBITAL NATURE OF THE LUMINESCENT EXCITED STATE OF ORTHOMETALATED TRANSITION METAL COMPLEXES

V.Balzani, M.Maestri, A.Melandri, D.Sandrini, L.Chassot, C.Cornioley-Deuschel, P.Jolliet, U.Maeder, and A.von Zelewsky

Chemistry Department "G. Ciamician", University of Bologna, ITALY
Institute FRAE-CNR, Bologna, ITALY
Institute of Inorganic Chemistry, University of Fribourg, SWITZERLAND

The study of the photochemical and photophysical properties of transition metal complexes is of great interest for theoretical reasons (i.e., for a better understanding of the "excited state dimension" of chemistry) as well as for practical applications (luminescent materials, photocatalytic processes etc.). In the last few years the attention of numerous research groups has been focussed on the search and characterization of transition metal complexes that can play the role of light absorption sensitizers (LAS) and/or light emission sensitizers (LES) for the interconversion between light energy and chemical energy via electron transfer reactions involving electronically excited states (Balzani 1983). To perform systematic experiments in this field as well as to arrive at practical devices we need a series of compounds covering a broad range of excited state energies, lifetimes, and oxidation-reduction potentials. The family of Ru(II)-polypyridine compounds, having as a prototype the famous $Ru(bpy)_3^{2+}$ complex, has proved to be very interesting for these purposes, and some hundreds Ru(II)-polypyridine compounds have been synthetized and studied in the last few years (Kalyanasundaram; Juris). Polypyridine complexes of Cr(III) (Jamieson), Rh(III) (De Armond), Ir(III) (Watts), and Os(II) (Sutin) have also been studied, but an ideal LAS and/or LES has not yet been found (Balzani 1986).

The current interest in the photochemical and photophysical properties of orthometalated complexes (Sprouse; King 1984, 1985; Finlayson; Maestri 1985, 1987; Chassot; Wakatsuki; Sandrini) is, on one side, a logic extension of the previously mentioned studies carried out on complexes containing polypyridine ligands; on the other side, this interest has been stimulated by the recent development of organometallic chemistry, a field that has so far contributed a relatively small number of studies concerning excited state reactivity and/or luminescence.

In transition metal complexes the excited state responsible for luminescence and bimolecular light induced processes is the lowest

Photochemistry and Photophysics
of Coordination Compounds, Ed. by H. Yersin/A. Vogler

excited state. The properties of such an excited state are strongly dependent on its orbital nature and on the proximity of other excited states. For the family of the Ru(II)-polypyridine complexes, suitable changes in the nature of the ligands may cause a change in the orbital nature of the lowest excited state and, more generally, may allow us "to tune" the excited state properties (Juris).

The number of orthometalated complexes that have been examined so far is not much large. Nevertheless, it is interesting to compare the available results to draw some preliminary conclusions on the possibility to tune their excited state properties. In this paper we focuss our attention on a series of closely related orthometalated complexes and we examine the trends shown by energies and lifetimes of the luminescent excited state.

Figure 1 shows the structural formulae and abbreviations of the orthometalated ligands. The full names of the ligands constituting the coordination sphere of the complexes examined are as follows: phpy = 2-phenylpyridine, thpy = 2-(2-thienyl)pyridine, bhq = benzo(h)-quinoline, bpy = 2,2'-bipyridine, phen = 1,10-phenanthroline.

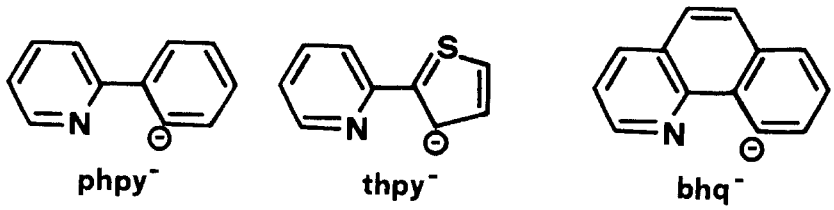

Figure 1 - Structural formulae of the orthometalated ligands

Table 1 summarizes the available data concerning absorption spectra at room temperature and luminescence spectra and lifetimes (at 77 K) of the complexes examined. It should be noted that for the mixed-ligand complexes the non-orthometalated ligands are not involved in the lowest energy excited state, although they may indirectly affect to some degree the excited state properties via electron withdrawing or electron donating effects on the metal.

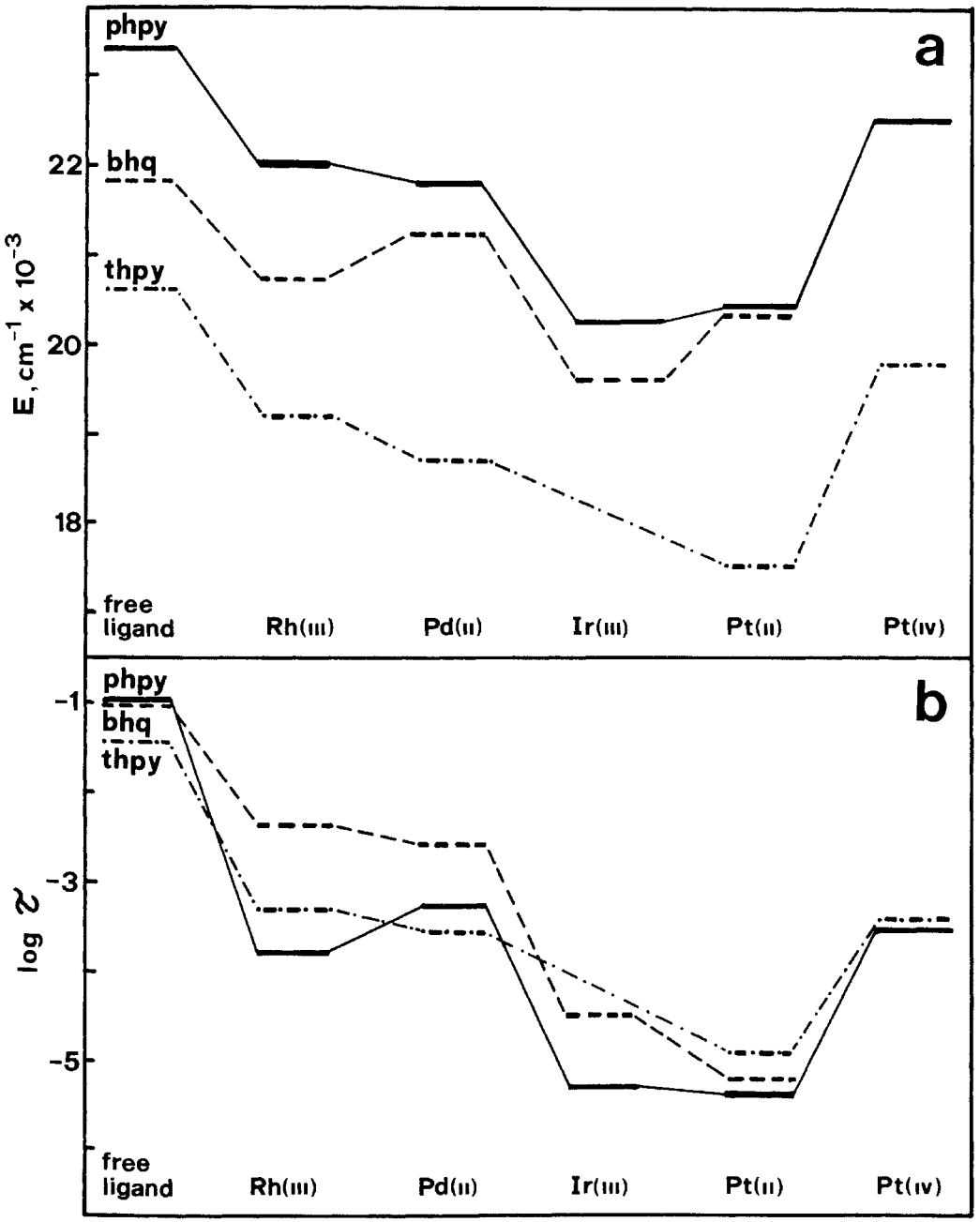

Figure 2 - Energy (a) and lifetime (b) of the luminescent excited states of the free protonated orthometalated ligands and of their complexes (see Table 1).

Figure 2a shows schematically the trend in the emission energy for the $phpy^-$, bhq^-, and $thpy^-$ complexes of Rh(III), Pd(II), Ir(III), Pt(II), and Pt(IV). For comparison purposes, the emission energy (phosphorescence) of the free protonated ligands are also shown. Figure 2b shows the trend in the luminescence lifetime of the same complexes. Information on the orbital nature (ligand centered, LC, or metal-to-ligand charge-transfer, MLCT) of the luminescent excited state can be drawn from the data reported in Table 1 and from their trends shown in Fig. 2. For the Pt(IV) complexes the emission energy is very close to (less than 1000 cm^{-1} red-shifted from) that of the free ligand and the luminescence lifetime is relatively long, indicating a heavy-atom perturbed LC phosphorescence. For the Ir(III) complexes the red-shift from the free ligand phosphorescence is very large (2000-3000 cm^{-1}) and the luminescence lifetimes are 10-60 times shorter than those of the analogous Pt(IV) complexes, showing that the emitting excited state is essentially MLCT in nature. This is also the case for the Pt(II) complexes whose emission occurs from slightly higher energy excited states with comparable lifetimes. For the Rh and Pd compounds the situation is more complex. The emission of the phpy complex of Rh(III) occurs at lower energy than that of the Pt(IV) complex and exhibits a shorter lifetime, in spite of the fact that Rh is lighter than Pt. These results suggest some mixing between LC and MLCT levels. For the bhq complex, however, the smaller red-shift from the free ligand emission and the very long lifetime point towards an essentially LC emission. The rigidity of the bhq ligand may cause some steric hindrance that increases the metal-ligand bond distance, thereby reducing the metal-ligand charge transfer interaction. For the Rh(III) complex with the flexible thpy ligand, the red shift from the ligand emission is higher (~1400 cm^{-1}); actually, the emission occurs ~500 cm^{-1} lower in energy than the LC emission of the Pt(IV) complex. This shows that there is some LC-MLCT mixing although the relatively long luminescence lifetime (which is also longer than that of the phpy complex) indicates a noticeable LC character. The fact that the lifetime of the Rh(III) thpy complex is longer than that of the analogous Pt(IV) complex (in spite of the apparent purer LC character of the latter) is likely due to the stronger heavy-atom effect in the Pt complex.

As to the Pd(II) complexes, the red shift from the emission of the Pt(IV) complexes indicates some LC-MLCT mixing. The fact that the lifetimes of the Pd(II) complexes are similar (for thpy) or even higher (for phpy) than those of the Pt(IV) complexes in spite of the

Table 1 - Absorption and emission data for some orthometalated complexes

Complex	Absorption[a]		Emission[b]		
	λ_{max}[c] (nm)	(ε)	λ_{max}[d] (nm)	τ (μs)	Ref.
$Rh(phpy)_2(bpy)^+$	367[e]	(8000)	454	170	Maestri 1987
$Rh(thpy)_2(bpy)^+$	379[e]	(9000)	521	500	Maestri 1987
$Rh(bhq)_2(phen)^+$	393[e]	(5500)	483[f]	4250	Ohsawa
$Pd(phpy)_2$	349	(9000)	458	480	g
$Pd(thpy)_2$	382	(7000)	536	280	g
$Pd(bhq)_2$	391	(6000)	472	2600	g
$[Ir(phpy)_2Cl]_2$[h]	434	(4200)	493[i]	4.8	Sprouse
$[Ir(bhq)_2Cl]_2$[h]	442	(5500)	510[i]	30	Sprouse
$Pt(phpy)_2$	402[j]	(12800)	491	4	Maestri 1985
$Pt(thpy)_2$	418[j]	(10500)	570	12	Maestri 1985
$Pt(bhq)_2$	421[j]	(9200)	492	6.5	Maestri 1985
$Pt(phpy)_2(CH_2Cl)Cl$	306	(15000)	444	300	Chassot
$Pt(thpy)_2(CH_2Cl)Cl$	344	(17000)	507	340	Chassot

a) Room temperature; CH_2Cl_2 solution, unless otherwise noted.
b) 77 K; propionitrile-butyronitrile 4:5 v/v mixture, unless otherwise noted.
c) Lowest energy absorption maximum.
d) Wavelength of the high energy feature.
e) MeOH solution
f) EtOH-MeOH 4:1 v/v mixture.
g) Maestri et al. unpublished results.
h) Substantially similar results have recently been obtained (Ohsawa) for $Ir(phpy)_2bpy^+$ and $Ir(bhq)_2phen^+$, with some complications due to dual emission.
i) EtOH-MeOH-CH_2Cl_2 4:1:1 v/v mixture.
j) Propionitrile-butyronitrile 4:5 v/v mixture.

purer LC nature of the latter can again be attributed to the different degree of heavy-atom perturbation. Finally, the fact that the Pd(II) bhq exhibits almost pure LC emission characteristics ($\sim$500 cm^{-1} red shift compared to the free ligand emission; very long lifetime) are likely due to the rigid nature of bhq which causes steric hindrance

and, as a consequence, prevents a sufficient closer approach for CT interaction between metal and ligands.

Acknowledgments. We would like to thank Mr. G. Gubellini for the drawings and Mr. V. Cacciari for technical assistence. Financial support from the Ministero della Pubblica Istruzione, the National Research Council of Italy, and the Swiss National Science Foundation is gratefully acknowledged.

References.

Balzani V, Bolletta F, Ciano M, Maestri M (1983) J Chem Educ 60: 447-450

Balzani V, Juris A, Scandola F (1986) in: Pelizzetti E, Serpone N (eds) Homogeneous and Heterogeneous Photocatalysis, D. Reidel Publishing Company, Dordrecht, p 1-27

Chassot L, von Zelewsky A, Sandrini D, Maestri M, Balzani V (1986) J Am Chem Soc 108: 6084-6085

DeArmond MK, Hillis JE (1971) J Chem Phys 54: 2247-2253

Finlayson MF, Ford PC, Watts RJ (1986) J Phys Chem 90: 3916-3922

Jamieson MA, Serpone N, Hoffman MZ (1981) Coord Chem Rev 39: 121-179

Juris A, Barigelletti F, Campagna S, Balzani V, Belser P, von Zelewsky A (to be published) Coord Chem Rev

Kalyanasundaram K (1982) Coord Chem Rev 46: 159-244

King KA, Finlayson MF, Spellane PJ, Watts RJ (1984) Riken Quarterly 78: 97-106

King KA, Spellane PJ, Watts RJ (1985) J Am Chem Soc 107: 1431-1432

Maestri M, Sandrini D, Balzani V, Chassot L, Jolliet P, von Zelewsky A (1985) Chem Phys Lett 122: 375-379

Maestri M, Sandrini D, Balzani V, Maeder U, von Zelewsky A (to be published 1987) Inorg Chem

Ohsawa Y, Sprouse S, King KA, DeArmond MK, Hanck KW, Watts RJ (to be published) J Phys Chem

Sandrini D, Maestri M, Balzani V, Chassot L, von Zelewsky A (submitted) J Am Chem Soc

Sprouse S, King KA, Spellane PJ, Watts RJ (1984) J Am Chem Soc 106: 6647-6653

Sutin N, Creutz C (1978) Adv Chem Ser 168: 1-27

Wakatsuki Y, Yamazaki H, Grutsch PA, Santham M, Kutal C (1985) J Am Chem Soc 107: 8153-8159

Watts RJ, Harrington J, van Houten J (1977) J Am Chem Soc 99: 2179-2187

CORRELATIONS BETWEEN OPTICAL AND ELECTROCHEMICAL PROPERTIES OF RU(II)-POLYPYRIDINE COMPLEXES: INFLUENCE OF THE LIGAND STRUCTURE

F.Barigelletti, A.Juris, V.Balzani, P.Belser, and A.von Zelewsky

Institute FRAE-CNR, Bologna, ITALY
Chemistry Department "G. Ciamician", University of Bologna, ITALY
Institute for Inorganic Chemistry, University of Fribourg, SWITZERLAND

The use of Ru(II)-polypyridine complexes as sensitizers in a number of light driven or light generating processes continues to be of interest (Juris). In this connection the correlations between optical and electrochemical properties (Ohsawa, Dodsworth) are much studied because they offer the opportunity to obtain absorption and emission energies from electrochemical potentials and viceversa. The basis for such correlations lies on the fact that the lowest energy Ru --> ligand transition involves the promotion of an electron from a metal centered π_M orbital to the lowest antibonding, "spatially isolated", ligand centered $^*\pi_L$ orbital which resembles the lowest $^*\pi$ orbital of the free ligand. The same metal centered and ligand centered orbitals that are involved in the metal-to-ligand transition are also involved in the oxidation and reduction processes, respectively. On these grounds it is clear that the ligand structure determines spectroscopic and electrochemical properties of complexes mainly because of the accepting ability of the LUMO orbital. This study employs EHMO calculations to correlate the above experimental quantities to the energy and symmetry properties of calculated LUMO's of free ligands.

The examined complexes are of the type $Ru(LL')_3^{2+}$ or $Ru(LL)_2(LL')^{2+}$, where LL' is a ligand easier to reduce than LL. For such complexes, the attention can be focussed on a Ru-LL' unit of C_{2v} symmetry. This is actually the symmetry of the Ru-LL' fragment which is present in the $Ru(LL)_2(LL')^{2+}$ complexes and is also an appropriate description for the monoreduced or excited $Ru(LL')_3^{2+}$ species because both processes involve population of a $^*\pi$ orbital localized in a single LL' ligand. A schematic MO diagram showing the orbital relevant to our discussion is shown in Fig. 1. Figure 2 shows the structural formula of the LL' ligands and Table 1 reports some calculated properties for the free ligands.

Figure 3 plots the reduction potential for the free ligands, $E_{1/2}(LL')$, and the reduction potential for the complexes, $E_{1/2}(red)$,

Photochemistry and Photophysics
of Coordination Compounds, Ed. by H. Yersin/A. Vogler

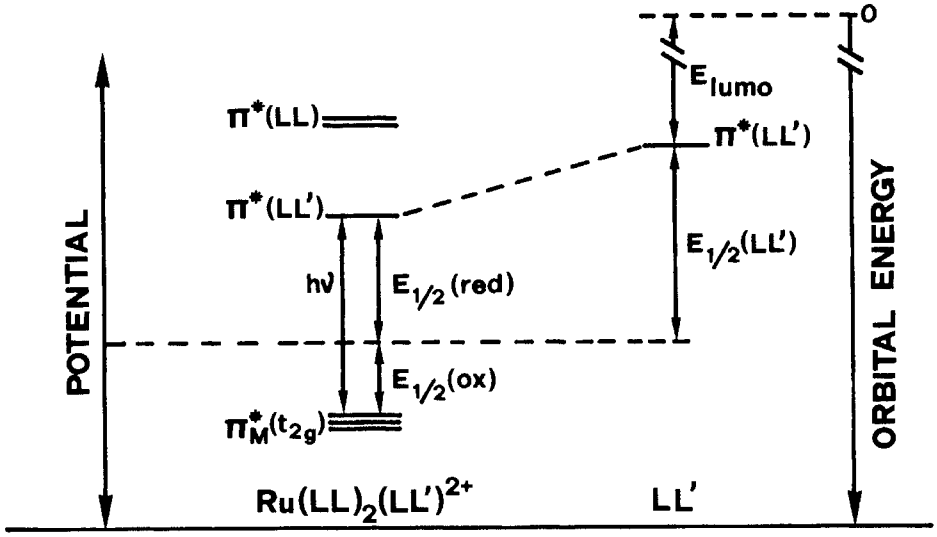

Fig. 1. Orbital diagram for the energy correlations between the calculated energy of the LUMO of LL', the electrochemical properties of the free ligand LL', and the spectroscopic and electrochemical properties of the complexes.

Table 1. Reduction Potential and Calculated Properties of the Lowest Unoccupied Molecular Orbital (LUMO) of the Free Ligands.

Ligand	$E_{1/2}(LL')$[a]	LUMO		
	V	energy/eV	(pN,pN)[b]	symmetry
a) i-biq	-2.20	-9.56	(0.35, 0.35)	ψ
b) bpy	-2.22	-9.71	(0.44, 0.44)	ψ
c) phen	-2.04	-9.77	(0.44, 0.44)	ψ
d) 4,4'-dpb	-2.06	-9.70	(0.41, 0.41)	ψ
e) bpym	-1.80	-9.94	(0.35, 0.35)	ψ
f) pq	-1.94	-10.01	(0.44, 0.34)	ψ
g) biq	-1.74	-10.19	(0.39, 0.39)	ψ
h) bpz	-1.70	-10.47	(0.45, 0.45)	ψ
i) DP	-1.18[c]	-10.66	(0.10, 0.10)	ψ
j) taphen	-1.26	-10.78	(0.12,-0.12)	χ

a) Room temperature data in acetonitrile, unless otherwise noted; b) MO atomic coefficients on chelating N positions; c) in dimethylformamide.

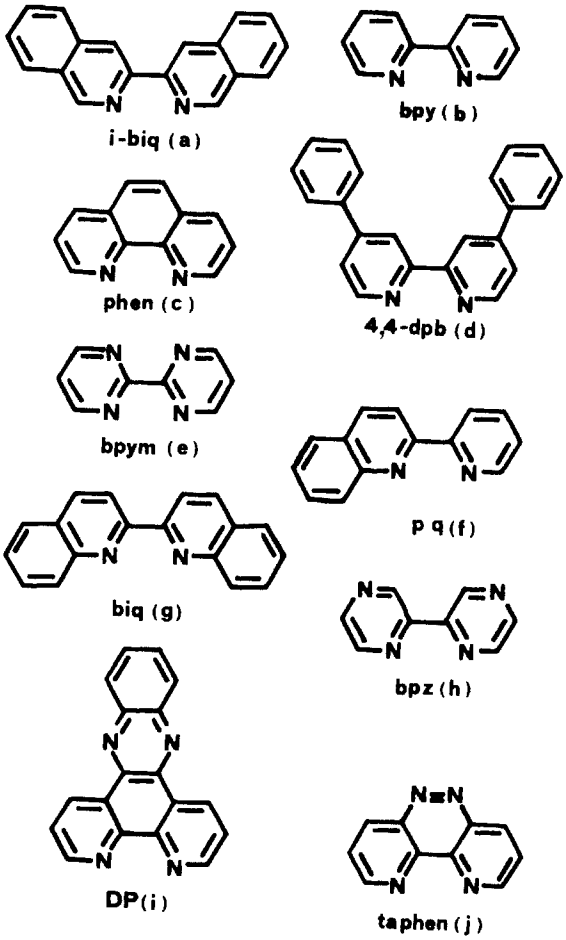

Fig. 2. Ligands (LL') and complexes: (a) i-biq and $Ru(i\text{-}biq)_3^{2+}$, (b) bpy and $Ru(i\text{-}biq)_2(bpy)^{2+}$, (c) phen and $Ru(phen)_3^{2+}$, (d) 4,4'-dpb and $Ru(bpy)_2(4,4'\text{-}dpb)^{2+}$, (e) bpym and $Ru(bpy)_2(bpym)^{2+}$, (f) pq and $Ru(bpy)_2(pq)^{2+}$, (g) biq and $Ru(bpy)_2(biq)^{2+}$, (h) bpz and $Ru(bpy)_2(bpz)^{2+}$, (i) DP and $Ru(bpy)_2(DP)^{2+}$, and (j) taphen and $Ru(bpy)_2(taphen)^{2+}$.

against the calculated $^*\pi$ (LL') LUMO of the free ligands. In both causes good correlations are found indicating that reduction occurs to the LUMO of the free ligand in the former case and to the LUMO of the complex (closely resembling that of the free ligand) in the latter

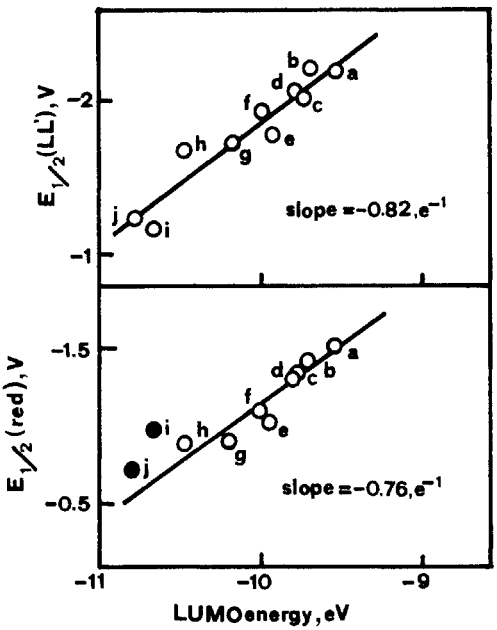

Fig. 3. See text.

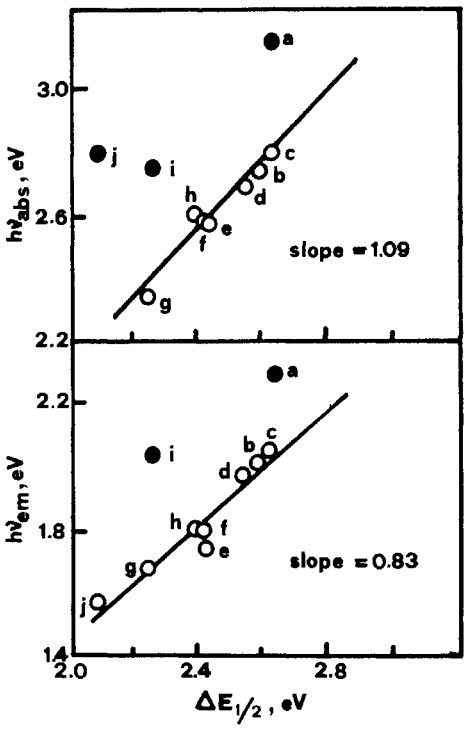

Fig. 4. See text.

case. As one can see the two correlations in Fig. 3 are characterized by different slopes. For the complexes this is likely due to the effect of interaction between occupied metal d orbitals and lowest lying unoccupied ligand orbitals of matching symmetry leading to stabilization of the former and destabilization of the latter. On the basis of energy separation arguments, the HOMO (metal centered) and LUMO (ligand centered) orbitals, Fig. 1, are expected to be most affected by this interaction.

Under C_{2v} symmetry and if a single configuration Ru --> LL' transition well approximates the excited state, the energy of the absorption (to the singlet) and emission (from the triplet) maxima of the MLCT transition involving the $^{*}\pi$(LL') LUMO is given by

$$h\nu_{abs}(S) = \Delta E_{1/2} + A$$
$$h\nu_{em}(T) = \Delta E_{1/2} + B$$

where $\Delta E_{1/2} = e[E_{1/2}(ox) - E_{1/2}(red)]$, $E_{1/2}(ox)$ is the oxidation potential of the complex, and A and B include terms that take into account solvation energies, inner and outer sphere barriers, and coulombic energies. Figure 4 shows the relation between the spectroscopic and electrochemical quantities. Linear relations are observed with a few exceptions (full points in the figures). A more detailed discussion concerning the reported deviations will be given elsewhere (Barigelletti).

As one can see the ligand structure apparently determines a number of properties of Ru-polypyridine complexes through the energy and symmetry of the $^{*}\pi$ (LL') LUMO. Based on the reported linear relations of Figures 3 and 4, it is suggested that EHMO calculations on free ligands can help in designing new complexes of the Ru-polypyridine family with predicted electrochemical and spectroscopic properties.

Acknowledgments. This work was supported by the Italian National Research Council and Ministero della Pubblica Istruzione and by the Swiss National Science Foundation.

References

Barigelletti F, Juris A, Balzani V, Belser P, von Zelewsky A (to be published)

Dodsworth ES, Lever ABP (1986) Chem Phys Lett 124: 152 and references therein

Juris A, Barigelletti F, Campagna S, Balzani V, Belser P, von Zelewsky A (to be published) Coord Chem Rev

Ohsawa Y, Hanck KW, DeArmond MK (1984) J Electroanal Chem 175: 229

TOWARDS A DYNAMIC MODEL FOR THE $RU(BPY)_3^{2+}$ SYSTEM

M.A.Collins and E.Krausz*

Research School of Chemistry, Australian National University, G.P.O.Box 4, Canberra 2601, AUSTRALIA

INTRODUCTION

The $Ru(bpy)_3^{2+}$ (RBY) chromophore/luminophore has been the subject of a great deal of study by a range of spectroscopic techniques. Some recent evidence, such as the time resolved luminescence of Ferguson and Krausz (FK) (1982, 1986a) magnetic circular polarization of luminescence (FK 1982, 1986a,b,c) anomalous Zeeman effects (FK 1987),(Krausz 1987), magnetic circular dichroism results of Ferguson, Krausz and Vrbancich (1986) and also solid phase excited state Raman by Krausz (1984), have pointed to the possibility of vibronic coupling in this system.

Summarizing our current ideas, much of the spectroscopy of RBY requires a delocalized description of the metal to ligand charge transfer excited state, yet other evidence, particularly excited state Raman measured in solution points to excitation of a single bipyridine ligand. Critical observations of luminescence changes in passing from rigid to liquid phases (FK 1986a,b,1987b) indicates an environmentally induced localization process. Some aspects of the luminescence below 10 K bear a remarkable resemblance to the changes in passing from rigid to fluid environments and in general provide evidence for strong vibronic coupling. Our contention is then, that although delocalized, the excitation has a tendency to localize, which becomes more pronounced in long lived excited states below 10 K and furthermore leads to the luminophore "digging itself a hole" in fluid environments. Thus some inherent tendency to localize is compensated by a relaxation of the environment, which itself causes a greater degree of localization etc..

In order to access the parent (vibronic) problem theoretically, a great deal of simplification of our descriptions of the system must be made. We are developing a model that contains the barest essentials of the known properties of RBY and yet can still be lead to a useful vibronic analysis. We consider a single, non-degenerate deformation mode of (each) bpy ligand and couple it to a simplified metal-ligand charge transfer excitation process. Potential surfaces of the resulting (total-molecule) modes are then derived along with vibronic energy levels. Some attempts at calculating intensity (Franck-Condon) factors between vibronic levels

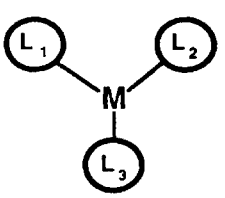

Figure 1. Model for vibronic analysis.

Photochemistry and Photophysics
of Coordination Compounds, Ed. by H. Yersin/A. Vogler

(at 0 K) are then made, in order to access the observed Stokes shift between absorption and emission. The relevance to existing experimental information is discussed and outlines of future developments given.

THEORY

Consider a trigonal arrangement of the metal M and three identical ligands $L_{1,2,3}$. In the ground electronic state, we consider just one vibrational degree of freedom associated with each ligand (or metal-ligand bond). We write

$$H_g = \sum_{n=1}^{3} p_n^2/2m + kq_n^2/2 + k'q_nq_{n-1} \quad (1)$$

where p_n is the momentum operator of the vibration on the nth ligand, q_n the vibrational coordinate, m the effective mass of the ligand vibration, k the force constant and k' is a force constant for terms proportional to q_nq_m. If all the normal modes of vibration in the ground state are degenerate, then no q_nq_m coupling terms will occur. We describe an electronic excited state of the ML_3 complex, in an exciton model, as a linear combination of excited states associated with each ligand. The excited state in our case refers to the MLCT state with the transferred electron occupying a π^* orbital.

Let $|g_n\rangle$ be the ground electronic state of ligand n and $|e_n\rangle$ the excited state of ligand n. Thus the electronic excited state is written as

$$|\Psi\rangle = c_1|e_1\rangle|g_2\rangle|g_3\rangle + c_2|g_1\rangle|e_2\rangle|g_3\rangle + c_3|g_1\rangle|g_2|e_3\rangle \quad (2)$$

a useful notation is $|g\rangle=|g_1\rangle|g_2\rangle|g_3\rangle$ and a_n^+ the raising operator which creates an excitation on the nth ligand (going from $|g_n\rangle$ to $|e_n\rangle$. Thus equation (2) becomes

$$|\Psi\rangle = \sum_{n=1}^{3} c_n a_n^+ |g\rangle \quad (3)$$

a_n is the reverse (destruction operator) and we assume that different states are orthonormal. Thus

$$\langle e_n|a_n^+a_n|e_n\rangle = \langle e_n|a_n^+|g_n\rangle = \langle e_n|e_n\rangle = 1 \quad (4)$$

and as no state exists below the ground state $a_n|g_n\rangle = 0$ so that

$$\langle g_n|a_n^+a_n|g_n\rangle = \langle e_n|a_n^+a_n|g_n\rangle = \langle g_n|a_n^+a_n|g_n\rangle = 0 \quad (5)$$

When the nth ligand is excited, the vibrational energy associated with q_n is changed: the Born-Oppenheimer (BO) potential energy surface for (say) ring

stretching is different for excited state bpy^- from ground state bpy. We denote the change in potential energy for the n'th ligand vibration as $\Delta V(q_n)$. Thus we can write the electronic Hamiltonian of the excited ML_3 complex as

$$H = H_g + \sum_{n=1}^{3} a_n^+ a_n \Delta V(q_n) \qquad (6)$$

The number operator $(a_n^+ a_n)$ will give the eigenvalue 1 if the nth ligand is excited so that the total energy will be changed by $\Delta V(q_n)$. We now consider the effect of resonant energy transfer. Since all three ligands are similar, electronic excitation can be transferred from one ligand to another. This sharing changes the total energy. The operator $a_{n-1}^+ a_n$ acting on $|\Psi\rangle$ moves the excitation from the nth to the n-1th ligand. Thus we arrive at our Hamiltonian

$$H = \sum_{n=1}^{3} \{p_n^2/2m + kq_n^2/2 + k' q_n q_{n-1} + a_n^+ a_n \Delta V(q_n) + M[a_{n-1}^+ a_n + a_n^+ a_{n-1}]\} \qquad (7)$$

where M is the energy gain (or loss) due to resonant energy transfer. Combining equations (3) and (7) we can write the BO energy surface as the expectation value of the Hamiltonian for the electronic state, neglecting the nuclear kinetic energy (p_n) in (7); treating the nuclear coordinates q_n as parameters we derive

$$\langle\Psi|H|\Psi\rangle = \sum_{n=1}^{3} kq_n^2/2 + k' q_n q_{n-1} + |c_n|^2 \Delta V(q_n) + M[c_n^* c_{n-1} + c_{n-1}^* c_n] = E \qquad (8)$$

Solving the secular equation $H|\Psi\rangle = \varepsilon|\Psi\rangle$ gives $E = \varepsilon + \sum kq_n^2/2 + k' q_n q_{n-1}$ where ε satisfies

$$\begin{bmatrix} \Delta V(q_1)-\varepsilon & M & M \\ M & \Delta V(q_2)-\varepsilon & M \\ M & M & \Delta V(q_3)-\varepsilon \end{bmatrix} \begin{pmatrix} c_1 \\ c_2 \\ c_3 \end{pmatrix} = 0 \qquad (9)$$

The cubic equation in ε is easily soluble if $\Delta V_{1,2,3}=0$, giving the electronic energies $\varepsilon_{1,2,3} = 2M, -M, -M$ (the $-M$ level is doubly degenerate). If ΔV is non vanishing, we assume it can be expanded in a power series

$$\Delta V(q) = v_0 + v_1 q + v_2 q^2 + \ldots \qquad (10)$$

for simplicity we truncate the series after the quadratic term; significant vibronic effects can be described at this level of approximation. The solutions to the cubic equation arising from the secular determinant can be evaluated, using this truncation, by considerable tedious but computer assisted algebraic manipulation, to obtain the energies $\varepsilon_{1,2,3}$

$$\varepsilon_1 = v_0 + 2M + v_1\rho_1/\sqrt{3} + v_2(\rho_1^2+\rho_2^2+\rho_3^2)/3 + v_1^2(\rho_2^2+\rho_3^2)/9M$$

$$\varepsilon_2 = v_0 - M + v_1\rho_1/\sqrt{3} + v_2(\rho_1^2 + r^2)/3 + |v_1|r/\sqrt{6} - r^2v_1^2/18M + [v_2|v_1|/3v_1 - v_1^2/18M]r^2\cos 3\theta \qquad (11)$$

$$\varepsilon_3 = v_0 - M + v_1\rho_1/\sqrt{3} + v_2(\rho_1^2+r^2)/3 - |v_1|r/\sqrt{6} - r^2v_1^2/18M + [-v_2|v_1|/3v_1 + v_1^2/18M]r^2\cos 3\theta$$

where $\rho_{1,2,3}$ are the normal coordinates with frequencies $\omega_{1,2,3}$ defined as

$$\rho_1 = (q_1+q_2+q_3)/\sqrt{3},\ \rho_2=(q_1-q_2/2-q_3/2)\sqrt{2}/\sqrt{3} \text{ and } \rho_3=(q_2-q_3)/\sqrt{2} \qquad (12)$$

and the polar coordinates have the usual definition, $\rho_2=r\cos\theta$ and $\rho_3=r\sin\theta$ The energy surface for ε_3 has minima at $r\neq 0$. The surface has three local minima as a function of θ, the well known Mexican hat surface, Fisher (1984).

Introducing dimensionless variables, and T being the nuclear kinetic energy operator, we write

$$h_1 = (T+\varepsilon_1-v_0-2M)/\hbar\omega_2\ ;\quad h_2 = (T+\varepsilon_2-v_0+M)/\hbar\omega_2\ ;\quad h_3 = (T+\varepsilon_3-v_0+M)/\hbar\omega_2$$

$$x_n = \sqrt{(m\omega_2/\hbar)}\rho_n\ ;\quad R = \sqrt{(m\omega_2/\hbar)}r\ ;\quad P_n = p_n/\sqrt{(m\omega_2\hbar)} \qquad (13)$$

$$\mu_1 = v_1/\sqrt{(3m\omega_2^3\hbar)}\ ;\quad \mu_2 = 2v_2/(3m\omega_2^2)\quad \mu_3 = v_1^2/(9Mm\omega_2^2)$$

In dimensionless polar coordinates P_R, R, θ, P_θ the nuclear dynamics are described by the three nuclear BO Hamiltonians

$$h_1 = [P_1^2+(\omega_1x_1/\omega_2)^2]/2+\mu_1x_1+\mu_2x_1^2/2+[P_R^2+P_\theta^2/R^2]/2+R^2[1/2+\mu_2/2+\mu_3]$$

$$h_2 = [P_1^2+(\omega_1x_1/\omega_2)^2]/2+\mu_1x_1+\mu_2x_1^2/2+[P_R^2+P_\theta^2/R^2]/2+R^2[1+\mu_2-\mu_3]/2 + |\mu_1|R/\sqrt{2}+[\mu_2|\mu_1|/\mu_1-\mu_3]R^2\cos(3\theta)/2 \qquad (14)$$

$$h_3 = [P_1^2+(\omega_1x_1/\omega_2)^2]/2+\mu_1x_1+\mu_2x_1^2/2+[P_R^2+P_\theta^2/R^2]/2+R^2[1+\mu_2-\mu_3]/2 - |\mu_1|R/\sqrt{2}+[-\mu_2|\mu_1|/\mu_1+\mu_3]R^2\cos(3\theta)/2$$

DISCUSSION

The three electronic eigenvalues $\varepsilon_{1,2,3}$ determine three electronic states at each nuclear configuration via the secular equations (9). These states form a complete

basis for the exact vibronic wavefunctions, Fisher (1984), which have yet to be evaluated. Here we discuss some features of the adiabatic nuclear dynamics and eigenstates determined by the derived BO Hamiltonians $h_{1,2,3}$

The nondegenerate vibration, with coordinate x_1, shows the same origin and frequency shifts in all three excited electronic states: The ground and excited state surfaces are as shown in Figure 2 unless $\mu_2 < -(\omega_1/\omega_2)^2$, when anharmonic terms are significant and the excited state surface may display a double well form. The displacement of the minimum, proportional to μ_1, will contribute to a progression of this mode in the absorption spectrum as well as a Stokes shift of the order of $(\omega_2\mu_1/\omega_1)^2-(\omega_2/\omega_1)$.

The vibrations with coordinates x_2 and x_3 are degenerate in the ground state and remain so in the state described by h_1; where only a frequency shift occurs. However these vibrations effect a Jahn-Teller distortion which splits the degeneracy of the electronic states of energy -M, to produce distinct BO Hamiltonians h_2 and h_3. If only <u>linear</u> electron-nuclear coupling is included, $\mu_2=\mu_3=0$, the degeneracy of the vibrational coordinate is still retained in both h_1 and h_2. The radial dependence of these potential energy surfaces is shown in Figure 3, clearly illustrating the displacement of the minimum in h_3. While vibronic coupling between states on these two surfaces will be significant for all vibrational levels, the lowest energy levels should be approximately described within the BO approximation if the energy splitting, proportional to μ_1^2, is sufficiently large. Assuming that $\mu_1 \geq 2$ and

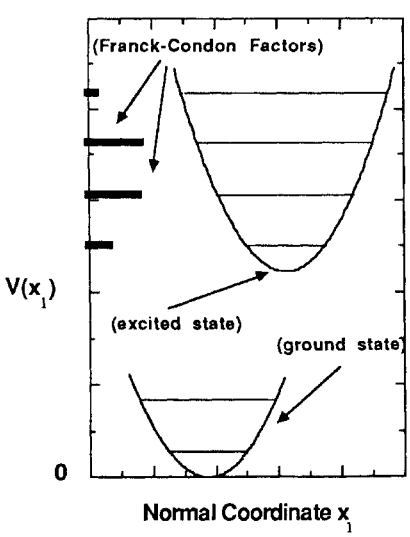

Figure 2 Potential energy as a function of the non-degenerate coordinate.

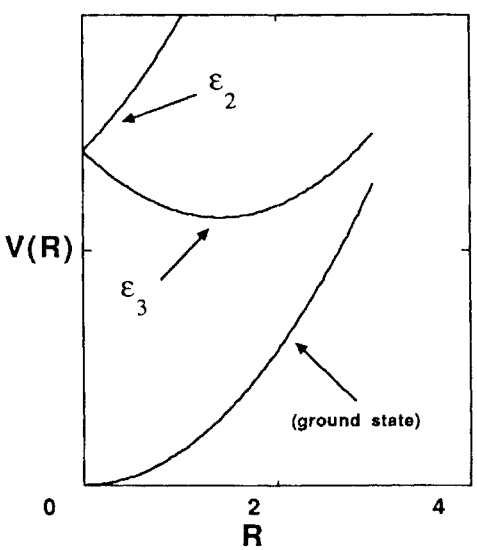

Figure 3 Potential energy as a function of the "Mexican Hat" radius.

$\mu_2,\mu_3 \neq 0$, the Jahn-Teller distortion is expected to produce a Stokes shift of the order of $3\mu_1^2/4-2$. Interestingly, this contribution to the total Stokes shift may be smaller that the contribution caused by the origin shift of the nondegenerate vibration x_1.

When $\mu_2=\mu_3=0$, the motion of the angular coordinate θ is that of a free rotor. However, the second order coupling constants μ_2 and μ_3 introduce a potential proportional to $\cos(3\theta)$ which hinders the rotational motion. For excited states which involve a electron transfer to the bpy ligand, we expect that $\mu_1,\mu_2>0$ and $\mu_3>0$, so that the two terms in h_3 proportional to $\cos(3\theta)$ may be of opposing signs. The direction of the distortion associated with this angle θ would depend on the actual magnitude of μ_2 and μ_3. We note that the angular potential energy is proportional to R^2, so that the $\cos(3\theta)$ term is much more significant in the third excited state where the origin shift increases the average value of R.

While the angular momentum is not constant when $\mu_2,\mu_3 \neq 0$, it fluctuates about a quantized value, (l^2, $l=1,2,3...$) when μ_2 and μ_3 are small. In this limit, the radial motion in h_3 can be approximately described in terms of the radial potential in Figure 3, while the angular motion is that of a <u>hindered</u> rotor at the average radius R. The wavefunctions of this hindered rotor may be obtained in terms of Mathieu functions, to describe the tunnelling and "free" states below and above the maxima in $\cos(3\theta)$. Without going into details the Franck Condon (FC) factors for transitions from the ground electronic/vibrational state, where $l=0$, to the rotor states of h_3 can be evaluated. It is straightforward to show that the FC factor is of the order of 1 if $l \simeq 0$ in ε_3. The factor is 0 if $l \simeq 1$, $(\mu_3-\mu_2|\mu_1|/\mu_1)^2$ if $l \simeq 2$ and so on. While one can infer from the form of the radial potential energy that the <u>radial</u> wavefunction FC factors for transitions to upper vibrational levels of ε_3 are favorable, only the component of these levels with $l \simeq 0$ are readily excited.

Localization corresponds to trapping within a single minimum of the $\cos(3\theta)$ potential well within the state described by h_3. Of course eigenstates retain the trigonal symmetry of the Hamiltonian so that no eigenstate can be localized within one well. Any localized wavefunction is therefore a time dependent state. If one considers the excitation to be initially localized, the corresponding wave packet will spread on a timescale determined by tunnelling between the equivalent minima in the $\cos(3\theta)$ potential. It is clear that this tunnelling time is long when μ_1 is large <u>and</u> $\mu_3-\mu_2|\mu_1|/\mu_1$ is large. The dominant influence is of the linear coefficient v_1.

FUTURE DIRECTIONS

Analytic solutions to the eigenstates and FC factors for the <u>radial</u> functions are difficult to evaluate. Numerical evaluation of the <u>full</u> vibronic problem is now

feasible as we have analytic forms for the electronic matrix elements and potential energy surfaces, together with a BO basis set. Numerical calculation will also allow evaluation of magnetic moments (and polarizations) of eigenstates. These properties in particular will be strongly influenced by vibronic coupling parameters and should allow a useful description of recent experiments to be developed.

REFERENCES

Ferguson J, Krausz E, (1982) The assignment of the Luminescent States of $Ru(bpy)_3^{2+}$. MCPL and Time-Resolved Luminescence at 2K, Chem Phys Lett 93: 21-25.

Ferguson J, Krausz E, (1986a) Time Resolved Luminescence and MCPL of $Ru(bpy)_3^{2+}$ in Glassy Solvents at the Fluid-Glass Transition, Chem Phys Lett 127: 551-556.

Ferguson J, Krausz E, (1986b) MCPL Evidence for the Transition from Delocalized to Localized Luminescent States of $Ru(bpy)_3^{2+}$ in Glass-Fluid Media, Inorg Chem 25: 3333-3335.

Ferguson J, Krausz E, (1986c) The Excitation Dependence of the Luminescence and MCPL of $Ru(bpy)_3^{2+}$ in Rigid Solutions. J Lumin 36: 129-141.

Ferguson J, Krausz E, (1987a) Magnetically Perturbed, Temperature-Dependent and Time Resolved Aspects of the Polarized Luminescence of $Ru(bpy)_3^{2+}$ Below 10 K. Chem Phys 112: 271-283.

Ferguson J, Krausz E, (1987b) Absorption, Luminescence and Magnetic Circular Polarized Luminescence of Dicarboethoxy Derivatives of $Ru(bpy)_3^{2+}$ in Rigid and Fluid Solutions: Evidence for Environmentally Induced Charge Localization. J Phys Chem 91: (in press).

Ferguson J, Krausz E, Vrbancich J, (1986) Magnetic Circular Dichroism and the Assignments of Metal-Ligand Charge Transfer States in $Ru(bpy)_3^{2+}$ and Related Systems, Chem Phys Lett 131: 463-467.

Fisher G,(1984) Vibronic Coupling, Academic Press, London.

Krausz E, (1984) Excited State Raman Spectra in the Luminescent States of $Ru(bpy)_3^{2+}$. Chem Phys Lett 116: 501-504.

Krausz E, (1987) Zeeman Effects in Absorption and Luminescence of the Zero Phonon lines in $Ru(bpy)_3(PF_6)_2$. Chem Phys Lett (in press).

BROAD-BAND EMISSION AND ZERO-PHONON LINES OF SINGLE-CRYSTAL $[Ru(bpy)_3](PF_6)_2$ - A COMPARISON

E.Gallhuber, G.Hensler, and H.Yersin

Institut für Physikalische und Theoretische Chemie, 8400 Regensburg, FRG

INTRODUCTION

In this paper we report on results of investigations on neat single-crystal $[Ru(bpy)_3](PF_6)_2$. For this compound the crystal structure has been determined[1]: The complex ions lie on D_3 sites and all molecular threefold axes are parallel to the crystallographic c axis. Thus, $[Ru(bpy)_3](PF_6)_2$ single crystals are well-suited for polarized spectroscopy, which allows grouptheoretical assignments of the excited states by use of the selection rules[2]. Moreover, single-crystal spectra may be much better resolved due to a reduction of inhomogeneous broadening. Indeed, at low temperatures it is possible to resolve the zero-phonon lines[3,4], which delivers considerably more information about the lowest exited states than had been deduced from the broad-band spectra of the complex diluted in organic glasses[5] or host matrices[6]. In the following we want to demonstrate the parallelism between the broad-band spectra and the zero-phonon lines of $[Ru(bpy)_3](PF_6)_2$ with respect to their temperature dependence and magnetic-field behavior.

TEMPERATURE DEPENDENCE

Broad-band Spectra

Figure 1 shows the temperature-dependent development of the total emission spectra ($E \perp c$, E = electric field vector) run at low spectral resolution. The main band at 1.4 K (band I) has its maximum at 585 nm. On temperature increase band II grows in on the blue side at 570 nm and becomes dominant above 2 K. The growing in of band II is accompanied by an intensity increase by a factor of about 4 to 5 up to 10 K.

This temperature dependence is readily interpreted by a two-state model[2,5,6], in which the transition from the second state is considerably more allowed than the transition from the lower one, and in which the different transitions involve different vibronic patterns as is shown schematically in the inset of Fig. 1. Thus, the blue shift on temperature increase results from a displacement of the centre of the

Photochemistry and Photophysics
of Coordination Compounds, Ed. by H. Yersin/A. Vogler

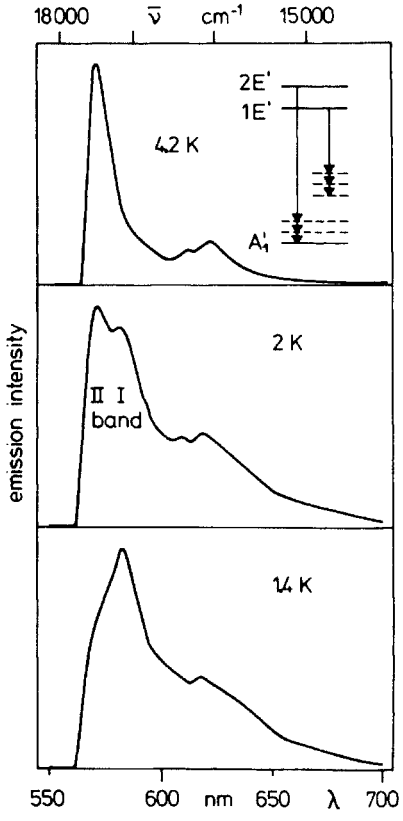

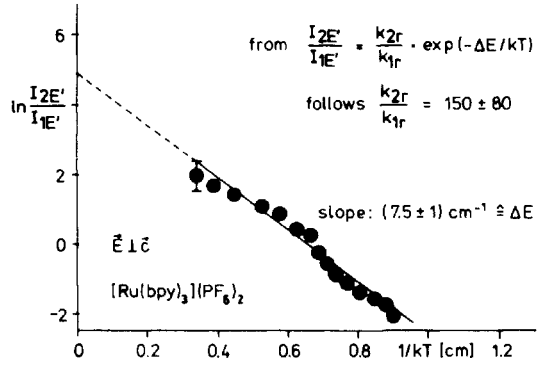

Fig. 2. Arrhenius plot of the ratio of the broad-band emission intensities of the two lowest excited states 1E' and 2E'. The spectra (see Fig. 1) were decomposed in analogy to the ref.[6]. As the spectral band shapes of the "pure" 1E' and 2E' spectra are not exactly known, the error limits for the slope and the intercept of the calculated straight line are considerable.

Fig. 1. E⊥c-polarized emission spectra of [Ru(bpy)$_3$](PF$_6$)$_2$ single crystals at low temperatures. The spectra are normalized to their maximum heights. The intensities of the corresponding E∥c-polarized spectra are generally weaker by a factor of at least 10.

unresolved vibronic distribution. As the low-temperature ($T \leq 10$ K) emission spectra are mainly E⊥c-polarized (the intensities of the corresponding E∥c-polarized spectra being weaker by a factor of at least 10) the two emitting states are assigned both to E' states (in the symmetry group D_3').

In order to obtain quantitative results, we analysed the emission spectra by decomposing them into two separate components due to emission from the two states 1E' and 2E', respectively. An Arrhenius plot of the intensity ratio of these two components is shown in Fig. 2. The straight line through the experimental points has a slope of (7.5 ± 1) cm^{-1}, which represents the activation energy for the thermal population of the second state from the lower one. Further, a value of about 5 is found for the intercept, from which a value of the order of hundred is obtained for the ratio k_{2r}/k_{1r} of the radiative rates for the two transitions under consideration.

A comparison of our single-crystal data to emission data of the complex diluted in a $[Zn(bpy)_3]SO_4$ matrix[6] shows that the temperature dependence of the spectra is identical and that the quantitative results are comparable. Therefore, it is near at hand to conclude that also in the neat material the emission properties can be described to base on excited complexes which are not subject to significant cooperative solid-state interactions (see also the ref.[7]).

Zero-phonon Lines

Under high resolution a sharp fine structure is observable on the very blue side of the emission bands of $[Ru(bpy)_3](PF_6)_2$ single crystals[3]. This fine structure essentially consists of a pair of narrow lines, denoted as lines I and II in Fig. 3, with halfwidths of 2 cm^{-1} and an energy separation of 6.9 cm^{-1}. The two lines are polarized with $E \perp c$, the intensity of the parallel polarization again is considerably weaker (by a factor of at least 20). Further, the intensities of the two lines exhibit a rather drastic temperature dependence: On tempera-

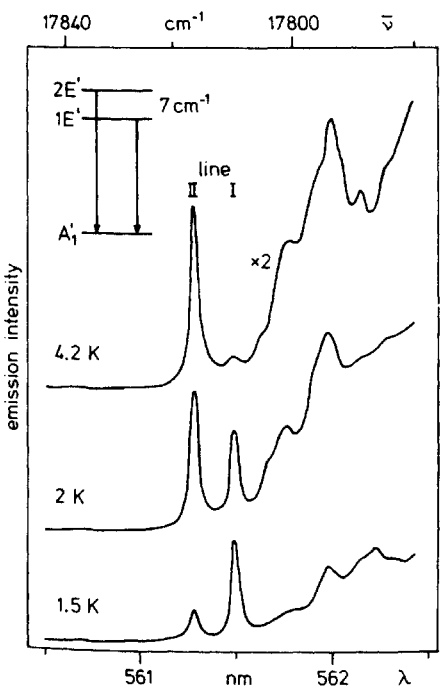

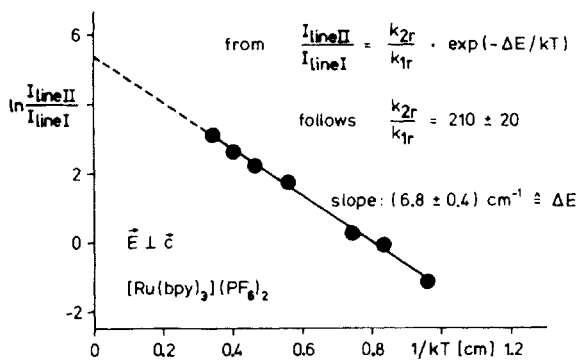

Fig. 4. Arrhenius plot of the intensity ratio of the two zero-phonon lines. Note that the calculated activation energy equals the spectral energy separation of the two lines and is in accordance with the value calculated from the temperature dependence of the broad-band spectra.

Fig. 3. High-energy part of the highly resolved $E \perp c$-polarized emission of single-crystal $[Ru(bpy)_3](PF_6)_2$. The intensities are comparable after multiplication with the given factor. The two zero-phonon lines are situated at 17809 cm^{-1} (line I) and 17816 cm^{-1} (line II).

ture increase from 1.5 K, the higher-energy line II grows in to the expense of line I (see Fig. 3).

As these two lines are the emission features to highest energy, they are assigned to the zero-phonon transitions from the two lowest emitting states (for further arguments see below and the ref.[3,4,7]). This means that the two lines directly reflect the properties of the exited electronic states. Moreover, by the detection of the zero-phonon lines we are able to give both the absolute energies of the two lowest charge-transfer transitions as well as the energy separation of these two states of $[Ru(bpy)_3](PF_6)_2$ directly from the spectra.

Figure 4 shows an Arrhenius plot of the intensity ratio of the two zero-phonon lines. A straight line is obtained with a slope of 6.8 cm^{-1} which is the same value as the observed spectral separation of the two lines. Assuming equal electron-phonon coupling strengths for the two transitions, the total emission intensities in the Boltzmann law may be replaced by the intensities of the zero-phonon lines. By this a value of about 210 is calculated for the ratio of the radiative rates (see Fig. 4). These values should be compared to the values obtained from the analysis of the broad-band spectra (see Fig. 2). Since they fit quite nicely, the parallelism in the temperature dependence of the broad-band emission and the zero-phonon line emission is clearly demonstrated.

The above model is further supported by the results shown in Fig. 5, from which it can be seen that there is a sharp line in the absorption as well as in the excitation spectrum just at the same energy position as the emission line II[4,7]. This is the result expected for a

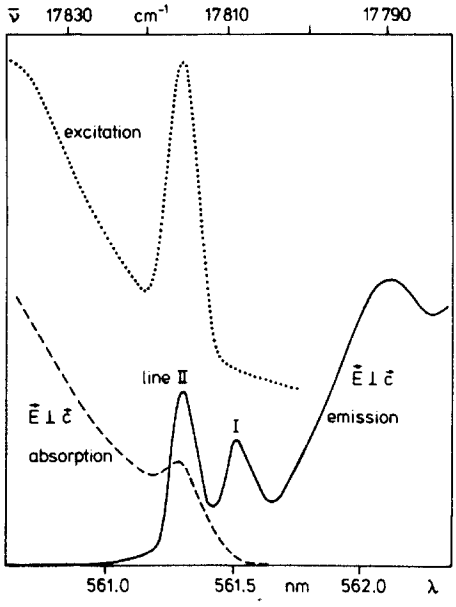

Fig. 5. Highly resolved emission, absorption and excitation spectra in the region of the zero-phonon lines for T = 2 K. In absorption as well as in excitation a sharp line is observed corresponding to emission line II, while this is not the case for line I (see text). The molar extinction coefficient of absorption line II is about 5 l/mol*cm (see the ref.[4]). The excitation line II is observed at the detection wavelength 570 nm as well as at 585 nm. Excitation into line II yields the same emission spectrum as is obtained for high-energy excitation (e.g. in the UV region).

zero-phonon line, because for a purely electronic transition absorption and emission necessarily coincide. The fact that there is no absorption and excitation line corresponding to the emission line I is immediately understood realizing that the radiative transition probability and thus the extinction coefficient is lower by more than two orders of magnitude compared to transition II.

MAGNETIC-FIELD BEHAVIOR

Broad-band Spectra

A magnetic field H oriented perpendicular to the c axis has drastic effects on the low-temperature emission spectra[8,9] as demonstrated in Fig. 6. It is observed that the blue band II grows in at T = 2 K, when the magnetic-field strength is raised. Thereby the total emission intensity is enhanced by a factor of about 5 up to H = 6 T, paralleling the development on temperature increase.

This result is interpreted by a mixing of the wavefunctions of the two lowest excited states under the action of the magnetic field[6,8,9]. Thus, the emission properties of the second state (for example the higher transition probability to the ground state) are effectively donated to the lower state (and vice versa). The small energy difference of about 10 cm^{-1} between the thermally induced band II (emitted by the higher state) and the magnetically induced band II (emitted by the lower state) cannot be detected in the broad-band spectra.

The extent of the mixing of the wavefunctions of the two interacting states can be estimated from the magnetic-field dependence of the broad-band emission: At a magnetic-field strength of 6 T, the mixing should be almost complete. That is the two states are predicted to display nearly equal photophysical properties in sharp contrast to the situation at zero magnetic field.

Zero-phonon Lines

Figure 7 shows that the magnetic-field effect is observed still more drastically with the zero-phonon emission lines[8,9]. At T = 4.5 K and zero magnetic field the emission is predominantly due to the thermally popu-lated second state and thus line I is only very weak (see Fig. 3). Application of a magnetic field ($H \perp c$) leads to the growing in of line I to the expense of line II. Concomitantly the two zero-phonon lines move apart.

As has been argued above, the magnetic field removes part of the forbiddeness of the transition from the lower state. Therefore, line I

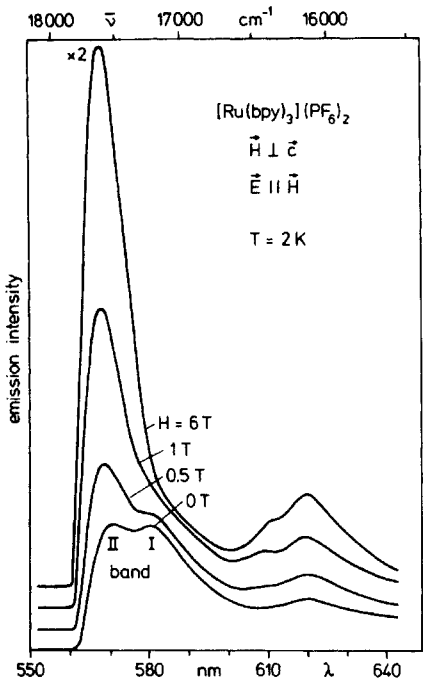

Fig. 6. Magnetic-field dependence the broad-band emission at 2 K. No magnetic-field effect was observed in E∥c = E⊥H (for H⊥c). As the magnetically induced effects for H∥c were very weak, they may interpreted to be due to slight misalignments of the crystals.

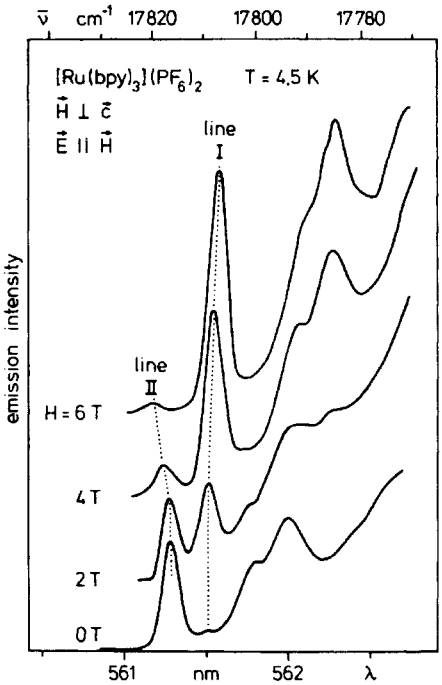

Fig. 7. Magnetic-field dependence of the zero-phonon emission lines at 4.5 K. Note the Zeeman effect and the rather drastic change of the line pattern. See the legend of Fig. 6 for further explanation.

gains intensity. Moreover, the interaction of the two states causes a Zeeman effect. Thus, the intensity of line II decreases further because of lower thermal population of the second state.

Figure 8 demonstrates that the energy separation ΔE of the zero-phonon lines increases from 7 cm^{-1} at zero field to 13 cm^{-1} at H = 6 T. Furthermore, the relation between energy separation and magnetic field is not linear, as it is expected for two (zero-field split) states interacting by the magnetical perturbation. With the knowledge of this plot the relative thermal populations of the two states can be calculated as a function of the magnetic-field strength. Then using the experimental results for the intensity ratio of the two zero-phonon lines the magnetic-field dependence of the ratio of the radiative rates is obtained. From Fig. 9 it is found that this ratio decreases from a value of about 210 (see Fig. 4) at zero magnetic field to a value of

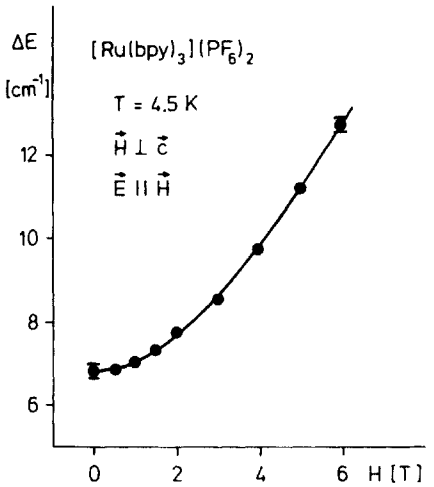

Fig. 8. Magnetic-field dependence of the energy separation ΔE between the two zero-phonon lines.

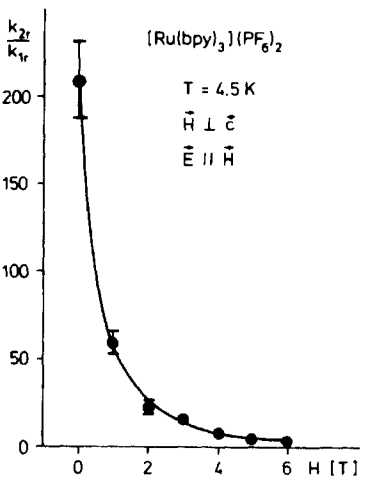

Fig. 9. Magnetic-field dependence of the ratio of the radiative rates for the transitions from the two lowest excited states.

roughly 2 at T = 6 T. This means that at 6 T the radiative transition probability from the lower state is nearly the same as that from the second state, confirming the prediction made from the magnetic-field behavior of the broad-band spectra.

In order to further support the interpretation of the observed magnetic-field effects, Fig. 10 shows an important issue. For the first time the effect of magnetic-field induced absorption is demonstrated[10]. Whereas the absorption line corresponding to the line I cannot be detected at zero magnetic-field this absorption line is induced by strong magnetic fields. The two absorption lines exhibit the same Zeeman effect as the two emission lines. At H = 6 T the extinction coefficients of the two absorption lines are nearly equal, which again indicates almost complete mixing of the wavefunctions.

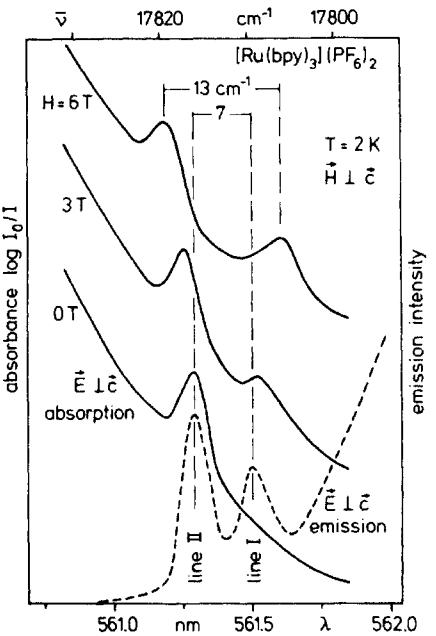

Fig. 10. Zero-phonon absorption for various magnetic-field strenghts. Line I is induced in absorption by magnetic fields. The line emission at zero field is shown for comparison.

CONCLUSION

By carrying out polarized spectroscopy on single crystals of neat $[Ru(bpy)_3](PF_6)_2$ it is possible to gain new information about the lowest excited states and the corresponding optical transitions of the $[Ru(bpy)_3]^{2+}$ chromophore. Especially, the detection of the zero-phonon lines in emission and absorption lead to direct insight into the photophysical behavior. It was found that the two lowest excited states are separated by 7 cm^{-1} and exhibit rather different emission properties, the radiative rate from the lower excited state being less by a factor of about 210 than that from the second state.

Strong magnetic fields couple the two states. At a magnetic-field strength of 6 T, the wavefunctions of the two states are almost completely mixed. As a consequence, their emission properties become very similar. Moreover, magnetically induced absorption is observed for the lower state.

Finally, the parallelism between the broad-band spectra and the zero-phonon lines with respect to their temperature dependence and their magnetic-field behavior was demonstrated, showing that the fine structure and the broad bands are coupled to the excited states of the same chromophores.

ACKNOWLEDGEMENTS

The authors thank Prof. Dr. G. Gliemann for support of this work. The "Studienstiftung des Deutschen Volkes" is acknowledged for financial grant by one of the authors (E.G.).

REFERENCES

(1) D.P. Rillema, D.S. Jones, H.A. Levy, J. Chem. Soc. Chem. Commun., 1979, 849.
(2) H. Yersin, E. Gallhuber, J. Am. Chem. Soc., 1984, 106, 6582.
(3) G. Hensler, E. Gallhuber, H. Yersin, Inorg. Chim. Acta, 1986, 113, 91.
(4) H. Yersin, E. Gallhuber, G. Hensler, Chem. Phys. Lett., 1987, 134, 497.
(5) G.D. Hager, G.A. Crosby, J. Am. Chem. Soc., 1975, 97, 7031.
(6) D.C. Baker, G.A. Crosby, Chem. Phys., 1974, 4, 428.
(7) H. Yersin, G. Hensler, E. Gallhuber, Inorg. Chim. Acta, 1987, in press.
(8) E. Gallhuber, G. Hensler, H. Yersin, J. Am. Chem. Soc.,1987, 109, in press.
(9) E. Gallhuber, G. Hensler, H. Yersin, XIth IUPAC Symposium on Photochemistry, Lisbon 1986, Volume of Abstracts, p. 384.
(10) G. Hensler, E. Gallhuber, H. Yersin, Inorg. Chem., 1987, in press.

MAGNETIC-FIELD EFFECTS AND HIGHLY RESOLVED VIBRONIC STRUCTURE OF $[Ru(bpy)_3]^{2+}$

H.Yersin, E.Gallhuber, and G.Hensler

Institut für Physikalische und Theoretische Chemie, 8400 Regensburg, FRG

INTRODUCTION

Up to now only little information is available for $[Ru(bpy)_3]^{2+}$ about the vibrational couplings to the electronic transitions between the ground state and the different excited states. More comprehensive data about the vibronic structures, for example, could deliver information about differences in equilibrium geometries of the ground state and the excited states or might allow a more reliable treatment of the nonradiative decay rates.[1,2] Moreover, a detailed knowledge about the vibronic components of the spectra is an essiatial requirement for a well-founded assignment of absorption or emission spectra.[3] But in most cases the published spectra are only badly resolved. This results mainly from a superposition of vibronic structures corresponding to different electronic transitions, from inhomogeneous broadening effects, and from relatively large electron phonon coupling strengths. However, under suitable conditions spectroscopic investigations with single crystals at low temperatures may deliver highly resolved spectra of the chromophores. Indeed, it has been shown that single crystals of $[Ru(bpy)_3]X_2$ (with $X = ClO_4$, PF_6) represent promising compounds[3,4] and it is subject of this paper to focus on their vibronic structures.

RESULTS and DISCUSSION

Fig. 1a reproduces the highly resolved emission of single-crystal $[Ru(bpy)_3](ClO_4)_2$ at T = 2 K. At the high energy side one observes two lines I and II, being $\Delta E = 8.2\ cm^{-1}$ apart (see the enlarged spectrum at the left hand side of the diagram). Both lines have been assigned to purely electronic zero-phonon transitions of Ru4d → bpyπ^* triplet CT-character. The main reason for a classification of these as 0-0 lines comes from the fact that emission and absorption are found exactly at the same energies. (For further arguments see ref.[4,5] and the discussion below.) These two lowest excited states |I> and |II> are (relative to the long emission lifetime) in thermal equilibrium.

Photochemistry and Photophysics
of Coordination Compounds, Ed. by H. Yersin/A. Vogler

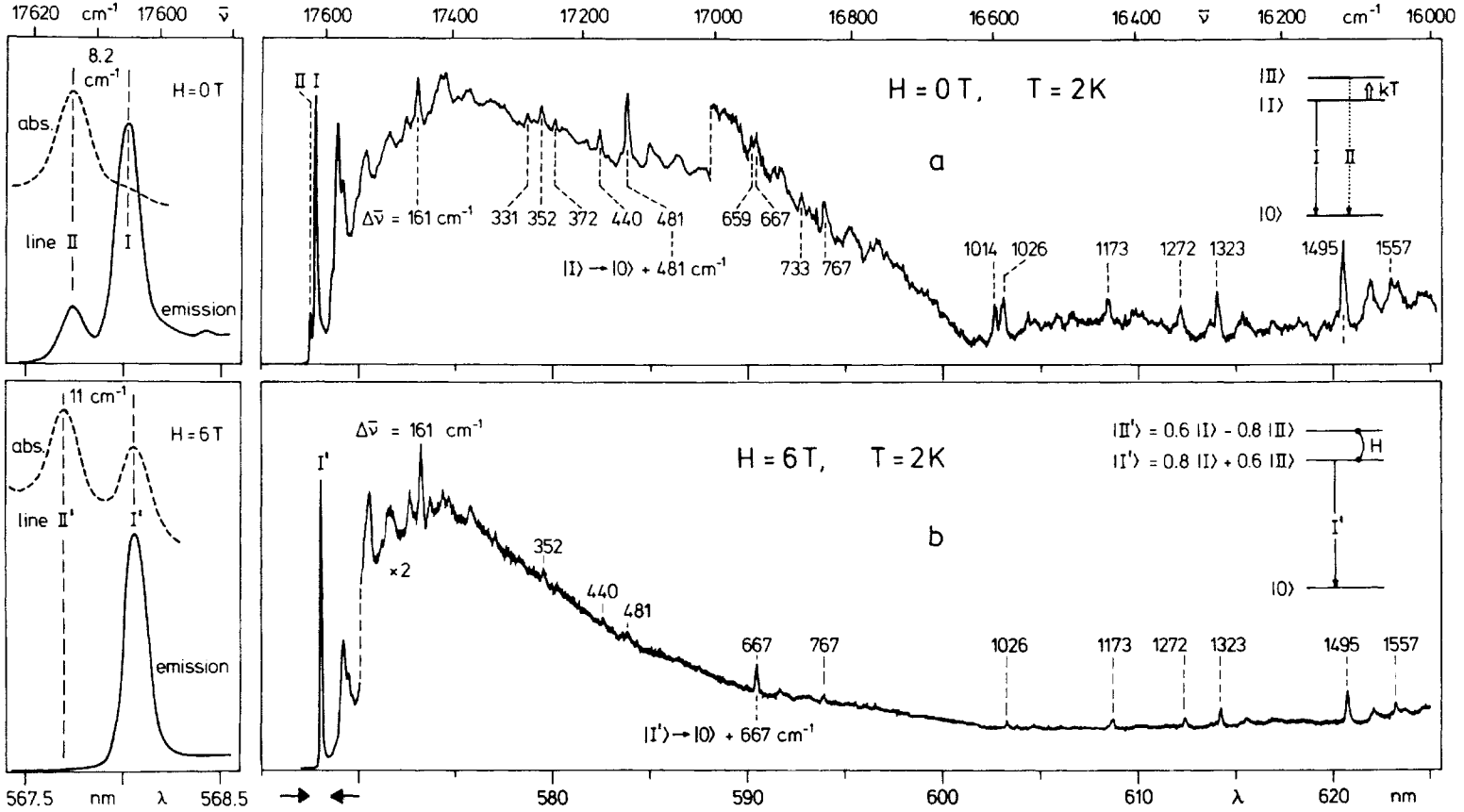

Figure 1. Emission and absorption (abs.) spectra of single-crystal $[Ru(bpy)_3](ClO_4)_2$ (T = 2 K) at H = 0 T and H = 6 T, respectively. The left hand scales of wavelengths are strongly enlarged. The states |I'> and |III'> result from the magnetic-field induced mixing of the wavefunctions (see the insets). The experimental conditions are summarized in ref.[4].

Therefore, at T = 2 K the emission from |II> is essentially frozen out and the spectrum results mainly from |I>.

The energies of the dominating peaks and their energy separations to line I (at 17605 cm^{-1}) are summarized in Table I and compared to the energies of Raman modes[6]. The good agreement between these energies safely allows to assign the observed modes to vibrational modes coupled to the zero-phonon transition. Further, this assignment is supported by the fact that the Raman intensities of just these modes are strongly enhanced in the resonance Raman experiment[6]. Moreover, the close correspondence between the energies of the vibronic peaks and the Raman modes also substantiates the assignment of line I as a zero-phonon transition.

Table I. Vibrational modes of $[Ru(bpy)_3](ClO_4)_2$ at T = 2 K

Emission peaks [cm^{-1}]	Energy separations [cm^{-1}]	Raman data [6] [cm^{-1}]	Resonance Raman enhancement factors [6] and remarks
17605 (line I)	0	-	zero-phonon line
17444	161	165	
17402	203	198	4
17274	331	337	8
17253	352	-	
17233	372	372	4
17165	440	(464)	(20)
17124	481	478	6 $\|I\rangle \rightarrow \|0\rangle + 481\ cm^{-1}$
16946	659	659	4
16938	667	668	150 $\|I'\rangle \rightarrow \|0\rangle + 667\ cm^{-1}$
16872	733	730	>5
16838	767	765	2
16591	1014	1012	4
16579	1026	1025	8
16432	1173	1173	20
16333	1272	1278	6
16282	1323	1317	12
16110	1495	1490	25
16048	1557	1558	58

With application of high magnetic fields one obtains a strong mixing of |II> and |I>, giving the perturbed lowest excited state |I'>. Due to the fact that the radiative decay rate from state |II> is much larger than from state |I>[4,5], the transition |I'> → |0> reflects mainly the spectroscopic properties of the original state |II>.[7-9]

Further, with increasing magnetic fields one expects a growing in of the zero-phonon absorption |0> → |I'> which is not observable for |0> → |I> at H = 0 T. Indeed, the enlarged part of the spectrum, reproduced in Fig. 1b, clearly shows the magnetic-field induced absorption to the very lowest excited state. Due to the Zeeman effect, the energy of |0> → |I'> is slightly shifted to lower energy and |0> → |II'> to higher energy, respectively, ΔE increasing from 8.2 cm^{-1} (at H = 0 T) to 11 cm^{-1} (at H = 6 T).[5,8] Also under high magnetic fields, these transitions occur at exactly the same energies in emission and absorption.

From the presented discussion it follows that the vibronic spectrum at T = 2 K and H = 6 T (Fig. 1b) is mainly governed by the wavefunction of state |II>. Thus, from a comparison of the vibronic structure at H = 0 T (Fig. 1a) with the structure at H = 6 T one finds that most of the observed promoting modes are the same for the two lowest excited states. However, one also finds distinct differences. For example, the 481 cm^{-1} mode is more strongly coupled to the transition |I> → |0> while the 667 cm^{-1} mode (and some low energy ones) distinctly promote the transition |II> → |0>. Since the distribution of the promoting modes is different for the two emitting states one can easily understand the blue shift of the non-resolved broad band spectra with application of high magnetic fields.[10]

The discussed properties of the two lowest excited states of $[Ru(bpy)_3]^{2+}$ suggest the occurrence of similar vibronic structures of the emission spectra at H = 6 T (T = 2 K) and at T ≈ 5 K (H = 0 T) (due to the thermal repopulation and the relatively high radiative rate constant of |II> ↔ |0>[5]). In fact, this is stated by experiment.

It is worthwhile to mention that the emission spectra from the two states |I> and |II> do not exhibit any pronounced progressions with regard to the vibrational modes, which are listed in Table I. This indicates very similar geometrical configurations of the states |0>, |I>, and |II> with respect to the corresponding normal coordinates.

Transitions between the ground state and higher lying excited states could exhibit different properties of the vibrational coupling. This has recently been shown for $[Ru(bpy)_3](PF_6)_2$ single crystals.[3] It

is found that the absorption spectrum to a state ($2A_2'$ see ref. 11) lying about 800 cm^{-1} above the lowest excited one, is dominated by a 1600 cm^{-1} (bpy-ring stretching) progression. From this progression one can conclude on a shift of the equilibrium position of this state compared to that of the ground state along the corresponding normal coordinate. (For example, the inter-ring C-C separation is estimated to change by about 0.02 Å [12])

CONCLUSION

This paper presents highly resolved emission spectra which allow detailed insight into the vibronic structure of the $[Ru(bpy)_3]^{2+}$ chromophore. It is shown by investigations under high magnetic fields that several distinct modes promote more strongly the transition from the very lowest excited state |I> while others couple more pronounced to the transition from |II>. Both states seem to have similar geometrical configurations compared to that of the ground state while for a higher lying excited state the equilibrium position is shifted with respect to a 1600 cm^{-1} bpy-ring stretching coordinate.

ACKNOWLEDGMENTS

The authors would like to express their thanks to Professor G. Gliemann for support of this work. The "Verband der Chemischen Indutrie" and the "Stiftung Volkswagenwerk" are acknowledged for financial support.

REFERENCES

[1] Kober, E.M.; Caspar, J.V.; Lumpkin, R.S.; Meyer, T.J. J. Phys. Chem. 1986, 90, 3722

[2] Kober, E.M.; Meyer, T.J. Inorg. Chem. 1985, 24, 106

[3] Yersin, H.; Gallhuber, E.; Hensler, G. Chem. Phys. Lett. 1987, 134, 497

[4] Gallhuber, E.; Hensler, G.; Yersin, H. Chem. Phys. Lett. 1985, 120, 445

[5] Gallhuber, E.; Hensler, G.; Yersin, H. Contribution in these Proceedings

[6] Poizat, O.; Sourisseau, C. J. Phys. Chem. 1984, 88, 3007

[7] Gliemann, G. Comments Inorg. Chem. 1986, 5, 263

[8] Hensler, G.; Gallhuber, E.; Yersin, H. Inorg. Chem. 1987, 26, in press

[9] Hensler, G.; Gallhuber, E.; Yersin, H. Contribution in these Proceedings

[10] Elfring, W.H.; Crosby, G.A. J. Am. Chem. Soc. 1981, 103, 2683. Baker, D.C.; Crosby, G.A. Chem. Phys. 1974, 4, 428

[11] Yersin, H.; Gallhuber, E. J. Am. Chem. Soc., 1984, 106, 6582

[12] Schönherr, T.; Degen, J.; Gallhuber, E.; Hensler, G.; Yersin, H. submitted

HIGHLY RESOLVED OPTICAL SPECTRA OF $[Os(bpy)_3]^{2+}$ DOPED INTO $[Ru(bpy)_3]X_2$

G.Hensler, E.Gallhuber, and H.Yersin

Institut für Physikalische und Theoretische Chemie, 8400 Regensburg, FRG

INTRODUCTION

Many investigations were carried out to describe the electronic properties of $[Ru(bpy)_3]^{2+}$ and $[Os(bpy)_3]^{2+}$ complexes due to their interesting photochemical and photophysical behavior. The recent discovery[1-4] of the electronic 0-0-transitions occuring between the lowest MLCT states and the ground state in neat single crystals, delivered the energy positions and separations of the lowest excited states of $[Ru(bpy)_3]^{2+}$. In this contribution we want to present highly resolved low-temperature emission spectra of $[Os(bpy)_3]^{2+}$ doped into $[Ru(bpy)_3]X_2$ ($X = PF_6$, ClO_4) single crystals. To our knowledge these extremely structured spectra are discussed here for the first time.

RESULTS and DISCUSSION

Figure 1a shows the $E \perp c$-polarized emission of $[Os(bpy)_3]^{2+}$ doped into $[Ru(bpy)_3](PF_6)_2$ (**E** = electric field vector, c = needle axis of the crystal). The emission of $[Ru(bpy)_3]^{2+}$ lies at higher energies and is not reproduced here (but see the two other contributions of the authors in these proceedings). Application of high magnetic fields $H \perp c$ ($E \parallel H$) leads to a drastic change of the overall spectrum (Fig. 1b). Fig. 2 reproduces the magnetic field dependence in the region of the high energy part of the emission. With increasing magnetic field the intensity of the dominating lines increases drastically up to a factor of about 10^3 (at H = 6 T).

The most conspicuous feature of these emission spectra is the occurrence of a triple structure. The energy separation between these lines is (37 ± 2) cm^{-1}. These transitions are interpreted to result from three different sites of the guest molecules in the host matrix. (The crystal structures of $[Ru(bpy)_3](PF_6)_2$ and $[Os(bpy)_3](PF_6)_2$ are not isomorphous.[5]) This interpretation is confirmed by the fact that with application of magnetic fields the triple structure is also

Photochemistry and Photophysics
of Coordination Compounds. Ed. by H. Yersin/A. Vogler

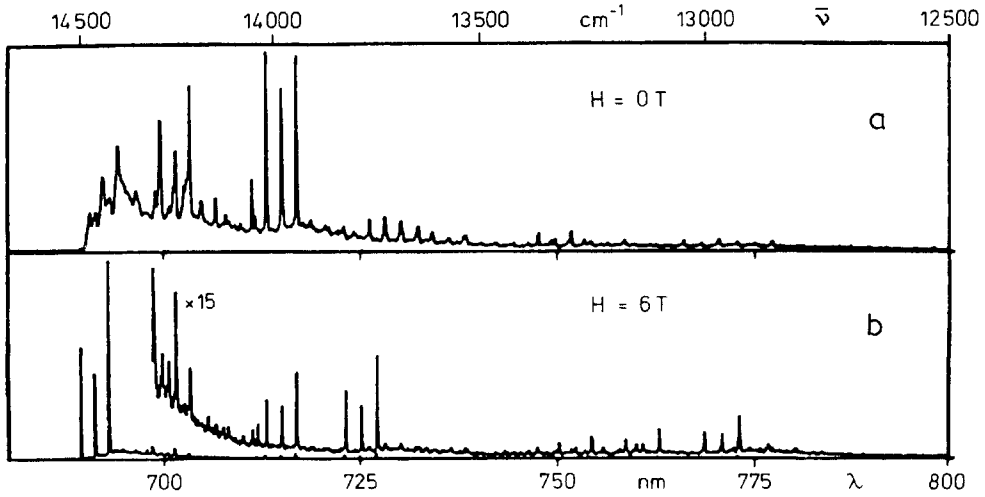

Fig. 1. E⊥c - polarized emission spectra of $[Os(bpy)_3]^{2+}$ doped into $[Ru(bpy)_3](PF_6)_2$ at H = 0 T and H = 6 T (T = 2 K, Ru:Os ≈ 100; λ_{ex} = 363.8 nm. For λ_{ex} = 632.8 nm the results are identical). The intensities are not comparable. The E∥c polarized emission intensity is weaker by a factor of about 80.

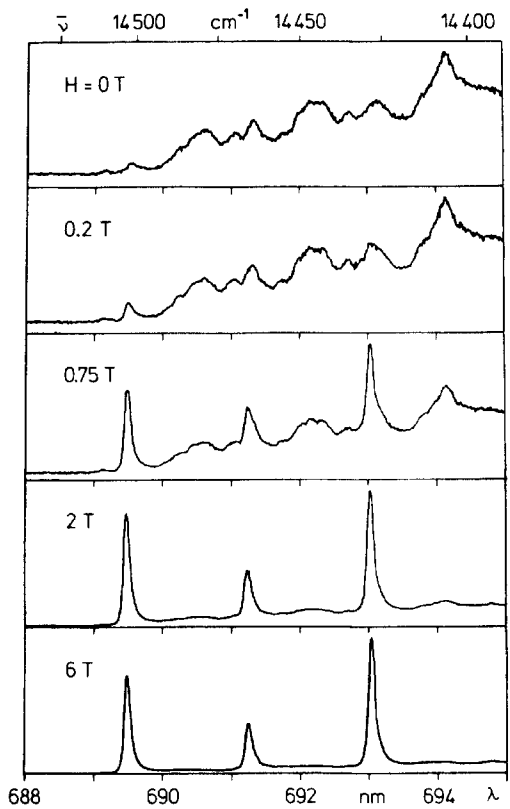

Fig. 2. Blue flank of the emission spectra of $[Os(bpy)_3]^{2+}$ doped into $[Ru(bpy)_3](PF_6)_2$ at various magnetic field strengths (E⊥c, H⊥c, E∥H). The half-width of the narrow lines appearing at higher field strengths is about 2 cm^{-1}.

observed in the absorption spectra at the corresponding energies. Further, this assignment was verified very recently by site selection measurements, leading to one-site emission spectra.

Consequently, the emission features of $[Os(bpy)_3]^{2+}$ doped into $[Ru(bpy)_3](PF_6)_2$ result from a superposition of the spectra of three different sites with the respective purely electronic transitions coupled to a large number of phonons and intramolecular vibrations, thus producing the pattern of a triple structure.

The changes under magnetic fields are interpreted in analogy to the behavior found for $[Ru(bpy)_3]X_2$ [6,7]. The lowest zero-phonon transition (for a specific site) is strongly forbidden but through magnetic-field induced admixture of wave functions of higher lying states into that of the lowest excited one this transition can get considerable oscillator strength mixed-in (see also ref.[8]).

Figure 3a shows the emission spectrum of $[Os(bpy)_3]^{2+}$ doped into $[Ru(bpy)_3](ClO_4)_2$. This spectrum is much simpler and seems to result from a distribution of relatively similar sites. ($[Os(bpy)_3](ClO_4)_2$ and $[Ru(bpy)_3](ClO_4)_2$ have isomorphous structures[5].) Furthermore, the emission is red-shifted by about 330 cm^{-1}, compared to the (PF_6)-compound, being in analogy to the corresponding $[Ru(bpy)_3]X_2$ salts[2,3]. The magnetic field effect (see Fig. 3b) is similar to that demonstrated in Fig. 1, but less drastic.

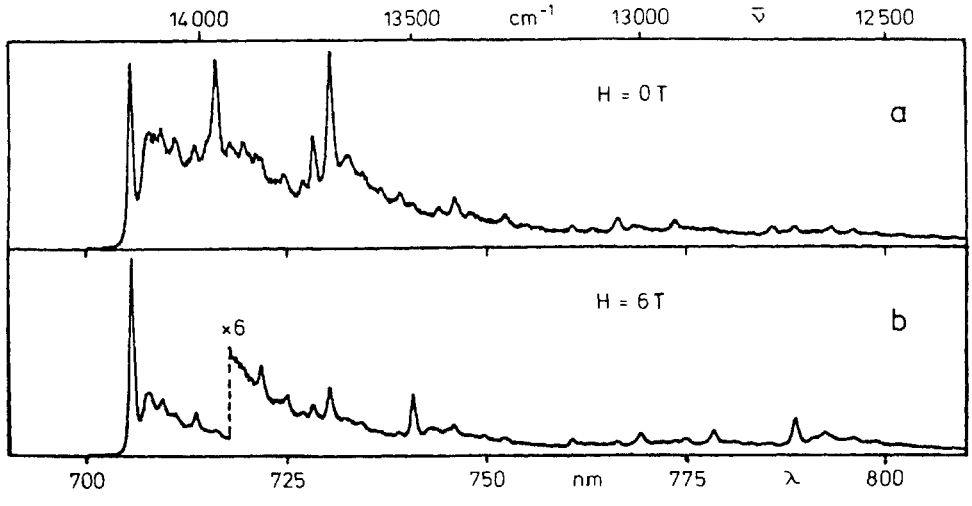

Fig. 3. Emission spectra of $[Os(bpy)_3]^{2+}$ doped into $[Ru(bpy)_3](ClO_4)_2$ at H = 0 T and H = 6 T (T = 2 K; Ru:Os ≈ 50). Intensities are not comparable.

Figure 4 delivers a synopsis of the temperature dependence of the emission of $[Os(bpy)_3]^{2+}$ doped into $[Ru(bpy)_3](ClO_4)_2$. At T = 2 K line I (at 14169 cm^{-1}) represents the transition of highest energy. With increasing temperature two further peaks appear, 61 cm^{-1} (line II) and 211 cm^{-1} (line III) at higher energies, respectively. These three transitions are detected in absorption at the same energies and therefore represent different zero-phonon lines[9].

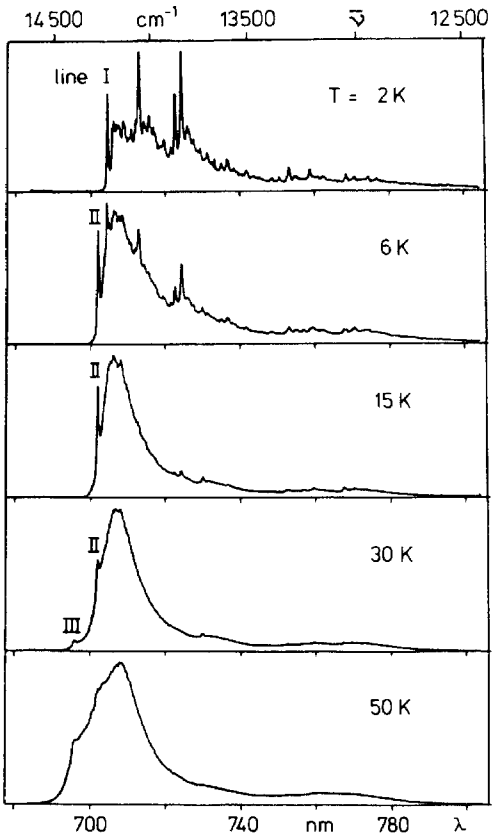

Fig. 4. Temperature dependence of the total emission spectra of $[Os(bpy)_3]^{2+}$ doped into crystalline $[Ru(bpy)_3](ClO_4)_2$.

Finally, we want to focus on the vibrational satellites observed in the emission spectra of $[Os(bpy)_3]^{2+}$ doped into $[Ru(bpy)_3](ClO_4)_2$. In Table I we compare the energies of vibrations coupled to the lowest electronic transition for the case of H = 0 T to IR and Raman data[10] of $[Ru(bpy)_3]^{2+}$ and Raman data[11] of $[Os(bpy)_3]^{2+}$. At zero magnetic field, several IR modes are present (e.g. 1126 cm^{-1}, 1244 cm^{-1}, 1445 cm^{-1}, 1564 cm^{-1}), while for H = 6 T those vibrations are dominant which show a strong Resonance Raman enhancement[10,11] (e.g. 1172 cm^{-1}, 1325 cm^{-1}, 1553 cm^{-1}). This result indicates that the vibronic

coupling of the transitions from different excited states to IR and Raman modes, respectively, is distinct.

Emission of $[Os(bpy)_3]^{2+}$ [cm^{-1}]	Vibrational satellites [cm^{-1}]	IR[10] of $[Ru(bpy)_3]^{2+}$ [cm^{-1}]	Raman[10] of $[Ru(bpy)_3]^{2+}$ [cm^{-1}]	Raman[11] of $[Os(bpy)_3]^{2+}$ [cm^{-1}]
line I 14169	0			
14009	160	-	-	-
13959	210	(195)	(198)	-
13924	245	-	252	-
13891	278	-	281	-
13850	319	-	-	-
13796	373	371	372	-
13751	418	421	-	-
13727	442	-	-	-
13687	482	(468)	(464)	-
13526	643	642	643	-
13496	673	658	658	-
13440	739	732	730	-
13402	767	774	765	-
13143	1026	1024	1025	1029
13100	1069	1066	1069	-
13044	1125	1121	-	-
13011	1158	1159	1160	-
12997[a]	1172	-	1173	1175
12925	1244	1243	-	-
12844[a]	1325	-	1317	1322
12724	1445	1441	-	-
12678	1491	1485	1490	1491
12616[a]	1553	-	1558	1558
12605	1564	1565	-	-
12561	1608	1600	1607	1610

Table I. Comparison of observed satellites in the emission spectra of $[Os(bpy)_3]^{2+}$ doped into $[Ru(bpy)_3](ClO_4)_2$ (at T = 2 K) with IR and Raman data of the $[Ru(bpy)_3]^{2+}$ and $[Os(bpy)_3]^{2+}$ complexes. The marked vibronic peaks (a) are weak at H = 0 T and strong at H = 6 T.

CONCLUSION

$[Ru(bpy)_3]X_2$ (with $X = PF_6$, ClO_4) represents an appropriate matrix for spectroscopic studies of $[Os(bpy)_3]^{2+}$. Due to weak electron-phonon coupling in this diluted crystalline system it is possible to obtain highly resolved emission and absorption[9] spectra of the guest complex. Three zero-phonon transitions occuring between three different electronic states and the ground state are detected.

Further, many vibronic satellites are resolved in the emission spectra, with the energy separations from the 0-0-transition in agreement with the energy values published for IR and Raman modes.

ACKNOWLEDGEMENT

The authors would like to express their thanks to Professor G. Gliemann for support of this work. The "Verband der Chemischen Industrie" and the "Stiftung Volkswagenwerk" are acknowledged for financial support.

REFERENCES

(1) H. Yersin, E. Gallhuber, G. Hensler, J. Physique (Paris), 1985, 46, p.C7-453.
(2) E. Gallhuber, G. Hensler, H. Yersin, Chem. Phys. Lett., 1985, 120, 445.
(3) G. Hensler, E. Gallhuber, H. Yersin, Inorg. Chim. Acta, 1986, 113, 91.
(4) H. Yersin, E. Gallhuber, G. Hensler, Chem. Phys. Lett., 1987, 134, 497.
(5) M. Zabel, University Regensburg, private communication.
(6) G. Hensler, E. Gallhuber, H. Yersin, Inorg. Chem., 1987, 26, in press.
(7) E. Gallhuber, G. Hensler, H. Yersin, J. Am. Chem. Soc., 1987, 109, in press.
(8) G. Gliemann, "Comments Inorg. Chem." 1986, 5, 263.
(9) H. Yersin, E. Gallhuber, G. Hensler, submitted for publication.
(10) O. Poizat, C. Sourisseau, J. Phys. Chem., 1984, 88, 3007.
(11) J. V. Caspar, T. D. Westmoreland, G. H. Allen, P. G. Bradley, T. J. Meyer, W. H. Woodruff, J. Am. Chem. Soc., 1982, 106, 3492.

EXCITED STATE BEHAVIORS OF RUTHENIUM(II) COMPLEXES AS STUDIED BY TIME RESOLVED AND TEMPERATURE AND SOLVENT DEPENDENT EMISSION SPECTRA

S.Tazuke, H.-B.Kim, and N.Kitamura

Research Laboratory of Resources Utilization, Tokyo Institute of Technology, 4259 Nagatsuta, Midori-ku, Yokohama 227, JAPAN

INTRODUCTION

Ruthenium(II) complexes are widely investigated electron transfer sensitizers (Kalyanasundaram 1982). The main reasons are ; i) the appropriate oxidation and reduction potentials, ii) the long excited state lifetime, iii) the negligible photoanation , and iv) the handy wavelength of photoabsorption. While the factors determining the properties mentioned above are in principle determined by energy levels of various electronic states and interactions between any two energy levels (i.e., transition moment, overlap, and coupling which decide absorption and radiative/nonradiative processes), the photophysics of Ru(II) complexes is not yet fully understood. The major parameters to determine the electronic state is certainly the nature of ligands. In the past, we synthesized a series of Ru(II) complexes with various diazadiimine ligands and showed that the redox potentials in the ground and excited states, the wavelength of absorption and emission, and the excited state lifetime could be altered (Kitamura 1983a, 1983b ; Kawanishi 1984 ; Tazuke 1985). While the redox potentials and the absorption and emission energies were correlated with ligand properties, the dynamics of the relaxation from the excited state was puzzling.

In this report, we are going to discuss the relaxation processes of excited $Ru(bpy)_3^{2+}$ and $RuL_2(CN)_2$ (L is 2,2'-bipyridine (bpy) or 1,10-phenanthroline (phen)). These are, firstly, solvent effects on relaxation processes, secondly, the relaxation processes from the initially populated excited ^{3}MLCT state by means of time-resolved emission spectroscopy. Through these investigations, we are trying to pin point the dynamics of the relaxation processes of the excited Ru(II) complexes.

I. SOLVENT EFFECTS ON EXCITED STATE PROPERTIES.

One way to modulate the MLCT excited state properties of metal complexes is the variation of solvents. As reported previously, both absorption and emission energies of $RuL_2(CN)_2$ (L=diimine ligands) show higher energy shift with increasing the Gutmann's solvent acceptor number, AN (Belser 1985). With increasing AN of solvents, σ-donor strength of the cyanide ligands decreases and consequently, the metal t_{2g} orbitals move to lower energy, bringing about the higher energy shift of both absorption and emission. Solvent effects on the redox potentials of $Ru(phen)_2(CN)_2$ are consistent with the interpretation (Kitamura 1987a). The reduction potential (i.e., the π^* energy of the phen ligand) is almost unaffected by solvents whereas the oxidation potential (i.e., the t_{2g} orbital on the metal) depends on solvent AN. The spectral data and the oxidation potentials are correlated as shown in Fig. 1.

Changes in energy levels should also influence the excited state lifetime. From the lifetime analysis by eq.(1), the temperature

Photochemistry and Photophysics
of Coordination Compounds, Ed. by H. Yersin/A. Vogler

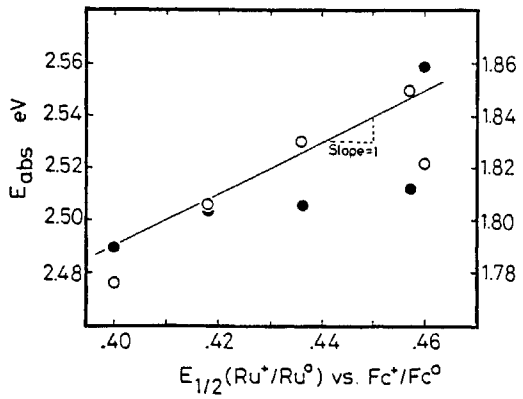

Fig.1 Relationship between E_{abs}(○) or E_{em}(●) and the oxidation potential of $Ru(phen)_2(CN)_2$.

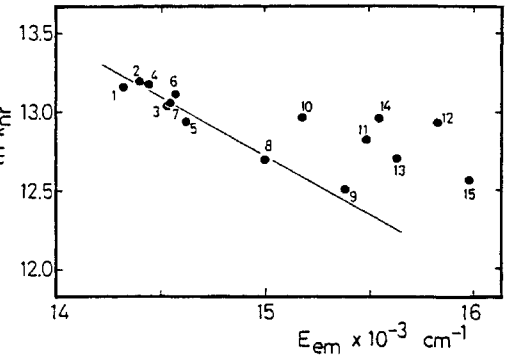

Fig. 2 Solvent effects on ln k_{nr}.

$$\tau^{-1} = k_r + k_{nr} + k'\exp(-\Delta E_a/RT) \qquad (1)$$

independent nonradiative rate constant, k_{nr}, and the activation energy of the emission lifetime, ΔE_a, were obtained. Figure 2 shows a ln k_{nr} vs emission energy (E_{em}) plot. The energy gap law (Meyer 1986) is applicable for a series of solvents while the data in hydrogen bonding solvents deviate from the linear relation. The hydrogen bonding interaction between the cyanide ligands and solvents is certainly important for the relaxation of excited $Ru(phen)_2(CN)_2$. On the other hand, there is a reasonable correlation between ΔE_a and AN (Fig. 3). The observed ΔE_a in low AN solvents is much smaller than the estimated energy difference between the d-d* and ^{3}MLCT states. The energy difference was reported to be 5000 cm^{-1} in an N,N-dimethylformamide/dichloromethane mixture (Belser 1985). Recently, the presence of the fourth MLCT excited state (MLCT') which lies 600-1000 cm^{-1} above ^{3}MLCT state was suggested (Kober 1984 ; Meyer 1986). In low AN solvents, the ^{3}MLCT state locates at lower energy as compared with that in high AN solvents so that the relaxation via d-d* is unlikely but proceeds through the MLCT' giving a small ΔE_a. With increasing AN of solvents, the relaxation proceeds via d-d* and the overall activation energy increases. However, it is experimentally not possible to divide overall ΔE_a into ΔE_a(d-d*) and ΔE_a(MLCT'). If both the d-d* and MLCT' states participates in the relaxation, photoanation in a series of solvents will be related to the fraction of decay via the d-d* state. The results in Table 1 agree with this view indicating that photoinduced ligand substitution is facilitated with increasing AN.

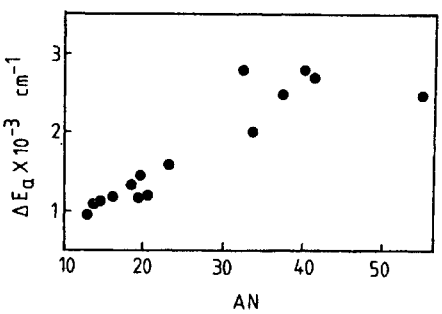

Fig. 3 Solvent effects on ΔE_a.

Table. 1 Photoreaction of $Ru(phen)_2(CN)_2$ with KSCN(0.1M).

Solvent	AN	Φ %[a]
N,N-dimethylacetamide	13.6	0.0
dimethylsulfoxide	19.3	13.7
N-methylformamide	32.1	14.5
methanol	41.3	27.4

a) Relative to the yield of $Ru(bpy)_3^{2+}$ in water.

II. TIME DEPENDENT SHIFT OF EMISSION.

Solvent dipole relaxation in the ^{3}MLCT excited state can be followed by time-resolved emission spectroscopy. Interrelation between the role of solvent dipole relaxation and localization/delocalization of an excited electron is a point of controversy. In the ns time regime, the emission spectrum of $Ru(bpy)_3^{2+}$ shows time-dependent (TD) shift at low temperature (Ferguson 1985 ; Kitamura 1986). This phenomenon was attributed to solvent dipole relaxation and probably, in part, to the transition from the charge delocalized excited state to the charge localized state. Although the TD shift slightly depends on the nature of a counter anion ($X=Cl^-$, ClO_4^-, or PF_6^-) of $Ru(bpy)_3X_2$ (Kitamura 1986), this discussion could not be applied to $RuL_2(CN)_2$, which shows even a bigger TD shift than $Ru(bpy)_3^{2+}$ as shown in Fig. 4. The TD shift is specifically observed in a narrow temperature range just below and above the glass transition temperature of the matrix (T_g). For quantitative discussion, we defined the rate of relaxation as the reciprocal of time required for half relaxation (k_r) and the Arrhenius polts are shown in Fig. 5. The plots are devided in two parts at 130 K. Below 130 K, the apparent activation energies for TD shift, ΔE_a, are 570 and 1360 cm^{-1} for $Ru(bpy)_3Cl_2$ and $Ru(bpy)_2(CN)_2$, respectively. The activation energy of viscous flow for an ethanol/methanol mixture below 120 K is 1900 cm^{-1} (Carlin 1985) so that the present ΔE_a values are too small to be ascribed to the activation energy for the phenomena related to the viscosity of the medium. Since the rate of relaxation depends on the nature of solvents, solvent dipole relaxation in the ^{3}MLCT excited state is primarily responsible for the TD shift.

As judged by the accumulated evidence that an excited electron in $Ru(bpy)_3^{2+}$ or analogous complexes is delocalized in rigid matrices while that is localized in fluid media, the TD shift in near T_g of the solvent should be closely related to solvent dipole relaxation of more precisely, solvent assisted electron localization. In ethanol/methanol at 150 K, the emission from $Ru(bpy)_3^{2+}$ obeys a single exponential function and the decay time is independent of the monitoring wavelength. However, for $Ru(bpy)_3^{2+}$ at 125 K, the decay profile observed at 580 nm does not agree with that monitored at 752 nm as shown in Fig. 6. Similar results have been reported by Ferguson et al. (1986a,1986b). The effects are more pronounced and complicated in the case of $Ru(phen)_2(CN)_2$ (Kitamura 1987b). The emission decay monitored at 580 nm is multi- or even non-exponential and the decay profile varies with the monitoring wavelengths (Fig. 7). The longer the monitoring wavelength, the longer the apparent emission lifetime. Furthermore, the wavelength dependent emission decay is observed at 150 K. The formation and destruction of the hydrogen bonding interaction between the cyanide ligands and alcoholic solvents around T_g (Kitamura 1987a) could be reflected on the emission decay profile. Although it is not clearly seen in Fig. 6 and 7, the emission from both complexes exhibits rise and decay when monitored above 700 nm. Since the emission spectrum shows TD shift at this temperature, the change in the emission decay profile with the monitoring wavelength is not surprising. However, taking the report of MCPL experiments (Ferguson 1986) into account, we conclude that the phenomena are closely related with the transition from the delocalized excited state to the localized one.

As we have already shown, the decay profile of the emission between 100 and 140 K is complicated and could not be fit in a single or multi-exponential mode. It is indeed non-exponential. The meaning of non-exponential decay should be understood in two ways. Firstly, because of the TD shift of emission, the decay profile monitored at a fixed wavelength provides a false feature. The total emission intensity integ-

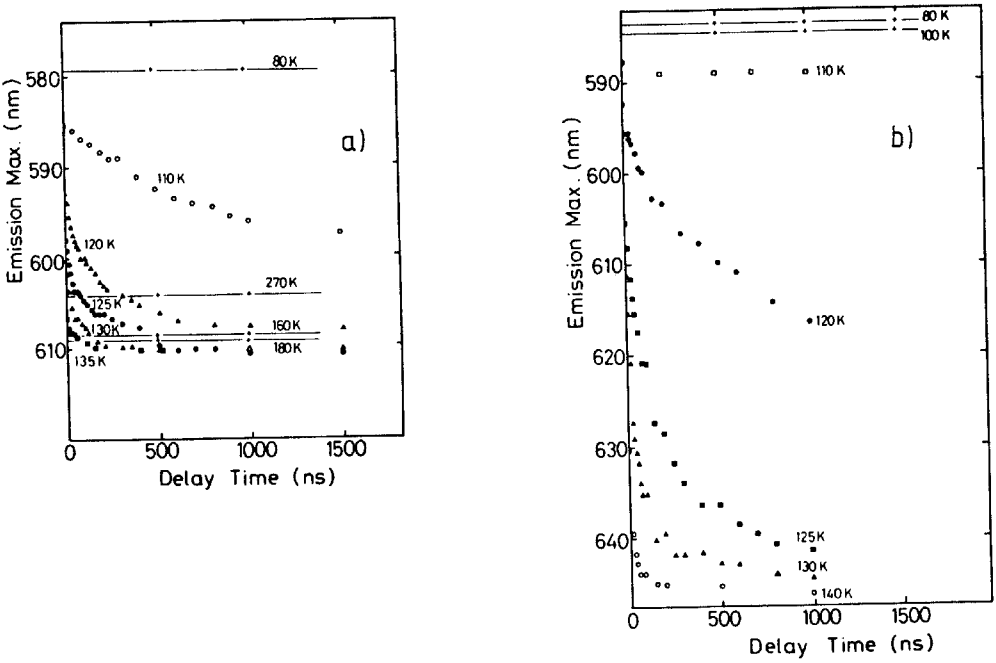

Fig. 4 Time and temperature dependence of the emission maximum of $Ru(bpy)_3Cl_2$ (a) and $Ru(bpy)_2(CN)_2$ (b) in an ethanol-methanol mixture.

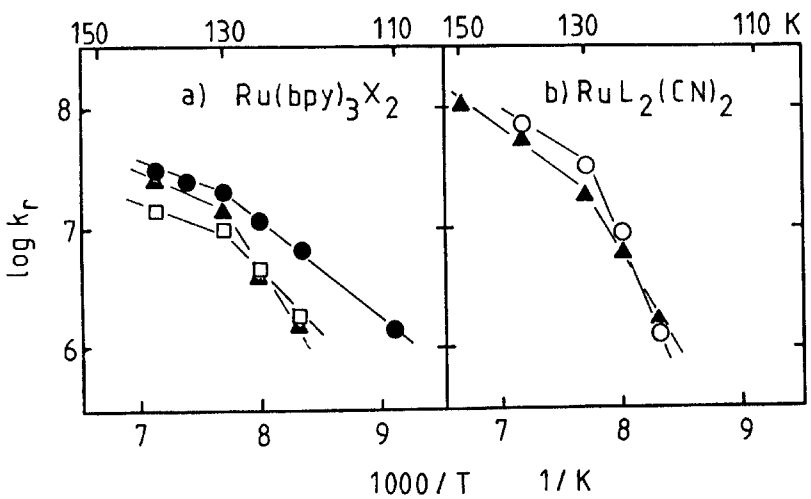

Fig. 5 Temperature dependence of k_r ; (a) X = Cl^-(●), ClO_4^-(▲), and PF_6^-(□), (b) L = bpy(○) and phen(▲).

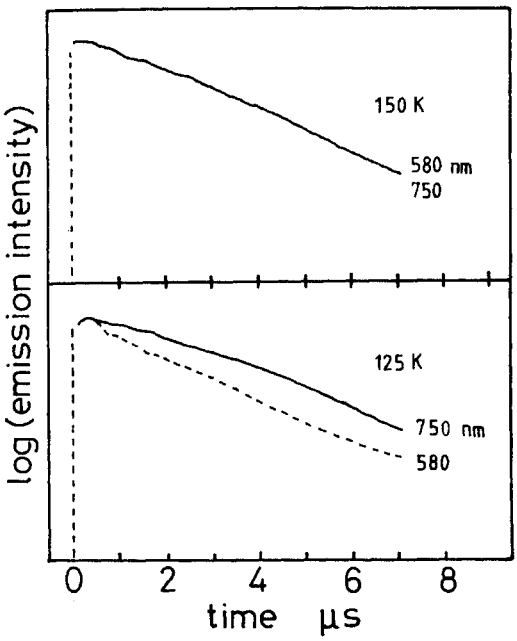

Fig. 6 Emission decay profile of $Ru(bpy)_3^{2+}$.

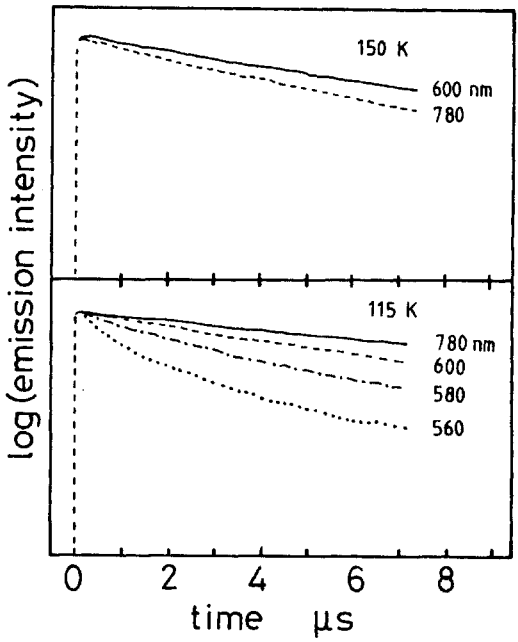

Fig. 7 Emission decay profile of $Ru(phen)_2(CN)_2$.

rated over the whole wavelength region must be plotted against time. Secondly, provided that the procedure mentioned above could be adopted, the decay profile might be multi-exponential. This is the true case of time-dependent rate. Such non-exponential decay has been discussed in a number of unimolecular fluorescence decay of organic compounds such as twisted intramolecular CT compounds (Heisel 1983, 1985a, 1985b) and intramolecular excimer/exciplex (Tazuke 1986). The work along this line is now in progress.

References

Belser P, Zelewsky AV, Juris A, Bargelletti F, Balzani V (1985) Excited state properties of some new ruthenium(II) cyano-polypyridine complexes in various solvents. Gazz Chim Ital 115: 723-729

Carlin CM, DeArmond MK (1985) Temperature-dependent photoselection-Intramolecular exciton motion in $[Ru(bpy)_3]^{2+}$. J Am Chem Soc 107: 53-57

Ferguson J, Krausz ER, Maeder M (1985) Charge localization in the luminescent state of $Ru(bpy)_3^{2+}$ in fluid solutions. J Phys Chem 89: 1852-1854

Ferguson J, Krausz E (1986a) Time-resolved luminescence and MCPL of $Ru(bpy)_3^{2+}$ in glassy solvents at the fluid-glass transition. Chem Phys Lett 127: 551-556

Ferguson J, Krausz E (1986b) MCPL evidence for the transition from delocalized to localized luminescent state of $Ru(bpy)_3^{2+}$ in glass-fluid media. Inorg Chem 25: 3333-3335

Heisel F, Miehe JA (1983) Dynamical study of twisted intramolecular charge transfer in p-dimethylaminobenzonitrile solutions. Chem Phys Lett 100 : 183-188

Heisel F, Miehe JA (1985a) p-Dimethylaminobenzonitrile solution. 1 Time-dependent rate in intramolecular electron transfer reaction. Chem Phys 98: 233-241.

Heisel F, Miehe JA, Martinho JMG (1985b) p-Dimethylaminobenzonitrile in polar solution. 2 Quantum yield measurements and quasi-stationary kinetic study of the electron transfer reaction. Chem Phys 98: 243-249

Kalyanasundaram K (1982) Photophysics, photochemistry and solar energy conversion with tris(bipyridyl)ruthenium(II) and its analogues. Coord Chem Rev 46: 159-244

Kawanishi Y, Kitamura N, Kim Y, Tazuke S (1984) Ligamd design of ruthenium(II) complexes aiming at efficient electron transport sensitization. Riken Sci Papers 78: 212-219

Kitamura N, Kawanishi Y, Tazuke S (1983a) Spectroscopic and electrochemical studies on ruthenium(II) complexes containing diazadiimine ligands. Chem Phys Lett 97: 103-106

Kitamura N, Kawanishi Y, Tazuke S (1983b) Highly efficient photo-reduction of methylviologen by tris(bis-diazadiimine)-ruthenium(II) complexes. Chem Lett : 1185-1188

Kitamura N, Kim HB, Kawanishi Y, Obata R, Tazuke S (1986) Time-resolved emission spectra of $Ru(bpy)_3Cl_2$ and cis-$Ru(bpy)_2(CN)_2$ at low temperature. J Phys Chem 90: 1488-1491

Kitamura N, Sato M, Kim HB, Obata R, Tazuke S (1987a) Solvatochromism in the excited state of cis-dicyanobis(1,10-phenanthroline)ruthenium(II) complex. Inorg Chem : submitted

Kitamura N, Kim HB, Sato M, Tazuke S. (1987b) In preparation

Kober EM, Meyer TJ (1984) An electronic structural model for the emitting MLCT excited states of $Ru(bpy)_3^{2+}$ and $Os(bpy)_3^{2+}$. Inorg Chem 23: 3877-3886

Meyer TJ (1986) Photochemistry of metal coordination complexes ; metal to ligand charge transfer excited states. Pure Appl Chem 58: 1193-1206

Tazuke S, Kitamura N, Kawanishi Y (1985) Problems of back electron transfer in electron transfer sensitization. J Photochem 29: 123-138

Tazuke S, Higuchi Y, Tamai No, Kitamura N, Tamai Na, Yamazaki I (1986) Formation and relaxation of excited complex in polymers. Macro-molecules 19: 603-606

THE LOWEST EXCITED STATES OF (Ru(2,2'-bipyrazine) (2,2'-bipyridine)$_2$)$^{2+}$

Hiroshi Kobayashi, Youkoh Kaizu, Kazuteru Shinozaki, and Hideyo Matsuzawa

Department of Chemistry, Tokyo Institute of Technology, O-okayama, Meguro-ku, Tokyo 152, JAPAN

PROTONATION AND DEPROTONATION OF EXCITED COMPLEXES

The lowest excited state of $[Ru(bpy)_2(CN)_2]$ (bpy, 2,2'-bipyridine) is the "metal-to-bipyridine" charge-transfer excited state. Absorption spectrum of the complex varies with protonation on the coordinated cyano groups in acidified media, while emission exhibits a spectrum of deprotonated species with a constant yield regardless of the hydrogen-ion concentrations $[H^+]$ in solution. A rapid, complete deprotonation follows excitation of the protonated species (Peterson 1976). In highly acidic H_2SO_4-methanol glass at 77 K, $[Ru(bpy)_2(CN)_2]$ as well as $[Ru(phen)_2(CN)_2]$ (phen, 1,10-phenanthroline) exhibits an emission band with vibrational structure which is very similar to the ligand $^3(\pi,\pi^*)$ emission band found with the corresponding Rh(III) tris-chelate complexes. It was proposed that the protonation in the rigid glass results in an inversion of the lowest charge-transfer and the ligand-localized $^3(\pi,\pi^*)$ excited states (Peterson 1978).
Recently we prepared anion complexes $[Rubpy(CN)_4]^{2-}$ and $[Ruphen(CN)_4]^{2-}$. The complexes exhibit metal-to-bipyridine or -phenanthroline charge-transfer bands very similar to those observed with $[Ru(bpy)_3]^{2+}$, $[Ru(bpy)_2(CN)_2]$ and their phenanthroline analogues. In dilute acidic solutions such as $[H^+] < 0.5$ M, one of the coordinated cyano groups is protonated and a fast, complete deprotonation follows excitation of the protonated complex. In the media 6 M > $[H^+]$ > 2 M a continuous blue shift of emission band and an increase of decay lifetime are observed with increasing $[H^+]$: the protonated excited complexes are rather long-lived than the deprotonated species. A further increase of $[H^+]$ results in an one-electron oxidation of the complex. A paramagnetic Ru(III) complex yielded in highly acidic media ($[H^+] > 8.3$ M) emits at ambient temperature an intense short-lived emission which has the structure observed with the ligand $^3(\pi,\pi^*)$ emission of $[Rh(bpy)_3]^{3+}$ at 77 K (Matsuzawa unpublished). NMR spectrum confirmed the spin-doublet state of the paramagnetic Ru(III) complex. By addition of OH^- to the acidic solution, the original Ru(II) complex is recovered. The intense short-lived emission from $[Ru(III)bpy(CN)_4]^-$ is assigned as a spin-allowed transition from the trip-doublet state of ligand $^3(\pi,\pi^*)$

Photochemistry and Photophysics
of Coordination Compounds, Ed. by H. Yersin/A. Vogler

origin. The interaction with spin doublet on the central metal ion makes all ligand singlets become doublets and triplets into doublets (trip-doublets) and quartets (trip-quartets). The protonation gives rise to an electron detachment but not an inversion of the lowest charge-transfer and the ligand-localized $^3(\pi,\pi^*)$ excited states. Both protonated and deprotonated forms of $[Ru(bpy)_2(4,7\text{-dihydroxy-}1,10\text{-phenanthroline})]^{2+}$ are emissive in aqueous solutions and the proton-dissociation constants in the ground and excited states are determined by spectral and lifetime measurements with varied $[H^+]$ in the media (Giordano 1978). The complex is more acidic in the excited state. On the other hand, excitation of $[Ru(bpy)_2(2,2'\text{-bipyridine-}4,4'\text{-dicarboxylic acid})]^{2+}$ decreases the acidity of carboxylic acid on one of coordinated bipyridines. Two different titration curves were obtained by absorption and emission intensity measurements and a displacement of the titration curves was attributed to a shift of the protonation equilibrium upon electronic excitation in the metal-to-ligand charge-transfer band (Giordano 1977).

EXCITED STATES OF $[Rubpz(bpy)_2]^{2+}$

The lowest excited state of $[Rubpz(bpy)_2]^{2+}$ (bpz, 2,2'-bipyrazine) is the "metal-to-bipyrazine" charge-transfer (MLCT) excited state. Irradiation of 457.9 nm line in the red component of the split visible MLCT band (band I, 20.5×10^3 cm^{-1}) shows a resonance Raman modes of bipyrazine, while irradiation of 406.7 nm line in the blue component band (band II, 24.8×10^3 cm^{-1}) exhibits those of bipyridine. $[Rubpz(bpy)_2]^{2+}$ exhibits emission from the lowest excited triplet state. Phosphorescence excitation spectra of $[Rubpz(bpy)_2]^{2+}$ doped in PVA films show a high positive polarization ($P \approx 2/5$) even at room temperature in the band I, which indicates the electronic excitation is localized within the coordinated bipyrazine. Phosphorescence band is in a mirror-image of the weak absorption band (16.2×10^3 cm^{-1}) by the second-derivative absorption spectrum to the red of the intense MLCT band (band I). The weak band is assigned as the spin-forbidden S-T (singlet-triplet) component band of "metal-to-bipyrazine" MLCT transition.

$[Rubpz(bpy)_2]^{2+}$ emits phosphorescence in solution even at room temperature: the lifetime and yield in H_2O at 25 °C are τ = 88 ns, ϕ = 0.006; D_2O, τ = 190 ns, ϕ = 0.012; CH_3OH, τ = 200 ns, ϕ = 0.026; CH_3CN, τ = 460 ns, ϕ = 0.027; propylenecarbonate, τ = 400 ns, ϕ = 0.026, respectively (Shinozaki unpublished). From the measured lifetimes and yields, the radiative (k_r) and nonradiative decay rate constants (k_{nr})

are evaluated according to $k_r = \phi\tau^{-1}$ and $k_{nr} = (1-\phi)\tau^{-1}$: H_2O, $k_r = 6.8\times10^4\ s^{-1}$, $k_{nr}=11.3\times10^6 s^{-1}$; D_2O, $k_r=6.3\times10^4\ s^{-1}$, $k_{nr}=5.2\times10^6\ s^{-1}$; CH_3OH, $k_r=6.7\times10^4\ s^{-1}$, $k_{nr}=4.9\times10^6\ s^{-1}$; CH_3CN, $k_r=5.9\times10^4\ s^{-1}$, $k_{nr}=2.1\times10^6\ s^{-1}$; propylenecarbonate, $k_r=6.5\times10^4\ s^{-1}$, $k_{nr}=2.4\times10^6\ s^{-1}$. The radiative rate is about $7\times10^4\ s^{-1}$ independent of the media. However, the lifetime is controlled by the rate of nonradiative relaxation which increases in protic solvents.

The lifetimes were measured in H_2O and D_2O as a function of temperature (Shinozaki unpublished). A plot of ln K ($\equiv 1/\tau$) against $1/k_BT$ well fits the equation $k=k^0\exp(-\Delta E/k_BT)$: $k^0_H=3.88\times10^7\ s^{-1}$, $\Delta E_H=270\ cm^{-1}$; $k^0_D=2.70\times10^7\ s^{-1}$, $\Delta E_D=340\ cm^{-1}$. Protic solvent molecules form hydrogen bonds with the peripheral nitrogens of coordinated bipyrazine. Even if the basicity of bipyrazine is increased by charge transfer from ruthenium to bipyrazine in the excited state, the hydrogen-bonded water protons or deuterons are oscillating in a minimum nearby water oxygen. From the plot of ln k_H/k_D *versus* $1/k_BT$, we obtained $(m_D/m_H)^{1/2}f^{\ddagger}/f_0=1.4$ and thus $f^{\ddagger}/f_0=1$. To form the nonemissive protonated species, the proton should be transferred to another minimum beyond an energy barrier ($\Delta E_H=270\ cm^{-1}$; $\Delta E_D=340\ cm^{-1}$). The protonated species $[RubpzH(bpy)_2]^{3+}$ emits no phosphorescence.

A semiempirical SCMO calculation was carried out on the (π,π^*) excited singlet and triplet states of coordinated bipyrazine. The $^{1,3}(\pi,\pi^*)$ excited states were also calculated on the two stages of protonation of the peripheral nitrogens. The lowest $^3(\pi,\pi^*)$ state of coordinated bipyrazine in $[RubpzH(bpy)_2]^{3+}$ ($11\times10^3\ cm^{-1}$) is lower than the lowest MLCT excited triplet state ($12\times10^3\ cm^{-1}$), while that of $[RubpzH_2(bpy)_2]^{4+}$ ($14\times10^3\ cm^{-1}$) is at around the MLCT excited state. The nonemissive $^3(\pi,\pi^*)$ excited state of coordinated bipyrazine is stabilized by protonation to one of the two nitrogens much lower than the lowest MLCT excited triplet. The quenching in the protonated complex is attributable to fast nonradiative relaxation in the nonemissive low-lying $^3(\pi,\pi^*)$ excited state of monoprotonated bipyrazine. In this particular case, it is not necessary to assume a thermal activation to the low-lying $^{1,3}(d,d^*)$ excited states which limits the lifetime of the excited complexes (Van Houten 1975, 1976; Allsopp 1978; Durham 1982; Casper 1983; Allen 1984).

PROTONATION OF $[Rubpz(bpy)_2]^{2+}$

In acidic media, $[Rubpz(bpy)_2]^{2+}$ is protonated on the peripheral nitrogens of coordinated bipyrazine. The monoprotonated species is predominant in $6.0\ M > [H^+] > 3.5\ M$, while the diprotonated species in

$[H^+] > 8.0$ M. The protonated complexes emit no phosphorescence. In a dilute acid solution such that no protonated species is detected by absorption measurements, the phosphorescence is partly quenched by H_3O^+ in solution. Two different titration curves are obtained as a function of pH by absorption and emission intensity measurements. However the displacement of the curves is not direct indication of the MLCT-induced enhancement of bipyrazine basicity. By measurements of the time-resolved repopulation of the ground-state species after pulse excitation, the excited-state lifetime of the nonemissive $^*[RubpzH(bpy)_2]^{3+}$ in acidic aqueous media was determined as 1.1 ns, which is rather short in contrast with that of $^*[Rubpz(bpy)_2]^{2+}$ (88 ns) (Shinozaki unpublished). Since the nonradiative relaxation process in the protonated species is so accelerated that the protonation equilibrium is not accomplished within the excited-state lifetime, the quenching in acidic media is governed by the rate of diffusion controlled encounter of H_3O^+ and the excited complex.
In a dilute acid solution where the ground-state species is exclusively $[Rubpz(bpy)_2]^{2+}$, the excited complex is quenched by the diffusion controlled protonation and thus $[Rubpz(bpy)_2]^{2+}$ is recovered by the proton dissociation following the deactivation. In fact, the recovery of $[Rubpz(bpy)_2]^{2+}$ is slower than the emission decay. Measurements determined the rate of proton dissociation ($k_{-2}=2\times10^8$ s^{-1}) of the $[RubpzH(bpy)_2]^{3+}$ yielded by the deactivation of excited species.

COMPLEX FORMATION IN THE EXCITED STATE

Absorption spectra vary with increasing concentration of hydrated Ag^+ ion $[Ag^+]$ in a solution of $[Rubpz(bpy)_2]^{2+}$. The first stage of the spectral variation is ascribed to the formation of $[RubpzAg(bpy)_2]^{3+}$, in which a hydrated Ag^+ ion is coordinated to one of the bipyrazine peripheral nitrogens. $[RubpzAg(bpy)_2]^{3+}$ emits to the red of the emission from $[Rubpz(bpy)_2]^{2+}$. Emission lifetimes were measured with $[Ag^+]$ varied within the first stage of complex formation. The ratio of the lifetimes in the absence and presence of Ag^+ ion, τ_0/τ, increases with $[Ag^+]$ but the plot of τ_0/τ against $\log[Ag^+]$ shows a plateau when $[Ag^+]$ is increased up to $2\sim4\times10^{-1}$ M. The lifetime of $[RubpzAg(bpy)_2]^{3+}$ at 25 °C was determined as 66 ns from the plateau value τ_∞. Emission spectrum varies with $[Ag^+]$, while it is invariant regardless of whether it is excited in the absorption band of $[Rubpz(bpy)_2]^{2+}$ or that of $[RubpzAg(bpy)_2]^{3+}$. This indicates the equilibrium of complex formation is accomplished in a shorter period than the time constant of the excited-state lifetimes.

From the decay lifetimes measured for a variety of [Ag^+], the complex-formation constant in the excited state was determined K^*=130 M^{-1} at 25 °C, μ=3.0 M. On the other hand, the formation constant in the ground state was obtained by absorption measurements as K=20 M^{-1} at 25 °C, μ=3.0 M. The complex formation in the excited state is appreciably promoted than that of the ground state, since the coordinated bipyrazine increases the basicity upon the MLCT electronic excitation.

References

Allen GH, White RP, Rillema DP, Meyer TJ (1984) Synthetic control of excited-state properties. Tris-chelate complexes containing the ligand 2,2'-bipyrazine, 2,2'-bipyridine, and 2,2'-bipyrimidine. J Am Chem Soc 106: 2613-2620.

Allsopp SR, Cox A, Kemp TJ, Reed WJ (1978) Inorganic photophysics in solution. Part-1. Temperature activation of decay processes in the luminescence of tris(2,2'-bipyridine)ruthenium(II) and tris(1,10-phenanthroline)ruthenium(II) ion. J Chem Soc Faraday Trans I 74: 1275-1289.

Casper JV, Meyer TJ (1983) Photochemistry of $Ru(bpy)_3^{2+}$. Solvent effects. J Am Chem Soc 105: 5583-5590.

Durham B, Casper JV, Nagle JK, Meyer TJ (1982) Photochemistry of $Ru(bpy)_3^{2+}$. J Am Chem Soc 104: 4803-4810.

Giordano PJ, Bock CR, Wrighton MS (1978) Excited state proton transfer of ruthenium(II) complexes of 4,7-dihydroxy-1,10-phenanthroline. Increased acidity in the excited state. J Am Chem Soc 100: 6960-6965.

Giordano PJ, Bock CR, Wrighton MS, Interrante LV, Williams RFX (1977) Excited state proton transfer of a metal complex: determination of the acid dissociation constant for a metal-to-ligand charge transfer state of a ruthenium(II) complex. J Am Chem Soc 99: 3187-3189.

Matsuzawa H, Kaizu Y, Kobayashi H (to be published) Preparation and emission spectra of $K_2[Rubpy(CN)_4]$ and $K_2[Ruphen(CN)_4]$.

Peterson SH, Demas JN (1976) Excited state acid-base reactions of transition metal complexes: Dicyanobis(2,2'-bipyridine)ruthenium(II) in aqueous acid. J Am Chem Soc 98: 7880-7881.

Peterson SH, Demas JN (1978) Excited-state acid-base reactions of dicyanobis(2,2'-bipyridine)ruthenium(II) and dicyanobis(1,10-phenanthroline)ruthenium(II). J Am Chem Soc 101: 6571-6577.

Shinozaki K, Kaizu Y, Hirai H, Matsuzawa H, Kobayashi H (to be published) Protonation and complex formation of $[Rubpz(bpy)_2]^{2+}$ in the lowest excited state.

Shinozaki K, Ohno O, Kaizu Y, Kobayashi H, Sumitani M, Yoshihara K (to be published) Excited-state lifetime of a nonemissive complex $[RubpzH(bpy)_2]^{3+}$.

Van Houten J, Watts RJ (1975) The effect of ligand and solvent deuteration on the excited state properties of the tris(2,2'-bipyridyl)ruthenium(II) ion in aqueous solution. Evidence for electron transfer to solvent. J Am Chem Soc 97: 3843-3844; (1976) Temperature dependence of the photophysical and photochemical properties of the tris(2,2'-bipyridyl)ruthenium(II) ion in aqueous solution. J Am Chem Soc 98: 4853-4858.

QUENCHING OF EXCITED $Ru(bpy)_3^{2+}$ WITH METHYLVIOLOGEN AT LOW TEMPERATURES

Cz.Stradowski and M.Wolszczak

Institute of Applied Radiation Chemistry, Technical University (Politechnika), 93-590 Lodz, Wroblewskiego 15, POLAND

There is a growing interest in the studies of electron transfer reactions,in which the reactants are separated by several molecular radii.Among them photoinduced electron transfer was intensely studied (Miller et al.1982).Well-know reaction transfer between excited $Ru(bpy)_3^{2+}$ (tris(2,2´-bipyridine)ruthenium(II) dication) and MV^{2+} (methylviologen, 1,1´-dimethyl-4,4´-bipyridinium dichloride) served as a model system (Milosavljevic and Thomas 1985).It has been demonstrated that methylviologen quenches the luminescence of $Ru(bpy)_3^{2+}$ in polymers at ambient (Milosavljevic and Thomas 1985) and low (Guarr et al.1985) temperatures.The quenching was ascribed to electron tunnelling over large distances (>10 A) from excited $Ru(bpy)_3^{2+}$ to methylviolgen.The similar interpretation was used to explain the quenching of $Ru(bpy)_3^{2+}$ in viscous liquid (Guarr et al.1983). However,the direct proof of electron transefer via long-range tunnelling,showing the accelleration of luminescence decay in the presence quencher at 77 K is still lacking.The aim of the present work was to study the quenching of luminescence in solid phase down to 77 K.

The luminescene of $Ru(bpy)_3^{2+}$ was studied in ethylene glycol-water mixture,2:1 by volume (EG/H_2O) and in several polymer foils.The preparation of the samples and luminescence measurements are described elsewhere (Stradowski and Wolszczak 1987).The Fig.1 summarizes the data of luminescence of $Ru(bpy)_3^{2+}$ in EG/H_2O as measured by time-resolved laser photolysis. The kinetics of the luminescence, observed after 10 ns laser pulse (λexc = 530 nm) was monitored at 610 nm.The decay of the luminescence was always monoexponential.The lifetimes of luminescence at temperatures 290-200 K are presented in Fig.1.It is evident that at temperatures 290-200 K the presence of the quencher accellerated markedly the decay of the luminescence.The system EG/H_2O is higly viscous and possibility of the diffusion of $Ru(bpy)_3^{2+}$ and MV^{2+} during the lifetime of luminescence is very limited. Nevertheless,one observs efficient quenching of luminescence under this conditions,which is favour of long-range tunnelling as a mechanism of quenching.On the other hand,below 200 K the presence of the quencher has very little or no effect on the rate of luminescence decay.The decay at 77 K was still monoexponential.The lifetime of the luminescence was 3.1 us,independent of the quencher addition up to 0.15 M MV^{2+}.Therefore,we conclude that at temperature range 77-200 K the dynamic quenching of luminescence of $Ru(bpy)_3^{2+}$ by methylviologen does not occur.In order to find out the quenching mechanism,the measurements of the dependence of luminescence intensity as a function of MV^{2+}concentration were carried out.The intensity of luminescence was measured with a conventional fluorimeter.The results are sumarized in Fig.2.Curve 1 in Fig.2 shows that at 77 K the quenching is very inefficient,and independent of the nature of the medium.In earlier studies the quenching of the luminescence of $Ru(bpy)_3^{2+}$ by MV^{2+} in solids was ascribed to long-range tunnelling of electron from excited $Ru(bpy)_3^{2+}$ to MV^{2+} (Milosavljevic and Thomas 1985;Guarr et al.1985).

Photochemistry and Photophysics
of Coordination Compounds, Ed. by H. Yersin/A. Vogler

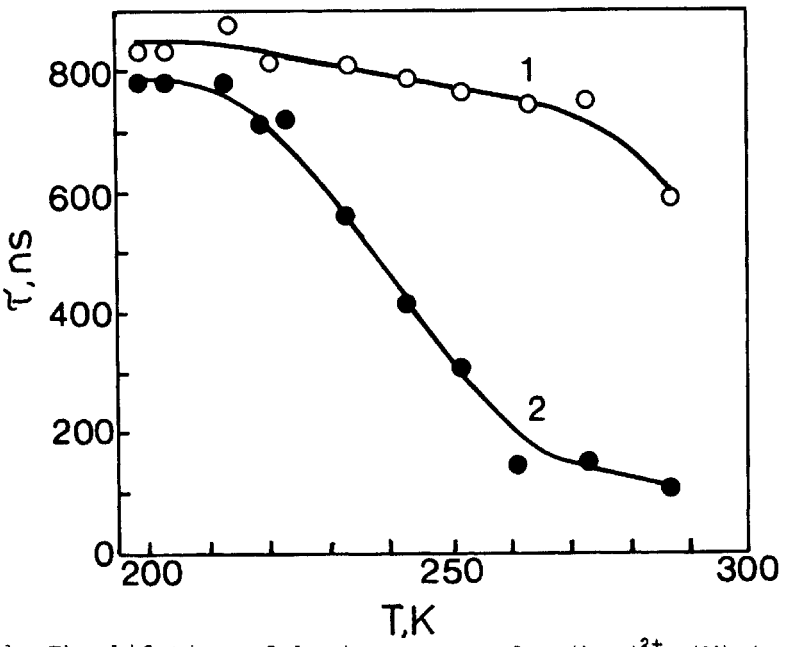

Fig. 1. The lifetime of luminescence of $Ru(bpy)_3^{2+}$ (τ) in ethylene glycol-water as a function of temperature (T).(1)-$Ru(bpy)_3^{2+}$ alone (2)-$Ru(bpy)_3^{2+}$ with 0.05 M methylviologen.

Present data show that this interpretation can not be used for data at 77 K.Three following observation are in disagreement with such interpretation:(1) The decay of luminescence of $Ru(bpy)_3^{2+}$ at 77 K was not accellerated in the presence of MV^{2+}(2) The quenching curve,shown in Fig.2,is well described by luminescence quenching in contact pairs. The radius of such contact pair,calculated from curve 1 in Fig.2 is 7.1 A,i.e less then sum of geometric radii of $Ru(bpy)_3^{2+}$ and MV^{2+} (10 A). Such result is meaningless from the point of view of long-range tunnelling.(3) Lack of any traces of $MV^{+\cdot}$ radical cation,that is the product of quenching at 77 K.Therefore,we postulate that the quenching of luminescence of $Ru(bpy)_3^{2+}$ by MV^{2+} at 77 K via long-range tunnelling is neglibile.Inefficiency of electron tunnelling between excited $Ru(bpy)_3^{2+}$ and MV^{2+} was assigned by Seefeld (Seefeld et al.1977) to high energy barrier between reactants (c.a. 2.5 eV).Thus,the quenching at 77 K in our system should be ascribed to "static" type of quenching, occuring within contact pairs formed in the ground state.The Perrin or static type of quenching occuring infinitely fast within an active sphere,results in a monoexponential luminescence decay and leads to a decrase of the initial intensity of luminescence.The lifetime of luminescence remains unaffected by this type of quenching.

On the other hand,the curves 2,3 and 4 in Fig.2 indicate that at room temperature the quenching in solid state is much more efficient then at 77 K.The same observation concerns viscous liquid at low temperatures (see Fig. 1).Obviously,the possibility of the diffusion of reactants during the lifetime of excited $Ru(bpy)_3^{2+}$ is very limited under conditions applied in the present work.Thus,we conclude that thermally activated electron tunnelling takes place.We have recorded some traces of $MV^{+\cdot}$ cation radical in polymer foils at room temperature,which additionally supports this suggestion.Let us discuss briefly some possible mechanisms of the thermal activation.

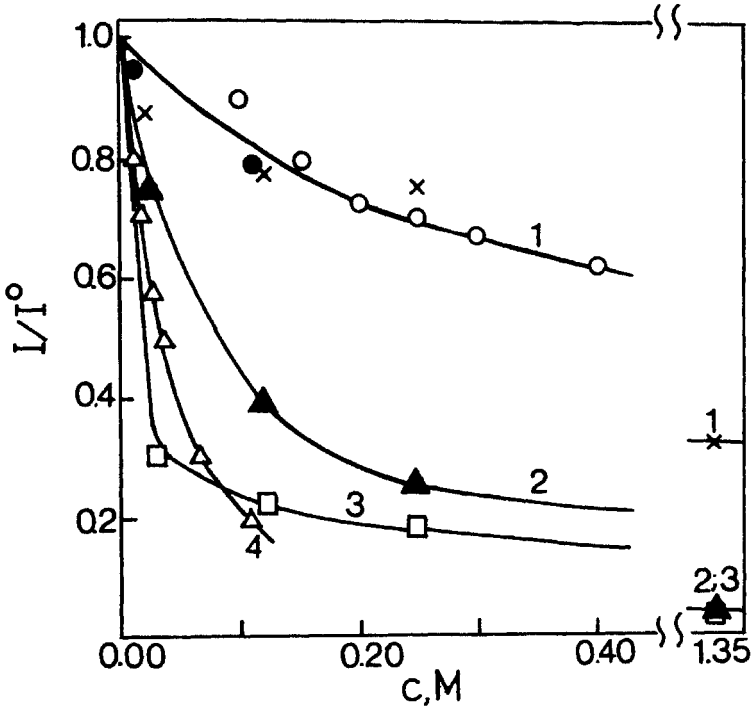

Fig. 2. Normalized intensity of luminescence of $Ru(bpy)_3^{2+}$ as a function of methylviologen concentration.Curve (1) at 77 K ((o) EG/H O,(•) cellophane,(x) poly(vinyl alcohol),curves 2,3 and 4 at room temperature ((▲) poly(vinyl alcohol) in vacuum,(□) poly(vinyl alcohol) in air,(Δ) dry cellophane).

The first mechanism involves the influence of temperature on electron energy levels of electron donor,excited $Ru(bpy)_3^{2+}$ .Thanks to the fine work of Yersin and Gallhuber (Yersin and Gallhuber 1984) one knows a great deal about energy levels of $Ru(bpy)_3^{2+}$ at various temperatures. However,the question of dynamics of electron localization onto one of bpy ligands at low temperatures in polar solvent is still unresolved (Ferguson et al.1985). The reorganisation of the solvation shell arround excited $Ru(bpy)_3^{2+}$ in a glass,polymeric film,or the solid state at low temperatures is long on the time scale for excited state decay (Meyer 1986).At higher temperatures reorganization of the medium is completed at times much shorter than the lifetime of luminescence. Relaxation time of the medium is several orders of magnitude smaller at room temperrature then at 77 K and energy level matching (making electron transfer efficient) could be much faster.

The second activation mechanism involves influence of temperature on energy levels in electron acceptor,i.e MV^{2+}.The energy gap between excited $Ru(bpy)_3^{2+}$ and $MV^{+\cdot}$cation radical is 0.4 eV (Milosavljevic and Thomas 1985).This amount of energy should be dissipated into the medium during electron transfer,mostly via phonon emission.This process is also believed to be thermally activated.

Both factors discussed above are dependent on the medium nature.This agrees well with curves in Fig.2.It is demonstrated that at room temperature the quenching is different in various media while at 77 K this is not case.

Additional proof for the crucial role of thermal activation in the quenching of excited Ru complexes can be inferred from the studies of $Ru(bpy)_2$ (N⟨⟩-⟨⟩N-Me)$_2^{4+}$ (Sullivan et al.1978).In this structure electron acceptor occupies a part of the ligand sphere of the complex. At 77 K the luminescence characteristics resembled those of $Ru(bpy)_3^{2+}$. At room temperature,however,much weaker,short-lived and red-shifted luminescence was observed.This effect was explained in terms of thermally activated electron transfer from bpy ligand to remote pyridinium site (Sullivan et al.1978).

Generally,the present observation suggest that the quenching of luminescence of $Ru(bpy)_3^{2+}$ by methylviologen at 77 K has mainly static character.At higher temperatures the quenching via thermally activated long-range tunnelling occurs in solid phase.The efficiency of this process depends significantly upon the nature of surrounding medium.

ACKNOWLEDGMENT

One of the authors (Cz.S) gratefully acknowledges the possibility to measure time-resolved luminescence at Max-Planck- Institut fur Strahlenchemie,Mulheim,W.Germany.

REFERENCES.

Ferguson J,Krausz ER,Maeder M (1985) Charge localization in the luminescent states of $Ru(bpy)_3^{2+}$ in fluid solutions.J Phys Chem 89:1852-1854.

Guarr T,McGuire M,Strauch S,McLendon G (1983) Collisionless photoinduced electron transfer from ruthenium tris(bipyridine)* homologues to methyl viologen (MV^{2+}) in rigid glycerol solution.J Am Chem Soc 105:616-618.

Guarr T,McGuire ME,McLendon G (1985) Long range photoinduced electron transfer in a rigid polymer.J Am Chem Soc 107:5104-5111.

Miller JR,Peeples JA,Schmitt MJ,Closs GL (1982) Long-distance fluorescence quenching by electron transfer in rigid solutions.J Am Chem Soc 104:6488-6493.

Milosavljevic BH,Thomas JK (1985) Photochemistry of compounds adsorbed into cellulose.5.Solid-state reduction of methylviologen photosensitized by tris(2,2´-bipyridine)ruthenium(II).J Phys Chem 89:1830-1835.

Meyer TJ (1986) Photochemistry of metal coordination complexes:metal to ligand charge transfer excited states.Pure Appl Chem 58:1193-1206.

Seefeld K-P,Mobius D,Kuhn H (1977) Electron transfer in monolayer with incorporated ruthenium (II) complexes.Helv Chim Acta 60:2608-2632.

Stradowski Cz,Wolszczak M (1987) Quenching of excited $Ru(bpy)_3^{2+}$ with methylviologen in solid phase.to be published.

Sullivan BP,Abruna HD,Finklea HO,Salmon DJ,Nagle JK,Meyer TJ (1978) Multiple emission from charge transfer excited states of ruthenium (II)-Polypyridine complexes.Chem Phys Lett 58:389-393.

Yersin H,Gallhuber E (1984) On the lowest excited states of $[Ru(bpy)_3](PF_6)_2$ single crystals. J Am Chem Soc 106:6582-6586.

KINETICS OF THE CHEMILUMINESCENT OXIDATION OF AQUEOUS BR^- BY $Ru(bipyr)_3^{3+}$

L.El-Sayed, D.Salkin Swaim, W.K.Wilmarth+, and A.W.Adamson*

Department of Chemistry, University of Southern California, Los Angeles, CA 90089-1062, USA

A number of examples of chemiluminescent, CL, redox reactions are now known, for which the emission comes from an excited state coordination compound. The best known case is that of the reduction of RuL_3^{3+}, L = 2,2'-bipyridine, by various reductants, with emission from the lowest charge transfer excited state of the product, $[RuL_3^{2+}]^*$ (Lytle, 1971; Gafney 1975; Martin 1972; Vogler 1981; Bolletta 1981, 1982; El-Sayed 1987). As other examples, emission from the doublet thexi state of CrL_3^{3+} has been observed on oxidation of CrL_3^{2+} by RuL_3^{3+} (Vogler 1981) as well as the CL oxidation of $Mo_6Cl_{14}^{3-}$ or reduction of $Mo_6Cl_{14}^{-}$ (El-Sayed 1987). Also, a pair of reactant species may be generated electrochemically, to give an emitting excited state product on back reaction (Bolletta 1982; Nocera 1984; Luong 1978, Rubinstein 1981). The typical CL reaction is fast however, and detailed kinetic studies are rare.

Wilmarth and co-workers (Stanbury 1980) were interested in non-complementary redox reactions, such as between a one-electron oxidant and a two electron reductant; such reactions involve radical intermediates and are often slow enough for conventional kinetic studies, which can yield useful information about the properties of such intermediates. An example is the oxidation of aqueous Br^- by $Fe(5\text{-Br-phen})_3^{3+}$ to give the Fe(II) complex and Br_2 (Salkin 1983) and in a joint study (El-Sayed 1983), the kinetics of the analogous reaction with RuL_3^{3+},

$$2\ RuL_3^{3+} + 2\ Br^- = 2\ RuL_3^{2+} + Br_2\ (\text{or}\ Br_3^-) \qquad (1)$$

has been investigated, along with that of the chemiluminescence, CL, that accompanies the analytical reaction. We report briefly here on this study, with emphasis on the latter aspect.

+ Posthumus contribution.
* To whom correspondence should be addressed.

Photochemistry and Photophysics
of Coordination Compounds, Ed. by H. Yersin/A. Vogler

EXPERIMENTAL

All chemicals used were of reagent grade or were carefully purified (as in the case of $[RuL_3](ClO_4)_2$; the solvent water used was distilled over sodium persulfate and the vapor passed through a tube at 800°C with oxygen carrier gas. Solutions of RuL_3^{3+} were prepared immediately before use by oxidizing an acidified RuL_3^{2+} solution with PbO_2 (the excess then filtered off). The oxidized complex was also prepared photochemically by photolysis of an aerated RuL_3^{2+} solution. No difference in kinetic behavior was observed.

Chemiluminescent intensities, both initial and as a function of time, were measured by means of a quantum counter having a chamber into which a solution of one reactant would be placed and a solution of the second reactant then injected under dark conditions. Various filters could be interposed between the window of the reaction chamber and the photomultiplier detector, so as to determine the CL spectrum. The analytical reaction was followed spectrophotometrically, from the growth of the absorbance of the RuL_3^{2+} product at 453 nm. Reacting mixtures were thermostatted to ± 0.1°C.

There is a slow reaction with water in the absence Br^- (Sutin 1976, 1983; Slawson 1976), which is slightly chemiluminescent. A relatively minor correction was made to both the analytical and the CL rate data to allow for this solvent reaction. Dissolved oxygen increases the CL of the solvent reduction but has little effect on the Br^- reduction.

RESULTS AND DISCUSSION

It was first established that the CL spectrum was essentially the same as that of the photoexcited emission from RuL_3^{2+} and also that the stoichiometry of the analytical reaction (1) was indeed being observed (to within about 10% precision).

Some plots of the decrease in CL intensity, I, with time are shown in Fig. 1, and some of the apparent first order rate constants, k_{CL}, are given in Table 1. Figures 2 and 3 illustrate that the rate law for the CL reaction is

$$I^\circ \text{ (initial CL intensity)} = (\text{constant})(Br^-)^3(RuL_3^{3+})^2 \qquad (2)$$

Separate studies (to be reported elsewhere) showed the rate law for the analytical reaction (1) to be

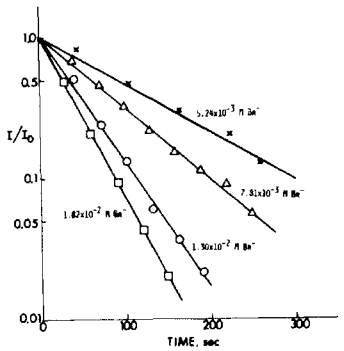

Fig. 1. Semi-logarithmic plot of chemiluminescence intensity vs. time for the Br^- reduction of $Ru(L)_3^{3+}$ in 0.053 M $HClO_4$.

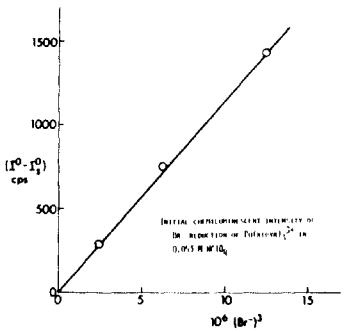

Fig. 2. Dependence of initial CL intensity (corrected for that due to solvent reduction) on (Br^-).

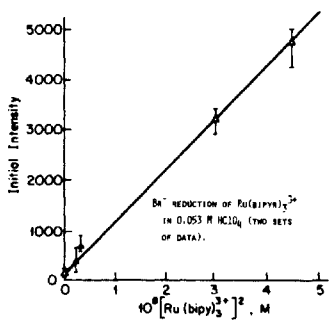

Fig. 3. Dependence of initial CL corrected intensity on (RuL_3^{3+}).

Table 1

Rate Constants for the Analytical and Chemiluminescent Reduction of $Ru(bipyr)_3^{3+}$ by Br^-.

t, °C	$10^2[Br^-]$	$10^2\ k_{CL}, s^{-1}$	$10^2\ k_{AN}, s^{-1}$	k_{CL}/k_{AN}
17.5	1.30	1.13 ± 0.1	0.49 ± 0.09	2.25
27.5	1.82	2.53 ± 0.15	1.69 ± 0.15	*
	1.30	1.53 ± 0.09	0.99 ± 0.03	*
	0.781	0.91 ± 0.07	0.578 ± 0.00	*
37.4	1.30	2.60 ± 0.10	1.13 ± 0.03	2.30

*Not parallel runs

$$- d \ln(RuL_3^{3+})/dt = k_{AN} = k_1(Br^-) + k_2(Br^-)^2 + k_3(Br^-)^3(RuL_3^{3+}) \quad (3)$$

It follows from Eqs. (2) and (3) that $-d(I/I^\circ)/dt = k_{CL} = 2\ k_{AN}$. This expectation is qualitatively confirmed by the data of Table 1, which give $k_{CL}/k_{AN} = 2.3 \pm 0.3$. The chemiexcitation yield was determined, using the luminol system as reference (Brundrett 1974), and found to be 4.2×10^{-5} moles of excited state, $[RuL_3^{2+}]^*$, produced per mole of RuL_3^{3+} reduced.

Our results indicate that the CL pathway is the same as one of the pathways for the analytical reaction, and that via this path, which is a minor one, only about 10^{-4} of reaction events produce excited state product. Note that the ΔG° for reaction (1) is only - 8 kcal, while $[RuL_3^{2+}]^*$ lies about 48 kcal above the ground state. Any mechanism for the CL path must therefore not only conform to the observed rate law, but must also contain a step which is sufficiently energetic to make excited state product formation possible. One possibility is that $Br_2^-\cdot$ radicals produced as intermediates in the analytical reaction can react with RuL_3^{3+} to form $[RuL_2(LBr)]^{2+}$, where LBr is some form of brominated bipyridine. Reaction of this last complex with another $Br_2^-\cdot$ radical could now have sufficient energy to give $[ML_3^{2+}]^*$ + Br_3^- as products. A detailed mechanism can be written such that the kinetics would conform to Eqs. (2) and (3).

The present system appears to be the only one reported for which a direct connection can be made approximately between the mechanisms of the analytical and corresponding CL reaction.

ACKNOWLEDGEMENT

This investigation was supported in part by a grant from the U.S. National Science Foundation.

REFERENCES

Bolletta F, Rossi A, Balzani V (1981) Chemiluminescence on Oxidation of Tris(2,2'-bipyridine)chromium(II): Chemical Generation of a Metal-Centered Excited State. Inorg Chim Acta 53: L23-24.

Bolletta F, Balzani V (1982) Oscillating Chemiluminescence from the Reduction of Bromate by Malonic Acid Catalyzed by Tris(2,2'-bipyridine)ruthenium(II). J Am Chem Soc 104: 4250-4251.

Bolletta F, Ciano M, Balzani V, Serpone N (1982) Polypyridine Transition Metal Complexes as Light Emission Sensitizers in the Electrochemical Reduction of the Persulfate Ion. Inorg Chim Acta 62: 207-213.

Brundrett RB, White EH (1974) Synthesis and Chemiluminescence of Derivatives of Luminol and Isoluminol. J Am Chem Soc 96, 7497-7502.

El-Sayed L (1983) Chemiluminescent Reactions Involving Coordination Compounds. Dissertation, University of Southern California.

El-Sayed L, Adamson AW (1987) Chemiluminescent Reactions of Ru(2,2'-bipyridine)$_3^{+1,+3}$ and $Mo_6Cl_{14}^{-1,-3}$. Inorg Chim Acta accepted.

Gafney HD, Adamson AW (1975) Chemiluminescence, An Illuminating Experiment. J Chem Educ 52: 480-481.

Luong JL, Nadjo L, Wrighton MS (1978) Ground and Excited State Electron Transfer Processes Involving fac-Tri-carbonylchloro(1,10-phenanthroline)rhenium(I). Electrogenerated Chemiluminescence and Electron Transfer Quenching of the Lowest Excited State. J Am Chem Soc 100: 5790-5795.

Lytle FE, Hercules DM (1971) Photobiol 13: 123.

Martin JE Hart EJ, Adamson AW, Gafney H, Halpern J (1972) Chemiluminescence from the Reaction of the Hydrated Electron with Tris(bipyridyl)ruthenium(III). J Am Chem Soc 94: 9238-9240.

Nocera DG, Gray HB (1984) Electrochemical Reduction of Molybdenum(II) and Tungsten(II) Halide Cluster Ions. Electrogenerated Chemiluminescence of $Mo_6Cl_{14}^{2-}$. J Am Chem Soc 106: 824-825.

Rubinstein I, Bard AJ (1981) Electrogenerated Chemiluminescence. 37. Aqueous Ecl Systems Based on Ru(2,2'- bipyridine)$_3^{2+}$ and Oxalate or Organic Acids. J Am Chem Soc 103: 512-516 and citations therein.

Salkin DS (1983) Outer Sphere Electron Transfer Reactions of Some Main Group Substrates. Dissertation, University of Southern California.

Slawson V, Adamson AW (1976) unpublished work.

Stanbury DM, Wilmarth WK, Khalaf S, Po HN, Byrd JE (1980) Oxidation of Thiocyanate and Iodide by Iridium(IV). Inorg Chem 19: 2715-2722.

Creutz C, Sutin N, (1976) Reaction of tris(bipyridine)ruthenium(III) with Hydroxide and its Application in a Solar Energy Storage System. Proc Nat Acad Sci USA 72: 2858-2862.

Sutin N, Creutz C (1983) private communication.

Vogler A, El-Sayed L, Jones RG, Namnath J, Adamson AW (1981) New Chemiluminescent Reactions Involving Coordination Compounds. Inorg Chim Acta 53: L35-L37.

SYNTHESIS AND PHOTOPHYSICAL STUDIES OF ORTHO-METALATED Pd(II) COMPLEXES INCLUDING TWO NOVEL Pd(II)/Rh(III) DIMERS

C.A.Craig, F.O.Garces, and R.J.Watts

Department of Chemistry, University of California, Santa Barbara, CA 93106, USA

INTRODUCTION

The photophysics of cyclopalladated compounds has received attention in the literature recently (Wakatsuki 1985). We were initially interested in exploring the photophysics of a complex prepared by Kasahara (1968); $[Pd(ppy)Cl]_2$. The electronic transitions of this dimeric complex as well as for several monomeric derivatives have been characterized as intra ligand transitions of the ortho-metalated 2-phenylpyridine (ppy) ligand (Craig 1987). Our attention was then focused on combining two different metals of non-equivalent valence into a single molecule. We report here the synthesis, characterization and photophysics of two novel mixed-metal organometallic complexes where palladium(II) and rhodium(III) have been coupled via a halide bridge.

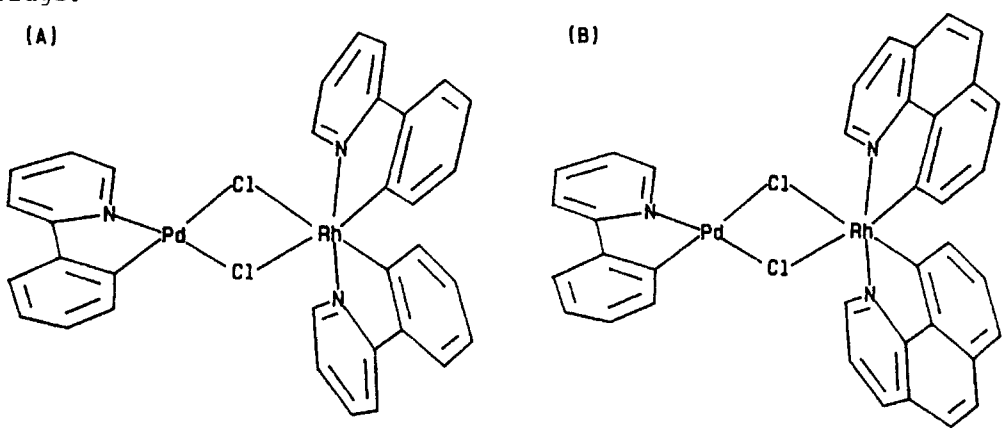

Figure 1. Structures of $[(ppy)Pd(Cl)_2Rh(ppy)_2]$ (A), and $[(ppy)Pd(Cl)_2Rh(bzq)_2]$ (B).

Ortho-metalated transition metal centers linked by a u-dichloro bridge, where the metal is Rh(III) or Ir(III), have been reported to cleave quite readily at the bridge when bidentate chelating ligands are brought in contact with the parent dimer in solution (Nonoyama 1974). Similar cleavage occurs in the presence of monodentate coordinating ligands or in solvents such as DMF, DMSO or acetonitrile resulting in monomeric derivatives of the parent complexes. Not surprisingly, this is true for Pd(II) as well (Cope 1965; Parshall 1969; Trofimenko 1972; Gutierrez 1980; Nonoyama 1982; Sprouse 1984). We utilized this technique to produce monomeric derivatives of the Pd(II) and Rh(III) ortho-metalated dimers $[Pd(ppy)Cl]_2$, $[Rh(ppy)_2Cl]_2$ and $[Rh(bzq)_2Cl]_2$ where: (ppy)=2-phenylpyridine and (bzq)=benzo[h]quinoline. When iradiated in equimolar proportion certain monomeric derivatives of these compounds combine to form heterometallic dichloro-bridged dimers. The newly prepared compounds have the following

Photochemistry and Photophysics
of Coordination Compounds, Ed. by H. Yersin/A. Vogler

formulas: $[(ppy)Pd(Cl)_2Rh(ppy)_2]$ (A), and $[(ppy)Pd(Cl)_2Rh(bzq)_2]$ (B), with proposed structures illustrated in Fig. 1. ^1H NMR for these novel complexes have been obtained and reveal complex splitting patterns. Photophysical data strongly suggests that the emitting states of (A) and (B) are principally ligand localized and each metal center retains its unique emitting manifold.

EXPERIMENTAL

Synthesis of $[(ppy)Pd(Cl)_2Rh(ppy)_2]$

$[Pd(ppy)Cl]_2$ (0.1441 g) was combined with (0.1567 g) $[Rh(ppy)_2Cl]_2$ (Nonoyama 1971) in 100 ml dichloromethane. Carbon monoxide was bubbled through this solution for three hours. The solution was then broad band irradiated with a 150 W Hg source for 1 hour and the dichloromethane evaporated using a flow of nitrogen gas. The residual yellow powder was dissolved in 125 ml of chloroform, filtered, and the chloroform evaporated. The solid was then recrystallized from dichloromethane and hexanes to give 0.2329 g fine needle crystals (90 % yield). Anal. Calculated for $[(ppy)Pd(Cl)_2Rh(ppy)_2]\cdot 1/2CH_2Cl_2$: C, 51.28; H, 3.18; N, 5.35. Found: C, 51.43; H, 3.12; N, 4.92.

Synthesis of $[(ppy)Pd(Cl)_2Rh(bzq)_2]$

The procedure was similar to that used for (A). $[Pd(ppy)Cl]_2$ and $[Rh(bzq)_2Cl]_2$ were combined in equimolar quantities, stirred in the presence of CO for 3 hours and then irradiated for 45 minutes. Upon obtaining the solid it was dissolved in dichloromethane and hexanes and passed through a column containing Sephadex LH-20 resin in order to separate the mixed metal dimer from unreacted starting materials. Mass spectral analysis gave the following peaks: 791,494,459,179,155. Anal. Calculated for $[(ppy)Pd(Cl)_2Rh(bzq)_2]\cdot 1/4CH_2Cl_2$: C, 55.10; H, 3.01; N, 5.17. Found: C, 55.25; H, 3.01; N, 4.76.

Absorption data were obtained with a Cary 15 spectrophotometer or HP 8452A Diode Array Spectrophotometer. Emission lifetime data were obtained with apparatus described elsewhere (Sprouse 1984). All ^1H NMR spectra were measured with a Nicolet NT-300 FT NMR spectrometer.

RESULTS AND DISCUSSION

Compounds (A) and (B) are formed following initial generation of $[Pd(ppy)COCl]$ and $[Rh(L)_2COCl]$ monomeric adducts of the parent dimers (L=(ppy) or (bzq)) (Craig 1987). We know from infrared data that irradiation of the solution containing the carbon monoxide monomers results in photolysis of the terminally bound carbon monoxide ligands on both palladium and rhodium. This suggests formation of two coordinatively unsaturated fragments which then recombine to form compounds (A) and (B). Preferential formation of the mixed metal species may be explained using simple steric arguments. We propose that the sterically hindered coordinatively unsaturated rhodium fragment combines readily with the less bulky palladium fragment. Attempts to repeat these reactions using $[Pd(ppy)Cl]_2$ and $[Ir(ppy)_2Cl]_2$ under identical conditions have been unsuccessful in forming the mixed metal species because of the difficulty in photolyzing CO off of the iridium. We feel that success in forming Pd(II)/Rh(III) dimers is due to facile CO loss under photolysis followed by dimerization.

Both of the mixed metal dimers exhibit unique ^1H NMR spectra which are not superposed spectra of the parent $[Pd(ppy)Cl]_2$ and $[Rh(L)_2Cl]_2$ dimers. ^1H NMR for both mixed metal complexes integrate for 24 protons. 2D COSY ^1H NMR have been obtained for (A) and (B) and from this data we are able to assign all of the chemical shifts in the proton NMR (Craig 1987).

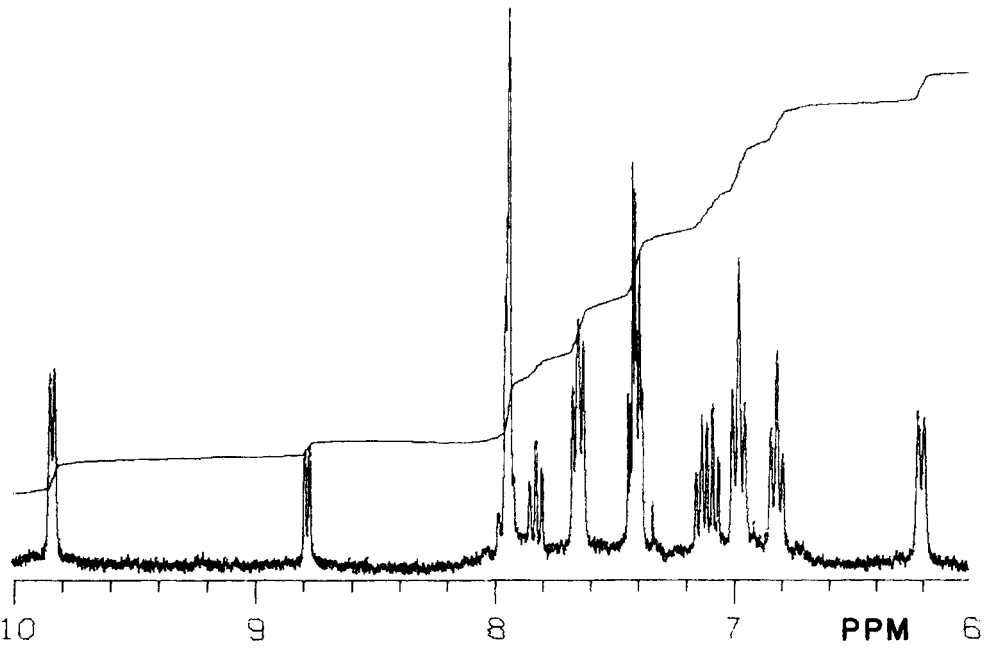

Figure 2. ^1H NMR of $[(ppy)Pd(Cl)_2Rh(ppy)_2]$, CD_2Cl_2 solvent

Room temperature absorption and 77 K emission data for (A) and (B) are shown in Fig. 3. Superposition of the starting dimer spectra with those of the Pd(II)/Rh(III) dimers illustrate obvious similarities between the mixed metal systems and their parent dimer complexes. The low temperature emission spectra of $[Pd(ppy)Cl]_2$ and $[Rh(L)_2Cl]_2$ have been assigned as intra ligand transitions (Sprouse 1984; Craig 1987).

The emission spectrum for complex (B) exhibits two distinguishable emission profiles. Lifetimes were obtained at the maximum peak intensity positions of 460 nm and 484 nm (see Table 1). The lifetime obtained at 484 nm is slightly less than that measured for $[Rh(bzq)_2Cl]_2$, whereas the lifetime at 460 nm is approximately double that of $[Pd(ppy)Cl]_2$. Due to the similarities of the two components of this emission spectrum to the parent dimer materials it appears as if each metal centered fragment of the hetero-dimetallic dimer retains the emission characteristics of its respective parent complex. The lifetime increase at 460 nm for complex (B) relative to $[Pd(ppy)Cl]_2$ could be explained by a decrease in the nonradiative rate of deactivation via the dichloro-bridge for Pd(ppy) which is now bound to a much heavier $Rh(bzq)_2$ species. The opposite effect is also observed for the rhodium portion of the dimer which is now coupled to a lighter palladium moiety. A second source of the lifetime differences might result from deactivation pathways via solvent-chloride bridge interac-

tion. The smaller palladium fragment coupled to the bulkier rhodium fragment would exclude solvent-chloride interaction relative to the $[Pd(ppy)Cl]_2$ dimer resulting in less non-radiative deactivation through this pathway. The $Rh(bzq)_2Cl$ portion of complex (B) would be solvated to a greater degree about the chloride bridge as a result of having the less sterically hindered palladium fragment bound to it. This would have the effect of increasing the solvent-chloride interaction relative to $[Rh(bzq)_2Cl]_2$ allowing for a greater degree of non-radiative deactivation resulting in a decrease in the lifetime at 484 nm.

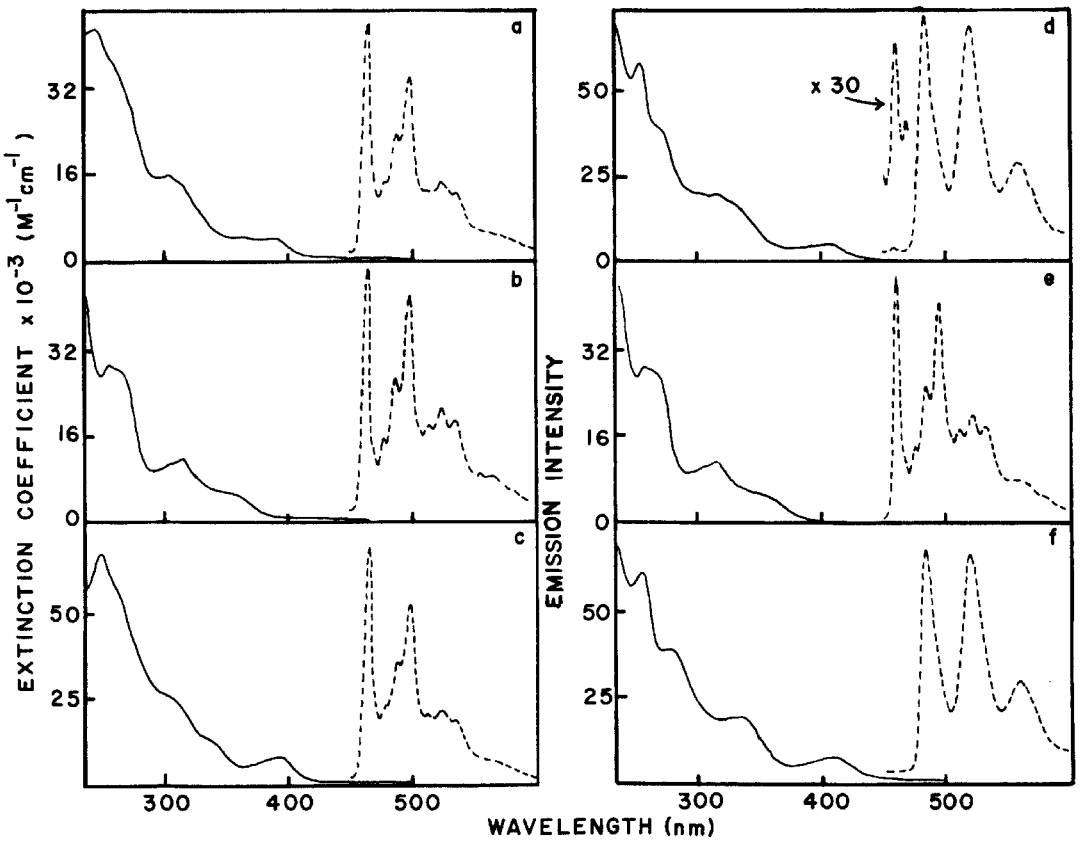

Figure 3. Absorption and 77 K emission spectra of, (a) $[(ppy)Pd(Cl)_2Rh(ppy)_2]$; (b) $[Pd(ppy)Cl]_2$; (c) $[Rh(ppy)_2Cl]_2$ (d) $[(ppy)Pd(Cl)_2Rh(bzq)_2]$; (e) $[Pd(ppy)Cl]_2$; (f) $[Rh(bzq)_2Cl]_2$

The emission spectra for dimer (A), $[Pd(ppy)Cl]_2$ and $[Rh(ppy)_2Cl]_2$ are nearly identical. The lifetimes of these compounds are also very similar. These results make it impossible for us to detect a double exponential decay for complex (A) and we therefore report a single lifetime. If this complex has non-equilibrated electronic excited states analogous to dimer (B), a lifetime which is near that of $[Rh(ppy)_2Cl]_2$ and $[Pd(ppy)Cl]_2$ would be expected. This lifetime would be a weighted average dependent on the quantum yield of emission for each half of the dimer. Exact quantum yields of the parent dimers are

not known at 77 K, however the 484-460 nm peak intensity ratios of the emission spectra for complex (B) and the absorptivity of $[Rh(ppy)_2Cl]_2$ versus $[Pd(ppy)Cl]_2$ suggests that the lifetime should be nearer to that of the $[Rh(ppy)_2Cl]_2$ dimer than the corresponding palladium dimer. Additionally the lifetime is expected to be less than the $[Rh(ppy)_2Cl]_2$ dimer (vida supra).

Table 1. Photophysical data for parent dimers, compounds (A) and (B) and for the free ligands (ppy) and (bzq)

	ABSORPTION FEATURES (nm)	77 K EMISSION E_{0-0} (nm)[b]	77 K LIFETIMES[b]
2-phenylpyridine	240, 295	440[a]	1.9(s)[a]
benzo[h]quinoline	278, 303 352, 364	480[a]	2.2(s)[a]
$[Pd(ppy)Cl]_2$	254, 265(sh) 305(sh), 315 365	460	116(us)
$[Rh(ppy)_2Cl]_2$	240, 310(sh) 333(sh), 380(sh) 393, 450	461	93(us)
$[Rh(bzq)_2Cl]_2$	255, 277, 330(sh), 390(sh) 410, 440(sh)	484	2.6(ms)
$[(ppy)Pd(Cl)_2Rh(ppy)_2]$	245, 265(sh) 305, 315(sh) 365, 393 455(sh)	460	85(us)
$[(ppy)Pd(Cl)_2Rh(bzq)_2]$	247, 257 305(sh), 315 408	460 484	237(us) 2.5(ms)

a. Phosphorescence
b. 4/1/1 V/V/V Ethanol/Methanol/Dichloromethane glass

CONCLUSION

Carbon monoxide is useful in cleaving u-dichloro-bridged systems of the types mentioned. This can be used as a method to derivatize these dimers (Ryabov 1985; Pfeffer 1981; Constable 1980). More importantly however, facile CO bridge cleavage followed by photolysis is a simple and efficient means with which to prepare mixed metal systems. The restriction at this point appears to be that the CO ligand must be somewhat photo labile. It may be possible however to overcome this by altering the ligand used in the cleavage reaction. This may actually become an advantage as one might imagine tailoring reaction and photolysis conditions as a method to selectively prepare mixed metal dimers.

The similarity of the absorption and emission spectra for (A) and (B) to those of $[Pd(ppy)Cl]_2$, $[Rh(ppy)_2Cl]_2$ and $[Rh(bzq)_2Cl]_2$, together with lifetime data is conclusive evidence that the lowest energy excited states of these novel dimers are intra ligand transitions of the ortho-metalated 2-phenylpyridine and benzo[h]quinoline ligands. It might have been expected that these new dimers would have one equilibrated excited state although evidence has been presented here arguing for non-equilibrated excited states in these complexes. We are currently attempting to prepare new dimers of this type using similar ortho-metalated dimer precursors.

ACKNOWLEDGMENT

This work was supported by the Office of Basic Energy Sciences, United States Department of Energy, Project DE-AT03-78ER70277

REFERENCES

Constable AG, McDonald WS, Sawkins LC, Shaw BL (1980) Transition-metal-carbon bonds. Part 45.[1] Attempts to cyclopalladate some aliphatic oximes, NN-dimethylhydrazones, ketazines and oxime O-allyl ethers. Crystal structures of $[Pd_2(CH_2C(CH_3)_2C(=NOH)CH_3)_2Cl_2]$ and $[Pd(CH_2C(=NNMe_2)C(CH_3)_3)(acac)]$. J C S Dalton 1992-2000

Cope AC, Siekman RW (1965) Formation of covalent bonds from platinum or palladium to carbon by direct substitution. J Am Chem Soc 87: 3272-3273

Craig CA, Garces FO, Watts RJ (1987) unpublished results.

Gutierrez MA, Newkome GR, Selbin J (1980) Cyclometallation. Palladium 2-arylpyridine complexes. J Organometal Chem 202: 341-350

Kasahara A (1968) Sigma-bonded 2-phenylpyridine palladium complex. Bull Chem Soc Jpn 41: 1272

Nonoyama M, Yamasaki K (1971) Rhodium(III) complexes of benzo[h]quinoline and 2-phenylpyridine. Nucl Chem Letters 7: 943-946

Nonoyama M (1974) Synthesis of several bis(benzo[h]quinoline-10-YL-N) rhodium(III) complexes. J Organometal Chem 82: 271-276

Nonoyama M (1982) Cyclopalladation and cyclorhodation of N-(3-thienyl)pyrazole. J Organometal Chem 229: 287-292

Parshall GW (1970) Intramolecular aromatic substitution in transition metal complexes. Acc Chem Res 3: 139-144

Pfeffer M, Grandjean D, Le Borgne G[1] (1981) Reactivity of cyclopalladated compounds. 6. Synthesis of heterodimetallic species with Pd-Co, Pd-Mo, or Pd-Fe bonds. X-ray crystal structure of (Dimethylphenylphosphine)tricarbonyl(n-cyclopentadienyl) molybdenum (8-methylquinoline-C,N)palladium(II)(Pd-Mo). Inorg Chem 20:4426-4429

Ryabov AD (1985) The application of cyclopalladated compounds in synthesis. 54: 153-170

Sprouse S, King KA, Spellane PJ, Watts RJ (1984) Photophysical effects of metal-carbon sigma bonds in ortho-metalated complexes of Ir(III) and Rh(III). J Am Chem Soc 106: 6647-6653

Trofimenko S (1973) Some studies of the cyclopalladation reaction. Inorg Chem 12: 1215-1221.

Wakatsuki Y, Yamazaki H, Grutsch PA, Santhanam M, Kutal C (1985) Study of intramolecular sensitization and other excited-state pathways in orthometallated azobenzene complexes of palladium(II). J Am Chem Soc 107: 8153-8159

PHOTOPROPERTIES OF ORTHO-METALATED Ir(III) AND Rh(III) COMPLEXES

K.A.King, F.O.Garces, S.Sprouse, and R.J.Watts

Department of Chemistry, University of California, Santa Barbara, CA 93106, USA

INTRODUCTION

Recent studies have served to provide initial characterizations of the photoproperties of a variety of ortho-metalated complexes of Ir(III) (Sprouse 1984; King 1984, 1985), Rh(III) (Balzani 1986; Sprouse 1984), Ru(II) (Reveco 1985; Constable 1986), Pt(II) (Maestri 1985; Chassot 1986), and Pd(II) (Wakatsuki 1985) with 2-phenylpyridine (ppy), benzo[h]quinoline (bzq) and related ligands. While a portion of the initial impetus for these studies followed from interest in the characterization of ortho-metalated complexes of the widely used ligand, 2,2'-bipyridine (bpy) (Watts 1977; Spellane 1983; Wickramasinghe 1981; Nord 1983; Braterman 1984; Skapski 1985; Cohen 1985; Slama-Schwok 1985; Grutsch 1986; Finlayson 1986), the more traditional ortho-metalating ligands such as ppy and bzq impart upon their metal complexes photoproperties quite distinct from those of either N,N'-chelated or N,C-ortho-metalated bpy complexes. Of particular significance is the ability of these traditional ortho-metalating ligands to impart upon their metal complexes the thermodynamic potential to function as strong reducing agents in their low-energy excited states. Analogous complexes of N,N'-chelating bpy tend to be far superior oxidizing agents but much poorer reducing agents in their low-energy excited states. Recent studies in our laboratory have focused upon ortho-metalated complexes of Ir(III) and Rh(III) with ppy as well as the methyl-substituted ligands 2-(p-tolyl) pyridine (ptpy) and 3-methyl-2-phenylpyridine (mppy). The structures of these ligands are illustrated in Fig. 1 below.

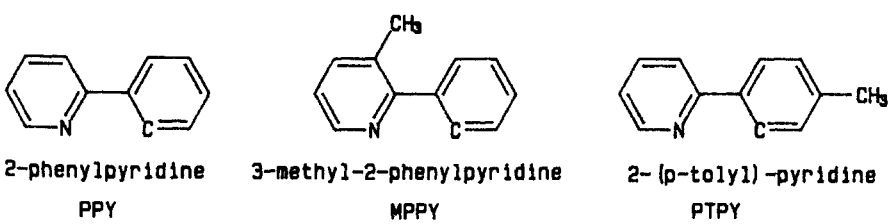

Figure 1. Structures of Ortho-metalating Ligands

These studies provide some initial insights into the relative effects of substitution of the phenyl and pyridyl rings on the photoproperties of ortho-metalated complexes of these ligands.

Photochemistry and Photophysics
of Coordination Compounds, Ed. by H. Yersin/A. Vogler

RESULTS AND DISCUSSION

A variety of monometallic complexes can be prepared (Nonoyama 1971, 1974) by facile reactions of chelating ligands with dimeric species of the type $[M(X\text{-}ppy)_2Cl]_2$, where X-ppy is ppy, ptpy or mppy. For these studies we chose to use bpy as the chelating ligand because its presence in the coordination sphere of the metal ion assures that both good sigma-donor (X-ppy) and pi-acceptor (bpy) ligands are simultaneously coordinated. Several interesting phenomena arise in complexes containing this combination, including: a) low-energy metal-to-ligand charge-transfer (MLCT) transitions; b) MLCT transitions in which a metal electron may be promoted to a pi* orbital of either bpy or the pyridine ring of ppy; and c) excited states capable of functioning as either good electron donors or electron acceptors.

Evidence for dual emissions arising from MLCT excited states associated with bpy and with ppy is found in the time-resolved emission spectrum of $Ir(ppy)_2(bpy)^+$ in low temperature glasses as illustrated in Fig. 2 below.

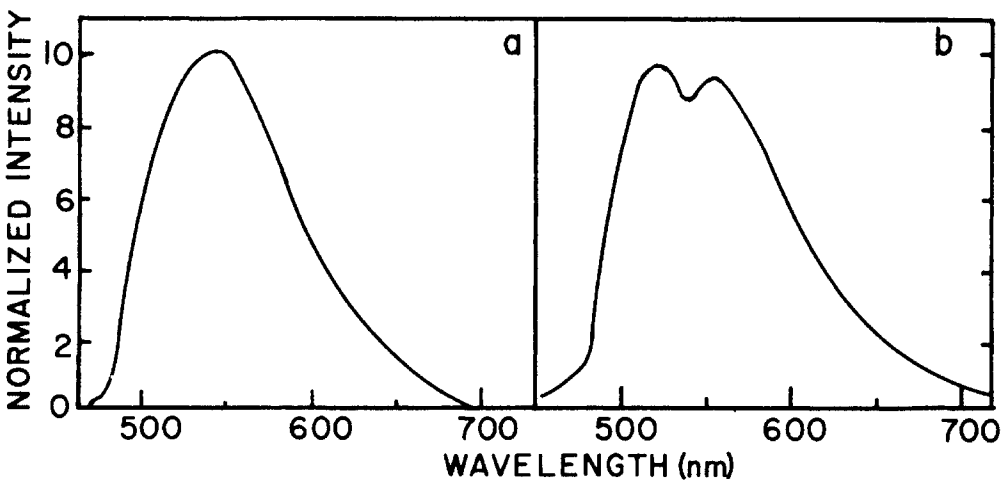

Figure 2. Time-resolved Emission Spectra of $Ir(ppy)_2(bpy)^+$ in Ethanol/Methanol at 77 K Excited at 377 nm with a Pulsed Nitrogen Laser. a) 100 ns after excitation; b) 15 μs after excitation.

Similar results have been found for $Ir(mppy)_2(bpy)^+$ and for $Ir(ptpy)_2(bpy)^+$. In each case the relatively unstructured emission at short delay times (100 ns) is the result of overlapping emissions of states resulting from charge-transfer of a metal electron to a chelating (MLCT/bpy) or ortho-metalating (MLCT/X-ppy) ligand. At longer delay times (10-15 μs) a more structured emission characteristic of the lower-energy MLCT/bpy state is evident. Further evidence for these assignments has been found by monitoring the emission spectra of the Ir(III) complexes as a function of excitation wavelength. In these measurements, excitation at wavelengths longer than 470 nm leads to the same structured MLCT/bpy emission as is seen in Fig. 2b above, while shorter wavelength excitation gives unstructured luminescence

characteristic of overlap of the higher energy MLCT/ppy and lower-energy MLCT/bpy emissions. $Rh(ppy)_2(bpy)^+$, on the other hand, displays a single emission characteristic of a ligand-localized state associated with ppy (LL/ppy) in both time-resolved emission spectroscopy and in excitation-emission spectroscopy. These results indicate that the intramolecular electron transfer (Meyer, 1978) from MLCT/ppy to MLCT/bpy is slow in Ir(III) complexes in rigid glasses whereas resonance energy transfer (Balzani, 1980) from (LL/bpy) to (LL/ppy) in the Rh(III) complex is rapid. The result is attributed to a viscosity dependent Franck-Condon barrier (Dellinger, 1975, 1976; Watts, 1978) to intramolecular electron transfer which arises from a large distortion of the MLCT(bpy) state relative to the ground state. Evidence for this distortion is found in the room temperature emissions of the Ir(III) complexes in fluid solutions, which display large Stoke's shifts and a single emission characteristic of the MLCT/bpy excited state under these conditions. In contrast, the LL/ppy and LL/bpy states in $Rh(ppy)_2(bpy)^+$ are relatively undistorted compared to the ground state, and resonance energy transfer proceeds rapidly without significant Franck-Condon barriers.

Half-wave potentials for the first oxidation and first reduction of several Ir(III) and Rh(III) complexes from cyclic voltammograms are compiled in Table 1 below.

Table 1. Half-wave Potentials for Ir(III) and Rh(III) Complexes in TEAH-saturated Acetonitrile at Room Temperature

	$E_{1/2}$[a], V vs SCE	
Complex	2+/1+	1+/0
$Ir(ppy)_2(bpy)^+$	1.28	-1.38
$Ir(mppy)_2(bpy)^+$	1.21	-1.41
$Ir(ptpy)_2(bpy)^+$	1.18	-1.42
$Rh(ppy)_2(bpy)^+$	1.60[b]	-1.38

a. A scan rate of 1.0 V/s was used in each measurement
b. Anodic peak potential of irreversible wave

The reductive process (+1/0) is reversible in all of the complexes which were studied, whereas the oxidative process is reversible in the Ir(III) complexes but irreversible in the Rh(III) complex. The reductive process is believed to occur at the bpy ligand whereas the oxidative process (+1/+2) is thought to be metal-centered in the Ir(III) complexes. The high potential oxidative process in the Rh(III) complex is irreversible and oxidation may occur at the ppy ligand in this instance. Variations of 100 mv in the $E_{1/2}$ values for the 1+/2+ oxidative process among the three Ir(III) complexes reflect the degree to which the methyl substituents enrich the electron density at the metal center.

By combining values of the potentials for the oxidative and reductive processes in Table 1 with estimates of the excited state energies of these complexes taken from low temperature emission maxima (2.34 V), standard electrochemical potentials for the luminescent excited state of each species can be estimated. This procedure leads to estimated values of $E°(2+/*1+)$ in the range -1.06 V vs SCE $[Ir(ppy)_2(bpy)^+]$ to

-1.16 V vs SCE [$Ir(ptpy)_2(bpy)^+$] and to values for E°(*1+/0) of about 0.95 V vs SCE for all four complexes. These estimates assume that entropy changes upon excitation are negligible, and although they are expected to provide adequate estimates of the thermodynamic driving force for excited state redox processes, they do not reflect kinetic limitations to electron transfer which might arise from Franck-Condon barriers or non-adiabatic behavior (Sutin 1983). In order to more fully characterize the kinetics of excited state oxidation and reduction reactions, Stern-Volmer studies of the quenching of the emission of $Ir(ppy)_2(bpy)^+$ by a series of oxidative quenchers (nitrobenzenes) (Bock 1975) and a series of reductive quenchers (phenylamines and methoxybenzenes) (Marshall 1984) were performed. The results of these studies are summarized in Fig. 3 below.

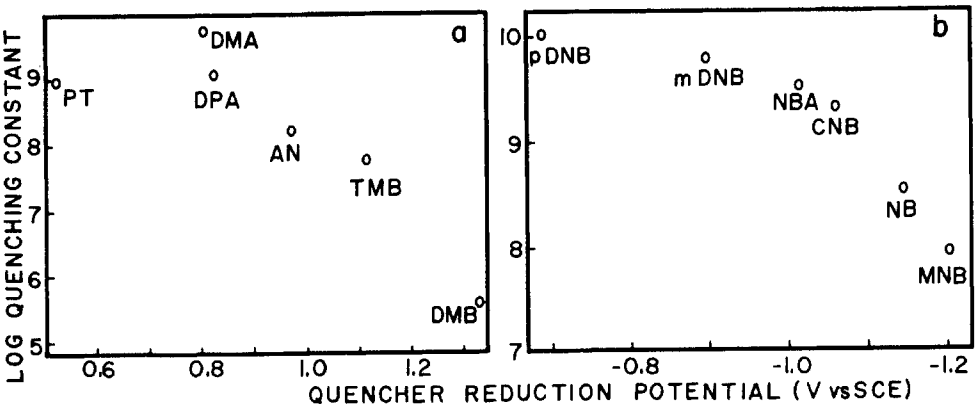

Figure 3. Stern-Volmer Quenching of $Ir(ppy)_2(bpy)^+$ in Acetonitrile by Reductive (a) and Oxidative (b) Quenchers.
(a) PT, Phenothiazine; DMA, N,N-dimethylaniline; DPA, diphenylamine; AN, aniline; TMB, 1,2,4-trimethoxybenzene; DMB, 1,4-dimethoxybenzene
(b) pDNB, p-Dinitrobenzene; mDNB, m-Dinitrobenzene; NBA, m-nitrobenzaldehyde; CNB, p-chloronitrobenzene; NB, nitrobenzene; MNB, p-methylnitrobenzene

Kinetic estimates of the excited state redox potentials taken from the breaking region between the diffusion controlled limit and the linear region indicate a value of E°(2+/*1+) of -1.1 V vs SCE and a value of E°(*1+/0) of +0.98 V vs SCE. These values are in good agreement with the thermodynamic estimates above, and the relatively narrow breaking region in the plots in Fig. 3 suggest that reorganizational barriers toward either oxidative or reductive electron transfer are small.

SUMMARY

Combined photophysical, photochemical, and electrochemical studies of these and related ortho-metalated complexes of a variety of transition metals indicate that this class of molecular species provides a useful basis for the study of effects of metal-carbon sigma-bonding on electron-transfer processes. While the covalent nature of these metal-carbon bonds may well assure strong electronic coupling of

excited states in these complexes, these bonds may also impose large geometric distortions on excited states associated with ligands trans- to them. The associated Frank-Condon barriers may, in viscous solvents, lead to dual emissions such as those observed in the Ir(III) complexes.

The strong sigma-donor abilities of ortho-metalating ligands greatly enriches the electron denisty at the metal center in their complexes, and leads to species which are often strong reducing agents in their excited states. When these ligands are combined with good electron accepting ligands, such as bpy, in the coordination sphere of a single metal, complexes which can be used as either excited state oxidizing or reducing agents result. Kinetic Stern-Volmer quenching studies indicate that these species do indeed participate in outer sphere electron transfer reactions with driving forces comparable to the values estimated from combined spectroscopic-electrochemical results. Ortho-metalated complexes show promise for application as photocatalysts where there is a need for substances which can absorb visible light and convert a large fraction of the absorbed energy into reducing power in relatively long-lived excited states.

ACKNOWLEDGMENT

This work was supported by the Office of Basic Energy Sciences, United States Department of Energy, Project DE-AT03-78ER70277

REFERENCES

Balzani V, (private communication 1986)
Balzani V, Bolleta F, Scandola F (1980) J Am Chem Soc 102: 2152-2163
Bock CR, Meyer TJ, Whitten DG (1975) J Am Chem Soc 97: 2909-2911
Braterman PS, Heath GA, MacKenzie AJ, Noble BC, Peacock RD, Yellowless LJ (1984) Inorg Chem 23: 3425-3426
Chassot L, von Zelewsky A, Sandrini D, Maestri M, Balzani V (1986) J Am Chem Soc 108: 6084-6085
Cohen H, Slama-Schwok A, Rabani J, Watts RJ, Meyerstein D (1985) J Phys Chem 89: 2465-2467
Constable EC, Holmes JM (1986) J Organomet Chem 301: 203-208
Dellinger B, Kasha M (1975) Chem Phys Lett 36: 410-414
Dellinger B, Kasha M (1976) Chem Phys Lett 38: 9-14
Finlayson MF, Ford PC, Watts RJ (1986) J Phys Chem 90: 3916-3922
Grutsch PA, Kutal C (1986) J Am Chem Soc 108: 3108-3110
King KA, Finlayson MF, Spellane PJ, Watts RJ (1984) Sci Pap Inst Phys Chem Res 78: 97-106
King KA, Spellane PJ, Watts RJ (1985) J Am Chem Soc 107: 1431-1432
Maestri M, Sandrini D, Balzani V, Chassot L, Jolliet P, von Zelewsky A (1985) Chem Phys Lett 122: 375-379
Marshall JL, Stobart SR, Gray HB (1984) J Am Chem Soc 106: 3027-3028
Meyer TJ (1978) Acc Chem Res 11: 94-100
Nonoyama M (1974) Bull Chem Soc Jpn 47: 767-768
Nonoyama M, Yamasaki K (1971) Inorg Nucl Chem Lett 7: 943-946
Nord G, Hazell A, Hazell RG, Farver O (1983) Inorg Chem 22: 3429-3434
Reveco P, Schmehl RH, Cherry WR, Fronczek FR, Selbin J (1985) Inorg Chem 24: 4078-4082
Skapski AC, Sutcliffe VF, Young GB (1985) J Chem Soc Chem Commun 609-611
Slama-Schwok A, Gershuni S, Rabani J, Cohen H, Meyerstein D (1985) J Phys Chem 89: 2460-2464

Spellane PJ, Watts RJ, Curtis CJ (1983) Inorg Chem 22: 4060-4062
Sprouse S, King KA, Spellane PJ, Watts RJ (1984) J Am Chem Soc 106: 6647-6653
Sutin N, Creutz C (1983) J Chem Ed 60: 809-814
Wakatsuki Y, Yamazaki H, Grutsch PA, Santhanam M, Kutal C (1985) J Am Chem Soc 107: 8153-8159
Watts RJ, Harrington JS, van Houten J (1977) J Am Chem Soc 99: 2179-2187
Watts RJ, Missimer D (1978) J Am Chem Soc 100: 5350-5357
Wickramasinghe WA, Bird PH, Serpone N (1981) J Chem Soc Chem Commun: 1284-1286

GROUND AND EXCITED STATE INTERACTIONS IN MULTIMETAL SYSTEMS

J.D.Petersen

Department of Chemistry, Clemson University, Clemson, SC 29634-1905, USA

This article discusses data from this and other laboratories with respect to the electronic communication across various aromatic, nitrogen heterocyclic ligands in polymetallic complexes. As the nature and complexity of the bridging ligand in transition metal comlexes increases our understanding of the factors that affect ground- and excited-state electronic coupling must be more fully understood. The majority of the work sited here is from our laboratories and has involved numerous graduate students and post-doctoral fellows, most notably Andrea Wallace, Karen Brewer, and Rory Murphy.

BACKGROUND

The excited-state reactivity of complexes related to $Ru(bpy)_3^{2+}$ (where bpy = 2,2'-bipyridine) has received considerable attention because of the long-lived, excited-state of this species at room temperature in fluid solution, and the ability of this complex and its derivatives to undergo fascile excited-state electron- or energy--transfer reactions. The fact that $Ru(bpy)_3^{2+}$ absorbs visible light (intense metal-to-ligand charge-transfer transition) has made it a prime candidate for a variety of solar-energy-driven, fuel production schemes.

Recently, the capabilities of these complexes have been expanded by the preparation and characterization of complexes like $Ru(dpp)_3^{2+}$ (where dpp = 2,3-bis(2'-pyridyl)pyrazine). Like the intensely studied $Ru(bpy)_3^{2+}$ center, $Ru(dpp)_3^{2+}$ absorbs visible light, has a long-lived, emissive, excited state, and is stable thermally in both oxidized and reduced forms. One advantage that $Ru(dpp)_3^{2+}$ has over $Ru(bpy)_3^{2+}$ is that the former is capable of binding an additional metal center to each of the dpp ligands to form thermally stable, polymetallic complexes. In addition, mixed-ligand, polymetallic complexes have been prepared using dpp and other related ligands such as 2,2'-bipyrimidine (bpm), and 2,3-bis(2'-pyridyl)quinoxaline(dpq). While polymetallic complexes afford the advantage that synthetically you can bring all reaction partners together in a single molecular unit (thus avoiding the inherent inefficiency of bimolecular processes), these systems are complex molecular units which are not well understood. The fact that some of these polymetallic systems emit at room temperature in fluid solution while other don't, and the inconsistent trends in electrochemistry in going from monometallic to bimetallic to polymetallic species have generated numerous and varied hypotheses on the existence and the nature of metal-metal communication in these ligand-bridged systems.

Photochemistry and Photophysics
of Coordination Compounds, Ed. by H. Yersin/A. Vogler

GROUND STATE COMMUNICATION

The electrochemistry of mono- di- and polymetallic complexes of three bridging ligands, bpm (2,2'-bipyrimidine), dpp and dpq are summmarized in Table I. In the first two data columns of Table I, some interesting trends are observed for the metal oxidations. The comparison of the $Ru^{III/II}$ couple in a monometallic complex with the first $Ru^{III/II}$ couple in the corresponding bimetallic analog shows slightly different behavior dependent on BL. In the case of BL = bpm, the first $Ru^{III/II}$ couple is 0.13 V more positive for the bimetallic $[Ru(bpy)_2]_2bpm^{4+}$ than the mono-metallic $Ru(bpy)_2bpm^{2+}$ complex. For the other BL entries in Table I the differences are much smaller (0.00-0.05 V). Gaffney and coworkers have attributed this to ground-state metal-metal communication in the bimetallic systems. When BL = bpm, good electronic communication is exhibitied between the two ruthenium centers causing the 0.13 V shift in potential and leading to loss of emission (room temperature, fluid solution) for the bpm-bridged bimetallic complex. On the other hand, dpp and dpq bridged species show only small potential shifts from monometallic analogs (0.00-0.05 V) due to a lack of ground-state communication, and thus the room temperature emission is observed in the polymetallic complexes and not quenched by the presence of the second metal center.

TABLE I. Electrochemistry of Mono-, Di-, Tri- and Polymetallic Complexes of Ruthenium Polyazine Complexes[a]

Complex	$E_{1/2}(1)^{ox}$ b)	$E_{1/2}(2)^{ox}$ c)	$E_{1/2}(1)^{red}$ d)
$Ru(bpy)_2bpm^{2+}$	1.40	--	-1.02
$[Ru(bpy)_2]_2bpm^{4+}$	1.53	1.69	-0.41
$Ru[(bpm)Ru(bpy)_2]_3^{8+}$	irreversible		
$Ru(bpy)_2dpp^{2+}$	1.33	--	-1.06
$[Ru(bpy)_2]_2dpp^{4+}$	1.38	1.56	-0.66
$Ru[(dpp)Ru(bpy)_2]_3^{8+}$	1.50[e]	1.8[f]	-0.56
$Ru(phen)_2dpp^{2+}$	1.39	--	-1.07
$[Ru(phen)_2]_2dpp^{4+}$	1.44	1.65	-0.64
$Ru[(dpp)Ru(phen)_2]_3^{8+}$	1.43[e]	1.8[f]	-0.5
$Ru(bpy)_2dpq^{2+}$	1.42	--	-0.77
$[Ru(bpy)_2]_2dpq^{4+}$	1.47	1.62	-0.37
$Ru(phen)_2dpq^{2+}$	1.42	--	-0.79
$[Ru(phen)_2dpq^{4+}$	1.48	1.64	-0.40

a) In acetonitrile with 0.1 M supporting electrolyte unless noted otherwise.
b) Potential for oxidation of first Ru(II) center (in V vs. SCE)
c) Potential for oxidation of second Ru(II) center where appropriate (in V vs. SCE).
d) Potential for first reduction of complex (in V vs. SCE).
e) Corresponds coulometrically to a three-electron process.
f) Outside solvent window.

For the tetrametallic complexes, the same trends are observed. With bpm as the bridging ligand, i.e., $Ru[(bpm)Ru(bpy)_2]_3^{8+}$, no room temperature emission is observed and the electrochemistry is irreversible. When dpp is the bridging ligand, the tetrametallic complexes emit at room temperature and have electrochemistry consistent with minimal communication between the peripheral metal centers. While resonance Raman studies may indicate that the high degree of electronic communication in bpm and lack of electronic communication in dpp and dpq bridged systems is due to ligand conformation, that may not be the total picture. Electrochemical oxidation of the bimetallic complexes of Fe(II) and Ru(II) show that the electronic communication as measured by comproportionation constant is roughly the same for bpm, dpp, and dpq systems (Table II).

Table II. [a]Comproportionation Constants for Various Bimetallic Complexes.

Complex	$E_{1/2}$, mV[b]	K_{com}
$[Ru(bpy)_2]_2bpm^{4+/5+/6+}$	160	5.1×10^2
$[Ru(bpy)_2]_2dpp^{4+/5+/6+}$	180	1.1×10^3
$[Ru(bpy)_2]_2dpq^{4+/5+/6+}$	150	3.4×10^2
$[Ru(phen)_2]_2dpp^{4+/5+/6+}$	210	3.5×10^3
$[Ru(phen)_2]_2dpq$	160	5.1×10^2
$[Fe(CN)_4]_2bpm^{4-/3-/2-}$	140	2.3×10^2
$[Fe(CN)_4]_2dpp^{4-/3-/2-}$	150	3.4×10^2

a) In acetonitrile with 0.1 M supporting electrolyte unless noted.
b) $E_{1/2}(2)^{ox}-E_{1/2}(1)^{ox}$ from Table I.

Thus, while emission studies indicate that extensive ground-state communication occurs only for bpm, the electrochemistry gives ambiguous results.

EXCITED STATE PROPERTIES

The bpm, dpp, and dpq monometallic complexes and the dpp and dpq bi- and tetrametallic complexes emit at room temperature in fluid solution with lifetimes in the 20 - 300 ns region. The emission is charge transfer in nature and involves the lowest energy π^* orbital (bpm, dpp or dpq) and the Ru d_π core. Regardless of the complexity of the system, the emission energy depends on whether the bpm, dpp, or dpq ligand is terminal or bridged and is not sensitive to the number of metal centers present (Table III). As an example of this phenomenon, all of the polymetallic complexes containing bridging dpp (Table III) have emission maxima between 746 and 772 nm.

TABLE III. Emission Maxima and Lifetimes of Mono-, Bi- and Tetrametallic Complexes in Acetonitrile at Room Temperature

Complex	λ_{max}^{em}, nm	τ, ns
Monometallics		
$Ru(bpm)_3^{2+}$	639	131
$Ru(bpy)_2bpm^{2+}$	710	76
$Ru(dpp)_3^{2+}$	623	183
$Ru(bpy)_2dpp^{2+}$	660	226
$Ru(phen)_2dpp^{2+}$	652	252
$Ru(dpq)_3^{2+}$	716	82
$Ru(bpy)_2dpq^{2+}$	766	71
$Ru(phen)_2dpq^{2+}$	756	83
dpp Polymetallics		
$[Ru(bpy)_2]_2dpp^{4+}$	756	134
$[Ru(phen)_2]_2dpp^{4+}$	746	153
$Ru(phen)_2dppRu(bpy)_2^{4+}$	752	113
$Ru[(dpp)Ru(bpy)_2]_3^{8+}$	772	89
$Ru[(dpp)Ru(phen)_2]_3^{8+}$	760	87
$Ru[(dpp)Ru(tpy)Cl]_3^{5+}$	758	50-200
dpq Polymetalilcs		
$[Ru(bpy)_2]_2dpq^{4+}$	822	<20
$[Ru(phen)_2]_2dpq^{4+}$	810	20
$Ru(phen)_2dpqRu(bpy)_2^{4+}$	820	<20

The data above indicate that very few parameters are necessary to determine emission energies in polymetallic centers. Thus, highly absorbing molecular fragments can be placed into supramolecular systems with controllable and predictable properties and utilized for visible-light intramolecular sensitization.

REFERENCES

Brauenstein C H, Baker A D, Strekas T C, Gafney H D (1984) Inorg Chem 23:857
Brewer K J, Murphy, Jr. W R, Spurlin S R, Petersen J D (1986) Inorg Chem 25:882
Dose E V, Wilson L J (1978) Inorg Chem 17:2660
Hunziker M, Ludi A (1977) J Am Chem Soc 99:7370
Navon G, Sutin N (1974) Inorg Chem 13:2159
Rillema D P, Mack K B (1982) Inorg Chem 21:3849
Rillema D P, Allen G, Meyer T J, Conrad D (1983) Inorg Chem 22:1617
Ruminski R R, Petersen J D (1982) Inorg Chem 21:3706

PHOTOPHYSICAL AND PHOTOCHEMICAL PROPERTIES OF RUTHENIUM(II) MIXED-LIGAND COMPLEXES: PRECURSORS TO HOMONUCLEAR AND HETERONUCLEAR MULTIMETAL COMPLEXES CONTAINING RUTHENIUM(II), PLATINUM(II), RHENIUM(I) AND RHODIUM(III)

D.P.Rillema* and H.B.Ross

Department of Chemistry, The University of North Carolina at Charlotte, Charlotte, NC 28223, USA

INTRODUCTION

The mononuclear ruthenium(II) complexes addressed in this report contain chelating ligands with remote bidentate coordination sites. These sites have been used in our laboratories to coordinate ruthenium(II), platinum(II) (Sahai 1986), rhenium(I) and rhodium(III). The photophysical properties of the mononuclear mixed-ligand ruthenium(II) complexes have indicated that photophysical properties of excited states can be synthetically controlled. These issues are addressed in this report along with radiative and substitution quantum yields, excited state redox potentials, and energy gap correlations.

MIXED-LIGAND COMPLEXES

Preparations

Ligands with remote nitrogen donors are shown in Fig. 1

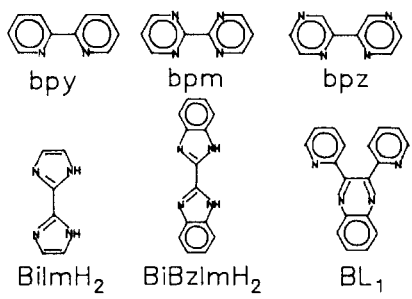

Figure 1. Heterocyclic Ligands

Abbreviations are as follows:
bpy = 2,2'-bipyridine
bpm = 2,2'-bipyrimidine
bpz = 2,2'-bipyrazine
BL_1 = 2,3-bis(2-pyridyl)quinoxaline
$BiImH_2$ = 2,2'-Biimidazole
$BiBzImH_2$ = 2,2'-Bibenzimidazole

The ligands bpy, bpm, bpz and BL_1 are π-acceptors; the ligands $BiImH_2$ and $BiBzImH_2$ are π-donors. These ligands form the basis for sequences such as $[Ru(bpy)_{3-n}(BL)_n]^{2+}$, where n = 1, 2 and 3 and BL is a bidentate chelating ligand.

The preparation of the ruthenium(II) mixed-ligand complexes has involved several thermal (Rillema 1982, 1983; Haga 1983) and photochemical procedures. One thermal method has involved formation of weakly coordinated acetone (eq. 1) followed by reaction with an excess of the desired bidentate ligand to give $[Ru(bpy)_2BL]^{2+}$. A more

$$Ru(bpy)_2Cl_2 + 2AgPF_6 \xrightarrow[\Delta]{S=CH_3\overset{O}{\overset{\|}{C}}CH_3} [Ru(bpy)_2S_2]^{2+} + 2\underline{AgCl} + 2PF_6^- \quad [1]$$

*Person to contact for reprints

Photochemistry and Photophysics
of Coordination Compounds, Ed. by H. Yersin/A. Vogler

general route to a variety of ruthenium(II) complexes has involved reaction of the appropriate ruthenium precursor complex with an excess of BL ligand in ethylene glycol according to eq. 2. Formation of ruthenium(II) complexes containing the bibenzimidazole ligand

$$\begin{matrix} Ru(bpy)_2Cl_2 \\ Ru(bpy)Cl_4 \\ RuCl_3\ 3H_2O \end{matrix} \xrightarrow[x\text{'s BL}, \Delta]{\text{ethylene glycol = EG}} \begin{matrix} [Ru(bpy)_2BL]^{2+} \\ [Ru(bpy)(BL)_2]^{2+} \\ [Ru(BL)_3]^{2+} \end{matrix} \qquad [2]$$

followed the procedures of Haga (1983), who used glycerol as the reaction medium rather than ethylene glycol.

Photochemical reactions were used to synthesize complexes that could not be obtained thermally. Ligand loss was effected in the presence of Cl^- and acetonitrile to yield an acetochloro intermediate (eq. 3), which then was reacted with an excess of the BL ligand via eq. 2

$$[Ru(bpz)_3]^{2+} \xrightarrow[CH_3CN]{h\nu,\ Cl^-} [Ru(bpz)_2(CH_3CN)Cl]^+ \qquad [3]$$

resulting in formation of $[Ru(bpz)_2(BL)]^{2+}$.

Ligand Loss Photochemistry: The Lowest π^* Energy Level vs. Monodentate Coordination

The energy of the ligand π^* levels are in the order BL_1 < bpz < bpm < bpy based on their respective reduction potentials of -1.56V, -1.76V, -1.99V and -2.21V vs. SSCE. For $[Ru(bpy)_3]^{2+}$ population of the metal to ligand charge transfer state reportedly "localizes" the electron on one of the bpy ligands (Dallinger 1979). It is reasonable, then, that in closely related systems decay would be to the ligand with the lowest π^* energy levels and this ligand would be lost upon photolysis. Reactions such as given in eq. 4 verified this hypothesis. Upon photolysis, the bpz (eq. 4) ligand was lost to give the appropriate

$$[Ru(bpz)_2(bpy)]^{2+} \xrightarrow[CH_3CN]{h\nu,Cl^-} [Ru(bpz)(bpy)(CH_3CN)Cl]^+ \xrightarrow[EG,\Delta]{bpm} [Ru(bpz)(bpy)(bpm)]^{2+} \qquad [4]$$

acetochloro complex. It was then reacted with bpm to produce the $[Ru(bpz)(bpy)(bpm)]^{2+}$ cation.

Photolysis of the monodentate acetochloro complexes, on the other hand, resulted in loss of acetonitrile as illustrated in eq. 5. Analogous results were reported by Pinnick (1983) for $[Ru(bpy)_2(CH_3CN)Cl]^+$

$$[Ru(bpz)_2(CH_3CN)Cl]^+ \xrightarrow[CH_3CN]{h\nu,Cl^-} [Ru(bpz)_2Cl_2] \qquad [5]$$

and suggested that energy transfer from the ^{3}MLCT energy manifold into the $d\sigma^*$ state labilizes the monodentate rather than the bidentate ligand. The stability of the bidentate ligand to photosubstitution most likely is due to the chelate effect.

Photochemical Quantum Yields, Radiative Lifetimes, and Radiative Quantum Yields

Data in Table 1 are arranged in descending order of emission energy maxima with the exception that the entry for $[Ru(bpy)_3]^{2+}$ is on the top for comparison to the others. Room temperature excited state lifetimes were found to vary from a little over a microsecond for $[Ru(bpz)_2(bpy)]^{2+}$ to a few nanoseconds for $[Ru(bpy)_2BL_1]^{2+}$. Radiative quantum yields reached a maximum of 0.042 for $[Ru(bpy)_3]^{2+}$ and a minimum of 1.8×10^{-5} for $[Ru(bpm)_2(CH_3CN)Cl]^{+}$. Photochemical substitutions were effected in acetonitrile solutions containing 1mM tetraethylammonium chloride (TEACl). The substitution quantum yields spanned the range from 0.35 for $[Ru(bpz)_3]^{2+}$ to $<1.0 \times 10^{-4}$ for $[Ru(bpy)_2BL_1]^{2+}$.

Ground State and Excited State Properties

A comparison of the ground state and excited state properties of the various complexes listed in Table 1 is illustrated in Fig. 2. The ground state redox potentials shown are for the $Ru^{3+/2+}$ and $Ru^{2+/+}$ couples, although the $Ru^{2+/+}$ couple actually involves the reduction of the most easily reduced coordinated ligand, e.g. $[Ru^{II}(bpz)(bpy)(bpm)]^{2+}/[Ru^{II}(bpz^{-})(bpy)(bpm)]^{+}$. As shown in Fig. 2, potentials for the $Ru^{2+/+}$ couple become more negative in the following order: $[Ru(BL_1)_3]^{2+/+} < [Ru(bpz)_3]^{2+/+} < [Ru(bpm)_3]^{2+/+} < [Ru(bpy)_3]^{2+/+}$. Potentials for the $Ru^{3+/2+}$ couple become more negative in the sequence: $[Ru(bpz)_3]^{3+/2+} < Ru(BL_1)_3^{3+/2+} < Ru(bpm)_3^{3+/2+} < Ru(bpy)_3^{3+/2+}$. In comparison to the other ligands, bpz stabilizes ruthenium(II) relative to ruthenium(III); the bpy ligand stabilizes ruthenium(II) relative to coordinated ligand reduction (Ru^{II}-BL^{-}). These effects are related to the stronger σ donor properties of bpy compared to bpz (pK_a of pyridine = 5.3 (Summers 1970); pK_a of pyrazine = 0.3 (Ford 1968)) and stronger π acceptor character of bpz relative to bpy. The σ and π properties of the bpm and BL_1 ligands fall in between these extremes.

Excited state $Ru^{2+*/+}$ and $Ru^{3+/2+*}$ potentials were determined by the difference between $E_{0,0}$-values (the energy difference between the zeroth vibrational level of the excited state emitting manifold and that of the zeroth vibrational level of the ground state) (Allen 1984; Rillema 1987) and the ground state redox potentials, e.g. $E^{2+*/+} = E_{0,0} - E^{2+/+}$; $E^{3+/2+*} = E^{3+/2+} - E_{0,0}$. The figure shows that the $[Ru(bpy)_3]^{3+/2+*}$ and $[Ru(bpy)_3]^{2+*/+}$ redox potentials are more negative than potentials of similar tris chelate ruthenium complexes. Furthermore, Fig. 2 shows that the $[Ru(BL_1)_3]^{3+/2+*}$ potential is a positive value whereas all other $Ru^{3+/2+*}$ potentials are negative quantities. In addition, the most positive $Ru^{2+*/+}$ couple is for $[Ru(bpz)_3]^{2+}$.

Energy Gap Correlations

Energy gap correlations are given in Figs. 3-5. The energy gap given by $\Delta E_{1/2}$ is the difference in potential between the $Ru^{3+/2+}$ and $Ru^{2+/+}$ redox couples. e.g. $\Delta E_{1/2} = E_{1/2}(Ru^{3+/2+}) - E_{1/2}(Ru^{2+/+})$. Recently we (Rillema 1987) showed that a linear correlation existed

Table 1. Luminescence Quantum Yields, Excited State Lifetimes and Photochemical Quantum Yields for Ru(II) Complexes Containing the Ligands bpy, bpz, bpm and BL_1.[a]

Compound	λ_{max}, nm[b]	τ_o, ns[c]	Φ_r[d]	Φ_p[e]
$Ru(bpy)_3^{2+}$	612	800	0.042	0.0021
$Ru(bpz)_3^{2+}$	610	795[f]	0.0339	0.35
$Ru(bpm)_3^{2+}$	619	131[f]	0.00283	0.043
$Ru(bpy)_2bpz^{2+}$	684	376[f]	0.00557	0.00017
$Ru(bpy)_2bpm^{2+}$	668	76[f]	0.00109	0.0003
$Ru(bpm)_2bpy^{2+}$	644	182[f]	0.00384	0.0016
$Ru(bpz)_2bpy^{2+}$	638	1099[f]	0.0400	0.0049
$Ru(bpz)_2bpm^{2+}$	618	276[f]	0.0405	0.24
$Ru(bpm)_2bpz^{2+}$	633	338[f]	0.0321	0.091
$Ru(bpy)(bpz)(bpm)^{2+}$	658	550[f]	0.0156	0.00038
$Ru(bpz)_2(CH_3CN)Cl^+$	725	—	0.00018	0.0052
$Ru(bpm)_2(CH_3CN)Cl^+$	732	—	0.000018	0.0007
$Ru(BL_1)_3^{2+}$	714	70	0.012	0.029
$Ru(BL_1)_2(bpy)^{2+}$	734	167	0.010	0.00076
$Ru(bpy)_2BL_1^{2+}$	770	15	0.002	< 0.0001

a. In acetonitrile, unless otherwise noted. T = 25 ±1° C

b. λ_{ex}= 436 nm, ±1 nm, λ_{max} uncorrected.

c. Data from Rillema (1987) and the MS thesis of George Allen, The University of North Carolina (1984).

d. Radiative Quantum Yield, ±5%, λ_{ex}= 436 nm.

e. Photochemical Quantum Yield, λ_{ex}= 436 nm, 1 mM TEACl.

f. Propylene Carbonate.

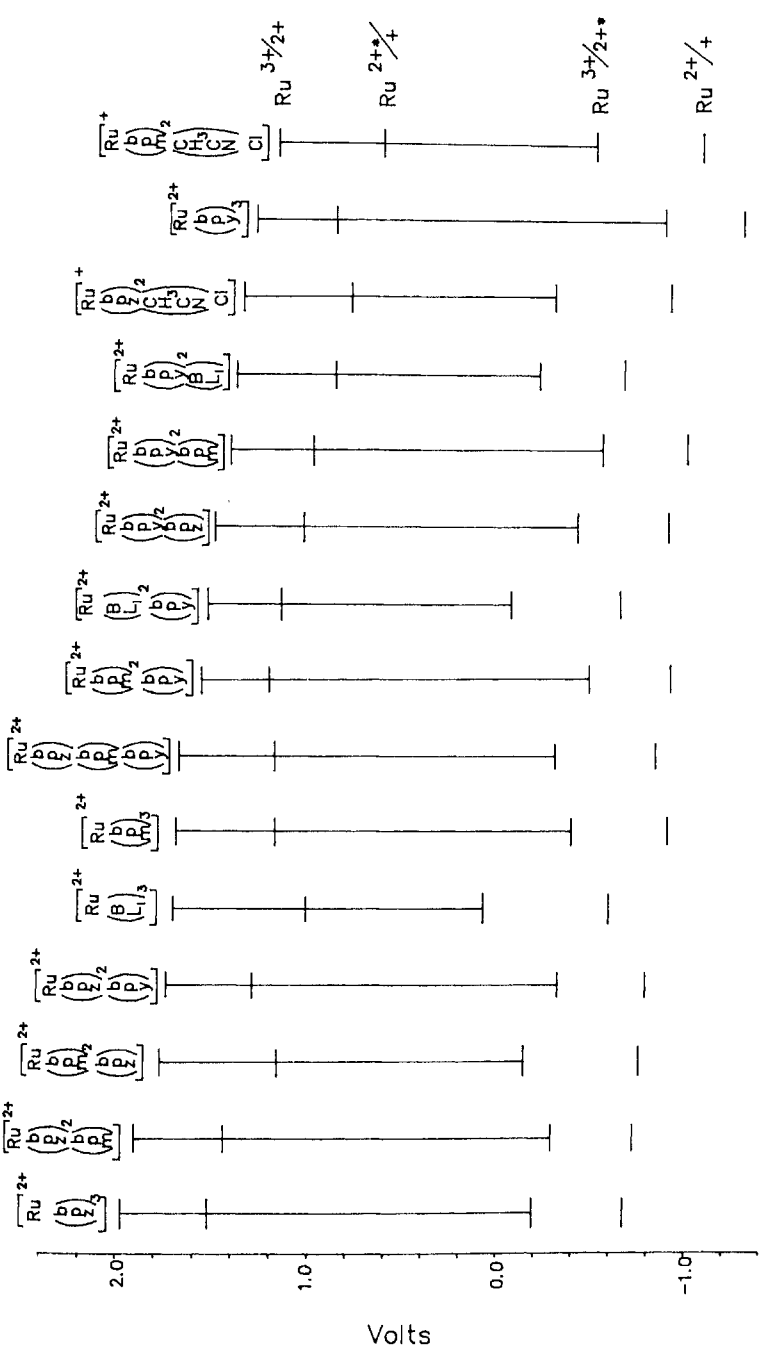

Figure 2. A Comparison of Excited State and Ground State Redox Potentials for the Compounds listed in Table 1. See text for calculations of excited state redox potentials. Ground state redox potential values for most of the compounds were taken from publications by Rillema (1983, 1987).

between $\Delta E_{1/2}$ and $E_{0,0}$. $\Delta E_{1/2}$ represents the outer sphere electron transfer analogue (eq. 6) of the inner sphere counterpart ($E_{0,0}$) as illustrated by eq. 7. Figure 3 illustrates these relationships,

$$(Ru^{III}BL)^{3+} + (Ru^{II}\text{-}BL^{-}) \longrightarrow 2(Ru^{II}BL)^{2+} \quad [6]$$

$$(Ru^{III}BL^{-})^{2+*} \longrightarrow 2(Ru^{II}BL)^{2+} \quad [7]$$

except corrected E_{em}-values were used rather than $E_{0,0}$. E_{em} is statistically less meaningful since it contains vibrational contributions that vary as $E_{0,0}$. Nevertheless, $\Delta E_{1/2}$ is more readily obtained from polarographic measurements, whereas $E_{0,0}$ determinations require spectral curve fitting analyses of luminescence spectra obtained at low temperatures.

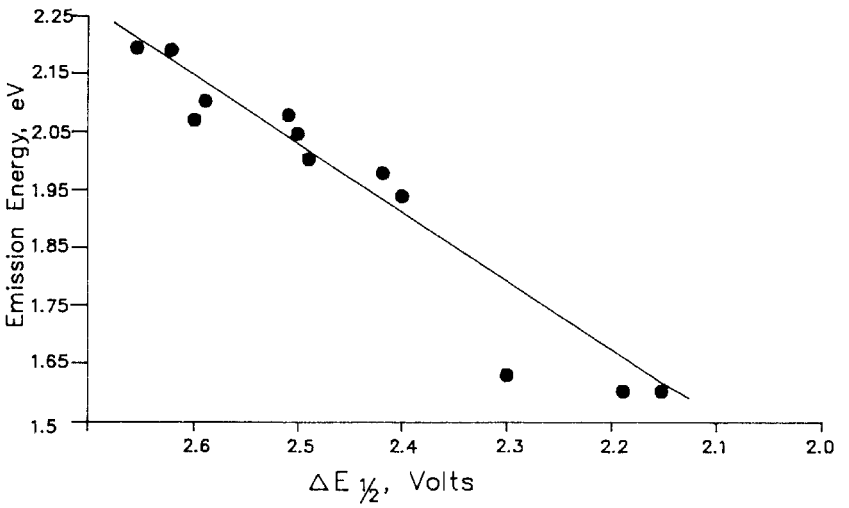

Figure 3. Correlation of Energy Gap ($\Delta E_{1/2}$) with Emission Energy. Redox potentials were taken from Fig. 2. Corrected emission energy maxima were taken from publications by Allen (1984) and Rillema (1987).

A correlation relevant to photosubstitution is shown in Fig. 4. This figure shows that for a series of closely related complexes, photosubstitution decreases as the energy gap decreases. The fact that bpm complexes correlate with bpz complexes demonstrates the close relationship of these two ligand systems. The BL_1 series, on the other hand, follows a trend (not shown) that is nearly parallel to the one shown in Fig. 4. The exponential nature of the trend is related to the energy barrier between the ^{3}MLCT state responsible for emission and the $d\sigma^*$ state responsible for photodissociation. The energy barrier can be rationalized in two ways. It can either be a kinetic barrier or an equilibrium barrier. In either case, both are exponential functions and would account for the logarithmic nature of the trend. The most likely mechanism for altering the energy of the barrier is lowering the ^{3}MLCT manifold and at the same time raising the $d\sigma^*$ energy manifold, since the metal-ligand distance is expected to be fairly constant in the series.

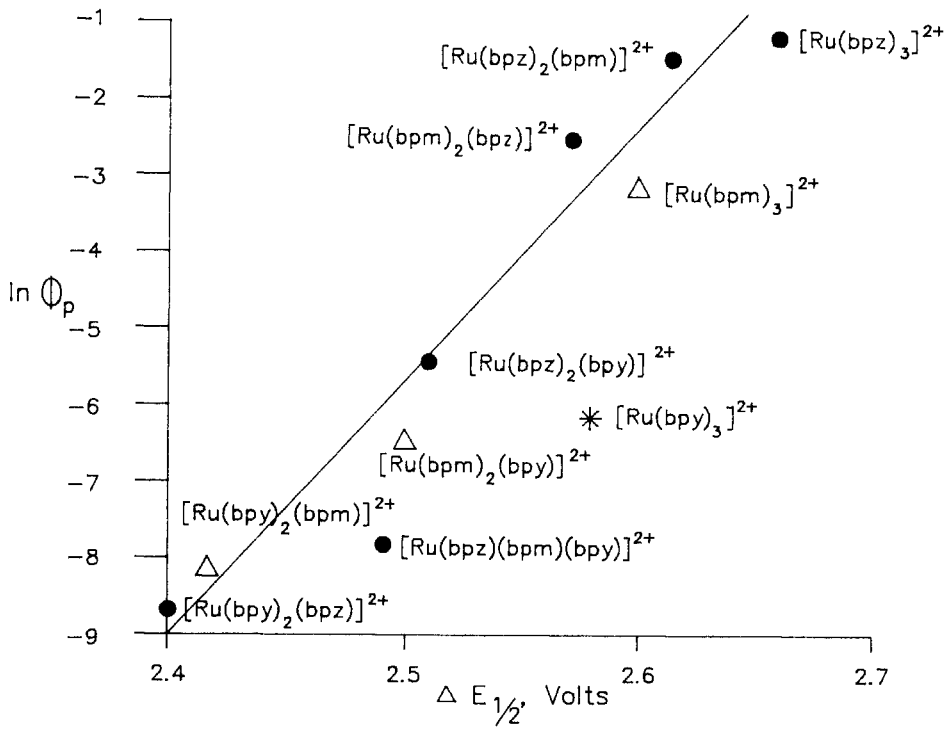

Figure 4. Correlation of Energy Gap ($\Delta E_{1/2}$) with ln Φ_p. Data are taken from Table 1 and Fig. 2.

While the photosubstitution behavior appears to be somewhat well behaved, the radiative processes occurring from the ^{3}MLCT states are less predictable. Figure 5 illustrates that the second member of the series, e.g. [Ru(bpz)$_2$(bpy)]$^{2+}$ and [Ru(bpm)$_2$(bpy)]$^{2+}$, have larger radiative quantum yields than their parents, [Ru(bpz)$_3$]$^{2+}$ and [Ru(bpm)$_3$]$^{2+}$. The bis-bipyridine analogues, on the other hand, have lower radiative quantum yields. This behavior is related to the complex nature of the ^{3}MLCT excited state and has been explained either by the localized orbital model approach (Braterman 1985; DeArmond

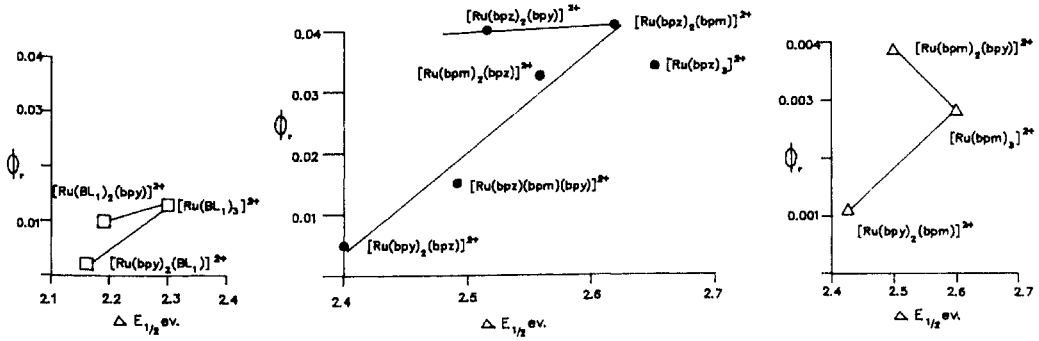

Figure 5. Dependence of Φ_r on the Energy Gap $\Delta E_{1/2}$. Data are taken from Table 1 and Fig. 2.

1985) or by the possible presence of a 4th MLCT state having greater singlet character (Rillema 1987). The ^{3}MLCT state has been shown to consist of three closely spaced states, which for $[Ru(bpy)_3]^{2+}$ have spacings of about 10 and 50 cm^{-1} (Hager 1975; Allsopp 1979). The localized orbital model places the 3rd ^{3}MLCT state about 1000 cm^{-1} above the other two in mixed-ligand complexes and population of this state is thought to lower the efficiency of the radiative process.

ACKNOWLEDGEMENTS

We thank the Office of Basic Energy Science of the Department of Energy under Grant No. DE-FG0584ER13263 for support and the National Science Foundation for the Perkin-Elmer Diode Array 3840 and the Luminescence 650-40 Spectrophotometers.

REFERENCES

Allen, GH, White RP, Rillema DP, Meyer TJ (1984) Synthetic control of excited-state properties. Tris-chelate complexes containing the ligands 2,2'-bipyrazine, 2,2'-bipyridine,and 2,2'-bipyrimidine. J Am Chem Soc 106: 2613-2620

Allsopp SR, Cox A, Kemp TJ, Reed WJ, Carasitti V, Traverso O (1979) Inorganic photophysics in solution. J Chem Soc, Faraday Trans 1 75: 353-362

Braterman PS, Heath GA, Yellowless LJ (1985) Absorption and emission in tris(2,2'-bipyridyl)ruthenium(II); effects of excited-state asymmetry. J Chem Soc, Dalton Trans: 1081-1086

Dallinger RF, Woodruff WH (1979) Time-resolved resonance raman study of the lowest ($d\pi^*$, ^{3}CT) excited state of tris(2,2'-bipyridine)ruthenium(II). J Am Chem Soc 101: 4391-4393

DeArmond MK, Hanck KW, Wertz DW (1985) Spaciously isolated redox orbitals - an update. Coord Chem Rev 65: 65-81

Ford P, Rudd, DeFP, Gaunder R, Taube H (1968) Synthesis and properties of pentaammine pyridineruthenium(II) and related pentaammineruthenium(II) complexes of aromatic nitrogen heterocycles. J Am Chem Soc 90: 1187-1194

Haga MA (1983) Synthesis and properties of tris(2,2'-bibenzimidazole)ruthenium(II) dication, $[Ru(BiBzImH_2)_3]^{2+}$. Inorg Chim Acta 77: L39-L41

Hager GD, Crosby GA (1975) Charge-transfer excited states of ruthenium(II) complexes. Quantum yield and decay measurements. J Am Chem Soc 97: 7031-7037

Pinnick D, Durham B (1984) Photosubstitution reactions of $Ru(bpy)_2XY^{n+}$ complexes. Inorg Chem 23: 1440-1445

Rillema DP, Mack KB (1982) The low-lying excited state in ligand π-acceptor complexes of ruthenium(II): Mononuclear and binuclear species. Inorg Chem 21: 3849-3854

Rillema DP, Allen G, Meyer TJ, Conrad D (1983) Redox properties of ruthenium(II) tris chelate complexes containing the ligands 2,2'-bipyrazine, 2,2'-bipyridine and 2,2'-bipyrimidine. Inorg Chem 22: 1617-1622

Rillema DP, Taghdiri DG, Jones DS, Keller CD, Worl LA, Meyer TJ, Levy HA (1987) Structure and redox and photophysical properties of a series of ruthenium heterocycles based on the ligand 2,3-bis(2-pyridyl)quinoxaline. Inorg Chem 26: 578-585

Sahai R, Rillema DP (1986) A novel hetero-oligomer containing one ruthenium(II) and three platinum(II) metal centers bridged by 2,3-bis(2-pyridyl)quinoxaline. J Chem Soc, Chem Commun: 1133-1134

Summers DB (1970) Chemistry handbook. 2nd edn. Willard Grant Press, Boston, p79

GROUND- AND EXCITED-STATE ACID-BASE EQUILIBRIA OF (2,2'-bipyridine)TETRACYANORUTHENATE(II)

M.T.Indelli, C.A.Bignozzi, A.Marconi, and F.Scandola

Dipartimento di Chimica dell'Università, Centro di Fotochimica CNR, 44100 Ferrara, ITALY

The novel mono-bpy $Ru(bpy)(CN)_4^{2-}$ complex has similar excited-state properties as the parent $Ru(bpy)_3^{2+}$: replacement of two bpy by four strong-field CN^- ligands keeps the "useful" emitting, long-lived d-π^* MLCT triplet as the lowest excited state (Bignozzi 1986). Owing to its simplicity this complex may be considered as a prototype for the class of Ru(II) polypyridine photosensitizers. Contrary to the $Ru(bpy)_3^{2+}$ case, however, the spectroscopic and photophysical properties of this complex are extremely sensitive to the environment: absorption spectra, emission spectra (both at room temperature and at 77 K) and excited-state lifetimes depend strongly on the solvent, nature and concentration of counterions and acidity. This behavior is consistent with the polar nature of the d-π^* transition and the inclination of the four cyanides towards outer-sphere donor-acceptor interactions(Balzani 1986).It has long been known (Schilt 1960) that complexes of the cis-M-$(LL)_2(CN)_2$ type (when LL represents a bipyridine ligand and M= Fe(II), Ru(II), Os(II)) protonate in acidic media. The effect of protonation on the photophysics of Ru(II) complex of this type (where LL=bpy and phen) has been thoroughly investigated in the last decade by Peterson and Demas(1979). The effect of protonation on the spectroscopic and photophysical properties of $Ru(bpy)(CN)_4^{2-}$ is now described.

At neutral pH, the complex is present as the fully deprotonated anionic form. Four consecutive protonation steps (eqs 1-4) can be envisioned leading to the fully protonated cationic species in highly acidic solutions (concentrated sulfuric acid).

$$Ru(bpy)(CN)_4^{2-} + H^+ \overset{K_1}{\rightleftharpoons} Ru(bpy)(CN)_3(CNH)^- \quad (1)$$

$$Ru(bpy)(CN)_3(CNH)^- + H^+ \overset{K_2}{\rightleftharpoons} Ru(bpy)(CN)_2(CNH)_2 \quad (2)$$

$$Ru(bpy)(CN)_2(CNH)_2 + H^+ \overset{K_3}{\rightleftharpoons} Ru(bpy)(CN)(CNH)_3^+ \quad (3)$$

$$Ru(bpy)(CN)(CNH)_3^+ + H^+ \overset{K_4}{\rightleftharpoons} Ru(bpy)(CNH)_4^{2+} \quad (4)$$

Figure 1 shows absorption spectra of the complex in water with varying concentration of H_2SO_4; definite blue shifts are observed in the visible region with increasing acidity, starting from pH 3. Up to $[H^+] \simeq 0.05$ M there is an isosbestic point which indicates that the solution consists of deprotonated and monoprotonated forms. A second isosbestic point is present in the 0.4M - 2M $[H^+]$ range where the mono- and diprotonated forms predominate. For 2M $>[H^+]<$5M slow precipitation of the diprotonated

Photochemistry and Photophysics
of Coordination Compounds, Ed. by H. Yersin/A. Vogler

uncharged form occurs. At $[H^+]>5M$ the redissolution of the precipitate indicates the formation of cationic species. In solutions of $[H_2SO_4]>18N$ further changes in the absorption spectrum are not observed, suggesting that the fully protonated cationic form is the only species present. It is important to note that in these highly acidic conditions the blue shift in the absorption spectrum in the visible region is so large that the d-π^* MLCT band is completely hidden by π-π^* ligand centered transitions.

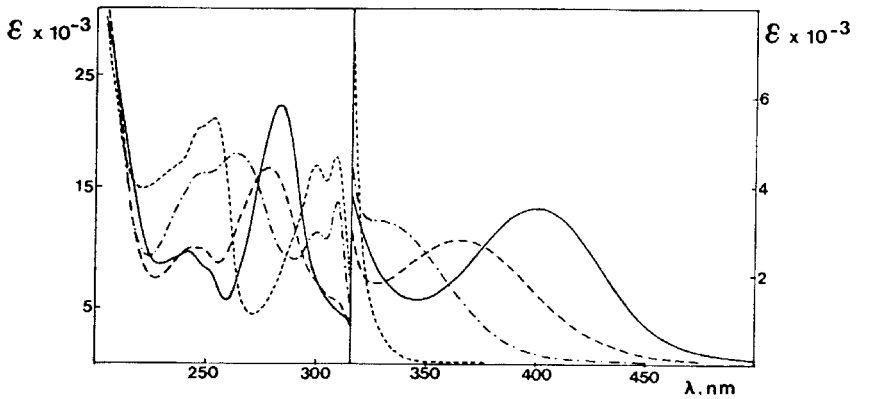

Figure 1. Absorption spectra of $Ru(bpy)(CN)_4^{2-}$ in aqueous H_2SO_4 solutions. Acid concentrations for each curve are: 0 (——), 0.5 N (- - - - -), 8 N (-·-·-), 36 N (·····).

Using the same procedure indicated by Demas (1979) for $Ru(LL)_2(CN)_2$ the following values for the association constants of the first (eq.1) and the second (eq.2) protonation step have been estimated from the spectral variations: K_1= 60 M^{-1} and K_2= 8 x10^{-2} M^{-1}. The calculated distribution and the absorption spectra of the unprotonated, mono- and diprotonated forms are shown in Fig. 2. The spectra of the protonated forms are quite similar in intensity and shape to that of the parent unprotonated form; the maximum of the visible band is blue shifted of about 2.5 kK upon each step of protonation.

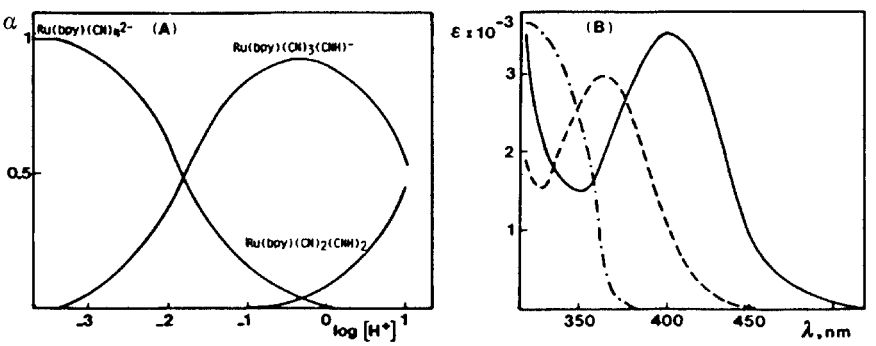

Figure 2. (a) Calculated distributions and (b) absorption spectra of $Ru(bpy)(CN)_4^{2-}$ (——), $Ru(bpy)(CN)_3(CNH)^-$(- - - - -)and $Ru(bpy)(CN)_2(CNH)_2$ (-·-·-·).

This fact is consistent with the d-π^* nature of the lowest transition and with the electron-withdrawing effect of the proton. The difference between the absorption maxima of the d -π^* band of the unprotonated and monoprotonated forms can be used to estimate the shift in the pK value in going from the ground to singlet excited state on the basis of Forster cycle calculations (Grabowski 1976); the magnitude of the shift is estimated to be about 5pK units.

As far as the emission results are concerned, no spectral shifts (λmax = 610 nm) nor changes in the emission lifetime (τ= 100 ns) were observed to occur in the 7-0 pH range. This result indicates that (i) the d- π^* triplet excited state is remarkably more acidic than the ground-state (as expected since the d-π^* transition leads to a decrease in electron density at the protonation site) and (ii) the proton-transfer excited-state equilibrium is fast with respect to excited-state deactivation (i.e. in the 3-0 pH range fast deprotonation of the excited state precedes the emission). In more acidic solutions (12N<[H_2SO_4]>1 N) a progressive blue shift and an increase in intensity in the emission spectrum were observed with increasing acidity indicating that excited-state protonation takes place. The onset of the shift in emission (pH$\lesssim$ 0) seems to indicate that the shift in the pK_1 of the triplet state with respect to ground state is smaller than that estimated for the singlet state from absorption. In Figure 3 are reported the emission spectra (normalised for intensity) of solutions of different acidity. As one can see, with further increase of H_2SO_4 concentration (H_2SO_4>14 N) the emission undergoes a dramatic change: it is further blue shifted and shoulders appear on the high energy portion of the d-π^* band. In concentrated sulfuric acid, a highly structured emission is present.

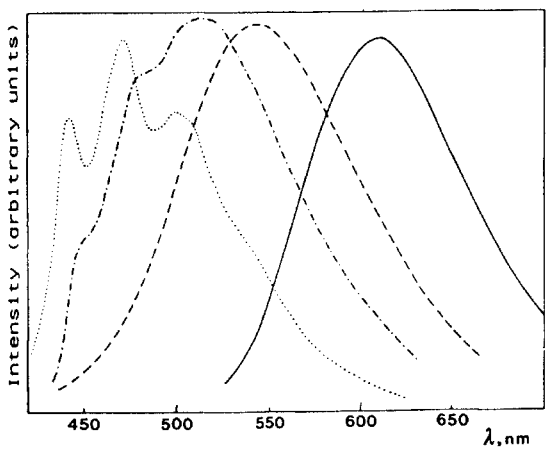

Figure 3. Room temperature emission spectra of $Ru(bpy)(CN)_4^{2-}$ in aqueous H_2SO_4 solutions. (——) H_2O, τ = 100 ns; (---) 12 N H_2SO_4 , τ = 300 ns; (-·-·) 15 N H_2SO_4, τ = 1.1 μs; (·····) concentrated H_2SO_4, τ = 100 μs.

The progressive shift to the blue with increasing acidity is accompanied by a progressive increase in emission lifetime (Fig. 4). An important observation is that in the whole range of acidities studied the emission decays were found to be strictly monoexponential, with lifetimes independent

on the emission wavelength. This result provides a further direct evidence of the fact that excited-state protonation equilibria are fast with respect to deactivation. In this kinetic limit the experimental rate constant ($k = 1/\tau$) of excited state deactivation is given by the following expression:

$$k = \sum_{n=0-4} \alpha_n \times 1/\tau\,(^*AH_n^{n+})$$

where $\tau(^*AH_n^{n+})$ are the lifetimes of the various protonated forms and $\alpha_n = [^*AH_n^{n+}] / \sum[^*AH_n^{n+}]$. In principle a plot of $1/\tau$ against $\log[H^+]$ could be used to evalued the excited-state pK values. Such a plot is shown in Fig. 4. It consist of three distinct regions: (i) a first region ($\tau < 200$ ns) of slowly decreasing $1/\tau$,(ii) a narrow region in which $1/\tau$ decreases sharply; (iii) a third region ($\tau > 10$ μs) of slowly decreasing $1/\tau$ These three regions correspond closely to the acidity ranges in which (i) only the unstructured emission is present, (ii) a transition is seen from the unstructure to structured emission, (iii) only the structured emission is present. The figure seems to indicate that several closely spaced excited state pKs are contained in the acidity range investigated and that $\tau(^*AH_n^{n+})$ values of various forms exhibiting the same type of emission increase slowly with the degree of protonation. It does not seem possible to obtain from these data a more detailed picture, in particular regarding the excited-state protonation step at which the switching between the two types of emission occurs.

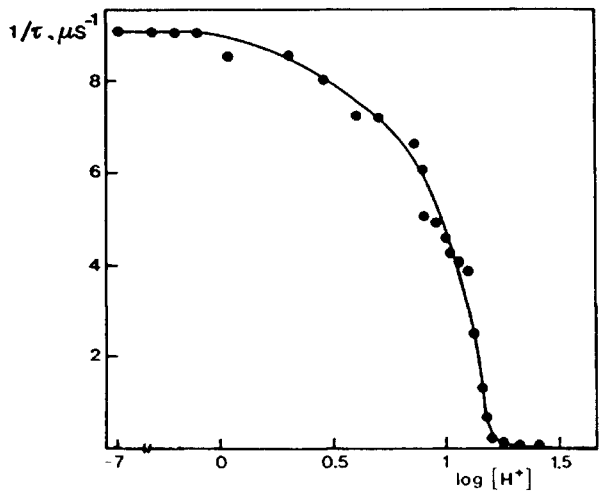

Figure 4. Emission lifetimes of $Ru(bpy)(CN)_4^{2-}$ in dearated aqueous H_2SO_4 solutions of different concentration.

As far as the orbital nature of structured emission is concerned, Figure 5 shows a comparison between the emission spectrum at 77 K of $Ru(bpy)(CN)_4^{2-}$ in concentrated sulfuric acid and the 77 K emission spectrum of $Rh(bpy)_3^{3+}$, which is known to consist of π-π^* ligand centered phosphorescence (Casterns 1970).

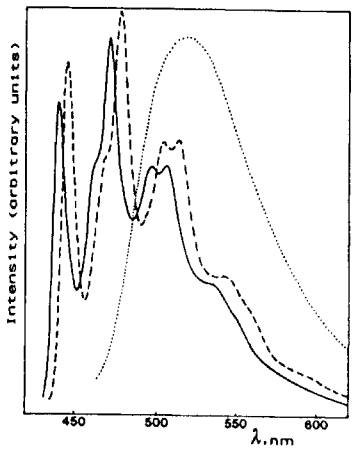

Figure 5. Low temperature 77 K emission spectra of (·····) $Ru(bpy)(CN)_4^{2-}$ in 9 M aqueous LiCl glass, (——) $Ru(bpy)(CN)_4^{2-}$ in concentrated H_2SO_4 and (-----) $Rh(bpy)_3^{3+}$ in concentrated H_2SO_4 glass.

Except for a slight energy shifting, the structure, vibrational progression and relative intensities of adjacent peaks are identical in the two spectra. Since the structured emission is virtually identical to that at 77 K we conclude definitely that the protonated form present in concentrated sulfuric acid exhibits a pure π-π^* phosphorescence. The very long lifetime (τ = 100 μs) confirms this assignment.This finding is interpreted in terms of the shifts in excited state energies depicted in Figure 6.

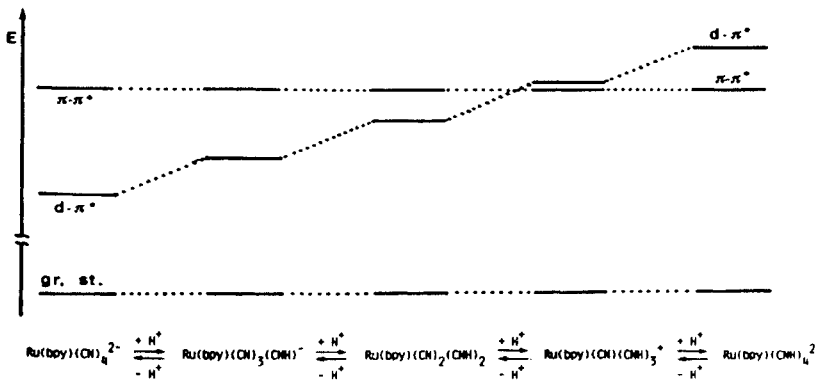

Figure 6. Change in the orbital nature of the lowest excited stae upon protonation of $Ru(bpy)(CN)_4^{2-}$.

The protonation at the cyanides decreases the electron density at the Ru center thus shifting to higher energy the Ru-LL MLCT excited state while leaving almost unaffected levels of π- π^* ligand centered orbital origin (Demas 1979, Balzani 1986). The energy spacing of d -π^* and π-π^* levels is strongly affected so that in H_2SO_4 concentrated the energy ordering of

the d-π^* and π-π^* levels is reversed and the π-π^* state becomes the lowest excited state. According to Demas (1976), $Ru(bpy)_2(CN)_2$ exhibits a similar π-π^* emission in concentrated H_2SO_4 at 77 K, but becomes nonluminescent at room temperature. This appears to be the first example of room temperature very long-lived π-π^* emission for a Ruthenium(II) polypyridine complex.

REFERENCES

Balzani, V.; Sabbatini, N.; Scandola, F. Chem. Rev. 1986 86, 319
Bignozzi, C.A.; Chiorboli, C.; Indelli, M.T.; Rampi Scandola, M.A.; Varani, G.; Scandola,F. J. Am. Chem. Soc. 1986, 108, 7872.
Carstens, D.H.W.; Crosby,G.A. J. Mol. Spectrosc. 1970 34, 113.
Grabowski, Z.R.; Grabowka, A. Z. Physik. Chem. Neue Folge 1976,101, 197.
Peterson, S.H.; Demas, J.N. J. Am. Chem. Soc. 1979, 101, 6571.
Schilt, A.A. J. Am. Chem. Soc. 1960, 82, 3000.
Schilt, A.A. J. Am. Chem. Soc. 1960, 82, 5779.

TOPIC 4

Photoredox Processes

KINETICS AND MECHANISM OF PHOTOCHEMICAL FORMATION OF A PYRAZINE BRIDGED Fe(II) PROTOPORPHYRIN POLYMERIC COMPOUND

C.Bartocci, A.Maldotti, R.Amadelli, and V.Carassiti

Centro di Fotochimica del CNR, Dipartimento di Chimica dell'Università di Ferrara, Via L. Borsari 46, 44100 Ferrara, ITALY

Introduction

Polymeric, electron rich ligand bridged Fe(II) macrocyclic compounds are expected to give rise to directional electron transfer through the iron atoms. In light of this peculiarity, they have been studied in view of their use as catalysts of redox processes of biological interest (Wang, 1960), as monodimensional electrical conductors (Schneider, 1983), as models in investigations concerning the light absorption properties of chlorophyll (Kats, 1973). The photochemical production of this type of compounds appears to be of some interest because it is possible to induce 'in situ' redox reactions in chemical as well as in biological systems, so ruling out undesirable secondary reactions. In the last years we have conducted investigations on the photoredox reactions of Fe(III) porphyrin complexes (Bartocci, 1980, 1983; Maldotti, 1983, 1985). We have observed that Fe(III) porphyrin compounds might be photoreduced, in the presence of nitrogenous bases, that are able to axially coordinate to Fe(II), to give Fe(II) porphyrin hexa-coordinated complexes (hemochromes). On the basis of this experience, we started an investigation in which the photoreduction of Fe(III) porphyrins were carried out in the presence of bifunctional nitrogenous ligands (e.g. pyrazine) to photochemically obtain ligand bridged Fe(II) porphyrin polynuclear compounds (Bartocci, 1986).

Results and discussion

The irradiation with at 320 nm of alkaline (pH 10), carefully deaerated solutions of Fe(III) Protoporphyrin IX (Hemin, Fe(III)PP) containing an excess of pyrazine (5000/1) leads to the appearance of an electronic spectrum (Fig. 1, spectrum a) which is quite similar to that of $Fe(II)PP(py)_2$ (py=pyridine), indicating that $Fe(II)PP(pyz)_2$ (pyz= pyrazine) is the photoreaction product. With less pyrazine ($<$ 100/1) the spectrum obtained is that shown in Fig. 1, spectrum b. The comparison with spectrum a indicates that, i) the Soret band (400 nm) and α and β bands (550 and 525 nm, respectively) are red shifted; ii) a sharp and intense band appears at 800 nm. A similar spectrum has been previously obtained by Fuhrop et al. (Fuhrop, 1980) upon reduction of Hemin in aqueous, pyrazine containing, solution and was attributed to a Fe(II)PP dimeric species in which the Fe(II) units were linked by pyrazine bridges. If, however, photochemical experiments were conducted in the presence of poly-L-lysine, which is known to form insoluble adducts with polynuclear Iron porphyrin compounds (Wang, 1960), a precipitate was obtained which presented an electronic spectrum identical with that obtained in solution during the irradiation (Fig. 1, spectrum b), providing evidence that polymeric ($[Fe(II)PPpyz]_n$) rather than dimeric species were formed in our conditions. Granted the polymeric nature of the compound obtained, the most interesting spectral characteristic of $[Fe(II)PPpyz]_n$ is the intense band at 800 nm. It was interpreted by Fuhrop (Fuhrop, 1980) as arising from an electron transfer between two porphyrin chromophores, favoured by the aromaticity of the bridge ligand. Alternatively, we have assigned the red band to a $Fe(II) \longrightarrow pyz$ charge transfer transition shifted toward lower energies with respect to $Fe(II)PP(pyz)_2$ by the delocalization of the pyrazine π system, caused by the polymerization. On the

Photochemistry and Photophysics
of Coordination Compounds, Ed. by H. Yersin/A. Vogler

basis of the results obtained up to now, a discrimination between the two interpretations is unachievable. It is certain, however, that the spectral behaviour is strictly connected to the aromaticity of the ligand, as confirmed by the absence of any red absorption observed when Fe(II) units are linked by the non aromatic piperazine (Bartocci, 1986).

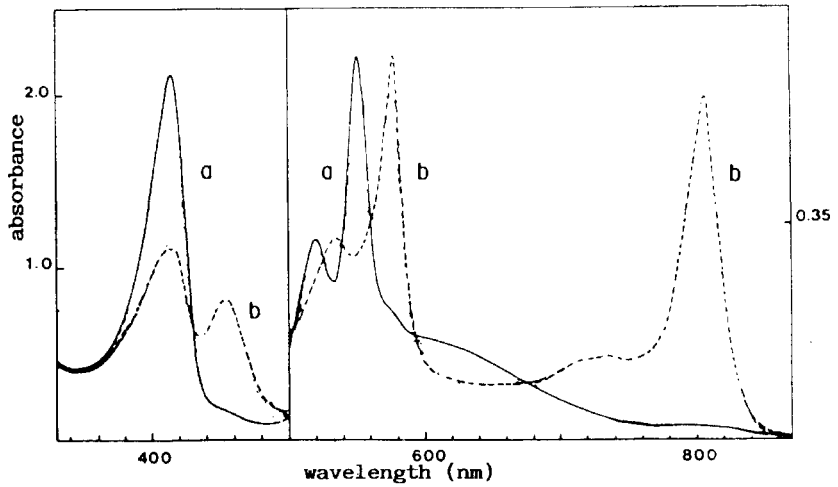

Fig. 1 - Electronic spectra monitored after 90 s irradiation at $\lambda > 320$ nm of Fe(III)PP solutions at pH$\sim$10: a) with a 5000 fold excess of pyrazine; b) with a 100 fold excess of pyrazine.

The photoreduction of Fe(III)PP was carried out with pyz/Fe concentration ratioes ranging from 5000/1 to 1/1. The results unequivocally indicate that the monomeric $Fe(II)PP(pyz)_2$ species is formed in any case, irrespective of the pyrazine concentration and that the polynuclear species is formed via a secondary thermal reaction, the rate of which increases with decreasing the pyrazine concentration. The kinetics of the secondary reaction was studied with pyz/Fe concentration ratioes ranging from 300/1 to 1,500/1. In these conditions the polymerization process is observed to be much slower than the reduction of Fe(III)PP. One can thus envisage that virtually all Fe(III)PP has been reduced when polymerization begins. The complete reduction of Fe(III)PP was performed with an excess of Sodium dithionite and the disappearance rate of $Fe(II)PP(pyz)_2$ was followed by monitoring the absorbance decrease at 550 nm. The results show that the polymerization follows a second order rate law. On this basis, we propose the following mechanism:

$$A \underset{}{\overset{K}{\rightleftharpoons}} B + pyz \qquad (1)$$

$$2B \xrightarrow{k_2} C \qquad (2)$$

$$B + A \xrightarrow{k_3} C' \qquad (3)$$

$$C + pyz \xrightarrow{k_4} C' \qquad (4)$$

$$C' + B \xrightarrow{k_5} D' \qquad (5)$$

$$C + B \xrightarrow{k_6} D \qquad (6)$$

$$C + A \xrightarrow{k_7} D' \qquad (7)$$

.....

where, A = Fe(II)PP(pyz)$_2$; B = Fe(II)PPpyz; C = Fe(II)PPpyzFe(II)PPpyz;
C' = pyzFe(II)PPpyzFe(II)PPpyz; D' = pyzFe(II)PPpyzFe(II)PPpyzFe(II)PPpyz;
D = Fe(II)PPpyzFe(II)PPpyzFe(II)PPpyz.

Supposing that Equilibrium 1 is very rapidly established, that, due to the excess of pyrazine, reactions 6 and 7 are negligible compared with reaction 5, and introducing the steady state approximation for C, C', D ...., Eq. 8 gives the rate of disappearance of A (Fe(II)PP(pyz)$_2$).

$$-d[A]/dt = (n-1)k_2K^2[A]^2/[pyz]^2 + (n-1)k_3K[A]^2/[pyz] \qquad (8)$$

where n is the number of the iron centers in the polymeric compound. Considering that the steady state concentration of intermediates C, C', D, ... are likely to be very low, n can be taken constant and representing the number of the monomeric units in the final product. Then, since the variation of the pyrazine concentration is negligible due to the excess of the basis with respect to Fe(II)PP(pyz)$_2$,

$$-d[A]dt = k_{obs}[A]^2 \text{ with } k_{obs} = (n-1)k_2K^2/[pyz]^2 + (n-1)k_3K/[pyz] \qquad (9)$$

The validity of kinetic expression 9 has been tested by plotting k_{obs} vs. pyz and then making the best fit of the experimental data to the form

$$y = a/[pyz]^2 + b/[pyz]$$

In Fig. 2 the good fit of the experimental points with the theoretical curve is evident.

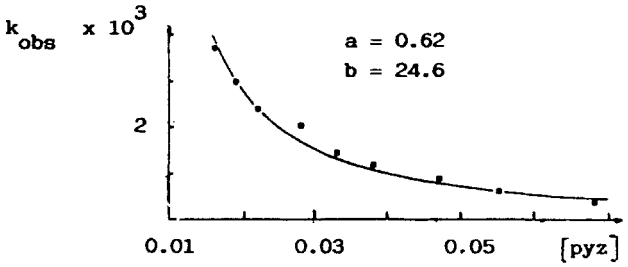

Fig. 2 - Best fit plot of experimental k_{obs} values to the form $y=a/[pyz]^2 + b/[pyz]$

Another peculiarity of the Fe(II)PP polynuclear compound is its reactivity with respect to oxygen: in alkaline solution (pH$\sim$10) the polymer is rapidly oxidized and disgregated to give the reactant Fe(III)PP. At pHs close to neutrality ($\sim$8) the

spectral behaviour after oxygenation is as follows: i) the spectrum exhibits the α and β bands decreased in intensity and the 800-nm absorption less intense and blue shifted; ii) the addition of an excess of dithionite reverts the spectrum to that of the reduced polymer; iii) the spectrum of Fe(III)PP is obtained back by adding ferricyanide. These results can be taken as an evidence that oxygen oxidizes $[Fe(II)PPpyz]_n$ to a Fe(II)-Fe(III) mixed valence porphyrin polynuclear compound. This compound appears to be stable for several days. It forms with poly-L-lysine a solid adduct that presents a spectrum identical with that observed in solution, giving evidence of its polymeric structure. The partial oxidation of $[Fe(II)PPpyz]_n$ by oxygen may be interpreted as arising from a different reactivity of the terminal Fe(II) atomswith respect to the oxidation, compared with the other ones. Thus, the mixed valence polymer should have the structure Fe(III)PPpyzFe(II)PPpyz....Fe(II)PP-pyzFe(III)PP. In this structure the pyrazine π system is expected to be less delocalized compared with that of the reduced polymer, so giving the reason of the observed diminution in intensity and the blue shift of the 800-nm band. The rapid and complete oxidation observed in alkaline solution is likely to be due to the pyrazine bridge breaking caused by OH^- which is known to be a good ligand for Fe(III) porphyrin species. Unfortunately, any attempt to isolate the mixed valence as well as the reduced polynuclear compounds failed because of the rapid oxidation and disgregation occurring as soon as the solids were separated from the excess of pyrazine.

References

Bartocci C, Scandola F, Ferri A, Carassiti V (1980) Photoreduction of Hemin in Alcohol-Containing Mixed Solvents. J Am Chem Soc 102: 7067-7072

Bartocci C, Maldotti A, Traverso O, Bignozzi CA, Carassiti V (1983) Photoreduction of Chlorohemin in Pure Pyridine. Polyhedron 2: 97-102

Bartocci C, Amadelli R, Maldotti A, Carassiti V (1986) Photoreduction of Fe(III) Protoporphyrin IX in Ethanol-Water solutions containing Bifunctional Ligands. Polyhedron 5: 1297-1301

Fuhrhop JH, Baccouche M, Bünzel M (1980) A Pyrazine-Bridged Heme Dimer Absorbing at 800 nm. Angew Chem Int Ed Engl 19: 322-323

Maldotti A, Bartocci C, Amadelli A, Carassiti V (1983) An ESR Spin Trapping Investigation on the Photoreduction of Chlorohemin in Mixed Solvents. Inorg Chim Acta 74: 275-278

Maldotti A, Bartocci C, Chiorboli C, Ferri A, Carassiti V (1985) The Role of Oxygen in the Mechanism of the Intramolecular Photoredox Reaction of Fe(III) Protoporphyrin IX in Alkaline Aqueous Ethanol. J Chem Soc Chem Comm: 881-882

Schneider O, Hanack M (1983) Axial polymerisiertes (Phtalocyaninato)eisen(II) mit Pyrazin, 4,4'-Bipyridin, 1,4-Diisocyanobenzol oder 1,4-Diazabicyclo(2.2.2)octan als Brückenliganden; Darstellung, Charakterisierung und elektrische Leitfähigkeiten Chem Ber 116: 2088-2108

Wang JH, Brinigar WS (1960) Design and Synthesis of a Catalyst for the Aerobic Oxidation of Cytochrome c. Proc Natl Acad Sci USA 46: 958-963

CHARGE-TRANSFER STATES AND TWO-PHOTON PHOTOCHEMISTRY OF $Cu(NN)_2^+$ SYSTEMS

R.M.Berger, A.K.Ichinaga, and D.R.McMillin

Department of Chemistry, Purdue University, West Lafayette, IN 47907, USA

Because Cu(I) has a d^{10} electronic configuration, the metal-centered absorption bands tend to occur in the UV spectral region. But because the Cu(II) oxidation state is quite accessible, metal-to-ligand charge-transfer (CT) absorption bands appear in the visible spectrum when the ligands present low-lying acceptor orbitals. For example, Cu(I) complexes involving chelating heteroaromatic ligands (NN ligands) such as bipyridine (bpy) or 1,10-phenanthroline (phen) or one of their derivatives are brightly colored. In fact, several different CT excited states are accessible in these systems. One reason is that the ligands present 2 low-lying acceptor levels which Orgel (1961) designated as χ and ψ orbitals. (They transform as symmetric and antisymmetric orbitals, respectively, under rotation about the two-fold axis (Fig. 1).) Further complexity arises in $Cu(NN)_2^+$ systems because the d shell of the metal is split into at least four sublevels. Finally, there is some evidence that a charge-transfer-to-solvent state can be populated when a high intensity pulsed laser source is used.

In this report we will attempt to assign the visible absorption bands of a series of copper phenanthrolines. As the CT spectra are poorly resolved, even at low temperatures, in most cases the spectra will be assigned under the assumption of the highest available symmetry which is D_{2d}. However, when phenyl groups are present in the 2,9 positions of the phenanthroline core, the complexes exhibit a significant distortion at low temperatures and in the solid state. This distortion is apparently favored by intramolecular interligand stacking interactions.

EXPERIMENTAL

The ligand abbreviations are as follows: 1,10-phenanthroline, phen; 2,9-dimethyl-1,10-phenanthroline, dmp; 2,9-dimethyl-4,7-diphenyl-1,10-phenanthroline, bcp; 2,9-diphenyl-1,10-phenanthroline, dpp; 2,4,7,9-tetraphenyl-1,10-phenanthroline, tpp. The ligands were obtained from commercial sources or prepared by a literature method (Dietrich-Buchecker etal. 1981), and the complexes were prepared as before (McMillin etal. 1977).

Absorption measurements were carried out with a Cary 17D spectrophotometer, and the low-temperature data were obtained with an Oxford Instruments DN-704 cryostat. A Nd:YAG laser (Quanta Ray DCR-1) served as a high intensity pulsed light source. For photolysis studies the sample was deoxygenated in a quartz cuvette and stirred during irradiation. The rep rate was 10 Hz, and the width at half height of each pulse was about 7 ns.

Photochemistry and Photophysics
of Coordination Compounds, Ed. by H. Yersin/A. Vogler

BAND ASSIGNMENTS IN D_{2d} SYMMETRY

In the energy level scheme depicted in Fig. 1 there are seven symmetry-allowed CT transitions. However, two transitions are expected to carry most of the intensity. This follows from the CT theory of Mulliken which predicts that the oscillator strength is mainly due to the charge-transfer term and is concentrated in

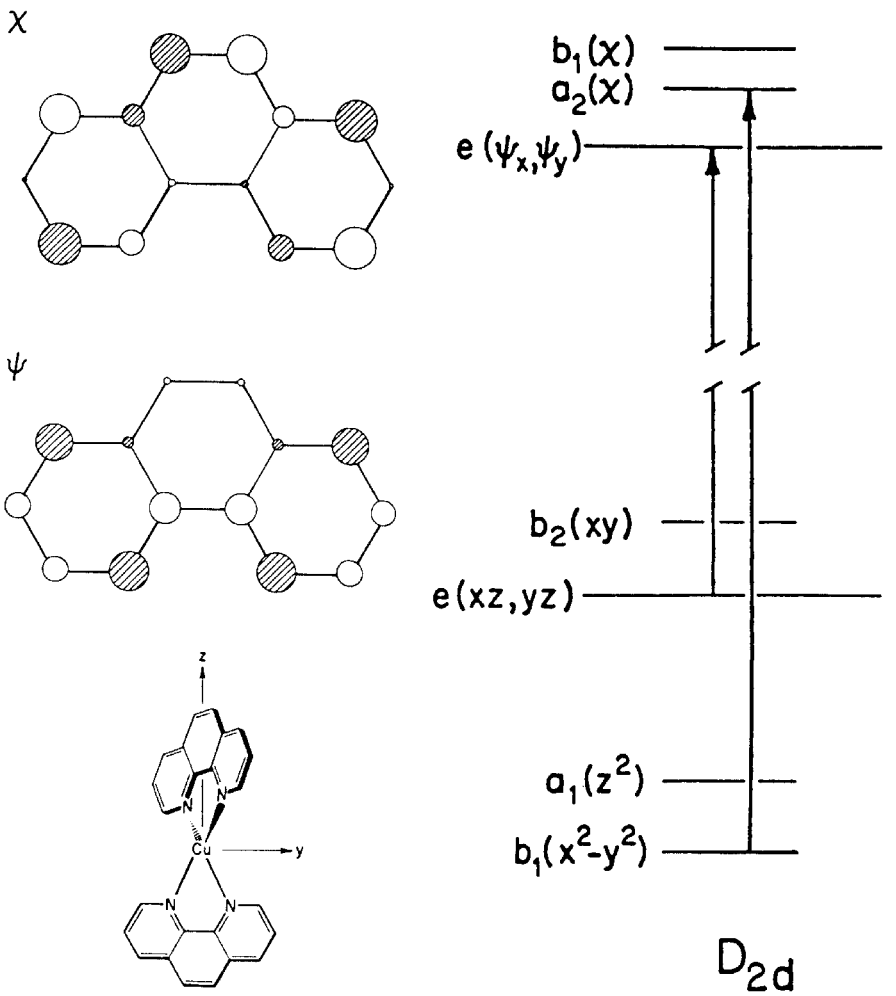

Figure 1. Upper left: The relative weights and phases of the $p\pi$ atomic orbitals in the χ^* and ψ^* orbitals of phen. Lower left: $Cu(phen)_2^{+}$ in D_{2d} symmetry. Right: one electron energy levels for $Cu(phen)_2^{+}$ in D_{2d} symmetry. The z-polarized CT transitions ($^1B_2 \longleftarrow {}^1A_1$) are indicated by arrows.

those transitions which are polarized along the axis joining the metal and the ligand centers (Mulliken 1952; Day and Sanders 1967; Phifer and McMillin 1986). When this is the z-axis, the symmetry labels are $e(xz,yz) \longrightarrow e(\psi^*)$ and $b_1(x^2-y^2) \longrightarrow a_2(\chi^*)$ where the asterisk indicates that π-antibonding orbitals of the ligand are involved.

The absorption spectrum of $Cu(dmp)_2^+$ at 90 K in a 4:1 ethanol/methanol glass is presented in Fig.2. The spectrum reveals a strong band at 460 nm with a vibronic satellite at 440 nm. In addition there is a weaker maximum at 390 nm and a shoulder at 510 nm. Similar spectra are obtained from $Cu(phen)_2^+$ and $Cu(bcp)_2^+$ (Table 1). If the bands are labeled as Bands I, II and III in order of increasing energy, the only unambiguous assignment is that the transition to $e(\psi^*)$ is contained in Band II. This follows because the transition to ψ^* is expected to be quite intense. In particular, it should be 2-3 times as intense as the transition to χ^* because the $2p\pi$ orbital of nitrogen participates more strongly in the ψ^* orbital (Phifer and McMillin 1986). Band III probably represents the partially resolved transition to χ^*. This assignment is in accord with the relative transition energies expected on the basis of Fig.1 and with the fact that an analogous transition is not resolved in the spectrum of bpy analogues where the χ^* orbital is known to occur at higher energies. If the symmetry is D_{2d}, Band I must be assigned as x,y-polarized. The relative intensity is consistent with this assignment, and there is a precedent for x,y-polarized transitions in the spectra of $W(CO)_4(NN)$ complexes (Staal etal. 1978). On the other hand, Band I could also acquire intensity from the charge transfer term if the complexes are subject to low-symmetry distortions in solution. In the solid state $Cu(phen)_2^+$ (Healy etal. 1985) and $Cu(dmp)_2^+$ (Dobson etal. 1984) have been found to adopt flattened structures with lattice-dependent angles between mean ligand planes which are significantly smaller than 90°. However, the flattening distortions have been connected with intermolecular stacking interactions which do not survive in solution (Goodwin etal. 1986). More experimental work will be needed to ascertain whether any low symmetry distortions occur in solution.

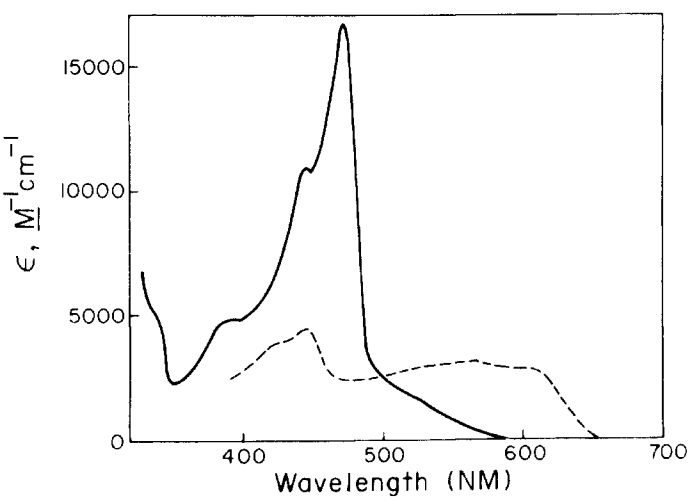

Figure 2. Absorption spectra of $Cu(dmp)_2^+$ (——) and $Cu(dpp)_2^+$ (---) at 90 K in a 4:1 ethanol/methanol glass.

Table 1. Electronic Absorption Data at 90 K

NN	band	λ, nm	ϵ^a	NN	band	λ, nm	ϵ^a
phen	I	500 (sh)		dpp	II'	550	3,000
	IIa	463	17,200		IIIa'	436	4,400
	IIb	435	12,500		IIIb'	413	3,900
	III	380	8,100				
				tpp	II'	590	9,800
dmp	I	510 (sh)			III'	460	10,300
	IIa	460	16,500				
	IIb	440	10,800				
	III	390	4,800				
bcp	I	540 (sh)					
	IIa	495	31,600				
	IIb	460	20,200				
	III	425	10,700				

[a]The ϵ values are not corrected for solvent contraction

LOW SYMMETRY SPECTRA

As can be seen in Fig. 2 the low-temperature absorption spectrum of $Cu(dpp)_2^{2+}$ has a very different shape in that two intense CT absorption bands are resolved in the visible region. If these bands can be assigned as transitions to the ψ^* and χ^* orbitals of the ligands, in view of the relative intensities the lower energy band would be assigned to the ψ^* transition. Extended Hückel calculations reveal that the presence of the phenyl groups has little effect on the relative energies of the ψ^* and χ^* orbitals, hence the increased spectral resolution probably reflects a change in the separation among the $d_{x^2-y^2}$ and the d_{xz} and d_{yz} orbitals. The splitting increase suggests a symmetry change, and in line with this argument a related complex of a catenand ligand has been shown to have a distorted, almost trigonal pyramidal coordination geometry in the solid state. In this case the relative positioning of the ligands appears to be determined by interligand stacking interactions (Cesario etal. 1985). Because intramolecular stacking is involved, the low symmetry structure might be expected to occur in solution as well. The $Cu(dpp)_2^+$ system also has phenyl substituents in the 2 and 9 positions, hence it might be expected to have a similar structure. Indeed, the copper catenate, $Cu(dpp)_2^+$ and $Cu(tpp)_2^+$ all exhibit similar low temperature absorption spectra. The indicated conclusion is that Cu(I) complexes of phenanthrcline ligands bearing 2,9-phenyl substituents are prone to low-symmetry distortions due to intramolecular, interligand stacking interactions. Because of the anticipated symmetry differences, primed and unprimed numerals are used to label the bands in Table 1. Parenthetically, we should note that in the limit of a large distortion it is not possible to attribute the separately resolved transitions to χ^* and ψ^* orbitals.

TWO PHOTON ABSORPTION

Although deaerated solutions of $Cu(dmp)_2^+$ in CH_2Cl_2 are quite photostable under room light and under exposure to 355 nm radiation from a 1000 W Xe arc lamp, Fig. 3 shows that the solutions are rapidly bleached when irradiated with a high intensity pulsed laser source. The bleaching is even more rapid when 354.7 nm light is used. Product analysis shows that the net reaction entails the oxidation of $Cu(dmp)_2^+$ to the Cu(II) state and the reduction of the solvent with concomitant formation of chloride. At relatively low powers (< 3 mJ per pulse at 354.7 nm) the rate of bleaching approximately depends on the square of the laser power. This establishes that the bleaching requires the absorption of two photons:

$$Cu(dmp)_2^+ + 2\ h\upsilon + CH_2Cl_2 \longrightarrow Cu(dmp)_2^{2+} + Cl^- + Prod. \quad (1)$$

At higher intensities the bleaching rate becomes a linear function of laser power because all of the $Cu(dmp)_2^+$ molecules in the irradiated volume have been driven into the relatively long-lived CT excited state. Consistent with this interpretation, saturation is much harder to achieve for $Cu(phen)_2^+$ which has a relatively short-lived CT excited state. The mechanistic details have yet to be established, but it is possible that two photon absorption populates a charge-transfer-to-solvent (CTTS) excited state. In any case the solvent dependence of the bleaching rate (CH_2Cl_2 > CH_3CN >> CH_3OH) parallels the reaction rates of the solvated electron with the same series of solvents. Moreover, CTTS transitions have been observed in the UV spectra of the radical anion forms of various aromatic systems (Joschek and Grossweiner 1966).

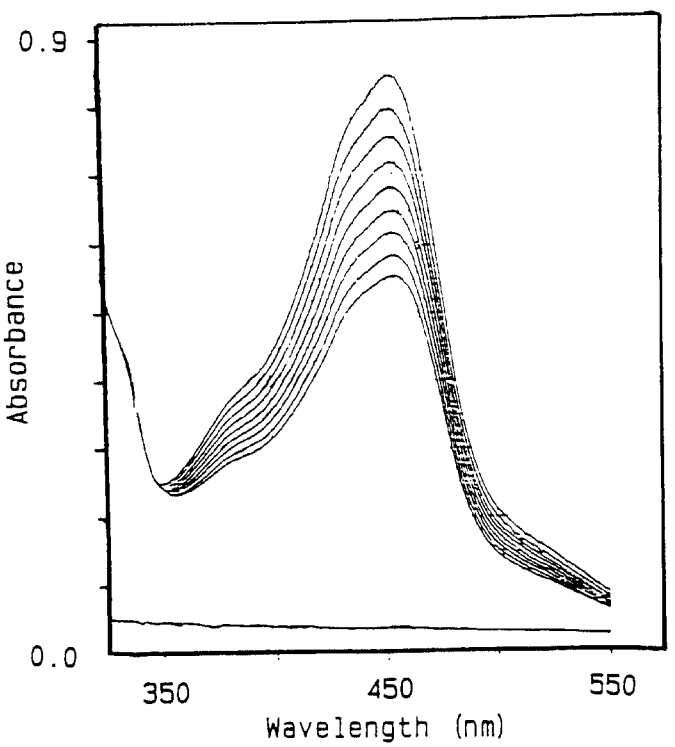

Figure 3. Photolysis of $Cu(dmp)_2^+$ at 20° in CH_2Cl_2. The sample was irradiated with 3.2 mJ pulses of 502.9 nm radiation for 1 min intervals where the repetition rate is 10 Hz.

ACKNOWLEDGMENT

This research was supported by the National Science Foundation through Grant No. CHE-8414267.

REFERENCES

Cesario M, Dietrich-Buchecker CO, Guilhem J, Pascard C, Sauvage, JP (1985) Molecular structure of a catenand and its copper(I) catenate: Complete overturn of the interlocked macrocyclic ligands by complexation. J Chem Soc Chem Commun 244-247.

Day R, Sanders N (1967) The spectra of complexes of conjugated ligands. Part II. Charge-transfer in substituted phenanthroline complexes: Intensities. J Chem Soc (A) 1536-1541

Dietrich-Buchecker CO, Marnot PA, Sauvage JP (1982) Direct synthesis of disubstituted aromatic polyimine chelates. Tet Lett 23: 5291-5294

Dobson JF, Green BE, Healy PC, Kennard CHL, Paskawatchai C, White AH (1984). The stereochemistry of bis(α,α'-diimine)-copper(I) complexes: The crystal amd molecular structures of bis(2,9-dimethyl-1,10-phenanthroline)copper(I) bromide hydrate, bis(4,4'6,6'-tetramethyl-2,2'-bipyridine)copper(I) chloride dihydrate, and bis(2,9-dimethyl-1,10-phenanthroline)copper(I) nitrate dihydrate (a redetermination). Aust J Chem 37: 649-659

Goodwin KV, McMillin DR, Robinson WR (1986) Crystal and molecular structure of $[Ag(tmbp)_2]BF_4$. Origin of flattening distortions in d^{10} complexes of the type $M(NN)_2^+$. Inorg Chem 25: 2033-2036

Healy PC, Engelhardt LM, Patrick VA, White AH (1985) Lewis-base adducts of group 1B metal(I) compounds. Part 19. Crystal structures of bis(1,10-phenanthroline)copper(I) perchlorate and dibromocuprate(I). J Chem Soc Dalton Trans 2541-2545

Joschek H-I, Grossweiner LI (1966) Optical generation of hydrated electrons from aromatic compounds. II. J Am Chem Soc 88: 3261-3268

McMillin DR, Buckner MT, Ahn BT (1977) A light-induced redox reaction of bis(2,9-dimethyl-1,10-phenanthroline)copper(I). Inorg Chem 16: 943-945

Mulliken, RS (1952) Molecular compounds and their spectra. II. J Am Chem Soc 74: 811-824

Orgel LE (1961) Double bonding in chelated metal complexes. J Chem Soc 3683-3686

Phifer CC, McMillin DR (1986) The basis of aryl substituent effects on charge-transfer absorption intensities. Inorg Chem 25: 1329-1333

Staal LH, Stufkens DJ, Oskam A (1978) A study of the electronic properties of $M(CO)_4DAB$ (M = Cr, Mo, W; DAB = diazabutadiene). I. Electronic absorption, resonance Raman, infrared, ^{13}C- and ^{15}N-NMR spectra. Inorg Chim Acta 26: 255-262

PHOTOINDUCED MULTIELECTRON REDOX REACTIONS IN THE $(PtCl_6)^{2-}$/ALCOHOL SYSTEM: VISIBLE LIGHT REDUCTION OF PLATINUM CENTERS

A.B.Bocarsly, R.E.Cameron, and Meisheng Zhou

Department of Chemistry, Princeton University, Princeton, N.J. 08544, USA

Although the photochemistry of octahedral haloplatinum (IV) complexes has been extensively investigated, it has always been viewed in terms of ligand substitution processes. However, the preference of platinum for the (II) and (IV) oxidation states,and the previous observation (Cox et al., 1972) that photoaquation of $[PtC\ell_6]^{2-}$ can involve a Pt(III) intermediate suggests that such complexes may be capable of photoinduced multielectron charge transfer. Such a capability has now been demonstrated in the photoinitiated reaction of $[PtC\ell_6]^{2-}$ with alcohols. Up to four electrons can be transferred in this process leading to the formation of platinum metal (Cameron and Bocarsly, 1986) and aldehydes or ketones depending on whether a primary or secondary alcohol is initially employed. Of special interest is the finding that primary alcohols are not overoxidized to the acid. Further aldehyde formation can be carried out catalytically by addition of $O_2/CuC\ell_2$ to the reaction mixture as a reoxidant of lower platinum oxidation states back to Pt(IV) (Cameron and Bocarsly, 1985).

The photochemical production of platinum metal is an unusual finding. The photochemistry of Pt(IV) is typified by an inability to generate platinum metal. Only recently has production of metal been noted. This was obtained by Vogler and Hlavatch (1983) who employed the relatively novel $[Pt(N_3)_6]^{2-}$ complex which generates N_2 and metal upon illumination. Since the ability to generate a well defined platinum surface is both scientifically novel and of practical interest with respect to heterogeneous catalysis and electronic lithography, photochemistry leading to this goal is of fundamental interest.

MECHANISM OF PLATINUM PHOTOREDUCTION

The four electron photoinduced reduction of $[PtC\ell_6]^{2-}$ in aqueous alcohol does not require heating and occurs at all wavelengths at which the complex absorbs light. Thus, irradiation at energies as low as 514 nm, reported to excite a $[PtC\ell_6]^{2-}$: $^1A_{1g} \longrightarrow {}^3T_{1g}$ ligand field transition (Swihart and Mason, 1970) yields platinum metal. A large variety of alcohol reactants undergo two electron oxidation in the presence of $[PtC\ell_6]^{2-}$. The reaction of $[PtC\ell_6]^{2-}$ with ethanol and 2-propanol are prototypical.

The fate of the platinum species in these reactions has been followed using ^{195}Pt-FTNMR and UV-visible spectroscopy. Figure 1 details the time dependence of the NMR sensitive platinum species during the photoreduction of $PtC\ell_6^{2-}$ by 2-propanol, along with organic product formation as determined by gas chromotography. As can be seen from these data the initially observed platinum photoproduct is a Pt(II) species identified as $PtC\ell_4^{2-}$ using UV-visible spectroscopy. There exists a fairly long induction period prior to metal formation. The exact length of this period depends on the light intensity employed, and the reagent concentrations. Once an initial amount of metal is produced the reaction rapidly goes to completion.

In general, platinum formation is not found to occur until a ~ 90% yield of $[PtC\ell_4]^{2-}$ has accumulated. This suggests that $[PtC\ell_6]^{2-}$ acts as an inhibitor toward platinum metal formation. In order to gain insight into this process the thermal reduction chemistry of $[PtC\ell_4]^{2-}$ was examined. $[PtC\ell_4]^{2-}$ was found to react with 2-propanol in a redox reaction to produce platinum metal

Photochemistry and Photophysics
of Coordination Compounds, Ed. by H. Yersin/A. Vogler

and acetone in a 1:1 stoichiometry. Addition of $[PtCl_6]^{2-}$ (or KCl) had a strong inhibiting effect on metal formation demonstrating the source of the $[PtCl_6]^{2-}$ inhibition. On the other hand, addition of high surface area platinum metal enhanced the reaction rate; thus, this reaction is autocatalytic in platinum metal. These two findings taken together explain the asymmetry of the Pt(II) versus time profile shown in Fig. 1.

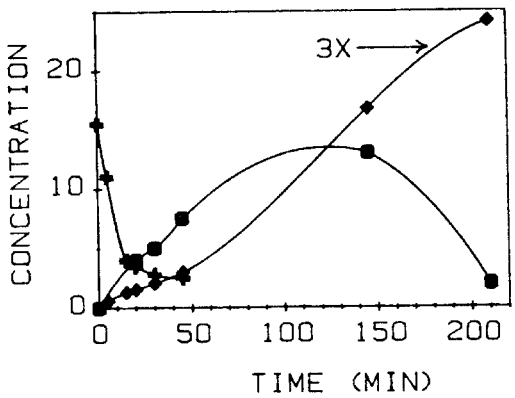

Figure 1: Product distribution for the reaction of $[PtCl_6]^{2-}$ with 2-propanol as a function of time. All concentrations are in millimolar. The "+" represents the $[PtCl_6]^{2-}$ concentration, "•" represents $[PtCl_4]^{2-}$, and "▲" represents one third of the total organic concentration. The latter is a sum of acetone and acetaldehyde concentrations. Metal is observed to form at ~ 150 minutes.

Unlike the reduction of $[PtCl_4]^{2-}$, which only yields acetone as the organic product, acetaldehyde is initially the major product during the photoreduction of $PtCl_6^{2-}$ by 2-propanol. Formation of this species is indicative of methyl free radical loss from 2-propanol. The existence of such a process is confirmed by reaction of t-butanol with $[PtCl_6]^{2-}$. This reaction yields acetone (again signifying methyl loss) and $[PtCl_4]^{2-}$, directly indicating that $[PtCl_6]^{2-}$ associated photochemistry is responsible for the formation of methyl free radicals. The existence of methyl free radicals introduces two major mechanistic implications. First, the oxygen based 2-propanol free radical, $^{\bullet}O\text{-}CH(Me)_2$, must be generated. This is unusual since it is the carbon based radical which is more stable. Second, the charge transfer chemistry must involve one electron processes. This latter conclusion is confirmed by the photochemical reaction of cyclobutanol with $[PtCl_6]^{2-}$. This alcohol is a known free radical clock (Meyer and Rocek, 1972) which produces ring opened products upon one electron oxidation. Our observation in this reaction of one electron oxidized organic products implicates a Pt(III) species as a primary photoproduct.

Since oxidation of an alcohol via an unstructured oxidant such as $Cl^{\bullet}$ (a possible reactive species in the present system) would lead to the thermodynamically favored carbon based free radical, the available data suggest that reaction proceeds via photoinduced formation of a platinum-alkoxy bond followed by optical homolysis to generate the indicated products as outlined below:

$$[PtCl_6]^{2-} \xrightarrow[R'RCH\text{-}OH]{h\nu} [PtCl_5(OCHRR')]^{2-} + HCl \qquad (1)$$

$$[PtCl_5(OCHRR') \xrightarrow{h\nu} [PtCl_5]^{2-} + {}^{\bullet}OCHRR' \qquad (2)$$

$$[PtCl_5]^{2-} + {}^{\bullet}OCHRR' \longrightarrow [PtCl_4]^{2-} + O{=}CRR' \quad (3a)$$

$$2[PtCl_5]^{2-} \longrightarrow [PtCl_4]^{2-} + [PtCl_6]^{2-} \quad (3b)$$

$${}^{\bullet}OCHRR' \longrightarrow O{=}CR + R' \quad (4)$$
(for R'=Me)

The existence of reactions 3a,b is speculative, however, consistent with the expected behavior of a Pt(III) species. Support for this mechanism comes from the observation that irradiation of isolated $[PtCl_x(OR)_{6-x}]^{2-}$ complexes (where R = 2-propyl) leads to platinum metal production. Thus, reaction (2) is directly verified. Metal formation is expected to proceed from the thermal reaction of the products of reaction (3) with the alcohol as discussed previously. Although this latter reaction proceeds via a thermal pathway, it is photochemically accelerated by visible light.

CATALYTIC PRODUCTION OF ALDEHYDES AND KETONES

Although the observation that aldehyde can be produced without overoxidation to the acid is synthetically interesting, the utilization of an expensive reagent ($K_2[PtCl_6]$) removes any synthetic appeal. In order to generate a synthetically useful process the reaction must be catalytic in platinum. Since reoxidation of platinum metal is difficult it is necessary to intercept an intermediate oxidation state of platinum. Further, it is desirable to trap the ${}^{\bullet}OCHRR'$ product prior to methyl loss in cases where this is a possible reaction pathway. This is accomplished by adding a $CuCl_2/O_2$ redox catalyst to the system. As shown in Table 1 under these conditions aldehyde and ketone products are generated in high yield without methyl loss or other free radical side products. Control experiments indicate that neither $CuCl_2/O_2$ alone nor $[PtCl_6]^{2-}/O_2$ alone produces a catalytic cycle.

Table I: Typical Product Yields[a]

Alcohol	Product	% Yield[b]	Φ[c]
Ethanol	Acetyldehyde	94	0.05
2-Propanol	2-Propanone	98	0.06
Cyclopentanol	Cyclopentanone	98	0.04
Cyclohexanol	Cyclohexanone	92	0.02
Cyclobutanol	Cyclobutanone	94	-
Benzyl Alcohol	Benzaldehyde	93	0.03
2-Hexanol	2-Hexanone	84	0.02
Cinnamyl Alcohol	Cinnamaldehyde	88	0.02

[a] 1:2 $K_2[PtCl_6]/CuCl_2$ catalyst. Reactions were carried out in acetonitrile, acetone, or water solvents.
[b] Reactions were carried out in an acetone solvent using a tungsten halogen source supplied with UV and IR cut-off filters.
[c] Quantum yield for product formation at 488 nm.

As can be seen from data in Table I this system is capable of carrying out the specific two electron oxidation of a wide variety of alcohols. Even low redox potential alcohols such as benzyl alcohol show no tendency to be overoxidized to the acid. Further, reactivity does not appear to be significantly influenced by the presence of sites of unsaturation near the alcohol functionality. Thus, as demonstrated using cinnamyl alcohol conjugated aldehydes can be generated in good yield. That cyclobutanone is produced in high yield from the corresponding alcohol indicates the process has a "two

electron" character to it. Presumably this radical clock is stabilized by the rapid loss of an electron to Cu^{2+}, a species known to be a fast radical trap. For the case of 2-propanol oxidation quantum yields as high as 0.15 have been observed for acetone formation using 488 nm light. Turnover numbers in excess of 150 have been observed when white light is employed with only a slight decrease in catalytic activity at the end of the reaction period. Catalyst stability is quite good.

The reaction is found to be fairly sensitive to the amount of $CuCl_2$ present. As the $CuCl_2$ concentration is increased the turnover rate is observed to increase linearly. This phenomenon appears to saturate at ~ 1:2 ratio of $CuCl_2$ to $[PtCl_6]^{2-}$. Addition of an excessive amount of $CuCl_2$ causes the solution to turn brown with a concomitant loss of catalytic activity. ^{195}Pt NMR studies demonstrate that Cu^{2+} cannot oxidize $[PtCl_4]^{2-}$. This result can be best explained by assuming that Cu^{2+} is oxidizing a Pt(III) chloride complex to regenerate $[PtCl_6]^{2-}$. Therefore the requirement of two equivalents of $CuCl_2$ can be understood in terms of its dual role as an oxidant of Pt(III) and a radical trap for $^{\bullet}OCHRR'$. The overall cycle is summarized in Fig. 2. The high product yields along with the lack of typical organic free radical products can best be explained by the existence of a binuclear (possibly chloro bridged) platinum-copper complex as the active catalytic species. Such a complex could provide the strong cage effect necessary to produce the observed product yield.

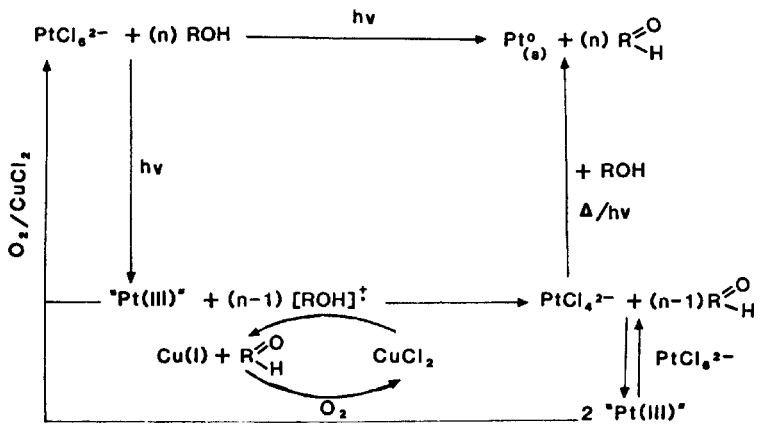

Figure 2: Mechanistic sequence for the reaction of $[PtCl_6]^{2-}/CuCl_2/O_2$ with primary alcohols and $[PtCl_6]^{2-}$ itself with primary alcohols.

Acknowledgment is made to the Donors of The Petroleum Research Fund, administered by the American Chemical Society for Support of this Research.

References:

Cameron, RE, Bocarsly AB (1985) Photoactivated oxidation of alcohols by oxygen. J Am Chem Soc 107: 6116-6117.

Cameron, RE, Bocarsly, AB (1986) Multielectron-photoinduced reduction of chloroplatinum complexes: Visible light deposition of platinum metal. Inorg Chem 25: 2910-2913.

Cox, LE, Peters, DG, Wehry, EL (1972) Photoaquation of Hexachloroplatinate(IV)> J Inorg Nucl Chem 34: 297-305.

Meyer, K, Rocek, J. (1972) One-electron vs. two-electron oxidations. Ce(IV) and cyclobutanol. J Am Chem Soc 94: 1209-1214.

Swihart, DL, and Mason, WR (1970) Electronic spectra of octahedral Pt(IV) complexes. Inorg Chem 9: 1749-1757.

Vogler, A, and Hlavatsch, J (1983) Photochemical four-electron redox reaction of hexaazidoplatinate(IV). Angew Chem Int Ed 22: 154-155.

DYNAMIC AND STATIC OUTER-SPHERE AND INNER-SPHERE QUENCHING PROCESSES

L.Checchi, C.Chiorboli, M.A.Rampi Scandola, and F.Scandola

Dipartimento di Chimica dell'Università, Centro di Fotochimica del CNR,
44100 Ferrara, ITALY

INTRODUCTION

Bimolecular quenching via energy or electron transfer of electronically excited states of coordination compounds in fluid solutions has been the subject of intesive investigations in the last ten years (Balzani 1978,Sutin 1979,Sutin 1980,Balzani 1981, Sutin 1982,Balzani 1983). The kinetics of such processes can be conveniently discussed by separating diffusive and reactive steps as shown in Scheme 1:

Scheme 1.

$$A + B \underset{1/\tau^\circ}{\overset{h\nu}{\rightleftharpoons}} {}^*A + B \underset{k_{-d}}{\overset{k_d}{\rightleftharpoons}} {}^*A\,B \xrightarrow{k_t} \begin{cases} A^+ + B^- \\ A + {}^*B \end{cases}$$

The reactive step taking place into the so-called precursor complex *A B, is considered as a unimolecular process. In most cases (A and B uncharged or with positive charge product)both the ground and excited state concentrations of A B are small and the constant k_t can be at best indirectly inferred from the second order quenching rate constant k_q. If, on the other hand, strong electrostatic attraction between A and B is operating (A and B of high and opposite charge), a sufficiently high concentration of the ground state precursor complex may be present to allow direct excitation of this species and observation of the unimolecular step.

Recently,studies of optically induced energy or electron transfer processes between transition metal centers covalently linked in a supermolecular structure have been performed (Vogler 1985, Bignozzi 1985, Curtis 1985). These processes are summarized in Scheme 2.

Scheme 2

$$A - B \underset{1/\tau^\circ}{\overset{h\nu}{\rightleftharpoons}} {}^*A - B \xrightarrow{k_t} \begin{cases} A^+ - B^- \\ A - {}^*B \end{cases}$$

If the supermolecule A - B forms in solution upon addition of A and B (or related species) and the covalent linkage does not change strongly the properties of the subunits, the locally-excited molecule can be viewed as a covalently linked precursor complex of the transfer process. From this viewpoint, a general kinetic scheme (Scheme 3) can represent photoinduced electron or energy transfer between A and B which are capable of electrostatic and/or covalent (usually called second sphere donor-acceptor) interaction.

Scheme 3

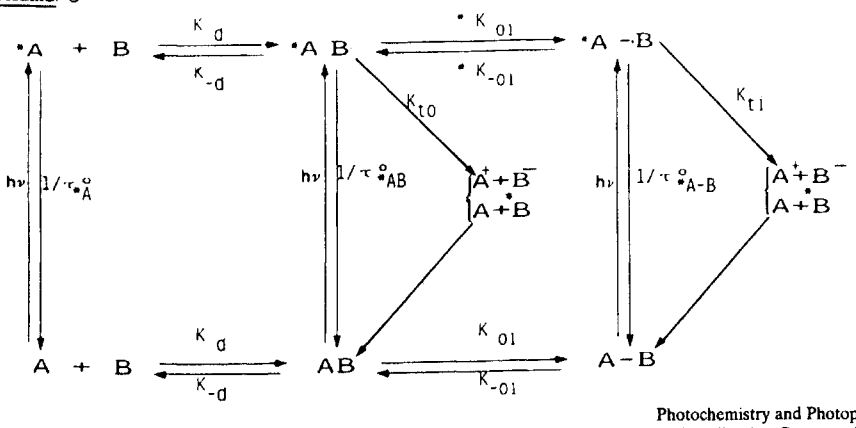

Photochemistry and Photophysics
of Coordination Compounds, Ed. by H. Yersin/A. Vogler

In this Scheme, $^*A\ B$ is the precursor complex of an outer-sphere transfer mechanism, while $^*A$ - B can be considered as the precursor complex of an inner-sphere transfer mechanism. Depending on the relative constants of the various ground-state species and on the relative rates of the excited-state processes, the complex kinetic behavior predicted by this Scheme may give rise to two experimental distinguishable situations (Balzani 1975, Rybak 1981, Frank 1983, White 1984): 1) if(i)the ground-state concentration of associated species is neglegible or (ii) the excited associated species undergo prompt dissociation ($k_{to}<k_{-d}$; $k_{ti}< k_{*-oi}$), the system behaves as if $^*A$ was the only excited species. In this case both emission intensity (I) and lifetime (τ) follow the same Stern-Volmer behavior: $\tau^\circ/\tau = I^\circ/I = 1+k_q\tau^\circ[B]$. In this case the quenching is usually called dynamic quenching;2) if(i)the ground state concentration of outer-sphere and/or inner-sphere associated species is high and (ii) their excited states react before dissociating ($k_{to}> k_{-d}$; $k_{ti}>k_{*-oi}$), a complex multiexponential decay is expected, with one or two short components whose lifetime is independent of B concentration, followed by a longer one that obeys Stern-Volmer law.
The intensity quenching is always larger than the lifetime quenching and usually follows a quadratic law of the type: $I^\circ/I= (1+k_q\tau^\circ[B])(1+K_A[B])$ where K_A is an "effective" association constant of all the present associated species. In this case the quenching is usually called static quenching. Studies in this field have been limited by the use of positive sensitizers for which a small number of negative quenchers is available. We report here the results of quenching studies involving recently synthetized, negatively charged photosensitizers, $Ir(QOSO_3)_3^{3-}$(Ballardini 1985) and $Ru(bpy)CN_4^{2-}$(Bignozzi 1986) and positively charged quenchers.

RESULTS and DISCUSSION

System I: $Ir(QOSO_3)_3^{3-}$ + $Cr(bpy)_3^{3+}$, $Cr(phen)_3^{3+}$(DMF, μ=0.01M TEAP)

The diffusional parameters have been estimated by numerical integration of the Debye-Smoluchowski, Eigen-Fuoss equations (Chiorboli 1986). They are reported in Table 1. The emission of $Ir(QOSO_3)_3^{3-}$is quenched by $Cr(bpy)_3^{3+}$ according to $I^\circ/I= (1+ k_q\tau^\circ[B])(1+K_A[B])$. By using the experimental value of the quenching constant obtained in laser lifetime measurements ($k_q=1.8\times10^{10}\ M^{-1}s^{-1}$) the association constant is obtained as $K_A=1.5\times10^3 M^{-1}$In single photon counting experiments, the emission decays are nonexponential as shown in Fig.1.

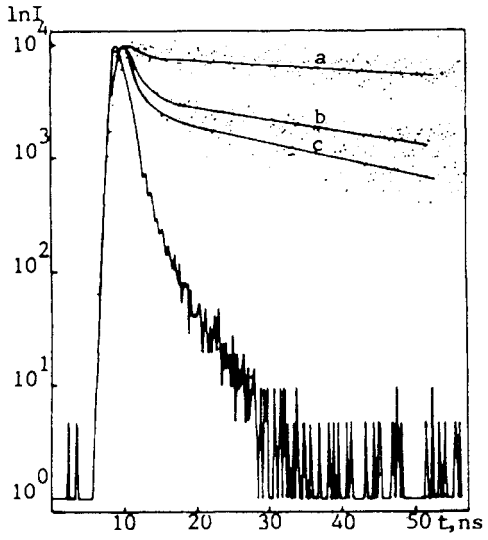

Fig. 1: Luminescence decay for $Ir(QOSO_3)_3^{3-}$ (1.4×10^{-4}M) with various concentrations of $Cr(bpy)_3^{3+}$ (a:2×10^{-4}M, b:4×10^{-4}M c:8×10^{-4}M), μ =0.01M TEAP.

The shorter component has a constant lifetime (τ^*_{AB} = 1 ± 0.3 ns) and a relative weight that increases with quencher concentrations. The longer component has a lifetime that decreases with quencher concentrations according to a Stern-Volmer kinetic (k_q=1.8x10^{10} $M^{-1}s^{-1}$).The absence of artifacts in the appearence of the short component is indicated by the strictly monoexponential decay obtained for similar systems having one of the partners as an uncharged species ($Ir(QOSO_3)_3^{3-}$ + benzoquinone, $Ir(QO)_3$ + $Cr(bpy)_3^{3+}$). Laser photolysis fails to give any proof for energy transfer or (more plausible) elecron transfer quenching mechanism. Similar results have been obtained using $Cr(phen)_3^{3+}$ as quencher.

The data can be interpreted in terms of Scheme 3 as follow:
i) the quenching mechanism is of the outer-sphere type ; (ii) the dynamic part of the quenching is diffusional (k_q=k_d), requiring k_{to}>k_{-d}, a condition that makes it possible to detect static quenching upon excitation of *A B;(iii) static quenching shows up both as a deviation of I°/I from $\tau°/\tau$ and as a double exponential decay. The short component of the decay (τ^*_{AB} ≅ 1ns) gives a direct measurement of k_{to}(few examples of direct measurements of k_{to} are available (Ballardini 1985)); (iv) the experimental K_A value obtained from I°/I vs $\tau°/\tau$ is higher than the calculated one, presumably because of compenetration effects.

System II : $Ir(QOSO_3)_3^{3-}$ + $Co(NH_3)_6^{3+}$,$Co(en)_3^{3+}$ (H_2O, μ=0.01 M NaCl)

The estimated diffusional parameters are reported in Table 1.

The emission decays in both laser and single photon counting experiments are appreciably monoexponential and give k_q= 1.7x10 M^{-1} s^{-1}. Emission intensity quenching gives small deviation of I°/I from Stern-Volmer behavior, smaller than that calculated from $I°/I=(1+k_q\tau°[B])(1+K_A[B])$ with the values of experimental k_q and calculated K_A. Laser photolysis fails to give any proof for energy or electron transfer mechanism for the quenching. Similar results have been obtained for the both quenchers. They can be interpreted in terms of Scheme 3 as follows:
i) the quenching mechanism is of the outer-sphere type; (ii) the k_q value is in somewhat smaller than k_d, implying that k_{to} may be of the same order of magnitude as k_{-d}(1x10^8 s^{-1});this makes it difficult to detect static quenching effects;(iii) in fact, very small static quenching is obtained as deviation of I°/I from $\tau°/\tau$.

System III :$Ru(bpy)CN_4^{2-}$ + $Cr(H_2O)_6^{3+}$ (H_2O, μ=0.6 M KNO_3)

The estimated values of diffusional parameters are reported in Table 1.
Aqueous solutions containing $Ru(bpy)CN_4^{2-}$ and $Cr(H_2O)_6^{3+}$ undergo slow absorption spectral changes indicating coordination of the complex to the cynide ligands $Ru(bpy)CN_4^{2-}$ chromophore(Demas 1977, Bignozzi 1985, Scandola 1986) according to:

$$Ru(bpy)CN_4^{2-} + Cr(H_2O)_6^{3+} \longrightarrow Ru(bpy)CN_4\text{-}Cr(H_2O)_5^{+} + H_2O$$

With the same kinetics the emission intensity of $Ru(bpy)CN_4^{2-}$ decreases with the time. Equilibrated solutions do not emit appreciably. It is possible to perform quenching experiments on solutions where the adduct formation is neglegible. The experiments give coincident I°/I and $\tau°/\tau$ Stern-Volmer plots, yielding k_q=1.6x10^8 $M^{-1}s^{-1}$ smaller than k_d. Laser photolysis does not supply any evidence for electron or energy transfer quenching mechanism. According to Scheme 3, we can conclude that:(i) the system evolves with the time from outer-sphere dynamic quenching to inner-sphere static quenching;(ii) the dynamic quenching has a k_q lower than the k_d value, implying that k_{to}< k_{-d} (estimated value k_{to}= 4x10^7 s^{-1});(iii) taking the lower limiting value from the lack of emission of the adduct, k_{ti}>10^9s^{-1}.

This system clearly shows the large increase in transfer rate constant observed upon going from outer to inner-sphere mechanism.

Table 1: Diffusional parameters calculated for the investigated systems.

A	B	$k_d, M^{-1}s^{-1}$	k_{-d}, s^{-1}	K_A, M^{-1}
$Ir(QOSO_3)_3^{3-}$	$Cr(bpy)_3^{3+}$	$1.8X10^{10}$	$1.2X10^{7}$	$1.5X10^{3}$
$Ir(QOSO_3)_3^{3-}$	$Cr(phen)_3^{3+}$	$1.8X10^{10}$	$1.2X10^{7}$	$1.5X10^{3}$
$Ir(QOSO_3)_3^{3-}$	$Co(NH_3)_6^{3+}$	$2.0X10^{10}$	$8.9X10^{7}$	$2.3X10^{2}$
$Ir(QOSO_3)_3^{3-}$	$Co(en)_3^{3+}$	$1.8X10^{10}$	$1.0X10^{8}$	$1.7X10^{2}$
$Ru(bpy)CN_4^{2-}$	$Cr(H_2O)_6^{3+}$	$8.7X10^{9}$	$2.0X10^{9}$	4.3

CONCLUSIONS

The possibility of measuring directly the rate constant of the unimolecular reactive step, taking advantage of ionic or donor-acceptor association, is restricted within a rather narrow window of conditions. In fact, with the "fast" Cr(III)reactants the reactive step of ion pair is at the limit of experimental detection, whereas with the Co(III)reactants the reactive step is already too slow to occur before dissociation of the excited ion pair. The large increase in the rate of unimolecular reactive step expected in going from the outer-sphere precursor complex to the inner-sphere adduct is clearly shown in the last system.

REFERENCES

-Ballardini,R.;Varani,G.;Indelli,M.T.;Scandola,F. J.Am.Chem.Soc.1986,25,3858.
-Ballardini,R.;Gandolfi,M.T.;Balzani,V. Chem.Phys.Lett.1985,119,459.
-Balzani,V.;Moggi,L.;Manfrin,M.F.;Bolletta,F.;Laurence,G.S. Coord.Chem.Rev.1975,15,321.
-Balzani,V.;Bolletta,F.;Gandolfi,M.T.;Maestri,M. Top.Curr.Chem.1978,75,1.
-Balzani,V.;Scandola,F. in"Photochemical Conversion and Storage of Solar Energy";J.S., Ed.; Academic Press : New York,1981,Chapter 4,p.97.
-Balzani,V.;Scandola,F. in"Energy Resources through Photochemistry and Catalysis", Graetzel,M.,Ed.; Academic Press: London,1983;Chapter1,p.1.
-Bignozzi,C.A.;Roffia,S.;Scandola,F. J.Am.Chem.Soc.1985,107,1644.
-Bignozzi,C.A.;Chiorboli,C.;Indelli,M.T.;Rampi Scandola,M.A.;Varani,G.;Scandola,F. J.Am.Chem.Soc.1986,108,7872.
-Chiorboli,C.;Scandola,F.;Kisch,H. J.Am.Chem.Soc.1986,90,2211.
-Curtis,J.C.;Bergstein,J.S.;Meyer,T.J. Inorg.Chem.1985,24,385.
-Demas,J.M.;Addington,J.W.;Peterson,S.H.;Harris,E.W. J.Phys.Chem.1977,81,1039.
-Frank,R.;Rau,H. J.Phys.Chem.1983,87,5181.
-Rybak,W.;Haim,A.;Netzel,T.L.;Sutin,N. J.Phys.Chem.1981,85,2856.
-Scandola,F.;Bignozzi,C.A.;Balzani,V. in"Homogeneous and Heterogeneous Photocatalysis" Pellizzetti,E. and Serpone,N.eds.; D.Reidel:Dordrecht,1986.
-Sutin,N. J.Photochem.1979,10,19.
-Sutin,N.;Creutz,C. Pure Appl.Chem.1980,52,2717.
-Sutin,N.;Creutz,C. J.Chem.Educ.1983,60,809.
-Vogler,A.;Osman,A.H.;Kunkely,H. Coord.Chem.Rev.1985,64,159.
-White,H.S.;Becker,W.G.;Bard,A.J. J.Phys.Chem.1984,88,1840.

PHOTOCHEMISTRY AND SPECTROSCOPY OF ION PAIR CHARGE TRANSFER COMPOUNDS

H.Hennig, D.Rehorek, and R.Billing

Sektion Chemie, Karl-Marx-Universität, Leipzig, GDR

Ion pairs of metal complexes characterized by spectroscopic ion pair charge transfer (IPCT) transitions have been described first time by Linhard (1944), but until now there are no systematic investigations concerning the general behaviour of this interesting class of compounds.

Examples of IPCT compounds based on metal complexes are still very rare (Balzani 1986). We have been able to prepare some further IPCT compounds which are distinguished by interesting photochemical and photocatalytic behaviour. Our investigations concern ion pair associates of copper(II)complexes and cobalt(III)ammines with tetraphenylborate (Hennig 1983; Rehorek 1979, 1980) as well as of cyanometallates with diphenyliodonium cations (Rehorek 1979; Billing 1985). These compounds are distinguished by spectroscopic transitions in the visible which can not be explained as the sum of the components forming the ion pairs but which are to consider as ion pair charge transfer transitions.

The excitation of these IPCT states leads to very efficient photo redox reactions in low-energy regions where the parent complexes alone (as $[Co(NH_3)_6]^{3+}$ and $[Mo(CN)_8]^{4-}$, for instance) show not any photo redox reactivity.
The high brutto quantum yield values concerning the formation of Co(II) and Mo(V) (1), (2) are due to the formation of both short-lived tetraphenylbor radicals and diphenyliodine radicals which contribute to overcome fast back electron transfer processes.

$$\{[Co(NH_3)_6]^{3+};B\emptyset_4^-\} \xrightarrow{h\cdot\nu} \{Co(NH_3)_6]^{2+};B\emptyset_4\cdot\} \longrightarrow .... \quad (1)$$

$$\{[Mo(CN)_8]^{4-};\emptyset_2I^+\} \xrightarrow{h\cdot\nu} \{Mo(CN)_8]^{3-};\emptyset_2I\cdot\} \longrightarrow .... \quad (2)$$

Systematic investigations of the IPCT phenomenon are rather complicated since all IPCT compounds of complex ions have been detected accidentally and the prediction of the energies of optical IPCT transitions of any ion pair combinations has been unsuccesful until now.

Photochemistry and Photophysics
of Coordination Compounds, Ed. by H. Yersin/A. Vogler

Therefore an increment system for predicting of the energy of IPCT transitions as proposed by us very recently (Billing 1985; Hennig 1986) might be useful to expand our knowledge of such second-sphere effects.

INCREMENT SYSTEM FOR PREDICTING OF THE ENERGY OF OPTICAL IPCT TRANSITIONS

Our increment system is based on the applicability of an energy cycle proposed by Cannon (1980) for the estimation of the energy of CT transitions (ΔG_{CT}) to IPCT compounds. Considering some common assumptions (3) can be derived which gives $\Delta G_{CT}(A^+,D^-)$ the energy of the optical IPCT transition:

$$\Delta G_{CT}(A^+,D^-) = \Delta G_E + \Delta G_{W'} - \Delta G_W + \Delta G_{FC} \qquad (3)$$

where ΔG_E are standard electrode potentials, ΔG_W and $\Delta G_{W'}$ work terms and ΔG_{FC} the reorganization energy. Following Marcus (1965) the reorganization energy can be considered as the arithmetic mean of the self-exchange of the both components forming the ion pair and the following expression can be obtained (4):

$$\Delta G_{CT}(A^+,D^-) = F[E^{\ominus}_{(D/D^-)} - E^{\ominus}_{(A^+/A)}] + 1/2[\Delta G_{FC}(A^+A) + \Delta G_{FC}(DD^-)] \qquad (4)$$

Expression (4) leads to the conclusion that $\Delta G_{CT}(A^+,D^-)$ consists of energy contributions of each of both ions independently on the kind of both components. Therefore the absolute values of the energy contributions can be substituted by increments of each ion. The contributions of the ions A^+ and D^- to $\Delta G_{CT}(A^+,D^-)$ can be defined as the sum of the increments of these ions in a certain solvent (as H_2O, for instance). Using the increments $I^{aq}_{A^+}$ and $I^{aq}_{D^-}$ equation (5) can be derived:

$$\Delta G_{CT}(A^+,D^-) = I_{A^+} + I_{D^-} \qquad (5)$$

For aqueous solutions the tropylium cation has been introduced as having a basis increment of nought (6):

$$I^{aq}_{trop^+} \stackrel{def}{=} 0 \qquad (6)$$

and for any donor anions D^- the increment values $I^{aq}_{D^-}$ are given by (7)

$$I^{aq}_{D^-} = \Delta G^{aq}_{CT}(trop^+,D^-) \qquad (7)$$

Analogously expression (8) can be applied to any acceptor cations A^+:

$$I^{aq}_{A^+} = \Delta G^{aq}_{CT}(A^+,D'^-) - I^{aq}_{D'^-} \qquad (8)$$

where D'^- is a reference anion with know increment value. For aqueous solutions hexacyanoferrate(II) has been proposed as a particularly suitiable reference anion.

Thus it is possible to estimate $\Delta G_{CT}(A^+,D^-)$ spectroscopically for any ion pair combinataions by using the proposed increment system. The ΔG_{CT} values estimated in this way are in fairly good agreement with the experimental results. However, if ion pair combinations give rise to thermal redox reactions with tropylium cations and hexacyanoferrate(II) anions, respectively, the increments I_{A^+} and I_{D^-} can not be obtained by spectroscopy. The same is to consider if the IPCT bands are covered by absorption bands of the reference or counter ions. However, due to the linear dependence of the increment values I_{A^+} and I_{D^-} on their standard electrode potentials, the increment values can be obtained also by using the appropriate redox potentials (Hennig 1986). The following equations (9), (10) can be used to estimate I_{A^+} and I_{D^-} electrochemically:

$$I_D^{aq} = 11{,}7 \cdot 10^3 cm^{-1} + 11{,}9\ E^{\ominus} \cdot 10^3 cm^{-1}V^{-1} \quad (9)$$

$$I_{A^+}^{aq} = -3{,}4 \cdot 10^3 cm^{-1} - 11{,}8\ E^{\ominus} \cdot 10^3 cm^{-1}V^{-1} \quad (10)$$

Relations (9) and (10) have been derived by regression calculations based on an appropriate number of ion pair combinations.

It has been shown that the increment system for predicting of optical IPCT transitions can be applied also to non-aqueous solvents (Hennig 1986). Using 6 different solvents (methanol, dimethylsulfoxide, dimethylformamide, acetone, acetonitrile, and dichloromethane) which represent a broad range of solvent polarity, a good agreement of $\Delta G_{CT}(A^+,D^-)$ values estimated experimentally and by using the increment values obtained for the appropriate solvent has been observed.

Solvent effects on the position of the maxima of IPCT bands can be estimated generally by using the following three parameter approach (Hennig 1986):

$$\Delta G_{CT}^{solv}(A^+,D^-) = C_o + C_1 \cdot AN + C_2 \cdot DN + C_3(1/n^2 - 1/\varepsilon) \quad (11)$$

where $(1/n^2 - 1/\varepsilon)$ stands for the solvent term, DN as the acceptor number and DN as the donor number and C_n as the coefficients of the three parameter approach.

However, it is to consider the increment system can be applied only to contact ion pairs and the position of the lowest energy IPCT band can be predicted only. Furtheron, we have been unable until now to prove the reliability of our increment system to such ion pair combinations consisting of donor cations (D^+) and acceptor anions (A^-) since there are no appropriate examples available.

Ion pairs distinguished by low-energy IPCT bands are of particular interest concerning the static spectral sensitization of photocata-

lytic systems based on light-sensitive coordination compounds and organometallics, respectively (Hennig 1985).

REFERENCES

Balzani V, Sabbatini N, Scandola F (1986) "Second-sphere" photochemistry and photophysics of coordination compounds. Chem Rev 86: 319 - 337

Billing R (1985) Untersuchungen zum spektralen, photochemischen und thermischen Verhalten von Ionenpaaren in Lösung - ein Beitrag zur statischen spektralen Sensibilisierung. Dissertation, Karl-Marx-Universität, Leipzig

Cannon RD (1980) Electron transfer reactions. Butterworth, London Boston, p. 277; see also Adv Inorg Radiochem 21: 253 (1978)

Hennig H, Walther D, Thomas P (1983) Über das photochemische Verhalten von Ionenpaarassoziaten des Typs $Co(NH_3)_5X$,$B(C_6H_5)_4$ bei Einstrahlung in den IPCT-Bereich. Z Chem 23: 446

Hennig H, Rehorek D, Archer RD (1985) Photocatalytic systems with light-sensitive coordination compounds and possibilities of their spectral sensitization - an overview. Coord Chem Rev 51: 1 - 53

Hennig H, Billing R, Benedix R (1986) Dreiparameterbeschreibung von Lösungsmitteleinflüssen auf Ionenpaar-Charge-Transfer-Banden. Monatsh Chem 117: 51 - 54

Hennig H, Benedix R, Billing R (1986) Inkrementsystem zur Beschreibung der Lage von Ionenpaar-Charge-Transfer-Banden in Wasser und nichtwäßrigen Lösungsmitteln. J prakt Chem 328: 829 - 840

Linhard M (1944) Über Lichtabsorption und Konstitution anorganischer Komplexsalze. I. Luteokobalt- und Luteochromsalze. Z Elektrochem 50: 224 - 238

Marcus RA (1965) On the theory of electron transfer reaction. VI. Unified treatment for homogeneous and electrode reaction. J chem Phys 43: 679 - 701

Rehorek D, Ackermann M, Hennig H, Thomas P (1979) Ungewöhnliche Photoredoxreaktionen von Bis(ferroin)kupfer(II)-tetraphenylboranaten. Z Chem 19: 149

Rehorek D, Salvetter J, Hantschmann A, Hennig H (1979) Photooxidation von Octacyanomolybdat(IV) durch langwellige Anregung. J prakt Chem 321: 159 - 160

Rehorek D, Schmidt D, Hennig H (1980) Langwellige spektrale Sensibilisierung der Photoreduktion von Cobalt(III)-Komplexen durch Ionenpaarbildung mit Tetraphenylborationen. Z Chem 20: 223 - 224

BACKWARD ELECTRON TRANSFER WITHIN GEMINATE RADICAL PAIR FORMED IN THE ELECTRON TRANSFER QUENCHING

Takeshi Ohno and Akio Yoshimura

Chemistry Department, College of Chemical Education, Osaka University, Osaka 560, JAPAN

Unfortunate low yields of redox products have been observed often in the bimolecular electron transfer quenching of phosphorescent compounds. The lowest yield of free radical formation in the bulk is of course zero, which have been observed in the electron transfer quenching of excited tris(2,2-bipyridine)ruthenium(II) by nitrobenzenes and quinones. Laser photolytic studies of triplet state quenching already have demonstrated (Ohno 1983) that every quenching of triplet excited state produces a geminate radical pair, which undergoes a fast backward electron transfer before its dissociation.

Since the geminate radical pair decays via two modes, backward electron transfer (BET) and dissociation to the bulk, the free radical yield (F) in the quenching can be expressed by using the two rate constants of k_b and k_{diff}. The formula is rearranged to another one,

$$F = k_{diff}/(k_{diff} + k_b)$$

in which k_b is expressed in terms of the observable quantity, F. The magnitude of k_{diff} is estimated to be around 10^{10} s^{-1} for a pair of similarly charged radicals by using Eigen's formula (1954), therefore, a variation of the radical yield in the range 5-90 % corresponds to a variation of k_b in the range of 10^9-$10^{11}s^{-1}$.

According to R.A.Marcus, the rate of ET reaction increases with exergonicity involved in the ET reaction in a low exergonic region, stops increasing and then decreases in a high exergonic region. An elaborate work by Scandola et al. (1984) has shown leveling off of the ET rates in a wide exergonic region. However, inspection of BET within a geminate radical pair could manifest a bell-shaped curve of ET rate with respect to ΔG°, because the variation of k_b in the range of 10^9-$10^{11}s^{-1}$ is reflected on the radical yields in the range of 5-90%. The radical yields in 1:1 CH_3CN-H_2O mixed solvent were obtained in the reductive quenching of Ru(4,7-diphenyl-1,10-phenanthroline)$_3^{2+}$ by some aromatic amines. The ratio, k_b/k_{diff}, are calculated from the free radical yields. On plotting log k_b/k_{diff} as a function of ΔG°, a bell-shaped curve was obtained with the maximum at -1.7 eV. A similar trend was obtained for reductive quenching of Ru(bpy)$_3^{2+}$ in the mixed solvent of CH_3CN and H_2O. The top of the bell-shaped curve lies at -1.7 eV again. The phosphorescent state of Cr(dp-phen)$_3^{3+}$ was also quenched by the aromatic amines and methoxybenzenes to produce the cation radical of the donor. A plot of k_b/k_{diff} as a function of G° appears to have a maximum at about

Photochemistry and Photophysics
of Coordination Compounds, Ed. by H. Yersin/A. Vogler

-1.7 eV. In the case of $Rh(dp\text{-}phen)_3^{3+}$, which has the triplet excited state localized in the dp-phen ligand as the lowest excited state, a bell-shaped curve on plotting log k_b/k_{diff} as a function of G° appeares to have the maximum at -1.8 eV.

The variation in the ratio of k_b/k_{diff} can be regarded as the variation in k_b since k_{diff} is approximately constant as long as the same charged reactants are used. This is the case for all the reactions mentioned here. The most important finding is that ΔG°, maximizing the rate k_b, is substantially more negative compared with ΔG° required for the nearly diffusion controlled rate. How can we explain such a large value in the theory of ET reaction.

Let me focus on the rate of ET within the geminate radical pair formed in the triplet quenching. A following equation comes from the golden rule of time-dependent perturbation theory. The integral represents electronic

$$k = 2\pi/\hbar \, \langle {}^1f|\mathcal{H}|{}^3i\rangle \, FC$$

coupling between the initial and the final states. The perturbation must contain spin-orbit coupling, because the ET process is accompanied by a spin-flip. FC is thermally averaged Franck-Condon integral, for which a famous formula has been proposed by R.A.Marcus in a classical way.

$$FC = \exp\left[-\lambda/4(1 + \Delta G^\circ_{if}/\lambda)^2\right]$$

λ and G°_{if} are the rearrangement energy and Gibbs function change involved in the ET, respectively. Following this equation, k_b has the maximum at $G^\circ = -\lambda$.

Since λ of the bimolecular ET is assumed to be the average of rearrangement energies for the self-exchange ET of the two reactants, we can estimate the λ of BET from the λ for the self-exchange ET of the reactants which are available in references. Though the λ for the amines used here are not available except for TMPD, it is most probable that they are smaller than 1 eV. Then it turns out that λ for BET between the reduced metal compound and the cation radical of the amine could be smaller than 1 eV. These small values of λ never fits to the observation.

Since free radical yield substantially are affected by the solvent polarity (not dielectric constant), it will be reasonable to apply the formulas of Kakitani and Mataga (1985), in which ionic species in polar solvent is solvated by solvent molecules in a specific way so that the frequency of solvent mode around the ionic species is much larger than that around the neutral solute molecule. This model causes enormous differences in the solvent mode depending Franck-Condon integral between "charge separation" process and "charge recombination" process: the solvent mode depending Franck-Condon integral remarkably modefies the intramolecular mode depending Franck-Condon integral to

shift the maximum of the rate in more exergonic region in the "charge recombination", while the former gives rise to a small shift of the maximum ΔG° in the "charge separation" process.

We are returning back to my cases of BET within geminate radical pair.

$$^{3}(^{2}RuL_{3}^{+}, {}^{2}TMPD^{+}) \rightarrow RuL_{3}^{2+} + TMPD$$

If you focus on the charge of the metal complex, the process can be regarded as "charge separation". And, if you focus on TMPD, the process can be regarded as "charge recombination". The whole aspect of these BET is interpreted to fall between the two extremes so that the maximum of k_{b} could be observed at a higher exergonicity compared with the prediction on the intramolecular mode depending Franck-Condon integral.

It is a pleasure to acknowledge a number of very illuminating discussion with Prof. N.Mataga of Osaka University and Prof. U.Steiner of Konstanz University. I thank Dr. T.Ulrich of Konstanz University for translating the manuscript.

Eigen M. (1954) Z.phys.Chem. NF 1, 176-200.
Indelli M.T, Ballardini R,Scandola F, (1984) J.Phys.Chem. 88, 2547-51.
Kakitani T, Mataga N, (1985) J.Phys.Chem. 89, 4752-7.
Ohno T, Kato S, Yamada A, Tanno T, (1983) J.Phys.Chem. 87, 775-81.

PHOTOCHEMISTRY OF COPPER COMPLEXES AND ITS CATALYTIC ASPECTS

J.Sýkora

Slovak Technical University, Department of Inorganic Chemistry,
812 37 Bratislava, CSSR

Within the vehement development of photochemistry of coordination compounds and its photocatalytic aspects in the past ten years /Hennig 1985/ a progress was made also in the field of copper photochemistry. The presented contribution summarizes and analyzes the current state in the field of photochemical behaviour of copper complexes mainly from the point of view of catalysis. The hitherto known photochemical reactions of copper coordination compounds are presented within the classification suggested in our laboratory. The state reached in some types of copper photochemical reactions is illustrated by purposefully selected representative examples; mainly results /after 1979/ not included in the latest review article in the field /Ferraudi 1981/ are preferred for discussion in this lecture.

Cu/I/ PHOTOCHEMISTRY

The variety of possibilities of photochemical Cu/I/ complexes behaviour is conditioned by the nature of photochemically active excited state/s/: MLCT, LMCT, CTTS and intraligand excited states, So that a many various redox reactions were observed as a consequence of deactivation of these excited states /e.g. photooxidation of Cu/I/ metal center accompanied by formation of solvated electron followed by H_2 production, photoinduced intramolecular electron transfer etc./. A number of photochemical processes where coordination compounds of Cu/I/ catalyze transformations of the organic substrates was reviewed recently by Salomon /1983/ and Kutal /1985/. According to Kutal's classification of olefin photo-transformations in the presence of Cu/I/ complexes three types of such phototransformation reactions can be distinquished

Type A $\mathrm{Cu/I/} \xrightarrow{h\nu} [\mathrm{Cu/I/}]^* \xrightarrow{+\text{olefin}} [\mathrm{Cu/I/\text{-}olefin}]^* \longrightarrow \mathrm{Cu/I/} + \text{olefin}'$

Type B $\mathrm{Cu/I/} + \text{olefin} \longrightarrow \mathrm{Cu/I/\text{-}olefin} \xrightarrow{h\nu} [\mathrm{Cu/I/\text{-}olefin}]^* \longrightarrow \mathrm{Cu/I/\text{-}olefin}'$

Type C $\text{olefin} \xrightarrow{h\nu} \text{olefin}^* \longrightarrow [\mathrm{Cu/I/\text{-}olefin}^*] \longrightarrow \mathrm{Cu/I/} + \text{olefin}'$

It is of interest to note that in connection with the possible application of photoisomerisation of olefins catalyzed by Cu/I/ complexes

Photochemistry and Photophysics
of Coordination Compounds, Ed. by H. Yersin/A. Vogler

applicable to the solar energy storage problem Sakaki /1984/ elaborated a Cu/I/ photocatalytic system efficiently working under visible-light irradiation.

Cu/II/ PHOTOCHEMISTRY

Photochemically active is usually spin-allowed charge transfer dublet excited state; observed photoredox reaction is often accompanied by rapid internal conversion to the lowest d-d dublet excited state or ground state, respectively. Ligand field excited states are photoinert. When spin-allowed intraligand excited state $Cu[L]^*$ is primarily populated, usually very rapid internal conversion to the photoactive dublet charge transfer excited state take place.
Based on published data on photochemical behaviour the Cu/II/ photochemistry can be classified /Sýkora 1982/ into three classes A, B, C where S=solvent, ligand L≠S, L_{ox}=oxidized ligand or solvent, respectively.

Class A
$$Cu/II/LS \xrightarrow{h\nu} Cu/I/S + L_{ox}$$
$$Cu/II/L_2S \xrightarrow{h\nu} Cu/I/L_2 + S_{ox}$$
$$Cu/II/LL'_2 \xrightarrow{h\nu} Cu/I/LL' + L'_{ox}$$
$$Cu/II/L_2 \xrightarrow{h\nu} Cu/I/L + L_{ox}$$
$$Cu/I/L \longrightarrow Cu^o + L_{ox}$$

Class B
$$Cu/II/L \xrightarrow{h\nu} Cu/III/...L^-$$

Class C
$$Cu/II/L \xrightarrow{h\nu} Cu/I/...L'_{ox}$$
$$Cu/I/...L'_{ox} \rightarrow Cu/II/ + L'$$
$$Cu/II/L_2 + S^* \longrightarrow [Cu/II/L_2..S^*] \longrightarrow Cu/I/L + L_{ox} + S$$
$$2Cu/I/L \longrightarrow Cu/II/L_2 + Cu^o$$
$$Cu/I/L + L_{ox} \rightarrow Cu/II/L_2 .$$
$$Cu/II/L + S^* \rightarrow Cu/I/L + S^+$$

The main attention of our research was concentrated upon the catalytic aspects of Cu/II/ halogenocomplexes photochemistry in order to use the data obtained in the field of phototransformations of organic substrates. The observed photosensitivity of these systems in the region of lowest spin-allowed charge transfer excited state results in the oxidation of Cl^- to $Cl^\cdot$ radical evidenced by pulsed laser flash photolysis as $Cl_2^{\cdot-}$ /Cervone 1979/. Besides a powerful oxidation agent--the radical $Cl^\cdot$ also Cu/I/ is formed, oxidable by dioxygen again to Cu/II/ thus closing the cycle. The presence of O_2 often regarded as a drawback in photochemical studies, is of significance in this case and makes it possible to increase the yields of oxidation products compared with those of systems irradiated under anaerobic conditions.

These results led us to suggest photoassisted catalytic reaction of the Cu/II/-Cu/I/ redox cycle, which would render possible the oxidation of organic substrates; e.g. aliphatic alcohols /Sýkora 1982/, unsubstituted and alkylsubstituted phenols /Engelbrecht 1986, Sýkora 1986/ - Fig. 1 /scheme suggested for photooxidation of phenols/.

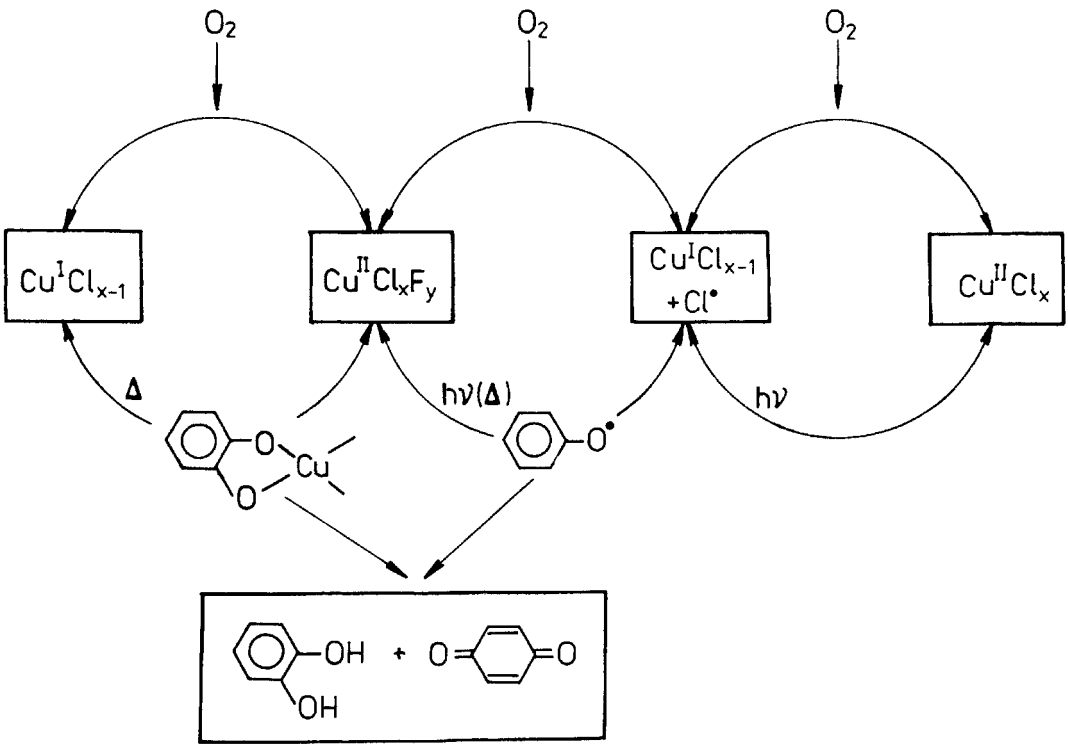

Fig. 1

It was found that selectivity of quinone formation can be regulated by composition of the system /the composition of copper complexes present in solution is of great importance/.
The possibilities of practical use of knowledge on copper coordination compounds photochemistry and photocatalysis in the field of polymer chemistry, photosynthesis of organic and coordination compounds, solar energy storage, photoelectrochemistry and others were reviewed recently /Hennig 1985; Sýkora 1986; Watanabe 1985; McMillin 1985/.

References

Cervone E, Diomedi-Camassei F, Giannini I, Sýkora J /1979/ Photoredox behaviour of chlorocopper/II/ complexes in acetonitrile: mechanism and quantum yields. J Photochem 11: 321-332

Engelbrecht P, Thomas Ph, Hennig H, Sýkora J /1986/ Photooxygenierung von Phenol in Gegenwart von Chlorocupraten. Z Chem 26: 137

Ferraudi G, Muralidharan S /1981/ Photochemical properties of copper complexes. Coord Chem Revs 36: 45-88

Hennig H, Rehorek D, Archer RD /1985/ Photocatalytic systems with light-sensitive coordination compounds and possibilities of their spectral sensibization-an overview. Coord Chem Revs 61: 1-53

Kutal C /1985/ Photochemistry of transition metal-organic systems. Coord Chem Revs 64: 191-206

McMillin DR, Kirchhoff JR, Goodwin KV /1985/ Exciplex quenching of photo-excited copper complexes. Coord Chem Revs 64: 83-92

Sakaki S, Okitaka I, Ohkubo K /1984/ Trans-cis isomerization of stilbene photocatalyzed by copper/I/ complexes. The first example of copper/I/ photocatalysis efficient under visible-light irradiation. Inorg Chem 23: 198-203

Salomon RG /1983/ Homogeneous metal-catalysis in organic photochemistry. Tetrahedron 39: 485-575

Sýkora J /1982/ Photochemical reactions of copper complexes and their catalytic aspects. Chem Listy 76: 1047-1067

Sýkora J, Kureková m, Engelbrecht P, Thomas Ph, Hennig H /1986/ Photooxidations catalyzed by copper complexes-a new route of preparation of mono- and dimethylbenzoquinones. Proc Symp Polygrafia Academica'86 373-375

Sýkora J, Jakubčová M, Cvengrošová Z /1982/ Photooxidation effect of cupric complexes on aliphatic alcohols in nonaqueous solutions. Collect Czech Chem Commun 47: 2061-2068

Sýkora J, Šima J /1986/ Photochemistry of coordination compounds. Veda, Bratislava

Watanabe T, Machida K, Suzuki H, Kobayashi M, Honda K /1985/ Photoelectrochemistry of metallochlorophylls. Coord Chem Revs 64: 207--224

INTRAMOLECULAR EXCITED STATE ELECTRON TRANSFER FROM NAPHTHALENE TO COBALT(III)

A.H.Osman and A.Vogler

Institut für Anorganische Chemie der Universität Regensburg, Universitätsstr. 31, 8400 Regensburg, FRG

Introduction

The majority of intramolecular photoredox processes of metal complexes which have been reported [1,2] takes place upon direct optical charge transfer (CT) excitation. As an alternative intramolecular photoredox processes may occur by an excited state electron transfer. An excited chromophoric group of a complex can undergo an electron transfer to or from another part of the same complex. While in intermolecular photoredox processes the structural arrangement of donor and acceptor in the encounter pair is not known intramolecular electron transfer occurs in a better defined environment. Although these features make it attractive to study intramolecular excited state electron transfer this subject has been largely neglected until a few years ago.

The recent interest in intramolecular excited state electron transfer is associated with attempts to understand the primary events of photosynthesis and to design model systems for the natural and an artificial photosynthesis. In the first step an excited state uphill electron transfer is required in order to convert light into chemical energy. In simple systems this first step is followed by a rapid downhill charge recombination. In the photosynthesis a charge separation is achieved by introducing a barrier for back electron transfer. Recently model compounds have been designed to study the charge separation in detail. A system which found much attention consists of a porphyrin as excited state electron donor which is linked covalently to a quinone as electron acceptor. In addition, a carotene may be attached as a donor to accomplish charge separation over large distances [3].

T. J. Meyer and his research group have investigated the light-induced charge separation in compounds which contain metal complexes as initially excited chromophores [4]. In these cases the charge recombination regenerated the starting com-

Photochemistry and Photophysics
of Coordination Compounds, Ed. by H. Yersin/A. Vogler

pounds. Under suitable conditions another secondary reaction may be rapid enough to compete with the charge recombination. As a result stable photoproducts can be formed.

In 1969 Adamson et al. studied a photoreaction of this type [5]. Upon intraligand (IL) excitation of $[Co^{III}(NH_3)_5TSC]^{2+}$ with TSC^- = trans-4-stilbene carboxylate the excited TSC-ligand transfers an electron to Co(III) [6]. The Co(II) releases its ligands before an efficient charge recombination takes place. A variety of other complexes of the type $[Co^{III}(NH_3)_5OOCR]^{2+}$ with R = aromatic group such as naphthyl shows qualitatively the same behavior as the TSC complex [7,8]. Excited state electron transfer from aromatic molecules to Co(III) ammines takes place also as an intermolecular reaction [8,9]. First observations were explained by the assumption that an energy transfer occurs to reactive CT states of the complex [9]. However, more recent investigations have shown that all results can be explained best by an excited state electron transfer mechanism [6-8].

In the present study the complexes $[2\text{-naphthyl-CONH-}(CH_2)_n\text{-}COOCo^{III}(NH_3)_5]^{2+}$ with n = 1 to 5 were investigated in order to learn more about the structural requirements for excited state electron transfer in this system.

Results and Discussion

Synthesis

The free ligands were synthesized by the reaction of 2-naphthoic acid and the benzyl esters of the amino acids:

$$\begin{aligned} &2\text{-naphthyl-COOH} + NH_2\text{-}(CH_2)_n\text{-}COOCH_2\text{-}C_6H_5 \\ \rightarrow\ &2\text{-naphthyl-CO-NH-}(CH_2)_n\text{-}COO\text{-}CH_2\text{-}C_6H_5 + H_2O \end{aligned}$$

Saponification yielded the protonated ligands which were converted by NaOH to the sodium salts $2\text{-naphthyl-CO-NH-}(CH_2)_n\text{-}COO^-Na^+$. The complexes $[2\text{-naphthyl-CONH-}(CH_2)_n\text{-}COOCo(NH_3)_5]^{2+}$ were obtained as perchlorates by the reaction of $[Co(NH_3)_5H_2O](ClO_4)_3$ and the sodium salts of the ligands. Recrystallization from acetone yielded analytically pure compounds.

Absorption Spectra

The electronic spectra of the sodium salts of the aqueous free ligands 2-naphthyl-CO-NH-$(CH_2)_n$-COO^-Na^+ show two absorption bands at λ_{max} = 310 nm and λ_{max} = 317 nm. Both bands which are of nearly the same intensity ($\epsilon \approx 1200$ L mol^{-1} cm^{-1}) are assigned to $\pi\pi^*$ transitions of the naphthyl group. In the complex cations [2-naphthyl-CO-NH-$(CH_2)_n$-$COOCo(NH_3)_5]^{2+}$ these intraligand (IL) bands appear with almost the same position and intensity. These results show unambiguously that the naphthaline moiety is an isolated chromophoric group of these complexes since coordination does not change the absorption spectrum of the free ligands. This observation is certainly not surprising because the aromatic π-electron system is separated by the saturated methylene groups (n = 1 to 5) from the Co^{3+} ion. In addition to the IL bands the first ligand field band of the complexes appears at λ_{max} = 504 nm (ϵ = 85).

Emission Spectra

Light absorption of the free ligands (λ_{exc} = 310 nm) is accompanied by an intense fluorescence (λ_{max} = 354 nm) which originates from the lowest-energy $\pi\pi^*$ singlet of the naphthyl group. The lifetime was not measured but is known to be approximately 10^{-8} s for related naphthaline derivatives [10]. This emission is largely but not completely quenched in the complexes. The integrated fluorescence intensity was reduced to 2.00 % (n = 1), 1.75 % (n = 2), 1.48 % (n = 3), 1.07 % (n = 4), and 1.62 % (n = 5).

Photochemistry

Upon light absorption by the IL bands (λ_{exc} = 333 nm) the aqueous complexes underwent a photoredox reaction. While Co(III) was reduced to Co^{2+} the oxidation products were not identified. In analogy to related cases [6-8] it is assumed that the naphthalene ligand was oxidized. The quantum yield of Co^{2+} formation was dependent on n: Φ = 0.084 (n = 1), 0.072 (n = 2), 0.034 (n = 3), 0.024 (n = 4), and

0.041 (n = 5). In the concentration range of 10^{-2} to 10^{-3} M complex the quantum yields were constant. It follows that under these conditions the photoredox reaction is certainly an intra- and not an intermolecular process.

Mechanism

Naphthalene is oxidized at $E_{1/2}$ = 1.72 V vs SCE [11]. At an excitation energy of 3.97 eV [12] the $\pi\pi^*$ singlet is now strongly reducing ($E_{1/2}$ = -2.25 V). Although these parameters are certainly somewhat different from those of the ligands 2-naphthyl-CO-NH$(CH_2)_2$-COO^- there is no doubt that for the complexes there is a large driving force for an electron transfer from the excited IL $\pi\pi^*$ singlet to the Co(III) center. Similar Co(III) complexes are reduced at E° = +0.06 V [13]. Fluorescence quenching and formation of Co^{2+} can then be described by the following reaction scheme (Nap = 2-naphthyl group, B = -CO-NH-$(CH_2)_2$-COO- peptide bridge, A = ammonia):

$$[\text{Nap-B-Co}^{III}\text{A}_5]^{2+} \xrightarrow{h\nu} [\text{Nap}^*\text{-B-Co}^{III}\text{A}_5]^{2+}$$

$$[\text{Nap}^*\text{-B-Co}^{III}\text{A}_5]^{2+} \xrightarrow{k_1} [\text{Nap-B-Co}^{III}\text{A}_5]^{2+} + h\nu$$

$$[\text{Nap}^*\text{-B-Co}^{III}\text{A}_5]^{2+} \xrightarrow{k_2} [\text{Nap-B-Co}^{III}\text{A}_5]^{2+} + \text{heat}$$

$$[\text{Nap}^*\text{-B-Co}^{III}\text{A}_5]^{2+} \xrightarrow{k_3} [\text{Nap}^+\text{-B-Co}^{II}\text{A}_5]^{2+}$$

$$[\text{Nap}^+\text{-B-Co}^{II}\text{A}_5]^{2+} \xrightarrow{k_4} [\text{Nap-B-Co}^{III}\text{A}_5]^{2+}$$

$$[\text{Nap}^+\text{-B-Co}^{II}\text{A}_5] \xrightarrow{k_5} Co^{2+} + 5NH_3 + \text{oxidized Nap-B}$$

On the basis of this reaction scheme kinetic equations can be derived:

$$\frac{\Phi^F_o}{\Phi^F_{Co(III)}} = 1 + \frac{k_3}{K_1 + k_2} = 1 + k_3 \cdot \tau_o$$

F_o and $F_{Co(III)}$ are the fluorescence intensities of the free and coordinated ligands. τ_o is the lifetime of the $\pi\pi^*$ singlet of the free ligand which was assumed

to be 10^{-8} s (see above). The efficiency of electron transfer (ET) from the excited IL singlet to Co(III) is then given by:

$$\Phi_{ET} = \frac{k_3}{k_3 + \tau^{-1}}$$

The quantum yield of Co^{2+} formation is not only determined by Φ_{ET} but also by rate constants of back electron transfer (k_4) and of the decay of the Co(II) complex (k_5).

$$\Phi_{Co^{2+}} = \frac{\Phi_{ET}\, k_5}{k_5 + k_4}$$

The rate constant k_5 is not known but is assumed to be larger than 10^6 s^{-1} [14]. It follows that the rate constants k_4 for back electron transfer can also not be obtained. However, relative rates k_4' were calculated assuming k_5 to be constant:

$$k_4' = \frac{k_4}{k_5} = \frac{\Phi_{ET}}{\Phi_{Co^{2+}}} - 1$$

Table 1.

Rate constants k_3 and quantum yields Φ_{ET} of excited state electron transfer, and relative rate constants k_4' of back electron transfer for [2-naphthyl-CO-NH-$(CH_2)_2$-COOCo$(NH_3)_5$]$^{2+}$.

n	$k_3 \times 10^{-9}$ s^{-1}	ET	k_4'
1	4.9	0.980	11
2	5.6	0.982	13
3	6.6	0.985	28
4	9.2	0.989	40
5	6.0	0.983	23

In contrast to the expectation it was found (Table 1) that the rate constant and efficiency of excited state electron transfer as well as the rate of back electron transfer drops from n = 1 to 4. This observation suggests that the actual distance between the naphthyl group and Co(III) decreases with increasing chain length of the peptide from n = 1 to 4. It is assumed that donor and acceptor come to a closer approach by an appropriate bending of the flexible peptide linkage. This back bonding may be favored by hydrogen bonding between coordinated ammonia and the carbonyl

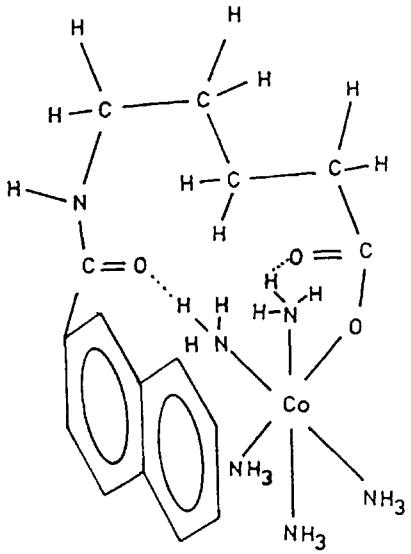

groups of the peptide. At n = 5 electron transfer becomes less efficient (Table 1). The donor-acceptor distance may now increase be an extension of the peptide.

References

1) Adamson, A. W.; Fleischauer, P. D. (Eds.) Concepts of Inorganic Photochemistry, Wiley, New York, 1975.
2) Balzani, V.; Carassiti, V. Photochemistry of Coordination Compounds, Academic Press, New York, 1970.
3) Gust, D.; Moore, T. A.; Liddell, P. A.; Nemeth, G. A.; Making, L. R.; Moore, A. L.; Barrett, D.; Pessiki, P. J.; Bensasson, R. V.; Rougée, M.; Chachaty, C.; De Schryver, F. D.; Van der Auweraer, M.; Holzwarth, A. R.; Conolly, J. S. J. Am. Chem. Soc. 1987, 109, 846 and ref. cited therein.
4) Chen, P.; Westmoreland, T. D.; Danielson, E.; Schanze, K. S.; Anthon, D.; Neveux, P. E.; Meyer, T. J. Inorg. Chem. 1987, 26, 1116 and ref. cited therein.
5) Adamson, A. W.; Vogler, A.; Lantzke, I. J. Phys. Chem. 1969, 73, 4183.
6) Vogler, A.; Kern, A. Z. Naturforsch. 1979, 34b, 271.
7) Kern A. Dissertation, Universität Regensburg, 1978.
8) Schäffl, S. Diplomarbeit, Universität Regensburg, 1984.
9) Scandola, M. A.; Scandola, F.; Carassiti, V. Mol. Photochem. 1969, 1, 403.

10) Berlman, I. B. Fluorescence Spectra of Aromatic Molecules, Academic Press, New York, 1971.
11) Eberson, L.; Nyberg, K. J. Am. Chem. Soc. 1966, 88, 1686.
12) Birks, J. B. Photophysics of Aromatic Molecules, Wiley, London, 1970.
13) Milazzo, G.; Caroli, S. Tables of Standard Electrode Potentials, Wiley, New York, 1978.
14) Simic, M.; Lilie, J. J. Am. Chem. Soc. 1974, 96, 291.

PHOTOCHEMISTRY OF COORDINATION COMPOUNDS OF MAIN GROUP METALS. REDUCTIVE ELIMINATION OF THALLIUM(III) COMPLEXES

A.Paukner, H.Kunkely, and A.Vogler

Institut für Anorganische Chemie der Universität Regensburg, Universitätsstr. 31, 8400 Regensburg, FRG

Introduction

The photochemistry of coordination compounds of the main group metals is a rather interesting but largely neglected part of inorganic photochemistry. Within a general approach to this subject we studied recently photoredox reactions of $[Sn(N_3)_6]^{2-}$ and $[Pb(N_3)_6]^{2-}$ [1]. These ions are examples of complexes containing a metal with an empty valence shell (s° electron configuration). Such compounds are characterized by low-energy ligand to metal charge transfer (LMCT) bands in their absorption spectra. Reductive elimination initiated by LMCT excitation seems to be the typical photoreaction of s° complexes. We extended now these investigations to Tl(III) complexes in order to test the general validity of this assumption.

There is not much known about the photochemistry of Tl(III) complexes [2,3]. Spectral assignments of electronic absorption bands were reported for a few tetrahalogeno complexes of Tl(III) [4,5]. In the present work we studied the photochemistry of $[Tl(N_3)_2Br_2]^-$, $[Tl(bipy)_2I_2]^+$ (bipy = 2,2'-bipyridyl), and $[Tl(acetate)_3]$ in some detail. Spectral assignments of absorption bands were supported by the photochemical behavior of these complexes.

Results and Discussion

The compounds $[As(C_6H_5)_4][Tl(N_3)_2Br_2]$ [6] and $[Tl(bipy)_2I_2]I$ [7], were prepared by literature procedures. $Tl(CH_3CO_2)_3 \times 1.5\ H_2O$ was purchased from Aldrich.

The absorption spectrum of $[Tl(N_3)_2Br_2]^-$ in acetonitrile displays a long-wavelength band at λ_{max} = 293 nm (ϵ = 10200 L mol^{-1} cm^{-1}). This band is assigned to a LMCT transition. Since azide and bromide have comparable optical electronegativities

Photochemistry and Photophysics
of Coordination Compounds, Ed. by H. Yersin/A. Vogler

it is difficult to distinguish between N_3^- → Tl(III) and Br^- → Tl(III) CT transitions. However, the photoreaction supports the former assignment. At shorter wavelength the typical absorption features of the counterion $[As(C_6H_5)_4]^+$ appear in the spectrum (λ_{max} = 271, 265, 259 nm) [6].

Upon irradiation of the LMCT band (λ_{irr} = 313 nm) of $[Tl(N_3)_2Br_2]^-$ in CH_3CN the evolution of nitrogen was observed. Simultaneously, the intensity of the LMCT band decreased. Finally, this absorption disappeared when the photolysis went to completion. In the later stages of the photolysis the solution became cloudy due to the formation of insoluble TlBr. These observations are consistent with a reductive elimination:

$$[Tl^{III}(N_3)_2Br_2]^- \xrightarrow{h\nu} Tl^{I}Br + Br^- + 3\ N_2$$

The disappearance of $[Tl(N_3)_2Br_2]^-$ was determined by the decrease of the extinction at λ_{max} = 293 nm. Upon irradiation at 313 nm the reductive elimination occured with a quantum yield of Φ = 0.3.

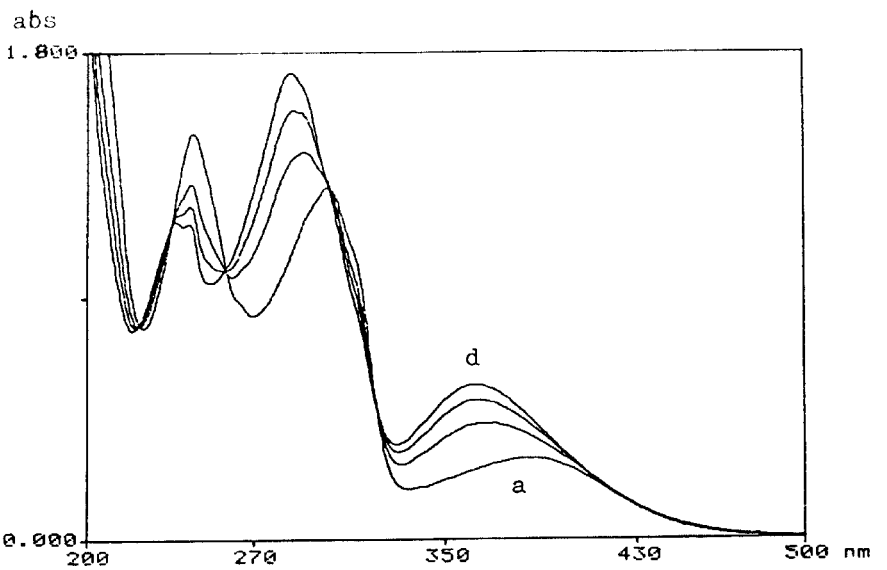

Fig. 1.

Spectral changes during the photolysis of $5.33 \cdot 10^{-5}$ M $[Tl(bipy)_2I_2]^+$ in CH_3CN at (a) 0 and (d) 200 s irradiation time, with λ_{irr} > 200 nm and a 1-cm cell.

The absorption spectrum of $[Tl(bipy)_2I_2]^+$ in CH_3CN (Fig. 1) consists of 3 bands at λ_{max} = 374 nm (ε = 4700), 302 nm (23210), and 244 nm (28200). The longest wavelength band at 374 nm may be due to a $J^- \rightarrow Tl(III)$ LMCT transition since $[TlI_4]^-$ shows such an absorption at λ_{max} = 397 nm [4,5]. However, the photochemical behavior of $[Tl(bipy)_2I_2]^+$ (see below) is not consistent with this assignment. As a reasonable alternative the band at 374 nm may be assigned to a $J^- \rightarrow$ bipy ligand to ligand (LL) CT transition. The complex $[Be(bipy)I_2]$ shows such a LLCT band at 368 nm (ε = 7000) [8]. The second band of $[Tl(bipy)_2I_2]^+$ at 302 nm should be assigned to the $\pi\pi^*$ intraligand (IL) transition of the bipy ligand which absorbs in this region. An $I^- \rightarrow Tl(III)$ LMCT transition could also contribute to this band since low-energy absorptions of this type are expected to appear near this wavelength [4,5]. The third absorption at 244 nm is certainly a $I^- \rightarrow Tl(III)$ LMCT band in agreement with the photochemical behavior of $[Tl(bipy)_2I_2]^+$.

Irradiation (λ_{max} > 200 nm) of $[Tl(bipy)_2I_2]^+$ in CH_3CN was accompanied by spectral changes (Fig. 1) which are consistent with a reductive elimination according to:

$$[Tl^{III}(bipy)_2I_2]^+ \rightarrow Tl^+ + 2\ bipy + I_2$$

In the photolyzed solution the absorption maximum at 360 nm is caused by I_2. The new band at 286 nm is apparently a superimposition of absorption maxima of I_2 (λ_{max} = 289 nm) and free bipy (λ_{max} = 280 nm). The presence of released bipy is also indicated by bands at λ_{max} = 235 and 243 nm.

In accordance with the assignments of the absorption bands of $[Tl(bipy)_2I_2]^+$ the quantum yields of the reductive elimination (Φ = 0.54 at λ_{irr} = 254 nm, 0.03 at 302 nm, and 2.9×10^{-3} at 366 nm) decreased with increasing wavelength of irradiation.

The photochemistry of some thallium(III) carboxylates of the type $Tl(RCOO)_3$ where R is a larger aliphatic group was studied by Kochi and Bethea [2]. The photolysis of these compounds in benzene solution led to the formation of Tl(I) and oxidation of carboxylate ($RCOO^- - e^- \rightarrow R\bullet + CO_2$).

In the present work we investigated the photolysis of $Tl(CH_3COO)_3$ which does not dissolve in benzene. In the solid state Tl(III) is essentially hexacoordinated by three chelating acetate ligands [9]. In aqueous solution the acetate ligands are partially substituted [10]. Since in acetonitrile such ligand substitutions are generally less efficient it is assumed that $Tl(CH_3COO)_3$ dissolves in CH_3CN without dissociation. The absorption spectrum of $Tl(CH_3COO)_3$ in acetonitrile (Fig. 2)

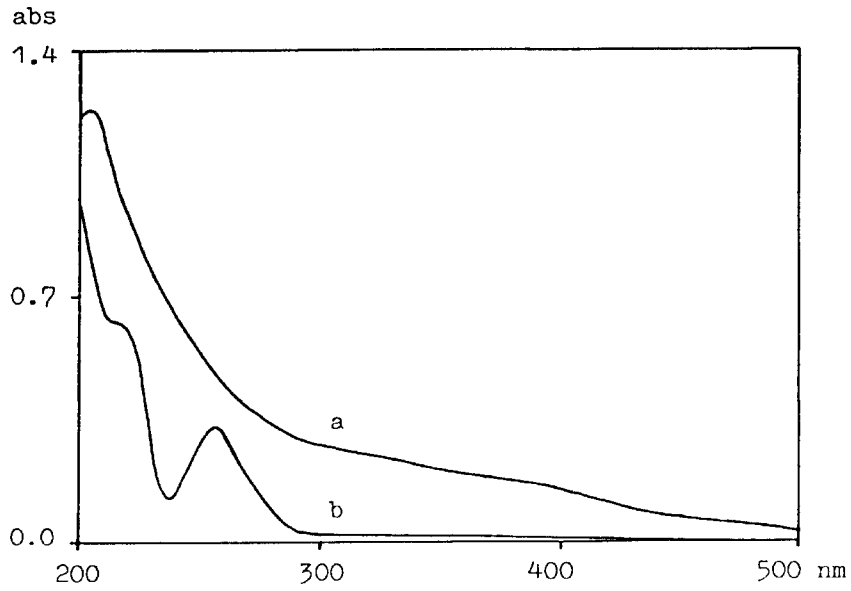

Fig. 2

Absorption spectra of 9.9×10^{-5} M $[Tl(CH_3COO)_3]$ (a) and its photolysis product (b) in CH_3CN, $\lambda_{irr} > 200$ nm, 1-cm cell

is rather featureless. The complex starts to absorb in the visible region. The absorption increases towards shorter wavelength. A maximum appears at 203 nm ($\varepsilon = 12430$) while shoulders occur at 240 nm ($\varepsilon = 6440$) and 395 nm ($\varepsilon = 1660$). These absorptions can certainly be assigned to acetate → Tl(III) LMCT transitions.

The spectral changes which accompanied the irradiation (white light from a high-pressure mercury arc) of $Tl(CH_3COO)_3$ in CH_3CN indicated the formation of Tl(I) acetate (Fig. 2) which shows absorption bands at $\lambda_{max} = 256$ nm and 214 nm. Although the oxidation products were not identified it is assumed that the reductive elimination takes place according to the equation:

$$Tl^{III}(CH_3COO)_3 \xrightarrow{h\nu} Tl^{I}(CH_3COO) + 2\ CO_2 + 2\ CH_3\cdot$$

The methyl radicals may undergo dimerization or other secondary reactions. At λ_{irr} = 254 nm the quantum yield for the disappearance of $Tl(CH_3COO)_3$ was Φ = 0.14. It dropped to Φ = 0.01 at λ_{irr} = 395 nm.

References

1) Vogler, A.; Quett, C.; Paukner, A.; Kunkely, H. J. Am. Chem. Soc. 1986, 108, 8263.
2) Kochi, J. K.; Bethea, T. W. J. Org. Chem. 1968, 33, 75.
3) Sagi, S. R.; Prakasa Raju, G. S.; Appa Rao, K.; Prasada Rao, M. S. Talanta 1982, 29, 413 and references cited therein.
4) Matthews, R. W.; Walton, R. A. J. Chem. Soc. A 1968, 1639.
5) Day. P.; Seal, R. H. J. Chem. Soc. Dalton 1972, 2054.
6) Beck, W.; Fehlhammer, W. P.; Pöllmann, P.; Schuierer, E.; Feldl, K. Chem. Ber. 1967, 100, 2335.
7) Sutton, G. J. Austr. J. Sci. Res., A 1951, 4, 654.
8) Coates, G. E.; Green, S. I. E. J. Chem. Soc. 1962, 3340.
9) Faggiani, R.; Brown, I. D. Acta Cryst. B 1978, 34, 2845.
10) Lee, A. G. The Chemistry of Thallium, Elsevier, Amsterdam 1971.

TOPIC 5

Organometallic Photochemistry

PHOTOPHYSICS AND PHOTOCHEMISTRY OF TUNGSTEN CARBYNE COMPLEXES

A.B.Bocarsly*, R.E.Cameron, A.Mayr*, and G.A.McDermott

Department of Chemistry, Princeton University, Princeton, NJ 08544, USA

Transition metal complexes that luminesce at room temperature in fluid solution upon excitation with visible light have attracted much attention since such species have low-lying excited states which may allow the utilization of optical energy in the preparation of useful chemical products. Despite this interest only few such species have been discovered. In most cases luminescence is associated with a charge transfer transition involving metal $d\pi$ electrons and the π^* orbital of ligated aromatic diimines. Here we describe some of the photophysical and photochemical properties of bis-donor ligand-substituted tungsten arylcarbyne complexes $[(W{\equiv}CAryl)X(CO)_2L_2]$ (X=halide, L=donor ligand) (Fischer 1977), a new class of luminescent organometallic species (Bocarsly 1985). The emissive excited state is associated with the lowest energy absorption band, which is assigned to a d-metal to $\pi^*(M{\equiv}CAryl)$ transition. Quenching experiments indicate that a significant amount of triplet character is associated with the emissive excited state. Bimolecular oxidative and reductive charge transfer quenching is also observed, demonstrating the excited state to be strongly reducing and oxidizing. Photoinduced associative ligand substitutions occur in these molecules (Cameron 1986).

ELECTRONIC ABSORPTION SPECTRA

The spectroscopic properties of tungsten carbyne complexes of the type $[(W{\equiv}CR)X(CO)_2L_2]$ are listed in Table 1. As a characteristic example the spectrum of $[(W{\equiv}CPh)Br(CO)_2(tmeda)]$ is shown in Fig. 1. The electronic absorption spectra for tungsten phenylcarbyne complexes of the type $[(W{\equiv}CPh)X(CO)_2L_2]$, where X = Cl, Br, I and L_2 = 2 pyridine (py), tetramethylethylene diamine (tmeda), and bisdiphenyl phosphinoethane (dppe), exhibit a fairly weak absorption at about 450 nm and a more intense absorption at about 350 nm. The lowest energy absorptions are assigned to $d_{xy} \rightarrow \pi(M{\equiv}C)^*$ transitions (z-axis coinciding with M≡C bond axis). For phenylcarbyne tungsten complexes the $\pi(M{\equiv}C)^*$ orbital is conjugated with the

Table 1. Electronic Absorption and Emission Data.

$[(W{\equiv}CR)X(CO)_2L_2]$ R	X	L_2	$d_{xy} \rightarrow \pi(M{\equiv}C)^*$ λ_{max} [nm], (ϵ [$M^{-1}cm^{-1}$])	$\pi(M{\equiv}C) \rightarrow \pi(M{\equiv}C)^*$ λ_{max} [nm], (ϵ [$M^{-1}cm^{-1}$])	Emission λ_{max} [nm]
Ph	Cl	tmeda	448 (393)	330 (5500)	640
Ph	Br	tmeda	450 (400)	327 (13000)	630
Ph	I	tmeda	454 (560)	—	630
Ph	Cl	2py	460 (1064)*	340 (17000)$^+$	625
Ph	Br	2py	460 (1086)*	350*$^+$	630
Ph	Cl	dppe	435 (368)	360 (10000	660
CMe_3	Cl	tmeda	364 (617)	270 (8000)	—
2-$C_{10}H_7$	Cl	2py	475	354$^+$	660

*shoulder

$^+$solvent dependent, values indicated are in nonpolar solvents.

Photochemistry and Photophysics
of Coordination Compounds, Ed. by H. Yersin/A. Vogler

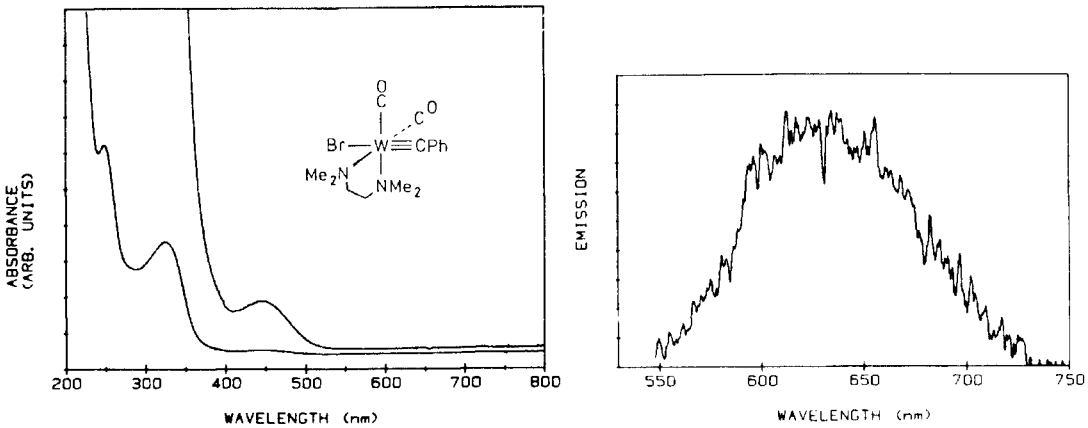

Figure 1. Electronic Absorption Spectrum and Emission Spectrum of $[(WCPh)Br(CO)_2(tmeda)]$.

π-system of the phenyl group. Molecular orbital calculations by Kostić and Fenske (1982) on the related compound $[(Cr{\equiv}CPh)Cl(CO)_4]$ indicate that this conjugation is significant. A similar assignment has been suggested by Vogler (1983) for $[(Os{\equiv}CPh)Cl(CO)(PPh_3)_2]$; although this complex has a different geometry from the tungsten systems, the lowest lying excited state seems to be similar in nature. Replacement of the phenyl group by a tert-butyl group results in a shift of the low energy absorption band toward the blue by about 85 nm. This is consistent with removal of the conjugation from the LUMO orbital, $\pi(M{\equiv}C)^*$. On the other hand, replacement of the phenyl group with a 2-naphthyl group leads to a red shift by about 15 nm, indicating an extension of the conjugated system. The nature of the donor ligands also significantly influences the low energy absorption. Replacing tmeda by two monodentate pyridine ligands causes a shift toward the red by about 10 nm, replacing tmeda by the phosphorous-based dppe ligand causes a blue shift by about 15 nm. Assuming that the energy of $\pi(M{\equiv}C)^*$ remains more or less unaffected by these ligand substitutions, the observed changes in absorption energies may be explained by a weak π-donor ability of the pyridine and a weak π-acceptor ability of dppe ligands, respectively. Replacing tmeda by 2,2´-bipyridine or by phenanthroline causes a significant red shift (38 nm) in the lowest absorption band of the tungsten carbyne system. However, by comparison with the absorption spectrum of $[W(CO)_4(bpy)]$ this electronic transition is believed to contain a large component of metal d $\rightarrow$ bpy π^* charge-transfer character. Variation of the halide ligand trans to the carbyne has only a minor effect on the position of the low energy absorption, ruling out these orbitals as the HOMO and further suggesting that the halide p-orbitals (lone pairs) are not significantly interacting with the metal center in these tungsten carbyne complexes.

The more intense absorption at about 350 nm for $[(W{\equiv}CPh)X(CO)_2L_2]$ is assigned to $\pi{\rightarrow}\pi^*$ transitions in the conjugated M≡CPh systems in analogy to the $\pi{\rightarrow}\pi^*$ absorption in diphenylacetylene (295 nm, 29000 cm^{-1} M^{-1}). In cases where the ligands L contain a π^* system, for example L=pyridine, there is also a component of the absorptivity in this region associated with an MLCT transition.

LUMINESCENCE IN ROOM TEMPERATURE FLUID SOLUTION

Several tungsten phenylcarbyne complexes of the type $[(W{\equiv}CPh)X(CO)_2L_2]$ have been found to luminesce at room temperature in fluid solution upon excitation with visible light. The emission spectrum of $[(W{\equiv}CPh)Br(CO)_2(tmeda)$ is shown in Fig. 1. It is typical for this class of compound, being structureless both at room temperature and at 77K in a frozen glass. This is indicative of a large degree of vibrational coupling similar to that observed for the solution emission of $[Ru(bpy)_3]^{2+}$

We associate the luminescence with the lowest energy absorption band at 450 nm based on the observed overlap of the emission onset with the low energy tail of the 450 nm absorption band. A large Stokes shift on the order of 180 nm is seen by all these emissive complexes. This may be due to significant stretching of the metal-carbon triple bond and/or bending of the carbyne ligand in the excited state. The quantum yield of emission (Φ_E)for the tungsten phenylcarbyne complexes is in the range of 10^{-3} in room temperature fluid solution, Table 1. Irradiation into the higher energy absorption peaks also leads to emission from the $\pi(M{\equiv}C)^*$ orbital of these complexes. Apparently, efficient nonradiative coupling between these higher energy states and the LUMO orbital exists. Consistent with this result is the finding that the radiative quantum yield for this system is wavelength-independent for all wavelengths tested.

Variation of the carbyne substituent R has a strong influence on the emission. If the phenyl group is replaced by a tert-butyl group, the complex is found not to emit in fluid solution. Absence of fluid solution emission under these conditions further suggests that conjugation of the metal-carbon triple bond and the phenyl π^* system is essential to obtain appreciable rate constants for radiative decay. Replacement of the phenyl group with a 2-naphthyl group leads to an extended metal-carbyne π^* system and correspondingly to a red shift in the emission band. The nature of the donor ligands L has only a small influence on the observed luminescence properties, provided the ligands do not contain low lying π^* orbitals themselves. As with the absorption spectra, varying the halide ligand trans to the carbyne has only a minor effect on the emission band. Donor ligands with low lying π^* orbitals strongly affect the emission. Introduction of 2,2´-bipyridine leads to total quenching of the fluid solution emission. With 1,10-phenanthroline an emissive complex is obtained, however, the luminescence is significantly red-shifted. For these complexes, the lowest energy excitation appears to be the $d_{xy} \rightarrow \pi^*(L_2)$ charge-transfer transition. Consistent with this assignment is the observation that the emission of the phenanthroline complex is blue shifted in more polar solvents, unlike the other tungsten phenylcarbyne emissions which show no solvent dependence.

The excited state lifetimes of all luminescent tungsten carbyne complexes were analyzed and are listed in Table 2. The relatively long lifetimes found for the emissive excited state suggest the transition to the ground state is forbidden.

Table 2. Emission Quantum Yields, Emission Lifetimes, and Radiative Rate Constants in Toluene at 298K.

$[(W{\equiv}CR)X(CO)_2L_2]$ R	X	L_2	$\Phi_E x10^4$	Lifetime[μsec]	Radiative Rate Constant $k_r = \Phi_E/\tau$[sec^{-1}]
Ph	Cl	tmeda	6.3	0.285	$2.3x10^3$
Ph	Br	tmeda	5.3	0.180	$2.96x10^3$
Ph	I	tmeda	1.5	0.220	$0.70x10^3$
Ph	Cl	2py	7.8	0.440	$1.8x10^3$
Ph	Cl	dppe	2.2	0.232	$0.93x10^3$
CMe_3	Cl	tmeda			

PHOTOREACTIVITY

Energy Transfer Quenching

The luminescence of the tungsten carbyne complexes in fluid solution is found to be easily quenched by a variety of organic triplet quenchers. As demonstrated in Table 3 the rate constants for quenching of the excited state of $[(W{\equiv}CPh)Br(CO)_2(py)_2]$ are dependent on the triplet energy of the organic molecule. The rate constants are close to diffusion limited until the triplet energy of the quencher rises above about 210 kJ/mol (572nm). Above 210 kJ/mol the rate constant drops off quickly. This suggests that the energy of the quenchable state is about 210

Table 3. Quenching of Emission in Toluene at 298K.

Quencher	Triplet Energy of Quencher [kJmole^{-1}]	Quenching Rate Constant k_q[M^{-1}sec^{-1}]x10^8
Anthracene	175.7	15.8
Pyrene	201.7	15.1
Benzil	223.8	13.8
2-Bromonaphthalene	252.3	3.9
Phenanthrene	259.0	4.0
Diphenylacetylene	261.5	2.5
Diphenyl	274.9	0.3
Fluroene	284.5	0.1

kJ/mol. This corresponds to the overlap region of the absorption and emission spectra suggesting the quenchable and emissive excited states are the same and further confirming π(M≡C)* as the emissive state.

Electron Transfer Quenching

Irradiation of [(W≡CPh)Cl(CO)$_2$(tmeda)] by 488 nm light in the presence of methylviologen dichloride (MV^{2+}) in oxygen-free acetonitrite solution leads to a change of color from yellow to blue. Changes in the visible absorption spectrum show that MV^+ has formed and the neutral carbyne complex has decreased in concentration. The excited tungsten phenylcarbyne complex is postulated to transfer one electron to MV^{2+}, generating MV^+ and $[(W{\equiv}CPh)Cl(CO)(tmeda)]^+$. The tungsten carbyne complex is not fully regenerated in the slow dark back-reaction. Since population of the lowest energy absorption band using 488 nm light induces the charge-transfer quenching, electron transfer is proposed to be occurring from the emitting excited state. The quantum yield for MV^+ production is found to be 0.032.

The complex [(W≡CPh)Cl(CO)$_2$(tmeda)] also undergoes reductive quenching with N,N,N´,N´-tetramethyl-p-phenylenediamine (tmpd). Irradiation of the carbyne complex with 488 nm light in the presence of tmpd in acetonitrile solution generates new absorptions at 612 and 564 nm corresponding to $[tmpd]^{\cdot +}$.

Photosubstitution

Irradiation of [(W≡CPh)Cl(CO)$_2$(dppe)] by 488 nm light in the presence of excess dppe in THF solution under N_2 leads to formation of a new product which was identified as [(W≡CPh)Cl(dppe)$_2$].

$$[(W{\equiv}CPh)Cl(CO)_2(dppe)] + dppe \xrightarrow{h\nu} [(W{\equiv}CPh)Cl(dppe)_2] + 2CO$$

The quantum yields for this reaction were shown to exhibit first order dependence on the concentration of the dppe ligand indicating an associative mechanism of lignd substitution. Ligand association may be facilitated in the excited state since transfer of an electron from the tungsten d_{xy} orbital to the π(M≡C)* orbital would make the tungsten center more electrophilic.

REFERENCES

Bocarsly AB, Cameron RE, Rubin H-D, McDermott GA, Wolff CR, Mayr A (1985) Inorg Chem 24: 3976-3978.

Cameron RE (1986) Ph.D. Thesis, Princeton University.

Fischer EO, Ruhs A, Kreissl FR (1977) Chem. Ber. 110: 805-815.

Kostić NM, Fenske RF (1982) Organometallics 1: 409-496.

Vogler A, Kisslinger J, Roper WR (1983) Z. Naturforsch. 386: 1506-1509.

THE PHOTOISOMERIZATION AND PHOTOSUBSTITUTION REACTIONS OF THE RUTHENIUM CLUSTER $HRu_3(CO)_{10}(\mu\text{-}COCH_3)$

A.E.Friedman and P.C.Ford*

Department of Chemistry, University of California, Santa Barbara, CA 93106, USA

Our recent research has been concerned with using photochemical techniques to prepare and study reactive organometallic intermediates of the type formed in active catalytic systems. Described here are the photoreactions of $HRu_3(CO)_{10}(\mu\text{-}COCH_3)$, its photoisomerization to form a new carbon-carbon bond from C_1 precursors, and its photosubstitution reactivity. This isomerization represents an unprecedented oxygen to carbon migration of a methyl group on the triruthenium cluster, a reaction of the type which finds some analogy in the catalytic isomerization of methyl formate to acetic acid (Pruett, 1982):

PHOTOISOMERIZATION OF $HRu_3(CO)_{10}(\mu\text{-}COCH_3)$

Photolysis (λ_{irr} = 313 nm) of a 10^{-4} M solution of $HRu_3(CO)_{10}(\mu\text{-}COCH_3)$ (I) in CO-saturated cyclohexane led to the electronic spectral changes shown in Fig. 1. The absorption peak (384 nm ϵ = 6900 M^{-1} cm^{-1}) characteristic of the starting cluster, diminished in intensity, accompanied by rising absorbance at longer wavelength. Isosbestic points were observed at 358 nm and 436 nm for > 40% reaction. Although the product infrared spectrum proved virtually identical with that of I, significant changes in the ^1H NMR (300 MHz) spectrum were evident. All three spectral properties (electronic, IR, NMR) are fully consistent with identification of the product as the $\mu\text{-}\eta^2$ acyl cluster $HRu_3(CO)_{10}(\mu\text{-}\eta^2\text{-}C(O)CH_3)$ (II). The result is an overall oxygen-to-carbon migration of the methyl group. (eq 1)

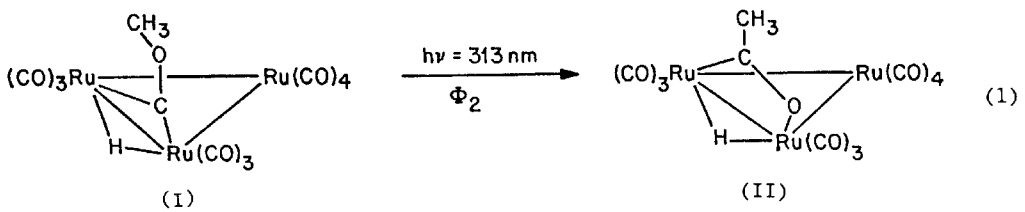

(I) (II) (1)

The quantum yield for this isomerization was found to be notably dependent both on the concentration of CO and on the wavelength of excitation. Although the resulting optical changes were the same for different λ_{irr}, the quantum yields in CO saturated cyclohexane ranged from < 10^{-5} at 405 nm to 4.9 x 10^{-2} at 313 nm (Fig. 2). Furthermore, the quantum yield varied linearly from 1.2 x 10^{-4} at P_{CO} = 0.0 to 4.9 x 10^{-2} at P_{CO} = 1.0 atm for 313 nm photolysis in cyclohexane. Prolonged photolysis produces cluster fragmentation in CO-saturated cyclohexane. The photolysis eventually gives $Ru(CO)_5$ plus the acetaldehyde. With authentic samples of $HRu_3(CO)_{10}(\mu\text{-}\eta^2\text{-}C(O)CH_3)$ the latter photoreaction was studied quantitativly and a wavelength independent quantum yield of 1.1 x 10^{-3} moles/ einstein was determined (313 nm irradiation, P_{co} = 1.0 atm, cyclohexane)

Photochemistry and Photophysics
of Coordination Compounds, Ed. by H. Yersin/A. Vogler

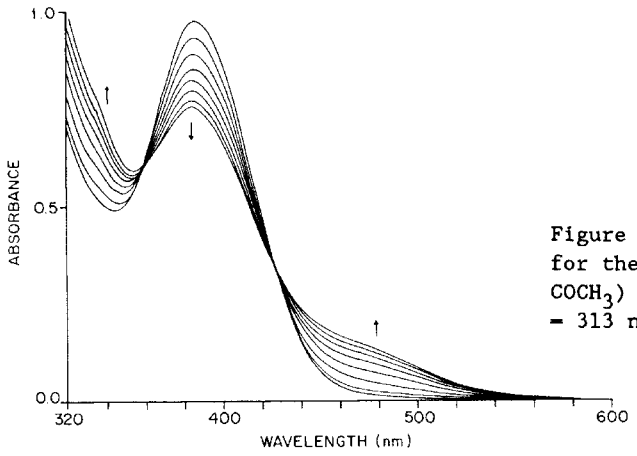

Figure 1. Electronic spectrial changes for the photolysis of $HRu_3(CO)_{10}(\mu\text{-}COCH_3)$ in cyclohexane P_{co} = 1 atm, λ_{irr} = 313 nm

Although additional carbon monoxide is not required by the stoichiometry of Eq. 2 this unusual reaction is promoted by the presence of CO. In earlier studies of the photolytic fragmentation of the triangular cluster $Ru_3(CO)_{12}$ (Desrosiers, 1986), a key step in the proposed mechanism was isomerization leading to heterolytic cleavage of a metal-metal bond with concomitant migration of a terminal CO to a bridging site. Such a transformation would open up a coordination site for a two electron donor such as carbon monoxide. In order to test this hypothesis, I was irradiated at 313 nm in neet THF under a blanket of N_2; the quantum yield for photoisomerization was enhanced by over an order of magnitude compared to the cyclohexane quantum yield under the same conditions, suggesting that THF as a donor could also promote this reaction.

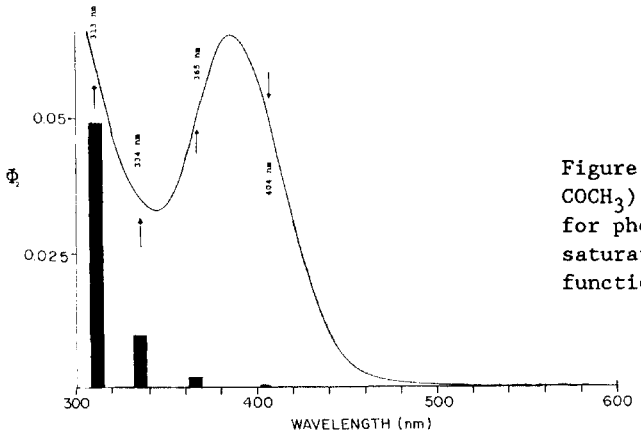

Figure 2. Spectrum of $HRu_3(CO)_{10}(\mu\text{-}COCH_3)$ in cyclohexane. Quantum yields for photoisomerization at 25°C CO-saturated cyclohexane represented as a function of irradiation wavelength

PHOTSUBSTITUTION OF $HRu_3(CO)_{10}(\mu\text{-}COCH_3)$

The photochemistry of $HRu_3(CO)_{10}(\mu\text{-}COCH_3)$ in the presence of $P(OCH_3)_3$ was investigated to examine, if possible, the photoisomerization with other two

electron donors. Photolysis (λ_{irr} = 313 nm) of $HRu_3(CO)_{10}(\mu\text{-}COCH_3)$ (10^{-4} M) with $P(OCH_3)_3$ (0.012 M) in N_2-saturated cyclohexane led to the electronic spectral changes shown in Fig. 3. The absorption band shifts to longer wavelength characteristic to phosphite substitution of the cluster. No isosbestic points were observed, an indication either of secondary photolysis or of nonconsistent stoichiometry. The analogous thermal reaction was studied by Dalton et al. (1985) and a pseudo-first order rate constant of 10^{-5} sec^{-1} was measured. The products of the photolysis were isolated and characterized to be the mono- and bis- phosphite substituted alkylidyne clusters, $HRu_3(CO)_9(\mu\text{-}COCH_3)P(OCH_3)_3$ and $HRu_3(CO)_8(\mu\text{-}COCH_3)(P(OCH_3)_3)_2$ with no evidence for alkyl migration. The quantum yield for the first 10% reaction was determined to be 0.22 moles/einstein. Notably the wavelength dependence observed for this photolysis was similar to that of the alkyl-migration; a value of 0.22 was measured at λ_{irr} = 313 and decreased to < 10^{-4} at λ_{irr} = 405 nm. In order to demonstrate that the bis-substituted cluster $HRu_3(CO)_8(\mu\text{-}COCH_3)(P(OCH_3)_3)_2$ is formed from secondary photolysis, an authentic sample of $HRu_3(CO)_9(\mu\text{-}COCH_3)P(OCH_3)_3$ was irradiated at 313 nm in the presence of $P(OCH_3)_3$ (0.012 M). The only product formed from this photolysis was the bis-substituted cluster with a quantum efficiency of 0.1 moles/einstein in N_2-saturated cyclohexane.

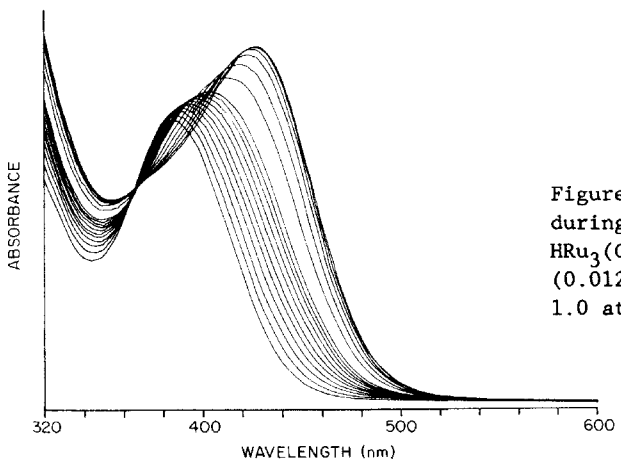

Figure 3. Sequential spectra recorded during the 313 nm photolysis of $HRu_3(CO)_{10}(\mu\text{-}COCH_3)$ plus $P(OCH_3)_3$ (0.012 M) in cyclohexane solution P_{co} = 1.0 atm

Photolysis of $HRu_3(CO)_{10}(\mu\text{-}COCH_3)$ (10^{-4} M) with $P(OCH_3)_3$ (0.012 M) in CO-saturated cyclohexane also yielded only substituted alkylidyne clusters with a quantum yield of 0.17 moles/einstein. No photoisomerization was noted in the presence of $P(OCH_3)_3$, in spite of the fact the reactivity involves the same excitation. One explanation is that upon photolysis an excited complex is formed that reacts by two pathways, one that leads to alkyl-migration while another, more dominant, pathway is responsible for substitution. A reaction commonly proposed in the photochemistry of transition metal carbonyls is labilization of carbon monoxide followed by trapping of the unsaturated intermediate by L. A similar scheme is proposed here. (Scheme 1)

Scheme 1

$$HRu_3(CO)_{10}(\mu\text{-}COCH_3) \xrightarrow{h\nu,\ \Phi_{II}} HRu_3(CO)_9(\mu\text{-}COCH_3) + CO$$

$$HRu_3(CO)_9(\mu\text{-}COCH_3) + S \rightleftharpoons HRu_3(CO)_9(\mu\text{-}COCH_3)S$$

$$HRu_3(CO)_9(\mu\text{-}COCH_3) + CO \xrightarrow{k_{co}} HRu_3(CO)_{10}(\mu\text{-}COCH_3)$$

$$HRu_3(CO)_9(\mu\text{-}COCH_3) + L \xrightarrow{k_L} HRu_3(CO)_9(\mu\text{-}COCH_3)L$$

An analogous mechanism was proposed for the photosubstitution reactions of the homoleptic trimer $Ru_3(CO)_{12}$. According to scheme 1 the quantum yield should respond to variation in [L] and [CO] as follows.

$$\Phi_s = \Phi_{II} \frac{k_L[L]}{k_{co}[CO] + k_L[L]} \qquad (2)$$

A plot of Φ_s^{-1} vs $[L]^{-1}$ should give Φ_{II}^{-1} as an intercept and $k_{co}[CO]/k_L$ as the slope. Such treatment of the data for 313 nm photolysis of $P(OCH_3)_3$ solutions (P_{co} = 1.0 atm) gave limiting Φ_s (i.e. Φ_{II}) of 0.223 and a k_{co}/k_L ratio of 4.06 under these conditions. The Φ_s (lim) agrees with the $P(OCH_3)_3$ independent values measured under N_2, i.e., 0.22. The value 4.06 for the discrimination ratio compares to 4:1 measured for the unsaturated complex $Ru_3(CO)_{11}$ (Desrosiers, 1986).

CONCLUDING REMARKS

The photochemistry of the ruthenium trimer $HRu_3(CO)_{10}(\mu\text{-}COCH_3)$ leads to photoisomerization or to photosubstitution products depending on the conditions. The photoisomerization has no thermal analogue, although Gavens, (1978) attempted to interconvert $HOs_3(CO)_{10}(\mu\text{-}COCH_3)$ to $HOs_3(CO)_{10}(\mu\text{-}\eta^2\text{-}C(O)CH_3)$ at 150°C in cyclohexane but no reaction occurred. Our own attempts to thermally isomerize $HRu_3(CO)_{10}(\mu\text{-}COCH_3)$ at 100°C in cyclohexane also failed to produce the acyl cluster. This is further evidence that photogenerated reactive intermediates may induce new reactivity that may not be thermally accessible. Isotopic labelling and flash photolysis studies are presently under way to further illuminate these mechanisms.

Acknowledgement: This work was supported by the National Science Foundation.

REFERENCES

Dalton DM, Barnett DJ, Duggan TP, Keister JB, Malik PT, Modi SP, Shaffer Mr Smesko SA (1985) *Organometallics* 4: 1854-1866

Desrosiers MF, Wink DA, Trautman R, Friedman AE, Ford PC (1986) *J. Am. Chem. Soc.* 108: 1917-1927

Gavens PD, Mays MJ (1978) *J. Organomet. Chem.* 162: 389-410

Pruett RL, Kacmarcik RT (1982) *Organometallics* 1: 1693-1699

MULTIPLE EMISSION FROM $(\eta^5\text{-}C_5H_5)Re(CO)_2L$ (L = A SUBSTITUTED PYRIDINE) COMPLEXES IN ROOM-TEMPERATURE SOLUTION

M.M.Glezen and A.J.Lees

Department of Chemistry, University Center at Binghamton,
State University of New York, Binghamton, NY 13901, USA

A great deal has been learned about the excited states and photophysical properties of organometallic complexes from their emission data in recent years [1]. In particular, complexes which emit in room-temperature solution yield valuable deactivation rate data under normally efficient photochemical conditions. On-going research in our laboratory has been concerned with the emission characteristics of metal carbonyl complexes in fluid solution; several of these systems are now known to exhibit room-temperature luminescence from low-lying metal to ligand charge-transfer (MLCT) excited states [2-4]. Recently, dual MLCT emission bands have been observed from $M(CO)_4(\alpha\text{-diimine})$ (M = Cr, Mo, W) complexes at room temperature [5,6]. This article reports absorption, emission and excitation data recorded from $(\eta^5\text{-}C_5H_5)Re(CO)_2L$ (L = a substituted pyridine) complexes; the results indicate unusual multiple luminescence features in room-temperature solution. Emission results obtained from $(\eta^5\text{-}C_5H_5)Re(CO)_2L$ (L = ammonia, piperidine) are also reported.

The $(\eta^5\text{-}C_5H_5)Re(CO)_2L$ derivatives, where L = pyridine (py), 4-methylpyridine (4-Mepy), 3,5-dichloropyridine (3,5-Cl_2py), 4-acetylpyridine (4-Acpy), 3-benzoylpyridine (3-Bzpy), 4-phenylpyridine (4-Phpy) and 4-benzoylpyridine (4-Bzpy), were synthesized by direct photolysis of the parent $(\eta^5\text{-}C_5H_5)Re(CO)_3$ complex in the presence of excess ligand, according to a previously published procedure [7]. Infrared and UV-visible spectra obtained for the product complexes were in good agreement with literature values. Electronic absorption spectra were recorded on a Hewlett-Packard 8450A diode-array spectrometer. Emission and excitation spectra were recorded on a SLM Instruments Model 8000/8000S spectrometer which incorporates a photon counting detector; these spectra were fully corrected for variations in instrument response as a function of wavelength. Emission lifetimes were recorded on a PRA System 3000 single-photon counting apparatus following excitation with the 357 nm line (1 ns pulsewidth) of a nitrogen flashlamp.

Figure 1 depicts the electronic absorption spectra recorded from these complexes in benzene at 20°C; these spectra are dominated by two intense low-lying bands, previously assigned to MLCT transitions [7]. Absorption data obtained from the $(\eta^5\text{-}C_5H_5)Re(CO)_2L$ series are shown in Table 1. In accordance with the MLCT assignment the energy of these transitions depend on the electron withdrawing character of the ligand substituent, following the order 4-Mepy > py > 4-Phpy > 3-Bzpy > 3,5-Cl_2py > 4-Bzpy > 4-Acpy. Moreover, these MLCT absorption features are very solvent sensitive, shifting to higher energies in more polar media, as demonstrated by the data of $(\eta^5\text{-}C_5H_5)Re(CO)_2$(4-Phpy) (see Table 2), [7,8].

Table 1. Electronic absorption data of $(\eta^5\text{-}C_5H_5)Re(CO)_2L$ complexes in hexane at 20°C.

L	Absorbance max (nm)	L	Absorbance max (nm)
4-Mepy	381,414	3,5-Cl_2py	434,506
py	392,448	4-Bzpy	474,558
4-Phpy	416,478	4-Acpy	478,552
3-Bzpy	404,510		

Photochemistry and Photophysics
of Coordination Compounds, Ed. by H. Yersin/A. Vogler

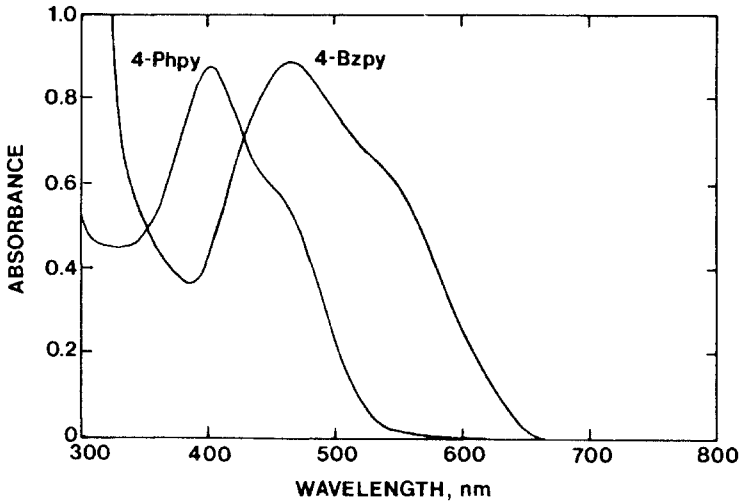

Figure 1. Electronic absorption spectra of $(\eta^5\text{-}C_5H_5)Re(CO)_2L$ (L = 4-Phpy and 4-Bzpy) in benzene at 20°C.

Table 2. Absorption and emission spectral data of $(\eta^5\text{-}C_5H_5)Re(CO)_2$(4-Phpy) in various solvents at 20°C.

Solvent	Absorbance max (nm)	Emission max (nm)[a]
hexane	416, 478	b
benzene	404, 458(sh)	506, 695
chloroform	390, 446(sh)	504(sh), 680
methylene chloride	386, 440(sh)	494, 675

[a]Emission spectra were corrected for variations in instrumental response as a function of wavelength. The excitation wavelength is 370 nm.
[b]Emission weakly observed in the 500-800 nm region.

Emission and excitation spectra obtained from the $(\eta^5\text{-}C_5H_5)Re(CO)_2L$ (L = 4-Phpy and 4-Bzpy) complexes are shown in Fig. 2 and the emission data for the 4-Phpy complex are summarized in Table 2. Each complex exhibits two broad emission features in room-temperature solution. The lower energy emission band is dependent on both the nature of substituent and solvent (see Tables 2 and 3) and, consequently, is assigned as a MLCT transition. Excitation spectra were not obtained from the lower energy emission bands of each complex. The emission and excitation data obtained from the higher energy component indicate that this state may also be assigned as a MLCT band, but it appears to be heavily mixed with intraligand (IL) character. For example, in the case of $(\eta^5\text{-}C_5H_5)Re(CO)_2$(4-Bzpy) complex the upper emission band exhibits structure resembling that of the free ligand (see Fig. 2). Furthermore, this emission band is unusually high in energy to be associated with the MLCT absorption, and the excitation spectrum provides further evidence that it originates from a state at higher energy. We were unable to observe room-temperature emission from the free 4-Phpy ligand and thus make a comparison of its emission and excitation spectra with those of the complex, however, it is noticeable that the excitation spectra recorded from the 4-Phpy and 4-Bzpy complexes are quite similar. Moreover, excitation spectra for either complex were observed to be solvent independent consistent with a IL contribution. Previously, multiple emission features involving MLCT and IL excited states have been observed from rhenium carbonyl complexes, but only in a low-temperature glass environment [9,10].

Table 3. Emission data of $(\eta^5\text{-}C_5H_5)Re(CO)_2L$ (L = 4-Phpy and 4-Bzpy) in deoxygenated benzene at 20°C.[a]

L	high-energy band			low-energy band		
	λ_{max} (nm)	$\phi(\times 10^{-4})$[b]	τ (ns)[c]	λ_{max} (nm)	$\phi(\times 10^{-4})$[b]	τ (ns)[c]
4-Phpy	506	25.2	13	695	8.41	45
4-Bzpy	495	8.51	25	655	3.28	155

[a]Emission spectra were corrected for variations in instrumental response as a function of wavelength. The excitation wavelength is 370 nm, unless otherwise stated.
[b]Absolute quantum yield data; measured relative to that of $Ru(bpy)_3^{2+}$ (ref. 11).
[c]Determined following excitation at 357 nm.

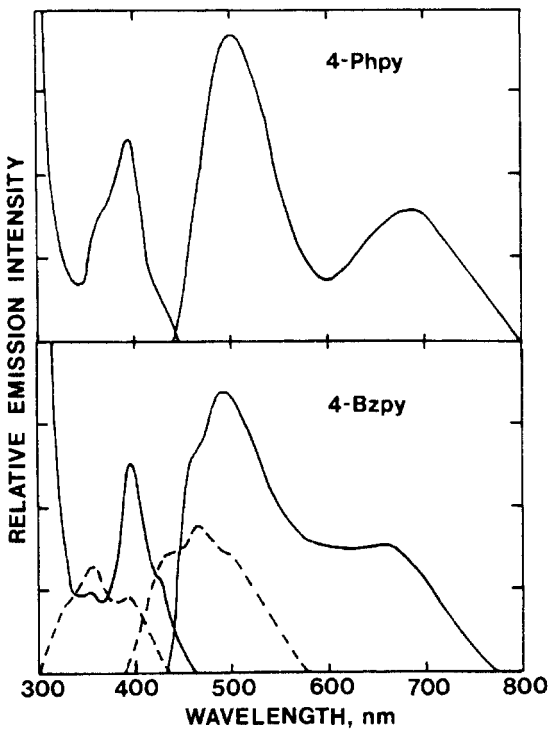

Figure 2. Corrected excitation and emission spectra of $(\eta^5\text{-}C_5H_5)Re(CO)_2L$ (L = 4-Phpy and 4-Bzpy) complexes in deoxygenated benzene at 20°C. Emission spectra were recorded with an excitation wavelength of 370 nm; excitation spectra were recorded at 506 nm (L = 4-Phpy) and 495 nm (L = 4-Bzpy), respectively. Corrected excitation and emission features of the free 4-Bzpy ligand (---) are also shown.

The closely related $(\eta^5\text{-}C_5H_5)Re(CO)L$ complexes, where L = NH_3 and pip (pip = piperidine), exhibit a single emission band in deoxygenated room-temperature benzene with maxima at 424 nm and 440 nm, respectively. Excitation spectra indicate that these emission bands are associated with the lowest lying excited states of these complexes. In the absence of a low-lying π^*-acceptor orbital (as in these NH_3 and pip derivatives) a LF excited state is attributed to be at lowest energy, although $M(d\pi)\rightarrow(\pi^*)CO$ and $M(d\pi)\rightarrow(\pi^*)C_5H_5$ transitions are thought to be close in energy and may contribute substantially to the excited state character [12-14]. Emission lifetimes were observed to be shorter than 1 ns for each complex, consistent with an excited state that contains LF character which can deactivate rapidly in room-temperature solution via efficient nonradiative processes. The photophysical characteristics of these systems are currently being further investigated.

ACKNOWLEDGEMENT. We are grateful to the Petroleum Research Fund, administered by the American Chemical Society, for their support of this research.

REFERENCES

1. A.J. Lees, Chem. Rev. (1987) in press.
2. S. Chun, E.E. Getty and A.J. Lees, Inorg. Chem. **23**, 2155 (1984).
3. A.J. Lees, J.M. Fobare and E.F. Mattimore, Inorg. Chem. **23**, 2709 (1984).
4. R.M. Kolodziej and A.J. Lees, Organometallics **5**, 450 (1986).
5. D.M. Manuta and A.J. Lees, Inorg. Chem. **25**, 1354 (1986).
6. P.C. Servaas, H.K. van Dijk, T.L. Snoeck, D.J. Stufkens and A. Oskam, Inorg. Chem. **24**, 4494 (1985).
7. P.J. Giordano and M.S. Wrighton, Inorg. Chem. **16**, 160 (1977).
8. D.M. Manuta and A.J. Lees, Inorg. Chem. **25**, 3212 (1986).
9. P.J. Giordano, S.M. Fredericks, M.S. Wrighton and D.L. Morse, J. Am. Chem. Soc. **100**, 2257 (1978).
10. P.J. Giordano and M.S. Wrighton, J. Am. Chem. Soc. **101**, 2888 (1979).
11. J. Van Houten and R.J. Watts, J. Am. Chem. Soc. **98**, 4853 (1976).
12. G.L. Geoffroy and M.S. Wrighton in "Organometallic Photochemistry," Academic Press: New York, 1979.
13. N.J. Gogan, C.-K. Chu, J. Organomet. Chem. **93**, 363 (1975).
14. D.L. Lichtenberger and R.F. Fenske, J. Am. Chem. Soc. **98**, 50 (1976).

PHOTOCHEMICALLY INDUCED C-C-BOND FORMATION IN THE COORDINATION SPHERE OF TRANSITION METALS

C.G.Kreiter and K.Lehr

Fachbereich Chemie der Universität Kaiserslautern, 6750 Kaiserslautern, FRG

Unsaturated hydrocarbons alter their reactivity fundamentally, when coordinated to transition metals and offer interesting possibilities for the organic synthesis. Nevertheless, the synthetic potential of readily available hydrocarbon complexes is far from being thoroughly investigated and used. A promising type of reactions is the photochemically induced C-C-bond formation between complexed and free hydrocarbons in the coordination sphere of transition metals.

We have shown several years ago, that tricarbonyl-η^6-1,3,5-cycloheptatriene-chromium(0) reacts with acyclic, conjugated dienes upon irradiation in a smooth [4 + 6]-cycloaddition, forming η^6-bicyclo[4.4.1]undeca-2,4,8-triene-tricarbonyl-chromium(0) complexes [1].

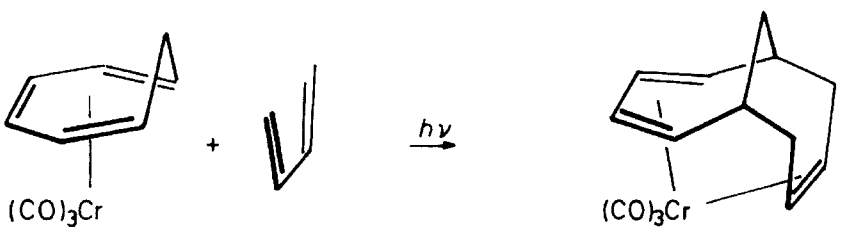

This reaction principle is limited however. Other complexes, related to $[Cr(CO)_3(\eta^6\text{-}C_7H_8)]$, and cyclic dienes show a different behaviour. 1,3-Cyclopentadiene or 1,3,5,7-cyclooctatetraene substitute the η^6-1,3,5-cycloheptatriene ligand photochemically. $[Cr(CO)_2(\eta^5\text{-}C_5H_5)(\eta^3\text{-}C_5H_7)]$ and $[Cr(CO)_3(\eta^6\text{-}C_8H_8)]$, respectively are formed in high yields. With spiro[4.4]nona-1,3-diene not the expected [6+4]-cycloadduct, but a [6+2]-cycloadduct is formed with an uneffected spiro system [2]. 1,3-Cyclohexadiene yields tricarbonyl-$\eta^{4:2}$-tricyclo-[6.3.2.$0^{2,7}$]trideca-3,5,9-triene-chromium(0). After a [4+2]-cycloaddition to the η^6-1,3,5-cycloheptatriene ligand, metal assisted 1,5-H shifts complete the reaction [2].

Tricarbonyl-η^6-1,3,5-cyclooctatriene-chromium(0) or tricarbonyl-η^6-1,3,5,7-cyclooctatetraene-chromium(0) do not react with dienes

Photochemistry and Photophysics
of Coordination Compounds, Ed. by H. Yersin/A. Vogler

photochemically at all. In $[Mo(CO)_3(\eta^6\text{-}C_7H_8)]$ and $[W(CO)_3(\eta^6\text{-}C_7H_8)]$, the homologue complexes to $[Cr(CO)_3(\eta^6\text{-}C_7H_8)]$, conjugated dienes substitute photochemically the 1,3,5-cycloheptatriene ligand.

Only complexes very closely related to $[Cr(CO)_3(\eta^6\text{-}C_7H_8)]$, like tricarbonyl-$\eta^6$-8,8-dimethylheptafulvene-chromium(0) [3], hexacarbonyl-$\eta^{6:6}$-heptafulvalene-dichromium(0), and hexacarbonyl-$\eta^{6:6}$-bi(2,4,6-cycloheptatrien-1-yl)dichromium(0) [4] show also [6+4]-cycloadditions with conjugated dienes [5 - 8].

Unexpectedly, tricarbonyl-η^6-8,8-dimethylheptafulvene-chromium(0) forms with 2,3-dimethyl-1,3-butadiene the dicarbonyl complex $[Cr(CO)_2(\eta^{3:5}\text{-}C_{14}H_{16}(CH_3)_2)]$, which at ambient conditions adds carbon monoxide [5, 6].

$$[Cr(CO)_3(\eta^6\text{-}C_{10}H_{12})] + C_4H_4(CH_3)_3 \longrightarrow [Cr(CO)_2(\eta^{3:5}\text{-}C_{14}H_{16}(CH_3)_2)] + CO$$

$$[Cr(CO)_2(\eta^{3:5}\text{-}C_{14}H_{16}(CH_3)_2)] + CO \longrightarrow [Cr(CO)_3(\eta^6\text{-}C_{14}H_{16}(CH_3)_2)]$$

The formation of $[Cr(CO)_2(\eta^{3:5}\text{-}C_{14}H_{16}(CH_3)_2)]$ and its smooth reaction with carbon monoxide sheds some light on the mechanism of the [6+4]-cycloaddition in the coordination sphere of chromium. Obviously, the photoreaction proceeds stepwise. First, the diene is coordinated to an activated complex and forms tricarbonyl-η^4-8,8-dimethylheptafulvene-η^2-diene-chromium(0). CC bond formation between C1 of the η^4-8,8-dimethylheptafulvene and C1 of the η^2-diene ligands produces the $\eta^{(5-n):(1+n)}$-1-(butene-1,2-diyl)-7-isopropylidenecycloheptadienyl ligand (n = 0, 2, 4). Different kinds of coordination have to be considered for this ligand in the intermediate. In most cases the intermediate immediately forms a second CC bond and yields the [6+4]-cycloadduct. Only intermediates of moderate stability like $[Cr(CO)_3(\eta^{3:3}\text{-}C_{14}H_{16}(CH_3)_2)]$ loose CO under photochemical conditions, and form $[Cr(CO)_2(\eta^{3:5}\text{-}C_{14}H_{16}(CH_3)_2)]$ [5, 6].

A new type of cycloaddition between simple, unsaturated hydrocarbons in the coordination sphere of a transition metal was found by incident. We have shown, that decacarbonyl-dimanganese(0) reacts photochemically at 253 K with 1,3-butadiene in n-hexane solution in an quite unusual way. After a short time of irradiation μ-$\eta^{3:1}$-2-butene-1-diyl-enneacarbonyl-dimanganese is the predominating reaction product [9, 10].

$$[Mn_2(CO)_{10}] + C_4H_6 \longrightarrow [Mn_2(CO)_9(\mu\text{-}\eta^{3:1}\text{-}C_4H_6)] + CO$$

The formation of $[Mn_2(CO)_9(\mu\text{-}\eta^{3:1}\text{-}C_4H_6)]$ can be rationalized by a stepwise attack of $[Mn(CO)_5\cdot]$ radicals to C1 and C4 of 1,3-butadiene to yield the intermediate $\{[(CO)_5MnC_4H_6Mn(CO)_5]\}$, which looses, like other carbonyl-η^1-enyl complexes CO and yields $[(CO)_4Mn(\mu\text{-}\eta^{3:1}\text{-}C_3H_4\text{-}CH_2)Mn(CO)_5]$.

When the photoreaction of decacarbonyl-dimanganese(0) is conducted with conjugated dienes, containing a chain of five or more carbon atoms, the reaction products differ substantially from those of the reaction with 1,3-butadiene. With E-, and Z-1,3-pentadiene the main reaction leads to mononuclear η^3-E-pentadienyl, and η^3-pentenyl tetracarbonyl-manganese complexes. In a kind of disproportionation hydrogen is transferred between two diene molecules [11, 12].

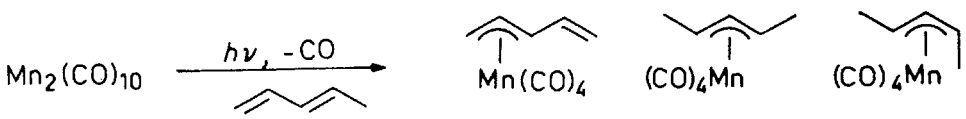

The reactions of $[Mn_2(CO)_{10}]$ with 1,3-pentadiene and its derivatives are easily understood, when intermediates, corresponding to $[Mn_2(CO)_9(\mu\text{-}\eta^{3:1}\text{-}C_4H_6)]$ are assumed. A hypothetical $[Mn_2(CO)_9(\eta^{3:1}\text{-}C_5H_8)]$ should be instable, with respect to a β-elimination, by which $[Mn(CO)_4(\eta^3\text{-}C_5H_7)]$ and pentacarbonyl-hydrido-manganese are formed.

$$[Mn_2(CO)_{10}] + C_5H_8 \longrightarrow \{[Mn_2(CO)_9(\eta^{3:1}\text{-}C_5H_8)]\} + CO$$

$$\{[Mn_2(CO)_9(\eta^{3:1}\text{-}C_5H_8)]\} \longrightarrow [Mn(CO)_4(\eta^3\text{-}C_5H_7)] + [Mn(CO)_5H]$$

In a further step, $[Mn(CO)_5H]$ reacts photochemically with free diene under loss of CO to $[Mn(CO)_4(\eta^3\text{-}C_5H_9)]$.

$$[Mn(CO)_5H] + C_5H_8 \longrightarrow [Mn(CO)_4(\eta^3\text{-}C_5H_9)] + CO$$

When E,E-2,4-hexadiene or 2,4-dimethyl-1,3-pentadiene are used instead of 1,3-butadiene in the reaction with $[Mn_2(CO)_{10}]$, tricarbonyl-manganese complexes were obtained as by-products with hydrocarbon ligands consisting from two diene molecules with one hydrogen less.

$$\tfrac{1}{2}\,[Mn_2(CO)_{10}] + 2\,C_6H_{10} \longrightarrow [Mn(CO)_3(C_{12}H_{19})] + 2\,CO + \{H\}$$

$$\tfrac{1}{2}\,[Mn_2(CO)_{10}] + 2\,C_7H_{12} \longrightarrow [Mn(CO)_3(C_{14}H_{23})] + 2\,CO + \{H\}$$

An X-ray diffraction study of [Mn(CO)$_3$($C_{14}H_{23}$)] shows the presence of an $\eta^{3:2}$-1,3,5,5,7-pentamethyl-2,6-cyclononadien-1-yl ligand in this complex [13, 14]. Similarily, an $\eta^{3:2}$-4,5,8-trimethyl-2,6-cyclononadien-1-yl ligand was prooven by the ^{1}H NMR spectrum for [Mn(CO)$_3$($C_{12}H_{19}$)]. The substitution patterns of both $\eta^{3:2}$-2,6-cyclononadien-1-yl ligands suggest a formal [5 + 4] cycloadditon of the dienes to η^5-2,4-hexadien-1-yl, and η^5-2,4-dimethyl-2,4-pentadien-1-yl tricarbonyl manganese complexes, respectively. Such complexes are readily formed from tetracarbonyl-η^3-E-2,4-pentadien-1-yl-manganese and related complexes on warming to 60 °C.

It is reasonable to assume, that a certain amount of [Mn(CO)$_4$(η^3-E-2,4-hexadien-1-yl)], and [Mn(CO)$_4$(η^3-E-2,4-dimethyl-2,4-pentadien-1-yl)] looses already during the irradiation CO. The hereby formed methyl substituted [Mn(CO)$_3$(η^5-2,5-pentadien-1-yl)] complexes, may react further with the excess of the dienes to the methyl substituted [Mn(CO)$_3$($\eta^{3:2}$-2,6-cyclononadien-1-yl)] complexes.

In order to proove this hypothesis, we irradiated [Mn(CO)$_3$(η^5-2,5-pentadien-1-yl)] and 1,3-butadiene with UV-light. In a fast, formal [5 + 4] cycloaddition, the simple [Mn(CO)$_3$($\eta^{3:2}$-2,6-cyclononadien-1-yl)] is formed good yield.

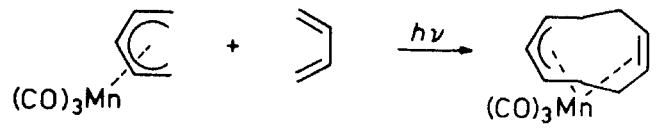

Again the question has to be answered, whether this reaction is generally applicable also to other dienes and other [Mn(CO)$_3$(η^5-dienyl)] complexes. With E-1,5-pentadiene, [Mn(CO)$_3$(η^5-C_5H_7)] reacts in a quite smoth reaction similarily. In contrast, Z-1,5-pentadiene reacts only when benzene is present in the reaction mixture as a catalyst.

In the first case [Mn(CO)$_3$($\eta^{3:2}$-exo-5-methyl-2,6-cyclononadien-1-yl)], in the second case the corresponding endo isomer is obtained.

A further system, we have investigated, is [Mn(CO)$_3$(η^5-cyclohexadienyl)]. With 1,3-butadiene, the only product is the chelate complex [Mn(CO)$_2$($\eta^{4:3}$-1-(3-buten-1,2-diyl)-2,4-cyclohexadiene)]. 2-Methyl-1,3-butadiene yields a mixture of [Mn(CO)$_3$($\eta^{3:2}$-3-methyl-bicyclo[4.3.1]-nona-3,8-dien-7-yl)] and [Mn(CO)$_2$($\eta^{4:3}$-1-(3-methyl-3-buten-1,2-diyl)-2,4-cyclohexadiene)]. Interstingly, the ratio between these two complexes varies with the reaction temperature. Low temperature

favours the formation of the $Mn(CO)_2$ complex. At room temperature predominantly the $Mn(CO)_3$ complex is obtained. 2,3-Dimethyl-1,3-butadiene adds cleanly to $[Mn(CO)_3(\eta^5\text{-cyclohexadienyl})]$ and $[Mn(CO)_3(\eta^{3:2}\text{-3,4-dimethyl-bicyclo[4.3.1]nona-3,8-dien-7-yl})]$ is obtained.

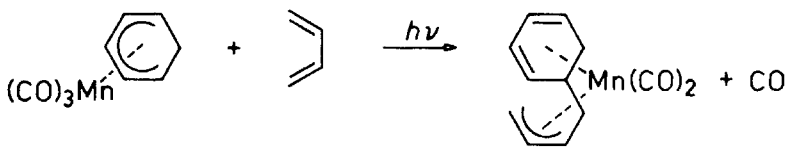

$$[Mn(CO)_3(\eta^5\text{-}C_6H_7)] + i\text{-}C_5H_8 \longrightarrow [Mn(CO)_3(\eta^{3:2}\text{-}CH_3C_9H_{12})]$$
$$[Mn(CO)_2(\eta^{4:3}\text{-}C_{11}H_{15})] + CO$$

$$[Mn(CO)_3(\eta^5\text{-}C_6H_7)] + (CH_3)_2C_4H_4 \longrightarrow$$
$$[Mn(CO)_3(\eta^{3:2}\text{-}(CH_3)_2C_9H_{11})]$$

These reactions show clearly, that it is possible to build photochemically bicyclo[4.3.1]nonane systems at manganese. There are good chances, to extend the reaction principle to systems distinctly different from the parent $Mn(CO)_3(\eta^5\text{-pentadienyl})$ complex.

There are also some informations about the mechanism of the reaction available. In a first step, photochemically a coordinatively unsaturated $\{[Mn(CO)_3(\eta^3\text{-dienyl})]\}$ intermediate is formed, which reacts with dienes to $\{[Mn(CO)_3(\eta^3\text{-dienyl})(\eta^2\text{-diene})]\}$. Formation of one C-C bond between the η^3-dienyl and η^2-diene ligands yields unstable $\{[Mn(CO)_3(\eta^{4:1}\text{-1-(endiyl)-2,4-diene})]\}$ or $\{[Mn(CO)_3(\eta^{2:3}\text{-1-(endiyl)-2,4-diene})]\}$. Formation of a second C-C bond leads to $[Mn(CO)_3(\eta^{3:2}\text{-2,6-cyclononadien-1-yl})]$, photochemically induced CO loss to $[Mn(CO)_2(\eta^{4:3}\text{-1-(endiyl)-2,4-diene})]$.

$$[Mn(CO)_3(\eta^5\text{-dienyl})] \longrightarrow \{[Mn(CO)_3(\eta^3\text{-dienyl})]\}$$

$$\{[Mn(CO)_3(\eta^3\text{-dienyl})]\} + \text{diene} \longrightarrow$$
$$\{[Mn(CO)_3(\eta^3\text{-dienyl})(\eta^2\text{-diene}]\}$$

$$\{[Mn(CO)_3(\eta^3\text{-dienyl})(\eta^2\text{-diene}]\} \longrightarrow$$
$$\{[Mn(CO)_3(\eta^{4:1}\text{-(endiyl)diene})]\}$$

$$\{[Mn(CO)_3(\eta^{4:1}\text{-(endiyl)diene})]\} \longrightarrow$$
$$[Mn(CO)_3(\eta^{3:2}\text{-2,6-cyclononadien-1-yl})]$$
$$[Mn(CO)_2(\eta^{4:3}\text{-(endiyl)diene})] + CO$$

1 S. Özkar, H. Kurz, D. Neugebauer, and C. G. Kreiter, J. Organometal. Chem., **160**, 115 (1978).

2 C. G. Kreiter, E. Michels, and H. Kurz, J. Organometal. Chem., **232**, 249 (1982).

3 J. A. S. Howell, B. F. G. Johnson, and J. Lewis, J. Chem. Soc., Dalton Trans. p. 293 (1974).

4 J. D. Munro, and P. L. Pauson, J. Chem. Soc., (1961) 3484.

5 E. Michels, and C. G. Kreiter, J. Organometal. Chem., **252**, C1 (1983).

6 E. Michels, W. S. Sheldrick, and C. G. Kreiter, Chem. Ber., **118**, 964 (1985).

7 C. G. Kreiter, and E. Michels, J. Organometal. Chem., **312**, 59 (1986).

8 C. G. Kreiter, E. Michels, and J. Kaub, J. Organometal. Chem., **312**, 221 (1986).

9 C. G. Kreiter, and W. Lipps, Angew. Chem., **93**, 191 (1981); Angew. Chem., Int. Ed. Engl., **20**, 201 (1981).

10 C. G. Kreiter, and W. Lipps, Chem. Ber., **115**, 973 (1982).

11 M. Leyendecker, and C. G. Kreiter, J. Organometal. Chem., **249**, C31 (1983).

12 C. G. Kreiter, and M. Leyendecker, J. Organometal. Chem., **280**, 225 (1985).

13 C. G. Kreiter, M. Leyendecker, and W. S. Sheldrick, unpublished.

14 C. G. Kreiter, Adv. Organometal. Chem., **26**, 297 (1986).

TRIPLET QUENCHING BY METAL CARBONYLS

M.Kucharska-Zon and A.J.Poë

The Department of Chemistry and Erindale College, University of Toronto, Mississauga, Ontario, L5L 1C6, CANADA

The quenching of triplet states by organometallic compounds is well established though not widely studied. Vogler (1970, 1975) reported benzophenone-photosensitized substitution reactions of $M(CO)_6$ (M = Cr, Mo, W) in benzene. It was postulated that triplet energy was transferred to the metal carbonyl, leading to CO dissociation. Ferrocene quenches triplet states of many organic molecules in benzene (Fry, 1966; Kikuchi, 1974; Farmilo, 1975) and it was concluded (Farmilo, 1975) that triplet energy transfer occurs to a distorted excited state of ferrocene. Traverso et al. (1978) showed that $M(\eta\text{-}C_5H_5)_2$ (M = Fe, Ru, Os) quench triplet uranyl ion in acetone by electron transfer as do several mononuclear carbonyls and one dinuclear one, $Mn_2(CO)_{10}$ (Sostero, 1979). It has also been shown (Fox, 1982) that triplet biacetyl, BA, is quenched by $Mn_2(CO)_{10}$ in CCl_4 and that this sensitizes the $Mn_2(CO)_{10}$ towards reaction with CCl_4 to form $Mn(CO)_5Cl$. The simplest explanation is that triplet energy transfer leads to homolysis of the Mn-Mn bond and reaction of the $Mn(CO)_5$ radicals with the solvent. $Re_2(CO)_{10}$ did not quench BA but $Re_2(CO)_8(PPh_3)_2$ did and was sensitized to formation of $Re(CO)_4(PPh_3)Cl$. We report here data for phosphorescence quenching of BA by a wide range of metal carbonyls, and a few examples of triplet benzil, BZ, quenching.

RESULTS

Phosphorescence intensities showed good agreement with Stern-Volmer kinetics. Values of k_q for BA in benzene are given in Table 1 together with values for the triplet energies, E(T), of the quenchers estimated by means of equ. (1) (Herkstroeter, 1966; Sandros, 1964)

$$k_q = k_m/\{1 + \exp. \Delta E(T)/RT\} \qquad (1)$$

where $\Delta E(T)$ is a measure of the extent to which the triplet energy of the quencher exceeds that of BA (19 700 cm^{-1}), and k_m is the maximum rate constant for triplet energy transfer taken as 1×10^{10} $M^{-1}s^{-1}$. This is close to the highest value of k_q observed here but lower than the 1.6×10^{10} $M^{-1}s^{-1}$ for a diffusion controlled rate constant

Photochemistry and Photophysics
of Coordination Compounds, Ed. by H. Yersin/A. Vogler

Table 1. Values of k_q [a] and E(T) for Quenching of Biacetyl by Metal Carbonyls in Benzene at ca. 23°C

Complex	k_q, $M^{-1}s^{-1}$	E(T), [b] cm^{-1}
$(\eta\text{-}C_5H_5)_2Fe_2(CO)_4$	9.9×10^9	18 760
$Os_3(CO)_9(PPh_3)_3$	9.4×10^9	19 139
$(\eta\text{-}C_5H_5)_2Mo_2(CO)_6$	6.2×10^9	19 600
$Ru_3(CO)_{12}$	5.8×10^9	19 630
$Co_4(CO)_{12}$	5.8×10^9	19 630
$Co_4(CO)_8(dppm)_2$ [c]	4.9×10^9	19 690
$Mn_2(CO)_{10}$	3.4×10^9	19 840
$Mn_2(CO)_8(P\text{-}n\text{-}Bu_3)_2$ [d]	2.6×10^9	19 910
$Mn_2(CO)_8(PPh_3)_2$ [d]	1.7×10^9	20 030
$Mn_2(CO)_8\{P(C_6H_{11})_3\}_2$ [d]	1.5×10^9	20,060
$Re_2(CO)_8(PPh_3)_2$ [d]	3.0×10^8	20 407
$Os_3(CO)_{12}$	1.9×10^8	20 500
$Re_2(CO)_8\{P(C_6H_{11})_3\}_2$ [d]	1.2×10^8	20 596
$Re_2(CO)_{10}$	ca. 5×10^6	21 254
$Mo(CO)_6$	ca. 4×10^5	21 740

[a] Estimated from the gradients, $k_q\tau$, of the Stern-Volmer plots and τ obtained by the method of Jones et al. (1980) based on data of Turro et al. (1980); [b] estimated from equ. (1) with $\Delta E(T) = E(T) - 19\ 700\ cm^{-1}$; [c] dppm = $Ph_2PCH_2PPh_2$; [d] bis axial complexes.

in benzene (Wagner, 1968). Some values of k_q for quenching of BZ are given in Table 2.

DISCUSSION

The values of E(T) given in Table 1 are likely to be lower limits since values of k_q are frequently found not to fall off with $\Delta E(T)$ as rapidly as predicted by equ.(1). This has been explained in terms of formation of geometrically distorted triplet states (Farmilo, 1975) or of thermal excitation of ground states (Engel, 1983) of the quenchers. Beach et al. (1968) assigned the lowest triplet state of $Mo(CO)_6$ an excitation energy of ca. 30 000 cm^{-1} rather than the

Table 2. Values of k_q[a] and E(T) for Quenching of Benzil by Some Metal Carbonyls in Benzene

Complex	$k_q(BZ)$, $M^{-1}s^{-1}$	E(T),[b] cm^{-1}	$k_q(BZ)/k_q(BZ)_{calcd}$[c]
$Mn_2(CO)_{10}$	1.06×10^8	19 430	6.6
$Co_4(CO)_8(dppm)_2$	1.25×10^9	18 810	54
$Os_3(CO)_{12}$	6.3×10^7	19 530	102
$Re_2(CO)_8(PPh_3)_2$	1.4×10^8	19 370	136
$Re_2(CO)_8\{P(C_6H_{11})_3\}_2$	2.1×10^8	19 290	528

[a] Estimated using τ = 80 μs (Flamigni, 1983); [b] estimated from equ. (1) with $\Delta E(T) = E(T) - 18\,500\ cm^{-1}$; [c] $k_q(BZ)_{calcd}$ is the value of k_q for BZ quenching calculated relative to that for BA quenching by use of equ. (1).

21 740 cm^{-1} derived here.

Another way of quantifying this effect is to compare the decrease of values of k_q with increasing values of $\Delta E(T)$ as indicated by studies with sensitizers of decreasing E(T). We have values of k_q for a few metal carbonyls with BZ (Table 2). For all but one carbonyl k_q for BZ quenching is less than that for BA quenching as expected from the 1 200 cm^{-1} lower excitation of triplet BZ. However, the ratio $k_q(BZ)/k_q(BA)$ is dependent on the nature of the carbonyl and, in one case it is actually greater than unity. Not only must this mean that deviations from equ. (1) are dependent on the nature of the quencher, which is not surprising in view of different possible distortions of excited states, but it must also mean that the deviations are different for different donors. This suggests the existence of rather specific effects on the energy transfer process which require further exploration.

The assumption of triplet energy transfer and not electron transfer is supported by the absence of clear correlations with redox potentials of the carbonyls. The effect of P-donor substituents on the values of k_q for $Mn_2(CO)_8L_2$ is very small whereas such substitution is known generally to have a very large effect on redox potentials (Arewgoda, 1982). The trends shown in Table 1 are quite pronounced. The only mononuclear carbonyl is very inefficient compared with all the multi-nuclear ones. The quenching efficiency of the multinuclear carbonyls decreases rapidly as the metal changes from the first to the second and third transition metal periods. The effect of P-donor substituents is quite small (and very slightly retarding) for carbonyls of the first row but substantially accelerating for third row carbonyls. Both cyclopentadienyl metal

carbonyls are very efficient quenchers. It will be interesting to see how these results correlate with triplet excitation energies of such complexes when they are obtained. It also remains to investigate the extent to which the quenching process sensititizes reactions of these carbonyls.

ACKNOWLEDGEMENTS

We thank the Natural Science and Engineering Research Council, Ottawa, Canada for support of this work, and M. K-Z. thanks the Technical University, Wroclaw, Poland for leave of absence.

REFERENCES

Arewgoda M, Rieger PH, Robinson BH, Simpson J, Visco SJ (1982) Paramagnetic Organometallic Molecules 12. J Am Chem Soc 104: 5633-5640 and references therein

Beach NA, Gray HB (1968) Electronic Structures of Metal Hexacarbonyls. J Am Chem Soc 90: 5713-5729

Engel PS, Woods TL, Page MA (1983) Quenching of Excited Triplet Sensitizers by Organic Peroxides. J Phys Chem 87: 10-13

Farmilo A, Wilkinson F (1975) Triplet State Quenching by Ferrocene. Chem Phys Lett 34: 575-580

Flamigni L, Barigelletti F, Dellonte S, Orlandi G (1983) Photophysical Properties of Benzil. J Photochem 21: 237-244

Fox A, Poë AJ, Ruminski R (1982) Photosensitized Fragmentation of Some Metal Carbonyls. J Am Chem Soc 104: 7327-7329

Fry AJ, Liu RSH, Hammond GS (1966) Mechanisms of Photochemical Reactions in Solution XLI. J Am Chem Soc 88: 4781-4782

Herkstroeter WG, Hammond GS (1966) Mechanisms of Photochemical Reactions in Solution XXXIX. J Am Chem Soc 88: 4769-4777

Jones G, Santhanam M, Chiang S-H (1980) Photoaddition of Biacetyl and Alkenes. J Am Chem Soc 102: 6088-6095

Kikuchi M, Kikuchi K, Kokubun H (1974) A study of Quenching of Triplets by Ferocene. Bull Chem Soc Japan 47: 1331-1333

Sandros K (1964) Transfer of Triplet State Energy in Fluid Solutions. Acta Chem Scand 18: 2355-2374

Sostero S, Traverso O, Di Bernardo P, Kemp TJ (1979) Quenching of Excited Uranyl Ion by Metal Carbonyls in Aprotic Solvents. J Chem Soc Dalton Trans: 658-660

Traverso O, Rossi R, Magon L, Cinquantini A, Kemp TJ (1978) The Quenching of Excited Uranyl Ion by d^6 Metallocenes. J Chem Soc Dalton Trans: 569-572

Turro NJ, Shima K, Chung G-J, Tanielian C, Kanfer S (1980) Photoreactions of Biacetyl and Tetramethylethylene. Tetrahedron Lett 21: 2775-2778

Vogler A (1970) Sensibilisierte Photolyse von $Cr(CO)_6$. Z Naturforsch B25: 1069-1070

Vogler A (1975) Concepts of Inorganic Photochemistry, Ed. Adamson AW, Fleischauer PD, Wiley, New York, p. 273

Wagner PJ, Kochevar I (1968) How Efficient is Diffusion Controlled Triplet Energy Transfer? J Am Chem Soc 90: 2232-2238

PHOTOEXCITATION OF $W(CO)_6$ SOLUTIONS CONTAINING α-DIIMINE LIGANDS. KINETICS AND MECHANISM OF CHELATION FOR A SERIES OF PHOTOPRODUCED $W(CO)_5$(α-DIIMINE) INTERMEDIATES

A.J.Lees, M.J.Schadt, and L.Chan

Department of Chemistry, University Center at Binghamton,
State University of New York, Binghamton, NY 13901, USA

Relatively little is presently known about the identity, structure, and reactivity of reaction intermediates in ligand photosubstitution processes of organometallic complexes. Direct spectral characterization of these intermediates and quantitative measurements of their reactivity have rarely been reported [1,2]. Recently, we have investigated the nature of reaction intermediates formed following photoexcitation of $W(CO)_6$ solutions that contain an α-diimine ligand [3-5]. Spectral evidence has been obtained for a reaction intermediate of the type, $W(CO)_5L$, where the normally bidentate α-diimine ligand is coordinated in a monodentate fashion. This article reports observed kinetic data and mechanistic behavior for the ring closure reaction of $W(CO)_5L$, where L is a series of α-diimine ligands. The α-diimines studied are 1,10-phenanthroline (phen), 2,2'-bipyridine (bpy), 1,4-diazabutadiene (dab), and 2-pyridinal-imine (py-im), or a derivative of these ligands.

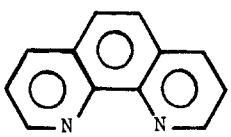

phen

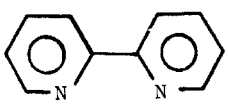

bpy

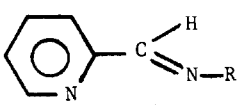

py-im

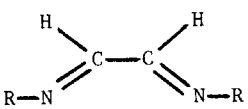

dab

A typical experiment consisted of c.a. 2 s irradiation with the 313 nm line of a 200 W Hg lamp of 5×10^{-4} M $W(CO)_6$ and 1×10^{-2} M α-diimine in deoxygenated benzene. Approximately 1×10^{-4} M $W(CO)_6$ undergoes photodissociation during this excitation; this value has been estimated by determining the incident light intensity using Ferrioxalate actinometry [6] and the quantum efficiency of $W(CO)_6$ [7]. The amount of photodissociation was determined accurately from the amount of $W(CO)_4L$ complex produced at the end of the kinetic experiment. Electronic absorption spectra were obtained throughout the reaction of $W(CO)_5L$ on a microprocessor-controlled diode-array Hewlett-Packard 8450A spectrometer. The rapid acquisition facilities of this equipment permitted spectra to be recorded within 2 s following photoexcitation. The shortest acquisition time and time intervals between subsequent spectral readings possible on this apparatus are 0.5 s and 1 s, respectively.

Figure 1 depicts the spectral sequence at 20°C following photoexcitation of $W(CO)_6$ in deoxygenated benzene containing 1×10^{-2} M bpy. The initial spectrum was recorded rapidly (c.a. 2 s) following photolysis and subsequent spectra were acquired every 15 s thereafter. The formation of $W(CO)_4$(bpy) product was recorded by the growth of its characteristic intense metal to ligand charge-transfer (MLCT) absorption centered at 514 nm. Sharp isosbestic points observed at 397 nm and 424 nm indicate that this thermal process apparently proceeds without interference from side or subsequent reactions.

Photochemistry and Photophysics
of Coordination Compounds, Ed. by H. Yersin/A. Vogler

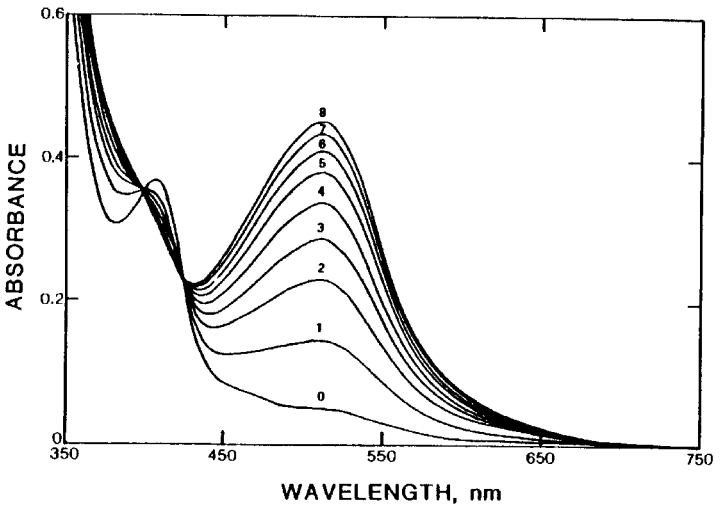

Figure 1. UV-visible spectral sequence recorded at 20°C following c.a. 2 s irradiation of a deoxygenated solution of 5 x 10^{-4} M $W(CO)_6$ and 1 x 10^{-2} M bpy in benzene: curve 0, initial spectrum recorded within 2 s after excitation; curves 1-8, spectra at subsequent 15 s intervals.

Figure 2 illustrates the difference UV-visible spectrum obtained by subtracting the absorption data of the unphotolyzed solution from that of the initial spectrum (curve 0 in Fig. 1). The spectral features of this difference spectrum are typical of those observed from a number of $W(CO)_5L$ complexes [8,9], as evidenced by the comparison with $W(CO)_5$(2-Phpy) (2-Phpy = 2-phenylpyridine). Thus, the initially formed intermediate is assigned to a $W(CO)_5$(bpy) species where the normally bidentate bpy ligand is coordinated in a monodentate manner. Importantly, a monodentate $W(CO)_5L$ intermediate was not observed when L = phen, in accordance with the rigid coplanar nature of this α-diimine ligand:

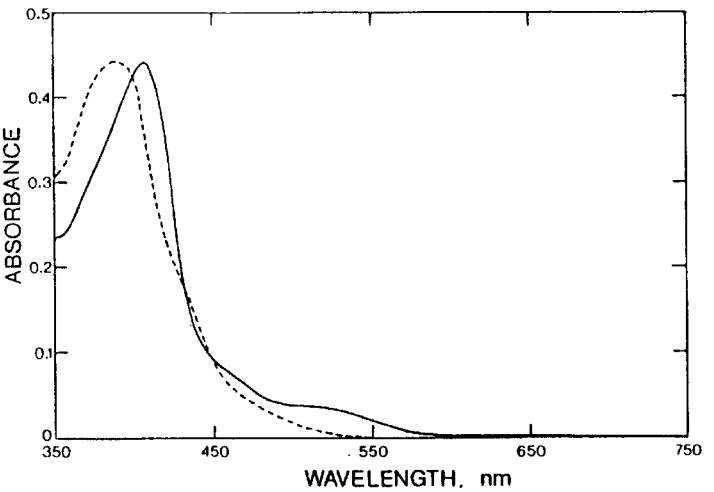

Figure 2. UV-visible difference spectrum (——) obtained by substracting spectral data of unphotolyzed solution from curve 0 in Fig. 1. For comparison the spectral features (---) of $W(CO)_5$(2-Phpy) are included; absorption is scaled arbitrarily to make maxima equal.

Reactions 1-3 are consistent with the experimental observations.

$$W(CO)_6 \underset{\Delta}{\overset{h\nu}{\rightleftharpoons}} W(CO)_5 + CO \qquad (1)$$

$$W(CO)_5 \xrightarrow[\alpha\text{-diimine}]{\Delta,\text{fast}} W(CO)_5(\alpha\text{-dimmine}) \qquad (2)$$

$$W(CO)_5(\alpha\text{-diimine}) \xrightarrow{\Delta,k_{obs}} W(CO)_4(\alpha\text{-diimine}) + CO \qquad (3)$$

Reaction rates have been determined for the ring closure reaction by monitoring the growth of the long-wavelength MLCT absorption of the corresponding $W(CO)_4L$ product. In each case the reactions were observed to be first order and independent of ligand concentration over a 1×10^{-3} - 1×10^{-2} M range. Determined rates and activation parameters for the phen, bpy, dab and py-im complexes are listed in Table 1.

Table 1. First-order rate constants at 20°C and derived activation energy parameters for the reaction of $W(CO)_5L$ to form $W(CO)_4L$ and CO.

Ligand (L)	k_{obs} (s^{-1})	ΔH^* (kcal mol^{-1})	ΔS^* (cal K^{-1} mol^{-1})
phen	>0.4[a]		
bpy	3.86×10^{-2}	19.2	0.5
4,4'-$(C_4H_9)_2$-bpy	1.58×10^{-2}	17.0	-8.6
1,4'-$(C_4H_9)_2$-dab	1.05×10^{-4}	19.1	-12.4
1,4'-$(C_3H_7)_2$-dab	1.79×10^{-5}	20.9	-8.9
py-(C_6H_5)-im	1.97×10^{-3}	10.9	-33.5
py-(C_4H_9)-im	1.50×10^{-5}	19.6	-13.6

[a]This value represents a lower limit as $W(CO)_5L$ intermediate was not observed.

The measured rate data illustrate a dependence on ligand class (phen > bpy > dab); this is interpreted in terms of steric constraints for the α-diimine coordination (see Fig. 3). When L = phen the nitrogen atoms are held coplanar and this results in a rapid ring closure mechanism following initial coordination. In contrast, the chelation of $W(CO)_5L$ complexes, where L = bpy or a dab derivative, is much slower. Theoretical and experimental studies on the conformation of the bpy and dab ligands have concluded that they exist in an approximately s-trans configuration in condensed phases [10-16]. Thus, these ligands must rotate about the central carbon-carbon bond to effect bidentate coordination; it has been estimated that the energy for the rotation is about 5 - 7 kcal mol^{-1} for either of these ligands [16,17].

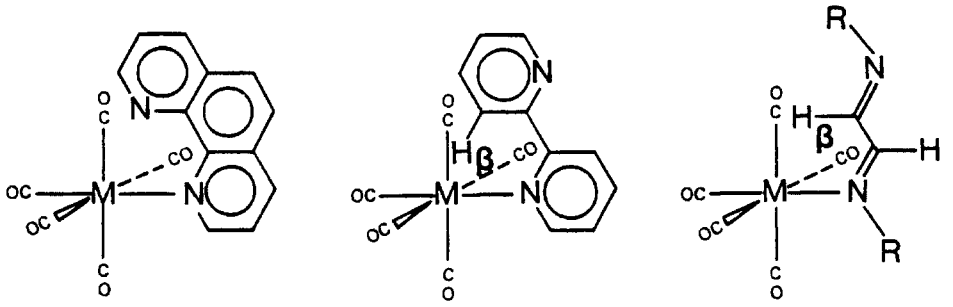

Figure 3. Stereochemistry of $W(CO)_5L$ derivatives (L = phen, bpy, and dab).

Therefore, although the $W(CO)_5L$ complexes containing dab ligands undergo ring closure much more slowly than the analogous bpy species, these large differences in rate data are not thought to be due to differences in the rotational energy barrier. Rather, it is more likely that these rate differences arise because of the varying interactions of the β-CH group in these ligands. Referring to Fig. 3 it can be seen that when L = bpy the β-CH group will interact substantially with the metal center and the carbonyl ligands, resulting in substantial electronic repulsion. This will tend to assist the twisting mechanism about the ligand C_2-C_2' bond that is required to achieve the cis-chelation geometry. When L = dab, the β-CH group is considerably less crowded and the $W(CO)_5$(dab) intermediate is much longer lived. In this connection, it is notable that monodentate dab complexes have been isolated with other transition-metal centers [17], but there are no reports of the analogous bpy complexes being stable.

Determined activation parameters (see Table 1) indicate that the ring closure reaction is enthalpy-controlled. For each of these ligand classes the rates of chelation are substantially greater than those previously reported for thermal substitution of either L or CO in $M(CO)_5L$ complexes, in which the entering species is an amine, phosphine, or arsenide ligand [18-20]. The more rapid chelation processes is attributed to a large contribution to the CO extrusion reaction by the associating ligand when it is already coordinated in a monodentate fashion.

The py-R-im ligands, perhaps not surprising, chelate at rates between the bpy and dab ligands. Importantly, a single rate constant is observed for each of these reactions and, therefore, only one chelation process is apparently involved in the mechanism [5]. However, the kinetic and activation energy data obtained depend substantially on the ligand substituent and relate closely to the steric hindrance about the aliphatic nitrogen atom. The data imply that the pyridine nitrogen atom initially scavenges the photoproduced $W(CO)_5$ species and that subsequent ring closure involves coordination by the free aliphatic nitrogen atom. Thus, when R = Ph chelation occurs much more rapidly than for the bulky R = tert-Bu. The derived activation energy parameters implicate that there are varying degrees of associative components in the transition states of the ring closure mechanism for these py-im ligands.

ACKNOWLEDGMENT. We are grateful to the Petroleum Research Fund, administered by the American Chemical Society, for support of this research.

REFERENCES

1. D.J. Darensbourg, Adv. Organomet. Chem. **21**, 113 (1982).
2. J.A.S. Howell and P.M. Burkinshaw, Chem. Rev. **83**, 557 (1983).
3. M.J. Schadt, N.J. Gresalfi and A.J. Lees, Inorg. Chem. **24**, 2942 (1985).
4. M.J. Schadt and A.J. Lees, Inorg. Chem. **25**, 672 (1986).
5. L. Chan and A.J. Lees, J. Chem. Soc. Dalton Trans. (1987) in press.
6. C.G. Hatchard and C.A. Parker, Proc. Roy. Soc. London, Ser. A., **235**, 518 (1956).
7. J. Nasielski and A. Colas, J. Organomet. Chem. **101**, 215 (1975); Inorg. Chem. **17**, 237 (1978).
8. M.S. Wrighton, H.B. Abrahamson and D.L. Morse, J. Am. Chem. Soc. **98**, 4105 (1976).
9. R.M. Dahlgren and J.I. Zink, Inorg. Chem. **16**, 3154 (1977).
10. C.W.M. Cumper, R.F.A. Ginman and A.I. Vogel, J. Chem. Soc. 1188 (1962).
11. K. Nakamoto, J. Phys. Chem. **64**, 1420 (1960).
12. P.H. Cureton, C.G. LeFevre and R.J.W. LeFevre, J. Chem. Soc. 1736 (1963).
13. S. Castellano, H. Gunther and S. Ebersole, J. Phys. Chem. **69**, 4166 (1965).
14. T. McL. Spotswood and C.I. Tanzer, Aust. J. Chem. **20**, 1227 (1967).
15. J.M. Kliegman and R.K. Barnes, Tetrahedron Lett. 1953 (1969).
16. R. Bendix, P. Birner, F. Birnstock, H. Hennig and H. Hofmann, J. Mol. Struct. **51**, 99 (1979).
17. G. van Koten and K. Vrieze, Adv. Organomet. Chem. **21**, 151 (1982).
18. D.J. Darensbourg and T.L. Brown, Inorg. Chem. **7**, 1679 (1968).
19. W.D. Covey and T.L. Brown, Inorg. Chem. **12**, 2820 (1973).
20. D.J. Darensbourg and J.A. Ewen, Inorg. Chem. **20**, 4168 (1981).

KINETICS AND MECHANISM OF C-H ACTIVATION FOLLOWING PHOTOEXCITATION OF $(\eta^5\text{-}C_5H_5)Ir(CO)_2$ IN HYDROCARBON SOLUTIONS

D.E.Marx and A.J.Lees

Department of Chemistry, University Center at Binghamton,
State University of New York, Binghamton, NY 13901, USA

The homogeneous catalytic activation of carbon-hydrogen bonds using transition metal complexes has been a challenging goal for organometallic chemists in the past few years. This process is of fundamental importance to the petrochemical industry, and has attracted considerable attention [1-7]. The activation of the C-H bonds of aromatics and saturated hydrocarbons is of particular interest because these are an abundant source of organic compounds but are normally inert due to their high C-H bond energies. Recently, it has been shown that $(\eta^5\text{-}C_5H_5)M(PMe_3)H_2$ (M = Rh, Ir) [8,9] and $(\eta^5\text{-}C_5R_5)Ir(CO)_2$ (R = H, Me) [10,11] undergo stoichiometric oxidative addition to the C-H bonds of benzene and alkanes under relatively mild photochemical conditions. This paper reports steady-state photolysis, quantum yield, and kinetic data for the C-H bond activation of a variety of hydrocarbon solvents by the photoexcited $(\eta^5\text{-}C_5H_5)Ir(CO)_2$ complex.

The synthesis of $(\eta^5\text{-}C_5H_5)Ir(CO)_2$ was performed according to that previously described, with minor modification [12]. All solvents were used as spectroscopic grade without further purification. Steady-state photolyses were carried out with the 366 line of an Ealing 200W medium pressure Hg lamp. The $(\eta^5\text{-}C_5H_5)Ir(CO)_2$ solutions were deoxygenated prior to the photolysis by purging for at least 15 min with purified nitrogen. Electronic absorption spectra were recorded in the dark on a microprocessor-controlled diode-array Hewlett-Packard 8450A UV-visible spectrophotometer. Infrared spectra were recorded on a Perkin-Elmer 283B spectrometer. The samples were recorded as solutions in a NaCl cell of 1 mm pathlength. Transient absorption spectra were obtained following excitation with the third harmonic of a Korad Nd glass laser (353 nm, 20 ns pulsewidth) [13,14].

Figure 1 illustrates the electronic absorption spectral sequence observed following 366 nm excitation of 2.2×10^{-3} M $(\eta^5\text{-}C_5H_5)Ir(CO)_2$ in deoxygenated benzene at 20°C. The conversion to product apparently occurs without interference from secondary photochemical or thermal processes, as evidenced by the clean spectral progression. IR spectral changes were recorded during this photolysis and are consistent with conversion of $(\eta^5\text{-}C_5H_5)Ir(CO)_2$ [2040(s) cm^{-1} (ν_{CO}), 1972(s) cm^{-1} (ν_{CO})] to $(\eta^5\text{-}C_5H_5)Ir(CO)(H)(C_6H_5)$ [2148(w) cm^{-1} (ν_{IrH}), 2003(s) cm^{-1} (ν_{CO})], as previously reported [10,11].

The quantum yield (ϕ) for this reaction has been calculated to be $3.0(\pm0.3) \times 10^{-2}$ in neat benzene. Table 1 lists quantum yield values determined for several solvents; the magnitudes of these yields reflect the relative selectivity of this photoexcited complex for the intermolecular activation of hydrocarbon C-H bonds. Recently, Janowicz and Bergman [8] have, from a series of competitive experiments, determined a relative rate of 4:1 for benzene:cyclohexane C-H activation following irradiation of $(\eta^5\text{-}C_5Me_5)Ir(PMe_3)(H)_2$ and Graham et al. [10] have reported a 2.5:1 ratio for benzene:cyclohexane C-H activation from the products formed following photoexcitation of $(\eta^5\text{-}C_5Me_5)\text{-}Ir(CO)_2$. The quantum yield data of Table 1 indicates that the aromatic hydrocarbons are activated more efficiently than the aliphatic molecules; thus the C-H bond activation may be facilitated by a π-interaction. Moreover, the exceptionally low value obtained for isooctane implies that steric factors could also be important in the C-H bond activation mechanism.

Photochemistry and Photophysics
of Coordination Compounds, Ed. by H. Yersin/A. Vogler

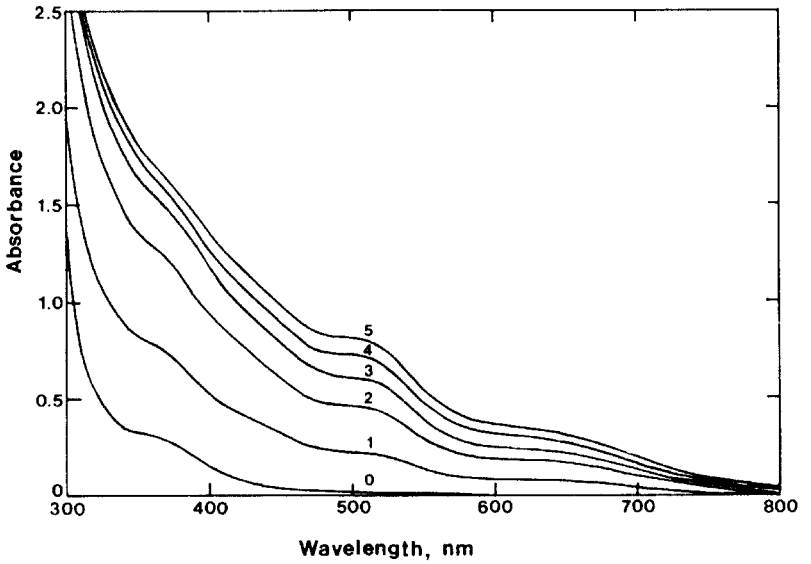

Figure 1. Electronic absorption changes accompanying the 366 nm photolysis (time intervals in h) of 2.2 x 10^{-3} M $(\eta^5\text{-}C_5H_5)Ir(CO)_2$ in N_2-purged benzene at 20°C.

Table 1. Quantum yields (ϕ) for the reaction of $(\eta^5\text{-}C_5H_5)Ir(CO)_2$ to $(\eta^5\text{-}C_5H_5)Ir(CO)(H)(R)$ products in various N_2-purged hydrocarbon solvents.[a]

RH	ϕ
benzene	0.03
toluene	0.026
n-heptane	0.015
n-pentane	0.014
cyclohexane	0.010
isooctane	0.006

[a]Reported values estimated to be accurate to ±10%; excitation wavelength is 366 nm.

Importantly, in neat perfluorobenzene no reaction was observed to take place over an 8 h photolysis period. Quantum yields (ϕ) for C-H activation of benzene were measured as a function of benzene concentration in perfluorobenzene at 20°C, and the data are listed in Table 2. The dependence of ϕ on $[C_6H_6]$ implies that the C-H activation reaction proceeds via a bimolecular process in which the association of a benzene molecule with the metal complex is the rate determining step. The experimental results are consistent with either of the two following mechanistic schemes, where S = perfluorobenzene.

$$(\eta^5\text{-}C_5H_5)Ir(CO)_2 \xrightarrow{h\nu} (\eta^5\text{-}C_5H_5)Ir(CO)_2^* \qquad (1)$$

Scheme 1

$$(\eta^5\text{-}C_5H_5)Ir(CO)_2^* \underset{k_2}{\overset{k_1,S}{\rightleftharpoons}} (\eta^5\text{-}C_5H_5)Ir(CO)(S) + CO \qquad (2)$$

$$(\eta^5\text{-}C_5H_5)Ir(CO)(S) \xrightarrow[C_6H_6]{k_3} (\eta^5\text{-}C_5H_5)Ir(CO)(H)(C_6H_5) + S \quad (3)$$

Scheme 2

$$(\eta^5\text{-}C_5H_5)Ir(CO)_2^* \underset{k_2}{\overset{k_1,S}{\rightleftharpoons}} (\eta^3\text{-}C_5H_5)Ir(CO)_2(S) \quad (4)$$

$$(\eta^3\text{-}C_5H_5)Ir(CO)_2(S) \xrightarrow[C_6H_6]{k_3} (\eta^5\text{-}C_5H_5)Ir(CO)(H)(C_6H_5) + CO + S \quad (5)$$

Quantum yields have been measured for C-H activation of benzene in perfluorobenzene solutions saturated with CO (c.a. 10^{-2} M [15]), and the data are shown in Table 2. The results illustrate that the effect of added CO on ϕ is negligible at any of the benzene concentrations measured. This observation argues against the mechanism involving initial CO dissociation from the photoexcited complex (Scheme 1). On the other hand, a hapticity change ($\eta^5 \rightarrow \eta^3$) mechanism (Scheme 2) would not be expected to be affected by the CO concentration. Low-temperature experiments previously carried out on the closely related $(\eta^5\text{-}C_5Me_5)Ir(CO)_2$ complex have provided additional support for a hapticity change mechanism; even after prolonged photolysis of this complex in Ar or N_2 matrices at 12 K no more than trace quantities of $(\eta^5\text{-}C_5Me_5)Ir(CO)$ have been observed [16].

Table 2. Quantum yields (ϕ) for the conversion of $(\eta^5\text{-}C_5H_5)Ir(CO)_2$ to $(\eta^5\text{-}C_5H_5)Ir(CO)(H)(C_6H_5)$ in perfluorobenzene at 293 K.[a]

$[C_6H_6]$, M	ϕ[b]	ϕ[c]
0.01	0.013	
0.025	0.017	0.015
0.05	0.018	
0.10	0.021	0.020
0.25	0.027	
0.50	0.029	0.028
11.3[d]	0.030	

[a]Reported values estimated to be accurate to ±10%; excitation wavelength is 366 nm.
[b]N_2-purged solutions.
[c]CO-saturated solutions (~10^{-2} M in dissolved CO concentration, see ref. 15).
[d]Neat benzene solvent.

Excitation of 3.8 x 10^{-3} M $(\eta^5\text{-}C_5H_5)Ir(CO)_2$ in N_2-purged benzene at 20°C with the third harmonic line of a Korad Nd glass laser (353 nm, 20 ns pulsewidth) produces an absorbance change immediately following the laser pulse that is depicted in Fig. 2. Approximately 1.1 x 10^{-4} M $(\eta^5\text{-}C_5H_5)Ir(CO)_2$ undergoes photodissociation following this excitation. This value has been determined from the laser pulse energy, the irradiated volume, absorbance, and quantum yield of $(\eta^5\text{-}C_5H_5)Ir(CO)_2$ in the transient absorption experiment. No further absorbance changes were observed. These absorption features closely match those obtained in the steady-state photolysis experiment and it is concluded that $(\eta^5\text{-}C_5H_5)Ir(CO)(H)(C_6H_5)$ has been formed. This result demonstrates that the intermolecular C-H activation of benzene by the photoexcited metal complex takes place on a very fast timescale (within the 20 ns laser pulse); thus, a lower limit for k_{app} = 4.4 (±0.9) x 10^6 M^{-1} s^{-1} ($k_{app} = k_{obs}/[C_6H_6]$) can be estimated for the C-H activation process. Any transient produced following photoexcitation is very short lived and rapidly scavenged by the solvent molecules present (neat benzene at 20°C is 11.3 M).

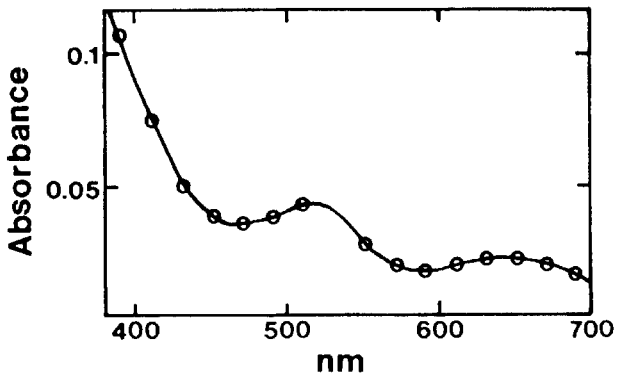

Figure 2. Photoproduct spectrum obtained in transient absorption experiment following 353 nm excitation of 3.8×10^{-3} M $(\eta^5\text{-}C_5H_5)Ir(CO)_2$ in benzene at 20°C.

Similar experiments have been carried out for $(\eta^5\text{-}C_5H_5)Ir(CO)_2$ in N_2-purged perfluorobenzene containing 5×10^{-3} M benzene. Immediately following excitation a transient with a broad absorbance (centered at 625 nm) was recorded, which subsequently decayed with $k_{obs} = 4.8(\pm 1.0) \times 10^6\ s^{-1}$ (thus $k_{app} = 9.6(\pm 1.9) \times 10^8\ M^{-1}\ s^{-1}$ to form the product $(\eta^5\text{-}C_5H_5)Ir(CO)(H)(C_6H_5)$. This transient absorption feature is assigned to the $(\eta^3\text{-}C_5H_5)Ir(CO)_2(S)$ species in accordance with the above analysis. Moreover, we were unable to observe absorbance changes representing product formation following laser photoexcitation of $(\eta^5\text{-}C_5H_5)Ir(CO)_2$ in neat perfluorobenzene; this result is consistent with the $\eta^3 \rightarrow \eta^5$ back reaction (see equation 4) taking place in the absence of scavenging benzene molecules.

ACKNOWLEDGMENT. We are grateful to the donors of the Petroleum Research Fund, administered by the American Chemical Society, for support of this research. We thank Ms. A. S. Lee for assistance with initial experiments and Prof. A. W. Adamson for use of the Nd glass laser and transient absorption equipment.

REFERENCES

1. G.W. Parshall, Acc. Chem. Res. **8**, 113 (1975).
2. A.E. Shilov and A.S. Shteinman, Coord. Chem. Rev. **24**, 97 (1977).
3. A.E. Shilov, Pure Applied Chem. **50**, 725 (1978).
4. G.W. Parshall, Catalysis **1**, 335 (1977).
5. D.E. Webster, Adv. Organomet. Chem. **15**, 147 (1977).
6. J.P. Collman and L.S. Hegedus, "Principles and Applications of Organotransition Metal Chemistry," University Science Books:Mill Valley, CA, 1980.
7. G.W. Parshall, "Homogeneous Catalysis," Wiley:New York, 1980.
8. A.H. Janowicz and R.G. Bergman, J. Am. Chem. Soc. **104**, 352 (1982).
9. W.D. Jones and F.J. Feher, Organometallics **2**, 686 (1983).
10. J.K. Hoyano and W.A.G. Graham, J. Am. Chem. Soc. **104**, 3723 (1982).
11. J.K. Hoyano, A.D. McMaster and W.A.G. Graham, J. Am. Chem. Soc. **105**, 7190 (1983).
12. E.O. Fischer and K.S. Brenner, Z. Naturforsh **16B**, 774 (1962).
13. A.J. Lees and A.W. Adamson, Inorg. Chem. **20**, 4381 (1982).
14. R. Fukuda, R.T. Walters, H. Mäcke and A.W. Adamson, J. Phys. Chem. **83**, 2097 (1979).
15. D.D. Lawson, Appl. Energy **6**, 241 (1980).
16. A.J. Rest, I. Whitwell, W.A.G. Graham, J.K. Hoyano, and A. McMaster, J. Chem. Soc. Chem. Commun. 624 (1984).

IDENTIFICATION OF H_2-, D_2-, N_2- BONDED INTERMEDIATES IN THE $Cr(CO)_6$ PHOTOCATALYZED HYDROGENATION REACTIONS

A.Oskam, R.R.Andréa, D.J.Stufkens, and M.A.Vuurman

Anorganisch Chemisch Laboratorium, University of Amsterdam,
Nieuwe Achtergracht 166, 1018 WV Amsterdam, THE NETHERLANDS

The mechanisms of photochemical reactions involving transition metal complexes have been the subject in several recent papers. Many attempts have been made to identify intermediates. This can be performed by studying parent molecules and primary photoproducts in inert matrices or solid glasses. Usually these intermediates can be characterized by IR and UV-visible spectroscopy. It is also possible to use flash photolysis in combination with fast resolved spectroscopy. This technique has the great advantage that reactions can be followed under normal conditions. This time-resolved techniques however have special restrictions as time and money consuming methods. Although matrix isolation spectroscopy is a very valuble technique for the identification and conformational analysis of primary photoproducts it has severe limitations in studying ongoing reactions because of lack of diffusion and mobility of the components.

A combination of the advantages of several methods is the use of liquid noble gases as solvents.These solvents do not absorb in the IR- and UV-visible spectral regions, are inert, can be used at various temperatures, show sufficient mobility of the components to study reactions, stabilize reactive intermediates of (photochemical) reactions long enough for spectral identification and do not show any site symmetry splittings.The solubility of most of the compounds in combination with a long pathlength in the sample cell is large enough for spectroscopic measurements. Several reports about IR, UV-visible, ESR and NMR-spectroscpic studies in solutions of liquid noble gases have appeared (Andréa 1986).

In order to stabilize primary photoproducts and study their thermal and photochemical reactions we have extended our experiments to solutions in liquid Xenon (LXe, 170-240K). This solvent is especially useful to look at the reaction mechanisms of $Cr(CO)_6$ photocatalyzed hydrogenation reactions of dienes. For this purpose a solution of $Cr(CO)_4$(norbornadiene) in LXe has been irradiated at 183K in the presence of H_2, D_2 and N_2. The photoproducts were mainly identified with FTIR. The CO-frequencies of the various photoproducts were

Photochemistry and Photophysics
of Coordination Compounds, Ed. by H. Yersin/A. Vogler

assigned with the use of the data obtained from irradiation experiments in N_2 and CH_4-matrices.

The infrared spectrum of $Cr(CO)_5H_2$ as an intermediate of the irradiation of $Cr(CO)_6$ and H_2 in liquid Xenon has been published before showing a $Cr(CO)_5$-pattern and an H_2-stretching vibration at 3030 cm^{-1} (Upmacis 1985). With D_2 instead of H_2 the same spectra appeared but with the D_2-stretching vibration at 2241 cm^{-1}, slightly higher than could be calculated for an uncoupled vibration. The corresponding N_2-experiment results in $Cr(CO)_5N_2$ with a N_2 frequency at 2237 cm^{-1} and after prolonged irradiation in $Cr(CO)_4(N_2)_2$, cis and trans with two different sets (a_1 + b_2 and a_u) of N_2-stretching frequencies (Turner 1983).

Irradiation $Cr(CO)_4$(norbornadiene) with H_2 or D_2 in order to identify a possible H_2-bonded intermediate of the catalyzed hydrogenation rection of norbornadiene no H_2- or D_2- stretching vibration of H_2 resp. D_2 as a ligand could be detected. The concentration of these intermediates simply was too low.

Because there were changes in the CO-stretching region during this photocatalyzed hydrogenation reaction we repeated this experiment with $Cr(CO)_4$(norbornadiene) and N_2. Here, three eventually four photo-products could be identified;

i.e. $Cr(CO)_3(N_2)^{ax}$(norbornadiene),

$Cr(CO)_3(N_2)^{eq}$(norbornadiene),

$Cr(CO)_4(N_2)(\eta^2$ norbornadiene),

and $Cr(CO)_3(N_2)_2(\eta^2$ norbornadiene). (see Figure)

Identification of these photoproducts were based on the assignments of the bands in the N_2- as well as in the CO-stretching region. At first the $Cr(CO)_3(N_2)$(norbornadiene) products (= 3) grow in and later on $Cr(CO)_4$ $(N_2)(\eta^2$ norbornadiene) (= 4) and $Cr(CO)_3(N_2)_2(\eta$-norbornadiene). (= 2).

The same experiments with H_2 or D_2 and ($Cr(CO)_4$(norbornadiene) in stead of N_2 show the same patterns in the CO-region. Therefore, we propose that the same type of products arise in these experiments. Complete proof of the assignments with ^{13}CO labeling experiments is in progress. $Cr(CO)_4$(norbornadiene) with H_2 and D_2 after prolonged irradiation in the presence of free norbornadiene shows no detectable intensity decrease of the parent bands of $Cr(CO)_4$(norbornadiene) at the very end and large bands which evidently belong to free norbornane.

Further experiments in liquid xenon to unraffle the mechanism of the catalyzed hydrogenation reaction of norbornadiene are in progress.

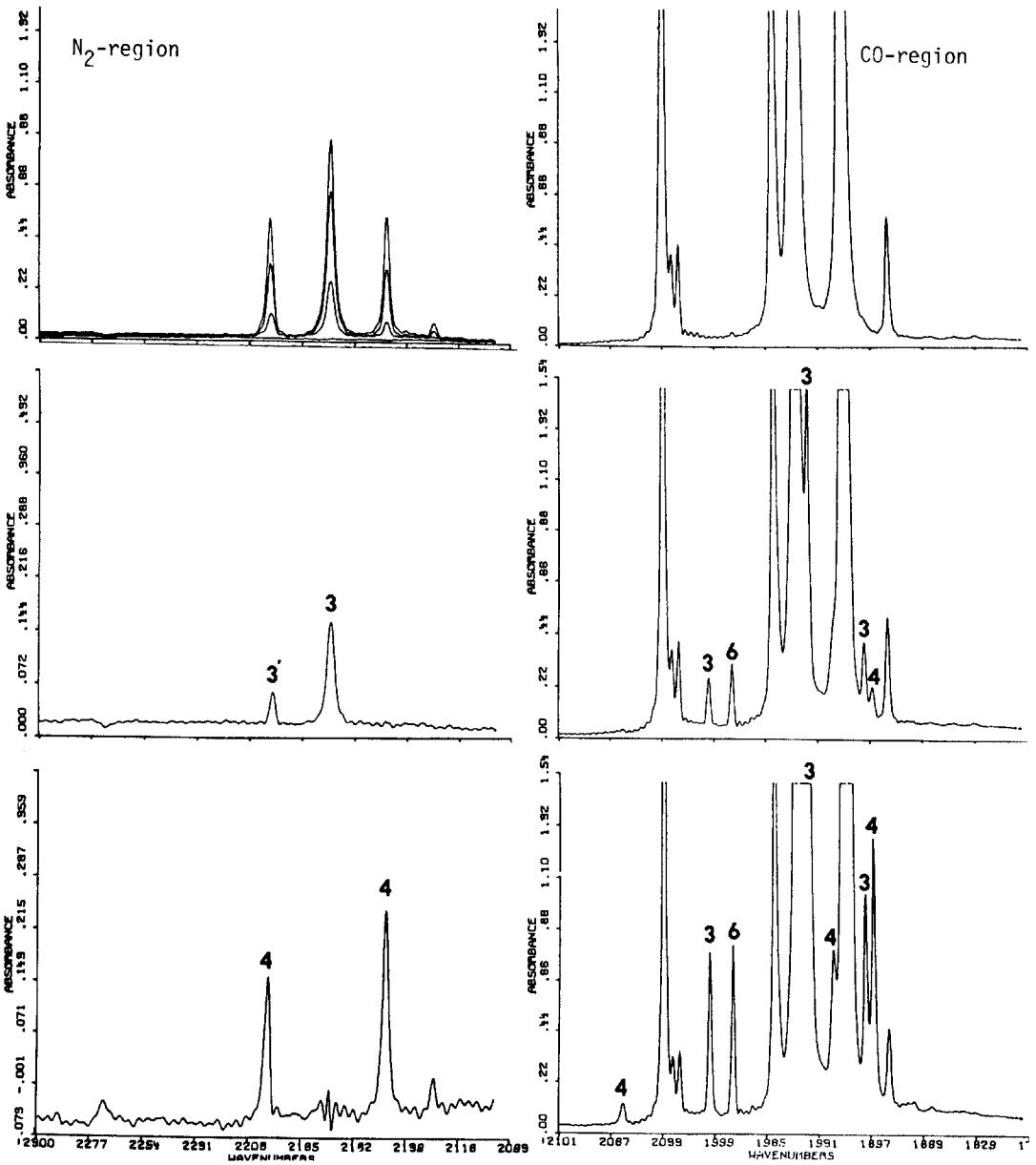

PRODUCTS: $6=Cr(^{12}CO)_6$

$4=Cr(^{12}CO)_4(\eta^2\text{-NBD})(N_2)$

$3=Cr(^{12}CO)_3(\eta^4\text{-NBD})(N_2{}^{ax})$

$3'=Cr(^{12}CO)_3(\eta^4\text{-NBD})(N_2{}^{eq})$

$2=Cr(^{12}CO)_3(\eta^2\text{-NBD})(N_2)$

Figure Photolysis of $Cr(CO)_4$(norbornadiene) with N_2

REFERENCES

Andréa RR, Luyten H, Vuurman MA, Stufkens DJ and Oskam A (1986) Applied Spectroscopy 40: 1184 and references therein

Turner JJ, Simpson MB, Poliakoff M, Maier II WB and Graham MA (1983) Inorg. Chem. 22: 911

Upmacis RK, Gadd GE, Poliakoff M, Simpson MB, Turner JJ, Whyman R, Simpson AF (1985) J.Chem. Soc. Chem. Commun. 27

SPECTROSCOPY AND PHOTOCHEMISTRY OF $Ni(CO)_2$(α-DIIMINE) COMPLEXES

P.C.Servaas, D.J.Stufkens, and A.Oskam

Anorganisch Chemisch Laboratorium, University of Amsterdam,
Nieuwe Achtergracht 166, 1018 WV Amsterdam, THE NETHERLANDS

INTRODUCTION

During the last ten years much attention has been paid in our laboratory to the spectroscopy, photochemistry and in some cases photophysics of low-valence transition metal α-diimine complexes. For most of these complexes the lowest excited state is metal to α-diimine charge transfer (MLCT) in character. Only in a few cases, viz. d^6-$M(CO)_4$(α-diimine) (M=Cr,Mo,W) (Balk 1980; van Dijk 1985) and recently d^8-$Fe(CO)_3$(α-diimine) (van Dijk, to be published; Kokkes 1984), a reaction was observed from these MLCT states, although the quantum yields of these reactions were always very low (ϕ<0.01). Because of these low quantum yields and because of the presence of close-lying reactive LF states, photochemical reactions normally occur from these latter states, especially at room temperature when these LF states become thermally occupied.

In order to investigate the steric and electronic effects on the MLCT photochemistry of α-diimine complexes without disturbing reactions from close-lying LF states taking place, we started a spectroscopic and photochemical study of the $Ni(CO)_2$(R-DAB) complexes. R-DAB represents the most simple α-diimine ligand 1,4-diaza-1,3-butadiene (=R-DAB; R-N=CH-CH=N-R). The results of this study are presented here.

RESULTS AND DISCUSSION

$Ni(CO)_2$(R-DAB) complexes could only be prepared for R-DAB ligands with bulky substituents R at the coordinating nitrogen atoms. This study is therefore confined to $Ni(CO)_2$(t-Bu-DAB) and $Ni(CO)_2$(2,6-iPr_2-Ph-DAB). Both complexes show an intensive absorption band in the visible region, with maxima in benzene at 19.34 kK for $Ni(CO)_2$(t-Bu-DAB) and at 18.48 kK for $Ni(CO)_2$(2,6-iPr_2-Ph-DAB). This band is assigned to a MLCT transition and it shows the characteristic solvent dependence of such a transition. The He(I) and He(II) photoelectron spectra of $Ni(CO)_2$(t-Bu-DAB), reported by Andréa (1985) pointed to a tetrahedral configuration of the metal-d orbitals. From MO calculations following the CNDO/S method, using known bond distances and angles of other

Photochemistry and Photophysics
of Coordination Compounds, Ed. by H. Yersin/A. Vogler

tetrahedral $Ni(CO)_2(\alpha\text{-diimine})$ complexes (von Hausen 1972; Sieler 1985), a MO scheme has been composed; the relevant part of which is shown in Figure 1.

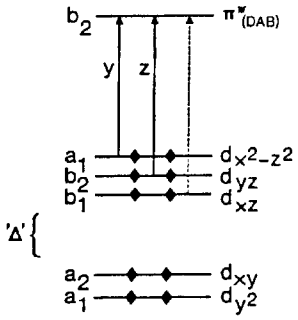

Figure 1.
MO-diagram of $Ni(CO)_2$(t-Bu--DAB)

The z-polarized $b_2 \rightarrow b_2^*$ MLCT transition will be the most strongly allowed transition in the absorption spectrum due to the strong overlap between the metal d_{yz} (b_2) and ligand π^* (b_2) orbitals involved. With the use of the resonance Raman (rR) technique it is possible to determine in detail the character of these MLCT transitions. For both $Ni(CO)_2$(R-DAB) complexes these spectra have been measured and some characteristic ones are shown in Fig. 2.

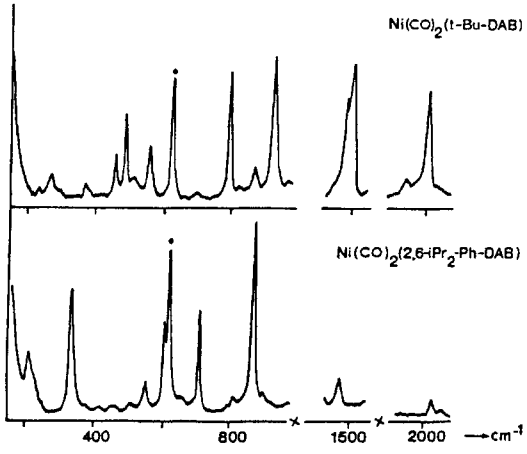

Figure 2.
rR spectra of $Ni(CO)_2$(R-DAB) complexes (in C_6H_6).

These spectra exhibit striking differences which at first sight indicate a change in CT-character of the main electronic transition. The appearance of an intensive band for ν^{sym}(CN) of the R-DAB ligand in the rR spectrum of $Ni(CO)_2$(t-Bu-DAB) is in accordance with a transition with considerable CT-character. This is also reflected in the observation of ν^{sym}(CO) at 2006 cm^{-1}. A rR effect for ν^{sym}(CO) was also found for the $M(CO)_4$(R-DAB) [M=Cr,Mo,W] complexes (Balk 1980) and had then been explained by a through space overlap between α-diimine- and CO-π* orbitals. Strong rR effects are also observed for two bands at 773 cm^{-1} and 913 cm^{-1}, respectively, belonging to bending modes of the $\overline{NiNCCN}$ moiety. Hardly any rR effect is observed for the metal-ligand stretching modes which means that none of these bonds is severely affected during this CT-transition. In summary we can say that the character of this transition as derived from the rR spectra is in accordance with that of the z-polarized $b_2 \rightarrow b_2^*$ transition derived from the MO-diagram, showing a large solvatochromism and therefore a large amount of CT-character.

The rR spectrum of $Ni(CO)_2$(2,6-iPr_2-Ph-DAB) differs appreciably from that of $Ni(CO)_2$(t-Bu-DAB) (see Fig. 4). The appearance of strong metal-ligand vibrations (ν^{sym}(Ni-N) at 206 cm^{-1} and ν^{sym}(Ni-C) at 321 cm^{-1}) and weak ligand vibrations (ν^{sym}(CN) at 1475 cm^{-1}) characterizes the transition as strongly metal (d_π)- ligand (π*) bonding to anti-bonding. However, such a strong rR effect for ν^{sym}(Ni-C) cannot arise from resonance of the exciting laser line with the $b_2 \rightarrow b_2^*$ transition of a quasi tetrahedral complex. There has to be a structural change with respect to the $Ni(CO)_2$(t-Bu-DAB) complex. Unfortunately, no single crystals of $Ni(CO)_2$(2,6-iPr_2-Ph-DAB) could be prepared for a X-ray structure determination. In order to find out how structural changes affect the rR-spectra of Ni-α-diimine complexes we measured the rR spectra of $Ni(R\text{-}DAB)_2$ complexes. These complexes have structures varying from tetrahedral $Ni(c\text{-}Hex\text{-}DAB)_2$ (Svoboda 1981) to pseudo planar $Ni(2,6\text{-}Me_2\text{-}Ph\text{-}DAB)_2$ (tom Dieck 1981), the latter having an angle between the two α-diimine ligands of 44.5°. The results are shown in Fig. 3.

These spectra show similar features as the spectra of the $Ni(CO)_2$(R-DAB) complexes in Fig. 2. The tetrahedral complex $Ni(c\text{-}Hex\text{-}DAB)_2$ shows a strong rR effect for ν^{sym}(CN) at 1496 cm^{-1} and weak effects for the M-L stretching modes. This result points to a transition with strong CT-character just as found for $Ni(CO)_2$(t-Bu-DAB). The pseudo planar complex $Ni(2,6\text{-}Me_2\text{-}Ph\text{-}DAB)_2$ on the other hand shows strong rR effects for the M-L stretching modes and a weak effect

for $\nu^{sym}(CN)$ which is in good agreement with the rR spectrum of $Ni(CO)_2(2,6\text{-}iPr_2\text{-}Ph\text{-}DAB)$. For reasons of comparison also the rR spectrum of the tetrahedral complex $Ni(4\text{-}Me\text{-}Ph\text{-}DAB)_2$ is presented in Fig. 3.

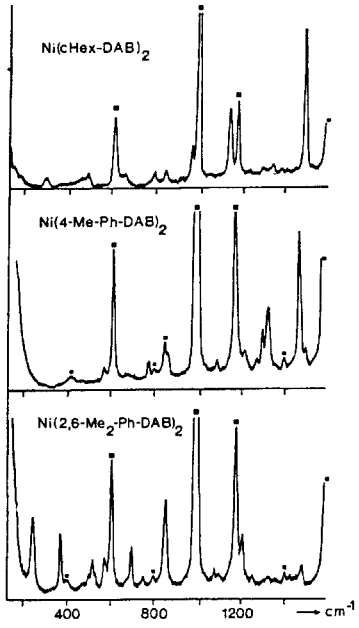

Figure 3.
rR spectra of $Ni(R\text{-}DAB)_2$ complexes (in C_6H_5).

This spectrum shows similar rR effects as the structural analogue $Ni(c\text{-}Hex\text{-}DAB)_2$, which means that the striking differences between the rR spectra of $Ni(c\text{-}Hex\text{-}DAB)_2$ and $Ni(2,6\text{-}Me_2\text{-}Ph\text{-}DAB)_2$ are primarily determined by the change of structure. Based on these results a MO scheme has been calculated for $Ni(CO)_2(2,6\text{-}iPr_2\text{-}Ph\text{-}DAB)$ assuming a distorted tetrahedral geometry (Fig. 4).

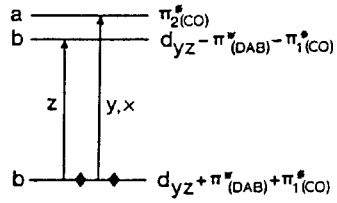

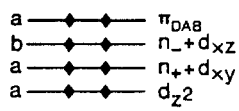

Figure 4.
MO diagram of $Ni(CO)_2$ - $(2,6\text{-}iPr_2\text{-}Ph\text{-}DAB)$.

It is obvious from Fig. 4 that during the main b→b* z-polarized CT-transition in particular the Ni-CO bonds are weakened as the result of the mixing of a π*-CO orbital in both the HOMO and LUMO. This change of Ni-CO bond character during the main transition is reflected in the photochemistry of this compound viz. release of CO as the primary photoprocess.

The photochemical behaviour of both $Ni(CO)_2$(R-DAB) complexes is shown schematically in Scheme I.

$Ni(CO)_2$(t-Bu-DAB)

1. + PR_3 (toluene) —190 K→ Ni(CO)(PR_3)(t-Bu-DAB)
2. + R'-DAB (toluene) —190 K→ $Ni(CO)_2$(R'-DAB)
3. CH_4 matrix 10 K ——→ (no CO dissociation)
4. pentane 168 K ——→ dinuclear complex

(high concentration)

↓↓

Breaking of a Ni-N bond

$Ni(CO)_2$(2,6-iPr_2-Ph-DAB)

1. + PR_3 (toluene) —190 K→ Ni(CO)(PR_3)(2,6-iPr_2-Ph-DAB)
2. + R'-DAB (toluene) —190 K→ Ni(R'-DAB)(2,6-iPr_2-Ph-DAB)
3. pentane 168 K ——→ no reaction

(high concentration)

↓↓

Breaking of a Ni-CO bond

Scheme I. Photochemistry of $Ni(CO)_2$(R-DAB).

Contrary to the $Ni(CO)_2$(2,6-iPr_2-Ph-DAB) complex $Ni(CO)_2$(t-Bu-DAB) shows Ni-N bond breaking leading to the formation of dimers when rather high concentrations of the complex are irradiated at 168 K in pentane. Irradiation causes the breaking of the weakest bond (Ni-N) whereas in the case of $Ni(CO)_2$(2,6-iPr_2-Ph-DAB) that particular bond is broken which is mostly affected upon excitation (Ni-CO). In conclusion it can be said that structural differences exist between $Ni(CO)_2$(R-DAB) complexes which strongly affect both the rR spectra and the photochemical behaviour.

REFERENCES

Andréa RR, Louwen JN, Kokkes MW, Stufkens DJ, Oskam A, (1985) He(I) and He(II) Photoelectron Spectra of Transition Metal Carbonyl Complexes containing a 1,4-diaza-1,3-butadiene ligand. J. Organomet. Chem. 281: 273-289.

Balk RW, Snoeck T, Stufkens DJ, Oskam A (1980) (Diimine)Carbonyl Complexes of Chromium, Molybdenum and Tungsten: Relationship between Resonance Raman Spectra and Photosubstitution Quantum Yields. Inorg. Chem. 19: 3015-3021.

tom Dieck H, Svoboda M, Greiser T (1981) Nickel(0)-bis(chelate) mit Aromatischen N-Substituenten, Z. Naturforsch. 36b: 823-832.

van Dijk HK, Servaas PC, Stufkens DJ, Oskam A (1985) Steric and Electronic Effects on the Quantum Yield of Photosubstitution of CO in $W(CO)_4$(α-diimine) Complexes. Inorg. Chim. Acta, 104: 179-183.

van Dijk HK, et. al., to be published.

von Hausen HD, Krogmann K (1972) Die Kristallstruktur von Dicarbonyl-diacetylbis(dimethylhydrazon)-Nickel(0). Z. Anorg. Allg. Chem. 389: 247-253.

Kokkes MW, Stufkens DJ, Oskam A (1984) Photochemistry of Tricarbonyl (α-diimine) iron complexes. J. Chem. Soc., Dalton Trans.: 1005-1017.

Sieler J, Than NN, Benedix R, Dinjus E, Walther D (1985) Kristallstruktur von 4,6-dimethyl-2,2'-dipyridyl-dicarbonylnickel(0). Z. Anorg. Allg. Chem. 522: 131-136.

Svoboda M, tom Dieck H, Krüger C, Tsay YH (1981) Nickel (0)-bis-(chelate) mit Aliphatischen N-Substituenten. Z. Naturforsch. 36b: 814-822.

$Fe(CO)_3$(R-DAB), A COMPLEX WITH TWO CLOSE-LYING REACTIVE EXCITED STATES

D.J.Stufkens, H.K.van Dijk, and A.Oskam

Anorganisch Chemisch Laboratorium, University of Amsterdam,
Nieuwe Achtergracht 166, 1018 WV Amsterdam, THE NETHERLANDS

INTRODUCTION

The complexes $Fe(CO)_3$(R-DAB)(R-DAB =1,4-diaza-1,3-butadiene;R-N=CH-CH-=N-R), having the structure shown in Fig. 1, possess an intensive absorption band at about 500 nm (Fig. 2). The Resonance Raman (RR) spectra, obtained by excitation into this band, only show RR effects for R-DAB and FeCO deformation modes (Kokkes 1983). This means that the transition involved has no MLCT character but that it is accompanied by a distortion of the complex. Similar results were obtained from m.o. calculations.

Although the lowest excited state (still called '^{3}MLCT' in Fig. 3) is therefore not expected to be reactive, fairly high quantum yields ($\phi \approx 0.2$) are found for the photosubstitution of CO by a nucleophile. This points to the presence of a close-lying reactive LF state and support for this assumption comes from the increase of ϕ upon going to higher energy excitation into the 500 nm band.

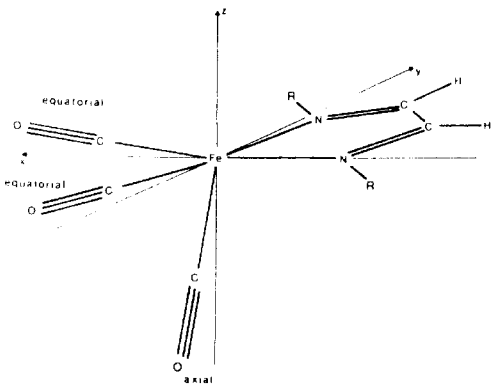

Figure 1.
Molecular Structure
of $Fe(CO)_3$(R-DAB)

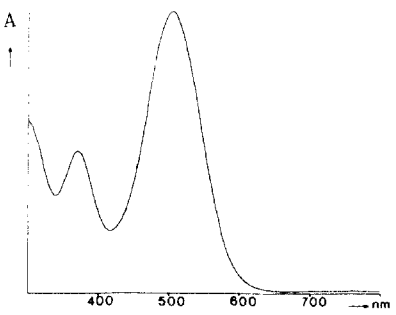

Figure 2
Absorption spectrum of
$Fe(CO)_3$(c-Hex-DAB) in toluene

Photochemistry and Photophysics
of Coordination Compounds, Ed. by H. Yersin/A. Vogler

The transition to the lowest ^{1}LF state is, at least in part, responsible for the absorption band at about 380 nm (Fig. 2). A tentative energy level diagram is shown in Fig. 3. At room temperature the photochemical reaction will preferably take place from the ^{3}LF state, which is much more reactive than ^{3}MLCT. At lower temperature, however, the ^{3}LF state will not be occupied when irradiation takes place at the low energy side of the 500 nm band. In that case only a reaction may occur from the ^{3}MLCT state. Higher energy excitation will, however, lead to occupation of ^{3}LF and to a reaction from that state. Thus, two different photochemical reactions may take place for these complexes at low temperatures , which will be discussed in detail.

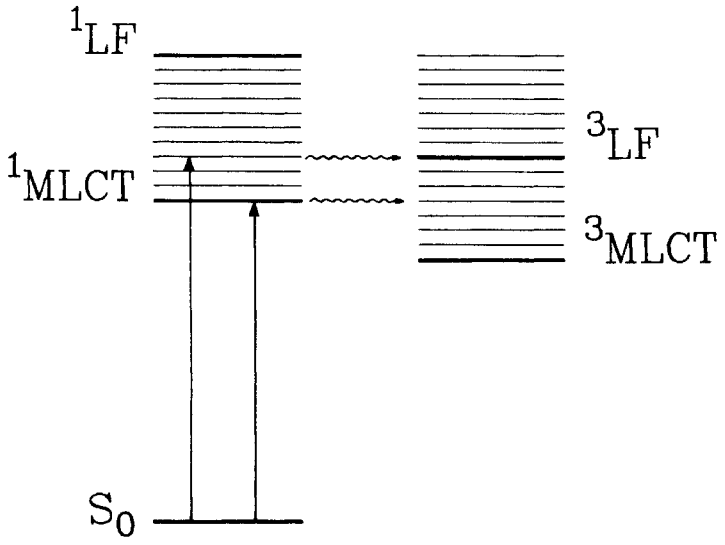

Figure 3. Tentative energy level diagram of $Fe(CO)_3$(R-DAB)

ROOM TEMPERATURE PHOTOCHEMISTRY WITH PHOSPHINES

Irradiation of $Fe(CO)_3$(R-DAB) in the presence of PR_3 causes the photosubstitution of a CO ligand. In the absence of a subtituting ligand no reaction is observed. For the photosubstitution reaction two mechanisms have been proposed (Fig. 4) (Kokkes 1984; Trogler 1986). In

the first mechanism the primary photoprocess is release of CO, in the second one a metal-nitrogen bond is broken first. Flashphotolysis may discriminate between these two mechanisms since substitution of CO by a solvent molecule (mechanism 1) will cause a shift of the 500 nm band to lower energy and breaking of a metal-nitrogen band (mechanism 2) will cause the disappearance of this band. The flashphotolysis results (excimer laser, λ = 308 nm) show that release of CO is the primary photoprocess for all complexes except for $Fe(CO)_3$(t-Bu-DAB). In the latter complex a metal-nitrogen bond is broken.

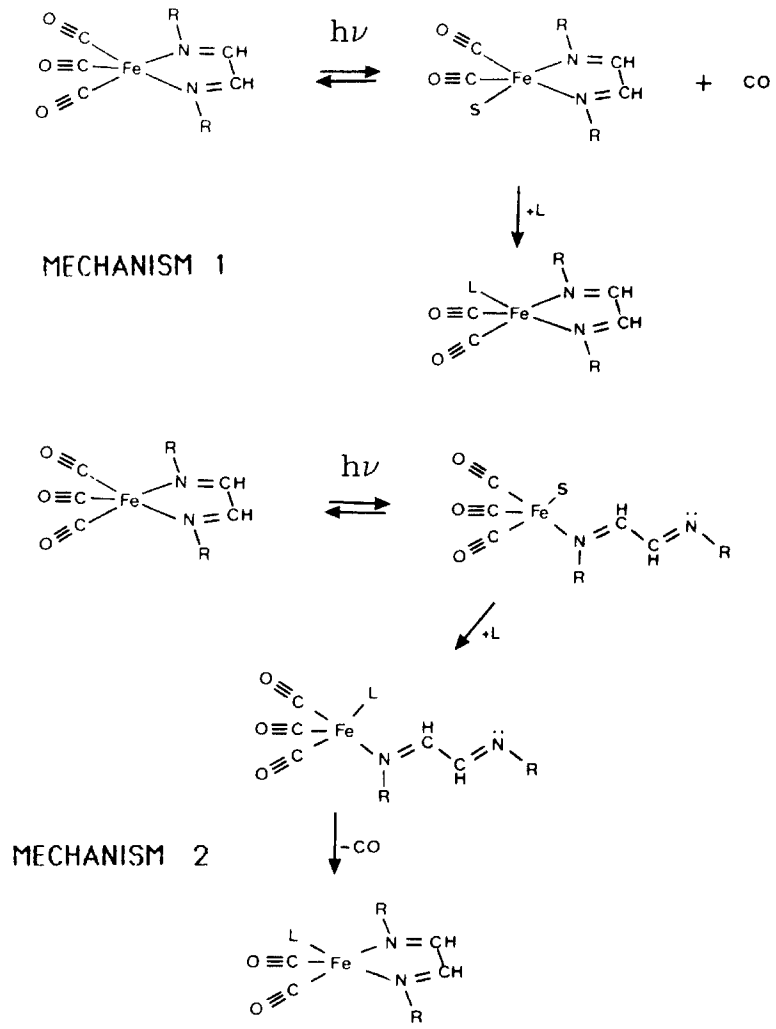

Figure 4. Possible mechanisms for the photosubstitutions of CO in $Fe(CO)_3$(R-(DAB)

By irradiation in n-pentane at 200K in the presence of $P(c\text{-}Hex)_3$, $Fe(CO)_3$(t-Bu-DAB) can be converted quantitatively into $Fe(CO)_3$(σ-N-t-Bu-DAB)($P(c\text{-}Hex)_3$), an intermediate in mechanism 2 in which the t-Bu-DAB is monodentately bonded to iron.

PHOTOLYSIS IN N-PENTANE (T=150K)AND IN LIQUID XENON (P=20BAR,T=170K)
The type of photochemical reaction in n-pentane at 150K depends on the substituent R of the R-DAB ligand and on the wavelength used. Excitation with $\lambda<500$ nm gives a dimeric photoproduct for all complexes except for $Fe(CO)_3$(t-Bu-DAB) which complex does not react. The formation of a dimer is evident from the concentration dependence of this reaction and from the appearance of a low CO-frequency in the bridging carbonyl region. This complex, presumably $Fe_2(CO)_5(R\text{-}DAB)_2$, will be formed by reaction of the primary photoproduct $Fe(CO)_2$(R-DAB)-(S) with the parent compound $Fe(CO)_3$(R-DAB). Upon irradiation with $\lambda>500$nm of an $Fe(CO)_3$(R-DAB) complex with not too bulky substituents R, a completely different reaction with low quantum yield is observed. The 500 nm band disappears and no new bands show up in the visible region. At the same time three new IR bands appear in the CO-stretching region at higher frequencies while no free CO is observed. This means that the photoproduct still contains the $Fe(CO)_3$ moiety. The shift to higher frequencies of the CO-stretching modes points to a decrease of the metal-CO π-backbonding which can only result from a concomitant decrease of π-backbonding to R-DAB. In order to find out whether this increase of π-backbonding to R-DAB is reflected in a frequency decrease of ν_s(CN) of this ligand, the reaction was performed in liquid Xenon (LXe) at 170K. LXe is a very inert solvent in which unstable photoproducts and intermediates can be stabilized (Andréa 1986). A further advantage of this solvent is its complete transparency in IR, Vis and UV. Figure 5 shows the IR spectral changes in the CO-stretching region upon photolysis of $Fe(CO)_3$(c-Hex-DAB) in LXe at 170K with $\lambda=565$ nm. Just as in n-pentane the CO-stretching modes shift to higher frequencies. At the same time ν_s(CN) is lowered in frequency from 1482 to 1364 cm^{-1} (See fig. 6). This increase of metal-R-DAB π-backbonding is explained with a change of coordination of this ligand from σ,σ-N,N' into η^4-CN,CN' as shown in Fig. 7. Support for this explanation is given by the comparison of this photoproduct $Fe(CO)_3$(η^4-R-DAB) with $Fe(CO)_3$(η^4-1,3-butadiene), which complex has nearly the same CO-stretching frequencies.

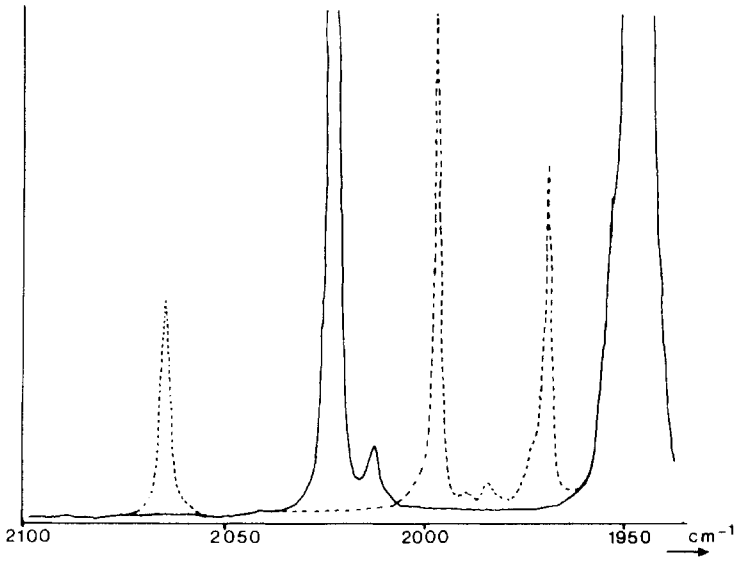

Figure 5. CO-stretching region of the IR spectra of $Fe(CO)_3$(c-Hex-DAB) (——)and its photoproduct (- - - -) in LXe upon irradiation with λ=565 nm at 170K.

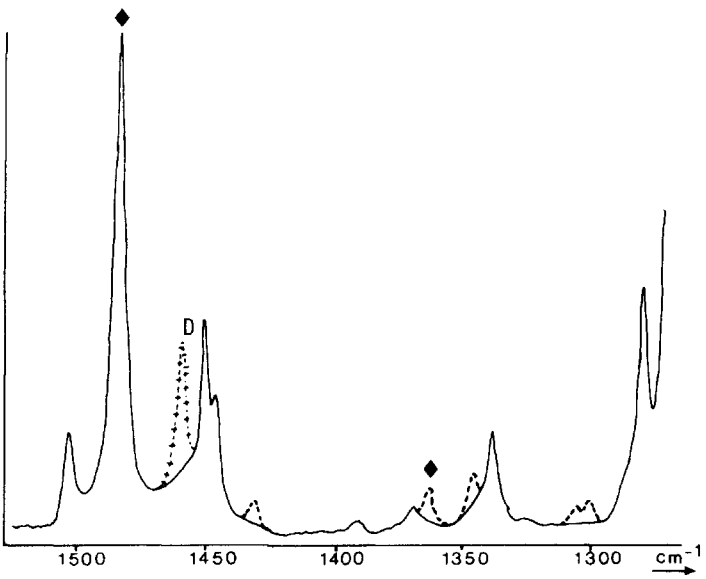

Figure 6. CN-stretching region of the IR spectra of $Fe(CO)_3$(c-Hex-DAB) (——) and its photoproduct (- - -) in LXe upon irradiation with λ=565 nm at 170K. ◆ represents ν_s(CN) of parent compound and photoproduct, D the same vibration of the dimer $Fe_2(CO)_5$(c-Hex-DAB)$_2$.

A similar reaction has been observed before by us in rare gas matrices at 10K (Kokkes 1984). The $Fe(CO)_3(\eta^4$-R-DAB) complexes are thermally unstable. At about 200K they react back to the parent compound.

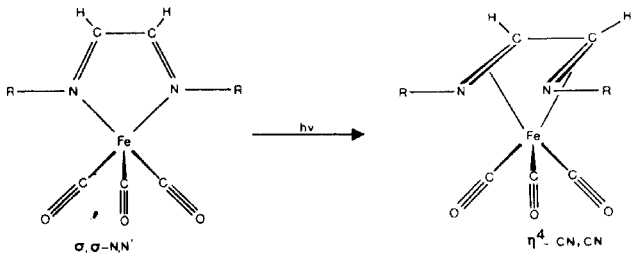

Figure 7. Structural change of $Fe(CO)_3$(c-Hex-DAB) upon photolysis in LXe at 170K with λ=565 nm

So two completely different photochemical reactions are observed at low temperatures depending on the wavelength used. The reaction at low energy, having a low quantum yield, takes place from the ^{3}MLCT state. The change of coordination of the R-DAB ligand, accompanying this reaction, agrees well with the RR effects observed for the deformation modes of the complex. The much more efficient reaction at higher energy takes place from a close-lying ^{3}LF state. Since this reaction at 150K already takes place upon irradiation with λ=500 nm, where no absorption to the lowest ^{1}LF state takes place, direct intersystem crossing from ^{1}MLCT to ^{3}LF is assumed to occur.

REFERENCES

Andréa RR, Luyten H, Vuurman MA, Stufkens DJ, Oskam A (1986) A Cryogenic Cell for Liquid Noble Gases. Appl. Spectroscopy 40: 1184-1190

Kokkes MW, Stufkens DJ, Oskam A (1983) Spectroscopic and Theoretical Studies of [$Fe(CO)_3$(1,4-diaza-1,3-butadiene)] Complexes. J. Chem. Soc., Dalton Trans.: 439-445

Kokkes MW, Stufkens DJ, Oskam A (1984) Photochemistry of Tricarbonyl (α-di-imine)iron Complexes. J. Chem. Soc., Dalton Trans.: 1005-1017

Trogler W (1986) Photochemical Production of Reactive Organometallics for Synthesis and Catalysis. In: Lever ABP (ed) Excited States and Reactive Intermediates, ACS Symposium Series 307. American Chemical Society, Washington, DC, p 177

THE PHOTOCATALYTIC METATHESIS REACTION OF OLEFINS

T.Szymańska-Buzar and J.J.Ziółkowski

Institute of Chemistry, University of Wrocław, 14, Joliot-Curie St.,
50-383 Wrocław, POLAND

INTRODUCTION

Structure of metal complex catalysts for olefin metathesis reaction and its mechanism are intensively studied since many years. Most of catalytic systems involve tungsten complexes combined with alkyl aluminium compound, $WCl_6/C_2H_5AlCl_2$. The currently accepted mechanism is based on carbene complex formation ($W{=}CH_2$) which next coordinates olefins in such a way that the metallocycle may be formed with high selectivity. However, the formation of the first carbene is still controversial. Highly active metathesis catalysts have been prepared only with Mo, W or Re soluble complexes. So, there is also some limitation to the metal. If metal carbonyls are used as catalyst precursors they are often activated photochemically or by addition of Lewis acid type cocatalysts.
Our earlier studies on photocatalytic systems containing $W(CO)_6$ in CCl_4 revealed that in initiation of metathesis reaction of olefin the key role is played by the donor $W(CO)_6$ - acceptor AX_n (CCl_4 or another halides of IIIb or IVb groups element) interactions (Borowczak, Szymańska-Buzar, Ziółkowski 1984). Such donor-acceptor interaction is competitive with that in which an olefin plays the role of the donor. Donor-acceptor interactions could produce the ion pair according to equation:

$$D + A \rightleftharpoons D\text{-}A \rightleftharpoons [\dot{D}^{+}\cdots\cdots\dot{A}^{-}]$$

For the same donor ($D = W(CO)_6$) the position of equilibrium depends on electron affinity of the acceptor ($A = AX_n$). Usually in the presence of a very strong acceptor (AX_n) the formation of C.T. complex could be observed:

$$W(CO)_6 + AX_n \rightleftharpoons [W(CO)_6 \cdot AX_n] \longrightarrow [\dot{W}^{\bullet}(CO)_6^{+}\cdots\cdots\dot{A}X_n^{-}]$$

In a case of weaker acceptors, the light may activate the donor (D) and facilitate its interaction with an acceptor in two ways:

$$W(CO)_6 \xrightarrow{h\nu} \begin{cases} W(CO)_6 \xrightarrow{AX_n} [\dot{W}^{\bullet}(CO)_6^{+}\cdots\cdots\dot{A}X_n^{-}] \\ W(CO)_5 \xrightarrow{AX_n} [(CO)_4W\text{-}CO \longrightarrow AX_n] \end{cases}$$
(-CO)

In this paper we are considering the effect of donor-acceptor interactions of $W(CO)_5L$ type donor (L = CO, py, PPh_3, Cl^-) with AX_n acceptor (AX_n = IIIb and IVab group element halides) on catalytic activity of the system in the light accelerated metathesis of olefins.

Photochemistry and Photophysics
of Coordination Compounds, Ed. by H. Yersin/A. Vogler

METATHESIS OF INTERNAL OLEFINS

The pent-2-ene metathesis reaction was studies with the photocatalytic system containing $W(CO)_5L$ type complexes and $ZrCl_4$. The results are shown in Table 1.

Table 1. Catalytic activity of $W(CO)_5L$ + $ZrCl_4$ system in photochemical metathesis reaction of pent-2-ene (after 30 min.). Reaction mixture contained: $[W(CO)_5L] = 3 \cdot 10^{-3}$ m·l^{-1}; $[ZrCl_4] = 3 \cdot 10^{-2}$ m·l^{-1} [pent-2-ene] = 0.3 m·l^{-1} in n-heptane or chlorobenzene, light source: mercury lamp HB-200, room temperature.

$W(CO)_5L$	pent-2-ene conversion (%)[a]	Oxidative potential $E_{1/2}$ (v)[b]	quantum yield of photosubstitution reaction[c]
$[Et_4N][W(CO)_5Cl]$	44(38)[d]	0.59	10^{-2}
$W(CO)_6$	36	1.86	1
$W(CO)_5py$	30	1.01	0.5
$W(CO)_5PPh_3$	24	1.23	0.3

a - % hex-3-ene x 2
b - Hershberger, Klinger, Kochi, 1982
c - Dahlgren, Zink, 1977
d - in darkness

Pent-2-ene metathesis by the $W(CO)_5L$-$ZrCl_4$ photocatalytic system is highly selective (the only products are but-2-ene and hex-3-ene). The trace amount of propylene and but-1-ene suggests the formation of the primary metallocarbenes as the result of decomposition of the metallocyclobutane complexes.

METATHESIS OF TERMINAL OLEFINS

Metathesis of terminal olefins is often preceded by isomerization reaction which may be favourable. In our photochemical system we have observed the various contribution of the reactions depending on the acceptor AX_n used. Results for $ZrCl_4$ are shown in Table 2. Pent-1-ene photochemical reactions depend mainly on a kind of metal (Table 3).

Table 2. Effect of $W(CO)_5L$ on pent-1-ene photochemical reaction in the presence of $ZrCl_4$ as catalyst (after 2 hrs).

$W(CO)_5L$	pent-1-ene (%)	pent-2-ene (%)	metathesis of pent-1-ene (%)[a]	co-metathesis of pent-1-ene[b] and pent-2-ene (%)	isomerization of pent-1-ene[c] (%)
$W(CO)_6$	25.6	6.5	44.6	23.2	18.1
$[Et_4N][W(CO)_5Cl]$	27.6	1.7	34.4	36.4	19.9
	(49.9)[d]	2.7	25.8	21.6	13.5
$W(CO)_5py$	37.3	3.3	45.8	13.6	10.1
$W(CO)_5PPh_3$	44.3	6.7	16.8	32.2	22.8

a - % oct-4-ene x 2
b - (% hex-2-ene + % hept-3-ene) x 2
c - (% pent-2-ene + % hept-3-ene + % hex-3-ene)
d - no light; reaction conditions: see legend under Table 1 [pent-1-ene] = 0.3 $m \cdot l^{-1}$

Table 3. Effect of $M(CO)_6$ on pent-1-ene photochemical reactions in presence of $ZrCl_4$ as cocatalyst (after 2h)

$M(CO)_6$	pent-1-ene (%)	pent-2-ene (%)	metathesis of pent-1-ene (%)	cometathesis of pent-1-ene and pent-2-ene (%)	izomerization of pent-1-ene (%)
$W(CO)_6$	25.6	6.5	44.6	23.2	18.1
$Mo(CO)_6$	22.6	51.8	traces	25.5	64.6
$Cr(CO)_6$	95.2	4.8	-	-	-

CONCLUSIONS

1. In photocatalytic metathesis and isomerization reactions of olefins the basic role is played by donor-acceptor properties of $M(CO)_5L$ and AX_n molecules, respectively. The most active system is that containing tungsten compound of lowest oxidation potential ($[Et_4N][W(CO)_5Cl]$) and halide AX_n of the highest electron affinity, $ZrCl_4$.

2. Formation of coordinatively unsaturated tungsten compounds suitable to bind the substrates (olefins) depends on photochemical reactivity of $W(CO)_5L$ species and interactions of AX_n-acceptor molecules with L ligand.

3. The internal and terminal olefin metathesis reactions catalyzed by $W(CO)_5L$-AX_n system are light-initiated. Terminal olefins undergo also double bond migration and cross metathesis with internal olefins.

REFERENCES

Borowczak D, Szymańska-Buzar T, Ziółkowski JJ (1984) The effect of light and role of donor-acceptor interactions in olefin metathesis. J Mol Catal 27: 355-365

Dohlgren RM, Zink JI (1977) Ligand substitution photochemistry of monosubstituted derivatives of tungsten hexacarbonyl. Inorg Chem 16: 3154-3161

Hershberger JW, Klinger RJ, Kochi JK (1982) Electron-transfer catalysis. Radical chain mechanism for the ligand substitution of metal carbonyls. J Am Chem Soc 104: 3034-3043

PHOTOCHEMICAL GENERATION OF NINETEEN-ELECTRON ORGANOMETALLIC COMPLEXES AND THEIR USE AS REDUCING AGENTS IN MICELLAR SYSTEMS

D.R.Tyler, V.MacKenzie, and A.S.Goldman

Department of Chemistry, University of Oregon, Eugene, OR 97403, USA

We have discovered a new class of organometallic complexes that are very powerful reducing agents. In some cases these reducing agents have oxidation potentials up to ≈ 2 volts (vs NHE). In addition to being quite powerful, the reducing agents are very versatile and they are easy to generate. Their versatility is demonstrated by their ability to reduce a wide variety of complexes, including organics, inorganics, classical coordination complexes, and organometallic species. Furthermore the reduction reactions can be carried out in aqueous or non-aqueous solvents. Perhaps the most remarkable feature of these reducing agents is their ease of generation; these species form simply by irradiating (generally $\lambda > 500$ nm) a metal-metal bonded carbonyl dimer in the presence of an appropriate ligand.

GENERATION OF NINETEEN-ELECTRON COMPLEXES

Our discovery of these powerful reductants was a result of our investigation into the photochemical disproportionation reactions of metal-metal bonded dimers.

In a series of papers, we established the pathway in Scheme I for the photochemical disproportionation of the $Cp_2Mo_2(CO)_6$ complex (Stiegman et al. 1983; Philbin et al. 1986a):

$$Cp_2Mo_2(CO)_6 \overset{h\nu}{\rightleftharpoons} 2\ CpMo(CO)_3 \qquad \text{initiation} \qquad [1]$$

$$CpMo(CO)_3 + L \overset{K_{eq}}{\rightleftharpoons} CpMo(CO)_3L \qquad [2]$$

$$CpMo(CO)_3L + Cp_2Mo_2(CO)_6 \longrightarrow CpMo(CO)_3L^+ + Cp_2Mo_2(CO)_6^- \qquad [3]$$

$$Cp_2Mo_2(CO)_6^- \longrightarrow CpMo(CO)_3^- + CpMo(CO)_3 \qquad [4]$$

$$CpMo(CO)_3L + CpMo(CO)_3 \longrightarrow CpMo(CO)_3L^+ + CpMo(CO)_3^- \qquad [5]$$

$$\text{Overall:}\quad Cp_2Mo_2(CO)_6 + L \longrightarrow CpMo(CO)_3^- + CpMo(CO)_3L^+ \qquad [6]$$

Scheme I

Photochemistry and Photophysics
of Coordination Compounds, Ed. by H. Yersin/A. Vogler

Analogous mechanisms operate in the disproportionation reactions of other metal-metal bonded dimers (Stiegman and Tyler 1984; Stiegman et al. 1986; Goldman and Tyler 1987).

Note that a key reaction intermediate in Scheme I is the 19-electron $CpMo(CO)_3L$ complex, formed in eq 2.[1] The formation of these 19-electron adducts is quite general as the following equation shows:

$$\underset{17}{ML_n} + L' \rightleftharpoons \underset{19}{ML_nL'} \qquad [7]$$

ML_n = $CpMo(CO)_3$, $CpW(CO)_3$, $Mn(CO)_5$, $CpFe(CO)_2$
L = phosphines, amines, halides, oxygen donors

(The thermodynamics of reaction 7 (Philbin et al. 1986b) and a molecular orbital interpretation of 19-electron complexes have been discussed elsewhere (Stiegman and Tyler 1986).

THE NINETEEN-ELECTRON COMPLEXES AS REDUCING AGENTS

Because the 19-electron complexes formed in the disproportionation reactions are capable of reducing metal-metal bonded dimers ($E_{1/2}$ = -1.4 V vs. Ag^+/Ag, $Mn_2(CO)_{10}$; -1.5 V, $Cp_2Mo_2(CO)_6$; -2.2 V, $Cp_2Fe_2(CO)_4$) they should be capable of reducing substrates with reduction potentials less negative than the metal-metal bonded dimers. This is indeed the case; irradiation of a metal-metal bonded dimer, a ligand, and a reducible substrate generally leads to a reduction of the substrate (and inhibition of the disproportionation chain mechanism). The following equation, using $Cp_2Fe_2(CO)_4$ as the dimer precursor and dppe (1,2-bis(diphenylphosphino)ethane) as the ligand, illustrates the overall process (Stiegman et al. 1984).

$$1/2\ Cp_2Fe_2(CO)_4 + dppe + S \xrightarrow{h\nu} CpFe(CO)(dppe)^+ + S^- \qquad [8]$$

In this reaction, irradiation of the $Cp_2Fe_2(CO)_4$ dimer ($\lambda > 500$ nm) yields a $CpFe(CO)_2$ radical which then reacts with dppe to form the 19-electron reducing agent CpFe(CO)(dppe). Some of the substrates, S, and their reduction potentials ($E_{1/2}$ or E_{pc} vs Ag/Ag^+) for which the reaction proceeds include $CpMo(CO)_3Cl$ (the product is $CpMo(CO)_3^-$) (-1.4 V), $[Ph_4P]_3[Fe(CN)_6]$ ($E_{1/2} > 0$), $Mn_2(CO)_{10}$ (the product is $Mn_2(CO)_5^-$) (-1.7 V), $Re_2(CO)_{10}$ (-2.3 V), Cp_2Co^+ (PF_6^- salt) ($E_{1/2}$ = -1.15 V vs NHE, CH_3CN), Bu-py^+ ($E_{1/2}$ = -1.30 V vs SCE) (the product is $(Bu\text{-}py)_2$) and methyl viologen ($E_{1/2}$ = -0.45 V vs NHE).

We have also demonstrated that systems of $Cp_2Fe_2(CO)_4$ and phosphorus ligands have utility as initiators of electron-transfer-catalyzed

---

1 The phrase "19-electron complex" is used to describe the adducts that form when 17-electron metal radicals react with 2-electron ligands. For further details, see reference 5 in Goldman and Tyler (1987).

(ETC) chain reactions (Bruce et al. 1983). Thus, for example, irradiation of a THF solution of $Ru_3(CO)_{12}$ (4 mM) ($E_{1/2}$ = -0.82 V vs Ag/AgCl), PMe_2Ph (4 mM), and only a catalytic amount of $Cp_2Fe_2(CO)_4$ (0.5 mM), initiates the ETC substitution in reaction 9. (Note that $Cp_2Fe_2(CO)_4$ is the only species in solution which absorbs light at the wavelengths used.) Similar results were obtained with $Os_3(CO)_{12}$ (3.0 mM) ($E_{1/2}$ = -1.16 V vs Ag/AgCl) and $Fe(CO)_5$.

$$Ru_3(CO)_{12} + PMe_2Ph \xrightarrow{Cp_2Fe_2(CO)_4,\ 500\ nm} Ru_3(CO)_{11}(PMe_2Ph) \quad [9]$$

REDUCTION OF CO_2

An extremely powerful reducing agent is formed by irradiation of $W_2(CO)_{10}^{2-}$ and PMe_2Ph, as the following reactions illustrate:

$$W_2(CO)_{10}^{2-} + PMe_2Ph + CO_2 \xrightarrow{h\nu} HCO_2^- + CO_3^{2-} + CO + W(CO)_5PMe_2Ph \quad [10]$$

$$1/2\ W_2(CO)_{10}^{2-} + PMe_2Ph + S \xrightarrow{h\nu} S^- + W(CO)_5PMe_2Ph \quad [11]$$

$S = C_6H_5C(O)C_6H_5$, $C_6H_5C(O)CH_3$

Presumably, the $W_2(CO)_{10}^{2-}$ dimer behaves similarly to the other M-M bonded dimers and upon irradiation forms the 19-electron $W(CO)_5PMe_2Ph^-$ complex which is the reducing agent. $E_{1/2}$ values for the $W(CO)_5PR_3$-type complexes are generally about -2.5 V so the oxidation potential of the $W(CO)_5PMe_2Ph^-$ species is quite extraordinary.

REDUCTIONS IN AQUEOUS SYSTEMS

One of the limitations of the 19-electron reducing agents is that they are generated and used in non-aqueous solvents. This limitation prevents the reduction of many interesting water-soluble substrates. To circumvent this problem, we recently demonstrated that the 19-electron complexes can be generated in micellar (or reverse micellar solutions) containing the water-soluble substrate. A typical procedure is the following. A benzene solution of $Cp_2Fe_2(CO)_4$ and PBu_3 is prepared and added to an aqueous solution containing a surfactant (typically didodecyldimethylammonium bromide) and the substrate. Irradiation (λ > 500 nm) then yields the reduced substrate:

$$Cp_2Fe_2(CO)_4/PBu_3/benzene + S \xrightarrow{h\nu} S^- + CpFe(CO)_2PBu_3^+ \quad [12]$$

S = methyl viologen, $Fe(CN)_6^{3-}$, $Ru(bpy)_3^{2+}$

Formation of the $CpFe(CO)_2PBu_3^+$ product suggests that the reducing agent is the photogenerated 19-electron $CpFe(CO)_2PBu_3$ species.

SUMMARY AND IMPLICATIONS OF THIS WORK

Nineteen-electron complexes form when metal-metal bonded dimers are irradiated in the presence of ligands. The 19-electron complexes are powerful and versatile reducing agents, and they can be used to reduce a variety of organics, inorganics and organometallic complexes in either aqueous or non-aqueous solvent systems. Recent studies from our lab have demonstrated that the reaction of a 17-electron species with a ligand to form the 19-electron species can be thermodynamically "downhill" (Philbin et al. 1986). Given this result, our demonstration of the facile formation of 19-electron species, and the widespread occurrence of 17-electron metal radicals in organometallic chemistry, we feel that 19-electron intermediates should be considered as potential intermediates in numerous reaction systems. In particular, chemists must be wary of ETC mechanisms initiated by electron-transfer from 19-electron complexes as was demonstrated herein. In addition, many radical chain mechanisms involving 17-electron radicals may actually involve ETC mechanisms initiated by electron-transfer from a 19-electron species.

Acknowledgment is made to the donors of The Petroleum Research Fund, administered by the American Chemical Society, the National Science Foundation, and the Air Force Office of Scientific Research for support of the research described in this paper.

REFERENCES

Bruce MI, Matison JG, Nicholson, BK (1983) Radical ion initiated syntheses of ruthenium cluster carbonyls containing tertiary phosphines, phosphates. J Organomet Chem 247: 321-343

Goldman AS, Tyler DR (1987) Nineteen-electron adducts in the photochemistry of $Cp_2Fe_2(CO)_4$. Inorg Chem 26: 253-259

Philbin CE, Goldman AS, Tyler DR (1986a) Back reactions in the photochemical disproportionation of $Cp_2Mo_2(CO)_6$. Inorg Chem 25: 4434-4436

Philbin CE, Granatir, CA, Tyler DR (1986b) Nineteen-electron adducts: measurement of ΔG^0 for the reactions of $CpMo(CO)_3$ with halide ligands. Inorg Chem 25: 4806-4807

Stiegman AE, Tyler DR (1984) Mechanism of the photochemical disproportionation of $Mn_2(CO)_{10}$. Inorg Chem 23: 527-529

Stiegman AE, Tyler DR (1988) Reactivity of seventeen- and nineteen-valence electron complexes in organometallic chemistry. Comm Inorg Chem. 5: 215-245

Stiegman AE, Stieglitz M, Tyler DR (1983) Mechanism of the low energy photochemical disproportionation reactions of $Cp_2Mo_2(CO)_6$. J Am Chem Soc 105: 6032-6037

Stiegman AE, Goldman AS, Leslie DB, Tyler DR (1984) Photochemically generated organometallic radicals as reducing agents. J Chem Soc Chem Commun 632-633

Stiegman AE, Goldman AS, Philbin CE, Tyler DR (1986) Photochemical disproportionation of $Mn_2(CO)_{10}$. Nineteen-electron intermediates and ligand and intensity dependence. Inorg Chem 25: 2976-2979

PROBING ORGANOMETALLIC PHOTOCHEMICAL MECHANISMS WITH QUINONES: PHOTOLYSIS OF $Mn_2(CO)_{10}$

A.Vlček, Jr.

The J.Heyrovský Institute of Physical Chemistry and Electrochemistry, Czechoslovak Academy of Sciences, Vlašská 9, 118 40 Prague 1, CSSR

INTRODUCTION

Quinones have been shown recently to be versatile redox-agents prone to react with a wide variety of reducing coordination and organometallic compounds. The mechanism and nature of the products of these reactions reflect the structure and chemical properties of the transition metal compound (Vlček, Jr. 1982, 1983a, 1986a; Hartl 1986). When quinones are employed as traps for photogenerated intermediates, the investigation of both the reaction product and mechanism of its formation can reveal important information on the nature of the intermediate (Vlček, Jr. 1985, 1986b).

The $Mn_2(CO)_{10}$ exhibits quite complicated photochemistry (Stiegman 1984a; Kobayashi 1985; Meyer 1985). Two primary photo-products, $Mn(CO)_5^{\bullet}$ and $Mn_2(CO)_9$ are formed. In donor solvents, a photodisproportionation to $Mn(CO)_3S_3^+$ and $Mn(CO)_5^-$ takes place via 19-electron $Mn(CO)_{6-m}(S)_m^{\bullet}$, m = 1-3, species formed by solvent (S) addition to $Mn(CO)_5^{\bullet}$. The presence of these species has been inferred mainly from the quantum yield measurements (Stiegman 1984b).

We have carried out the photolysis of $Mn_2(CO)_{10}$ in the presence of ortho- and para-quinones in order to investigate the nature of the aforementioned photointermediates and also to prove the utility of quinones as radical-traps in complicated photoreactions.

RESULTS AND DISCUSSION

The reactivity of quinones with individual intermediates of the $Mn_2(CO)_{10}$ photodisproportionation will now be discussed :

1. No evidence for previously postulated (Foster 1980) thermal and/or photochemical electron transfer between undissociated $Mn_2(CO)_{10}$ and quinones was found.

2. No reaction between $Mn_2(CO)_9$ primary photoproduct and quinones has been observed. (The photoreactivity between $Mn_2(CO)_{10}$ and quinones described below can be quenched by CCl_4, which is known (Hepp 1983) to be much more effective quencher for $Mn(CO)_5^{\bullet}$ than for $Mn_2(CO)_9$.)

Photochemistry and Photophysics of Coordination Compounds, Ed. by H. Yersin/A. Vogler

3. The $Mn(CO)_5^{\bullet}$ has been found to react readily with o-quinones (3,5--di-tert.butyl-1,2-benzoquinone, phenanthrenequinone and o-chloranil) producing Mn^I complexes with chelated o-semiquinone radical anions (SQ = $Q^{\bullet-}$), i.e. $Mn(CO)_4(SQ)$ that is formed in both inert (CH_2Cl_2, toluene) and donor (THF, CH_3CN, 10^{-1}M pyridine in toluene) solvents. Substituted $Mn(CO)_3(S)(SQ)$ species are also produced in the latter solvents. The intensity of corresponding ESR signals (Abakumov 1982; Vlček, Jr. 1986b) increase linearly with the irradiation time. These complexes are apparently formed by an oxidative addition of o-quinones to $Mn(CO)_5^{\bullet}$ producing primarily $Mn(CO)_5(SQ)$ species containing SQ ligand bound by one oxygen atom only (Tumanskij 1981).

No direct reaction between $Mn(CO)_5^{\bullet}$ and p-quinone (2,6-di-tert. butyl-1,4-benzoquinone, p-DBQ takes place. No photoreaction between $Mn_2(CO)_{10}$ and p-DBQ has been found in noncoordinating solvents, whereas more complex behaviour was found in donor solvents (vide infra).

4. The $Mn(CO)_5^{\bullet}$ was postulated to coordinate solvent molecules producing coordinatively saturated $Mn(CO)_{6-m}(S)_m^{\bullet}$, m = 1-3, species that is supposed to play crucial role in the photodisproportionation of $Mn_2(CO)_{10}$ (Stiegman 1984b). These species is known (Meyer 1985; Hepp 1981) to reduce substrates whose reduction potentials are comparable to those of quinones. This 19-electron species can be trapped by p-DBQ : At the begining of irradiation, an intense unresolved ESR signal (g = 2.0051) is formed. In the course of irradiation, its intensity passes through a maximum and then rapidly decreases concomitantly with the appearance of another 13-line signal (g = 2.0048, a_{Mn} = 0.15 mT, a_H = 0.08 mT). This latter signal does not appear when the irradiation was interrupted after the formation of the former. Under low-intensity irradiation, only the formation of the unresolved signal was observed. These results point to the presence of two successive photoreactions that can be interpreted as follows : the $Mn(CO)_{6-m}(S)_m^{\bullet}$ species undergoes an electron transfer with p-DBQ producing a $[Mn(CO)_{6-m}(S_m)^+] \cdot [p\text{-DBSQ}]$ ion-pair characterized by an unresolved ESR signal whose g-value is identical with that of free p-DBSQ (Vlček, Jr. 1986b). This ion-pair undergoes a second photochemical step in which either the solvent or, more probably, a CO-ligand dissociates from the $Mn(CO)_{6-m}(S)_m^+$ part of the ion-pair. The vacant site is then occupied by p-DBSQ anion-radical that acts as an O-bound ligand. In accord with this interpretation only the unresolved ESR signal is observed in the presence of pyridine. Apparently,

strongly coordinating pyridine competes effectively with p-DBSQ for the free coordination site after the second photolytic step.

CONCLUSIONS

Quinones proved to be excellent trapping agents that can be used even to investigate separately several intermediates in a complicated organometallic photoreaction. To gather all available information, not only the nature of the products of the trapping reactions but also the mechanism of their formation has to be followed.

With the use of quinones, the presence and expected chemical properties of key intermediates of the $Mn_2(CO)_{10}$ photodisproportionation was confirmed. The primary radical photoproduct $Mn(CO)_5^{\bullet}$ can either add oxidatively a quinone molecule or coordinate a solvent molecule producing a 19-e^- species reacting via electron-transfer. Despite the similar electron-transfer properties of ortho and para quinone isomers (Vlček, Jr. 1983b), the o-quinones strongly prefer the oxidative addition pathway, whereas their para-isomers react via an electron-transfer provided that the organometallic compound allows for both reactivity paths.

LITERATURE

Abakumov GA, Cherkasov VK, Shalnova KG, Teplova IA, Razuvaev GA (1982) o-Semiquinolate complexes of manganese and rhenium. J Organomet Chem 236: 331-341

Foster T, Chen KS, Wan JKS (1980) An ESR study of the reactions of decacarbonyldimanganese, trimethyltinpentacarbonylmanganese and decacarbonyldirhenium with quinones. J Organomet Chem 184: 113-124

Hartl F, Vlček Jr. A (1986) Oxidative addition of quinones to planar cobalt(II) complexes. Inorg Chim Acta 118: 57-63

Hepp FA, Wrighton MS (1981) Photochemistry of metal-metal bonded complexes. J Am Chem Soc 103: 1258-1261

Hepp FA, Wrighton MS (1983) Relative importance of metal-metal bond scission and loss of carbon monoxide from photoexcited dimanganese decacarbonyl. J Am Chem Soc 105: 5934-5935

Kobayashi T, Yasufuku K, Iwai J, Yesaka H, Noda H, Ohtani H (1985) Laser photolysis study on dimanganese and dirhenium decacarbonyls. Coord Chem Revs 64: 1-19

Meyer TJ, Caspar JV (1985) Photochemistry of metal-metal bonds. Chem Rev 85: 187-218

Stiegman AE, Tyler DR (1984a) Nonhomolytic cleavage pathways in the photochemistry of metal-metal carbonyl dimers. Acc Chem Res 17: 61-66

Stiegman AE, Tyler DR (1984b) Mechanism of the photochemical disproportionation of $Mn_2(CO)_{10}$. Inorg Chem 23: 527-529

Tumanskij BL, Sarbasov K, Solodovnikov SP, Bubnov NN, Prokofev AI, Kabachnik MI (1981) Issledovanie vzaimodeistva pentacarbonylo manganca s ortokinonami. Dokl Akad Nauk USSR 259: 611-615

Vlček Jr A, Klíma J, Vlček AA (1982) Coordinated p-benzosemiquinone radical: formation of $[Co(CN)_5(2,6\text{-di-}Bu^t\text{-}1,4\text{-semiquinone})]^{3-}$. Inorg Chim Acta 58: 75-81

Vlček Jr A, Klíma J, Vlček AA (1983a) The Parallelism in the mechanisms of the one-electron oxidative additions of ortho and para-quinones to $Co(CN)_5^{3-}$. Inorg Chim Acta 69: 191-197

Vlček Jr A, Bolletta F (1983) Oxidative quenching of $Rubipy_3^{2+}$ quinones. Inorg Chim Acta 76: L227-L229

Vlček Jr A (1985) Mechanism of organometallic radical trapping. The oxidative addition of quinones to photogenerated $CpTiCl_2^{\cdot}$. J Organomet Chem 297: 43-49

Vlček Jr A (1986a) Redox reactivity of photogenerated $Cr(CO)_5$ species: formation of $[Cr^{III}(o\text{-semiquinone})_3]$ complexes. Inorg Chem 25: 522--526

Vlček Jr A (1986b) Mechanism of the photochemistry of $Mn_2(CO)_{10}$ in the presence of para- and ortho-quinones. J Organomet Chem 306: 63-75

LASER FLASH PHOTOLYSIS OF PHOSPHINE-SUBSTITUTED DIMANGANESE CARBONYL COMPOUNDS

K.Yasufuku, N.Hiraga, K.Ichimura*, and T. Kobayashi*

Institute of Physical and Chemical Research, Wakoshi, Saitama 351, JAPAN
* Department of Physics, University of Tokyo, Bunkyoku, Tokyo 113, JAPAN

Introduction

There has been considerable interest in the photochemical reaction of metal-metal bonded dimetal carbonyls, $L(OC)_4M\text{-}M(CO)_4L$. Two primary processes, (1) metal-metal bond homolysis to produce radical fragments and (2) CO dissociation without metal-metal bond cleavage, were well established in the cases of M = Mn, L = CO (Yesaka 1981, 1983; Rothberg 1982; Hepp 1983; Church 1984) and M=Re, L=CO (Yasufuku 1984). The ratio of the processes (1)/(2) and the effect of irradiation wavelength were evaluated for M=Mn, L=CO (Kobayashi 1985).

$$L(OC)_4M\text{-}M(CO)_4L \xrightarrow{h\nu} \begin{cases} 2\ \cdot M(CO)_4L & \text{Process(1)} \\ M_2(CO)_7L_2 + CO & \text{Process(2)} \end{cases}$$

The occurrence of the process(2) has been of rather unexpected event because of the suggestion of the process(1) being a sole consequence of photoexcitation based on a simple MO scheme. In one particular case, no metal-metal bond photocleavage has been proven for the formation of $Mn_2(CO)_{10}$ from the compound, $Me_2Sn[Mn(CO)_5]_2$ (Yasufuku, unpublished result). Thus, it is of particular interest to study on the substituent effect of phosphorus ligands on the photochemistry of the dimanganese carbonyls (L=phosphines and phosphites): on the radical recombination reaction [Process(5)], on the reaction of $Mn_2(CO)_7L_2$ with CO [Process (6)], and on the ratio of the processes (1)/(2).

$$2\ \cdot Mn(CO)_4L \xrightarrow{k_5} L(OC)_4Mn\text{-}Mn(CO)_4L \qquad \text{Process(5)}$$

$$Mn_2(CO)_7L_2 + CO \xrightarrow{k_6} \text{"} \qquad \text{"} \qquad \text{Process(6)}$$

Ligand effects of some phosphorus ligands on the processes(5) and (6) were reported separately (Walker, Herrick 1984), however, no information on the ratios of the processes(1)/(2) has been available. Here we describe the effects of the phosphorus ligands on the whole photochemistry of the title compounds and another process newly found in the cases of L having only n-alkyl substituents.

Experimental

The third harmonics (355 nm) of a Q-switched Nd:YAG laser was used as an excitation light source. Stationary and pulsed Xe lamp (350 W) and $W\text{-}I_2$ lamp were used as monitoring light sources. The excitation light beam was aligned coaxially with the monitoring light path (l=0.1 cm) at the desired wavelength. Compounds used were synthesized by following the reported methods. Sample solutions were prepared in vacuo. Solvent (cyclohexane, benzene, or 2-methyltetrahydrofuran) stored on K-Na alloy was added in the sample compartment after measuring its volume and the sample cells were hermetically sealed. Then, CO or Ar gas was admitted into them through a side arm with a teflon stop cock.

Photochemistry and Photophysics
of Coordination Compounds, Ed. by H. Yersin/A. Vogler

Results and Discussion

As does the parent compound (L=CO), $L_2Mn_2(CO)_8$ show the transient absorptions at around 550 nm and 800 nm. A solid line in Fig.1 shows the transient spectrum of L=P(n-Bu)$_3$ observed in cyclohexane 1 μs after 355 nm excitation. It represents the common appearances of the transient absorption for all L. The absorbances around at 800 nm disappear by following the second order kinetics under either Ar or CO atomosphere and the decay changes into the pseudo-first order when CCl_4 is present in the systems (Fig.2a and 2b for L=P(n-Bu)3).

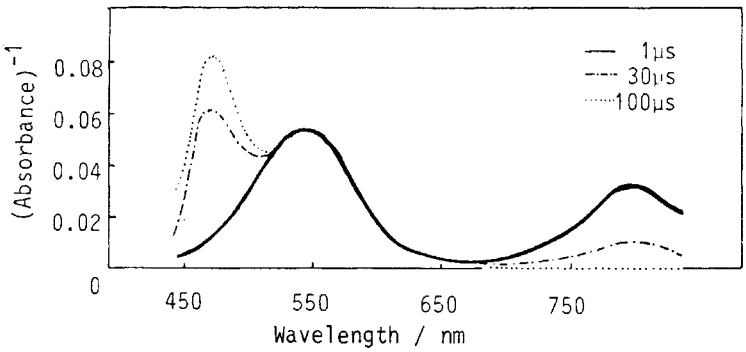

Figure 1. Transient absorption spectra of L=P(n-Bu)$_3$ in cyclohexane 1, 30, and 100 μs after 355 nm excitation.

On the other hand, the absorbances around at 550 nm have longer life time under Ar atomosphere, but their decay becomes faster and follows the first order kinetics (Fig.2c for L=P(n-Bu)$_3$). Addition of CCl_4 has no effect on their decay kinetics. These evidences show that the two processes (1) and (2) also take place concurrently in these systems.

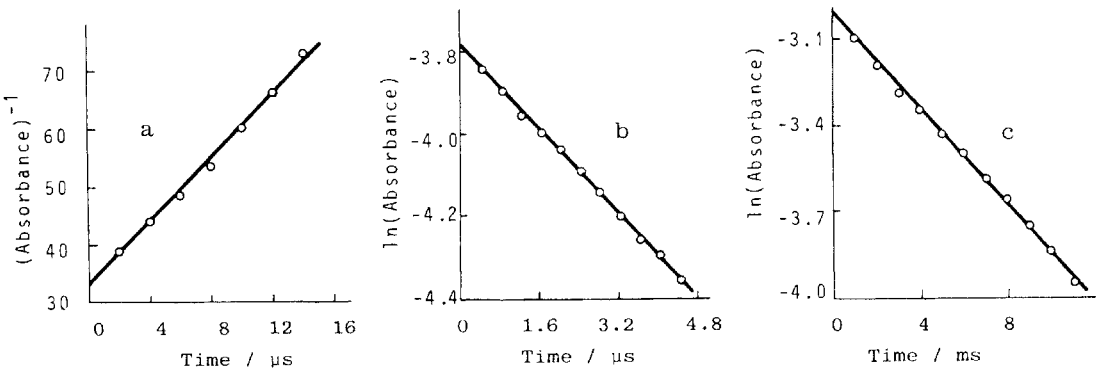

Figure 2. Time dependence of absorption of L=P(n-Bu)$_3$ under 1 atm. of CO in cyclohexane after 355 nm excitation observed at: (a) 800 nm, (b) 800 nm in the presence of 4.2×10^{-2} mol l^{-1} of CCl_4, and (c) 550 nm.

The second order rate constants of the processes(5) and (6) for each L were determined and listed in Table 1 together with those reported by Brown(1984). The values of k_5 were obtained based on the radical concentrations estimated from the transient decrease of the starting absorbances at 380 nm which also follow stepwise recovery corresponding to the processes(5) and (6). The k_6 values were derived from the pseudo first order rate constants obtained under 1 atomospheric pressure of CO (by using [CO] in cyclohexane = 1×10^{-2} mol l^{-1}).

Ligand Effect on the Processes(5) and (6)

The values obtained here and those of Brown's are fairly in good agreement. These show that the ligand bulkiness mainly governs the rates of both processes(5) and (6). Since these phosphorus ligands all occupy the axial positions to the Mn-Mn bond, the effect in k_5 may be explained by repulsion between the equatrial CO ligands on each Mn atoms through which the phosphorus ligands influence the stability of the metal-metal bond in the ground state.

The appearance of rather significant steric effect in k_6 indicates that the equatorial ligand, CO, is photoeliminated so that the axial phosphorus ligand may block the site for CO re-ligation. If the axial ligand was eliminated, the k_6 might be larger and closer to the value of the case L=CO.

Table 1. Bimolecular Rate Constants for Radical Recombination of $\cdot Mn(CO)_4L$, k_5, for Recombination of $Mn_2(CO)_7L_2$ with CO, k_6, and Relative Ratio of the Processes (1) and (2).

L	k_5 *1	k_6 *1	Ratio *2 (1)/(2)	θ *3
CO	9×10^8	4×10^5 (3×10^5)	1.1	95
$P(OEt)_3$	4×10^8	4×10^3	2.2	109
$P(OPh)_3$	2×10^8 (9×10^7)	3×10^4	1.0	130
$P(Oi\text{-}Pr)_3$	2×10^8	3×10^4 (4×10^4)	1.8	130
PEt_3	9×10^8	7×10^3	0.8	132
$P(n\text{-}Pr)_3$	5×10^8	7×10^3	1.7	132
$P(n\text{-}Bu)_3$	2×10^8 (1×10^8)	7×10^3 (9×10^3)	1.1	132
$P(i\text{-}Bu)_3$	7×10^7 (2×10^7)	2×10^3 (2×10^3)	1.4	143
PPh_3	(1×10^7)			144
$P(i\text{-}Pr)_3$	3×10^6 (4×10^6)	2×10^2 (1×10^2)	1.3	160

Values in parenthesis (Walker and Herrick 1984)
*1 mol^{-1} dm^3 s^{-1}; *2 Of the systems by 355 nm excitation;
*3 Ligand steric parameters (Tolman 1977)

Effect on the Ratio of the Processes (1)/(2)

In addition to the above observations, the ratio in the occurrence of the processes(1) and (2) could be determined for each L (Table 1). The values are a little scattered in the range of 0.8-2.0, however it can be safely noted that in the photochemical event, the phosphorus ligand may not affect on the excited state nature of the metal-metal bonding. This is in quite contrast with the ground state events mentioned above. For example, the compound of $L=P(i\text{-}Pr)_3$, which undergoes very facile metal-metal bond cleavage in the dark, shows almost the same in the ratio of the processes (1)/(2) to those of the thermally very stable analogs.

Occurrence of a Third Process

Bisides aforementioned ligand effects, a new phenomenon has been observed in the photolysis of $L=P(n\text{-}Bu)_3$. Another transient absorption with λ_{max} around 470 nm grows in 100 μs and disappears within 2 ms (Fig. 3).

The absorbance at 380 nm recovers with three steps and the kinetics of each step corresponds to the process(5), the disappearance of the absorption at 470 nm, and the process(6) under CO atomosphere showing that the third compornent decays also back the starting compound. Both the growth and decay of the absorbance at 470 nm follow the first order kinetics and the covering gas (Ar or CO) has no effect on the kinetics. Solvent (cyclohexane, benzene, or tetrahydrofuran) does not almost affect it's rate. Addition of CCl_4 quenches the occurrence of the third compernent. These facts strongly suggest the presence of a third process to give an unknown intermediate which may secondary give the compornent with λ_{max} at 470 nm. It deserves further study on the nature of the new process, but noteworthy is that the third compornents appear only in the cases of L=PR_3, R= n-alkyl. When R=Me, i-Pr, or Ph, the primary processes are simply (1) and (2).

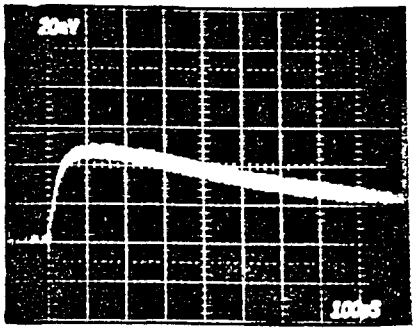

Figure 3. Growth and decay of the absorbance at 470 nm: 1 div.= 100 μs.

References

Yesaka H, Kobayashi T, Yasufuku K, Nagakura S (1981) Laser Photolysis of Dimanganese Decacarbonyl. Reza-Kagaku Kenkyu 3: 97-99

Yesaka H, kobayashi T, Yasufuku K, Nagakura S (1983) Laser Photolysis Study of the Photosubstitution in Dimanganese Decacarbonyl. J Am Chem Soc 105: 6249-6252

Rothberg LJ, Cooper NJ, Peters KS, Vaida V (1982) Picosecond Dynamics of Solution-Phase Photofragmentation of $[Mn_2(CO)_{10}]$. J Am Chem Soc 104: 3536-3537

Hepp AF, Wrighton MS (1983) Relative Importance of Metal-Metal Bond Scission and Loss of Carbon Monoxide from Photoexcited Dimanganese Decacarbonyl: Unsaturated, CO-Bridged Dinuclear Species in Low-Temperature Alkane Matrices. J Am Chem Soc 105: 5934-5935

Church SP, Hermann H, Grevels F-W, Schaffner K (1984) The Primary Photoproducts of $Mn_2(CO)_{10}$: Direct I.R. Observation and Decay Kinetics of $Mn(CO)_5$ and $Mn_2(CO)_9$ in Hydrocarbon Solution at Room Temperature. J Chem Soc Chem Commun 785-786

Yasufuku K, Noda H, Iwai J, Ohtani H, Hoshino M, Kobayashi T (1985) Laser Photolysis Study of Dirhenium Decacarbonyl: Evidence for a Non-radical Primary Process. Organometal 4: 2174-2176

Kobayashi T, Ohtani H, Noda H, Teratani S, Yamazaki H, Yasufuku K (1986) Excitation Wavelength Dependence of Photodissociation and the Secondary Laser Pulse Photolysis of Dimanganese Decacarbonyl. Organometal 5: 110-113

Yasufuku K, Noda H, Onaka S, Teratani S, Kobayashi T (to be published) Laser Flash Photolysis Study of Dimethylbis[pentacarbonylmanganese]-tin(II), 2(Mn-Sn).

Walker HW, Herrick RS, Olsen RJ, Brown TL (1984) Flash Photolysis Studies of Dinuclear Manganese Carbonyl Compounds. Inorg Chem 23: 3748-3752

Herrick RS, Brown TL (1984) Flash Photolytic Investigation of Photoinduced Carbon Monoxide Dissociation from Dinuclear Manganese Carbonyl Compounds. Inorg Chem 23: 4550-4553

Tolman CA (1977) Steric Effects of Phosphorus Ligands in Organometallic Chemistry and Homogeneous Catalysis. Chem Rev 77: 313-348

TOPIC 6

Methods, Applications, and Other Aspects

ELECTRON TRAPPING IN COLLOIDAL TiO_2 PHOTOCATALYSTS: 20 ps TO 10 ns KINETICS

C.Arbour, D.K.Sharma, and C.H.Langford

Canadian Centre for Picosecond Laser Flash Photolysis, Concordia University, 1455 West, de Maisonneuve, Montreal (Quebec) H3G 1M8, CANADA

ABSTRACT

The trapping of excess electrons in surface sites in < 0.05 um colloidal particles of TiO_2 in acid media has a time constant near 2 ns, independently of the excess electron population being produced by injection from an excited dye or hole scavenging. It is suggested that this relatively long lived state is one involved in electron transfer to solution acceptors in photocatalytic processes.

INTRODUCTION

Titanium dioxide photocatalysis has been studied since the 1930's. The effort to avoid degradation of organic matrices containing the oxide as a white pigment stimulated an active program of "anti-photocatalytic" research. The results were methods to deactivate TiO_2 surfaces. Since the striking report of the photoassisted electrolysis of water by Fujishima and Honda in 1972, the direction of research has reversed. Beyond photolysis of water, major initiatives have included the Krautler-Bard (1977) photo-Kolbe reaction and photochemical degradation of refractory chlorinated aromatics introduced by Carey et al. (1976) and Carey and Oliver (1980).

The development of techniques for working with colloidal photocatalytic TiO_2 by Duonghong et al. (1981) has made it possible to analyze the elementary events which occur in photocatalytic reactions using the tools of flash photolysis. There are two essential questions which must be addressed in analysis of either photoxidation or photoreduction: what is the rate of interfacial electron transfer, and what is the fate of carriers generated in TiO_2?

Early work indicated that fast electron transfer occurs with adsorbed partners. Early subnanosecond studies confirmed electron injection from Erythrosin B in CH_3CN in less than 250 ps (Kamat and Fox, 1983) and injection from adsorbed excited tetrasulfonato copper phthalocyanine in less than 100 ps (Kirk et al. 1984). It will be reported below that hexasulfonated tris (phenanthroline)ruthenium(II) captures holes from excited TiO_2 in less than 50 ps.

The fate of carriers in TiO_2 was first elucidated by flash photolysis studies by Henglein (1982) and Bahnemann et al. (1984). An electron spectrum in TiO_2 (pH = 1.5) was established by electron injection from radiolytically generated organic radicals. This spectrum has a peak near 625 nm and a shoulder near 500 nm. The exact shape of the spectrum varies with details of the preparation of the colloids. This spectrum was also generated by adsorption of polyvinyl alcohol (PVA) on the TiO_2 followed by direct irradiation of the colloid at 347 nm. PVA yields the electron spectrum by scavenging holes, h^+, to allow an electron build-up in preference to recombination. The reaction with PVA is "rapid" on the time scale of 15 ns. The decay of the electron signal is slow on microsecond time scale unless an electron acceptor is present in the solution. Henglein et al. assumed that electrons are trapped near the surface.

The nature of a trapped electron remaining after steady-state irradiation is elucidated by ESR recorded at 77 K (Howe and Graetzel,

Photochemistry and Photophysics
of Coordination Compounds, Ed. by H. Yersin/A. Vogler

1985). Two signals are observed which may be assigned to Ti^{3+}. A small signal is associated with interstitial ions in anatase. The larger signal resembles Ti^{3+} in silicate glasses and shows an environmental sensitivity (e.g. pH response) suggestive of a surface location.

As Bahnemann et al. (1984) summarized the matter: "photocatalytic reactions in TiO_2 sols can be achieved with sizable yields only if two scavengers are present (one for e^-, one for h^+) and at least one of them is adsorbed on the colloidal particles. It is the adsorbed scavenger which determines the yield of the reaction of the non-adsorbed one". Recombination can be fast, scavenging by adsorbed molecules can be fast, and trapped excess carriers can be long lived.

Recently, Rothenberger et al. (1985) have provided direct picosecond information on the recombination process in the absence of scavengers. Using a 25 ps pulse of about 2.5 mw power at 355 nm (Nd/YAG third harmonic), a transient is produced which decays with a time constant of less than 500 ps. The decay is a second order process depending on the square of the number of photons initially absorbed. The decay is attributed to hole-electron recombination. The interesting point is that the spectrum does not agree with the spectrum of the surface trapped electron reported before or the spectrum of electrons seen at pH = 3 after steady state or long pulse irradiation by Kolle, Moser, and Graetzel (1985). The transient which arises in the absence of scavenging has a maximum at an energy near but to the blue of 600 nm and does not drop sharply toward the blue.

The spectrum obtained in the absence of scavengers appears promptly at a 20 ps probe pulse delay and decays in a second order process. It is a flat band with a maximum somewhat to the blue of the other spectra obtained at longer times. It seems probable that there are two forms of transients associated with carriers in TiO_2. One is produced promptly on excitation with greater than band gap photons. The other arises after development of an excess electron population and has a long lifetime.

EXPERIMENTAL

TiO_2 colloids were prepared by the slow addition of $TiCl_4$ to cold water. Concentrations were varied between 1.0 and 16 g/L. The pH of solutions was near 1 and were not raised. The size of the particles varied as a function of both the concentration and the details of preparation. The particle size estimation was based on the shift to the blue of the absorption edge as the particle size becomes small as described by Nozik (13). The procedure was calibrated by dynamic light scattering studies of parallel preparations. (We thank Prof. Janos Fendler for assistance with these measurements and access to his equipment.)

The dyes were the tetrasulfonated copper phthalocyanine used previously (Kirk et al., 1984), a hexasulfonate derivative of trisphenanthrolineruthenium(II) which is tetraanionic and was the generous gift of Dr. Ann English, and commercial erythrosin.

Picosecond flash photolysis experiments were carried out using a Nd/YAG mode locked laser in the second and third harmonic modes (562 nm and 355 nm). The pulse width is 30 ps and the zero of time is adjusted at the maximum when 50% of the pulse has passed. A fraction of the fundamental of the excitation pulse is passed through a cell containing D_2O to generate a continuum pulse useful for probing the absorption spectrum from 425 to 675 nm. The probe pulse, which has the same time profile as the excitation pulse, is delayed from 20 ps to 10 ns from the centre of the excitation pulse. Each spectrum is the result of averaging ten shots.

RESULTS

a. **Absorption spectra.** The particle size of the TiO_2 may be monitored by recording the absorption spectrum of TiO_2. Up to a particle size of 0.025 um, the observed band edge shifts toward the red. This is illustrated by the spectra shown in Fig. 1 for samples of TiO_2 at concentrations of 1.0 to 16 g/L. In addition to the increase of concentration, this series reflects an increase of particle size and the red shift is observable. The particle size range in our experiments was calibrated by the study of independently prepared samples which were examined by dynamic light scattering.

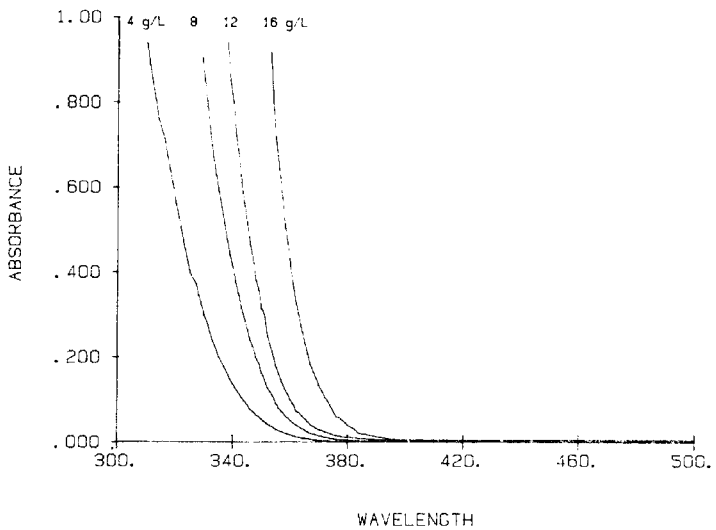

Figure 1. The absorption spectra of TiO_2 colloids. Absorptivity is given in absorbance/gm.

b. **Picosecond flash photolysis.** Figure 2 exhibits the spectrum obtained on flashing TiO_2 alone. The transient observed is present promptly 20 ps after the 355 nm pulse. Its decay is nearly complete within 1 ns. These observations are entirely concordant with those of Rothberger et al. (1985).

Figure 3 shows a representative transient spectrum for a sample of TiO_2 of 1.3 g/L with 6.7 X 10^{-5} M tetrasulfonated copper phthalocyanine ($CuPcS^{4-}$) adsorbed on the oxide (as demonstrated by the fact that the colour of the dye may be removed along with the colloid by filtration or centrifugation). Initially (20 ps), bleaching of the dye and excited state absorption centred at 520 nm are observable. At 100 ps, bleaching and new absorbances are in approximate balance and the absorbance change lies near zero at all wavelengths. Subsequently, the strong absorption in the red grows in.

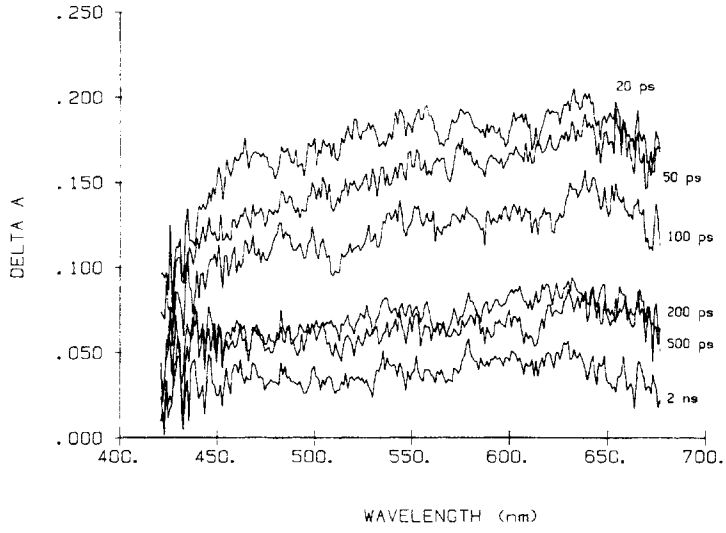

Figure 2. Subnanosecond transients in TiO_2 after irradiation with 2.5 mJ, 20 ps half width, Nd/YAG third harmonic pulses at 355 nm. The particle size is near 500 A. The concentration is 18 g/L.

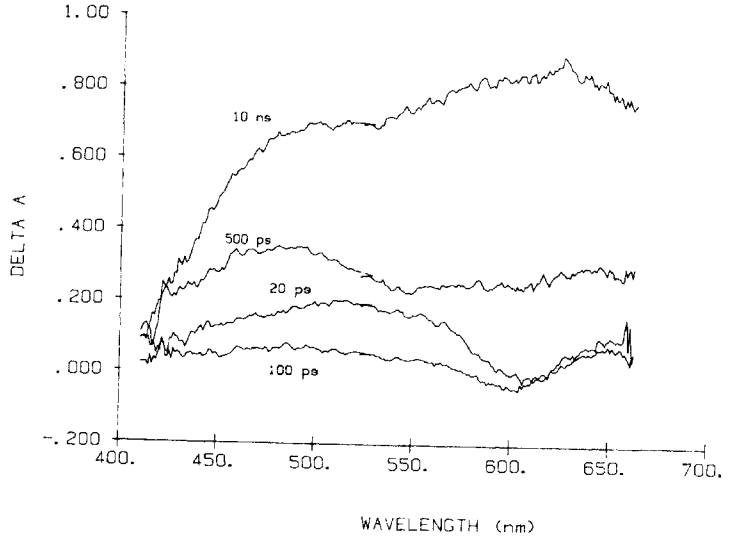

Figure 3. Transient spectra under spectrometer conditions of previous figure for TiO_2 - $CuPcS_4^-$ system.

Figure 4 presents a representative experiment using the anionic Ru(II) complex adsorbed on TiO_2. In the particular case, the solution contains 2.5 X 10^{-5} M hexasulfonated tris(phenanthroline)ruthenium(II) ($Ru(phen)_3S^{4-}$) adsorbed onto 4.0 g/L of TiO_2 of approximately 50 A particle size. In this system, the colloid has a band gap absorbance at 355 nm of 0.20. The Ru(II) complex has an absorbance of 0.08. At 20 ps, absorbance due to direct excitation of TiO_2 is observable. It decays rapidly. The red band observed previously has grown considerably at 5ns.

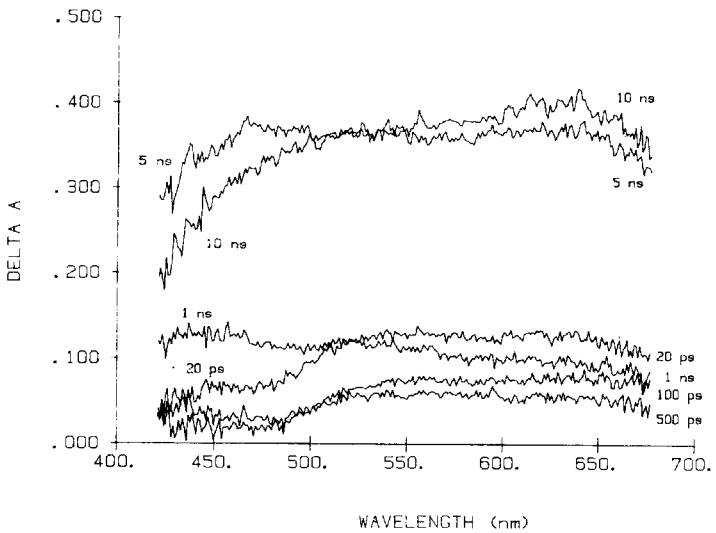

Figure 4. Transient spectra for $Ru(phen)_3S^{4-}$ - TiO_2 system under spectrometer conditions of Figure 2.

Figure 5 shows a final set of transients for 1.2 X 10^{-6} M erythrosin adsorbed onto 4.0 g/L TiO_2. Bleaching at the center of the spectrum due to the loss of the strong absorption of the dye depresses the spectrum at all times recorded, but the growth of red transient is again observable.

The growth of the signal in the red has been evaluated kinetically using 625 nm as the monitoring wavelength. In eight solutions of the $CuPcS^{4-}$ over the particle size range the rate constant was 8 6 X 10^8 s^{-1}. For four samples of colloids sensitized with the Ru(II) complex, the rate constant was 6.5 1 X 10^8 s^{-1}. For the single particle size used with erythrosin the rate constant was 5.5 1 X 10^8 s^{-1}. The rate constants are indistinguishable as the sensitizer varies. In contrast, there may be some real variation with particle preparation, although this is not established. Although it is difficult to correct the spectra for the spectra of the sensitizers, the extinction coefficient of the red band is approximately 2 X 10^4 M^{-1} cm^{-1}.

It is also important to observe that the kinetics are the same whether the primary absorber is the sensitizer or the TiO_2 colloid itself.

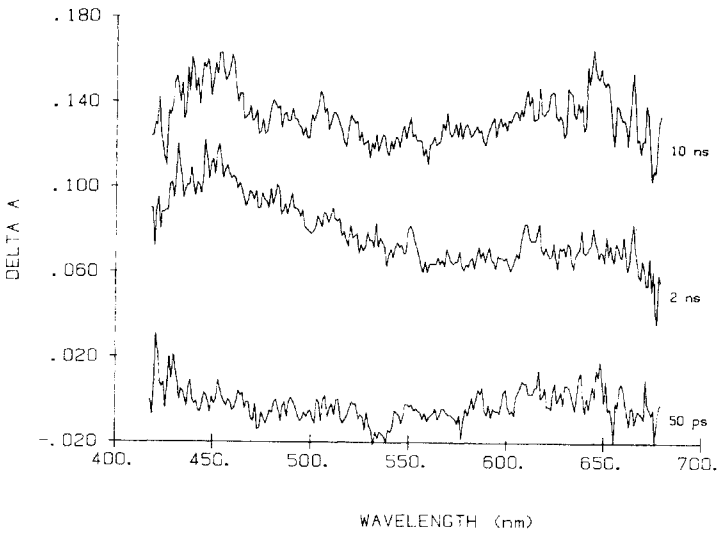

Figure 5. Transient spectra for the erythrosin -- TiO_2 system.

DISCUSSION

There are three aspects of the present experiments which can be analyzed to lead to a reasonable interpretation. These are the kinetics of the growth of the signal in the red, the extinction coefficient of the red band, and the spectral shape of the absorbance. The first point is the kinetic behaviour.

In all three cases, the choice of sensitizer is unimportant to the rate of growth of the red band. Nevertheless, a sensitizer is important to the growth of the red band. The role of the sensitizer is to ensure an excess of electrons. Analysis of the energetics of each of the sensitizers indicates that they can participate in two processes. The excited dyes are capable of injecting electrons into the conduction band of TiO_2. Similarly, a hole in the TiO_2 valence band can oxidize the dyes. Thus, either or both of the excitation processes taking place can lead to development of excess electrons in the colloid.

There are two possibilities for the origin of the red transient with a "grow in" time of ~2 ns which are consistent with the independence of the sensitizer. Either the process is a trapping process in the colloid or it is the formation of a solvated electron in the solution. The intensity of the red transient is greater than the transient produced initially or when TiO_2 alone is excited. The observed value is very close to that reported for a solvated electron (14). However, the absorption maximum is not identical to solvated electron spectra in water. Moreover, the rate constant for proton quenching of a hydrated electron is 2.1×10^{10} M^{-1} s^{-1} (Hart, 1965). In a solution at pH = 1, the lifetime of a solvated electron should be near one ns. The solvated electron explanation seems to be excluded.

In contrast, an extinction coefficient near that of the solvated electron and a spectrum with peaks similar to those first described by Bahnemann et al. (1984) at 500 nm and 625 nm is consistent with the ESR evidence for a Ti^{3+} species in the surface of the particle. The two bands are reasonably those of a TiO_6 d-d band and a broadened red shifted band corresponding to delocalization of the acceptor

orbital. It appears that the band which grows in with a time constant of ~2 ns is related to bands associated with electron transfer from TiO_2.

It is important to realize that "surface" states of hydrous oxides colloids may not be entirely like surface states of crystals. Hydrous oxide colloids may be "water swollen gels" with the entire structure of a small particle in contact with "solvent" and accessible as a site for adsorption of a sensitize. Thus, the state which is described may not correspond to a state in crystalline TiO_2.

A final question presents itself. What is the nature of the rapidly decaying signal seen when electrons and holes are generated in equal numbers? This is not a question to which a definitive answer can be given from the available evidence. However, one possibility does suggest itself. A spectrum for excess holes was presented early on (Bahnemann et al., 1984). It includes a band in the blue.A combination of that band envelope and a gently rising absorbance to the red could produce the broad envelope of the sort seen in a situation where a sum of an electron and a hole spectrum should be expected.

REFERENCES

Bahnemann, D., Henglein, A., Lilie, J., and Spanhel, L., (1984), J. Phys. Chem., 88, 207.

Carey, J.H., Lawrence, J., and Tosine, H.M., (1976), Bull. Envir. Contam. Toxic., 16, 697.

Carey, J.H. and Oliver, B.G., (1980), Water Poll. Res. J. Canada, 15, 157.

Duonghong, D., Borgarello, E., and Graetzel, M., (1981), J. Amer. Chem. Soc, 103, 4685.

Fujishima, A. and Honda, K., (1972), Nature, 238, 37.

Hart, E.J., (1965), "The Solvated Electron", ACS Advances in Chemistry, American Chemical Society, Washington, DC., p.51.

Henglein, A., (1982), Ber. Bunsenges., 86, 241.

Howe, R.F. and Graetzel, M., (1985), J. Phys. Chem., 89, 4495.

Kamat, P.V. and Fox M.A., (1983), Chem. Phys. Letts., 102, 379.

Kirk, A.D., Langford, C.H., Saint-Joly, C., Sharma, D.K., and LeSage, R., (1984), JCS Chem Comms., 961.

Kolle, U., Moser, J., and Graetzel, M., (1985), Inorg. Chem., 24, 2253.

Krautler, B. and Bard, A.J., (1977), J. Amer. Chem. Soc., 99, 7729.

Nozik, A. et al., (1985), J. Phys. Chem., 89, 397.

Rothenberger, G., Moser, J., Graetzel, M., Serpone, N., and Sharma, D.K., (1985), J. Amer. Chem. Soc., 107, 8054.

THE RADIATION SENSITIVITY OF SELECT METAL CHELATE POLYMERS: MECHANISTIC CHANGES AT HIGHER ENERGIES

R.D.Archer, C.J.Hardiman, and A.Y.Lee

Department of Chemistry, University of Massachusetts, Amherst, MA 01003, USA

INTRODUCTION

Our interest in the radiation sensitivity of heavy metal polymers was first sparked by the goal of enhanced miniaturization of integrated circuit (IC) chip features. As the features of IC chips get closer and closer together at the submicron level, microlithographic techniques must use higher energy photons (or electrons, etc.) than are currently used.[1] Otherwise, diffraction effects by the photons which pass through adjacent features blur the features and allow short circuits. The thin organic polymer films, which are normally used as lithographic resists, suffer from an inability to absorb all of the higher energy radiation. The unabsorbed radiation backscatters from the oxide layer which is normally between the resist and the semiconductor.

Heavy atom-containing polymer films should have an enhanced sensitivity to applied radiation because of the atomic number (Z) dependence of the photoelectric effect which has an atomic absorption coefficient which is Z^4 or greater (Evans 1972) whereas photon scattering by heavy atoms only has a Z^2 dependence. To test this concept,[2] we synthesized and tested a number of uranyl dicarboxylate polymers for gamma-ray

---

1 Visible and ultraviolet radiation passed through masks or projected onto the surface provide the mass production necessary for the low cost devices currently on the market. Although electron beam lithography can provide higher resolution, the throughput rate and backscattering problems suggest that x-ray or low-energy gamma-ray methodology is needed. For more details see either of two recent review volumes (Thompson 1983, 1984)

2 Polymers with main group heavy elements have shown increased sensitivity using the empirical method of determining solubilities before and after radiation (Webb 1979; Haller 1979). Such sensitivities are based on the dose per unit area required to dissolve the irradiated polymer with 1/2 of the unirradiated polymer still on the substrate (for a positive resist and vice versa for a negative resist). They are solvent and laboratory dependent, cf. Thompson (1983, 1984), and are not as fundamental as G values.

Photochemistry and Photophysics
of Coordination Compounds, Ed. by H. Yersin/A. Vogler

sensitivity. From the extensive literature on uranyl carboxylate photochemistry, cf. Burrows (1974), we anticipated CO_2 evolution, possibly mixed with hydrogen abstraction (Rehorek 1982). Much to our surprise, a sizable number of the uranyl polymers show no CO_2 loss during ^{137}Cs irradiation, but they crosslink with very high efficiency instead.

METHODOLOGY

The irradiation studies were conducted with a cesium-137 gamma photon source (662 keV) with dose rates of 0.022 to 0.073 Mrad/hr based on Fricke dosimetry (Hine 1956; Getoff 1962). Corrections for different mass absorption cross sections between the dosimeter and the uranyl polymers were made subsequently using literature data (Mann 1960) interpolated when necessary. Samples were irradiated in vacuo using sealed Pyrex or quartz tubes. Molecular weight analysis of the polymers before and after irradiation were conducted via gel permeation (or size exclusion) chromatography (GPC) in N-methylpyrrolidone (NMP) solutions on Ultrastyragel columns, which had been calibrated with polystyrene standards (in NMP). Gas chromatography-mass spectroscopy (GCMS), electron spin resonance (ESR), Fourier transform nuclear magnetic resonance (NMR) and infrared (IR), and ultraviolet-visible (UVV) spectroscopies were used to help elucidate the products.

G values were determined using the method of Charlesby (1954, 1960, 1964) and reiterated by Dole (1973):

$$1/\bar{M}_n' = 1/\bar{M}_n^{\,o} + (G_s - G_x)(r/100N_a) \qquad [1]$$

where $\bar{M}_n^{\,o}$ is the number-average molecular weight before irradiation,
$\bar{M}_n'$ is the number-average molecular weight after irradiation,
G_s is the number of chemical scissions per 100 electron volts,
G_x is the number of crosslinks per 100 electron volts,
r is the radiation dose in electron volts per gram, and
N_a is Avogadro's number.

Converted to Megarads (Mrad) the equation becomes:

$$1/\bar{M}_n' = 1/\bar{M}_n^{\,o} + (G_s - G_x)(1.04 \times 10^{-6} R) \qquad [2]$$

These equations are based on random scission and crosslinking processes, random initial molecular weight distributions ($\bar{M}_w/\bar{M}_n = 2$), and with G_s and G_x dose independent. Even for non-ideal systems, they provide the best guide possible to the magnitude of the radiation effects, and the dose dependence is apparent from plots of $1/\bar{M}_n$ vs dose in Mrad.

The synthesis and characterization of the uranyl dicarboxylates is detailed elsewhere (Archer 1987; Hardiman 1987). The essential synthetic reaction is

$$UO_2(O_2CCH_3)_2{\cdot}(H_2O)_2 + HO_2CRCO_2H \xrightarrow{C_2H_6SO} [UO_2(O_2CRCO_2)]_n + CH_3CO_2H \qquad [3]$$

The molecular weights have been determined by GPC, viscosity, and NMR end-group analysis. Solid-state ^{13}C-NMR has also been used (Archer 1987) to confirm the coordination modes of the carboxylate ligands to the uranyl ion. The results are as anticipated from IR results (Hardiman 1987); that is, both monodentate and bidentate carboxylate coordination occur such that 7-coordination predominates in polymers with either one or two moles of solvent coordinated to the uranyl ion.

URANYL POLYMERS WHICH APPEAR TO EXCLUSIVELY CROSSLINK

As anticipated, the uranyl dicarboxylate polymers are very sensitive to gamma-ray irradiation. The data for four branched alkyl, one alkene, and one aromatic dicarboxylates which appear to exclusively crosslink, with no evidence of CO_2 evolution, are summarized in Table 1. Whereas the entire absorption for the lighter elements (0.257, 1.54, 2.04, and 4.09 barns/atom for H, C, O, and S, respectively) is of the Compton type, for uranium 50% is photoelectric absorption (47.7 barns/atom total). Thus, the uranium atom constitutes from 50 to 58% of the absorption in the unit at this energy (662 keV), but only modifies the mass absorption coefficient for the polymer by about 13 to 16% relative to water, the absorber of the Fricke dosimeter. Organic polymers are typically lower than water; e.g., poly(methyl methacrylate), PMMA, is 0.083 cm^2/g using the same numbers, or 17 to 20% lower than the uranyl polymers. However, on a repeating unit basis, the uranyl polymers absorb from 600 to 700% as much radiation as PNMA (G = 1.3) and organic polymers with G values as high as 10 are known (Thompson 1984).

None of the species in Table 1 show any tendency for scission, thus, the G_s-G_x value is essentially $-G_x$. With increased dose levels, all exhibit lower G_x values--a logical consequence of fewer effective crosslinks. Extra crosslinks between the same chains do not increase the molecular weight any further. The values in the table are for 2 Mrad doses (or 3 Mrad for the succinate and phthalate derivatives as no curvature was observed until above 3 Mrad for these two species). The extremely high G_x value for the tetrapimelate derivative must be related to the mobility of the longer alkyl chain coupled with stabilized tertiary radicals coupled with efficient energy transfer.

Table 1. Gamma-ray Sensitivity of Negative Resist Uranyl Polymers

Empirical Formula Unit[a] (bridging carboxylate)	$\bar{M}_n$[b]	G_s-G_x[c]	μ/ρ[d]	G_s-G_x[e]
$UO_2\ O_2CC(CH_3)_2CH_2CO_2\ (C_2H_6SO)$ (2,2-dimethylsuccinate)	9,000[g]	-14[g]	0.100	-12[g]
$UO_2\ O_2CC(CH_3)_2CH_2CH_2CO_2\ (C_2H_6SO)$ (2,2-dimethylglutarate)	48,000[f]	-3.1[f]	0.100	-2.7[f]
$UO_2\ O_2CCH_2C(CH_3)_2CH_2CO_2\ (C_2H_6SO)$ (3,3-dimethylglutarate)	12,000[g]	-8.0[g]	0.100	-6.9[g]
$UO_2\ O_2CC(CH_3)_2(CH_2)_3C(CH_3)_2CO_2\ (C_2H_6SO)$ (2,2,6,6-tetramethylpimelate)	12,000[g]	-43[g]	0.099	-37[g]
$UO_2(Z\text{-}O_2CH{=}CHCO_2)(C_2H_6SO)_{1.75}$ (maleate)	9,300	-3.3	0.099	-2.9
$UO_2(o\text{-}O_2CC_6H_4CO_2)(C_2H_6SO)_2$ (phthalate)	17,800[g]	-3.7[g]	0.097	-3.3[g]

[a]Repeating unit of polymer chain including solvation
[b]$\bar{M}_n$ of samples not irradiated; based on GPC in NMP with polystyrene standards, or by NMR end-group analysis if so indicated
[c]Measured net G value using equation 2 and GPC after ^{137}Cs irradiation
[d]Mass absorption coefficients in cm^2/g for 662 keV irradiation
[e]Corrected G values relative to Fricke dosimeter(0.086 cm^2/g for ^{137}Cs)
[f]Polymer has poor $\bar{M}$ distribution and poor agreement with end-group detn
[g]$\bar{M}$ values for this polymer--end-group calibrated by NMR

URANYL POLYMERS WHICH UNDERGO SCISSION WITH GAMMA RADIATION

On the other hand, uranyl polymers with three different thio-bridged ligands and fumarate all show large G_s values upon irradiation as noted in Table 2. The cleanest one is the polymeric uranyl thiodiglycolate, which shows no tendency toward crosslinking; that is, G_s-G_x is probably a true measure of G_s. The GPC's of the others show evidence for both scission and crosslinking; thus G_s is larger than the G_s-G_x value shown. Unfortunately, they are so sensitive to radiation that reliable independent values are impossible to obtain. These high G_s-G_x values for the thio-bridged polymers would be even higher if the polystyrene-equivalent molecular weights were used instead of the NMR

Table 2. Gamma-ray Sensitivity of Positive Resist Uranyl Polymers[f]

Empirical Formula Unit[a] (bridging carboxylate)	$\bar{M}_n$[b]	G_s-G_x[c]	μ/ρ[d]	G_s-G_x[e]
$UO_2(O_2CCH_2SCH_2CO_2)(C_2H_6SO)_2$ (thiodiglycolate)	14,000[g]	56[g]	0.097	50[g]
$UO_2(O_2CCH_2SSCH_2CO_2)(C_2H_6SO)_{1.5}$ (dithiodiglycolate)	12,000[g-j]	300[g-j]	0.097	280[g-j]
$UO_2(O_2CCH_2SCH_2SCH_2CO_2)(C_2H_6SO)_2$ (methylenebis thioglycolate)	15,000[g,h]	103[g,h]	0.096	93[g,h]
$UO_2(E\text{-}O_2CCH{=}CHCO_2)(C_2H_6SO)_2$ (fumarate)	26,000[h,i]	63[h,i]	0.098	55[h,i]

[a-e]Same as Table 1

[f]G values based on first 0.5 to 0.6 Mrad only

[g]M adjusted to agree with NMR end-group analysis

[h]Polymer undergoes both scission and crosslinking

[i]$\bar{M}$ distribution poor; results very approximate

[j]Polymer very sensitive to radiation--nonirradiated samples change $\bar{M}$ distribution significantly during irradiation of other samples

end-group determined weights. Specifically, thiodiglycolate, dithiodiglycolate, and methylenebis thioglycolate were originally calculated to have G_s-G_x values of about 100, 400, and 160, respectively, using the polystyrene-equivalent calibrations. These polymers absorb from about 5 to 7 times as much energy per polymer unit as an organic polymer (such as PMMA) with a molecular weight of 100 at this energy. Even so, with the ligands that have two sulfur atoms per repeating unit, extremely high sensitivity to this gamma radiation occurs. At low dose level, where PMMA shows only a very small change in molecular weight distribution, these uranyl species have drastically modified molecular weight distribution. GCMS results indicate S-C scission for methylenebis thioglycolate and S-S scission in dithiodiglycolate. And ESR results indicate appreciable spin density on sulfur atoms for the same polymers with no evidence for uranium(V), even at -77°K.

The above results with uranyl polymers led us to synthesize linear cobalt(III) polymers containing two ß-diketones bridged with S atoms (-S-, -SS-, -SO-, & $-SO_2-$) for bridges and leucine as a nonpolymerizable third

bidentate ligand, which allows the synthesis of linear coordination polymers. These and similar VO^{2+} ß-diketonates bridged with sulfur atoms (Archer 1986) show radiation effects which are both wavelength and state/solvent dependent. For example, instead of reduction to cobalt(II), gamma irradiation produces facile C-S scission in the cobalt-(III) polymers. Space limitations precludes further details.

ACKNOWLEDGEMENTS

The financial support of the U.S. Office of Naval Research and helpful interactions with Professors J.C.W. Chien (Univ. Massachusetts) and N. Getoff (Univ. Wien) are gratefully acknowledged.

REFERENCES

Archer RD, Tramontano VJ, Lee AY, Grybos R (1986) Thio-, dithio- and sulfoxo-bis-ß-diketonate metal chelate polymers. International Conference on Coordination Compounds, Athens, Greece

Archer RD, Dickenson LC, Lee AY, Ochaya VO, Chien JCW (1987) Monodentate and bidentate carbonyl coordination in coordination polymers of uranium (to be published)

Burrows HD, Kemp TJ (1974) The photochemistry of the uranyl ion. Chem Soc Rev 3: 139-165

Charlesby A (1954) Molecular weight changes in degradation on long-chain polymers. Proc Royal Soc London, Ser A 224: 120

Charlesby A (1960) Atomic radiation and polymers. Pergamon, Oxford

Charlesby A, Moore N (1964) Comparison of gamma and ultra-violet radiation effects in polymethylmethacrylate at higher temperature. Int J Appl Radiat Isot 15: 703-708

Dole M (1973) The radiation chemistry of macromolecules, Vol 2. Academic Press, New York

Evans RD (1972) Amer inst phys hdbk, 3rd ed. McGraw-Hill, NY, sec 3, p 209

Getoff N (1962) Fortschritte der Strahlenchemie wäßriger Lösungen. Österr Chem Ztg 63: 91-98

Haller I, Feder R, Hatzakis M, Spiller EA (1979) Copolymers of methyl methacrylate and methacrylic acid and their metal salts as radiation sensitive resists. J Electrochem Soc 126: 154-161

Hardiman CJ, Archer RD (1987) Dioxouranium(VI) carboxylate polymers: synthesis and characterization of tractable coordination polymers and evidence for rigid rod conformation. Macromol (in press)

Hine GJ, Brownell GL (eds) (1956) Radiation dosimetry. Academic Press, New York

Mann RA (1960) Gamma ray cross section data. General Electric Aircraft Propulsion Dept, Cincinatti

Rehorek D, Puaux JP (1982) Formation of radicals during the photolysis of uranyl salts in aliphatic carboxylic acids. Radiochem. Radioanal. Lett 52: 29-35

Thompson LF, Willson CG, Bowden MJ (eds) (1983) Introduction to microlithography: theory, materials & processing, ACS Symposium Series No. 219. American Chemical Society, Washington, DC

Thompson LF, Willson CG, Frechet JMJ (eds) (1984) Microlithography: radiation sensitive polymers, ACS Symposium Series No. 266. American Chemical Society, Washington DC

Webb DJ, Hatzakis M (1979) Metal methacrylates as sensitizers for poly-(methyl methacrylate) electron resists. J Vac Sci Technol 16: 2008-2013

TEMPERATURE DEPENDENT EMISSION OF COPPER PORPHYRINS IN LIQUID SOLUTION

Motoko Asano, Osamu Ohno, Youkoh Kaizu, and Hiroshi Kobayashi

Department of Chemistry, Tokyo Institute of Technology, O-okayama, Meguro-ku, Tokyo 152, JAPAN

INTRODUCTION

Copper porphyrins exhibit a short-lived phosphorescence at ambient temperature. Fluorescence is quenched for a prompt intersystem crossing to the lowest excited triplet state caused by the interactions of an unpaired electron in the highest copper $d\sigma$ orbital and the $^{1,3}(\pi,\pi^*)$ excited configurations. The interaction makes all singlets become doublets and triplets split into doublets ("trip-doublet") and quartets ("trip-quartet") (Ake 1969; Smith 1968).

An energy gap between the lowest trip-quartet and trip-doublet was estimated as 260~330 cm^{-1} for PCu (P: porphin) by high resolutional emission and absorption measurements at low temperature (Noort 1976; Bohandy 1980). The measurements of zero-field and Zeeman splittings of the trip-quartet state of PCu provided knowledge on the structure of the trip-quartet (Van Dorp 1975; Van Dijk 1979, 1981).

The relaxation processes at room temperature of excited copper porphyrin have been studied by use of pico-second flash photolysis technique (Kobayashi 1979; Kim 1984). Copper protoporphyrin in the lowest excited "sing-doublet" ($^2S_1$) state relaxes into the lowest "trip-doublet" ($^2T_1$) state within 8 ps and then to a thermal equilibrium state of $^2T_1$ and the lowest "trip-quartet" ($^4T_1$) state with a time constant of 450-460 ps (Kobayashi 1979). The phosphorescence observed at room temperature is ascribed to a delayed $^2T_1$ emission caused by a thermal activation from $^4T_1$ state to $^2T_1$ state.

The emission band of OEPCu (OEP: 2,3,7,8,12,13,17,18-octaethylporphin) in both toluene and poly(methyl methacrylate) film increases prominence but shows only a slight shift with decreasing temperature. The emission spectrum of TPPCu (TPP: 5,10,15,20-tetraphenylporphin) in polymer film is rather invariant with temperature (300~77 K) and well corresponds to the spectrum in toluene rigid glass at 77 K. On the other hand, a bell-shaped emission is observed in toluene solution at room temperature and the band shifts to the red with decreasing temperature down to 200 K.

In this paper, we discuss the structure of the trip-doublet and trip-quartet states in four copper porphyrins in toluene liquid solution on the basis of the decay lifetimes and emission yields measured with decreasing temperature not so as to freeze the medium.

S-T ABSORPTION SPECTRA OF COPPER(II) PORPHYRINS

Copper porphyrins exhibit absorption bands very similar to those observed with the corresponding diamagnetic porphyrins. However these particular paramagnetic porphyrins do exhibit a weak additional absorption band (OD ca. 0.1 is observed with an almost saturated solu-

Photochemistry and Photophysics
of Coordination Compounds, Ed. by H. Yersin/A. Vogler

tion of 10^{-3} M) to the red of the Q band. The weak band forms a mirror image of the emission observed at room temperature. The absorption band is assigned to a S-T (sing-doublet-to-trip-doublet) transition.

TEMPERATURE DEPENDENCE OF EMISSION IN OEPCu AND TFPPCu

The trip-doublet emission of OEPCu and TFPPCu (TFPP: 5,10,15,20-tetra-(pentafluorophenyl)porphin) in liquid media 10 times increases its intensity persisting the spectral profile upon temperature down from 300 K to 200 K. Lifetime increases from 105 ns (OEPCu), 68 ns (TFPPCu) at 300 K to 1200 ns (OEPCu), 1250 ns (TFPPCu) at 200 K, respectively. A scheme is given for the relaxation process of the excited species as in figure 1. Assuming that a photostationary state is obtained, the yield of emission from the trip-doublet is

figure 1

$$\phi_2 = k_{2r} \cdot \phi_{isc} \cdot \frac{K + k_4/k_3}{k_2 K + k_4 (k_2/k_3 + 1)} , \qquad (1)$$

where $K = \frac{1}{2}\exp(-\frac{\Delta E}{kT}) = \frac{k_{-3}}{k_3}$, $\phi_{isc} = \frac{k_1}{k_0' + k_1}$.

Since $k_3 >> k_2 >> k_4$ and thus $1 + k_2/k_3 \fallingdotseq 1$ and $K + k_4/k_3 \fallingdotseq K$, the equation (1) is rewritten as

$$\phi_2 = k_{2r} \cdot \phi_{isc} \cdot \frac{K}{k_2 K + k_4} . \qquad (2)$$

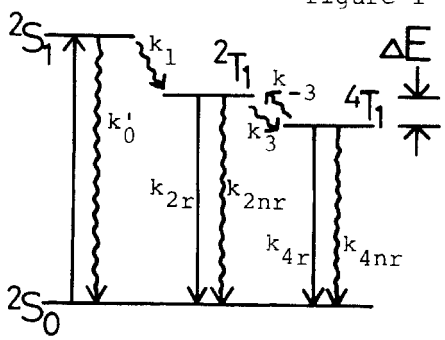

$k_2 = k_{2r} + k_{2nr}$, $k_4 = k_{4r} + k_{4nr}$

On the other hand, the decay rate of emission is described as

$$[^2T_1] = C_1 e^{-\alpha t} + C_2 e^{-\beta t} ,$$

$$\begin{pmatrix} \alpha \\ \beta \end{pmatrix} = \frac{1}{2}\{k_2 + k_3 + k_4 + k_{-3} \pm \sqrt{\{(k_2 + k_3) - (k_4 + k_{-3})\}^2 + 4k_3 k_{-3}}\} .$$

The observed decay corresponds to the slow component β. Since $k_3, k_{-3} >> k_2, k_4$, the lifetime is given by

$$\frac{1}{\tau} = \beta = \frac{k_2 K + k_4}{1 + K} . \qquad (3)$$

From the equations (2) and (3), it follows that

$$\tau/\phi = k_{2r} \cdot \phi_{isc} (1 + K)/K. \qquad (4)$$

Here the temperature variation of the ratio τ/ϕ is attributable only to the equilibrium constant K, since k_{2r} and ϕ_{isc} are less dependent on temperature. Using the least-squares method, the values of K are evaluated as a function of temperature, from which the energy gap (ΔE) between the $^2T_1$ and $^4T_1$ states can be determined according to the relationship $K = \frac{1}{2}\exp(-\Delta E/kT)$: OEPCu, 310 cm^{-1}; TFPPCu, 390 cm^{-1}.

TEMPERATURE DEPENDENCE OF EMISSION IN TPPCu AND T(EtO)PPCu

TPPCu shows a bell-shaped emission band at room temperature, however the emission profile varies and the band peak shifts to the red with reducing temperature. The lifetime, on the other hand, increases with

decreasing temperature down to 250 K while it decreases upon further cooling : 300 K, 29 ns; 250 K, 39 ns; 200 K, 27 ns. The emission of T(EtO)PPCu(T(EtO)PP: 5,10,15,20-tetra(*p*-ethoxyphenyl)porphin) also shows a small red shift at low temperature. The lifetime of this copper porphyrin simply decreases with decreasing temperature : 300 K, 17 ns; 200 K, 13.5 ns. In these two copper porphyrins, the emission intensity in toluene solution is much less than that in polymer film but varies only to a lesser extent with temperature in contrast with OEPCu. Temperature dependence of emission spectra and decay lifetimes of TPPCu and T(EtO)PPCu can not be described by means of the simple dissipation kinetics as in figure 1.

STRUCTURE OF THE TRIP-DOUBLET AND TRIP-QUARTET STATES IN COPPER PORPHYRINS

The absorption bands of a typical metalloporphyrin are ascribed to the lowest (π,π^*) transitions which arise from the highest occupied a_{2u} and a_{1u} orbitals in accidental degeneracy to the lowest vacant degenerate e_g orbital pair. The lowest excited singlet states are as 50-50 admixtures of $^1(a_{1u}e_g)$ and $^1(a_{2u}e_g)$, while the lowest excited triplet states are approximately a single configuration $^3(a_{1u}e_g)$ or $^3(a_{2u}e_g)$.

In the case of paramagnetic copper porphyrins, however, an unpaired electron in copper $d_{x^2-y^2}$ (b_{1g}) orbital migrates into the porphyrin nitrogens. Exchange interactions of the unpaired electron with porphyrin LUMO's and HOMO's give rise to a mixing between porphyrin lowest (π,π^*) excited singlets and triplets.

The exchange interactions between copper b_{1g} orbital and porphyrin LUMO e_g orbitals, HOMO a_{2u} and a_{1u} orbitals were evaluated: $(b_1e|eb_1)$ = 200~250 cm^{-1}, $(b_1a_2|a_2b_1)$ = 300~350 cm^{-1}, while $(b_1a_1|a_1b_1)$ = 0 since the a_{1u} orbital has no population on the nitrogens (Asano unpublished).

In OEPCu and TFPPCu, the lowest trip-quartet and trip-doublet are mainly of $|^{4,2}(b_1{}^3(a_1e))>$ origin, whereas in TPPCu and T(EtO)PPCu $|^{4,2}(b_1{}^3(a_2e))>$ turns out to be lower than $|^{4,2}(b_1{}^3(a_1e))>$. There is only a small energy gap between the $^4T_1$ and $^2T_1$ states in OEPCu (330 cm^{-1}) and TFPPCu (350 cm^{-1}), while a greater gap in TPPCu (~700 cm^{-1}) and T(EtO)PPCu (~800 cm^{-1}). Since observed decay rate from $^2T_1$ is about ~30 ns in TPPCu and ~20 ns in T(EtO)PPCu, a Boltzmann equilibrium between the lowest excited states is not established. On the other hand, the second excited states $^4T_2$ and $^2T_2$ are far from the $^2T_1$ state in OEPCu and TFPPCu, while those of TPPCu and T(EtO)PPCu are close to $^2T_1$ state.

CONCLUSION

The lowest excited trip-doublet and trip-quartet configurations of OEPCu and TFPPCu are mainly $|^{2,4}(b_1{}^3(a_1e))>$, while those of TPPCu and T(EtO)PPCu are $|^{2,4}(b_1{}^3(a_2e))>$. An energy gap between $^2T_1$ and $^4T_1$ was obtained 300~400 cm^{-1} for OEPCu and TFPPCu by kinetics study and the $^2T_1$ and $^4T_1$ states are in a Boltzmann equilibrium. In case of TPPCu and T(EtO)PPCu, temperature dependence of emission spectrum and lifetime is very anomalous in toluene solution.

A possible interpretation is as follows. Rotation of peripheral phenyl groups can cause delocalization of π-electrons of the porphyrin macrocycle to the substituents. It follows that the transition energies vary with temperature in liquid solution since the rotation depends on temperature. It is noted that a_{1u} orbital has no population on the *meso*-carbons to which phenyl substituents are bonding, while a_{2u} orbital does have. In TPPCu and T(EtO)PPCu, anomalous temperature dependence of emission spectrum and decay lifetime is attributable to the variation of phenyl groups rotation. In fact, spectrum of these copper porphyrins in polymer film, which is coincident with that in toluene rigid glass at 77 K, persists its profile and shows no shift with decreasing temperature. However, in case of TFPPCu, the lowest excited trip-doublet and trip-quartet configurations $|^{2,4}(b_1{}^3(a_1e))>$ are less influenced by the rotation and *ortho*-fluoro substituents of phenyl groups may inhibit it.

References

Ake RL, Gouterman M (1969) Porphyrins XIV. Theory for the luminescent state in VO, Co, Cu complexes. Theoret Chim Acta 15: 20-42.

Asano M, Ohno O, Kaizu Y, Kobayashi H (to be published) The lowest excited states of copper porphyrins.

Bohandy J, Kim BF (1980) Temperature dependence of Mg porphin, Cu porphin, and Pd porphin luminescence. J Chem Phys 73: 5477-5481.

Kim D, Holten D, Gouterman M (1984) Evidence from picosecond transient absorption and kinetics studies of charge-transfer states in copper(II) porphyrins. J Am Chem Soc 106: 2793-2798.

Kobayashi T, Huppert D, Straub KD, Rentzepis PM (1979) Picosecond kinetics of copper and silver protoporphyrins. J Chem Phys 70: 1720-1726.

Noort M, Jansen G, Canters GW, van der Waals JH (1976) High resolution spectra of palladium, platinum and copper porphyrins in *n*-octane crystals. Spectrochim Acta 32: 1371-1375.

Smith BE, Gouterman M (1968) Quartet luminescence from copper porphyrins. Chem Phys Lett 2: 517-519.

Van Dijk N, van der Waals JH (1979) Radiative decay of metastable quartet state of copperporphin. Mol Phys 38: 1211-1223.

Van Dijk N, Noort M, van der Waals JH (1981) Zeeman spectroscopy of the $^4E_u \rightarrow {}^2B_{1g}$ phosphorescence of copper porphin in an *n*-alkane single crystal. I. The energy problem, II. The intensity problem. Mol Phys 44: 891-911, 913-923.

Van Dorp WG, Canters GW, van der Waals JH (1975) The lowest quartet state of copper porphin: Zeeman experiments at 4.2 K. Chem Phys Lett 35: 450-456.

PRESSURE EFFECTS ON NONRADIATIVE DEACTIVATION FROM METAL COMPLEX EXCITED STATES IN SOLUTION

P.C.Ford and J.DiBenedetto

Department of Chemistry, University of California, Santa Barbara, CA 93106, USA

This article summarizes some observations in this and other laboratories regarding the effect of pressure on rates of nonradiative deactivation from metal complex excited states (ES) in fluid solutions. Studies here (partially in collaboration with Henry Offen at UCSB and with Rudi van Eldik at the University of Frankfurt, FRG) have been concerned with using pressure effects to probe photoreaction mechanisms and other properties of metal complex excited states (Ford 1986, DiBenedetto and Ford 1985). Nonradiative deactivation often is the principal pathway for excited state decay; thus understanding or, at least, determining the sensitivity of this pathway to such a systemic perturbation is crucial to interpreting the pressure effects on other excited state processes.

ACTIVATION VOLUMES

The application of hydrostatic pressure changes a number of parameters for a solution phase reaction which will be reflected in the reaction dynamics. Application of transition state theory leads to an activation volume defined according to

$$(1) \quad \Delta V_i^{\ddagger} = -RT\left(\frac{d(\ln k_i)}{dP}\right)_T$$

where k_i is the rate constant for a process of interest. Describing the pressure dependence of the reaction rate as an activation "volume" provides a convenient, qualitative perception of the distortions that may be occurring along the reaction coordinate of a molecular process. However, this view may be misleading since pressure may perturb other systemic parameters including solvent density, viscosity and dielectric constant, which may profoundly influence the reaction dynamics. Despite this qualification, the use of measured partial molar volumes and activation volumes as defined according to eq. 1 allows the construction of reaction volume profiles which have provided valuable insights into the natures of the mechanisms of numerous thermal reactions (van Eldik 1986).

The situation with excited states is somewhat more complicated. Analysis of ES dynamics according to transition state theory can only be valid for slower processes where the relevant states have achieved vibrational equilibration with the medium. In addition, the partial molar volumes of short-lived electronic states cannot be measured by the conventional methodologies, adding a further element of uncertainty into the interpretation. The unimolecular decay of a single ES may be summarized in terms of three types of processes, reaction to products (rate constant k_p), radiative deactivation (k_r) and nonradiative deactivation (k_n), each of which possibly a composite of several competing mechanisms. The sum of the decay rate constants $k_d = \Sigma k_i$ is equal to the inverse of the lifetime τ while the quantum yield ϕ_i of a particular process is described by the product of ϕ_{ic}, k_i and τ, where ϕ_{ic} is the efficiency of forming the relevant state via internal conversion/intersystem crossing. Values of k_i thus can be determined as functions of pressure from the corresponding values of ϕ_i, ϕ_{ic} and τ.

Photochemistry and Photophysics
of Coordination Compounds, Ed. by H. Yersin/A. Vogler

PHOTOREACTION $\Delta V^{\ddagger}$'s

This approach was used successfully to determine $\Delta V^{\ddagger}$ values for the ligand labilization pathways from the ^3E ligand field (LF) state of the halopentaamminerhodium(III) ions (eq. 2, A = NH_3 or ND_3, X = Cl or Br) (Weber 1983, 1984).

$$(2)\quad [RhA_5X^{2+}]^* + H_2O \longrightarrow \begin{cases} RhA_5(H_2O)^{3+} + X^- \\ RhA_4(H_2O)X^{2+} + A \end{cases}$$

A volume profile for the chloride complex is represented in Fig. 1 where it is seen that, while $\Delta V^{\ddagger}$ for NH_3 loss from the LF excited state is large and positive, consistent with a limiting dissociative mode for this excited state substitution mechanism, $\Delta V^{\ddagger}$ for Cl^- loss from the same species is negative. This seemingly contradictory result is easily explained in terms of solvent contraction around the transition state of the latter pathway owing to the creation of charge (dissociation of Cl^- leaves a +3 rhodium(III) fragment). The volume differences between the $\Delta V^{\ddagger}$'s of the two pathways are indeed close to the differences in the partial molar volumes of the reaction products. Thus, it was concluded that the pressure effects on the LF excited state substitution rates for this and related Rh(III) complexes were consistent with the proposed dissociative mechanism.

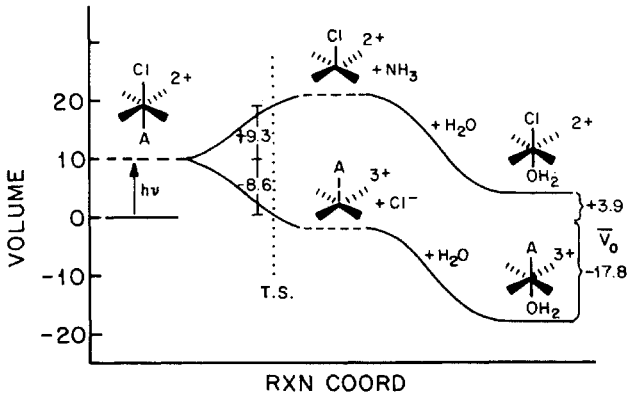

Figure 1 Volume profile diagram for the competitive photoaquation of NH_3 and of Cl^- from $Rh(NH_3)_5Cl^{2+}$ in aqueous solution via a proposed limiting dissociative mechanism.

PHOTOPHYSICAL $\Delta V^{\ddagger}$'s

Pressure effects on radiative deactivation have not been widely explored for metal complexes in solution, in part because emission quantum yields are often (not always!) small. Limited studies in solution are consistent with the changes in k_r correlating with pressure induced changes in the square of the solvent refractive index as predicted by the Strickler-Berg equation (Drickamer 1982).

With regard to nonradiative deactivation, pressure effects on k_n would depend on the detailed mechanism. Deactivation from a particular ES may occur directly to the ground state or by crossing over to another ES (e.g., one of different orbital parentage) which deactivates more efficiently. For an individual state, k_n is determined by vibrational and electronic factors. Vibronic coupling has been analyzed in terms of the "weak" and "strong" coupling limits. The former case has a relatively small displacement of the ES potential energy surface, thus

k_n is dominated by the high frequency molecular modes and is predicted to increase exponentially as ΔE between the ground and excited states decreases (the "energy gap law"). The strong-coupling limit involves a larger displacement of the ES potential energy surface (at least one normal mode) relative to the acceptor state such that the surfaces cross not far from the minimum of the higher state. According to theory, strong-coupling should show an Arrhenius type temperature dependence while weak-coupling should be essentially temperature independent. Strong coupling can also be associated with chemical deactivation pathways, thus may contribute to k_n in those cases where unimolecular reactions of the ES are common.

In general one might expect that weak coupling should show a rather small sensitivity to pressure. Changes in hydrostatic pressure may perturb the ES energy by compression of the complex or changing the solvent dielectric constant, and k_n should respond to $-\Delta E$ exponentially. For example, Salman and Drickamer (1982) investigated the pressure effects on the metal to ligand charge transfer (MLCT) phosphorescence spectra, lifetimes and quantum yields for the complexes $ReCl(CO)_3(phen)$ and $ReCl(CO)_3(4,7\text{-}Ph_2phen)$ as functions of pressure in several solvents. By systematic variation of solvent properties with pressure, they demonstrated a linear relationship between $\ln(k_n)$ and ΔE indicative of a weak-coupling deactivation mechanism for each complex. Values of $\Delta V_n^{\ddagger}$ can be calculated for each complex in the various solvents, and for the polar solvents dimethyl formamide and acetonitrile, these are quite small, 0 to +1 $cm^3/mol.$, but in m-xylene $\Delta V_n^{\ddagger}$'s are larger reflecting the greater compressibility of that solvent.

A similar observation has been made for the $Ru(bpy)_3^{2+}$ cation in polar solvents at ambient temperature. Early studies over the range 0.1 to 230 MPa indicated that $\Delta V_n^{\ddagger}$ is small and negative (Kirk 1980). Subsequent experiments (Fetterolf 1985) confirmed the small $\Delta V_n^{\ddagger}$ under these conditions but also demonstrated a dramatic temperature sensitivity for $\Delta V_n^{\ddagger}$ (see below).

Given that the strong-coupling mechanism is often closely associated with unimolecular reactions of the ES, one might expect a correlation between pressure effects experienced by the rates of chemical deactivation and the associated contributions to nonradiative deactivation rates. This appears to be the case for the Rh(III) ammine systems discussed above. Pressure effects on k_n values for the lowest LF states give measurable $\Delta V_n^{\ddagger}$ values which parallel those of the predominant photosubstitution reactions both in magnitude and sign (Weber 1983). Such an observation may indicate a substantial strong-coupling component to the k_n mechanism as proposed earlier as an explanation of temperature effects on apparent nonradiative deactivation rates of hexaamminerhodium(III) (Petersen 1974). We have found that a plot of $\Delta V_n^{\ddagger}$ vs $\phi_X \cdot \Delta V_X^{\ddagger} + \phi_A \cdot \Delta V_A^{\ddagger}$ (the ordinate representing the sum of the ES reaction activation volumes weighted by their respective ambient pressure quantum yields) is linear for the halopentaammine complexes. Although the quantitative significance of this plot has yet to be delineated, the correlation between $\Delta V_n^{\ddagger}$ and the weighted contributions of the photosubstution pathways is clearly suggestive of the contributions of strong-coupling pathways to the deactivation modes.

A Rh(III) complex which does not fit the above correlation is <u>trans</u>-$Rh(cyclam)(CN)_2^+$ (cyclam = 1,4,8,11-tetraazacyclotetradecane), <u>which</u> is inactive toward photosubstitution but has a remarkably long lived LF emission in ambient aqueous solution (8.1 usec) (Miller

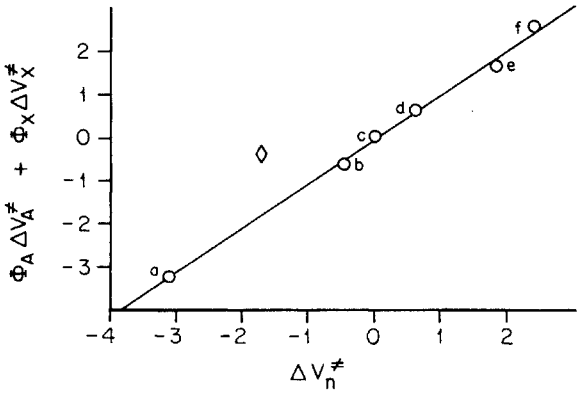

FIGURE 2: Plot of $\Delta V_n^{\neq}$ vs the summed products $\Delta V_A^{\neq}\phi_A + \Delta V_X^{\neq}\phi_X$ for Rh(III) complexes

a: $Rh(ND_3)_5Cl^{2+}$ in D_2O
b: $Rh(NH_3)_5Cl^{2+}$ in $HCONH_2$
c: $Rh(NH_3)_5Cl^{2+}$ in DMSO
d: $Rh(NH_3)_5Cl^{2+}$ in DMF
e: $Rh(NH_3)_5Br^{2+}$ in H_2O
f: $Rh(ND_3)_5Br^{2+}$ in D_2O
diamond: $Rh(bpy)_2Cl_2^{+}$ in H_2O

1983). The lack of photoreactivity may be attributed to the lowest energy LF ES being the $^3A_2$. For this state, ligand labilization, expected to be equatorial in analogy to the $Rh(NH_3)_5CN^{2+}$ ion (Skibsted 1983), is blocked by the cyclam macrocycle. We have found that under pressure τ is shortened and $\Delta V_d^{\neq} = -4.4$ cm^3/mol, and we interpret this as suggesting that the modes necessary for strong-coupling from the $^3A_2$ state also involve distortion along the macrocycle constrained equatorial metal-ligand bonds. Thus, the negative $\Delta V_n^{\neq}$ value may indicate the role of an alternative deactivation pathway, the crossing of the system to the higher energy ^3E state from which nonradiative deactivation occurs. A negative $\Delta\bar{V}$ for the $^3A_2$ --> ^3E transition might be explained in terms of solvation contributions to $\bar{V}$ of the latter state owing to the more ionic nature of the Rh-CN bond in the latter state.

A strong coupling mechanism with significant volume changes would certainly be expected if the thermally relaxed ES has a considerably different structure than does the ground state. An example is the four coordinate Ni(II) complex $Ni(dppe)Cl_2$ (dppe = 1,2-bis(diphenylphosphino)ethane) for which pressure effects on nonradiative decay (Amir-Ebrahimi 1984) gave $\Delta V_d^{\neq} = -10$ cm^3/mol. This was interpreted as indicating that the transition state for deactivation more closely resembles the square planar diamagnetic d^8 ground state than the less tightly solvated tetrahedral, triplet ES. The high spin/low spin relaxation of Fe(II) chelates, e.g., $Fe(pyim)_3^{2+}$ (pyim = 2-(2-pyridyl)imidazole) is somewhat analogous, although in this case radial contraction rather than coordination sphere twisting was argued to be responsible for the negative $\Delta V_n^{\neq}$'s (DiBenedetto, Arkle etc. 1985).

As suggested above, nonradiative deactivation may occur via crossing to another ES from which deactivation is much more rapid. In such a case, there may also be volume differences between the two ES. This is dramatically demonstrated by the emission spectrum of the iridium(III) cation $Ir(Mephen)_2Cl_2^{+}$ in DMF (Fig. 3) which emits from two states (Fig. 4). For this system, it is evident that increased pressure leads to enhanced charge transfer emission (550 nm) at the expense of LF emission (720 nm) with little or no shifts apparent in the peak maxima. The spectral changes were attributed to shifts in the relative populations of the two ES owing to partial molar volume differences between the LF and MLCT states (DiBenedetto 1984). A plot of the log of the CT/LF intensity ratio vs P proved linear. From the slope and the assumption that the ratio of the radiative rate constants is pressure independent, an apparent volume difference of

4.2 cm^3/mol between the states was calculated according to eq. 3, the LF ES being the larger. That the LF state is the larger is consistent with the population of antibonding orbitals in that ES leading to extensions of the M-L bonds.

$$(3) \qquad \Delta\bar{V}_{app} = -RT\left(\frac{d(\ln(k_r^{ct}/k_r^{lf}))}{dP}\right) + \Delta\bar{V}_{eq}$$

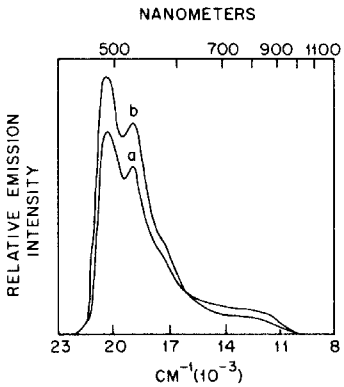

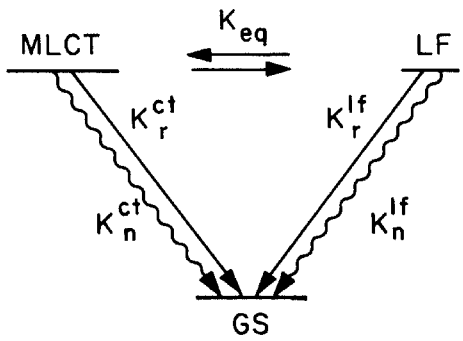

FIGURE 3 (left): Emission spectrum of $Ir(Mephen)_2Cl_2^+$ in DMF at 0.1 MPa (a) and at 300 MPa (b) showing the increase in the MLCT emission intensity at the expense of the longer wavelength LF emission at the higher pressure.

FIGURE 4: Scheme for luminescence from two emitting states of different orbital parentages. K_{eq} defined as equal to [MLCT]/[LF]

For $Ir(Mephen)_2Cl_2^+$, the MLCT is the lower energy state yet the two ES are in thermal equilibrium as evidenced by the wavelength independent emission lifetimes. Lifetime measurements in DMF solution show that the application of pressure decreases the deactivation rates with the $\ln(k_d)$ vs P plot giving the $\Delta V_d^{\ddagger}$ value +4.0 $\pm$ 0.2 cm^3/mol. The unimolecular deactivation rate constant k_d is related to the various constants noted in Fig. 4 according to eq. 4. However, since the k_r's are much smaller than the k_n's and, for such d^6 complexes, nonradiative deactivation is generally much faster from LF states than from MLCT states, k_d simplifies to $k_n^{lf}(1 + K_{eq})^{-1}$. For the limiting case $K_{eq} >> 1$, eq. 5 would hold, thus the $\Delta V_n^{\ddagger}$ value of +4.0 cm^3/mol is consistent with this model.

$$(4) \qquad k_d = \frac{K_{eq}(k_r^{ct} + k_n^{ct}) + k_n^{lf} + k_r^{lf}}{1 + K_{eq}}$$

$$(5) \qquad \Delta V_d^{\ddagger} = -RT[d(\ln k_n^{lf})/dP] - \Delta\bar{V}_{eq}$$

A two state model has also been proposed to explain pressure effects on the deactivation rates of $Ru(bpy)_3^{2+}$.[3] Small $\Delta V_n^{\ddagger}$'s were found at low temperatures, but a value of +7.5 cm^3/mol was the case for 70% aqueous solutions (Fetterolf 1985). This was explained in terms of

two competing nonradiative processes, slow weak-coupling directly from the emissive MLCT state and competitive thermal promotion to a nonluminescent, higher energy LF state from which nonradiative deactivation is extremely rapid.

CONCLUDING REMARKS

The above has been concerned with the pressure effects experienced by the nonradiative deactivation from metal complex excited states. Substantial effects often result from the involvement of several ES, so that apparent $\Delta V_n^{\ddagger}$'s may reflect differences between two ES rather than the distortions inherent to a specific deactivation mode. Nonetheless, it appears to be a safe conclusion that those systems for which a weak-coupling nonradiative deactivation mechanism is dominant, pressure effects on k_n are small (as are temperature effects). In contrast, deactivation by strong-coupling paths not only is temperature dependent, but may also be much more pressure dependent, since these appear to involve much more distortion prior to the deactivation event. Recently, we have extended our investigations to dinuclear complexes. Given that lowest energy ES for many of these derive from electron promotion between orbitals delocalized between the two centers, substantial distortions of the metal-metal bonds often result. An intriguing subset is that where both metal centers have the d^8 configuration such that the highest occupied MO is M-M antibonding but the LUMO is M-M bonding, thus the lowest ES has a significantly shorter M-M bond than the ground state (Marshall 1986). Preliminary pressure studies (Fetterolf 1987) have shown that the phosphorescence lifetimes in acetonitrile of the tetrabridged ion $Pt_2(\mu\text{-pop})_4^{4-}$ (pop is $P_2O_5H_2^{2-}$) are little affected by pressure ($\Delta V_n^{\ddagger} = -1.6$ cm^3/mol) but the dibridged complex $Ir_2(\mu\text{-pz})_2(COD)_2$ (pzH is pyrazole, COD is cyclooctadiene) has a substantially positive $\Delta V_n^{\ddagger}$ (4.6 cm^3/mol). These observations suggest that $Pt_2(POP)_4^{4-}$ deactivates by a weak-coupled pathway while the iridium dimer involves strong-coupling deactivation. The much greater temperature dependence of k_d for the latter species is fully consistent with this model.

Acknowledgement: This research was supported by the US National Science Foundation (CHE84-19283 and INT83-04030)

REFERENCES:

Amir-Ebrahimi V, McGarvey J (1984) Inorg Chem Acta 89: L39
DiBenedetto J, Arkle V, Goodwin H, Ford PC (1985) Inorg Chem 24: 455
DiBenedetto J, Ford PC (1985) Coord Chem Rev 64: 361-382
DiBenedetto J, Watts RJ, Ford PC (1984) Inorg Chem 23: 3039-3040
Drickamer HG (1982) Ann Rev Phys Chem 33: 25-47
Ford PC (1986) Chpt 6 in Inorganic High Pressure Chemistry. van Eldik R (ed), Elsevier, Amsterdam
Fetterolf ML, Offen HW (1985) J Phys Chem 89: 3320-3323
Fetterolf ML, Yang YY, Offen HW, Freidman A, Ford PC (1987) manuscript in preparation
Kirk AD, Porter GB (1980) J. Phys Chem 84: 2998-2999
Marshall AL, Stiegman AE, Gray HB (1986) ACS Symp Ser 307: 166-176
Miller DB, Miller PK, Kane-Maguire NAP (1983) Inorg Chem 22: 3832
Petersen JD, Ford PC (1974) J Phys Chem 78: 1144-1149
Salman OA, Drickamer HG (1982) J Phys Chem 77: 3337-3343
Skibsted LH, Ford PC (1983) Inorg Chem 22: 2749-2453
van Eldik R (ed, 1986) Inorganic High Pressure Chemistry, Kinetics and Mechanisms. Elsevier, Amsterdam
Weber W, van Eldik R, Kelm H, DiBenedetto J, Ducommun Y, Offen H, Ford PC (1983) Inorg Chem 22: 623-628
Weber W, DiBenedetto J, Offen H, van Eldik R, Ford P (1984) Inorg Chem 23: 2033-2038

HETEROGENEOUS PHOTOCATALYSIS BY METAL SULFIDE SEMICONDUCTORS

H.Kisch, W.Hetterich, and G.Twardzik

Institut für Anorganische Chemie der Universität Erlangen-Nürnberg
Egerlandstr. 1, 8520 Erlangen, FRG

Metallized semiconductor powders like titanium dioxide and cadmium sulfide may photocatalyze the reduction of water and reactions of organic compounds. In the latter case no new materials were obtained (Fox 1983) except in the dehydrodimerization of cyclic ethers by photoexcited zinc sulfide (Bücheler 1982; Zeug 1985; Yanagida 1985). This reaction affords from 2,5-dihydrofuran (2,5-DHF) and 2,3-dihydrofuran (2,3-DHF) the hitherto unknown compounds 1 - 3 in preparative amounts, and from THF the 2,2'-bitetrahydrofuryl (4) without traces of the 2,3'-isomer. Their formation is coupled to hydrogen evolution from water which occurs without a noble metal catalyst. In the following we report how the reaction

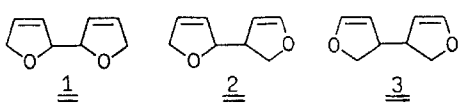

1 2 3

Scheme 1

of 2,5-DHF depends on the method of catalyst preparation, on the concentration of water, 2,5-DHF and zinc sulfide, and on the substitution of zinc sulfide by cadmium sulfide or homogeneous solutions of ZnS/CdS. Competition and inhibition experiments give some basic insights into the nature of interfacial electron transfer processes.

The sulfides were prepared by addition of sodium sulfide to zinc sulfate at room temperature (ZnS-A) or by the reaction of zinc sulfate

Photochemistry and Photophysics
of Coordination Compounds, Ed. by H. Yersin/A. Vogler

with thiourea (Kurian 1972) in alkaline solution at 80°C (ZnS-B). All samples were obtained as amorphous powders containing various amounts of cubic zinc sulfide. The sulfides ZnS-B have surface areas of 10 - 15 m^2/g (BET-method) and exhibit strong photocorrosion. EDAX-analysis shows that the ratio of Zn/S on the surface increases from 1.00/0.83 to 1.00 /0.68 when the sulfide is precipitated from a solution with the ratio Zn^{2+}/OH^- = 1/5 ($ZnS\text{-}B_1$) and 1/10 ($ZnS\text{-}B_2$), respectively. The higher content of zinc oxide, as indicated by the higher zinc to sulfur ratio, increases photocorrosion and decreases the reaction rate by 50% as compared to $ZnS\text{-}B_1$.

All zinc sulfides prepared exhibit at room temperature luminescence upon front-face illumination. Maxima in the emission spectra at 430, 670 nm originate from zinc sulfide, at 500 nm from the latter and traces of zinc oxide, and at 600 nm from an impurity of Mn(II). No obvious correlation is found between slight changes in the emission spectra and photocatalytic activity.

When the four sulfides $ZnS\text{-}A_{1-4}$ are precipitated from solutions containing different concentrations of ammonia, the initial rates are 7, 0, 7, and 19 ml H_2/h for the molar ratios Zn^{2+}/NH_3 = 1/0, 1/7, 1/20 and 1/30, respectively. Diffuse reflectance spectra of $ZnS\text{-}A_{1-3}$ contain the bandgap absorption at 354 nm, which indicates the presence of interstitial Zn^{2+} and Zn(0) (Kurian 1972). $ZnS\text{-}A_4$ has this absorption at 336 nm which is equal to the literature value of pure zinc sulfide. The interstitial atoms promote electron-hole recombination and thus the lower catalytic activity of $ZnS\text{-}A_{1-3}$ becomes explainable. When the ammonia concentration is too low, as in the case of $ZnS\text{-}A_2$, the alkaline medium induces the formation of zinc oxide which inhibits the reaction; the ratio Zn/S on the surface is 1.00/0.87, 1.00/0.55 and 1.00/0.83 in the case of $ZnS\text{-}A_1$, $ZnS\text{-}A_2$ and $ZnS\text{-}A_4$, respectively. Induction times are

longer with the less active samples pointing to a possible removal of interstitial atoms and surface oxide at this initial stage of the reaction. The rate induced by ZnS-A_4 is about three times that obtained by ZnS-B_1 and its catalytic activity persists much longer. This may be due to the larger specific surface of the sulfides ZnS-A (100 - 130 m^2/g) However, other properties of the surface like porosity seem to be also important and there is no simple correlation between surface area and photocatalytic activity.

Homogeneous solutions of platinized ZnS/CdS induce a decrease of the initial rate when the amount of cadmium is increased (Fig.1). This may be due to the concomitant decrease of the reducing and oxidizing power

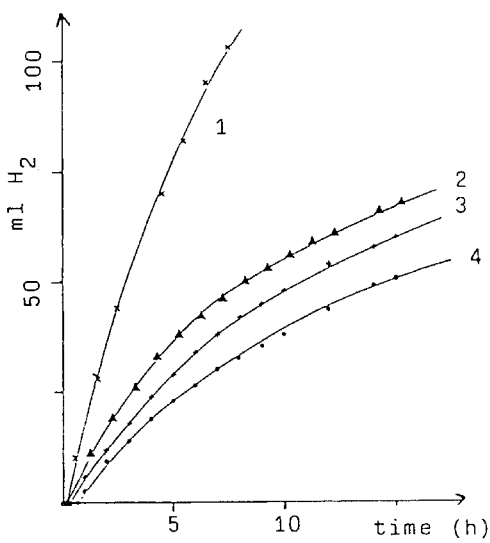

Fig.1: Rate of hydrogen evolution as function of irradiation time; 0.3 mmol of catalyst suspended in 120 ml of 2,5-DHF/H_2O = 1/14 (v/v); 1: ZnS-A_4, 2: $Zn_{0.2}Cd_{0.8}S$/Pt, 3: $Zn_{0.1}Cd_{0.9}S$/Pt, 4: CdS/Pt

of the photogenerated electrons and holes, respectively; the flatband positions of zinc and cadmium sulfide are at -1.6 and -0.7 V (pH=7), the bandgap energies at 3.65 and 2.4 eV, respectively. In the case of CdS/Pt the reaction occurs also with visible light.

Competition experiments between 2,5-DHF and THF were conducted with the catalyst ZnS-A_4. Since the reaction rate of 2,5-DHF is ten times that of THF, dehydrodimers of the latter and cross-products should be formed when THF is present in a tenfold excess over 2,5-DHF. The fact that these products appear only if the ratio THF/2,5-DHF is at least 100/1, points to specific adsorption effects. When the ratio is about 300/1, the dehydrodimer of THF , **4**, is the major product in the case of equal amounts of zinc sulfide and 2,5-DHF; contrary, **1** - **3** are formed predominantly when 2,5-DHF is present in a threefold excess over the sulfide (case a). When the ratio THF/2,5-DHF is increased to 1000/1 and that of 2,5-DHF/ZnS is decreased to 0.3, **4** becomes the main product and **1** - **3** are formed only in traces (case b). The reaction stops in case a after all 2,5-DHF has been consumed but continues with a slower rate, due to reaction of THF, in case b. The difference may be rationalized by the assumption that 2,5-DHF covers all adsorption sites when present in excess over zinc sulfide, and that THF cannot use these sites for adsorption nor replace adsorbed 2,5-DHF or **1** - **3**. Contrary, when 2,5-DHF is present in lower concentrations (case b) there seems some free surface available for adsorption of THF and the reaction continues through oxidation of THF when all 2,5-DHF has reacted. These experiments demonstrate that chemoselectivity can be introduced by proper selection of the ratio of substrate to catalyst.

The better adsorption of 2,5-DHF is further supported by the Langmuir-type dependence of the rate on the concentrations of 2,5-DHF, THF and water; after an initial linear increase a plateau of maximum rate is

reached at concentrations of 1.5, 6 and 15 M, respectively. From the plot of reciprocal rates versus reciprocal concentrations, equilibrium constants of adsorption are obtained as 10, 0.5 and 0.6 M^{-1} for 2,5-DHF THF and water, respectively.

From these experimental results a mechanistic scheme is proposed wherein photophysical processes and the adsorption equilibrium of water are omitted for the sake of simplification (Scheme 2); $\square_{ZnS}$ symbolizes an

$RH + \square_{ZnS}$	$\rightleftharpoons$	RH_{ad}	(1)
ZnS	$\xrightarrow{h\nu}$	$ZnS(e^-,h^+)$	(2)
$H_2O_{ad} + ZnS(e^-,h^+)$	$\longrightarrow$	$ZnS(h^+) + 1/2\ H_2 + OH^-_{ad}$	(3)
OH^-_{ad}	$\rightleftharpoons$	OH^-	(4)
$RH_{ad} + ZnS(h^+)$	$\longrightarrow$	$RH^{+\cdot}_{ad} + ZnS$	(5)
$RH^{+\cdot}_{ad}$	$\longrightarrow$	$R^{\cdot}_{ad} + H^+_{ad}$	(6)
H^+_{ad}	$\rightleftharpoons$	H^+	(7)
$R^{\cdot}_{ad}$	$\longrightarrow$	$1/2\ R_{2\,ad}$	(8)
$1/2\ R_{2\,ad}$	$\rightleftharpoons$	$1/2\ R_2$	(9)
$R^{\cdot}_{ad}$	$\rightleftharpoons$	$R^{\cdot}$	(10)
$R^{\cdot}$	$\longrightarrow$	$1/2\ R_2$	(11)

Scheme 2

empty adsorption site, and solvated species are shown without an index. The photogenerated electron-hole pair (step 2) reduces water to hydrogen (3) and the remaining holes oxidize the adsorbed ether (1,5) to the radical cation. Deprotonation should be fast due to the high hydration

energy of the proton (6,7). The radical R$^{\cdot}$ may dimerize in the adsorbed (8,9) and/or fully solvated state (10,11) to the final products. The fact that the diastereomers of the dehydrodimers are formed in equal amounts points to the latter possibility. Interfacial electron transfer (3,5) seems to be strongly coupled as indicated by the inhibition of both hydrogen and dehydrodimer formation in the presence of electron scavengers like N_2O or zinc chloride. The more efficient removal of conduction band electrons by the scavenger should increase the stationary hole concentration. This may induce oxidation of $RH^{+\cdot}$ or R$^{\cdot}$ by a second hole, preventing dimerization. A further possibility is that the inhibition occurs at a surface site where no ether species is adsorbed.

References

Bücheler J, Zeug N, Kisch H (1982) Zinksulfid als Katalysator der heterogenen Photoreduktion von Wasser. Angew.Chem. 94: 792

Fox MA (1983) Organic Heterogeneous Photocatalysis: Chemical Conversions Sensitized by Irradiated Semiconductors. Acc.Chem.Res. 16: 314 - 321

Kurian A, Suryanarayana CV /1972) Studies on a new method of preparation of zinc sulfide useful for luminescent phosphors. J.Appl.Electrochem. 2: 223 - 229

Yanagida S, Azuma T, Midori Y, Pac Ch, Sakurai H (1985) Semiconductor Photocatalysis. Part 4. Hydrogen Evolution and Photoredox Reactions of Cyclic Ethers Catalyzed by Zinc Sulfide. J.Chem.Soc.Perkin Trans II 1985: 1487 - 1493

Zeug N, Bücheler J, Kisch H (1985) Catalytic Formation of Hydrogen and C-C Bonds on Illuminated Zinc Sulfide Generated from Zinc Dithiolenes. J.Am.Chem.Soc. 107: 1459 -1465

INORGANIC PHOTOINITIATORS FOR PHOTOLITHOGRAPHIC APPLICATIONS

C.Kutal* and C.G.Willson**

* Department of Chemistry, University of Georgia, Athens, GA 30602, USA
**IBM Almaden Research Center, 650 Harry Rd., San Jose, CA 95120, USA

INTRODUCTION

Photolithography is used extensively in the microelectronics industry to generate three-dimensional patterns in a solid substrate such as single crystal silicon (Willson 1983; Bowden 1984). Figure 1 illustrates the sequence of steps that comprise the typical photolithographic process. The substrate initially is coated with a thin layer of a photosensitive material, termed a **resist**, and then exposed to light through a mask containing transparent and opaque areas that define the desired pattern. The transparent areas transmit light which causes a photochemical reaction in the resist, thereby affording a means of differentiating the exposed and unexposed regions. Preferential dissolution of the unexposed resist in a suitable developing solvent, for example, creates a negative tone image of the mask on the substrate surface (a positive tone image results if the exposed resist dissolves preferentially in the developer). This image, in turn, can be transferred into the substrate via a chemical and/or physical etching process in which the areas not protected by the resist are attacked by the etchant. The final step involves stripping away the resist to yield a negative tone relief image in the substrate that replicates the pattern of the mask.

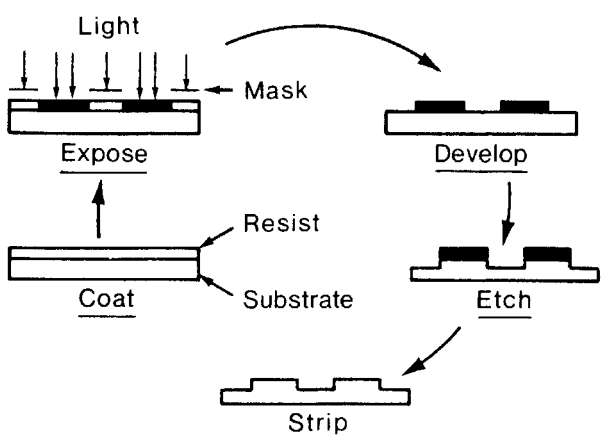

Figure 1. Sequence of steps in the photolithographic process.

Photochemistry and Photophysics
of Coordination Compounds, Ed. by H. Yersin/A. Vogler

Resists composed of a functionalized polymer and a photoinitiator have been a mainstay of the photolithographic process for a number of years. The generalized response of this type of system to light can be summarized by eq. 1 and 2. Absorption of a photon by the

$$P \xrightarrow{h\nu} I \qquad [1]$$

$$I + \text{polymer} \longrightarrow \text{modified polymer} \qquad [2]$$

photoinitiator P results in its conversion to one or more reactive species I. Subsequent thermal reaction of I with the polymer causes the change in solubility or other properties that form the basis for distinguishing between exposed and unexposed areas. Since the photoinitiator and the polymer serve different functions, it is possible to optimize the properties of one without affecting the desirable features of the other. This inherent flexibility of a two-component system greatly simplifies the task of designing radiation-sensitive materials.

The majority of commercially-important photoinitiators are nonmetallic compounds which generate radicals and/or strong acids upon irradiation. The latter species play the role of I in eq. 1 and 2 and react with the functionalized polymer via well-precedented radical or cationic pathways. Examples of commonly-used nonmetal initiators include benzoin and benzoin ethers, benzyl ketals, benzophenones plus hydrogen atom donors, and "onium" salts belonging to the aryldiazonium, triarylsulfonium, and diaryliodonium families (Gatechair 1983; Vesley 1986). In contrast, little information currently exists concerning the use of transition metal complexes as photoinitiators for the reactions of functionalized polymers. This oversight is surprising, since several classes of complexes appear to be well-suited for this role. Exemplary in this regard are the classical acidopentamminecobalt(III) complexes, $Co(NH_3)_5X^{+2}$, where X is Cl, Br, I or other uninegative group. In addition to their ease of synthesis, these complexes resist decomposition by air, moisture, and heat (>100°C), absorb strongly in the ultraviolet spectral region, and undergo quantum efficient photodecomposition from a ligand-to-metal (X to Co) charge transfer excited state. As described by eq. 3, this intramolecular redox reaction in aqueous solution generates the aquated cobalt(II) cation (a Lewis acid),

$$Co(NH_3)_5X^{+2} \xrightarrow{h\nu} Co^{+2}_{(aq)} + 5NH_3 + X^{\cdot} \qquad [3]$$

the X· radical, and five molecules of ammonia (a Lewis base) (Balzani 1970; Endicott 1975). One or more of these chemically distinct species could play the role of I in eq. 2 and initiate useful chemistry in a functionalized polymer.

To test this possibility, we selected $[Co(NH_3)_5Br](ClO_4)_2$ as the photoinitiator owing to its strong absorption in the deep-ultraviolet region, while the commercially-available resin, COP (Fig. 2), served as the functionalized polymer. The latter is a copolymer of glycidyl methacrylate and ethyl acrylate which has found use as a negative electron-beam resist (Thompson 1974, 1975). The epoxide group situated on the glycidyl side chain is susceptible to ring opening both by acidic and basic reagents and thus is a logical site for crosslink formation (Lee 1967). As discussed in the next section, the COP-$[Co(NH_3)_5Br](ClO_4)_2$ system proved to be of considerable interest as a photoresist.

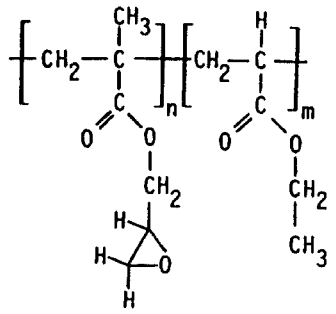

n/m = 0.74

$\frac{M_w}{M_n} = 2.2$

$M_n = 0.6 \times 10^5$ (by gpc)

Figure 2. Structure and properties of COP sample used in this study.

RESULTS AND DISCUSSION

While resists of varying composition have been investigated (Kutal 1987), the results summarized here refer specifically to a formulation containing 9 wt % of COP and 1 wt % of $[Co(NH_3)_5Br](ClO_4)_2$ dissolved in a 1:3 (v:v) solvent mixture of N-methyl-2-pyrrolidinone/chlorobenzene. Following filtration through a 0.2 μm filter, this solution was spin-coated onto quartz and silicon wafers and the solvent removed by heating at 62°C for 3-4 minutes. Films of COP-$[Co(NH_3)_5Br](ClO_4)_2$ prepared by this procedure were 0.5 μm thick and, when examined under a microscope at 1500x magnification, showed no evidence of aggregation of the cobalt salt. The electronic absorption spectrum of a film above 250 nm is essentially that of $Co(NH_3)_5Br^{+2}$, since COP absorbs very weakly in this wavelength region. Exposing a film to 254 nm radiation causes a bleaching of the intense Br-to-Co charge transfer absorption band (λ_{max} = 258 nm) in the complex. This behavior is consistent with the occurrence of a photoredox process which, in analogy to the aqueous solution photochemistry of the complex (eq. 3), generates one or more weakly-absorbing cobalt(II) species. While a detailed characterization of the photoproducts has yet to be undertaken, we would expect the reduced metal to remain coordinated to a number of ammonia molecules since such complexes are known to persist in the solid state at room temperature (Wendlandt 1967). Dissociation of ammonia may occur, however, especially when the polymer film is heated.

A film exposed to >60 mJ/cm^2 of 254 nm radiation dissolves completely away from the underlying wafer upon being sprayed for 15 seconds with a 5:3 mixture of 2-butanone/ethanol. In contrast, heating a comparably irradiated film at 68°C for 6.5 minutes renders it insoluble in this solution. Since heating, by itself, does not cause insolubilization, it appears that one or more of the photodecomposition products of $[Co(NH_3)_5Br](ClO_4)_2$ react(s) with COP in a thermally-activated process which crosslinks the epoxy resin. Experiments designed to elucidate the mechanism of crosslinking suggest that one or perhaps both of the following paths (Fig. 3) play(s) an important role: (i) reaction of the basic ammonia

molecule with pendant epoxide groups on adjacent polymer chains, (ii) coordination of a cationic cobalt species to the oxygen atom of an epoxide ring followed by nucleophilic attack of a second epoxide.

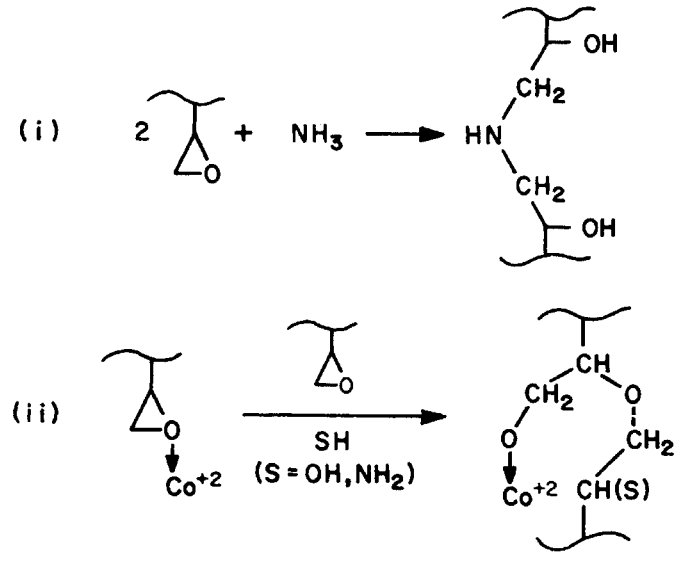

Figure 3. Mechanisms for the crosslinking of COP: (i) base initiated, (ii) cation initiated.

Dose-response measurements on COP-$[Co(NH_3)_5Br](ClO_4)_2$ films reveal that 20-25 mJ/cm^2 of 254 nm radiation is sufficient to cause detectable gel formation, while one-half of the ultimate film thickness can be achieved with 35-40 mJ/cm^2. Figure 4 displays the line-space pattern obtained upon exposing a film in contact with a chrome mask to a 40 mJ/cm^2 dose, baking at 68°C for 6.5 minutes, and then developing with 2-butanone/ethanol. Despite some swelling of the negative tone images by the developer, 1-2 micron resolution can be obtained.

Films of pure COP are insensitive to 254 nm radiation since, as noted earlier, the resin exhibits negligible absorption at this wavelength. Photochemistry does occur upon prolonged irradiation at shorter wavelengths, but quite interestingly, it results in degradation of the polymer chains. Consequently, upon development, the exposed areas of the film dissolve away. Thus, quite apart from extending the effective photosensitivity of the system to a convenient wavelength, the incorporation of $[Co(NH_3)_5Br](ClO_4)_2$ into a film of COP changes the basic response of the material from positive tone to negative tone. Moreover, the ability to image a COP-$[Co(NH_3)_5Br](ClO_4)_2$ film with both photons and electrons (recall that COP, itself, is a sensitive e-beam resist) offers the prospect

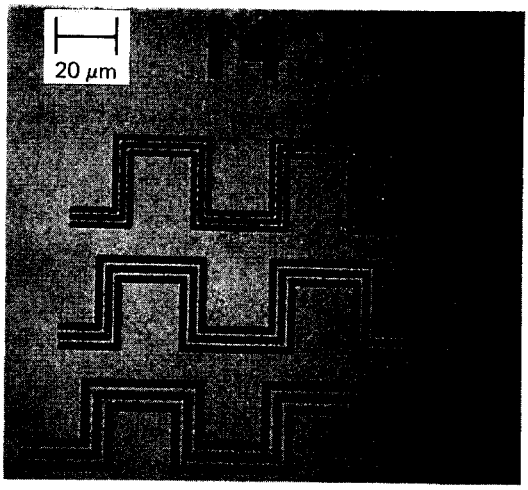

Figure 4. Optical photomicrograph of pattern obtained upon 254-nm exposure and development of a COP-$[Co(NH_3)_5Br](ClO_4)_2$ film.

of "hybrid" lithography (Imamura 1984) whereby relatively large patterns are first printed with uv light and then very fine patterns are delineated with a focused electron beam.

The interesting chemical and lithographic properties of the COP-$[Co(NH_3)_5Br](ClO_4)_2$ system provide a promising indication that new classes of radiation sensitive materials can result from the proper combination of an inorganic initiator and a functionalized polymer. The design of such materials, their fundamental chemistry, and their potential application are topics that we are continuing to pursue.

REFERENCES

Balzani V, Carassiti V (1970) Photochemistry of coordination compounds. Academic Press, London New York, p 193

Bowden MJ (1984) A perspective on resist materials for fine-line lithography. In: Thompson LF, Willson CG, Frechet JMJ (eds) Materials for microlithography. American Chemical Society, Washington, D.C., p 39

Endicott JF (1975) Charge-transfer photochemistry. In: Adamson AW, Fleischauer PD (eds) Concepts of inorganic photochemistry. Wiley-Interscience, New York London, p 81

Gatechair LR, Wostratzky D (1983) Photoinitiators: an overview of mechanisms and applications. J Radiat Curing 10:4-18

Imamura S, Tamamura T, Kogure O (1984) Chloromethylated poly(napthyl methacrylate) as electron beam and photoresist. Polymer J 16: 391-400

Kutal C, Willson CG (1987) Photoinitiated crosslinking and image formation in thin polymer films containing a transition metal compound. J Electrochem Soc in press

Lee H, Neville K (1967) Handbook of epoxy resins. McGraw-Hill, New York, Chap 5

Thompson LF, Feit ED, Heidenreich RD (1974) Lithography and radiation chemistry of epoxy containing negative electron resists. Polym Eng Sci 14: 529-533

Thompson LF, Ballantyne JP, Feit ED (1975) Molecular parameters and lithographic performance of poly(glycidyl methacrylate-co-ethyl acrylate): a negative electron resist. J Vac Sci Technol 12: 1280-1283

Vesley GF (1986) Mechanisms of the photodecomposition of initiators. J Radiat Curing 13:4-10

Wendlandt WW, Smith JP (1967) The thermal properties of transition-metal ammine complexes. Elsevier, New York, Chap 4

Willson CG (1983) Organic resist materials-theory and chemistry. In: Thompson LF, Willson CG, Bowden MJ (eds) Introduction to microlithography. American Chemical Society, Washington, D.C., p 88

PHOTOCHEMICAL BEHAVIOUR OF LUMINESCENT DYES IN SOL-GEL AND BORIC ACID GLASSES

R.Reisfeld*, M.Eyal*, R.Gvishi*, and C.K.Jørgensen**

* Department of Inorganic Chemistry, Hebrew University, Jerusalem, ISRAEL
**Section de Chimie, Université de Genève, 1211 Geneva 4, SWITZERLAND

Fluorescence of organic colorants is generally enhanced by high viscosity of the surrounding medium,having much fewer energetic collisions with the excited state,and perhaps also preventing large distortions along unsymmetrical vibrational modes.However,this is not simply determined by the macroscopic viscosity (Lewis and Calvin 1939) since cool glycerol is much more effective than a lubricating oil at the same low temperature. We are here studying fluorescein,belonging to the category of xanthene dyes (the heterocyclic xanthene is two benzene rings connected with two bridges in ortho-position,one being an oxygen atom and the other CH_2) like the various substituted eosine and rhodamine modifications.In many cases,their quantum yield η is above 0.9,and corresponding to their very strong absorption bands in the visible,the life-time τ of fluorescein is only 4 nanoseconds in water and alcohols (Martin 1975).

Lewis,Lipkin and Magel (1941) studied fluorescein in glasses formed by melting boric acid $B(OH)_3$ and removing water vapor to a composition close to $B_{20}O_{27}(OH)_6$.From the point of view of protonation discussed below,the absorption maximum at 436 nm makes this glass comparable to aqueous acid with pH below 1,but the luminescence is superposed a very slow decay of the first triplet state ("phosphorescence") reaching τ = 3 seconds at liquid air besides a non-exponential singlet emission at higher energy. Following Jabłoński (1935),Lewis et al. (1941) distinguish the "beta process" of triplet emission from the "alpha process" of exceptionally slow emission from the first excited singlet state,enhanced by increasing temperature.We call the alpha process "delayed fluorescence" since it is due to the thermal excitation of the long-lived triplet state to the first excited singlet,with an Arrhenius activation energy agreeing with the spectroscopic energy difference 3000 cm^{-1}.Another complication for the luminescence is the appearance (in strong illumination) of two new absorption bands at 650 and 505 nm due to transitions from the quasi-stationary concentration of the lowest triplet to two much higher triplet states.

Photochemistry and Photophysics
of Coordination Compounds, Ed. by H. Yersin/A. Vogler

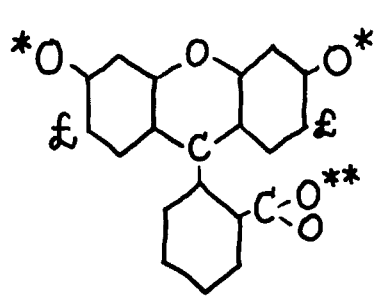

flu(C) cation: *each one H; ** one H

flu(N) neutral molecule(quinonic form;in equilibrium with lactonic tautomer in less polar solvents): *one of two has H; ** one H

flu(A) anion with one negative charge: *one of two has H

flu(D) di-anion with two negative charges: no additional H

flu(MA)is a neutral compound;each £ has H replaced by HgO_2CCH_3

The consecutive pK values for the deprotonation C→N→A→D in water (Zanker and Peter 1958;Leonhardt et al. 1971) are 2.2, 4.4 and 6.7. Hence,the di-anion is prevailing for all pH above 8.Contrary to many excited singlet states of heterocyclic compounds studied by Förster, the third pK = 6.7 only decreases marginally to 6.9 in the excited state.The C absorption maximum shifts smoothly from 436 nm in 0.5 molar to 431 nm in 7.4 molar perchloric acid (where the emission maximum occurs at 482 nm).It should be noted that differing conditions of hydrogen bonding in 7 solvents (Martin 1975) shift both the absorption and emission maxima of the di-anion within 7 percent.There is no sign of isosbestic points,as is also true in the case of $IrBr_6^{-2}$ in organic solvents (Jørgensen 1962).The almost identical behaviour of 6-hydroxy-9-phenyl-fluoron (Martin 1975) shows that the carboxyl group plays no essential rôle in fluorescein.

Contrary to boric acid glasses,the triplet state does not form to any large extent in these deuterated solvents,though the probability of internal conversion (non-radiative de-excitation) is then multiplied by 0.6 to 0.7 (Martin and Lindqvist 1973).The triplet life-time is 4.5 ms in acids and 20 ms at pH = 12,less than a percent of the value for boric acid glass (Carmichael and Hug 1986).Correspondingly, η = 0.31 for the neutral (N) and 0.93 for the di-anion (D) (Weber and Teale 1958). We find η = 0.23 at pH = 1 (cation C) showing the absorption maximum at 437 nm, η = 0.92 at pH = 6 in water (mixture of A and D,479 nm)and η = 0.92 at pH = 13 (D,490 nm).

Heat-sensitive colorants can be incorporated in Vycor glass (Mack et al. 1983) and in gel glasses (Reisfeld 1984;Levy et al. 1984) where, for instance,the silica cage modifies the spectra of trapped rhodamine 6 G and strongly enhances its photostability (Avnir et al.

1984).Recently,we have incorporated fluorescein derivatives (in methanolic solution) in a glass prepared by controlled hydrolysis of $Si(OCH_3)_4$ at 60°C for 48 hours.The glasses obtained are of good optical quality,transparent above 340 nm,and of densities 1.15 to 1.2 g/ml (Reisfeld et al. 1987).Also thin sol-gel glass films prepared by the method of Avnir,Kaufman and Reisfeld (1985) show η = 0.9 after light absorption in a maximum at 455 nm.If heated to 200°C,the absorption shifts to 490 nm,resembling the effect of deprotonation.Fluorescein substituted by two mercury acetate groups,flu(MA)in the scheme above, shows rapid transformation of the first excited singlet to the lowest triplet state,as a typical relativistic "heavy-atom" effect.The time-evolution of the emissibn spectrum of flu(MA) in boric acid glass is roughly invariant intensity of the 570 nm emission for a few milliseconds,followed by a slow decay (at room temperature) with τ=2.8$\pm$0.5 seconds,the τ value Lewis et al.(1941) found for 570 nm emission of fluorescein in boric acid glass at 60 K,to be compared with about 1 s at 300 K.These measurements are rendered difficult by the photochemical dissociation of the two MAgroups.Nevertheless,the observed 490 nm emission from flu(MA) has less than a-quarter of the intensity at 570 nm after at least 0.01 s has elapsed since the illumination stopped.

The luminescence of fluorescein in glasses prepared at moderate temperatures may have several applications.It seems rather probable that flat-plate luminescent solar concentrators (transporting emitted light by a series of total reflections out to a rim covered with a photovoltaic material) are only a competitive alternative to flat-plate silicon coverage,if combined with some organic materials (Reisfeld and Jørgensen 1982;Reisfeld et al. 1983;Neuroth and Haspel 1986).Lasers involving 4f and 3d group ions may also be combined with thin films containing organic luminophores (Reisfeld 1983 and 1985).Fluorescein-doped boric acid glass shows non-linear optical properties applicable to phase conjugation devices (Kramer et al. 1986).

Acknowledgements:
This work was supported by the National Council of Research and Development,Israel.

Avnir D,Levy D,Reisfeld R (1984) J.Phys.Chem. 88: 5956-5959
Avnir D,Kaufman V R,Reisfeld R (1985) J.Non-Cryst.Solids 74: 395-406
Carmichael T,Hug G L (1986) Triplet-triplet absorption spectra of organic molecules in condensed phases. J.Phys.& Chem.Ref.Data (Nat.Bur.Stand.,Washington DC) 15: 1.
Jabłoński A (1935) Z.Physik 94: 38-46
Jørgensen C K (1962) J.Inorg.Nucl.Chem. 24: 1587-1594
Kramer M A,Tompkin W R,Boyd R W (1986) Phys.Rev. A 34: 2026-2031
Leonhardt H,Gordon L,Livingston R (1971) J.Phys.Chem. 75: 245-249
Levy D,Reisfeld R,Avnir D (1984) Chem.Phys.Lett. 109: 593-597
Lewis G N,Calvin M (1939) Chem.Rev. 25: 273-328
Lewis G N,Lipkin D,Magel T T (1941) J.Am.Chem.Soc. 63: 3005-3018
Mack H,Reisfeld R,Avnir D (1983) Chem.Phys.Lett. 99: 238-239
Martin M M,Lindqvist L (1973) Chem.Phys.Lett. 22: 309-312
Martin M M (1975) Chem.Phys.Lett. 35: 105-111
Neuroth M,Haspel R (1986) Glasses for luminescent solar concentrators. Proc.SPIE-86,Opt.Mater.Technol.Energy Effic.Solar Energy Conversion 653: 88-92
Reisfeld R,Jørgensen C K (1982) Structure and Bonding 49: 1-36
Reisfeld R (1983) Chem.Phys.Lett. 95: 93-95
Reisfeld R,Manor N,Avnir D (1983) Solar Energy Materials 8: 399-409
Reisfeld R (1984) J.Electrochem.Soc. 131: 1360-1364
Reisfeld R (1985) Chem.Phys.Lett. 114: 306-308
Reisfeld R,Eyal M,Gvishi R (1987) Chem.Phys.Lett.,submitted
Weber G,Teale F W J (1958) Trans.Faraday Soc. 54: 640-648
Zanker V,Peter W (1958) Chem.Ber. 91;572-580

INDUSTRIAL APPLICATIONS OF ORGANOMETALLIC PHOTOCHEMISTRY

A.Roloff, K.Meier, and M.Riediker

Central Research Laboratories, CIBA-GEIGY AG, 4002 Basle, SWITZERLAND

INTRODUCTION

In an attempt to understand and improve the inorganic photochemistry of the photographic process numerous scientists in industrial laboratories studied the interaction of light with silver halides. Another form of imaging however has recently gained a lot of attention. Photopolymerisation methods for the manufacture of printed and integrated circuits are studied in great detail (Steppan et al. 1982). It is in this area that organometallic photochemistry has been put to work (Curtis et al. 1986). Two examples from our own research laboratories shall demonstrate the usefulness of organometallic photochemistry for imaging systems.

TITANOCENE PHOTOINITIATORS

A number of titanium(IV)-complexes have been described as light sensitive and some have been claimed as photoinitiators (Zucchini et al. 1971; Kaeriyama, Shimura 1972).
The photochemistry of bis-cyclopentadienyl-titanium-diphenyl (1) has been extensively studied (Peng, Brubaker 1978; Rausch et al. 1978; Tung, Brubaker 1981).

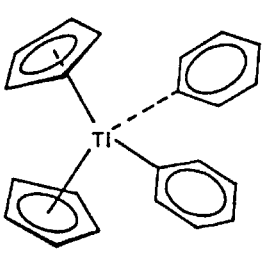

1

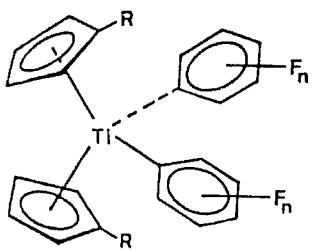

2

Photoinitiators however must be thermally stable and offer advantages over conventional radical UV-initiators. During our work with titanium complexes we discovered enhanced thermal and oxidative stability as well as a very efficient curing rate when a fluorinated aryl ligand is introduced into the complex (2) (Riediker et al. 1983; Roloff, Meier, Riediker 1986). The synthesis of these complexes was easily achieved according to the literature procedure (Chaudhari, Treichel, Stone 1964).
The photochemistry of the fluorinated compounds (2) however proved to be totally different from what was known about the phenyl derivative (1). Rausch (1978) had found that benzene and diphenyl were formed as the major products when the complex was irradiated in solution.

Photochemistry and Photophysics
of Coordination Compounds, Ed. by H. Yersin/A. Vogler

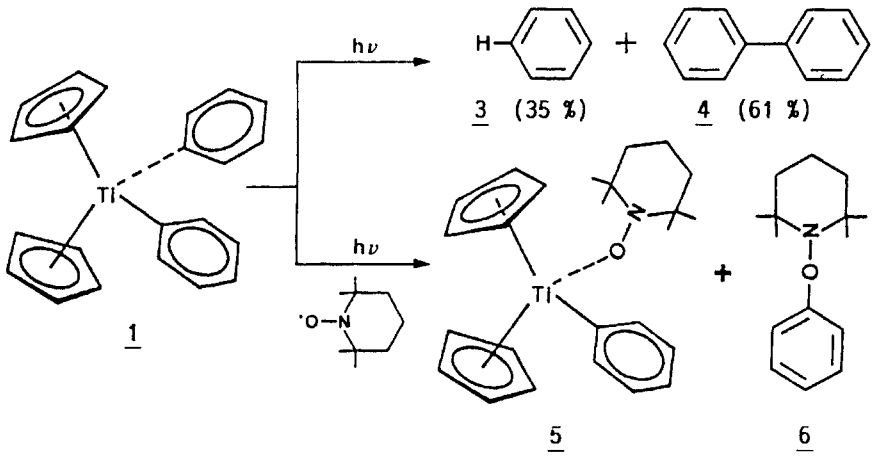

We were able to trap the radicals formed by homolysis of the Ti-aryl bond with the aid of a radical scavenger (Roloff, Meier, Riediker 1986). From the photoreaction of the fluorinated compound (7) however no organic radicals could be trapped. Pentafluorophenyl substituted cyclopentadienes (8) were observed as the main organic products and a titanium-fragment which had reacted with two radical scavengers (9) was isolated.

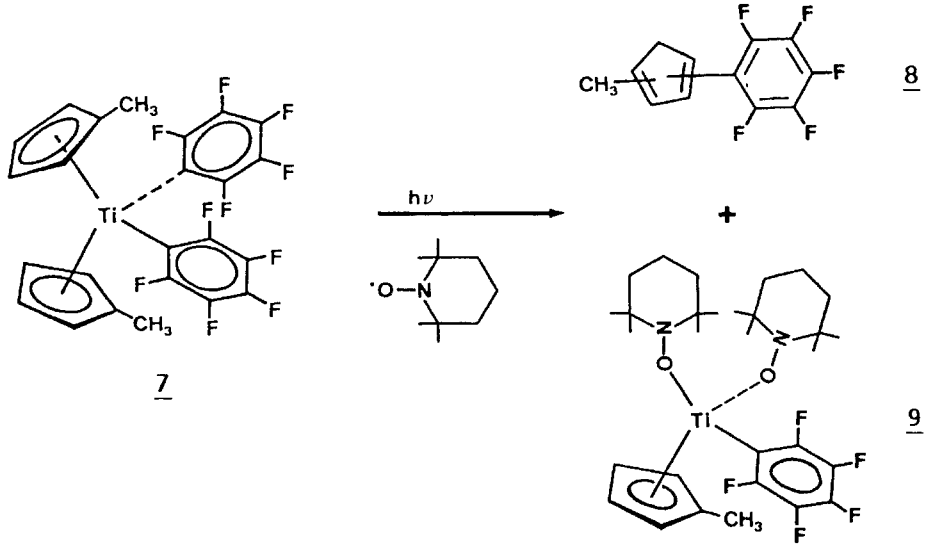

We are currently investigating the source of polymerisation initiation. Nevertheless are these titanium based photoinitiators among those with the greatest curing speed for vinyl polymerisation. They are applicable in the manufacture of permanent coatings and integrated circuits. Due to their absorption in the visible and their bleaching they can be applied in the curing of thicker layers as they are required for the application as planarising dielectrics between metal layers (Rohde et al. 1985, 1986). Their pronounced absorption in the region between 400 and 600 nm opens an opportunity to use these photoinitiators in laser-lithography. The main emissions of an argon laser are exactly in the region of the charge-transfer band of our titanium photoinitiators.

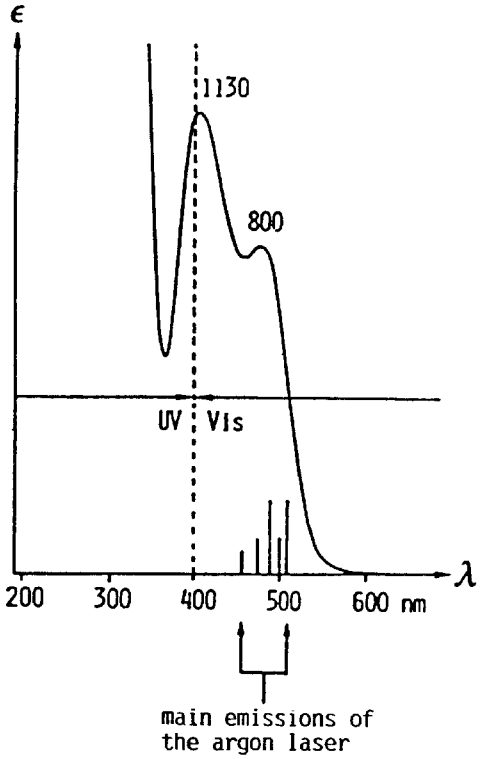

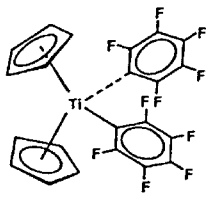

10

Fig. 1. Absorption spectrum of (10) with main emission lines of the argon laser.

IRON-ARENE PHOTOINITIATORS

In recent years the photocrosslinking of epoxides has become a field of increasing interest (Delzenne 1979; Green, Stark 1981). Crosslinked polyethers with their favourable properties such as thermal stability, mechanical strength, and chemical resistance thus became available for coating and imaging applications. In contrast to free radical polymerisation of vinylic substrates the cationic polymerisation of epoxy resins is not inhibited by oxygen (Lohse, Zweifel 1986). Several types of cationic photoinitiators have been described in the literature (Schlesinger 1974; Crivello 1977, 1981). A number of organometallic compounds have also been tested for this purpose (Brown et al. 1976; Curtis et al. 1986). So far most of the cationic photoinitiators have had certain drawbacks which with-held them from achieving a major break-through. In many cases there is a lack in thermal stability.
Our new iron-arene photoinitiators (11) can overcome most of these shortcomings (Meier et al. 1982; Meier, Zweifel 1985, 1986).

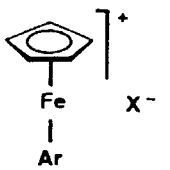

11

Ar: η^6-bound arene ligand

X: non nucleophilic anion like PF_6^-, AsF_6^-, BF_4^-

The preparation of these compounds was described by Nesmeyanov (1963) and he already studied the photochemical behaviour of these complexes (Nesmeyanov 1970).

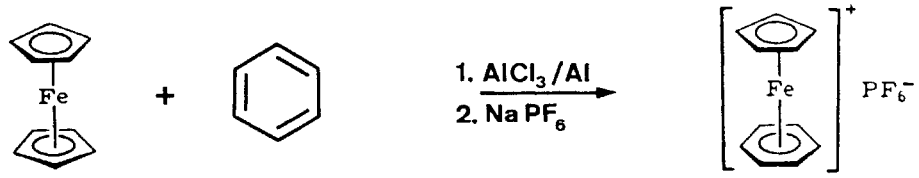

12 13

Gill and Mann (1980, 1981) studied ligand exchange reactions replacing the arene ligand by another three suitable ligands.

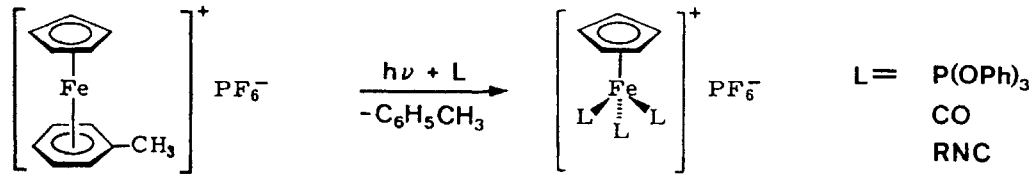

14 15

We have shown that the ligand is photolytically removed from the complex and the resulting Lewis-acid can start the epoxide polymerisation. We were however not successful in isolating the proposed intermediate (16).

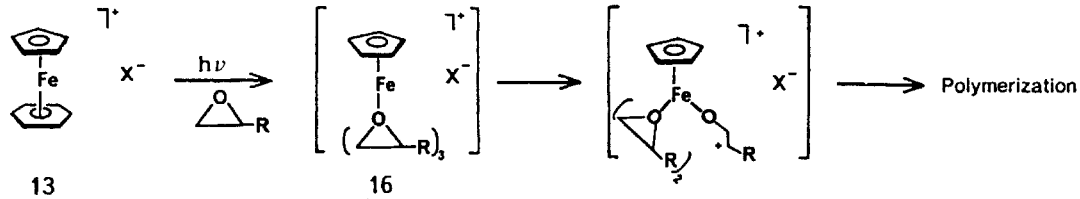

13 16

Fig. 2. Postulated mechanism for epoxide polymerisation initiation.

In a model experiment the photolysis of the toluene complex (15) in presence of ethylene oxide yielded the crystalline paramagnetic solid (17) with a chemical yield of 80 % (Meier, Rihs 1985). This led us to believe, that after photolytically removing the arene ligand an epoxide can serve as a suitable substitute.

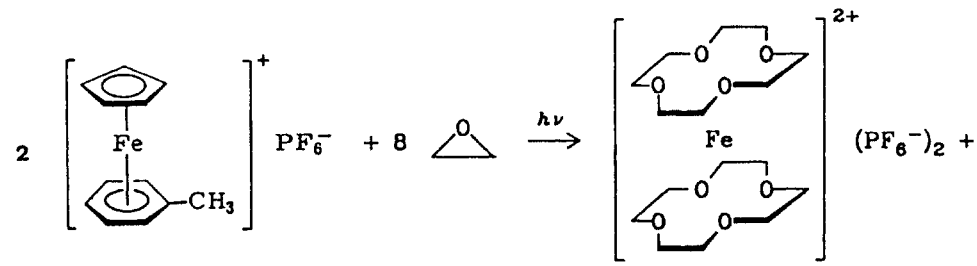

14 17

Subsequently ring opening can take place within the coordination sphere of the complex and thus start polymerisation. The process however requires temperatures of about 100°C. This temperature can be lowered, if as shown in fig. 3 the iron(II) is oxidised to iron(III). This then will execute the polymerisation process at about 50°C (Lohse, Zweifel 1986).

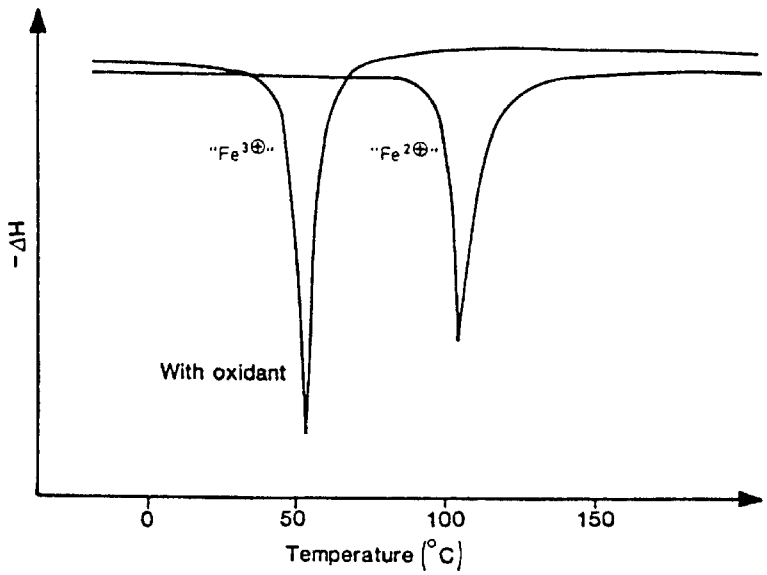

Fig. 3. DSC diagram of epoxide polymerisations with 2.5 % photoinitiator in the presence and in absence of the oxidant cumene hydroperoxide.

Cationic polymerisation with iron-arene complexes must therefore be considered a dual step process: 1. liberation of the active initiator by photolysis and 2. heat treatment to obtain complete polymerisation.

CONCLUSION

Organometallic photochemistry has practically not been used in industrial processes so far. The two examples of using organometallic photochemistry for polymerisation initiation seem only the beginning of exploiting a so far unused field.

REFERENCES

Brown DLS, Connor JA, Dobinson B, Stark BP (1976) Organometal carbonyl compounds of iron, molybdenum, and manganese as photosensitisers of the anhydride cure of epoxy resins. Angew Makromol Chem 50: 9

Chaudhari MA, Treichel PM, Stone FGA (1964) Pentafluorophenyl derivatives of transition metals. J Organometal Chem 2: 206

Crivello JV, Lam JHW (1977) Diaryliodonium Salts. A new class of photoinitiators for cationic polymerisation. Macromolecules 10: 1307

Crivello JV (1984) Applications of photoinitiated cationic polymerisation to the development of new photoresists. ACS Symp Ser 242: 3

Curtis H, Irving E, Johnson BFG (1986) Organometallic photoinitiated polymerisations. Chem in Britain 22: 327

Delzenne GA (1979) Organic photochemical imaging systems. Adv Photochem 11:1

Gill TP, Mann KR (1980) Photochemical generation of a reactive transition metal fragment. Inorg Chem 19: 3007
Gill TP, Mann KR (1981) Synthetic applications of the photolysis of the cyclopentadienyliron-(p-xylene) cation. J Organometal Chem 216: 65
Green GE, Stark BP (1981) Photopolymer systems and their applications. Chem in Britain 17: 228
Kaeriyama K, Shimura Y (1972) Photopolymerisation with the use of titanocene dichloride as sensitizer. J Polymer Sci: Polymer Chem Edit 10: 2833
Lohse F, Zweifel H (1986) Photocrosslinking of epoxy resins. Adv in Polymer Sci 78: 61
Meier K, Bühler N, Zweifel H, Berner G, Lohse F (1982) Härtbare, Metallocenkomplexe enthaltende Zusammensetzungen, daraus erhältliche aktivierbare Vorstufen und deren Verwendung. Eur Pat Appl N° 0 094 915
Meier K, Rihs G (1985) Reactions in the ligand sphere of iron(II): synthesis of crown ethers. Angew Chem Int Ed Eng 24: 858
Meier K, Zweifel H (1985) Imaging with cationic organometallic photoinitiators. Polymer Preprints 26: 347
Meier K, Zweifel H (1986) Imaging with iron arene photoinitiators. J Imaging Sci 30: 174
Nesmeyanov AN, Vol'kenau NA, Shilovtseva LS (1963) Exchange of ligands in ferocene. Dokl Akad Nauk SSSR 149: 615
Nesmeyanov AN, Vol'kenau NA, Shilovtseva LS (1970) Photodisproportionation of arene-cyclopentadienyl derivatives of iron. Dokl Akad Nauk SSSR 190: 857
Peng M, Brubaker CH (1978) Photochemical generation of reactive titanium (II) species. Inorg Chim Acta 26: 231
Rausch MD, Boon WH, Mintz EA (1978) Photochemical investigations of some di-η^5-cyclopentadienyl-diaryltitanium compounds. J Organomet Chem 160: 81
Riediker M, Roth M, Bühler N, Berger J (1983) Metallocene und photopolymerisierbare Zusammensetzung, enthaltend diese Metallocene. Eur Pat Appl N° 0 122 223
Rohde O, Riediker M, Schaffner A (1985) Recent advances in photoimagable polyimides. Proc SPIE-Int Soc Opt Eng 539: 175
Rohde O, Riediker M, Schaffner A (1986) High resolution, high photospeed polyimide for thick film applications. Solid State Technol 1986: (9) 109
Roloff A, Meier K, Riediker M (1986) Synthetic and metal organic photochemistry in industry. Pure and Appl Chem 58: 1267
Schlesinger SI (1974) Photopolymerisation of epoxides. Photogr Sci Eng 18: 387
Steppan H, Buhr G, Vollmann H (1982) Resisttechnik - ein Beitrag zur Chemie der Elektronik. Angew Chem 94: 417
Tung HS, Brubaker CH (1981) Photochemical decomposition of (diphenyl)-bis(η^5-pentamethylcyclopentadienyl)titanium and the zirconium analogs. Inorg Chim Acta 52: 197
Zucchini U, Albizati E, Giannini U (1971) Synthesis and properties of some titanium and zirconium benzyl derivatives. J Organometal Chem 26: 357

SYNTHESIS AND CHARACTERIZATION OF A μ-oxo-diruthenium COMPLEX AS A PRECURSOR TO AN EFFICIENT WATER OXIDATION CATALYST

F.P.Rotzinger, S.Munavalli[1a], P.Comte, J.K.Hurst[1b], and M.Grätzel

Institut de Chimie Physique, Ecole Polytechnique Fédérale
1015 Lausanne, SWITZERLAND

A precursor to a highly active molecular water oxidation catalyst has been prepared by controlled potential electrolysis of *cis*- $Ru^{II}(H_xL)_2(H_2O)_2$ in 0.5 M H_2SO_4. The deprotonated ligand L^{2-} is the 2,2'-bipyridyl-5,5'-dicarboxylate anion. The dimers $(H_xL)_2(H_2O)Ru^{III}ORu^{III}(H_2O)(H_xL)_2$ (blue) and $(H_xL)_2(H_2O)Ru^{III}ORu^{IV}(H_2O)(H_xL)_2$ (orange) were characterized by cyclic voltammetry, resonance Raman and UV-vis spectroscopy. In 0.5 M H_2SO_4, Ce^{IV} and Co^{3+} oxidize water rapidly to molecular oxygen in presence of this dimer. In comparison to other similar μ-oxo-Ru dimers this complex is a much more durable and efficient water oxidation catalyst.

INTRODUCTION

Strong oxidants such as e. g. Ag^{2+}, Co^{3+} and Ce^{IV} oxidize water only slowly in acidic solution despite of the large driving force, because the one electron oxidation of water leads to the very unstable hydroxyl radical. A simultaneous oxidation of two water molecules concerted with O-O bond formation, *viz.* $2\ H_2O \rightarrow H_2O_2 + 2\ e + 2\ H^+$, would avoid the formation of hydroxyl radicals and therefore, a much lower energy of activation would be required for water oxidation. A binuclear complex exhibiting e. g. two coordinated hydroxide ligands could achieve this goal:

$$\begin{array}{llll} M^{n+}\text{-}O\text{-}M^{n+} & \rightarrow & M^{n-1}\text{-}O\text{-}M^{n-1} & + 2\ H^+ \\ | \quad | & & | \quad | & \\ HO \quad OH & & O \text{———} O & \end{array}$$

The complex $(bpy)_2(H_2O)Ru^{III}\text{-}O\text{-}Ru^{III}(H_2O)(bpy)_2^{4+}$ was recently studied in detail by Gilbert et. al. (1985) and found to be a precursor to a water oxidation catalyst, indeed. Unfortunately, this compound has a low turnover number.

We found that by using the 2,2'-bipyridyl-5,5'-dicarboxylic acid ligand (H_2L) instead of 2,2'-bipyridine (bpy), a more efficient water oxidation catalyst is obtained.

---

[1] Invited professor, on leave of absence from:

a) The Chemical Research and Development Center of the United States Army, Edgewood, Maryland 21010.

b) The Department of Chemistry, Oregon Graduate Center, Beaverton, Oregon 97006.

Photochemistry and Photophysics
of Coordination Compounds, Ed. by H. Yersin/A. Vogler

SYNTHESIS AND CHARACTERIZATION

Attempts to prepare the $(HL)_2Ru(H_2O)_2$ (HL: monodeprotonated H_2L ligand) directly from "$RuCl_3 \cdot 3\ H_2O$" and the ligand failed, presumably because the desired product polymerizes via displacement of coordinated water by carboxylate. $(H_xL)_2Ru^{II}(H_2O)_2$ in 0.5 M H_2SO_4 ($1 < x \leq 2$) was prepared as follows:

$$\text{"}RuCl_3 \cdot 3\ H_2O\text{"} \xrightarrow{L',EtOH} RuL'_2Cl_2 \cdot H_2O$$

(L': 2,2'-bipyridyl-5,5'-dicarboxylic acid diethyl ester)

$$RuL'_2Cl_2 \cdot H_2O \xrightarrow[H_2O/EtOH]{NEt_3} Ru(H_2L)_2Cl_2 \cdot 2.5\ H_2O$$

$$Ru(H_2L)_2Cl_2 \cdot 2.5\ H_2O \xrightarrow[0.5\ M\ H_2SO_4]{Ag^+} (H_xL)_2Ru^{II}(H_2O)_2$$

$(H_xL)_2Ru^{II}(H_2O)_2$ forms $Ru^{II}(H_2L)_2SO_4 \cdot 4\ H_2O$ on standing in 0.5 M H_2SO_4 for a couple of weeks. The IR spectrum shows that sulfate acts as a bidentate chelating ligand. From this behavior and the CV (exhibiting $E_{1/2}$ = 0.78 V for the diaqua complex and a small wave at $E_{1/2}$ = 0.61 V for the sulfato complex) we conclude that sulfato complexes must also exist in solution.

Electrolysis of $(H_xL)_2Ru^{II}(H_2O)_2$ at 1.1 V (SCE) produced the corresponding Ru^{III} complex which then was dimerized by heating to 40°C and keeping the potential at 1.1 V. The primarily formed dimers are presumably sulfato complexes exhibiting $E_{1/2}$ = 0.68 and 0.87 V. The sulfato dimers were subsequently reduced at 0.65 V which lead to the diaqua complex $(H_xL)_2(H_2O)Ru^{III}\text{-}O\text{-}Ru^{III}(H_2O)(H_xL)_2$ which is oxidized reversibly to the corresponding $Ru^{III}\text{-}Ru^{IV}$ dimer at 0.98 V. This complex slowly oxidizes water to molecular oxygen. The sulfato complexes of the $Ru^{III}\text{-}Ru^{IV}$ dimer are reformed, if the solution is again electrolyzed at 1.1 V.

The thus obtained $Ru^{III}\text{-}Ru^{III}$ and $Ru^{III}\text{-}Ru^{IV}$ dimers were further characterized by UV-vis spectroscopy. The former complex exhibits λ_{max} at 654 nm with ε = 18000 $M^{-1}cm^{-1}$ whereas the latter has λ_{max} at 500 nm with ε = 17000 $M^{-1}cm^{-1}$. These maximas are red-shifted compared to those of the corresponding bpy analogs (Gilbert et. al. 1985).

The Raman spectra of the $Ru^{III}\text{-}Ru^{III}$ and $Ru^{III}\text{-}Ru^{IV}$ dimers show ν_s at 375 and 381 cm^{-1}, respectively. These vibrations are resonance enhanced and typical to ν_s(M-O-M) (Plowman et. al 1984, Burke et. al. 1978, San Filippo et. al. 1976 and Campbell et. al. 1980). Further evidence for the proposed structures and oxidation states were obtained

from chemical reductions of $(H_xL)_2(H_2O)Ru^{III}$-O-$Ru^{IV}(OH)(H_xL)_2$ with ascorbic acid. Addition of one equivalent of reductant to the Ru^{III}-Ru^{IV} dimer lead to the Ru^{III}-Ru^{III} dimer which was converted to two moles of $(H_xL)_2Ru^{II}(H_2O)_2$ upon addition of two equivalent.of reductant. At pH ≈ 3 the Ru^{III}-Ru^{III} dimer precipitates after addition of acetone. The solid analyzes as $Ba[(HL)(L)(H_2O)Ru^{III}$-O-$Ru^{III}(H_2O)(L)(HL)]\cdot 13\ H_2O$.

The *trans* isomers of the $(bpy)_2Ru^{II/III}(H_2O)_2^{2+/3+}$ complexes are thermodynamically unstable, but they can be generated by irradiation of the corresponding *cis* complexes (Durham et. al 1980). Since our preparations have been carried out in the dark, the monomers are expected to be present in the *cis* configuration. Dimerization of the *cis* complex, however, can still lead to two isomers, the racemate and the meso form. The crystal structure of $[(bpy)_2(H_2O)Ru^{III}$-O-$Ru^{III}(H_2O)(bpy)_2](ClO_4)_4\cdot 2\ H_2O$ is known (Gilbert et. al. 1985), and this compound is racemic.

The solution of $(H_xL)_2(H_2O)Ru^{III}$-O-$Ru^{III}(H_2O)(H_xL)_2$ in 0.5 M H_2SO_4 prepared by the procedure described above exhibits, in addition to the prominent wave at 0.98 V, an additional small wave at ≈ 0.9 V (SCE) in the CV. We assume that the wave at ≈ 0.9 V is due to small amounts of another isomer (eventually the meso form). Also, the isomer produced in large amounts is less soluble in acetone/H_2O at pH ≈ 3.

PROPOSED WATER OXIDATION MECHANISMS

a) Mechanism proposed by Gilbert et. al. (1985):
Based on CV using a glassy carbon electrode Gilbert et. al. (1985) postulate a three electron oxidation of the $(bpy)_2(H_2O)Ru^{III}$-O-$Ru^{III}(H_2O)(bpy)_2$ complex to the corresponding Ru^{V}-O-Ru^{V} dimer which restores the Ru^{III}-O-Ru^{III} dimer by reductive elimination of molecular oxygen. We assume that this mechanism is not established, because we were unable to obtain the three electron wave using In doped SnO_2 electrode.

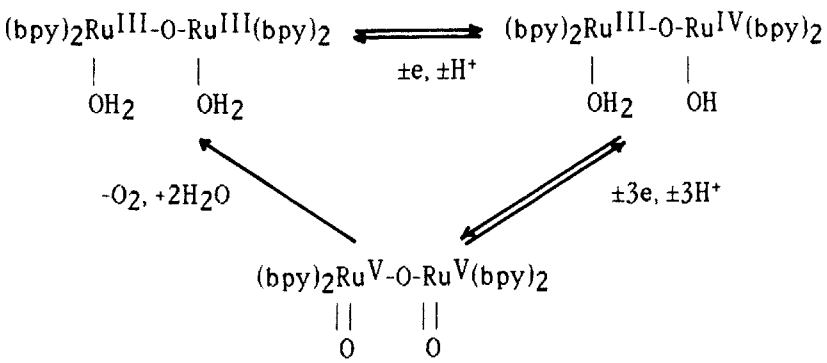

b) Alternative Mechanism:
Only the $(H_xL)_2(H_2O)Ru^{III}$-O-$Ru^{III}(H_2O)(H_xL)_2$ complex and the corresponding Ru^{III}-O-Ru^{IV} dimer can be observed by UV-vis spectroscopy and CV. Therefore, we propose that formation of the Ru^{IV}-O-Ru^{IV} dimer is slow and/or thermodynamically unfavorable, but this presumably very reactive species forms a μ-oxo, μ-peroxo complex which would quickly form molecular oxygen upon oxidation and reform the Ru^{III}-O-Ru^{III} dimer.

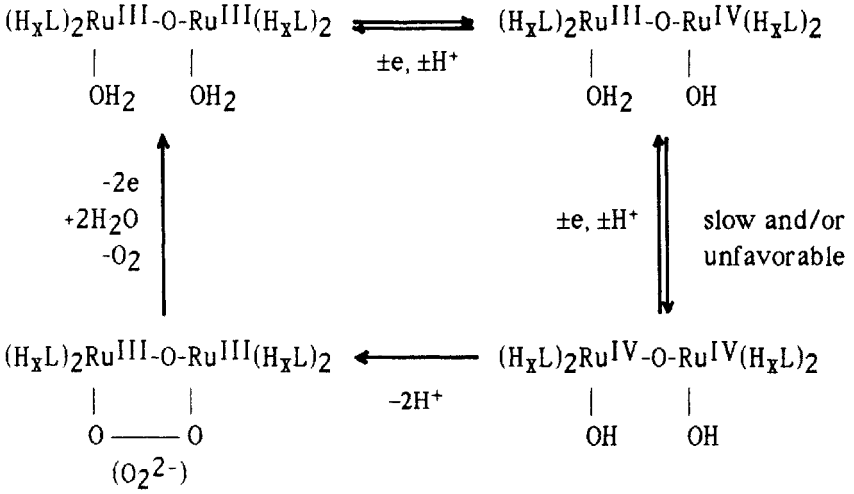

REFERENCES

Burke J J, Kincaid J R, Spiro T G (1978) J Am Chem Soc 100: 6077.

Campbell J R, Clark R J H (1980) J Chem Soc Faraday Trans II 76: 1103.

Durham B, Wilson S R, Hodgson D J, Meyer T J (1980) J Am Chem Soc 102: 600.

Gilbert J A, Eggleston D S, Murphy W R, Geselowitz D A, Gersten S W, Hodgson D J, Meyer T J (1985) J Am Chem Soc 107: 3855.

Plowman J E, Loehr T M, Schauer C K, Anderson O P (1984) Inorg Chem 23: 3553.

San Filippo J Jr, Grayson R L, Sniadock H T (1976) Inorg Chem 15: 1103.

THE APPLICATION OF DIFFUSE REFLECTANCE LASER FLASH PHOTOLYSIS TO METAL PHTHALOCYANINES IN AN OPAQUE ENVIRONMENT

F.Wilkinson and C.J.Willsher

Department of Chemistry, University of Technology, Loughborough, LE11 3TU, UK

Since its initial discovery, the elegant technique of flash photolysis has been continually refined in response to developments in the instrumentation for capturing very fast signals and in the shortening of the excitation pulse. A recent development has been our work to extend flash photolysis to opaque and highly-scattering substances; for such samples the transient species generated by an exciting pulse is interrogated by means of monitoring light which has been diffusely reflected from the sample. We have used 'Diffuse Reflectance Flash Photolysis' (DRFP) to detect transient absorption from the triplet state of a number of chromophores in a wide variety of different opaque environments, such as hydrocarbons adsorbed on γ-alumina, (Kessler, Wilkinson, 1981) ketones in microcrystalline form (Wilkinson, Willsher, 1984) and intercalated in the channels of the synthetic zeolite 'silicalite' (Wilkinson, Willsher, Casal, Johnston, Scaiano, 1986), and in the dyestuff Rose Bengal chemically attached to a polymer substrate (Wilkinson, Willsher, Pritchard, 1984). We have also shown that pulse radiolysis can be carried out on opaque substances by using the diffuse reflection from the sample to monitor transients formed by ionising radiation (Wilkinson, Willsher, Warwick, Land, Rushton, 1984), and recently we have extended DRFP to follow processes initiated by a picosecond excitation source (Wilkinson, Willsher, Leicester, Barr, Smith, 1986).

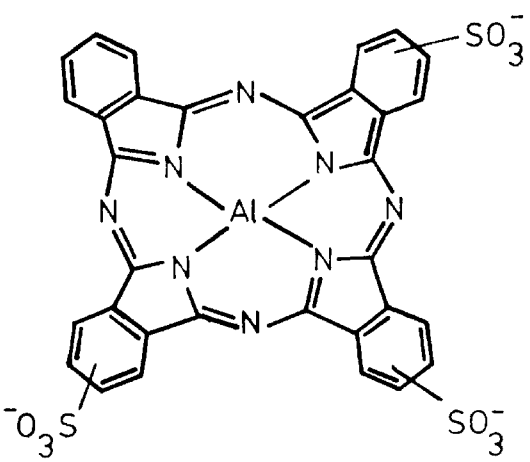

Aluminium Sulphonated Phthalocyanine (ALPCS)

Photochemistry and Photophysics of Coordination Compounds, Ed. by H. Yersin/A. Vogler

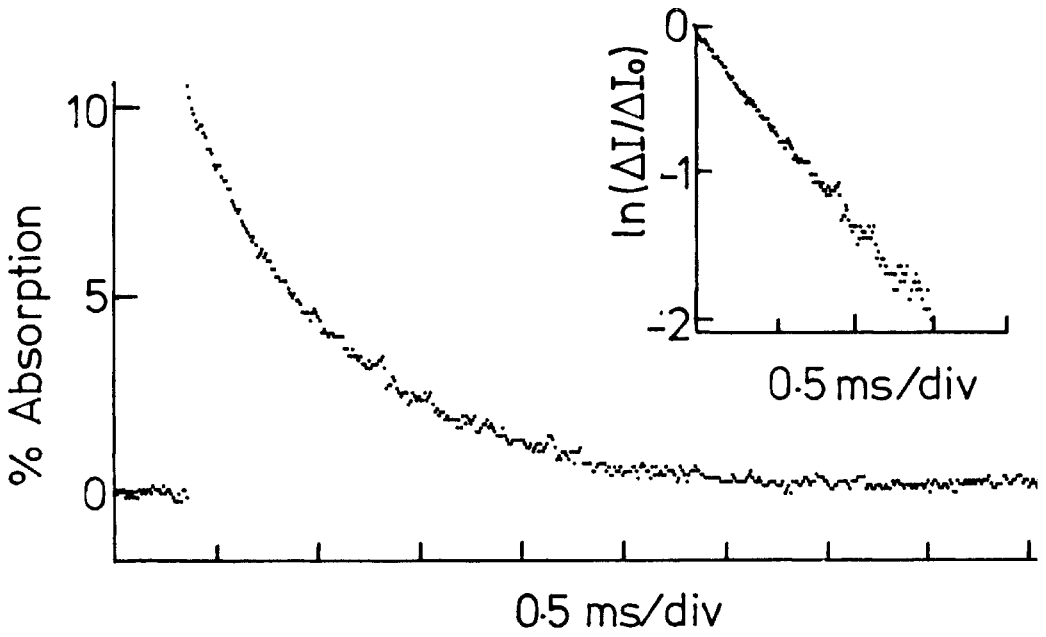

Figure 1. Decay of the triplet-triplet absorption at 510 nm of ALPCS dyed into a dry, N_2-purged cotton fabric. λ_{exc} = 354 nm.

We shall disuss briefly DRFP studies of a metal phthalocyanine, namely ALPCS dyed into a woven cotton fabric. The transient difference spectrum can be assigned as arising mainly from the triplet state of ALPCS (Wilkinson, Willsher, 1985). The decay of the triplet, which depicted in figure 1, follows a first order rate law where τ is in the region of 1 ms. This lifetime is somewhat longer than that observed for triplet ALPCS in water, where τ ranges between 250 and 50 μs, depending on the pH of the solution (Darwent, McCubbin, Phillips, 1982). Quenching by O_2 of triplet ALPCS is not observed in a dry fabric, and an oxygen effect can be seen only when the cotton is soaked with water. The deactivation of the oxygen-quenched triplet is shown in fig. 2 but the decay cannot be fitted by a pseudo-first order rate law, which suggests that the quenching process is inefficient. In an aqueous solution, however, oxygen quenching does occur quite efficiently, with $k_q = (2.0+0.1) \times 10^9$ dm^3 mol^{-1} s^{-1} (Darwent, McCubbin, Phillips, 1982). It is interesting to note that electron donors such as cysteine or p-benzohydroquinone have no effect on the decay of triplet ALPCS, even when the cotton fabric is water-saturated and concentrations of donor as high as 10^{-1} M are used in the solutions employed to load the dyed fabric with donor molecules. It is reported than in solution

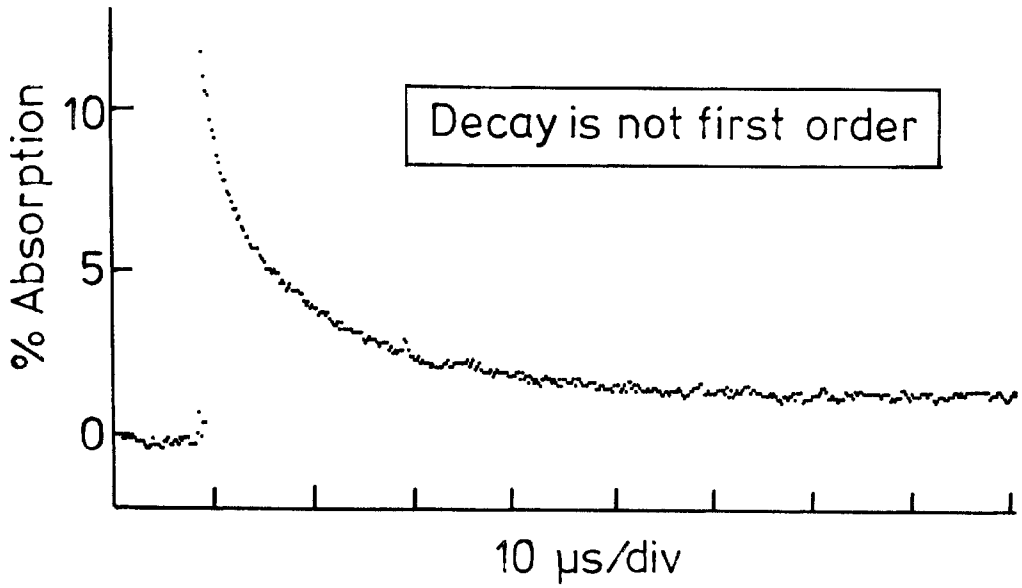

Figure 2. Decay of the triplet-triplet absorption at 510 nm of ALPCS dyed into cotton fabric which is water-saturated and oxygen-purged following pulsed excitation at 354 nm.

k_q = 5.5 x 10^8 dm^3 mol^{-1} s^{-1} for quenching with p-benzohydroquinone that leads to the formation of the phthalocyanine radical anion, (Darwent, McCubbin, Phillips, 1982); this species is not detected in the dyed fabric. These observations suggest that ALPCS is quite inaccessible when incorporated in cotton fibres, and water is necessary to observe quenching by oxygen. Even so, quenching by oxygen is not totally efficient, and larger molecules such as cysteine and p-benzohydroquinone cannot interact with the chromophore to any measurable extent, and therefore the electron transfer reactions which are known to occur in a less restricted environment are insignificant within the fibres of a cotton fabric.

CJW gratefully acknowledges support from the European Office of the US Army under Contract No. DAJA 45-85-C-0010 and wishes to thank the Department of Chemistry of LUT for financial assistance to attend this Conference.

References:

Darwent JR, McCubbin I, Phillips D (1982) Excited Singlet and Triplet State Electron-transfer Reactions of Aluminium(III) Sulphonated Phthalocyanine. J. Chem. Soc. Faraday Trans 2 78 347-357.

Kessler R, Wilkinson F (1981) Diffuse Reflectance Triplet-Triplet Absorption Spectroscopy of Aromatic Hydrocarbons Chemisorbed on γ-alumina. J. Chem. Soc. Faraday Trans 1 77 309-320.

Wilkinson F, Willsher CJ (1984) Detection of Triplet-Triplet Absorption in Microcrystalline Benzophenone by Diffuse Reflectance Laser Flash Photolysis, Chem.Phys.Lett. 104 272-276 and Triplet-Triplet Absorption in Microcrystalline Benzil Detected by Diffuse Reflectance Laser Flash Photolysis, Appl. Spectros. 38 897-901.

Wilkinson F, Willsher CJ (1985) Detection of Transient Absorption in a Dyed Cotton Fabric and in Semiconductor Powders by Diffuse Reflectance Laser Flash Photolysis, J. Chem. Soc. Chem. Comm. 142-143.

Wilkinson F, Willsher CJ, Casal HL, Johnston LJ, Scaiano JC (1986) Intrazeolite Photochemistry IV. Studies of Carbonyl Photochemistry on the Hydrophobic Zeolite Silicalite using Time-Resolved Diffuse Reflectance Techniques, Can. J. Chem, 64 539-544.

Wilkinson F, Willsher CJ, Leicester PA, Barr JRM, Smith MJC (1986) Picosecond Diffuse Reflectance Laser Flash Photolysis, J.Chem.Soc.Chem.Comm. 1216-1217.

Wilkinson F, Willsher CJ, Pritchard RB (1985) Laser Flash Photolysis of Dyed Fabrics and Polymers - I - Rose Bengal as a Photosensitising Dye, Eur. Polym. J. 21 333-341.

Wilkinson F, Willsher CJ, Warwick P, Land EJ, Rushton FAP (1984) Diffuse Reflectance Pulse Radiolysis of Opaque Samples, Nature 311 40-42.

QUENCHING OF SINGLET OXYGEN BY COBALT COMPLEXES

T.Vidóczy and S.Németh

Central Research Institute for Chemistry of the Hungarian Academy of Sciences, Pusztaszeri ut 59-67, 1025 Budapest, HUNGARY

Certain coordination compounds are efficient quenchers of singlet ($^1\Delta_g$) oxygen (Wilkinson 1981), referred to firstly by Carlsson (1974). Afterwards experiments were aimed to obtain a better insight into the polymer stabilizing efficiency of these compounds (Allen 1984). In spite of these results, however, no general theory emerged which could explain the large differences in the quenching ability of the various coordination compounds. The only study of the substituent effect on the ligands has not been evaluated kinetically (Kajitani 1985). Therefore we undertook a systematic study of the quenching of singlet oxygen by coordination compounds, starting with a series of cobalt complexes.

Quenching rate constants were determined by the widely accepted method of measuring the consumption of a singlet oxygen acceptor, 1,3-diphenyl-isobenzofuran (DPhBF) in both the absence and the presence of the quencher (Merkel 1974). Singlet oxygen was generated by a flashlamp pumped dye laser (Rhodamine 6G) using methylene blue (MB) as a sensitizer. Neutral density filters were employed to control the pulse intensity in order to keep the consumption of the acceptor below 10%. Under such conditions the consumption of the acceptor, being the measure of the disappearance of singlet oxygen, follows first order kinetics. The increase in the apparent first order rate constantdivided by the concentration of the quencher (Q) yields the quenching rate constant to be determined.

The accuracy of the measuremens is higher, if the lifetime of singlet oxygen is longer in the solvent employed. Therefore a mixture of 90% dichloromethane and 10% methanol was used.

Typical experimental result is shown in Fig. 1, where the main diagram represents the original data points, whereas the inset shows the straight line fitted to the evaluated points.

All cobaloximes were prepared according to the modified Schrauzer (1968) method. All chemicals were of analytical grade, diphenylglyoxime was recrystallized before use (m.p.: 240-1°C). In every case 0.02 mol of dimethylglyoxime or diphenylglyoxime, 0.02 mol of LiOH and 0.012 mol of the appropriate axial ligand were dissolved in 100 ml of boiling ethanol, and 0.01 mol of $Co(ClO_4)_2.6H_2O$ were added under intensive stirring. Oxygen was bubbled through the solution for 2 hours. The precipitates were filtered off, washed ether and dried. When TLC analysis indicated the presence of impurities, the solids were recrystallized from ethanol-water mixture. The complexes were characterized by their IR spectra.

$Ph_3PCo(Hdmg)_2OH$: yield 32%; IR (in cm^{-1}): 3094, 1556, 1483, 1437, 1248, 1104-1084 (broad), 752, 698, 517.

Photochemistry and Photophysics of Coordination Compounds. Ed. by H. Yersin/A. Vogler

$Et_3NCo(Hdmg)_2OH$: yield 22%; IR: 2941, 2904, 1562, 1460 (br), 1384, 1210 (br), 1113, 974, 750, 503.

$pyCo(Hdmg)_2OH$: yield 19%; IR: 3101, 3094, 3027, 3011, 2894, 1608, 1566, 1493, 1450, 1242, 1229, 1108, 977, 773, 750 (br), 698, 511.

$Ph_3PCo(Hdpg)_2OH$: yield 44%; IR: 3022, 1482, 1440, 1262, 1117, 1088 (br), 993, 889, 740, 695, 622, 514.

$pyCo(Hdpg)_2OH$: yield 31%; IR: 3031, 1610, 1491, 1453, 1446, 1302 (br), 1132, 896, 766, 740, 692, 628.

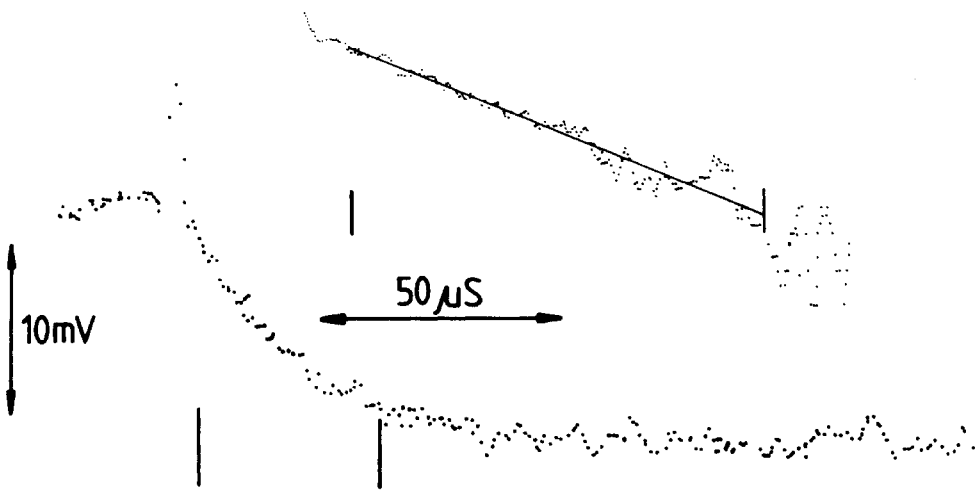

Figure 1
Results of a typical measurement. [DPhBF] = $2.21 \cdot 10^{-5}$ mol·dm^{-3}, [Q] = $1.91 \cdot 10^{-4}$ mol·dm^{-3}, calculated rate constant = 44700±720 s^{-1}

The results of our measurements are summarized in Table 1. The results show clearly that both the equatorial and the axial ligands exert a decisive effect on the quenching ability of the complex. Comparing the values obtained with the dimethylglyoxime series it can be assumed that a correlation exists between the sigma donor potential of the axial ligand and the rate constant for quenching; the same holds for the corresponding dimethylglyoxime and diphenylglyoxime pairs. This hypothesis will be tested in the next series of experiments.

Table 1
Rate constants for quenching of singlet oxygen by cobalt complexes

Complex	$k_q \cdot 10^{-6}$ $dm^3 \cdot mol^{-1} \cdot s^{-1}$
$Co(acac)_3$	650±50
$Et_3NCo(Hdmg)_2OH$	150±20
$pyCo(Hdmg)_2OH$	45±10
$pyCo(Hdpg)_2OH$	20± 6
$Ph_3PCo(Hdmg)_2OH$	<5
$Ph_3PCo(Hdpg)_2OH$	<5
Ph_3P	5±0.5
H_2dmg	1±0.5

Hdmg: monoanion of dimethylglyoxime; Hdpg: monoanion of diphenylglyoxime; py: pyridine; NEt_3: triethylamine; PPh_3: triphenylphosphine; acac: acetylacetonate monoanion.

One of the authors (T. V.) gratefully acknowledges the helpful discussions with professor Dezső Gál.

References:

Allen NS, Chirinos-Padron A, Appleyard JH (1984) Photo-stabilizing action of metal chelate stabilizers in polypropylene-Part VI: importance of singlet oxygen quenching and UV screening, and flash photolysis studies. Polym. Degr. Stab. 6: 31-45

Carlsson DJ, Suprunch T, Wiles DM (1974) Quenching of singlet oxygen by transition-metal chelates. Can J Chem 52: 3728-3734

Kajitani M, Yoshida Y, Akiyama T, Sugimori A (1985) Effects of substituents in the aryl moiety of bis(1,2-diaryl-1,2-ethylenedithiolato)nickel on the quenching of singlet oxygen and the reaction with singlet oxygen. Nippon Kagaku Kaishi 1985: 433-437

Merkel PB, Kearns DR (1971) Direct measurement of the lifetime of $^1\Delta$ oxygen in solution. Chem Phys Lett 12: 120-124

Schrauzer GN (1968) Bis(dimethylglyoximato)cobalt complexes ("Cobaloximes"). In: Jolly WL (ed) Inorganic synthesis volume XI, McGraw-Hill Book Company, New York San Francisco Toronto London Sydney, p 61

Wilkinson F, Brummer JG (1981) Rate constants for the decay and reaction of the lowest electronically excited singlet state of molecular oxygen in solution. J Phys Chem Ref Data 10: 809-998

RECENT ADVANCES IN INORGANIC AND ORGANOMETALLIC PHOTOLITHOGRAPHY

R.E.Wright

Corporate Research Laboratory, 3M, St. Paul, MN 55144, USA

During the last decade there has been a rapid growth in the number of publications dealing with commercially related applications of inorganic and organometallic photochemistry. The majority of these relate to lithography, specifically photoinitiators, photocrosslinking agents, and microlithography. There are far fewer examples of systems that have actually been commercialized, however. This paper is intended to both inform and stimulate inorganic and organometallic photochemists so that they will be more aware of the current 'hot' topics in all three areas of research. Several excellent references are available on conventional lithography (Brinckman 1978; Roffey 1982; Thompson 1983; Pappas 1985). For any commercial system containing inorganic or organometallic components to succeed, it must meet several requirements. First and most important, the system must meet strict toxicological guidelines both for the ultimate user and for the environment. It must also be economical. Air stability is a concern since special handling is otherwise required and finally, the system must offer advantages over more conventional or traditional alternatives.

The utility of most lithographic systems arises from photochemically induced solubility differences. Insolubilization may occur by formation of an insoluble polymer from a soluble monomer or else by formation of a crosslinked polymer from soluble oligomers or low molecular weight polymers. Conventional photopolymers are usually cured by one of two routes. Acrylate and related monomers are cured by free radical initiators whereas epoxides require cationic initiation. If either inorganic or organometallic initiators are to be utilized, they will most likely be limited to those few cases where some definite increase in performance is observed. Since small quantities of initiator are needed, the other requirements for success, except air stability, can be largely ignored.

Lithographic systems in which insolubilization occurs as a result of crosslink formation are treated separately since there is no chain reaction. A single event gives rise to a single stoichiometric chemical reaction. Several metal-containing systems, described below, have been shown to offer advantages over conventional organic ones but since larger quantities of the photoactive species are necessary, the other restrictions become much more important.

Another area where inorganic and organometallic photochemists can make significant contributions is microlithography. As the name implies, microlithography is a subset of lithography that is defined by resolution limits. The fabrication of microelectronic circuits is the principal goal. High resolution is required with both speed and cost being of secondary concern. Current efforts are pushing below one micron resolution and the market is primed for major breakthroughs in this area. The ultimate resolution is of course limited by the wavelength.

Photochemistry and Photophysics
of Coordination Compounds, Ed. by H. Yersin/A. Vogler

PHOTOPOLYMERS

A recent review (Curtis 1986) presents an excellent introduction to organometallic photoinitiators. The ability of some dinuclear transition metal carbonyl complexes to initiate free radical polymerizations has been known for some time (von Gustorf 1966). More recently, complexes which generate organic radicals directly upon photolysis have been investigated (Geoffrey 1979). So far, there have been no clear cut advantages demonstrated in using inorganic or organometallic free radical initiators over traditional organic systems.

In curing of epoxides, a great deal of industrial research has been going on. Several patents have either issued or been applied for in this area (Irving 1983; Palazzotto 1984; Yates 1984). Most of the efforts have dealt with cationic initiators. The mechanism has not been clearly elucidated but appears to involve the formation of coordinatively unsaturated cationic metal complexes arising from loss of a ligand. This area continues to be an active area of research.

PHOTOCROSSLINK FORMATION

Since no chain reaction is involved in formation of crosslinks, efficient photoreactions are a prerequisite. Transition metal carbonyl complexes, where quantum yields are typically near unity, have therefore received the most attention. Toxicity problems associated with metal carbonyls in general have hindered progress in this area. Furthermore, homoleptic metal carbonyls tend to have appreciable vapor pressures at room temperature and thus present a considerable stability problem. One possible way to circumvent these problems was first suggested by Pittman (1971) when he showed that some metal carbonyl complexes, especially those containing arene or cyclopentadiene groups, could be easily incorporated into polymer backbones by appropriate functionalization. The synthetic route to a typical organometallic polymer precursor is outlined below. Polymers containing pendant transition metal carbonyl complexes of this type have been found to be useful as lithographic systems (Wright 1985).

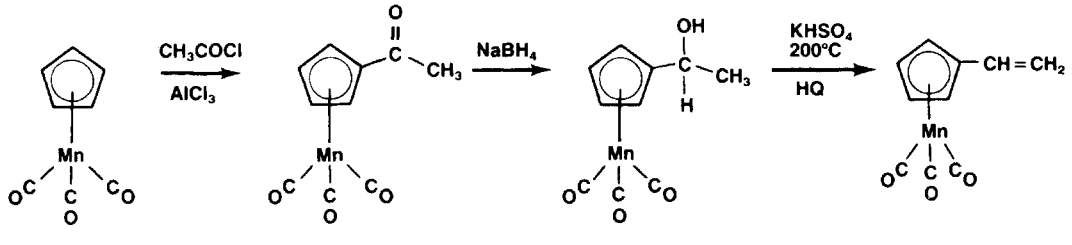

The functionalized polymers can be crosslinked several different ways. In the presence of bidentate ligands such as pyrazine, 4,4'-bipyridyl, and ethylenediammine, irradiation results in crosslink formation and insolubilization in the exposed areas. Furthermore, if the bridging ligand contains conjugation such that the metals are in electronic communication, highly colored images result. Resolution better than 1000 line pair per millimeter was achieved in some cases. The proposed mechanism of crosslink formation is shown below. Note that the method is inherently slow because crosslink formation requires two separate metal centers to undergo -CO loss before the bridge can form. There is also an orientation requirement for crosslinks of this type

to occur. The organometallic photopolymers are useful either as negative resist materials in which the unexposed areas are removed by wet development or alternatively, the image can be fixed by heating the film at some temperature at which the excess ligand can be driven off to give a non-silver imaging system.

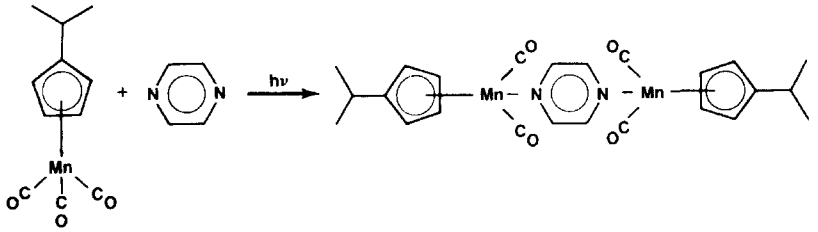

In an attempt to increase the speed of the system, both the organometallic moiety and a nucleophile were incorporated in the polymer backbone. The resulting photopolymers were found to become insoluble after much shorter exposure times. Spectroscopic evidence supports a mechanism involving photochemical loss of -CO followed by coordination of the nucleophile. Others (Purbrick 1981) have investigated the use of transition metal carbonyl complexes as components in compositions containing nucleophilic polymers. These systems also crosslink upon irradiation, although it appears that oxygen plays an important role in the mechanism of crosslink formation. In all likelihood, both mechanisms are operative. Several advantages of organometallic photopolymers have been shown. The best solvent was found to be dilute H_3PO_4 containing a small amount of an inorganic salt such as $CuSO_4$. Elimination of the need for organic developers is a major benefit. Adhesion of the photopolymers to aluminum substrates was found to be considerably better than observed using traditional organic photopolymers which usually require addition of an adhesion promoting layer. This often makes the final printing plate humidity and/or temperature sensitive. The organometallic photopolymers do not require addition of an adhesion promoter. The ability of coordinatively unsaturated metal carbonyl complexes to bind to oxide surfaces is known and it is assumed that a similar mechanism is operative at the oxide/photopolymer interface. Humidity and temperature stability of the organometallic photopolymers is excellent.

MICROLITHOGRAPHY

Microlithography is a third area that is capturing the attention of photochemists. High resolution is required by the electronics industry for generation of photoresists and microcircuit fabrication. Recent work by Kutal and Willson (1986) has shown that $[Co(NH_3)_5Br](ClO_4)_2$ can be used to photocrosslink a copolymer of glycidyl methacrylate and ethyl acrylate, a well known negative resist (Thompson 1983). A combination of photochemical and thermal steps is proposed for the mechanism. The exposed films displayed features with 1-2 micron resolution after development.

The ability to photochemically generate conductive metal films with micron scale resolution has recently been demonstrated (Montgomery 1986). Backside irradiation through a quartz substrate which is in contact with a solution containing a dinuclear metal carbonyl and a soluble silver salt caused cleavage of the metal carbonyl to give radicals which then reduced the silver cations to silver metal on the

substrate. Film thickness was limited to less than a few hundred angstroms by the decreasing transmittance of the substrate as the metal film deposited. Copper and palladium were also used although the quality of the films was poorer and the power requirements higher. The need for transparent substrates, intimate contact of the substrate with the solution, and the relatively thin films formed are all drawbacks of the technology.

SUMMARY

Excellent opportunities exist for the inorganic and organometallic photochemist to contribute to areas of reprographic lithography. Applications are available for virtually any combination of performance attributes, including speed, resolution, and spectral response. Furthermore, use of metal-containing components may lead to unanticipated benefits that could have significantly greater impact. It remains for the photochemist to be more aware of the opportunities and consider possible applications of his efforts.

REFERENCES

Brinckman E, Delzenne G, Poot A, Willems J (1978) Unconventional imaging processes, 1st edn. Focal Press Limited, London New York

Curtis H, Irving E, Johnson BFG (1986) Organometallic photoinitiated polymerizations. Chem Brit 22: 327-329

Geoffrey GL, Wrighton MS (1979) Organometallic photochemistry, 1st edn. Academic Press, New York London Toronto Sydney San Francisco, pp 300-325

Irving E, Johnson BFG, Meier K (1983) Photopolymerization with organometallic salts. EP 0094914 A2

Kutal C, Willson CG (to be published) Photoinitiated crosslinking and image formation in thin polymer films containing a transition metal compound. J Electrochem Soc

Montgomery RK, Mantei TD (1986) UV laser deposition of metal films by photogenerated free radicals. Appl Phys Lett 48: 493-495

Palazzotto MC, Hendrickson WA (1984) Energy polymerizable compositions containing organometallic initiators. EP 0109851 A2

Pappas SP (ed) (1985) UV curing: science and technology, 1st edn. Technology Marketing Corp., Norwalk, CT

Pittman CU (1977) Vinyl polymerization of organic monomers containing transition metals. In: Becker EI, Tsutsui, M (eds) Organometallic reactions. Interscience, New York, 1-61

Purbrick MD, Wagner HM (1981) Transition metal-carbonyl derivatives as photopolymerization initiators and photocrosslinking agents in photoresists. J Photo Sci 29: 230-235

Roffey CG (1982) Photopolymerization of surface coatings. Wiley, New York

Thompson LF, Willson CG, Bowden MJ (1983) Introduction to lithography. In: ACS Symposium Series, No. 219. Am Chem Soc, Washington, DC

von Gustorf EK, Henry MC, Di Pietro C (1966) Photochemische umsetzung von $Fe(CO)_5$ mit vinylchlorid, styrol, propylen, und vinylathylather. Z Naturforsch 21B: 42-45

Wright RE (1985) Radiation-sensitive compositions of polymers containing a π-metal carbonyl complex of conjugated polyolefin. US 4503140

Yates RL (1984) Photoactivated catalytic polymerization of monoepoxides. US 4479858

AUTHOR INDEX